ISSN 1007-9327 (print)
ISSN 2219-2840 (online)

World Journal of *Gastroenterology*

World J Gastroenterol 2017 August 21; 23(31): 5645-5828

Published by Baishideng Publishing Group Inc

World Journal of Gastroenterology

A peer-reviewed, online, open-access journal of gastroenterology and hepatology

Editorial Board

2014-2017

The *World Journal of Gastroenterology* Editorial Board consists of 1375 members, representing a team of worldwide experts in gastroenterology and hepatology. They are from 68 countries, including Algeria (2), Argentina (7), Australia (31), Austria (9), Belgium (11), Brazil (20), Brunei Darussalam (1), Bulgaria (2), Cambodia (1), Canada (25), Chile (4), China (165), Croatia (2), Cuba (1), Czech (6), Denmark (2), Egypt (9), Estonia (2), Finland (6), France (20), Germany (58), Greece (31), Guatemala (1), Hungary (14), Iceland (1), India (33), Indonesia (2), Iran (10), Ireland (9), Israel (18), Italy (194), Japan (149), Jordan (1), Kuwait (1), Lebanon (7), Lithuania (1), Malaysia (1), Mexico (11), Morocco (1), Netherlands (5), New Zealand (4), Nigeria (3), Norway (6), Pakistan (6), Poland (12), Portugal (8), Puerto Rico (1), Qatar (1), Romania (10), Russia (3), Saudi Arabia (2), Singapore (7), Slovenia (2), South Africa (1), South Korea (69), Spain (51), Sri Lanka (1), Sudan (1), Sweden (12), Switzerland (5), Thailand (7), Trinidad and Tobago (1), Tunisia (2), Turkey (55), United Kingdom (49), United States (180), Venezuela (1), and Vietnam (1).

Gordon Stanley Howarth, *Roseworthy*
Seungha Kang, *Brisbane*
Alfred King Lam, *Gold Coast*
Ian C Lawrance, *PerthFremantle*
Barbara Anne Leggett, *Brisbane*
Daniel A Lemberg, *Sydney*
Rupert W Leong, *Sydney*
Finlay A Macrae, *Victoria*
Vance Matthews, *Melbourne*
David L Morris, *Sydney*
Reme Mountifield, *Bedford Park*
Hans J Netter, *Melbourne*
Nam Q Nguyen, *Adelaide*
Liang Qiao, *Westmead*
Rajvinder Singh, *Adelaide*
Ross Cyril Smith, *StLeonards*
Kevin J Spring, *Sydney*
Debbie Trinder, *Fremantle*
Daniel R van Langenberg, *Box Hill*
David Ian Watson, *Adelaide*
Desmond Yip, *Garran*
Li Zhang, *Sydney*

Austria

Felix Aigner, *Innsbruck*
Gabriela A Berlakovich, *Vienna*
Herwig R Cerwenka, *Graz*
Peter Ferenci, *Wien*
Alfred Gangl, *Vienna*
Kurt Lenz, *Linz*
Markus Peck-Radosavljevic, *Vienna*
Markus Raderer, *Vienna*
Stefan Riss, *Vienna*

Belgium

Michael George Adler, *Brussels*
Benedicte Y De Winter, *Antwerp*
Mark De Ridder, *Jette*
Olivier Detry, *Liege*
Denis Dufrane Dufrane, *Brussels*
Sven M Francque, *Edegem*
Nikos Kotzampassakis, *Liège*
Geert KMM Robaeys, *Genk*
Xavier Sagaert, *Leuven*
Peter Starkel, *Brussels*
Eddie Wisse, *Keerbergen*

Brazil

SMP Balzan, *Santa Cruz do Sul*
JLF Caboclo, *Sao jose do rio preto*
Fábio Guilherme Campos, *Sao Paulo*
Claudia RL Cardoso, *Rio de Janeiro*
Roberto J Carvalho-Filho, *Sao Paulo*
Carla Daltro, *Salvador*
José Sebastiao dos Santos, *Ribeirao Preto*
Eduardo LR Mello, *Rio de Janeiro*
Sthela Maria Murad-Regadas, *Fortaleza*
Claudia PMS Oliveira, *Sao Paulo*
Júlio C Pereira-Lima, *Porto Alegre*
Marcos V Perini, *Sao Paulo*
Vietla Satyanarayana Rao, *Fortaleza*
Raquel Rocha, *Salvador*
AC Simoes e Silva, *Belo Horizonte*
Mauricio F Silva, *Porto Alefre*
Aytan Miranda Sipahi, *Sao Paulo*
Rosa Leonôra Salerno Soares, *Niterói*
Cristiane Valle Tovo, *Porto Alegre*
Eduardo Garcia Vilela, *Belo Horizonte*

Brunei Darussalam

Vui Heng Chong, *Bandar Seri Begawan*

Bulgaria

Tanya Kirilova Kadiyska, *Sofia*
Mihaela Petrova, *Sofia*

Cambodia

Francois Rouet, *Phnom Penh*

Canada

Brian Bressler, *Vancouver*
Frank J Burczynski, *Winnipeg*
Wangxue Chen, *Ottawa*
Francesco Crea, *Vancouver*
Jane A Foster, *Hamilton*
Hugh J Freeman, *Vancouver*
Shahrokh M Ghobadloo, *Ottawa*
Yuewen Gong, *Winnipeg*
Philip H Gordon, *Quebec*
Rakesh Kumar, *Edmonton*
Wolfgang A Kunze, *Hamilton*
Patrick Labonte, *Laval*
Zhikang Peng, *Winnipeg*
Jayadev Raju, *Ottawa*
Maitreyi Raman, *Calgary*
Giada Sebastiani, *Montreal*
Maida J Sewitch, *Montreal*
Eldon A Shaffer, *Alberta*
Christopher W Teshima, *Edmonton*
Jean Sévigny, *Québec*
Pingchang Yang, *Hamilton*
Pingchang Yang, *Hamilton*
Eric M Yoshida, *Vancouver*
Bin Zheng, *Edmonton*

Chile

Marcelo A Beltran, *La Serena*
Flavio Nervi, *Santiago*
Adolfo Parra-Blanco, *Santiago*
Alejandro Soza, *Santiago*

China

Zhao-Xiang Bian, *Hong Kong*
San-Jun Cai, *Shanghai*
Guang-Wen Cao, *Shanghai*
Long Chen, *Nanjing*
Ru-Fu Chen, *Guangzhou*
George G Chen, *Hong Kong*
Li-Bo Chen, *Wuhan*
Jia-Xu Chen, *Beijing*
Hong-Song Chen, *Beijing*
Lin Chen, *Beijing*
Yang-Chao Chen, *Hong Kong*
Zhen Chen, *Shanghai*
Ying-Sheng Cheng, *Shanghai*
Kent-Man Chu, *Hong Kong*
Zhi-Jun Dai, *Xi'an*
Jing-Yu Deng, *Tianjin*
Yi-Qi Du, *Shanghai*
Zhi Du, *Tianjin*
Hani El-Nezami, *Hong Kong*
Bao-Ying Fei, *Hangzhou*
Chang-Ming Gao, *Nanjing*
Jian-Ping Gong, *Chongqing*
Zuo-Jiong Gong, *Wuhan*
Jing-Shan Gong, *Shenzhen*
Guo-Li Gu, *Beijing*
Yong-Song Guan, *Chengdu*
Mao-Lin Guo, *Luoyang*
Jun-Ming Guo, *Ningbo*
Yan-Mei Guo, *Shanghai*
Xiao-Zhong Guo, *Shenyang*
Guo-Hong Han, *Xi'an*
Ming-Liang He, *Hong Kong*
Peng Hou, *Xi'an*
Zhao-Hui Huang, *Wuxi*
Feng Ji, *Hangzhou*
Simon Law, *Hong Kong*
Yan-Chang Lei, *Hangzhou*
Yu-Yuan Li, *Guangzhou*
Meng-Sen Li, *Haikou*
Shu-De Li, *Shanghai*
Zong-Fang Li, *Xi'an*
Qing-Quan Li, *Shanghai*
Kang Li, *Lasa*
Han Liang, *Tianjin*
Xing'e Liu, *Hangzhou*
Zheng-Wen Liu, *Xi'an*
Xiao-Fang Liu, *Yantai*
Bin Liu, *Tianjin*
Quan-Da Liu, *Beijing*
Hai-Feng Liu, *Beijing*
Fei Liu, *Shanghai*
Ai-Guo Lu, *Shanghai*
He-Sheng Luo, *Wuhan*
Xiao-Peng Ma, *Shanghai*
Yong Meng, *Shantou*
Ke-Jun Nan, *Xi'an*
Siew Chien Ng, *Hong Kong*
Simon SM Ng, *Hong Kong*
Zhao-Shan Niu, *Qingdao*
Di Qu, *Shanghai*
Ju-Wei Mu, *Beijing*
Rui-Hua Shi, *Nanjing*
Bao-Min Shi, *Shanghai*
Xiao-Dong Sun, *Hangzhou*
Si-Yu Sun, *Shenyang*
Guang-Hong Tan, *Haikou*
Wen-Fu Tang, *Chengdu*
Anthony YB Teoh, *Hong Kong*
Wei-Dong Tong, *Chongqing*
Eric Tse, *Hong Kong*
Hong Tu, *Shanghai*

Stavros Gourgiotis, *Athens*
Leontios J Hadjileontiadis, *Thessaloniki*
Thomas Hyphantis, *Ioannina*
Ioannis Kanellos, *Thessaloniki*
Stylianos Karatapanis, *Rhodes*
Michael Koutsilieris, *Athens*
Spiros D Ladas, *Athens*
Theodoros K Liakakos, *Athens*
Emanuel K Manesis, *Athens*
Spilios Manolakopoulos, *Athens*
Gerassimos John Mantzaris, *Athens*
Athanasios D Marinis, *Piraeus*
Nikolaos Ioannis Nikiteas, *Athens*
Konstantinos X Papamichael, *Athens*
George Sgourakis, *Athens*
Konstantinos C Thomopoulos, *Patras*
Konstantinos Triantafyllou, *Athens*
Christos Triantos, *Patras*
Georgios Zacharakis, *Athens*
Petros Zezos, *Alexandroupolis*
Demosthenes E Ziogas, *Ioannina*

Guatemala

Carlos Maria Parellada, *Guatemala*

Hungary

Mihaly Boros, *Szeged*
Tamás Decsi, *Pécs*
Gyula Farkas, *Szeged*
Andrea Furka, *Debrecen*
Y vette Mandi, *Szeged*
Peter L Lakatos, *Budapest*
Pal Miheller, *Budapest*
Tamás Molnar, *Szeged*
Attila Olah, *Gyor*
Maria Papp, *Debrecen*
Ferenc Sipos, *Budapest*
Miklós Tanyi, *Debrecen*
Tibor Wittmann, *Szeged*

Iceland

Tryggvi Bjorn Stefánsson, *Reykjavík*

Indiad

Brij B Agarwal, *New Delhi*
Deepak N Amarapurkar, *Mumbai*
Shams ul Bari, *Srinagar*
Sriparna Basu, *Varanasi*
Runu Chakravarty, *Kolkata*
Devendra C Desai, *Mumbai*
Nutan D Desai, *Mumbai*
Suneela Sunil Dhaneshwar, *Pune*
Radha K Dhiman, *Chandigarh*
Pankaj Garg, *Mohali*
Uday C Ghoshal, *Lucknow*
Kalpesh Jani, *Vadodara*
Premashis Kar, *New Delhi*
Jyotdeep Kaur, *Chandigarh*
Rakesh Kochhar, *Chandigarh*
Pradyumna K Mishra, *Mumbai*
Asish K Mukhopadhyay, *Kolkata*
Imtiyaz Murtaza, *Srinagar*
P Nagarajan, *New Delhi*
Samiran Nundy, *Delhi*
Gopal Pande, *Hyderabad*
Benjamin Perakath, *Vellore*
Arun Prasad, *New Delhi*
D Nageshwar Reddy, *Hyderabad*
Lekha Saha, *Chandigarh*
Sundeep Singh Saluja, *New Delhi*
Mahesh Prakash Sharma, *New Delhi*
Sadiq Saleem Sikora, *Bangalore*
Sarman Singh, *New Delhi*
Rajeev Sinha, *Jhansi*
Rupjyoti Talukdar, *Hyderabad*
Rakesh Kumar Tandon, *New Delhi*
Narayanan Thirumoorthy, *Coimbatore*

Indonesia

David Handojo Muljono, *Jakarta*
Andi Utama, *Jakarta*

Iran

Arezoo Aghakhani, *Tehran*
Seyed Mohsen Dehghani, *Shiraz*
Ahad Eshraghian, *Shiraz*
Hossein Khedmat, *Tehran*
Sadegh Massarrat, *Tehran*
Marjan Mohammadi, *Tehran*
Roja Rahimi, *Tehran*
Farzaneh Sabahi, *Tehran*
Majid Sadeghizadeh, *Tehran*
Farideh Siavoshi, *Tehran*

Ireland

Gary Alan Bass, *Dublin*
David J Brayden, *Dublin*
Ronan A Cahill, *Dublin*
Glen A Doherty, *Dublin*
Liam J Fanning, *Cork*
Barry Philip McMahon, *Dublin*
RossMcManus, *Dublin*
Dervla O'Malley, *Cork*
Sinead M Smith, *Dublin*

Israel

Dan Carter, *Ramat Gan*
Jorge-Shmuel Delgado, *Metar*
Eli Magen, *Ashdod*
Nitsan Maharshak, *Tel Aviv*
Shaul Mordechai, *Beer Sheva*
Menachem Moshkowitz, *Tel Aviv*
William Bahij Nseir, *Nazareth*
Shimon Reif, *Jerusalem*
Ram Reifen, *Rehovot*
Ariella Bar-Gil Shitrit, *Jerusalem*
Noam Shussman, *Jerusalem*
Igor Sukhotnik, *Haifa*
Nir Wasserberg, *Petach Tiqwa*
Jacob Yahav, *Rehovot*
Doron Levi Zamir, *Gedera*
Shira Zelber-Sagi, *Haifa*
Romy Zemel, *Petach-Tikva*

Italy

Ludovico Abenavoli, *Catanzaro*
Luigi Elio Adinolfi, *Naples*
Carlo Virginio Agostoni, *Milan*
Anna Alisi, *Rome*
Piero Luigi Almasio, *Palermo*
Donato Francesco Altomare, *Bari*
Amedeo Amedei, *Florence*
Pietro Andreone, *Bologna*
Imerio Angriman, *Padova*
Vito Annese, *Florence*
Paolo Aurello, *Rome*
Salavtore Auricchio, *Naples*
Gian Luca Baiocchi, *Brescia*
Gianpaolo Balzano, *Milan*
Antonio Basoli, *Rome*
Gabrio Bassotti, *San Sisto*
Mauro Bernardi, *Bologna*
Alberto Biondi, *Rome*
Ennio Biscaldi, *Genova*
Massimo Bolognesi, *Padua*
Luigi Bonavina, *Milano*
Aldo Bove, *Chieti*
Raffaele Bruno, *Pavia*
Luigi Brusciano, *Napoli*
Giuseppe Cabibbo, *Palermo*
Carlo Calabrese, *Bologna*
Daniele Calistri, *Meldola*
Vincenza Calvaruso, *Palermo*
Lorenzo Camellini, *Reggio Emilia*
Marco Candela, *Bologna*
Raffaele Capasso, *Naples*
Lucia Carulli, *Modena*
Renato David Caviglia, *Rome*
Luigina Cellini, *Chieti*
Giuseppe Chiarioni, *Verona*
Claudio Chiesa, *Rome*
Michele Cicala, *Roma*
Rachele Ciccocioppo, *Pavia*
Sandro Contini, *Parma*
Gaetano Corso, *Foggia*
Renato Costi, *Parma*
Alessandro Cucchetti, *Bologna*
Rosario Cuomo, *Napoli*
Giuseppe Currò, *Messina*
Paola De Nardi, *Milano*
Giovanni D De Palma, *Naples*
Raffaele De Palma, *Napoli*
Giuseppina De Petro, *Brescia*
Valli De Re, *Aviano*
Paolo De Simone, *Pisa*
Giuliana Decorti, *Trieste*
Emanuele Miraglia del Giudice, *Napoli*
Isidoro Di Carlo, *Catania*
Matteo Nicola Dario Di Minno, *Naples*
Massimo Donadelli, *Verona*
Mirko D'Onofrio, *Verona*
Maria Pina Dore, *Sassari*
Luca Elli, *Milano*
Massimiliano Fabozzi, *Aosta*
Massimo Falconi, *Ancona*

Ezio Falletto, *Turin*
Silvia Fargion, *Milan*
Matteo Fassan, *Verona*
Gianfranco Delle Fave, *Roma*
Alessandro Federico, *Naples*
Francesco Feo, *Sassari*
Davide Festi, *Bologna*
Natale Figura, *Siena*
Vincenzo Formica, *Rome*
Mirella Fraquelli, *Milan*
Marzio Frazzoni, *Modena*
Walter Fries, *Messina*
Gennaro Galizia, *Naples*
Andrea Galli, *Florence*
Matteo Garcovich, *Rome*
Eugenio Gaudio, *Rome*
Paola Ghiorzo, *Genoa*
Edoardo G Giannini, *Genova*
Luca Gianotti, *Monza*
Maria Cecilia Giron, *Padova*
Alberto Grassi, *Rimini*
Gabriele Grassi, *Trieste*
Francesco Greco, *Bergamo*
Luigi Greco, *Naples*
Antonio Grieco, *Rome*
Fabio Grizzi, *Rozzano*
Laurino Grossi, *Pescara*
Simone Guglielmetti, *Milan*
Tiberiu Hershcovici, *Jerusalem*
Calogero Iacono, *Verona*
Enzo Ierardi, *Bari*
Amedeo Indriolo, *Bergamo*
Raffaele Iorio, *Naples*
Paola Iovino, *Salerno*
Angelo A Izzo, *Naples*
Loreta Kondili, *Rome*
Filippo La Torre, *Rome*
Giuseppe La Torre, *Rome*
Giovanni Latella, *L'Aquila*
Salvatore Leonardi, *Catania*
Massimo Libra, *Catania*
Anna Licata, *Palermo*
C armela Loguercio, *Naples*
Amedeo Lonardo, *Modena*
Carmelo Luigiano, *Catania*
Francesco Luzza, *Catanzaro*
Giovanni Maconi, *Milano*
Antonio Macrì, *Messina*
Mariano Malaguarnera, *Catania*
Francesco Manguso, *Napoli*
Tommaso Maria Manzia, *Rome*
Daniele Marrelli, *Siena*
Gabriele Masselli, *Rome*
Sara Massironi, *Milan*
Giuseppe Mazzarella, *Avellino*
Michele Milella, *Rome*
Giovanni Milito, *Rome*
Antonella d'Arminio Monforte, *Milan*
Fabrizio Montecucco, *Genoa*
Giovanni Monteleone, *Rome*
Mario Morino, *Torino*
Vincenzo La Mura, *Milan*
Gerardo Nardone, *Naples*
Riccardo Nascimbeni, *Brescia*
Gabriella Nesi, *Florence*
Giuseppe Nigri, *Rome*
Erica Novo, *Turin*
Veronica Ojetti, *Rome*
Michele Orditura, *Naples*
Fabio Pace, *Seriate*
Lucia Pacifico, *Rome*
Omero Alessandro Paoluzi, *Rome*
Valerio Pazienza, *San Giovanni Rotondo*
Rinaldo Pellicano, *Turin*
Adriano M Pellicelli, *Rome*
Nadia Peparini, *Ciampino*
Mario Pescatori, *Rome*
Antonio Picardi, *Rome*
Alberto Pilotto, *Padova*
Alberto Piperno, *Monza*
Anna Chiara Piscaglia, *Rome*
Maurizio Pompili, *Rome*
Francesca Romana Ponziani, *Rome*
Cosimo Prantera, *Rome*
Girolamo Ranieri, *Bari*
Carlo Ratto, *Tome*
Barbara Renga, *Perugia*
Alessandro Repici, *Rozzano*
Maria Elena Riccioni, *Rome*
Lucia Ricci-Vitiani, *Rome*
Luciana Rigoli, *Messina*
Mario Rizzetto, *Torino*
Ballarin Roberto, *Modena*
Roberto G Romanelli, *Florence*
Claudio Romano, *Messina*
Luca Roncucci, *Modena*
Cesare Ruffolo, *Treviso*
L ucia Sacchetti, *Napoli*
Rodolfo Sacco, *Pisa*
Lapo Sali, *Florence*
Romina Salpini, *Rome*
Giulio Aniello, *Santoro Treviso*
Armando Santoro, *Rozzano*
Edoardo Savarino, *Padua*
Marco Senzolo, *Padua*
Annalucia Serafino, *Rome*
Giuseppe S Sica, *Rome*
Pierpaolo Sileri, *Rome*
Cosimo Sperti, *Padua*
Vincenzo Stanghellini, *Bologna*
Cristina Stasi, *Florence*
Gabriele Stocco, *Trieste*
Roberto Tarquini, *Florence*
Mario Testini, *Bari*
Guido Torzilli, *Milan*
Guido Alberto Massimo, *Tiberio Brescia*
Giuseppe Toffoli, *Aviano*
Alberto Tommasini, *Trieste*
Francesco Tonelli, *Florence*
Cesare Tosetti Porretta, *Terme*
Lucio Trevisani, *Cona*
Guglielmo M Trovato, *Catania*
Mariapia Vairetti, *Pavia*
Luca Vittorio Valenti, *Milano*
Mariateresa T Ventura, *Bari*
Giuseppe Verlato, *Verona*
Marco Vivarelli, *Ancona*
Giovanni Li Volti, *Catania*
Giuseppe Zanotti, *Padua*
Vincenzo Zara, *Lecce*
Gianguglielmo Zehender, *Milan*
Anna Linda Zignego, *Florence*
Rocco Antonio Zoccali, *Messina*
Angelo Zullo, *Rome*

Japan

Yasushi Adachi, *Sapporo*
Takafumi Ando, *Nagoya*
Masahiro Arai, *Tokyo*
Makoto Arai, *Chiba*
Takaaki Arigami, *Kagoshima*
Itaru Endo,*Yokohama*
Munechika Enjoji, *Fukuoka*
Shunji Fujimori, *Tokyo*
Yasuhiro Fujino, *Akashi*
Toshiyoshi Fujiwara, *Okayama*
Yosuke Fukunaga, *Tokyo*
Toshio Fukusato, *Tokyo*
Takahisa Furuta, *Hamamatsu*
Osamu Handa, *Kyoto*
Naoki Hashimoto, *Osaka*
Yoichi Hiasa, *Toon*
Masatsugu Hiraki, *Saga*
Satoshi Hirano, *Sapporo*
Keiji Hirata, *Fukuoka*
Toru Hiyama, *Higashihiroshima*
Akira Hokama, *Nishihara*
Shu Hoteya, *Tokyo*
Masao Ichinose, *Wakayama*
Tatsuya Ide, *Kurume*
Masahiro Iizuka, *Akita*
Toshiro Iizuka, *Tokyo*
Kenichi Ikejima, *Tokyo*
Tetsuya Ikemoto, *Tokushima*
Hiroyuki Imaeda, *Saitama*
Atsushi Imagawa, *Kan-onji*
Hiroo Imazu, *Tokyo*
Shuji Isaji, *Tsu*
Toru Ishikawa, *Niigata*
Toshiyuki Ishiwata, *Tokyo*
Soichi Itaba, *Kitakyushu*
Yoshiaki Iwasaki, *Okayama*
Tatehiro Kagawa, *Isehara*
Satoru Kakizaki, *Maebashi*
Naomi Kakushima, *Shizuoka*
Terumi Kamisawa, *Tokyo*
Akihide Kamiya, *Isehara*
Osamu Kanauchi, *Tokyo*
Tatsuo Kanda, *Chiba*
Shin Kariya, *Okayama*
Shigeyuki Kawa, *Matsumoto*
Takumi Kawaguchi, *Kurume*
Takashi Kawai, *Tokyo*
Soo Ryang Kim, *Kobe*
Shinsuke Kiriyama, *Gunma*
Tsuneo Kitamura, *Urayasu*
Masayuki Kitano, *Osakasayama*
Hirotoshi Kobayashi, *Tokyo*
Hironori Koga, *Kurume*
Takashi Kojima, *Sapporo*
Satoshi Kokura, *Kyoto*
Shuhei Komatsu, *Kyoto*
Tadashi Kondo, *Tokyo*
Yasuteru Kondo, *Sendai*
Yasuhiro Kuramitsu, *Yamaguchi*
Yukinori Kurokawa, *Osaka*
Shin Maeda, *Yokohama*
Koutarou Maeda, *Toyoake*

Hitoshi Maruyama, *Chiba*
Atsushi Masamune, *Sendai*
Hiroyuki Matsubayashi, *Suntogun*
Akihisa Matsuda, *Inzai*
Hirofumi Matsui, *Tsukuba*
Akira Matsumori, *Kyoto*
Yoichi Matsuo, *Nagoya*
Y Matsuzaki, *Ami*
Toshihiro Mitaka, *Sapporo*
Kouichi Miura, *Akita*
Shinichi Miyagawa, *Matumoto*
Eiji Miyoshi, *Suita*
Toru Mizuguchi, *Sapporo*
Nobumasa Mizuno, *Nagoya*
Zenichi Morise, *Nagoya*
Tomohiko Moriyama, *Fukuoka*
Kunihiko Murase, *Tusima*
Michihiro Mutoh, *Tsukiji*
Akihito Nagahara, *Tokyo*
Hikaru Nagahara, *Tokyo*
Hidenari Nagai, *Tokyo*
Koichi Nagata, *Shimotsuke-shi*
Masaki Nagaya, *Kawasaki*
Hisato Nakajima, *Nishi-Shinbashi*
Toshifusa Nakajima, *Tokyo*
Hiroshi Nakano, *Kawasaki*
Hiroshi Nakase, *Kyoto*
Toshiyuki Nakayama, *Nagasaki*
Takahiro Nakazawa, *Nagoya*
Shoji Natsugoe, *Kagoshima City*
Tsutomu Nishida, *Suita*
Shuji Nomoto, *Naogya*
Sachiyo Nomura, *Tokyo*
Takeshi Ogura, *Takatsukishi*
Nobuhiro Ohkohchi, *Tsukuba*
Toshifumi Ohkusa, *Kashiwa*
Hirohide Ohnishi, *Akita*
Teruo Okano, *Tokyo*
Satoshi Osawa, *Hamamatsu*
Motoyuki Otsuka, *Tokyo*
Michitaka Ozaki, *Sapporo*
Satoru Saito, *Yokohama*
Naoaki Sakata, *Sendai*
Ken Sato, *Maebashi*
Toshiro Sato, *Tokyo*
Tomoyuki Shibata, *Toyoake*
Tomohiko Shimatani, *Kure*
Yukihiro Shimizu, *Nanto*
Tadashi Shimoyama, *Hirosaki*
Masayuki Sho, *Nara*
Ikuo Shoji, *Kobe*
Atsushi Sofuni, *Tokyo*
Takeshi Suda, *Niigata*
M Sugimoto, *Hamamatsu*
Ken Sugimoto, *Hamamatsu*
Haruhiko Sugimura, *Hamamatsu*
Shoichiro Sumi, *Kyoto*
Hidekazu Suzuki, *Tokyo*
Masahiro Tajika, *Nagoya*
Hitoshi Takagi, *Takasaki*
Toru Takahashi, *Niigata*
Yoshihisa Takahashi, *Tokyo*
Shinsuke Takeno, *Fukuoka*
Akihiro Tamori, *Osaka*
Kyosuke Tanaka, *Tsu*
Shinji Tanaka, *Hiroshima*
Atsushi Tanaka, *Tokyo*
Yasuhito Tanaka, *Nagoya*
Shinji Tanaka, *Tokyo*
Minoru Tomizawa, *Yotsukaido City*
Kyoko Tsukiyama-Kohara, *Kagoshima*
Takuya Watanabe, *Niigata*
Kazuhiro Watanabe, *Sendai*
Satoshi Yamagiwa, *Niigata*
Takayuki Yamamoto, *Yokkaichi*
Hiroshi Yamamoto, *Otsu*
Kosho Yamanouchi, *Nagasaki*
Ichiro Yasuda, *Gifu*
Yutaka Yata, *Maebashi-city*
Shin-ichi Yokota, *Sapporo*
Norimasa Yoshida, *Kyoto*
Hiroshi Yoshida, *Tama-City*
Hitoshi Yoshiji, *Kashihara*
Kazuhiko Yoshimatsu, *Tokyo*
Kentaro Yoshioka, *Toyoake*
Nobuhiro Zaima, *Nara*

Jordan
Khaled Ali Jadallah, *Irbid*

Kuwait
Islam Khan, *Kuwait*

Lebanon
Bassam N Abboud, *Beirut*
Kassem A Barada, *Beirut*
Marwan Ghosn, *Beirut*
Iyad A Issa, *Beirut*
Fadi H Mourad, *Beirut*
AIa Sharara, *Beirut*
Rita Slim, *Beirut*

Lithuania
Antanas Mickevicius, *Kaunas*

Malaysia
Huck Joo Tan, *Petaling Jaya*

Mexico
Richard A Awad, *Mexico City*
Carlos R Camara-Lemarroy, *Monterrey*
Norberto C Chavez-Tapia, *Mexico City*
Wolfgang Gaertner, *Mexico City*
Diego Garcia-Compean, *Monterrey*
Arturo Panduro, *Guadalajara*
OT Teramoto-Matsubara, *Mexico City*
Felix Tellez-Avila, *Mexico City*
Omar Vergara-Fernandez, *Mexico City*
Saúl Villa-Trevino, *Cuidad de México*

Morocco
Samir Ahboucha, *Khouribga*

Netherlands
Robert J de Knegt, *Rotterdam*
Tom Johannes Gerardus Gevers, *Nijmegen*
Menno Hoekstra, *Leiden*
BW Marcel Spanier, *Arnhem*
Karel van Erpecum, *Utrecht*

New Zealand
Leo K Cheng, *Auckland*
Andrew Stewart Day, *Christchurch*
Jonathan Barnes Koea, *Auckland*
Max Petrov, *Auckland*

Nigeria
Olufunmilayo Adenike Lesi, *Lagos*
Jesse Abiodun Otegbayo, *Ibadan*
Stella Ifeanyi Smith, *Lagos*

Norway
Trond Berg, *Oslo*
Trond Arnulf Buanes, *Krokkleiva*
Thomas de Lange, *Rud*
Magdy El-Salhy, *Stord*
Rasmus Goll, *Tromso*
Dag Arne Lihaug Hoff, *Aalesund*

Pakistan
Zaigham Abbas, *Karachi*
Usman A Ashfaq, *Faisalabad*
Muhammad Adnan Bawany, *Hyderabad*
Muhammad Idrees, *Lahore*
Saeed Sadiq Hamid, *Karachi*
Yasir Waheed, *Islamabad*

Poland
Thomas Brzozowski, *Cracow*
Magdalena Chmiela, *Lodz*
Krzysztof Jonderko, *Sosnowiec*
Anna Kasicka-Jonderko, *Sosnowiec*
Michal Kukla, *Katowice*
Tomasz Hubert Mach, *Krakow*
Agata Mulak, *Wroclaw*
Danuta Owczarek, *Kraków*
Piotr Socha, *Warsaw*
Piotr Stalke, *Gdansk*
Julian Teodor Swierczynski, *Gdansk*
Anna M Zawilak-Pawlik, *Wroclaw*

Portugal
Marie Isabelle Cremers, *Setubal*
Ceu Figueiredo, *Porto*
Ana Isabel Lopes, *LIsbon*
M Paula Macedo, *Lisboa*
Ricardo Marcos, *Porto*
Rui T Marinho, *Lisboa*
Guida Portela-Gomes, *Estoril*

Filipa F Vale, *Lisbon*

Puerto Rico

Caroline B Appleyard, *Ponce*

Qatar

Abdulbari Bener, *Doha*

Romania

Mihai Ciocirlan, *Bucharest*
Dan LucianDumitrascu, *Cluj-Napoca*
Carmen Fierbinteanu-Braticevici, *Bucharest*
Romeo G Mihaila, *Sibiu*
Lucian Negreanu, *Bucharest*
Adrian Saftoiu, *Craiova*
Andrada Seicean, *Cluj-Napoca*
Ioan Sporea, *Timisoara*
Letiţia Adela Maria Streba, *Craiova*
Anca Trifan, *Iasi*

Russia

Victor Pasechnikov, *Stavropol*
Vasiliy Ivanovich Reshetnyak, *Moscow*
Vitaly Skoropad, *Obninsk*

Saudi Arabia

Abdul-Wahed N Meshikhes, *Dammam*
M Ezzedien Rabie, *Khamis Mushait*

Singapore

Brian KP Goh, *Singapore*
Richie Soong, *Singapore*
Ker-Kan Tan, *Singapore*
Kok-Yang Tan, *Singapore*
Yee-Joo Tan, *Singapore*
Mark Wong, *Singapore*
Hong Ping Xia, *Singapore*

Slovenia

Matjaz Homan, *Ljubljana*
Martina Perse, *Ljubljana*

South Korea

Sang Hoon Ahn, *Seoul*
Seung Hyuk Baik, *Seoul*
Soon Koo Baik, *Wonju*
Soo-Cheon Chae, *Iksan*
Byung-Ho Choe, *Daegu*
Suck Chei Choi, *Iksan*
Hoon Jai Chun, *Seoul*
Yeun-Jun Chung, *Seoul*
Young-Hwa Chung, *Seoul*
Ki-Baik Hahm, *Seongnam*
Sang Young Han, *Busan*
Seok Joo Han, *Seoul*
Seung-Heon Hong, *Iksan*
Jin-Hyeok Hwang, *Seoungnam*
Jeong Won Jang, *Seoul*
Jin-Young Jang, *Seoul*
Dae-Won Jun, *Seoul*
Young Do Jung, *Kwangju*
Gyeong Hoon Kang, *Seoul*
Sung-Bum Kang, *Seoul*
Koo Jeong Kang, *Daegu*
Ki Mun Kang, *Jinju*
Chang Moo Kang, *Seodaemun-gu*
Gwang Ha Kim, *Busan*
Sang Soo Kim, *Goyang-si*
Jin Cheon Kim, *Seoul*
Tae Il Kim, *Seoul*
Jin Hong Kim, *Suwon*
Kyung Mo Kim, *Seoul*
Kyongmin Kim, *Suwon*
Hyung-Ho Kim, *Seongnam*
Seoung Hoon Kim, *Goyang*
Sang Il Kim, *Seoul*
Hyun-Soo Kim, *Wonju*
Jung Mogg Kim, *Seoul*
Dong Yi Kim, *Gwangju*
Kyun-Hwan Kim, *Seoul*
Jong-Han Kim, *Ansan*
Sang Wun Kim, *Seoul*
Ja-Lok Ku, *Seoul*
Kyu Taek Lee, *Seoul*
Hae-Wan Lee, *Chuncheon*
Inchul Lee, *Seoul*
Jung Eun Lee, *Seoul*
Sang Chul Lee, *Daejeon*
Song Woo Lee, *Ansan-si*
Hyuk-Joon Lee, *Seoul*
Seong-Wook Lee, *Yongin*
Kil Yeon Lee, *Seoul*
Jong-Inn Lee, *Seoul*
Kyung A Lee, *Seoul*
Jong-Baeck Lim, *Seoul*
Eun-Yi Moon, *Seoul*
SH Noh, *Seoul*
Seung Woon Paik, *Seoul*
Won Sang Park, *Seoul*
Sung-Joo Park, *Iksan*
Kyung Sik Park, *Daegu*
Se Hoon Park, *Seoul*
Yoonkyung Park, *Gwangju*
Seung-Wan Ryu, *Daegu*
Il Han Song, *Cheonan*
Myeong Jun Song, *Daejeon*
Yun Kyoung Yim, *Daejeon*
Dae-Yeul Yu *Daejeon*

Spain

Mariam Aguas, *Valencia*
Raul J Andrade, *Málaga*
Antonio Arroyo, *Elche*
Josep M Bordas, *Barcelona*
Lisardo Boscá, *Madrid*
Ricardo Robles Campos, *Murcia*
Jordi Camps, *Reus*
Carlos Cervera *Barcelona*
Alfonso Clemente, *Granada*
Pilar Codoner-Franch, *Valencia*
Fernando J Corrales, *Pamplona*
Fermin Sánchez de Medina, *Granada*
Alberto Herreros de Tejada, *Majadahonda*
Enrique de-Madaria, *Alicante*
JE Dominguez-Munoz, *Santiago de Compostela*
Vicente Felipo, *Valencia*
CM Fernandez-Rodriguez, *Madrid*
Carmen Frontela-Saseta, *Murcia*
Julio Galvez, *Granada*
Maria Teresa García, *Vigo*
MI Garcia-Fernandez, *Málaga*
Emilio Gonzalez-Reimers, *La Laguna*
Marcel Jimenez, *Bellaterra*
Angel Lanas, *Zaragoza*
Juan Ramón Larrubia, *Guadalajara*
Antonio Lopez-Sanroman, *Madrid*
Vicente Lorenzo-Zuniga, *Badalona*
Alfredo J Lucendo, *Tomelloso*
Vicenta Soledad Martinez-Zorzano, *Vigo*
José Manuel Martin-Villa, *Madrid*
Julio Mayol, *Madrid*
Manuel Morales-Ruiz, *Barcelona*
Alfredo Moreno-Egea, *Murcia*
Albert Pares, *Barcelona*
Maria Pellise, *Barcelona*
José Perea, *Madrid*
Miguel Angel Plaza, *Zaragoza*
María J Pozo, *Cáceres*
Enrique Quintero, *La Laguna*
Jose M Ramia, *Madrid*
Francisco Rodriguez-Frias, *Barcelona*
Silvia Ruiz-Gaspa, *Barcelona*
Xavier Serra-Aracil, *Barcelona*
Vincent Soriano, *Madrid*
Javier Suarez, *Pamplona*
Carlos Taxonera, *Madrid*
M Isabel Torres, *Jaén*
Manuel Vazquez-Carrera, *Barcelona*
Benito Velayos, *Valladolid*
Silvia Vidal, *Barcelona*

Sri Lanka

Arjuna Priyadarsin De Silva, *Colombo*

Sudan

Ishag Adam, *Khartoum*

Sweden

Roland G Andersson, *Lund*
Bergthor Björnsson, *Linkoping*
Johan Christopher Bohr, *Örebro*
Mauro D'Amato, *Stockholm*
Thomas Franzen, *Norrkoping*
Evangelos Kalaitzakis, *Lund*
Riadh Sadik, *Gothenburg*
Per Anders Sandstrom, *Linkoping*
Ervin Toth, *Malmö*
Konstantinos Tsimogiannis, *Vasteras*
Apostolos V Tsolakis, *Uppsala*

Switzerland

Gieri Cathomas, *Liestal*
Jean Louis Frossard, *Geneve*
Christian Toso, *Geneva*
Stephan Robert Vavricka, *Zurich*
Dominique Velin, *Lausanne*

Thailand

Thawatchai Akaraviputh, *Bangkok*
P Yoysungnoen Chintana, *Pathumthani*
Veerapol Kukongviriyapan, *Muang*
Vijittra Leardkamolkarn, *Bangkok*
Varut Lohsiriwat, *Bangkok*
Somchai Pinlaor, *Khaon Kaen*
D Wattanasirichaigoon, *Bangkok*

Trinidad and Tobago

B Shivananda Nayak, *Mount Hope*

Tunisia

Ibtissem Ghedira, *Sousse*
Lilia Zouiten-Mekki, *Tunis*

Turkey

Inci Alican, *Istanbul*
Mustafa Altindis, *Sakarya*
Mutay Aslan, *Antalya*
Oktar Asoglu, *Istanbul*
Yasemin Hatice Balaban, *Istanbul*
Metin Basaranoglu, *Ankara*
Yusuf Bayraktar, *Ankara*
Süleyman Bayram, *Adiyaman*
Ahmet Bilici, *Istanbul*
Ahmet Sedat Boyacioglu, *Ankara*
Züleyha Akkan Cetinkaya, *Kocaeli*
Cavit Col, *Bolu*
Yasar Colak, *Istanbul*
Cagatay Erden Daphan, *Kirikkale*
Mehmet Demir, *Hatay*
Ahmet Merih Dobrucali, *Istanbul*
Gülsüm Ozlem Elpek, *Antalya*
Ayse Basak Engin, *Ankara*
Eren Ersoy, *Ankara*
Osman Ersoy, *Ankara*
Yusuf Ziya Erzin, *Istanbul*
Mukaddes Esrefoglu, *Istanbul*
Levent Filik, *Ankara*
Ozgur Harmanci, *Ankara*
Koray Hekimoglu, *Ankara*
Abdurrahman Kadayifci, *Gaziantep*
Cem Kalayci, *Istanbul*
Selin Kapan, *Istanbul*
Huseyin Kayadibi, *Adana*
Sabahattin Kaymakoglu, *Istanbul*
Metin Kement, *Istanbul*
Mevlut Kurt, *Bolu*
Resat Ozaras, *Istanbul*
Elvan Ozbek, *Adapazari*
Cengiz Ozcan, *Mersin*
Hasan Ozen, *Ankara*
Halil Ozguc, *Bursa*
Mehmet Ozturk, *Izmir*
Orhan V Ozkan, *Sakarya*
Semra Paydas, *Adana*
Ozlem Durmaz Suoglu, *Istanbul*
Ilker Tasci, *Ankara*
Müge Tecder-ünal, *Ankara*
Mesut Tez, *Ankara*
Serdar Topaloglu, *Trabzon*
Murat Toruner, *Ankara*
Gokhan Tumgor, *Adana*
Oguz Uskudar, *Adana*
Mehmet Yalniz, *Elazig*
Mehmet Yaman, *Elazig*
Veli Yazisiz, *Antalya*
Yusuf Yilmaz, *Istanbul*
Ozlem Yilmaz, *Izmir*
Oya Yucel, *Istanbul*
Ilhami Yuksel, *Ankara*

United Kingdom

Nadeem Ahmad Afzal, *Southampton*
Navneet K Ahluwalia, *Stockport*
Yeng S Ang, *Lancashire*
Ramesh P Arasaradnam, *Coventry*
Ian Leonard Phillip Beales, *Norwich*
John Beynon, *Swansea*
Barbara Braden, *Oxford*
Simon Bramhall, *Birmingham*
Geoffrey Burnstock, *London*
Ian Chau, *Sutton*
Thean Soon Chew, *London*
Helen G Coleman, *Belfast*
Anil Dhawan, *London*
Sunil Dolwani, *Cardiff*
Piers Gatenby, *London*
Anil T George, *London*
Pasquale Giordano, *London*
Paul Henderson, *Edinburgh*
Georgina Louise Hold, *Aberdeen*
Stefan Hubscher, *Birmingham*
Robin D Hughes, *London*
Nusrat Husain, *Manchester*
Matt W Johnson, *Luton*
Konrad Koss, *Macclesfield*
Anastasios Koulaouzidis, *Edinburgh*
Simon Lal, *Salford*
John S Leeds, *Aberdeen*
JK K Limdi, *Manchester*
Hongxiang Liu, *Cambridge*
Michael Joseph McGarvey, *London*
Michael Anthony Mendall, *London*
Alexander H Mirnezami, *Southampton*
J Bernadette Moore, *Guildford*
Claudio Nicoletti, *Norwich*
Savvas Papagrigoriadis, *London*
Sylvia LF Pender, *Southampton*
David Mark Pritchard, *Liverpool*
James A Ross, *Edinburgh*
Kamran Rostami, *Worcester*
Xiong Z Ruan, *London*
Frank I Tovey, *London*
Dhiraj Tripathi, *Birmingham*
Vamsi R Velchuru, *Great Yarmouth*
Nicholas T Ventham, *Edinburgh*
Diego Vergani, *London*
Jack Westwood Winter, *Glasgow*
Terence Wong, *London*
Ling Yang, *Oxford*

United States

Daniel E Abbott, *Cincinnati*
Ghassan K Abou-Alfa, *New York*
Julian Abrams, *New York*
David William Adelson, *Los Angeles*
Jonathan Steven Alexander, *Shreveport*
Tauseef Ali, *Oklahoma City*
Mohamed R Ali, *Sacramento*
Rajagopal N Aravalli, *Minneapolis*
Hassan Ashktorab, *Washington*
Shashi Bala, *Worcester*
Charles F Barish, *Raleigh*
P Patrick Basu, *New York*
Robert L Bell, *Berkeley Heights*
David Bentrem, *Chicago*
Henry J Binder, *New Haven*
Joshua Bleier, *Philadelphia*
Wojciech Blonski, *Johnson City*
Kenneth Boorom, *Corvallis*
Brian Boulay, *Chicago*
Carla W Brady, *Durham*
Kyle E Brown, *Iowa City*
Adeel A Butt, *Pittsburgh*
Weibiao Cao, *Providence*
Andrea Castillo, *Cheney*
Fernando J Castro, *Weston*
Adam S Cheifetz, *Boston*
Xiaoxin Luke Chen, *Durham*
Ramsey Cheung, *Palo Alto*
Parimal Chowdhury, *Little Rock*
Edward John Ciaccio, *New York*
Dahn L Clemens, *Omaha*
Yingzi Cong, *Galveston*
Laura Iris Cosen-Binker, *Boston*
Joseph John Cullen, *Lowa*
Mark J Czaja, *Bronx*
Mariana D Dabeva, *Bronx*
Christopher James Damman, *Seattle*
Isabelle G De Plaen, *Chicago*
Punita Dhawan, *Nashville*
Hui Dong, *La Jolla*
Wael El-Rifai, *Nashville*
Sukru H Emre, *New Haven*
Paul Feuerstadt, *Hamden*
Josef E Fischer, *Boston*
Laurie N Fishman, *Boston*
Joseph Che Forbi, *Atlanta*
Temitope Foster, *Atlanta*
Amy E Foxx-Orenstein, *Scottsdale*
Daniel E Freedberg, *New York*
Shai Friedland, *Palo Alto*
Virgilio George, *Indianapolis*
Ajay Goel, *Dallas*
Oliver Grundmann, *Gainesville*
Stefano Guandalini, *Chicago*
Chakshu Gupta, *St. Joseph*
Grigoriy E Gurvits, *New York*

World Journal of Gastroenterology

Contents

Weekly Volume 23 Number 31 August 21, 2017

Contents

World Journal of Gastroenterology
Volume 23 Number 31 August 21, 2017

AIMS AND SCOPE

World Journal of Gastroenterology (*World J Gastroenterol*, *WJG*, print ISSN 1007-9327, online ISSN 2219-2840, DOI: 10.3748) is a peer-reviewed open access journal. *WJG* was established on October 1, 1995. It is published weekly on the 7th, 14th, 21st, and 28th each month. The *WJG* Editorial Board consists of 1375 experts in gastroenterology and hepatology from 68 countries.

The primary task of *WJG* is to rapidly publish high-quality original articles, reviews, and commentaries in the fields of gastroenterology, hepatology, gastrointestinal endoscopy, gastrointestinal surgery, hepatobiliary surgery, gastrointestinal oncology, gastrointestinal radiation oncology, gastrointestinal imaging, gastrointestinal interventional therapy, gastrointestinal infectious diseases, gastrointestinal pharmacology, gastrointestinal pathophysiology, gastrointestinal pathology, evidence-based medicine in gastroenterology, pancreatology, gastrointestinal laboratory medicine, gastrointestinal molecular biology, gastrointestinal immunology, gastrointestinal microbiology, gastrointestinal genetics, gastrointestinal translational medicine, gastrointestinal diagnostics, and gastrointestinal therapeutics. *WJG* is dedicated to become an influential and prestigious journal in gastroenterology and hepatology, to promote the development of above disciplines, and to improve the diagnostic and therapeutic skill and expertise of clinicians.

INDEXING/ABSTRACTING

World Journal of Gastroenterology (*WJG*) is now indexed in Current Contents®/Clinical Medicine, Science Citation Index Expanded (also known as SciSearch®), Journal Citation Reports®, Index Medicus, MEDLINE, PubMed, PubMed Central and Directory of Open Access Journals. The 2017 edition of Journal Citation Reports® cites the 2016 impact factor for *WJG* as 3.365 (5-year impact factor: 3.176), ranking *WJG* as 29th among 79 journals in gastroenterology and hepatology (quartile in category Q2).

NAME OF JOURNAL
World Journal of Gastroenterology

ISSN
ISSN 1007-9327 (print)
ISSN 2219-2840 (online)

LAUNCH DATE
October 1, 1995

FREQUENCY
Weekly

EDITORIAL OFFICE
Jin-Lei Wang, Director
Yuan Qi, Vice Director
Ze-Mao Gong, Vice Director
World Journal of Gastroenterology
Baishideng Publishing Group Inc
7901 Stoneridge Drive, Suite 501,
Pleasanton, CA 94588, USA
Telephone: +1-925-2238242
Fax: +1-925-2238243
E-mail: editorialoffice@wjgnet.com
Help Desk: http://www.f6publishing.com/helpdesk
http://www.wjgnet.com

PUBLISHER
Baishideng Publishing Group Inc
7901 Stoneridge Drive, Suite 501,
Pleasanton, CA 94588, USA
Telephone: +1-925-2238242
Fax: +1-925-2238243
E-mail: bpgoffice@wjgnet.com
Help Desk: http://www.f6publishing.com/helpdesk
http://www.wjgnet.com

PUBLICATION DATE
August 21, 2017

INSTRUCTIONS TO AUTHORS
Full instructions are available online at http://www.wjgnet.com/bpg/gerinfo/204

ONLINE SUBMISSION
http://www.f6publishing.com

World Journal of Gastroenterology

Submit a Manuscript: http://www.f6publishing.com

World J Gastroenterol 2017 August 21; 23(31): 5645-5649

DOI: 10.3748/wjg.v23.i31.5645

ISSN 1007-9327 (print) ISSN 2219-2840 (online)

EDITORIAL

Direct-acting antiviral agents against hepatitis C virus and lipid metabolism

Tatsuo Kanda, Mitsuhiko Moriyama

Tatsuo Kanda, Mitsuhiko Moriyama, Division of Gastroenterology and Hepatology, Department of Medicine, Nihon University School of Medicine, Tokyo 173-8610, Japan

Author contributions: Kanda T and Moriyama M contributed to all aspects of this paper.

Conflict-of-interest statement: Kanda T and Moriyama M declare no conflict of interest related to this publication.

Manuscript source: Invited manuscript

Correspondence to: Tatsuo Kanda, MD, PhD, Associate Professor, Division of Gastroenterology and Hepatology, Department of Medicine, Nihon University School of Medicine, 30-1 Oyaguchi-Kamicho, Itabashi-ku, Tokyo 173-8610, Japan. kandat-cib@umin.ac.jp
Telephone: +81-3-39728111
Fax: +81-3-39568496

Received: May 26, 2017
Peer-review started: May 28, 2017
First decision: June 23, 2017
Revised: July 4, 2017
Accepted: July 22, 2017
Article in press: July 24, 2017
Published online: August 21, 2017

Abstract

Hepatitis C virus (HCV) infection induces steatosis and is accompanied by multiple metabolic alterations including hyperuricemia, reversible hypocholesterolemia and insulin resistance. Total cholesterol, low-density lipoprotein-cholesterol and triglyceride levels are increased by peginterferon and ribavirin combination therapy when a sustained virologic response (SVR) is achieved in patients with HCV. Steatosis is significantly more common in patients with HCV genotype 3 but interferon-free regimens are not always effective for treating HCV genotype 3 infections. HCV infection increases fatty acid synthase levels, resulting in the accumulation of fatty acids in hepatocytes. Of note, low-density lipoprotein receptor, scavenger receptor class B type I and Niemann-Pick C1-like 1 proteins are candidate receptors that may be involved in HCV. They are also required for the uptake of cholesterol from the external environment of hepatocytes. Among HCV-infected patients with or without human immunodeficiency virus infection, changes in serum lipid profiles are observed during interferon-free treatment and after the achievement of an SVR. It is evident that HCV affects cholesterol metabolism during interferon-free regimens. Although higher SVR rates were achieved with interferon-free treatment of HCV, special attention must also be paid to unexpected adverse events based on host metabolic changes including hyperlipidemia.

Key words: Cholesterol; Hepatitis C virus; Interferon-free; Lipid metabolism

Core tip: Eradication of hepatitis C virus (HCV) decreases the rate of complications, including liver-related and liver-unrelated death, and improves patient quality of life. Individuals infected with HCV have an increased risk of cardiovascular diseases and intracerebral hemorrhage, which are both associated with lipid metabolism. HCV infection causes abnormal host lipid metabolism. Treatment with interferon-based and interferon-free regimens has an impact on the

eradication of HCV, as well as lipid abnormalities, during treatment and after treatment. Further observations are needed to determine the long-term effects on lipid metabolism caused by HCV and by eradication of the virus.

Kanda T, Moriyama M. Direct-acting antiviral agents against hepatitis C virus and lipid metabolism. *World J Gastroenterol* 2017; 23(31): 5645-5649 Available from: URL: http://www.wjgnet.com/1007-9327/full/v23/i31/5645.htm DOI: http://dx.doi.org/10.3748/wjg.v23.i31.5645

INTRODUCTION

Hepatitis C virus (HCV) encodes at least 10 viral proteins, which include structural (core, E1, E2 and p7) and non-structural (NS2, NS3, NS4A, NS4B, NS5A and NS5B) proteins[1]. HCV is a leading cause of cirrhosis and hepatocellular carcinoma in the United States and Japan. Eradication of HCV is important for preventing death due to these liver diseases.

Associations of HCV with host lipoproteins have been reported[2]. Hepatocytes take up low-density lipoproteins (LDLs) and very low-density lipoproteins through LDL receptors. Antibodies to the HCV envelope may disrupt the HCV lipid-containing envelope[3]. These antibodies could provide an efficient mode of viral entry into liver cells[2]. HCV core protein colocalizes with apolipoprotein AII at the surface of lipid droplets, suggesting a relationship between the expression of HCV core protein and cellular lipid metabolism[4]. HCV infection or core protein expression also increases the expression of sterol regulatory element binding protein 1c and its target, fatty acid synthase (FASN), which are both involved in lipid synthesis[5].

Although interferon-free regimens could result in higher sustained virologic response (SVR) rates, Endo *et al*[6] reported that serum cholesterol levels were significantly increased during combination treatment with the HCV NS5B inhibitor sofosbuvir and the HCV NS5A inhibitor ledipasvir, compared with those during interferon-included regimens[7]. Of interest, the authors also observed that regardless of the regimens, total cholesterol, LDL cholesterol and high-density lipoprotein (HDL) cholesterol levels increased post-treatment[6].

HCV AND LIPID METABOLISM

HCV increases FASN levels[5], resulting in the accumulation of fatty acids in hepatocytes (Figure 1). Fatty acids are needed for cell growth, cell adhesion, extracellular matrix formation, cell migration and cell invasion, which are essential for cancer development. Synthesis of cholesterol requires 3-hydroxy-3-methylglutaryl coenzyme A (HMG-CoA) reductase. Among HMG-CoA reductase inhibitors, fluvastatin is an anti-HCV reagent that is used in combination with interferons[8]. Steatosis and abnormal lipid metabolism caused by HCV infection may enhance lipid droplet formation in hepatocytes[9-11]. Lipid droplets, which store neutral lipids, are required for the formation of infectious HCV particles[11].

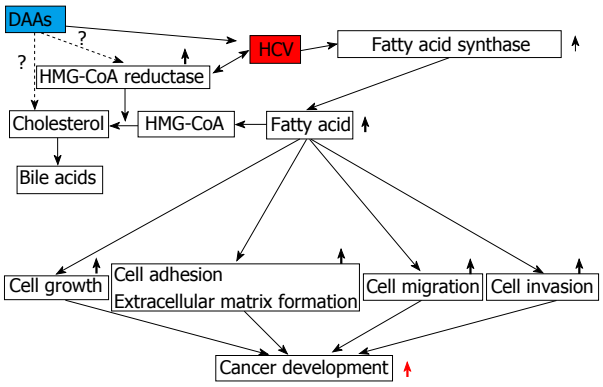

Figure 1 Hepatitis C virus and fatty acid synthesis. DAAs: Direct-acting antiviral agents; HCV: Hepatitis C virus; HMG-CoA, 3-hydroxy-3-methylglutaryl coenzyme A.

ADVANCED LIVER FIBROSIS AND LIPID METABOLISM

In most cells, the major source of new sterol is endogenous synthesis from acetyl-CoA[12]. HMG-CoA is formed from acetyl-CoA and acetoacetyl-CoA[12]. There are at least 4 mechanisms for acquiring cholesterol: (1) *de novo* synthesis within the cells and uptake of unesterified or esterified cholesterol from the external environment *via;* (2) the LDL receptor (LDLR); (3) scavenger receptor class B type I (SR-BI); or (4) Niemann-Pick C1-like 1 protein (NPC1L1)[13]. HDL particles containing apoA-I can be bound by SR-BI in hepatocytes and endocrine cells[13]. Interestingly, LDLR, SR-BI and NPC1L1 are candidate receptors that may be involved in HCV[14-16].

The total cholesterol pool in a human is 2.2 g/kg body weight. There is a continuous flow of cholesterol from the endoplasmic reticulum to the cell membrane and then from the plasma membrane to the liver and intestine[13]. In humans, the flux of cholesterol through the whole body is approximately 10 mg/d per kilogram body weight[17], although the half-life of plasma cholesterol is only a few days[13]. The serum lipids, total cholesterol, cholesteryl ester, LDL cholesterol and HDL cholesterol levels were significantly lower in HCV-related cirrhosis patients than in controls. HCV-related cirrhosis severely impairs liver lipid metabolism[18] (Figure 2). The serum total cholesterol level is an independent predictor of significant fibrosis[19]. When evaluating serum total cholesterol levels, liver function should also be checked (Figure 2).

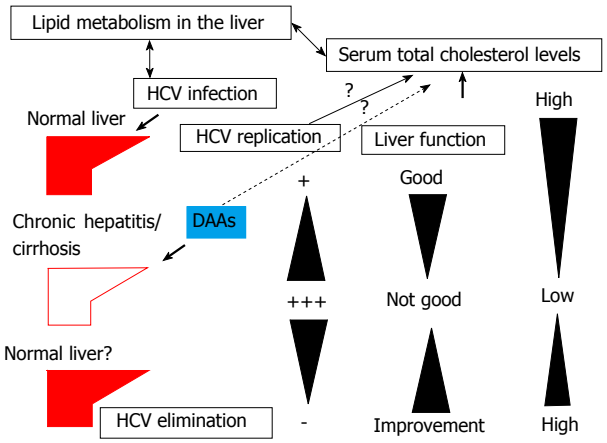

Figure 2 Effects of hepatitis C virus infection on liver function and liver lipid metabolism. DAAs: Direct-acting antiviral agents; HCV: Hepatitis C virus.

LIPID METABOLISM DURING TREATMENT WITH INTERFERON-BASED REGIMENS AGAINST HCV

Total cholesterol, LDL cholesterol and triglyceride levels are increased by peginterferon and ribavirin combination therapy when an SVR is achieved in patients with HCV genotype 1[20]. HCV eradication is closely related to lipid metabolism in patients treated with interferon-based regimens. Lange *et al*[21] examined the serum lipid profiles of 575 European HCV genotype 1-infected patients before, during and after treatment with peginterferon-α-2a (180 μg/wk) and ribavirin (1000-1200 mg/d) for 48 wk. The authors found substantial pretreatment hypocholesterolemia with a nonresponse to interferon-α-based therapy, and lower pretreatment cholesterol levels were an independent predictor of not attaining an SVR[21]. After treatment-induced HCV eradication, the median cholesterol levels increased above baseline. Kuo *et al*[22] reported that chronic HCV infection is associated with hypocholesterolemia and hypotriglyceridemia, and these conditions can be reversed by successful antiviral therapy.

HCV GENOTYPE 3

Serfaty *et al*[23] reported that hypobetalipoproteinemia is prevalent and associated with steatosis, especially in patients infected with HCV genotype 3. It has been reported that HCV, particularly genotype 3, is associated with steatosis. Poynard *et al*[24] reported that an SVR, achieved with interferon-based regimens, is associated with a reduction in steatosis in HCV genotype 3 patients, as well as a correction of serum cholesterol levels at baseline. Steatosis is significantly more common in HCV genotype 3 patients than in those with other HCV genotypes, and in patients treated with peginterferon alpha-2a plus ribavirin, an SVR is associated with reduction of steatosis[25]. New treatments using HCV NS3/4A protease inhibitors have limited activity against HCV genotype 3[26]. HCV NS5B and HCV NS5A inhibitors have also performed poorly in HCV genotype 3 patients[26].

LIPID METABOLISM DURING TREATMENT WITH INTERFERON-FREE REGIMENS AGAINST HCV

Endo *et al*[6] studied 276 patients with chronic HCV genotype 1b infection who were treated with interferon-free regimens. Of these 276 patients, 141 were treated with the HCV NS5A inhibitor daclatasvir plus the HCV NS3/4A inhibitor asunaprevir for 24 wk[27,28] and 135 were treated with sofosbuvir plus ledipasvir for 12 wk[6].

In the daclatasvir plus asunaprevir-SVR group, the total cholesterol levels were significantly increased throughout the observation period, and the total cholesterol levels were significantly increased at 4 wk after treatment and 12 wk after treatment, compared with those at the end of treatment (EOT)[6]. Serum LDL cholesterol levels increased after the EOT. HDL cholesterol was significantly increased throughout the treatment period, but there were no significant changes in serum triglyceride levels[6].

In the sofosbuvir plus ledipasvir-SVR group, the total cholesterol levels were markedly increased from the early stage of therapy and lasted until the EOT[6]. The total cholesterol levels were sharply decreased after the EOT ($P < 0.001$). Changes in the LDL cholesterol levels were quite similar to those found in the total cholesterol levels. After the EOT, the HDL cholesterol levels were decreased compared to those during therapy ($P < 0.001$), but there were no significant changes in triglyceride levels[6]. Hashimoto *et al*[29] also reported that the increase in cholesterol levels during treatment was much greater in the sofosbuvir plus ledipasvir-SVR group than in daclatasvir plus asunaprevir-SVR group. The authors also observed that a rapid increase in the serum LDL cholesterol concentration during the interferon-free treatment was associated with the type of regimen and decrease in the HCV core protein level. Morales *et al*[30] also reported that there was a significant increase in the LDL and total cholesterol levels after treatment, compared to the pre- and post-treatment laboratory data from 52 patients receiving sofosbuvir-based regimens, but there was no change in body mass index between pre-and post-treatment. Among HIV/HCV coinfected patients, an increase in LDL cholesterol was observed after an SVR was achieved with interferon-free treatment[31].

CONCLUSION

HCV infection induces steatosis and is accompanied by multiple metabolic alterations, such as hyperuricemia, reversible hypocholesterolemia, insulin resistance, arterial hypertension and visceral adipose tissue

expansion[32-34]. Eradication of HCV with interferon-free regimens increases total cholesterol levels. Because of the worsening nutritional status as an adverse event of interferon-based regimens, it is difficult to examine the effects of HCV on serum lipid profiles[6]. It is evident that HCV affects cholesterol metabolism during interferon-free regimens because these regimens have no influence on the nutritional status of the host[6]. The increase in cholesterol levels during treatment was much greater in the sofosbuvir plus ledipasvir-SVR group than in the daclatasvir plus asunaprevir-SVR group[6,29]. Although higher SVR rates were achieved with interferon-free treatment of HCV, special attention must also be paid to unexpected adverse events based on host metabolic changes.

REFERENCES

1 **Kanda T**, Imazeki F, Yokosuka O. New antiviral therapies for chronic hepatitis C. *Hepatol Int* 2010; **4**: 548-561 [PMID: 21063477 DOI: 10.1007/s12072-010-9193-3]

2 **Prince AM**, Huima-Byron T, Parker TS, Levine DM. Visualization of hepatitis C virions and putative defective interfering particles isolated from low-density lipoproteins. *J Viral Hepat* 1996; **3**: 11-17 [PMID: 8736235 DOI: 10.1111/j.1365-2893.1996.tb00075.x]

3 **Hijikata M**, Shimizu YK, Kato H, Iwamoto A, Shih JW, Alter HJ, Purcell RH, Yoshikura H. Equilibrium centrifugation studies of hepatitis C virus: evidence for circulating immune complexes. *J Virol* 1993; **67**: 1953-1958 [PMID: 8383220]

4 **Barba G**, Harper F, Harada T, Kohara M, Goulinet S, Matsuura Y, Eder G, Schaff Z, Chapman MJ, Miyamura T, Bréchot C. Hepatitis C virus core protein shows a cytoplasmic localization and associates to cellular lipid storage droplets. *Proc Natl Acad Sci USA* 1997; **94**: 1200-1205 [PMID: 9037030 DOI: 10.1073/pnas.94.4.1200]

5 **Bose SK**, Kim H, Meyer K, Wolins N, Davidson NO, Ray R. Forkhead box transcription factor regulation and lipid accumulation by hepatitis C virus. *J Virol* 2014; **88**: 4195-4203 [PMID: 24478438 DOI: 10.1128/JVI.03327-13]

6 **Endo D**, Satoh K, Shimada N, Hokari A, Aizawa Y. Impact of interferon-free antivirus therapy on lipid profiles in patients with chronic hepatitis C genotype 1b. *World J Gastroenterol* 2017; **23**: 2355-2364 [PMID: 28428715 DOI: 10.3748/wjg.v23.i13.2355]

7 **Kanda T**, Yasui S, Nakamura M, Suzuki E, Arai M, Ooka Y, Ogasawara S, Chiba T, Saito T, Haga Y, Takahashi K, Sasaki R, Wu S, Nakamoto S, Tawada A, Maruyama H, Imazeki F, Kato N, Yokosuka O. Real-World Experiences with the Combination Treatment of Ledipasvir plus Sofosbuvir for 12 Weeks in HCV Genotype 1-Infected Japanese Patients: Achievement of a Sustained Virological Response in Previous Users of Peginterferon plus Ribavirin with HCV NS3/4A Inhibitors. *Int J Mol Sci* 2017; **18**: 906 [PMID: 28441362 DOI: 10.3390/ijms18050906]

8 **Ikeda M**, Abe K, Yamada M, Dansako H, Naka K, Kato N. Different anti-HCV profiles of statins and their potential for combination therapy with interferon. *Hepatology* 2006; **44**: 117-125 [PMID: 16799963 DOI: 10.1002/hep.21232]

9 **Moriya K**, Yotsuyanagi H, Shintani Y, Fujie H, Ishibashi K, Matsuura Y, Miyamura T, Koike K. Hepatitis C virus core protein induces hepatic steatosis in transgenic mice. *J Gen Virol* 1997; **78** (Pt 7): 1527-1531 [PMID: 9225025 DOI: 10.1099/0022-1317-78-7-1527]

10 **Nakamura M**, Kanda T, Nakamoto S, Miyamura T, Jiang X, Wu S, Yokosuka O. No correlation between PNPLA3 rs738409 genotype and fatty liver and hepatic cirrhosis in Japanese patients with HCV. *PLoS One* 2013; **8**: e81312 [PMID: 24349054 DOI: 10.1371/journal.pone.0081312]

11 **Miyanari Y**, Atsuzawa K, Usuda N, Watashi K, Hishiki T, Zayas M, Bartenschlager R, Wakita T, Hijikata M, Shimotohno K. The lipid droplet is an important organelle for hepatitis C virus production. *Nat Cell Biol* 2007; **9**: 1089-1097 [PMID: 17721513 DOI: 10.1038/ncb1631]

12 **Spady DK**, Dietschy JM. Sterol synthesis in vivo in 18 tissues of the squirrel monkey, guinea pig, rabbit, hamster, and rat. *J Lipid Res* 1983; **24**: 303-315 [PMID: 6842086]

13 **Dietschy JM**, Turley SD. Thematic review series: brain Lipids. Cholesterol metabolism in the central nervous system during early development and in the mature animal. *J Lipid Res* 2004; **45**: 1375-1397 [PMID: 15254070 DOI: 10.1194/jlr.R400004-JLR200]

14 **Monazahian M**, Böhme I, Bonk S, Koch A, Scholz C, Grethe S, Thomssen R. Low density lipoprotein receptor as a candidate receptor for hepatitis C virus. *J Med Virol* 1999; **57**: 223-229 [PMID: 10022791]

15 **Scarselli E**, Ansuini H, Cerino R, Roccasecca RM, Acali S, Filocamo G, Traboni C, Nicosia A, Cortese R, Vitelli A. The human scavenger receptor class B type I is a novel candidate receptor for the hepatitis C virus. *EMBO J* 2002; **21**: 5017-5025 [PMID: 12356718 DOI: 10.1093/emboj/cdf529]

16 **Sainz B Jr**, Barretto N, Martin DN, Hiraga N, Imamura M, Hussain S, Marsh KA, Yu X, Chayama K, Alrefai WA, Uprichard SL. Identification of the Niemann-Pick C1-like 1 cholesterol absorption receptor as a new hepatitis C virus entry factor. *Nat Med* 2012; **18**: 281-285 [PMID: 22231557 DOI: 10.1038/nm.2581]

17 **Orth M**, Bellosta S. Cholesterol: its regulation and role in central nervous system disorders. *Cholesterol* 2012; **2012**: 292598 [PMID: 23119149 DOI: 10.1155/2012/292598]

18 **Vere CC**, Streba CT, Streba L, Rogoveanu I. Lipid serum profile in patients with viral liver cirrhosis. *Med Princ Pract* 2012; **21**: 566-568 [PMID: 22722340 DOI: 10.1159/000339206]

19 **Sud A**, Hui JM, Farrell GC, Bandara P, Kench JG, Fung C, Lin R, Samarasinghe D, Liddle C, McCaughan GW, George J. Improved prediction of fibrosis in chronic hepatitis C using measures of insulin resistance in a probability index. *Hepatology* 2004; **39**: 1239-1247 [PMID: 15122752 DOI: 10.1002/hep.20207]

20 **Tada S**, Saito H, Ebinuma H, Ojiro K, Yamagishi Y, Kumagai N, Inagaki Y, Masuda T, Nishida J, Takahashi M, Nagata H, Hibi T. Treatment of hepatitis C virus with peg-interferon and ribavirin combination therapy significantly affects lipid metabolism. *Hepatol Res* 2009; **39**: 195-199 [PMID: 19054155 DOI: 10.1111/j.1872-034X.2008.00439.x]

21 **Lange CM**, von Wagner M, Bojunga J, Berg T, Farnik H, Hassler A, Sarrazin C, Herrmann E, Zeuzem S. Serum lipids in European chronic HCV genotype 1 patients during and after treatment with pegylated interferon-α-2a and ribavirin. *Eur J Gastroenterol Hepatol* 2010; **22**: 1303-1307 [PMID: 20729742 DOI: 10.1097/MEG.0b013e32833de92c]

22 **Kuo YH**, Chuang TW, Hung CH, Chen CH, Wang JH, Hu TH, Lu SN, Lee CM. Reversal of hypolipidemia in chronic hepatitis C patients after successful antiviral therapy. *J Formos Med Assoc* 2011; **110**: 363-371 [PMID: 21741004 DOI: 10.1016/S0929-6646(11)60054-5]

23 **Serfaty L**, Andreani T, Giral P, Carbonell N, Chazouillères O, Poupon R. Hepatitis C virus induced hypobetalipoproteinemia: a possible mechanism for steatosis in chronic hepatitis C. *J Hepatol* 2001; **34**: 428-434 [PMID: 11322205 DOI: 10.1016/S0168-8278(00)00036-2]

24 **Poynard T**, Ratziu V, McHutchison J, Manns M, Goodman Z, Zeuzem S, Younossi Z, Albrecht J. Effect of treatment with peginterferon or interferon alfa-2b and ribavirin on steatosis in patients infected with hepatitis C. *Hepatology* 2003; **38**: 75-85 [PMID: 12829989 DOI: 10.1053/jhep.2003.50267]

25 **Reddy KR**, Govindarajan S, Marcellin P, Bernstein D, Dienstag JL, Bodenheimer H Jr, Rakela J, Messinger D, Schmidt G, Ackrill A, Hadziyannis SJ. Hepatic steatosis in chronic hepatitis C: baseline host and viral characteristics and influence on response to therapy with peginterferon alpha-2a plus ribavirin. *J Viral*

Hepat 2008; **15**: 129-136 [PMID: 18184196 DOI: 10.1111/j.1365-2893.2007.00901.x]
26 **Ampuero J**, Romero-Gómez M, Reddy KR. Review article: HCV genotype 3 - the new treatment challenge. *Aliment Pharmacol Ther* 2014; **39**: 686-698 [PMID: 24612116 DOI: 10.1111/apt.12646]
27 **Kumada H**, Suzuki Y, Ikeda K, Toyota J, Karino Y, Chayama K, Kawakami Y, Ido A, Yamamoto K, Takaguchi K, Izumi N, Koike K, Takehara T, Kawada N, Sata M, Miyagoshi H, Eley T, McPhee F, Damokosh A, Ishikawa H, Hughes E. Daclatasvir plus asunaprevir for chronic HCV genotype 1b infection. *Hepatology* 2014; **59**: 2083-2091 [PMID: 24604476 DOI: 10.1002/hep.27113]
28 **Kanda T**, Yasui S, Nakamura M, Suzuki E, Arai M, Haga Y, Sasaki R, Wu S, Nakamoto S, Imazeki F, Yokosuka O. Daclatasvir plus Asunaprevir Treatment for Real-World HCV Genotype 1-Infected Patients in Japan. *Int J Med Sci* 2016; **13**: 418-423 [PMID: 27279790 DOI: 10.7150/ijms.15519]
29 **Hashimoto S**, Yatsuhashi H, Abiru S, Yamasaki K, Komori A, Nagaoka S, Saeki A, Uchida S, Bekki S, Kugiyama Y, Nagata K, Nakamura M, Migita K, Nakao K. Rapid Increase in Serum Low-Density Lipoprotein Cholesterol Concentration during Hepatitis C Interferon-Free Treatment. *PLoS One* 2016; **11**: e0163644 [PMID: 27680885 DOI: 10.1371/journal.pone.0163644]
30 **Morales AL**, Junga Z, Singla MB, Sjogren M, Torres D. Hepatitis C eradication with sofosbuvir leads to significant metabolic changes. *World J Hepatol* 2016; **8**: 1557-1563 [PMID: 28050236 DOI: 10.4254/wjh.v8.i35.1557]
31 **Townsend K**, Meissner EG, Sidharthan S, Sampson M, Remaley AT, Tang L, Kohli A, Osinusi A, Masur H, Kottilil S. Interferon-Free Treatment of Hepatitis C Virus in HIV/Hepatitis C Virus-Coinfected Subjects Results in Increased Serum Low-Density Lipoprotein Concentration. *AIDS Res Hum Retroviruses* 2016; **32**: 456-462 [PMID: 26559180 DOI: 10.1089/AID.2015.0170]
32 **Lonardo A**, Adinolfi LE, Restivo L, Ballestri S, Romagnoli D, Baldelli E, Nascimbeni F, Loria P. Pathogenesis and significance of hepatitis C virus steatosis: an update on survival strategy of a successful pathogen. *World J Gastroenterol* 2014; **20**: 7089-7103 [PMID: 24966582 DOI: 10.3748/wjg.v20.i23.7089]
33 **González-Reimers E**, Quintero-Platt G, Rodríguez-Gaspar M, Alemán-Valls R, Pérez-Hernández O, Santolaria-Fernández F. Liver steatosis in hepatitis C patients. *World J Hepatol* 2015; **7**: 1337-1346 [PMID: 26052379 DOI: 10.4254/wjh.v7.i10.1337]
34 **Chang ML**. Metabolic alterations and hepatitis C: From bench to bedside. *World J Gastroenterol* 2016; **22**: 1461-1476 [PMID: 26819514 DOI: 10.3748/wjg.v22.i4.1461]

P- Reviewer: Guerrieri F, Ikura Y **S- Editor**: Qi Y **L- Editor**: A
E- Editor: Huang Y

World Journal of Gastroenterology

Submit a Manuscript: http://www.f6publishing.com

World J Gastroenterol 2017 August 21; 23(31): 5650-5668

DOI: 10.3748/wjg.v23.i31.5650

ISSN 1007-9327 (print) ISSN 2219-2840 (online)

REVIEW

Liquid biopsy in patients with hepatocellular carcinoma: Circulating tumor cells and cell-free nucleic acids

Wataru Okajima, Shuhei Komatsu, Daisuke Ichikawa, Mahito Miyamae, Takuma Ohashi, Taisuke Imamura, Jun Kiuchi, Keiji Nishibeppu, Tomohiro Arita, Hirotaka Konishi, Atsushi Shiozaki, Ryo Morimura, Hisashi Ikoma, Kazuma Okamoto, Eigo Otsuji

Wataru Okajima, Shuhei Komatsu, Daisuke Ichikawa, Mahito Miyamae, Takuma Ohashi, Taisuke Imamura, Jun Kiuchi, Keiji Nishibeppu, Tomohiro Arita, Hirotaka Konishi, Atsushi Shiozaki, Ryo Morimura, Hisashi Ikoma, Kazuma Okamoto, Eigo Otsuji, Division of Digestive Surgery, Department of Surgery, Kyoto Prefectural University of Medicine, Kyoto 602-8566, Japan

Author contributions: Okajima W and Komatsu S contributed equally to this work; Okajima W and Komatsu S wrote the manuscript; Ichikawa D and Otsuji E helped to draft the manuscript; Miyamae M, Ohashi T, Imamura T, Kiuchi J, Nishibeppu K, Arita T, Konishi H, Morimura R, Shiozaki A, Ikoma H and Okamoto K collected the literature.

Conflict-of-interest statement: The authors have no conflicts of interest to report.

Data sharing statement: Technical appendix and study data are available from the corresponding author at skomatsu@koto.kpu-m.ac.jp (Shuhei Komatsu) under the permission of Shuhei Komatsu. Participants gave informed consent for data sharing. No additional data are available.

Manuscript source: Invited manuscript

Correspondence to: Shuhei Komatsu, MD, PhD, Division of Digestive Surgery, Department of Surgery, Kyoto Prefectural University of Medicine, 465 Kajii-cho, Kawaramachihirokoji, Kamigyo-ku, Kyoto, 602-8566, Japan. skomatsu@koto.kpu-m.ac.jp
Telephone: +81-75-2515527
Fax: +81-75-2515522

Received: January 28, 2017
Peer-review started: February 8, 2017
First decision: March 3, 2017
Revised: April 14, 2017
Accepted: July 4, 2017
Article in press: July 4, 2017
Published online: August 21, 2017

Abstract

Hepatocellular carcinoma (HCC), with its high incidence and mortality rate, is one of the most common malignant tumors. Despite recent development of a diagnostic and treatment method, the prognosis of HCC remains poor. Therefore, to provide optimal treatment for each patient with HCC, more precise and effective biomarkers are urgently needed which could facilitate a more detailed individualized decision-making during HCC treatment, including the following; risk assessment, early cancer detection, prediction of treatment or prognostic outcome. In the blood of cancer patients, accumulating evidence about circulating tumor cells and cell-free nucleic acids has suggested their potent clinical utilities as novel biomarker. This concept, so-called "liquid biopsy" is widely known as an alternative approach to cancer tissue biopsy. This method might facilitate a more sensitive diagnosis and better decision-making by obtaining genetic and epigenetic aberrations that are closely associated with cancer initiation and progression. In this article, we review recent developments based on the available literature on both circulating tumor cells and cell-free nucleic acids in cancer patients, especially focusing on Hepatocellular carcinoma.

Key words: Hepatocellular carcinoma; Biomarker; Liquid biopsy; Circulating tumor cells; Cell-free nucleic acids

Core tip: Accumulating evidence about circulating tumor cells and cell-free nucleic acids in the blood of cancer patients has suggested their potent clinical utilities as novel biomarker. This concept, so-called "liquid biopsy" is widely known as an alternative approach to cancer tissue biopsy. This method might facilitate a more sensitive diagnosis and better decision-making by obtaining genetic and epigenetic aberrations that are closely associated with cancer initiation and progression. In this article, we review recent developments based on the available literature on both circulating tumor cells and cell-free nucleic acids in cancer patients, especially focusing on Hepatocellular carcinoma.

Okajima W, Komatsu S, Ichikawa D, Miyamae M, Ohashi T, Imamura T, Kiuchi J, Nishibeppu K, Arita T, Konishi H, Shiozaki A, Morimura R, Ikoma H, Okamoto K, Otsuji E. Liquid biopsy in patients with hepatocellular carcinoma: Circulating tumor cells and cell-free nucleic acids. *World J Gastroenterol* 2017; 23(31): 5650-5668 Available from: URL: http://www.wjgnet.com/1007-9327/full/v23/i31/5650.htm DOI: http://dx.doi.org/10.3748/wjg.v23.i31.5650

INTRODUCTION

Hepatocellular carcinoma (HCC) is the sixth most common cancer worldwide, but it ranks as the second most common cause of cancer-related death worldwide[1]. Despite recent development of a diagnostic and treatment method, the prognosis of HCC remains poor. Even in major advanced economies, the mortality rates have been increasing. Although HCC is a typical viral infection-related malignancy derived from chronic hepatitis B and C[2,3], HCC has also been strongly associated with lifestyle. Excessive alcohol consumption, obesity, and type 2 diabetes are strongly associated with the carcinogenesis and development of HCC[4-7]. Both the proportion and number of HCC patients with non-viral etiologies have been increasing on a global scale. Therefore, defining the target population should be added to screening as the most important clinical issues.

Early screening of patients for HCC has been reported to confer a survival benefit[8,9]. Patients who are identified early have multiple treatment options leading to improved outcomes. However, in clinical settings, only approximately 30% to 40% of patients with HCC can get effective treatment at the right time[10], and few molecules have been used as clinical biomarkers for HCC. Alpha-fetoprotein (AFP), AFP lectin fraction (AFP-L3), and des-γ-carboxy prothrombin (DCP, also known as proteins induced through vitamin K deficiency or antagonist-Ⅱ, PIVKA-Ⅱ) have been used as conventional serum tumor markers. However, these markers often show false-positive results, and lack sufficient sensitivity and specificity[11-13]. Therefore, to provide optimal treatment for each patient with HCC, more precise and effective biomarkers are urgently needed. Accumulating evidence of liquid biopsy might facilitate a more sensitive diagnosis and individualized decision-making in the duration of treatment of HCC.

In various cancers, many studies have demonstrated a large number of genetic and epigenetic aberrations contribute to carcinogenesis and their clinical utility[14-18]. Traditionally, these tumor-linked alterations has been provided from tissue samples of HCC patients. However, conventional procedures for tissue sampling from HCC patients is not always be conducted due to their clinical difficulties such as anatomical reasons, invasive nature, and/or the patient's poor hepatic status[19,20]. Because of such backgrounds, conventional procedures have some problems: (1) Results from a single biopsy could provide considerably restricted information; and (2) they could not reflect current cancer status, such as treatment sensitivity and therapeutic efficiency. Detecting circulating tumor cells (CTCs) and/or circulating cell-free nucleic acids (cfNAs) in the blood of cancer patients could provide us a so-called "liquid biopsy", which would realize repeated samplings and reflecting the characteristics and dynamics of tumor[21-24].

To date, many study groups have revealed the possibility of CTCs and cfNAs in the blood, as blood-based biomarkers, for several types of cancers[21-24]. These novel biomarkers are thought to have great potential and could provide more detailed individualized decision-making during HCC treatment, including the following; risk assessment, early cancer detection, prediction of treatment or prognostic outcome. In this article, based on the available literature, we review the histological backgrounds, recent developments and prospects for the future of liquid biopsy, particularly focusing on Hepatocellular carcinoma.

BIOLOGY AND DETECTION OF CIRCULATING TUMOR CELLS

CTCs are generally recognized as the "seeds" of tumors, which are shed into peripheral blood from a tumor *in situ* and eventually establish metastatic tumors in other organs[20]. Therefore, theoretically, circulating tumor cells (CTCs) are useful markers for early diagnosis. In 1869, Ashworth initially demonstrated the presence of CTCs[25] in the blood of breast cancer patient. This patients has widespread breast cancer, and the cells similar to those in the primary breast cancer had been detected in her blood. Afterwards, to validate Ashworth's remarks, many researches have challenged to investigate peripheral blood of various cancer patients to identify CTCs.

However, the effort has been hampered by some

difficulties. The problem is that the earlier the stage is, the less the cells are. Namely, the cell tends to be proportional to tumor volume. Moreover, CTCs have estimated infrequencies of approximately 1-10 CTCs in a background of millions of blood cells in patients with metastatic diseases[26]. In addition, less than 0.01% of CTCs introduced into the circulation survive to produce metastases. Furthermore, in phenotype, as well as genotype, CTCs are considered to be quite heterogeneous[27-29]. As CTCs are thought to be derived from the primary cancer or metastases, they are rarely present in patients with non-neoplastic disorders healthy person[30]. Therefore, the performance such as sensitivity and specificity of detection technique should be achieved to a proper level, precise detection of CTCs has been a major problem in this field for researchers.

TECHNIQUES FOR ISOLATION, ENRICHMENT, AND IDENTIFICATION OF CTCS

In recent years, various CTC isolation and enrichment technologies have emerged, their approaches are generally categorized into two methods.

Physical methods

Physical methods mainly depend on the physical properties of CTCs, such as density, size, migratory capacity, deformability and electric charge[31]. Most CTCs originate from epithelial tumors are thought to larger than other blood cells, several filtration-based techniques has been developed[32,33]. However, substantial difference has been demonstrated in cell size not only in an individual cancer patient but also in different cancer patients[34-36]. Thus, novel techniques adopting multiple filters have been studied to solve these issues and improve accuracy of enrichment of CTCs[37,38]. These micro device could isolate cancer cells using their physical properties such as size continuously and deformability. For example, Mohamed *et al*[37] designed a micro-machined device, which had arrays of four successively narrower channels, were able to fractionate cancer cells without interference from the blood cells. Those novel techniques could have substantial possibilities, their utility should be validated in the future.

Biological methods

Another approach is biological methods, which mainly rely on antigen-antibody binding and antibodies against tumor-specific biomarkers including epithelial cell adhesion molecule (EpCAM), human epidermal growth factor receptor2 (Her2), and prostate-specific antigen (PSA) that are typically used in CTCs purification[39]. Currently, Cell-Search™ (Veridex LLC, NJ, United States) is the most commonly used CTC platform. In this platform, immunomagnetic beads coated with EpCAM antibodies capture CTCs, followed by immunostaining with two positive markers, which are cytokeratins 8/18/19 for cytoplasmic epithelium and 4′,6′-diamidino-2-phenylindole hydrochloride for nucleic acids, and a negative marker, leukocyte-specific CD45. Its utility as a clinical indicator has been shown in the patients with metastatic breast, prostate, and colon cancers[40-45]. Therefore, this system has been the only CTC platform to be approved by the United States Food and Drug Administration. However, it could not capture CTCs that have increased the malignant potential, caused by the acquisition of an epithelial-mesenchymal transition (EMT). Concerning the detection and isolation capability and the clinical utility of CTCs, many challenges remain. To overcome its insufficient capability and accuracy, advanced technologies have emerged. "CTC-chip" is the representative technology without being influenced by the heterogeneity of them. It is a unique microfluidic platform, capable of efficient and selective separation of viable CTCs from peripheral whole blood samples, mediated by the interaction of target CTCs with antibody (EpCAM)-coated micro-posts[46]. Most recently, CTC-Chip was reported to detect CTCs with high accuracy by using tumor-specific markers, such as human epidermal growth factor (HER2) in breast cancer or prostate-specific antigen (PSA) in prostate cancer, in addition to epithelial markers[46,47]. Another unique approach was reported by Saucedo-Zeni *et al*[48] They captured and enriched CTCs from medical Seldinger guidewire, which were inserted into cubital veins. Despite these advances, the methodology of isolation and enrichment of CTCs has been in the process of development.

The identification process is generally conducted after the isolation and enrichment process. To identify genetic aberrations and other biological characteristics of CTCs, several methodologies, such as immunocytochemistry and molecular techniques, have been used. Conventionally, immunostaining using 4′,6′-diamidino-2-phenylindole hydrochloride as a nuclear stain, CK as an epithelial marker, and CD45 as a hematopoietic marker has been commonly adopted[49]. In various molecular approaches, quantitative reverse transcription-polymerase chain reaction (RT-PCR) has been widely used to identify the molecular characteristics of CKs, CEA, and other markers[50].

CTC DETECTION AND ITS CLINICAL RELEVANCE IN HCC PATIENTS

In the past decades, CTCs in HCC patients have been intensively studied. Table 1 is the summary of previously demonstrated candidates. As described in the last paragraph, these approaches are generally categorized into two methods: physical and biological methods.

Table 1 Circulating tumor cells in hepatocellular carcinoma

Ref.	HCC patients	Ethnicity	Background liver status	Patient background	Controls	Methodology	Positive rate
Matsumura, *et al*[51], 1999	88	Japan	HCV: 85%, HBV: 6%	Pre and post (TAE or PEI)	NA	RT-PCR (AFP)	63.0%
Mou *et al*[56], 2002	30	China	HBV: 100% LC: 100%	Pre resection	25 (HV: 25)	RT-PCR (MAGE1/3)	43.3%
Witzigmann *et al*[55], 2002	85	Germany	NA	Pre, during, post (Resection: 24, LT: 10, TACE: 13, No treatment: 38)	116 (OLT: 50, HD: 39, HV: 27)	RT-PCR (AFP)	28.0%
Vona *et al*[31], 2004	44	France	LC: 89%	Pre/post resection: 22 Unresectable: 22	107 (HV: 38, HD: 69)	ISET	52.2%
Jeng *et al*[53], 2004	81	China	HBV: 77%, HCV: 38% LC: 69%	Pre and post resection	50 (HV: 30, HD: 20)	RT-PCR (AFP)	23.4%
Cillo *et al*[52], 2004	50	Italy	HCV: 50%,HBV: 12% HCV and HBV: 6% Alcohol: 10% LC: 84%	Pre (Resection: 17, LT: 9, PT: 17) No treatment: 7	50 (HD: 6, OT: 44)	RT-PCR (AFP)	40.0%
Kong *et al*[59], 2009	343	South Korea	HBV: 78%, HCV: 10% Alcohol: 6% LC: 52%	Pre (Resection: 12, TACE: 224, RFA: 44, Chemotherapy: 12, Radiotherapy: 12, No treatment: 39)	NA	RT-PCR (AFP) (hTERT)	59.5% 14.0%
Fan *et al*[69], 2011	82	China	HBV: 80%	Pre and post resection	NA	CellSearch™	68.3%
Xu *et al*[70], 2011	85	China	HBV: 84%, HCV: 7% HBV and HCV: 5% nonB, nonC: 4%	Pre Resection: 63 Clinical Diagnosis: 22	71 (HD: 37, HV: 20, OT: 14)	CellSearch™	81.0%
Liu *et al*[67], 2013	60	China	HBV: 93% LC: 93%	Pre resection	NA	Flow cytometry	50.0%
Yao *et al*[57], 2013	123	China	HBV: 72% LC: 93%	NA	276 (HV: 30, HD: 196, OT: 50)	RT-PCR (GPC-3)	70.77%
Sun *et al*[73], 2013	123	China	HBV: 75% LC: 76%	Pre/post resection	NA	CellSearch™	66.6%
Schulze *et al*[72], 2013	59	Germany	Alcohol: 38% HBV: 17%, HCV: 13% LC: 89%	Pre (resection or systemic therapy)	19 (HD: 19)	CellSearch™	30.5%
Li *et al*[71], 2013	60	China	HBV: 92%, HCV: 3% nonB, nonC: 7% LC: 88.7%	NA	30 (HD: 10, HV: 10, OT: 10)	CellSearch™	76.6%
Bahnassy *et al*[68], 2014	70	Egypt	HCV: 100%	NA	63 (HD: 30, HV: 33)	Flow cytometry (CK19, CD90, 133) RT-PCR (Telomerase, MAGE1/3)	73.0%, 49.8%, 69.5% 55.7%, 60.0%, 62.9%
Li *et al*[76], 2014	27	China	NA	NA	61 (HD: 34, HV: 15, OT: 12)	CellSearch™	88.9%
Mu *et al*[78], 2014	62	China	HBV: 95.2%	NA	22 (HD: 7, HV: 15)	CellSearch™	48.3%
Fang *et al*[74], 2014	42	China	LC: 55%	Pre and post TACE	20 (HV: 10, HD: 10)	CellSearch™	52.3%
Morris *et al*[77], 2014	52	United Kingdom	Alcohol: 38%, HBV: 8% Diabetes: 12%	No treatment	NA	CellSearch™ ISET	28% 100%
Guo *et al*[75], 2014	299	China	HBV: 90% LC: 90%	Pre/post (Resection: 157, TACE: 76, RFA: 66)	120 (HV: 71, HD: 25, BT: 24)	CellSearch™	42.6%
Choi *et al*[58], 2015	81	South Korea	HBV: 80%, HCV: 11% Alcohol: 4% LC: 59%	Pre and post (Resection: 64, LT: 17)	16 (LHD: 16)	RT-PCR (K19, CD44)	22.2%
Kelley *et al*[19], 2015	20	Caucasian: 55%, Asian: 35%, American: 10% (African-5%) (Native-5%)	HBV: 25%, HCV: 45% HBV and HCV: 10% Alcohol: 5% NAFLD: 10%	NA	10 (HD: 10)	CellSearch™	40.0%
Wang *et al*[79], 2016	42	China	HBV: 81%, HCV: 2% nonB, nonC: 17%	NA	NA	CTC-Chip	59.5%
Zhang *et al*[207], 2016	36	China	NA	NA	NA	CTC-Chip	100%

NA: Not applicable; LC: Liver cirrhosis; NAFLD: Non-alcoholic fatty liver disease; TAE: Trans-arterial embolization; PEI: Percutaneous ethanol injection; LT: Liver transplantation; TACE: Trans-catheter arterial chemoembolization; RFA: Radiofrequency ablation; PT: Percutaneous treatment; HV: Healthy volunteers; HD: Hepatic disease without evidence of HCC; OLT: Other malignant liver tumors; BT: Benign tumor; OT: Other cancerous disease; LHD: Liver healthy donors; RT-PCR: Reverse transcriptase polymerase chain reaction; ISET: Isolation by size of epithelial tumor cells.

Physical methods

Vona *et al*[31] first reported the isolation by size of epithelial tumor cell (ISET) method to detect CTCs in HCC patients. By cytomorphologic analysis, they demonstrated that the spontaneous circulation of CTCs in peripheral blood reflects tumor progression and tumor spread in patients with HCC. Compared with expensive and cumbersome molecular techniques, ISET is a unique, inexpensive methodology. In this method, we can apply the cytopathological diagnosis of tumor cells, which were widely used in clinical oncology, as peripheral blood samples without any special equipment[32]. However, ISET device is still hard to release CTCs from the membrane. This may limit the application of downstream genetic analysis.

Biological methods

The presence and clinical utility of CTCs in HCC was first reported by Matsumura *et al*[51] using RT-PCR. They demonstrated the following. (1) the presence of alpha-fetoprotein (AFP) messenger RNA (mRNA) in peripheral blood could be a marker of circulating HCC cells; (2) the status of AFP mRNA in blood were investigated at entry, extrahepatic metastasis developed more frequently among the AFP mRNA-positive patients than among the AFP mRNA-negative patients; and (3) after treatment, AFP mRNA was investigated, and cumulative metastasis-free survival and overall survival were significantly better in patients whose AFP mRNA became negative after treatment than in patients with persistently positive AFP mRNA. In summary, they demonstrated that the presence or absence of AFP mRNA in blood (CTCs' positivity) could be a predictor of outcome in patients with HCC.

Following this study, the clinical utility of peripheral AFP mRNA was validated by other groups[52,53]; however, the significance as prognostic marker has not been adequately confirmed[54,55]. Thus, other tumor-specific molecules in the bloodstream, such as MAGE-1, MAGE3[56], glypican-3 (GPC-3)[57], keratin 19 (K19), cluster of differentiation 44 (CD44)[58], and hTERT[59] mRNA, have been investigated for markers of circulating HCC cells. For example, MAGE gene transcripts have been considered as HCC-specific markers[60]. Mou *et al*[56] demonstrated that detection of MAGE transcripts in blood with a follow-up survey could predict the prognosis and monitor the response to therapy. GPC-3 is a membrane-anchored heparin sulfate proteoglycan, known to be a reliable biomarker for HCC[61]. Yao *et al*[57] demonstrated that GPC-3 mRNA abnormality is useful as clinical biomarkers from early cancer detection to evaluating metastasis. Furthermore, K19 and CD44 have been shown to be cancer stem cell markers in HCC[62-65], their significance of prognostic factor in peripheral blood were also demonstrated by Choi *et al*[58]. However, HCC associated genes were not always candidates for the markers of CTCs. Although serum human telomerase reverse transcriptase protein (hTERT) mRNA expression has been suggested as a potential candidate diagnostic marker for HCC[66], the significance as prognostic marker has not been adequately confirmed[59].

Liu et *al*[67] and Bahnassy *et al*[68] used flow cytometry to analyze intercellular adhesion molecule 1 (ICAM-1) expression, cytokeratin 19, CD133, and CD90 in HCC blood samples and demonstrated their prognostic value. Among various techniques, EpCAM-based Cell-Search™ is currently the most widely used CTC platform[19,69-78]. Using this method, Sun *et al*[73] collected blood samples from 123 HCC patients who underwent curative resection and suggested that $EpCAM^+$ CTCs could be useful for real-time parameter for monitoring treatment response and be also used for therapeutic target in HCC recurrence. Guo *et al*[75] collected blood samples from 299 HCC patients with various kinds of treatment and 120 control subjects, and demonstrated that this method could be useful in early decision-making to tailor the most effective antitumor strategies. Most recently, Wang *et al*[79] suggested that novel CTC-Chip platform might be a new method for a simple and efficient detection of CTCs in HCC patients. They created biocompatible and transparent Hydroxyapatite/chitosan nanofilm coated by aptamer for carbohydrate sialyl Lewis Xto and demonstrated that it could be useful as prognostic marker.

Overall, the usefulness of CTCs as biomarkers in HCC might be practically guaranteed. However, several challenges that must be overcome remain. Firstly, it is possible that etiological differences of patients and controls, such as background liver disease, haptic status, and race, could be responsible for the heterogeneity of the results. Secondly, a novel methodology for the detection should be provided for solving the problem of the rarity and heterogeneity of CTCs. Thirdly, the techniques and results of past research have greatly differed. Consequently, a large-scale validation using patients with homogeneous backgrounds and development of a unified methodology are required for future applications.

BIOLOGY AND DETECTION OF CELL-FREE NUCLEIC ACIDS

cfNAs in peripheral blood of cancer patients, comprised of DNA, mRNA, and miRNA, are known to come from apoptotic and necrotic cells or are released from living eukaryotic cells[21]. The first discovery of cfNAs in human peripheral blood was in 1948 by Mandel and Metais[80]. However, their work did not gain attention for a long time due to insufficient understanding of that new concept, completely different from conventional ones. Cell free DNAs were first discovered by Leon *et al*[81] in the serum of cancer patients in 1977. They also suggested it could be a clinical indicator of treatment

outcome, showing decreased cfDNA levels in response to radiotherapy. Since then, numerous alterations in cfNAs have been demonstrated in various cancer patients. Cell free DNA with cancer characteristics was first discovered by Vasioukhin *et al*[82] in 1989. Tumours can shed DNA into the circulation. Their discovery indicated the possibility that cancers could release DNA into the blood of the cancer patients. This hypothesis was validated in the plasma of cancer patients: *KRAS* mutation in the pancreatic cancer patients[83] and *NRAS* mutation in the leukemia patients[84].

The state of RNA in the blood is easy-to degrade by the presence of endogenous ribonuclease, however, cell-free RNA has been demonstrated in blood. The presence of cfRNA was first discovered in 1999 from the serum of patients with nasopharyngeal carcinoma[85] and malignant melanoma[86]. Afterwards, many study group have demonstrated the presence and utility of mRNA in the blood of various cancer patients[87-89].

In 2008, Mitchell *et al*[90] first demonstrated that circulating microRNAs (miRNAs) in patients with solid cancers could be a promising biomarker. Since then, circulating noncoding RNAs have been intensively studied. Among them, miRNAs has especially gained attention. Other noncoding RNAs, such as small nucleolar RNA (snoRNA), small nuclear RNA (snRNA), piwi-interacting RNA (piRNA), and long noncoding RNA (lncRNA), have been also expected to be biomarkers, however, there are few studies of these. In the future, further research will probably be necessary.

CIRCULATING CELL-FREE DNA DETECTION AND ITS CLINICAL RELEVANCE IN HCC PATIENTS

Circulating cfDNA, a naturally occurring biological material, is generally considered to be a potential novel biomarker for a long time[91]. These abnormalities can be divided into two changes, such as quantitative changes and qualitative changes. Quantitative changes appear as higher concentrations of total circulating cfDNA, qualitative changes are gene mutations, DNA copy number variations, tumor-specific methylation, microsatellite instability (MSI) and loss of heterozygosity. Thus, analysis of circulating cell-free DNA in the plasma/serum can be mainly categorized into two strategies. One of these strategies is to measure the quantity of cell-free DNA in circulation. The other strategy is to detect tumor-specific genetic aberrations. Most researchers have adopted studies the later one as liquid biopsy[92-95].

Table 2 is the summary of previously demonstrated candidates. Some researchers have adopted a quantitative analysis[96-102]. Huang *et al*[100] and Chen *et al*[99] demonstrated that plasma DNA or serum DNA levels were significantly higher in HCC patients and they were associated with a poorer prognosis; however, it has not become a mainstream of cfDNA studies because the elevated levels of cfDNA were not specific for HCC. Although single nucleotide mutation[103] and copy number variation[95,104] were representative changes for the qualitative strategy, the "methylation pattern" has been the most intensively investigated. Initially, the presence and the clinical utility of circulating cell-free DNA in HCC was reported by Wong *et al*[105]. Using methylation-specific PCR, they analyzed p15 methylation patterns in three kinds of samples such as plasma, serum, and tissues surgically resected from HCC patients and showed the following: (1) in the blood samples, methylated p15 sequences were detected in 25% of patients with p15 methylation in the tissue; (2) nearly all patients showing p15 and p16 methylation in the tissue had detectable methylation abnormalities in their blood samples; and (3) clinical metastasis or recurrence were developed in the patients with p15/p16 methylation. In summary, these epigenetic markers could serve as diagnostic and prognostic markers. As previous studies revealed that changes of DNA methylation exited in various malignancies and played an important role in carcinogenesis[106,107], following this study, many researchers investigated the cfDNA methylation profile in HCC patients[108-124]. For example, Iyer *et al*[115] compared the tumor methylation profile for tumor suppressor genes, such as APC, FHIT, p15, p16, and E-cadherin, and in tumor tissues and plasma from the same HCC patients, and demonstrated that concordance between the two types of specimens was statistically significant for all five genes. It suggested that plasma DNA reliably predicts methylation events in tissue DNA; therefore, plasma DNA could be used for methylation studies. Huang *et al*[116] analyzed the plasma methylation status of four genes (APC, GSTP1, RASSF1A, and SFRP1) and showed the sufficient diagnostic value of cfDNAs. Although the area under the receiver-operation characteristic curve (AUC-ROC) for an individual gene was not adequate, the combination analysis of these four genes indicated higher AUC (0.933) in discriminating HCC from the normal control. Furthermore, they demonstrated methylated RASSF1A in plasma could be an independent prognostic factor for overall survival.

MS-PCR has been widely used for methylation research, because it provides a rapid and simple method with high sensitivity and accuracy. More recently, droplet digital PCR[125-128] and genome-wide high-throughput sequencing[128,129] has been reported as a further accurately detection tools for rare and multiple types of mutations in circulating DNA. These novel approaches has revealed that genetic aberrations in cell-free DNA gained from the bloodstream of cancer patients and drug resistance were correlating[130-132]. It is required that the potent clinical utility of cell-free DNA, such as risk assessment, early cancer detection, prediction of drug resistance and prognostic outcome,

Table 2 Circulating cell-free DNA in hepatocellular carcinoma

Ref	HCC patients	Sample	Ethnicity	Background liver	Controls	cfDNA abnormalities Methodolgy	Target
Wong *et al*[105], 2000	25 15	Plasma/serum Buffy coat	Hong-Kong	HBV: 88% HCV: 2%	55 (HD: 35, HV: 20) 35 (HD: 15, HV: 20)	Methylation MS-PCR	P16
Wong *et al*[108], 2003	29/22 29	Plasma/serum Buffy coat	Hong Kong	NA	50 (HD and HV) 35 (HD: 15, HV: 20)	Methylation MS-PCR	P16INK4A
Chu *et al*[109], 2004	46	Serum	Korea	HBV: 65% HCV: 22%	23 (HD: 23)	Methylation MS-PCR	P16INK4A
Yeo *et al*[110], 2005	40	Plasma	Hong-Kong	HBV: 83%	10 (HV: 10)	Methylation MS-PCR	RASSF1A
Iizuka *et al*[96], 2006	52	Serum	Japan	HCV: 100%	46 (HD: 30, HV: 16)	Quantitative analysis Real-time PCR	GSTP1
Ren *et al*[97], 2006	79	Plasma	China	HBV: 85% LC: 86%	40 (HD: 20, HV: 20)	Quantitative analysis Real-time PCR Allelic imbalance analysis	NA D8S258 and D8S264
Zhang *et al*[112], 2007	50	Serum	Taiwan	HBV: 22% HCV: 16%	50 HV: 50	Methylation MS-PCR	P15, P16
Tan *et al*[111], 2007	8	Serum	Singapore	NA	72 (OT: 62, HV: 10)	Methylation MS-PCR	RUNX3
Chan *et al*[113], 2008	85	Serum	Hong-Kong	HBV: 92%	135 (HD: 63, HV: 72)	Methylation RT-PCR	RASSFIA
Chang *et al*[114], 2008	19	Plasma	China	HBV: 89%	17 (LC: 17)	Methylation MS-PCR	APC, GSTP1, RASSF1A, P16, E-cadherin
Iyer *et al*[115], 2010	28	Plasma	Egypt	HCV: 79% HNV: 18%	NA	Methylation MS-PCR	APC, FHIT, P15, P16 and E-cadherin
Yang *et al*[98], 2011	60	Plasma	China	NA	50 (HD: 21, HV: 29)	Quantitative analysis FQ-PCR	hTERT
Szymańska *et al*[103], 2011	14	Plasma	China	Mostly HBV	NA	Single nucleotide mutation SOMA	R249S (TP53 mutation)
Iizuka *et al*[117], 2011	220	Serum	Japan	HCV: 100%	202 (HD: 202)	Methylation MS-PCR	SPINT2, SRD5A2
Huang *et al*[116], 2011	72	Plasma	China	HBV: 85%	37 (HD: 37)	Methylation MSRE-qPCR	APC, GSTP1, RASSF1A, and SFRP1
Huang *et al*[100], 2012	72	Plasma	China	HBV: 85%	115 (HD: 74, HV: 41)	Quantitative analysis Real-time PCR	NA
Chen *et al*[99], 2012	80	Serum	China	HBV: 100%	130 (HD: 80, HV: 50)	Quantitative analysis Real-time PCR	NA
Mohamed *et al*[118], 2012	40	Serum	Egypt	HCV: 100%	60 (HD: 40, HV: 20)	Methylation Real-time PCR	RASSF1A
Chen *et al*[101], 2013	39	Serum	China	HBV: 79%	45 (HV: 45)	Quantitative analysis Real-time PCR	NA
Piciocchi *et al*[102], 2013	66	Plasma	Italy	HCV: 51% Alcohol: 27%	76 (HD: 76)	Quantitative analysis Real-time PCR	hTERT
Chan *et al*[95], 2013	4	Plasma	China	NA	20 (HD: 4, HV: 16)	Copy number variation MPS	NA
Sun *et al*[119], 2013	43	Serum	China	HBV: 86%	50 (HD: 24, HV: 26)	Methylation MS-PCR	TFPI2
Zhang *et al*[120], 2013	37	Serum	China	HBV: 100%	33 (HD: 33)	Methylation Bead Chip, Hot-start PCR, Pyrosequencing	DBX2, THY1
Huang *et al*[122], 2014	66	Serum	United States	HCV: 100% HCV and HBV: 6%	43 (HD: 43)	Methylation Pyrosequencing, MS-PCR	INK4A
Han *et al*[121], 2014	160	Serum	China	HBV: 22%	133 (HD: 88, HV: 45)	Methylation MS-PCR	TRG5
Ji *et al*[123], 2014	121	Serum	China	HBV: 83%	68 (HD: 37, HV: 31)	Methylation MS-PCR	MT1M
Kuo *et al*[124], 2014	40	Plasma	Taiwan	NA	34	Methylation MS-PCR	HOXA9
Jiang *et al*[104], 2015	90	Plasma	Hong-Kong	NA	135 (HD: 103, HV: 32)	Copy number variation CAZA	NA

NA: Not applicable; HD: Hepatic disease without evidence of HCC; HV: Healthy volunteers; RT-PCR: Reverse transcriptase polymerase chain reaction; SOMA: Short oligonucleotide mass analysis; CAZA: Chromosome arm-level z-score analysis; MPS: Massively parallel sequencing; MS-PCR: Methylation-specific PCR; RT-PCR: Real time polymerase chain reaction; MSRE-qPCR: Methylation-sensitive restriction enzymes-based quantitative PCR; FQ-PCR: Real-time quantitative fluorescent polymerase chain reaction.

could be demonstrated in the patients with HCC.

CIRCULATING CELL-FREE MRNA IN PLASMA/SERUM AND HCC

Although RNA is fragile, easily degraded by ribonuclease (RNase) and the concentration of RNase in plasma/serum is known to be elevated in cancer patients[133], many researchers have successfully demonstrated the stable presence of cell-free mRNAs in the bloodstream of cancer patients. Recently, novel mechanistic insights have been gained that these RNAs can be incorporated into other surrounding such as exosomes, microvesicles and multivesicles, which considered to be sufficiently protected from the degradation by RNases and released from the cellular surface to the blood[134]. There are many studies of cell-free mRNA in the blood of patients with various solid cancers, and most of them targeted the mRNAs in plasma/serum whose up-regulation were previously validated in cancer tissues[87-89,135-137]. Regarding HCC, several study groups investigate mRNA in peripheral blood mononuclear cells as a marker for the detection of CTCs[51-53,55-57,59]; however, the quantity of cell-free mRNAs in plasma/serum is exceedingly small. Further studies of cell-free mRNA in patients with HCC may provide new knowledge to the research field of liquid biopsy.

CIRCULATING NONCODING RNA IN PLASMA/SERUM

Although as much as 80% of genomic DNA had already demonstrated to be transcribed into RNAs[138], the Human Genome Project revealed that the open reading frames of protein genes is only 2% of the 3.2 billion bases[139,140]. It can be paraphrased as there are only a very few human genomic DNAs that actually code proteins. It is gradually reveled that various noncoding RNAs (ncRNAs) play crucial roles in several cellular processes in the transition from DNA to protein. Therefore, the expression patterns of ncRNAs could be promising molecular biomarkers in novel diagnostic techniques[141].

For circulating ncRNAs, particular attention has been paid to miRNAs. MiRNAs are small non-coding RNAs that play crucial roles in various cellular processes. A single miRNA could regulate the expression of genes as follows: A guide strand of mature miRNA is taken into the RNA-induced silencing complex and then hybridizes to the 3′-untranslated region of their target mRNAs to translate or degrade these mRNAs. Thus, miRNAs have occupied important place in all cellular processes, some alterations in miRNA expression has come to draw a lot of attention in the association with various disease. Particularly, some researchers have demonstrated that specific miRNAs could act like oncogenes or tumor suppressors. Several studies in recent years on this subject have also shown that some extracellular miRNAs were generated from both cell lysis and active secretion[21,142,143]. Furthermore, several researchers have detected miRNAs in the plasma/serum in a remarkably stable form. In this regard, Kosaka *et al*[143] proved that secretory mechanisms and intercellular transfer of microRNAs in living cells. A group of miRNAs is packaged into small membrane vesicles called exosomes and released through a ceramide-dependent secretory machinery. Furthermore, miRNAs are remarkably stable form in plasma as they bind to certain proteins, such as argonaute 2 and high-density lipoproteins[144]. Therefore, all circulating miRNAs, regardless of whether they are taken into certain protein complexes and/or cell-derived microvesicles, has been thought to be sufficiently protected against the degradation by RNases in the bloodstream. These findings of recent years have pioneered a novel research field in cancer science.

In 2008, Mitchell *et al*[90] first reported that circulating miRNAs could be useful for stable blood-based markers for cancer detection. Since then, circulating miRNAs in the blood of cancer patients have been intensively studied to validate their potential as biomarkers. Table 3 is the summary of previously demonstrated candidates. In 2010, Li *et al*[145] first demonstrated that serum miRNAs expression profile could be useful as novel noninvasive biomarkers for the distinction between HBV infection and HBV-positive HCC. Since then, several research groups have reported the potential utility of miRNAs circulating in plasma/serum in clinical applications. Concerning circulating miRNAs in HCC, more than 70 miRNAs have been thought to be useful for biomarkers[145-195]. Some miRNAs had been used in combination with AFP, conventional serum tumor marker, to improve diagnostic accuracy[158,171,177,188,191,195]. Moreover, one miRNA could influence various mRNAs, more and more miRNAs and related mRNAs continues to be reported by numerous research groups. However, they are not always superimposable due to the large variances in the results. Thus, to realize more accurate diagnosing, some researchers have tried to use miRNAs in combination. Zhou *et al*[150] using the unique panel consisting of 7 mRNAs (miR-122, -192, -21, -223, -26a, -27a, and -801), based on the expression in plasma, could differentiate HCC from healthy (AUC = 0.941), chronic hepatitis B (AUC = 0.842), and cirrhosis (AUC = 0.884). More recently, Tan *et al*[166] reported that a combination of eight miRNAs could provide high diagnostic accuracy for HCC.

In terms of diagnosis, it should fully consider that HCC is an extremely prominent cancer among high-risk group patients. Patients who are already infected with HBV and HCV, and/or liver cirrhosis are at risk of developing liver cancer; however, some candidate miRNAs could not discriminate HCC patients from patients with liver chronic hepatitis, or cirrhosis[146,147,149,160,162,179,187]. They were useful for detecting HCC from general population, but not suitable for further screening, narrowing down patients

Table 3 Circulating cell-free microRNA in hepatocellular carcinoma

miR	Expression	Sample	HCC patients	Ethnicity	Background liver	Controls	Value	Ref.
miR-1	Up	Serum	195	Germany	HCV: 45%, Alcohol: 33%, HBV: 17%	54 (HD: 54)	P	Köberle *et al*[155] 2013
miR-10b	Up	Blood	27	China	Alcohol: 23%	81 (HD: 81)	D	Jiang *et al*[175] 2015
miR-15b	Up	Serum	153	China	HBV: 88%	59 (HD: 29, HV: 39)	D	Liu *et al*[152] 2012
miR-15b-5p	Down	Plasma	37	China	NA	60 (HD: 29, HV: 31)	D	Chen *et al*[170] 2015
miR-16	Down	Serum	105	United States	HCV: 64%, HBV: 20%	178 (HD: 107, HV: 7)	D	Qu *et al*[148] 2011
			90	China	NA	60 (HV: 60)	D	Ge *et al*[161] 2014
			40	Egypt	HCV: 100%	60 (HD: 40, HV: 20)	D	El-Abd *et al*[174] 2015
miR-17-5p	Up	Serum	136	China	NA	NA	P	Zheng *et al*[159] 2013
			8	Turkey	HCV: 100%	84 (HD: 56, HV: 28)	D	Oksuz *et al*[178] 2015
miR-18a	Up	Serum	101	China	HBV: 100%	90 (HD: 30, HV: 60)	D	Li *et al*[151] 2012
	Up	Serum	20	South Korea	HBV: 70%	40 (HD: 40)	D	Sohn *et al*[179] 2015
miR-19a	Down	Serum	112	Egypt	HCV: 100%	167 (HD: 125, HV: 42)	D	Motawi *et al*[177] 2015
miR-21	Up	Plasma	457	China	HBV:100%	477 (HD: 310, HV: 167)	D	Zhou *et al*[150] 2011
			136	Japan	HCV:68%, HBV: 23%	80 (HD: 30, HV: 50)	D, P	Tomimaru *et al*[153] 2012
		Serum	101	China	HBV: 75%	137 (HD: 48, HV: 89)	D	Xu *et al*[149] 2011
			136	China	HBV: 95%	NA	P	Liu *et al*[164] 2014
			97	China	HBV: 62%	30 (HV: 30)	D, P	Wang *et al*[180] 2015
			23	Egypt	HCV: 87%, HBV: 13%	17 (HD: 17)	D	Amr *et al*[186] 2016
	Down	Serum	70	China	HBV: 100%	72 (HD 48, HV: 24)	D	Qi *et al*[147] 2011
			90	China	NA	60 (HV: 60)	D, P	Ge *et al*[161] 2014
			52	China	HBV: 63%, HCV: 4%	85 (HD: 42, HV: 43)	D	Zhuang *et al*[195] 2016
miR-22	Down	Serum	192	Egypt	HCV: 100%	192 (HD: 192)	D	Zekri *et al*[194] 2016
miR-24-3p	Up	Serum	84	China	HBV: 100%	77 (HD: 31, HV: 46)	D, P	Meng *et al*[165] 2014
miR-26a	Down	Plasma	457	China	HBV: 100%	477 (HD: 310, HV: 167)	D	Zhou *et al*[150] 2011
		Serum	52	China	HBV: 63%, HCV: 4%	85 (HD42, HV: 43)	D	Zhuang *et al*[195] 2016
miR-26a-5p	Down	Serum	261	China	HBV: 100%	406 (HD 233, HV: 173)	D	Tan *et al*[166] 2014
miR-27a	Down	Plasma	457	China	HBV: 100%	477 (HD: 310, HV: 167)	D	Zhou *et al*[150] 2011
miR-29b	Down	Serum	192	Egypt	HCV: 100%	192 (HD: 192)	D	Zekri *et al*[194] 2016
miR-30c	Down	Serum	242	China	HCV: 63%	NA	P	Liu *et al*[176] 2015
miR-30c-5p	Down	Serum	8	Turkey	HCV: 100%	84 (HD: 56, HV: 28)	D	Oksuz *et al*[178] 2015
miR-34a	Up	Serum	112	Egypt	HCV: 100%	167 (HD: 125, HV: 42)	D	Motawi *et al*[177] 2015
miR-92a-3p	Up	Plasma	20	Turkey	HBV: 100%	74 (HD: 46, HV: 28)	D	Giray *et al*[162] 2014
miR-96	Up	Serum	104	China	HBV: 100%	400 (HD: 280, HV: 120)	D	Chen *et al*[171] 2015
miR-101	Up	Serum	25	China	HBV: 100%	20 (HV: 20)	D	Fu *et al*[154] 2013
	Down	Serum	67	China	HBV: 100%	170 (HD: 140, HV: 3,)	D	Xie *et al*[167] 2014
			20	South Korea	HBV: 70%	40 (HD: 40)	D	Sohn *et al*[179] 2015
			52	China	HBV: 63%, HCV: 4%	85 (HD: 42, HV: 43)	D	Zhuang *et al*[195] 2016
miR-106b	Up	Blood	27	China	Alcohol: 23%	81 (HD: 31, HV: 50,)	D	Jiang *et al*[175] 2015
miR-122	Up	Serum	70	China	HBV: 100%	72 (HD: 48, HV: 24,)	D	Qi *et al*[147] 2011
			101	China	HBV: 75%	137 (HD: 48, HV: 89,)	D	Xu *et al*[149] 2011
			195	Germany	HCV: 45%, Alcohol: 33%, HBV: 17%	54 (HD: 54)	P	Köberle *et al*[155] 2013
			30	Egypt	HCV: 100%	70 (HD: 60, HV: 10)	D	El-Garem *et al*[160] 2014
			136	China	HBV: 95%	NA	P	Liu *et al*[164] 2014
			192	Egypt	HCV: 100%	192 (HD: 192)	D	Zekri *et al*[194] 2016
	Down	Plasma	457	China	HBV: 100%	477 (HD: 310, HV: 167)	D	Zhou *et al*[150] 2011
		Serum	20	South Korea	HBV: 70%	40 (HD: 40)	D	Sohn *et al*[179] 2015
			122	China	NA	NA	P	Xu *et al*[181] 2015
miR-122a	Down	Serum	85	China	HBV: 88%	HV (HV: 85)	D	Luo *et al*[156] 2013
miR-122-5p	Up	Plasma	20	Turkey	HBV: 100%	74 (HD: 46, HV: 28)	D	Giray *et al*[162] 2014
		Plasma	120	South Korea	HBV: 100%	NA	P	Cho *et al*[172] 2015
		Serum	120	China	HBV: 100%	DN: 30	D	Hung *et al*[189] 2016
	Down	Serum	261	China	HBV: 100%	406 (HD: 233, HV: 173)	D	Tan *et al*[166] 2014
miR-125b	Down	Plasma	64	China	HBV: 100%	178 (HD: 122, HV: 56)	D	Chen *et al*[187] 2016
miR-125b-5p	Up	Plasma	20	Turkey	HBV: 100%	74 (HD: 46, HV: 28)	D	Giray *et al*[162] 2014
miR-126	Up	Plasma	59	India	HBV: 100%	38 (HD: 20, HV: 18)	D	Ghosh *et al*[188] 2016
	Down	Serum	23	Egypt	HCV: 100%	55 (HD: 55)	D	Khairy *et al*[190] 2016
miR-128-2	Up	Serum	222	China	HBV: 87%	NA	P	Zhuang *et al*[184] 2015
miR-129	Down	Serum	23	Egypt	HCV: 100%	55 (HD: 55)	D	Khairy *et al*[190] 2016
miR-130a	Up	Serum	112	Egypt	HCV: 100%	167 (HD: 125, HV: 42)	D	Motawi *et al*[177] 2015
miR-130b	Up	Serum	153	China	HBV: 88%	59 (HD: 29, HV: 30)	D	Liu *et al*[152] 2012
miR-139	Down	Plasma	31	China	NA	31 (HD: 31)	D, P	Li *et al*[163] 2014
miR-141-3p	Up	Serum	261	China	HBV: 100%	406 (HD: 233, HV: 173)	D	Tan *et al*[166] 2014
miR-143	Up	Serum	95	China	NA	245 (HD: 118, HV: 127)	D	Zhang *et al*[168] 2014
miR-143-3p	Up	Plasma	59	India	HBV: 100%	38 (HD: 20, HV: 18)	D	Ghosh *et al*[188] 2016
miR-146a	Up	Serum	112	Egypt	HCV: 100%	167 (HD: 125, HV: 42)	D	Motawi *et al*[177] 2015

miR-150	Down	Serum	120	China	HBV: 100%	230 (HD: 110, HV: 120)	D, P	Yu *et al*[183] 2015
miR-155	Down	Serum	23	Egypt	HCV: 100%	55 (HD: 55)	D	Khairy *et al*[190] 2016
miR-181a	Down	Blood	27	China	Alcohol: 23%	81 (HD: 31, HV: 50)	D	Jiang *et al*[75] 2015
miR-181b	Up	Serum	192	Egypt	HCV: 100%	192 (HD: 192)	D	Zekr *et al*[194] 2016
miR-182	Up	Serum	103	China	NA	135 (HD: 95, HV: 40)	D, P	Chen *et al*[169] 2015
miR-192	Up	Plasma	457	China	HBV: 100%	477 (HD: 310, HV: 167)	D	Zhou *et al*[150] 2011
		Serum	112	Egypt	HCV: 100%	167 (HD: 125, HV: 42)	D	Motawi *et al*[177] 2015
miR-192-5p	Down	Serum	261	China	HBV: 100%	406 (HD: 233, HV: 173)	D	Tan *et al*[166] 2014
miR-195	Down	Serum	112	Egypt	HCV: 100%	167 (HD: 125, HV: 42)	D	Motawi *et al*[177] 2015
			20	South Korea	HBV: 70%	40 (HD: 40)	D	Sohn *et al*[179] 2015
miR-199a	Down	Serum	105	United States	HCV: 64%, HBV: 20%	178 (HD: 107, HV: 71)	D	Qu *et al*[148] 2011
			40	Egypt	HCV: 100%	60 (HD: 40, HV: 20)	D, P	El-Abd *et al*[174] 2015
			78	China	NA	156 (HV: 156)	D	Yin *et al*[182] 2015
			23	Egypt	HCV: 87%, HBV: 13%	17 (HD: 17)	D	Amr *et al*[186] 2016
miR-199a-3p	Down	Serum	192	Egypt	HCV: 100%	192 (HD: 192)	D	Zekri *et al*[194] 2016
miR-199a-5p	Down	Serum	261	China	HBV: 100%	406 (HD: 233, HV: 173)	D	Tan *et al*[166] 2014
miR-200a	Up	Serum	136	China	HBV: 95%	NA	P	Liu *et al*[176] 2015
miR-203	Down	Serum	23	Egypt	HCV: 100%	55 (HD: 55)	D	Khairy *et al*[190] 2016
miR-203a	Down	Serum	242	China	HCV: 63%	NA	P	Liu *et al*[176] 2015
miR-206	Up	Serum	261	China	HBV: 100%	406 (HD: 233, HV: 173)	D	Tan *et al*[166] 2014
miR-215	Up	Serum	95	China	NA	245 (HD: 118, HV: 127)	D	Zhang *et al*[168] 2014
miR-218	Down	Serum	156	China	HBV: 72%	162 (HD: 98, HV: 64)	D, P	Yang *et al*[193] 2016
miR-221	Up	Serum	20	South Korea	HBV: 70%	40 (HD: 40)	D	Sohn *et al*[179] 2015
			192	Egypt	HCV: 100%	192 (HD: 192)	D	Zekri *et al*[194] 2016
	Down	Serum	30	Egypt	HCV: 100%	70 (HD: 60, HV: 10)	D	El-Garem *et al*[174] 2014
miR-222	Up	Serum	70	China	HBV: 100%	72 (HD: 48, HV: 24)	D	Qi *et al*[147] 2011
			20	South Korea	HBV: 70%	40 (HD: 40)	D	Sohn *et al*[179] 2015
miR-223	Up	Serum	70	China	HBV: 100%	72 (HD: 48, HV: 24)		Qi *et al*[147] 2011
		Serum	101	China	HBV: 75%	137 (HD: 48, HV: 89)	D	Xu *et al*[149] 2011
	Down	Plasma	457	China	HBV: 100%	477 (HD: 310, HV: 167)	D	Zhou *et al*[150] 2011
		Serum	23	Egypt	HCV: 100%	55 (HD: 55)	D	Khairy *et al*[190] 2016
miR-223-3p	Down	Plasma	20	Turkey	HBV: 100%	74 (HD: 46, HV: 28)	D	Giray *et al*[162] 2014
		Serum	8	Turkey	HCV: 100%	84 (HD: 56, HV: 28)	D	Oksuz *et al*[178] 2015
miR-224	Up	Plasma	107	Japan	HCV: 41%, HBV: 18%, Alcohol: 15%	102 (HD: 27, HV: 75)	D, P, T	Okajima *et al*[192] 2016
		Serum	20	South Korea	HBV: 70%	40 (HD: 40)	D	Sohn *et al*[179] 2015
			182	China	HBV: 87%	NA	D, P	Zhuang *et al*[185] 2015
			122	China	HBV: 100%	157 (HD: 135, HV: 22)	D	Lin *et al*[191] 2016
miR-224-5p	Up	Serum	136	China	HBV: 95%	NA	P	Liu *et al*[164] 2014
miR-296	Up	Serum	112	Egypt	HCV: 100%	167 (HD: 125, HV: 42)	D	Motawi *et al*[177] 2015
miR-302c-3p	Down	Serum	8	Turkey	HCV: 100%	84 (HD: 56, HV: 28,)	D	Oksuz *et al*[178] 2015
miR-331-3p	Up	Serum	103	China	NA	135 (HD: 95, HV: 40)	D, P	Chen *et al*[169] 2015
miR-335	Down	Serum	125	China	NA	250 (HD: 125, HV: 125)	D, P	Cui *et al*[173] 2015
miR-338-5p	Up	Plasma	37	China	NA	60 (HD: 29, HV: 31)	D	Chen *et al*[170] 2015
miR-375	Up	Serum	120	China	HBV: 100%	393 (HD: 183, HV: 210)	D	Li *et al*[145] 2010,
	Down		78	China	NA	156 (HV: 156)	D	Yin *et al*[182] 2015.
miR-433-3p	Up	Serum	261	China	HBV: 100%	406 (HD: 233, HV: 173)	D	Tan *et al*[166] 2014
miR-483-5p	Up	Serum	69	United States	HCV: 63%, HBV: 14%	69 (HV: 69)	D	Shen *et al*[157] 2013
			112	China	NA	141 (HD: 56, HV: 85)	D	Zhang *et al*[158] 2013
miR-500a	Up	Serum	112	China	NA	141 (HD: 56, HV: 85)	D	Zhang *et al*[158] 2013
miR-764	Up	Plasma	37	China	NA	60 (HD: 29, HV: 31)	D	Chen *et al*[170] 2015
miR-801	Up	Plasma	457	China	HBV: 100%	477 (HD: 310, HV: 167)	D	Zhou *et al*[150] 2011
miR-885-5p	Up	Serum	46	China	HBV: 72%	105 (HD: 64, HV: 24, GC: 17)	D	Gui *et al*[146] 2011
			192	Egypt	HCV: 100%	192 (HD: 192)	D	Zekri *et al*[194] 2016
miR-1228-5p	Up	Serum	261	China	HBV: 100%	406 (HD: 233, HV: 173)	D	Tan *et al*[166] 2014
let-7b	Up	Serum	120	China	HBV: 100%	30 (DN: 30)	D	Hung *et al*[189] 2016
let-7f	Down	Serum	90	China	NA	60 (HV: 60)	D, P	Ge *et al*[161] 2014

NA: Not applicable; HV: Healthy volunteers; HD: Hepatic disease without evidence of HCC; GC: Gastric cancer; DN: Dysplastic nodule; D: Diagnostic marker; P: Prognostic marker; T: Treatment outcome marker.

who already have some risks for HCC. Recently, Zhou *et al*[150], Okusuz *et al*[178], Lin *et al*[191], and Zekri *et al*[194] defined three subgroups of healthy volunteers, with patients with chronic hepatitis and cirrhosis as controls. Most recently, Motawi *et al*[177] and our group[192] set subgroups according to fibrosis stage. To demonstrate the clinical utility for diagnosis, it is necessary to select appropriate controls.

Accumulating evidence of circulating cell-free miRNAs made clear their clinical utility as prognostic biomarker as well as a marker for the detection of HCC[184,196-205]. In terms of the two types of curative treatment, Zheng *et al*[159] demonstrated that the level of serum miR-17-5p could serve as a novel prognostic

marker for HCC patients who underwent surgical resection, and Cho *et al*[172] demonstrated that high plasma miR-122 expression was associated with poor overall survival in patients with HBV-related HCC who underwent radiofrequency ablation (RFA). In terms of the treatment for unresectable HCC, trans-arterial chemoembolization (TACE), Liu *et al*[164] demonstrated that miR-200a was the independent prognostic factor associated with survival.

Most recently, our group found that miR-224 may be an indicator of residual tumor in non-surgical treatment, such as percutaneous ablation therapy and/or TACE, although this was preliminary result because the number of cases was small[192]. Despite accumulating evidence, we should recognize that several challenges remain for clinical application. Regarding inter- and intra-individual variation, the kind of blood samples such as serum, plasma or all blood for better clinical application of miRNAs as a liquid-based biomarker, many issues should be addressed. Furthermore, it is necessary to build a consensus what molecule is suitable for clinical application.

Recent research has demonstrated that several noncoding RNAs regulate oncogenic and/or tumor-suppressive functions. PTEN[150,180], Stathmin1[150], RUNX3[152], Rho-kinase 2[164], Mcl-1[167], SOX9[167], p21/E2F5[175], FNDC3B[168], VEGF[177], TP53INP1[169], LIN28B[187], ADAM17[194], ISRE[194], CDKN1B/p27[194], CDKN1C/p57[194], TIMP3[194], HDAC4[194], and mTOR[194], have been demonstrated to have cancer-related functions, and validated as targets for specific miRNAs in the blood of patients with HCC[206]. The noncoding RNAs, such as lncRNA, snoRNA, snRNA, and piRNA, in the blood of patients with HCC remain unexplored. We hope further studies of circulating noncoding RNAs based on the knowledge of recent years in HCC will shed more light on this research field.

CONCLUSION

Blood-based molecular biomarkers, the most typical one of the so-called liquid biopsy, are promising as diagnostic, therapeutic and/or prognostic markers for HCC because researchers has got over their clinical difficulties such as anatomical reasons, invasive nature, and/or the patient's poor hepatic status. Although the clinical utility of liquid biopsy in HCC has been practically guaranteed by many research groups, there remains large variance in the results. The lack of a standardized technical approach has contributed to the lack of consensus. The techniques adopted, patient's hepatic status, sample type, storage conditions and target molecules have differed according to study groups. Thus, large-scale study, which is performed in a uniform methodology through all processes, is required. Another important reason is the etiological difference in each cohort. HCC is a marked regional clustering cancer, the background liver is different for each study group. For example, as indicated in each of the Tables, while all patients were infected with HBV in some reports from China and South Korea, all patients infected with HCV in other reports from Egypt. Their results were too biased by sample characteristics, it is desirable to be validated in another cohort before further clinical application.

The utility of the current serum biomarkers, such as AFP, AFP-L3, and proteins induced through vitamin K deficiency, and imaging modalities, such as ultrasonography, computed tomography, and gadolinium ethoxybenzyl diethylenetriamine pentaacetic acid-enhanced liver magnetic resonance imaging (GdEOB-DTPA-enhanced MRI) is far from satisfactory. What is now required is less invasive and repeatable methodology. Accumulating evidence of liquid biopsy might facilitate a more sensitive diagnosis and individualized decision-making in the duration of treatment of HCC. A challenge is how to achieve further development based on recent studies. Many issues should be addressed before these promising results can be translated into a real clinical settings.

REFERENCES

1 **Ferlay J**, Soerjomataram I, Dikshit R, Eser S, Mathers C, Rebelo M, Parkin DM, Forman D, Bray F. Cancer incidence and mortality worldwide: sources, methods and major patterns in GLOBOCAN 2012. *Int J Cancer* 2015; **136**: E359-E386 [PMID: 25220842 DOI: 10.1002/ijc.29210]

2 **Parkin DM**. The global health burden of infection-associated cancers in the year 2002. *Int J Cancer* 2006; **118**: 3030-3044 [PMID: 16404738 DOI: 10.1002/ijc.21731]

3 **Tateishi R**, Okanoue T, Fujiwara N, Okita K, Kiyosawa K, Omata M, Kumada H, Hayashi N, Koike K. Clinical characteristics, treatment, and prognosis of non-B, non-C hepatocellular carcinoma: a large retrospective multicenter cohort study. *J Gastroenterol* 2015; **50**: 350-360 [PMID: 24929638 DOI: 10.1007/s00535-014-0973-8]

4 **Calle EE**, Rodriguez C, Walker-Thurmond K, Thun MJ. Overweight, obesity, and mortality from cancer in a prospectively studied cohort of U.S. adults. *N Engl J Med* 2003; **348**: 1625-1638 [PMID: 12711737 DOI: 10.1056/NEJMoa021423]

5 **Donato F**, Tagger A, Gelatti U, Parrinello G, Boffetta P, Albertini A, Decarli A, Trevisi P, Ribero ML, Martelli C, Porru S, Nardi G. Alcohol and hepatocellular carcinoma: the effect of lifetime intake and hepatitis virus infections in men and women. *Am J Epidemiol* 2002; **155**: 323-331 [PMID: 11836196]

6 **El-Serag HB**, Tran T, Everhart JE. Diabetes increases the risk of chronic liver disease and hepatocellular carcinoma. *Gastroenterology* 2004; **126**: 460-468 [PMID: 14762783]

7 **Mayans MV**, Calvet X, Bruix J, Bruguera M, Costa J, Estève J, Bosch FX, Bru C, Rodés J. Risk factors for hepatocellular carcinoma in Catalonia, Spain. *Int J Cancer* 1990; **46**: 378-381 [PMID: 2168342]

8 **van Meer S**, de Man RA, Coenraad MJ, Sprengers D, van Nieuwkerk KM, Klümpen HJ, Jansen PL, IJzermans JN, van Oijen MG, Siersema PD, van Erpecum KJ. Surveillance for hepatocellular carcinoma is associated with increased survival: Results from a large cohort in the Netherlands. *J Hepatol* 2015; **63**: 1156-1163 [PMID: 26100498 DOI: 10.1016/j.jhep.2015.06.012]

9 **Zhang BH**, Yang BH, Tang ZY. Randomized controlled trial of screening for hepatocellular carcinoma. *J Cancer Res Clin Oncol* 2004; **130**: 417-422 [PMID: 15042359 DOI: 10.1007/s00432-004-0552-0]

10 **Llovet JM**, Di Bisceglie AM, Bruix J, Kramer BS, Lencioni R,

Zhu AX, Sherman M, Schwartz M, Lotze M, Talwalkar J, Gores GJ; Panel of Experts in HCC-Design Clinical Trials. Design and endpoints of clinical trials in hepatocellular carcinoma. *J Natl Cancer Inst* 2008; **100**: 698-711 [PMID: 18477802 DOI: 10.1093/jnci/djn134]

11 **Sterling RK**, Jeffers L, Gordon F, Venook AP, Reddy KR, Satomura S, Kanke F, Schwartz ME, Sherman M. Utility of Lens culinaris agglutinin-reactive fraction of alpha-fetoprotein and des-gamma-carboxy prothrombin, alone or in combination, as biomarkers for hepatocellular carcinoma. *Clin Gastroenterol Hepatol* 2009; **7**: 104-113 [PMID: 18849011 DOI: 10.1016/j.cgh.2008.08.041]

12 **Tateishi R**, Yoshida H, Matsuyama Y, Mine N, Kondo Y, Omata M. Diagnostic accuracy of tumor markers for hepatocellular carcinoma: a systematic review. *Hepatol Int* 2008; **2**: 17-30 [PMID: 19669276 DOI: 10.1007/s12072-007-9038-x]

13 **Yoon YJ**, Han KH, Kim DY. Role of serum prothrombin induced by vitamin K absence or antagonist-II in the early detection of hepatocellular carcinoma in patients with chronic hepatitis B virus infection. *Scand J Gastroenterol* 2009; **44**: 861-866 [PMID: 19391065 DOI: 10.1080/00365520902903034]

14 **Herman JG**, Baylin SB. Gene silencing in cancer in association with promoter hypermethylation. *N Engl J Med* 2003; **349**: 2042-2054 [PMID: 14627790 DOI: 10.1056/NEJMra023075]

15 **Yoo CB**, Jones PA. Epigenetic therapy of cancer: past, present and future. *Nat Rev Drug Discov* 2006; **5**: 37-50 [PMID: 16485345 DOI: 10.1038/nrd1930]

16 **Sharma S**, Kelly TK, Jones PA. Epigenetics in cancer. *Carcinogenesis* 2010; **31**: 27-36 [PMID: 19752007 DOI: 10.1093/carcin/bgp220]

17 **Ozen C**, Yildiz G, Dagcan AT, Cevik D, Ors A, Keles U, Topel H, Ozturk M. Genetics and epigenetics of liver cancer. *N Biotechnol* 2013; **30**: 381-384 [PMID: 23392071 DOI: 10.1016/j.nbt.2013.01.007]

18 **Coppedè F**, Lopomo A, Spisni R, Migliore L. Genetic and epigenetic biomarkers for diagnosis, prognosis and treatment of colorectal cancer. *World J Gastroenterol* 2014; **20**: 943-956 [PMID: 24574767 DOI: 10.3748/wjg.v20.i4.943]

19 **Kelley RK**, Magbanua MJ, Butler TM, Collisson EA, Hwang J, Sidiropoulos N, Evason K, McWhirter RM, Hameed B, Wayne EM, Yao FY, Venook AP, Park JW. Circulating tumor cells in hepatocellular carcinoma: a pilot study of detection, enumeration, and next-generation sequencing in cases and controls. *BMC Cancer* 2015; **15**: 206 [PMID: 25884197 DOI: 10.1186/s12885-015-1195-z]

20 **Yin CQ**, Yuan CH, Qu Z, Guan Q, Chen H, Wang FB. Liquid Biopsy of Hepatocellular Carcinoma: Circulating Tumor-Derived Biomarkers. *Dis Markers* 2016; **2016**: 1427849 [PMID: 27403030 DOI: 10.1155/2016/1427849]

21 **Schwarzenbach H**, Hoon DS, Pantel K. Cell-free nucleic acids as biomarkers in cancer patients. *Nat Rev Cancer* 2011; **11**: 426-437 [PMID: 21562580 DOI: 10.1038/nrc3066]

22 **van de Stolpe A**, Pantel K, Sleijfer S, Terstappen LW, den Toonder JM. Circulating tumor cell isolation and diagnostics: toward routine clinical use. *Cancer Res* 2011; **71**: 5955-5960 [PMID: 21896640 DOI: 10.1158/0008-5472.CAN-11-1254]

23 **Alix-Panabières C**, Pantel K. Circulating tumor cells: liquid biopsy of cancer. *Clin Chem* 2013; **59**: 110-118 [PMID: 23014601 DOI: 10.1373/clinchem.2012.194258]

24 **Crowley E**, Di Nicolantonio F, Loupakis F, Bardelli A. Liquid biopsy: monitoring cancer-genetics in the blood. *Nat Rev Clin Oncol* 2013; **10**: 472-484 [PMID: 23836314 DOI: 10.1038/nrclinonc.2013.110]

25 **Ashworth TR**. A case of cancer in which cells similar to those in the tumours were seen in the blood after death. *Aust Med J* 1869; **14**: 146-149

26 **Miller MC**, Doyle GV, Terstappen LW. Significance of Circulating Tumor Cells Detected by the CellSearch System in Patients with Metastatic Breast Colorectal and Prostate Cancer. *J Oncol* 2010; **2010**: 617421 [PMID: 20016752 DOI: 10.1155/2010/617421]

27 **Fidler IJ**. Metastasis: quantitative analysis of distribution and fate of tumor emboli labeled with 125 I-5-iodo-2'-deoxyuridine. *J Natl Cancer Inst* 1970; **45**: 773-782 [PMID: 5513503]

28 **O'Flaherty JD**, Gray S, Richard D, Fennell D, O'Leary JJ, Blackhall FH, O'Byrne KJ. Circulating tumour cells, their role in metastasis and their clinical utility in lung cancer. *Lung Cancer* 2012; **76**: 19-25 [PMID: 22209049 DOI: 10.1016/j.lungcan.2011.10.018]

29 **Luzzi KJ**, MacDonald IC, Schmidt EE, Kerkvliet N, Morris VL, Chambers AF, Groom AC. Multistep nature of metastatic inefficiency: dormancy of solitary cells after successful extravasation and limited survival of early micrometastases. *Am J Pathol* 1998; **153**: 865-873 [PMID: 9736035 DOI: 10.1016/s0002-9440(10)65628-3]

30 **Allard WJ**, Matera J, Miller MC, Repollet M, Connelly MC, Rao C, Tibbe AG, Uhr JW, Terstappen LW. Tumor cells circulate in the peripheral blood of all major carcinomas but not in healthy subjects or patients with nonmalignant diseases. *Clin Cancer Res* 2004; **10**: 6897-6904 [PMID: 15501967 DOI: 10.1158/1078-0432.ccr-04-0378]

31 **Vona G**, Estepa L, Béroud C, Damotte D, Capron F, Nalpas B, Mineur A, Franco D, Lacour B, Pol S, Bréchot C, Paterlini-Bréchot P. Impact of cytomorphological detection of circulating tumor cells in patients with liver cancer. *Hepatology* 2004; **39**: 792-797 [PMID: 14999698 DOI: 10.1002/hep.20091]

32 **Vona G**, Sabile A, Louha M, Sitruk V, Romana S, Schütze K, Capron F, Franco D, Pazzagli M, Vekemans M, Lacour B, Bréchot C, Paterlini-Bréchot P. Isolation by size of epithelial tumor cells: a new method for the immunomorphological and molecular characterization of circulatingtumor cells. *Am J Pathol* 2000; **156**: 57-63 [PMID: 10623654 DOI: 10.1016/s0002-9440(10)64706-2]

33 **Zheng S**, Lin H, Liu JQ, Balic M, Datar R, Cote RJ, Tai YC. Membrane microfilter device for selective capture, electrolysis and genomic analysis of human circulating tumor cells. *J Chromatogr A* 2007; **1162**: 154-161 [PMID: 17561026 DOI: 10.1016/j.chroma.2007.05.064]

34 **Coumans FA**, van Dalum G, Beck M, Terstappen LW. Filter characteristics influencing circulating tumor cell enrichment from whole blood. *PLoS One* 2013; **8**: e61770 [PMID: 23626725 DOI: 10.1371/journal.pone.0061770]

35 **Coumans FA**, van Dalum G, Beck M, Terstappen LW. Filtration parameters influencing circulating tumor cell enrichment from whole blood. *PLoS One* 2013; **8**: e61774 [PMID: 23658615 DOI: 10.1371/journal.pone.0061774]

36 **Marrinucci D**, Bethel K, Bruce RH, Curry DN, Hsieh B, Humphrey M, Krivacic RT, Kroener J, Kroener L, Ladanyi A, Lazarus NH, Nieva J, Kuhn P. Case study of the morphologic variation of circulating tumor cells. *Hum Pathol* 2007; **38**: 514-519 [PMID: 17188328 DOI: 10.1016/j.humpath.2006.08.027]

37 **Mohamed H**, Murray M, Turner JN, Caggana M. Isolation of tumor cells using size and deformation. *J Chromatogr A* 2009; **1216**: 8289-8295 [PMID: 19497576 DOI: 10.1016/j.chroma.2009.05.036]

38 **Tan SJ**, Yobas L, Lee GY, Ong CN, Lim CT. Microdevice for the isolation and enumeration of cancer cells from blood. *Biomed Microdevices* 2009; **11**: 883-892 [PMID: 19387837 DOI: 10.1007/s10544-009-9305-9]

39 **Krebs MG**, Metcalf RL, Carter L, Brady G, Blackhall FH, Dive C. Molecular analysis of circulating tumour cells-biology and biomarkers. *Nat Rev Clin Oncol* 2014; **11**: 129-144 [PMID: 24445517 DOI: 10.1038/nrclinonc.2013.253]

40 **Cristofanilli M**, Budd GT, Ellis MJ, Stopeck A, Matera J, Miller MC, Reuben JM, Doyle GV, Allard WJ, Terstappen LW, Hayes DF. Circulating tumor cells, disease progression, and survival in metastatic breast cancer. *N Engl J Med* 2004; **351**: 781-791 [PMID: 15317891 DOI: 10.1056/NEJMoa040766]

41 **Danila DC**, Heller G, Gignac GA, Gonzalez-Espinoza R, Anand A, Tanaka E, Lilja H, Schwartz L, Larson S, Fleisher M, Scher HI. Circulating tumor cell number and prognosis in progressive castration-resistant prostate cancer. *Clin Cancer Res* 2007;

13: 7053-7058 [PMID: 18056182 DOI: 10.1158/1078-0432.ccr-07-1506]
42 **Hayes DF**, Cristofanilli M, Budd GT, Ellis MJ, Stopeck A, Miller MC, Matera J, Allard WJ, Doyle GV, Terstappen LW. Circulating tumor cells at each follow-up time point during therapy of metastatic breast cancer patients predict progression-free and overall survival. *Clin Cancer Res* 2006; **12**: 4218-4224 [PMID: 16857794 DOI: 10.1158/1078-0432.ccr-05-2821]
43 **Riethdorf S**, Fritsche H, Müller V, Rau T, Schindlbeck C, Rack B, Janni W, Coith C, Beck K, Jänicke F, Jackson S, Gornet T, Cristofanilli M, Pantel K. Detection of circulating tumor cells in peripheral blood of patients with metastatic breast cancer: a validation study of the CellSearch system. *Clin Cancer Res* 2007; **13**: 920-928 [PMID: 17289886 DOI: 10.1158/1078-0432.ccr-06-1695]
44 **Sastre J**, Maestro ML, Puente J, Veganzones S, Alfonso R, Rafael S, García-Saenz JA, Vidaurreta M, Martín M, Arroyo M, Sanz-Casla MT, Díaz-Rubio E. Circulating tumor cells in colorectal cancer: correlation with clinical and pathological variables. *Ann Oncol* 2008; **19**: 935-938 [PMID: 18212090 DOI: 10.1093/annonc/mdm583]
45 **Shaffer DR**, Leversha MA, Danila DC, Lin O, Gonzalez-Espinoza R, Gu B, Anand A, Smith K, Maslak P, Doyle GV, Terstappen LW, Lilja H, Heller G, Fleisher M, Scher HI. Circulating tumor cell analysis in patients with progressive castration-resistant prostate cancer. *Clin Cancer Res* 2007; **13**: 2023-2029 [PMID: 17404082 DOI: 10.1158/1078-0432.ccr-06-2701]
46 **Nagrath S**, Sequist LV, Maheswaran S, Bell DW, Irimia D, Ulkus L, Smith MR, Kwak EL, Digumarthy S, Muzikansky A, Ryan P, Balis UJ, Tompkins RG, Haber DA, Toner M. Isolation of rare circulating tumour cells in cancer patients by microchip technology. *Nature* 2007; **450**: 1235-1239 [PMID: 18097410 DOI: 10.1038/nature06385]
47 **Stott SL**, Hsu CH, Tsukrov DI, Yu M, Miyamoto DT, Waltman BA, Rothenberg SM, Shah AM, Smas ME, Korir GK, Floyd FP, Gilman AJ, Lord JB, Winokur D, Springer S, Irimia D, Nagrath S, Sequist LV, Lee RJ, Isselbacher KJ, Maheswaran S, Haber DA, Toner M. Isolation of circulating tumor cells using a microvortex-generating herringbone-chip. *Proc Natl Acad Sci USA* 2010; **107**: 18392-18397 [PMID: 20930119 DOI: 10.1073/pnas.1012539107]
48 **Saucedo-Zeni N**, Mewes S, Niestroj R, Gasiorowski L, Murawa D, Nowaczyk P, Tomasi T, Weber E, Dworacki G, Morgenthaler NG, Jansen H, Propping C, Sterzynska K, Dyszkiewicz W, Zabel M, Kiechle M, Reuning U, Schmitt M, Lücke K. A novel method for the in vivo isolation of circulating tumor cells from peripheral blood of cancer patients using a functionalized and structured medical wire. *Int J Oncol* 2012; **41**: 1241-1250 [PMID: 22825490 DOI: 10.3892/ijo.2012.1557]
49 **Lustberg MB**, Balasubramanian P, Miller B, Garcia-Villa A, Deighan C, Wu Y, Carothers S, Berger M, Ramaswamy B, Macrae ER, Wesolowski R, Layman RM, Mrozek E, Pan X, Summers TA, Shapiro CL, Chalmers JJ. Heterogeneous atypical cell populations are present in blood of metastatic breast cancer patients. *Breast Cancer Res* 2014; **16**: R23 [PMID: 24602188 DOI: 10.1186/bcr3622]
50 **Pantel K**, Alix-Panabières C, Riethdorf S. Cancer micrometastases. *Nat Rev Clin Oncol* 2009; **6**: 339-351 [PMID: 19399023 DOI: 10.1038/nrclinonc.2009.44]
51 **Matsumura M**, Shiratori Y, Niwa Y, Tanaka T, Ogura K, Okudaira T, Imamura M, Okano K, Shiina S, Omata M. Presence of alpha-fetoprotein mRNA in blood correlates with outcome in patients with hepatocellular carcinoma. *J Hepatol* 1999; **31**: 332-339 [PMID: 10453948]
52 **Cillo U**, Navaglia F, Vitale A, Molari A, Basso D, Bassanello M, Brolese A, Zanus G, Montin U, D'Amico F, Ciarleglio FA, Carraro A, Bridda A, Burra P, Carraro P, Plebani M, D'Amico DF. Clinical significance of alpha-fetoprotein mRNA in blood of patients with hepatocellular carcinoma. *Clin Chim Acta* 2004; **347**: 129-138 [PMID: 15313150 DOI: 10.1016/j.cccn.2004.04.032]
53 **Jeng KS**, Sheen IS, Tsai YC. Does the presence of circulating hepatocellular carcinoma cells indicate a risk of recurrence after resection? *Am J Gastroenterol* 2004; **99**: 1503-1509 [PMID: 15307868 DOI: 10.1111/j.1572-0241.2004.30227.x]
54 **Lemoine A**, Le Bricon T, Salvucci M, Azoulay D, Pham P, Raccuia J, Bismuth H, Debuire B. Prospective evaluation of circulating hepatocytes by alpha-fetoprotein mRNA in humans during liver surgery. *Ann Surg* 1997; **226**: 43-50 [PMID: 9242336]
55 **Witzigmann H**, Geissler F, Benedix F, Thiery J, Uhlmann D, Tannapfel A, Wittekind C, Hauss J. Prospective evaluation of circulating hepatocytes by alpha-fetoprotein messenger RNA in patients with hepatocellular carcinoma. *Surgery* 2002; **131**: 34-43 [PMID: 11812961]
56 **Mou DC**, Cai SL, Peng JR, Wang Y, Chen HS, Pang XW, Leng XS, Chen WF. Evaluation of MAGE-1 and MAGE-3 as tumour-specific markers to detect blood dissemination of hepatocellular carcinoma cells. *Br J Cancer* 2002; **86**: 110-116 [PMID: 11857021 DOI: 10.1038/sj.bjc.6600016]
57 **Yao M**, Yao DF, Bian YZ, Wu W, Yan XD, Yu DD, Qiu LW, Yang JL, Zhang HJ, Sai WL, Chen J. Values of circulating GPC-3 mRNA and alpha-fetoprotein in detecting patients with hepatocellular carcinoma. *Hepatobiliary Pancreat Dis Int* 2013; **12**: 171-179 [PMID: 23558072]
58 **Choi GH**, Kim GI, Yoo JE, Na DC, Han DH, Roh YH, Park YN, Choi JS. Increased Expression of Circulating Cancer Stem Cell Markers During the Perioperative Period Predicts Early Recurrence After Curative Resection of Hepatocellular Carcinoma. *Ann Surg Oncol* 2015; **22** Suppl 3: S1444-S1452 [PMID: 25791790 DOI: 10.1245/s10434-015-4480-9]
59 **Kong SY**, Park JW, Kim JO, Lee NO, Lee JA, Park KW, Hong EK, Kim CM. Alpha-fetoprotein and human telomerase reverse transcriptase mRNA levels in peripheral blood of patients with hepatocellular carcinoma. *J Cancer Res Clin Oncol* 2009; **135**: 1091-1098 [PMID: 19184104 DOI: 10.1007/s00432-009-0549-9]
60 **Chen CH**, Huang GT, Lee HS, Yang PM, Yan MD, Chen DS, Sheu JC. High frequency of expression of MAGE genes in human hepatocellular carcinoma. *Liver* 1999; **19**: 110-114 [PMID: 10220740]
61 **Filmus J**, Capurro M. The role of glypican-3 in the regulation of body size and cancer. *Cell Cycle* 2008; **7**: 2787-2790 [PMID: 18787398 DOI: 10.4161/cc.7.18.6672]
62 **Chiba T**, Kita K, Zheng YW, Yokosuka O, Saisho H, Iwama A, Nakauchi H, Taniguchi H. Side population purified from hepatocellular carcinoma cells harbors cancer stem cell-like properties. *Hepatology* 2006; **44**: 240-251 [PMID: 16799977 DOI: 10.1002/hep.21227]
63 **Kim H**, Choi GH, Na DC, Ahn EY, Kim GI, Lee JE, Cho JY, Yoo JE, Choi JS, Park YN. Human hepatocellular carcinomas with "Stemness"-related marker expression: keratin 19 expression and a poor prognosis. *Hepatology* 2011; **54**: 1707-1717 [PMID: 22045674 DOI: 10.1002/hep.24559]
64 **Yang ZF**, Ho DW, Ng MN, Lau CK, Yu WC, Ngai P, Chu PW, Lam CT, Poon RT, Fan ST. Significance of CD90+ cancer stem cells in human liver cancer. *Cancer Cell* 2008; **13**: 153-166 [PMID: 18242515 DOI: 10.1016/j.ccr.2008.01.013]
65 **Yin S**, Li J, Hu C, Chen X, Yao M, Yan M, Jiang G, Ge C, Xie H, Wan D, Yang S, Zheng S, Gu J. CD133 positive hepatocellular carcinoma cells possess high capacity for tumorigenicity. *Int J Cancer* 2007; **120**: 1444-1450 [PMID: 17205516 DOI: 10.1002/ijc.22476]
66 **Miura N**, Maeda Y, Kanbe T, Yazama H, Takeda Y, Sato R, Tsukamoto T, Sato E, Marumoto A, Harada T, Sano A, Kishimoto Y, Hirooka Y, Murawaki Y, Hasegawa J, Shiota G. Serum human telomerase reverse transcriptase messenger RNA as a novel tumor marker for hepatocellular carcinoma. *Clin Cancer Res* 2005; **11**: 3205-3209 [PMID: 15867214 DOI: 10.1158/1078-0432.ccr-04-1487]
67 **Liu S**, Li N, Yu X, Xiao X, Cheng K, Hu J, Wang J, Zhang D, Cheng S, Liu S. Expression of intercellular adhesion molecule 1 by hepatocellular carcinoma stem cells and circulating tumor cells. *Gastroenterology* 2013; **144**: 1031-1041.e10 [PMID: 23376424

DOI: 10.1053/j.gastro.2013.01.046]
68 **Bahnassy AA**, Zekri AR, El-Bastawisy A, Fawzy A, Shetta M, Hussein N, Omran D, Ahmed AA, El-Labbody SS. Circulating tumor and cancer stem cells in hepatitis C virus-associated liver disease. *World J Gastroenterol* 2014; **20**: 18240-18248 [PMID: 25561791 DOI: 10.3748/wjg.v20.i48.18240]
69 **Fan ST**, Yang ZF, Ho DW, Ng MN, Yu WC, Wong J. Prediction of posthepatectomy recurrence of hepatocellular carcinoma by circulating cancer stem cells: a prospective study. *Ann Surg* 2011; **254**: 569-576 [PMID: 21892074 DOI: 10.1097/SLA.0b013e3182300a1d]
70 **Xu W**, Cao L, Chen L, Li J, Zhang XF, Qian HH, Kang XY, Zhang Y, Liao J, Shi LH, Yang YF, Wu MC, Yin ZF. Isolation of circulating tumor cells in patients with hepatocellular carcinoma using a novel cell separation strategy. *Clin Cancer Res* 2011; **17**: 3783-3793 [PMID: 21527564 DOI: 10.1158/1078-0432.CCR-10-0498]
71 **Li YM**, Xu SC, Li J, Han KQ, Pi HF, Zheng L, Zuo GH, Huang XB, Li HY, Zhao HZ, Yu ZP, Zhou Z, Liang P. Epithelial-mesenchymal transition markers expressed in circulating tumor cells in hepatocellular carcinoma patients with different stages of disease. *Cell Death Dis* 2013; **4**: e831 [PMID: 24091674 DOI: 10.1038/cddis.2013.347]
72 **Schulze K**, Gasch C, Staufer K, Nashan B, Lohse AW, Pantel K, Riethdorf S, Wege H. Presence of EpCAM-positive circulating tumor cells as biomarker for systemic disease strongly correlates to survival in patients with hepatocellular carcinoma. *Int J Cancer* 2013; **133**: 2165-2171 [PMID: 23616258 DOI: 10.1002/ijc.28230]
73 **Sun YF**, Xu Y, Yang XR, Guo W, Zhang X, Qiu SJ, Shi RY, Hu B, Zhou J, Fan J. Circulating stem cell-like epithelial cell adhesion molecule-positive tumor cells indicate poor prognosis of hepatocellular carcinoma after curative resection. *Hepatology* 2013; **57**: 1458-1468 [PMID: 23175471 DOI: 10.1002/hep.26151]
74 **Fang ZT**, Zhang W, Wang GZ, Zhou B, Yang GW, Qu XD, Liu R, Qian S, Zhu L, Liu LX, Wang JH. Circulating tumor cells in the central and peripheral venous compartment - assessing hematogenous dissemination after transarterial chemoembolization of hepatocellular carcinoma. *Onco Targets Ther* 2014; **7**: 1311-1318 [PMID: 25071374 DOI: 10.2147/OTT.S62605]
75 **Guo W**, Yang XR, Sun YF, Shen MN, Ma XL, Wu J, Zhang CY, Zhou Y, Xu Y, Hu B, Zhang X, Zhou J, Fan J. Clinical significance of EpCAM mRNA-positive circulating tumor cells in hepatocellular carcinoma by an optimized negative enrichment and qRT-PCR-based platform. *Clin Cancer Res* 2014; **20**: 4794-4805 [PMID: 25009297 DOI: 10.1158/1078-0432.CCR-14-0251]
76 **Li J**, Chen L, Zhang X, Zhang Y, Liu H, Sun B, Zhao L, Ge N, Qian H, Yang Y, Wu M, Yin Z. Detection of circulating tumor cells in hepatocellular carcinoma using antibodies against asialoglycoprotein receptor, carbamoyl phosphate synthetase 1 and pan-cytokeratin. *PLoS One* 2014; **9**: e96185 [PMID: 24763545 DOI: 10.1371/journal.pone.0096185]
77 **Morris KL**, Tugwood JD, Khoja L, Lancashire M, Sloane R, Burt D, Shenjere P, Zhou C, Hodgson C, Ohtomo T, Katoh A, Ishiguro T, Valle JW, Dive C. Circulating biomarkers in hepatocellular carcinoma. *Cancer Chemother Pharmacol* 2014; **74**: 323-332 [PMID: 24923562 DOI: 10.1007/s00280-014-2508-7]
78 **Mu H**, Lin KX, Zhao H, Xing S, Li C, Liu F, Lu HZ, Zhang Z, Sun YL, Yan XY, Cai JQ, Zhao XH. Identification of biomarkers for hepatocellular carcinoma by semiquantitative immunocytochemistry. *World J Gastroenterol* 2014; **20**: 5826-5838 [PMID: 24914343 DOI: 10.3748/wjg.v20.i19.5826]
79 **Wang S**, Zhang C, Wang G, Cheng B, Wang Y, Chen F, Chen Y, Feng M, Xiong B. Aptamer-Mediated Transparent-Biocompatible Nanostructured Surfaces for Hepotocellular Circulating Tumor Cells Enrichment. *Theranostics* 2016; **6**: 1877-1886 [PMID: 27570557 DOI: 10.7150/thno.15284]
80 **Mandel P**, Metais P. [Not Available]. *C R Seances Soc Biol Fil* 1948; **142**: 241-243 [PMID: 18875018]
81 **Leon SA**, Shapiro B, Sklaroff DM, Yaros MJ. Free DNA in the serum of cancer patients and the effect of therapy. *Cancer Res* 1977; **37**: 646-650 [PMID: 837366]
82 **Vasioukhin V**, Anker P, Maurice P, Lyautey J, Lederrey C, Stroun M. Point mutations of the N-ras gene in the blood plasma DNA of patients with myelodysplastic syndrome or acute myelogenous leukaemia. *Br J Haematol* 1994; **86**: 774-779 [PMID: 7918071]
83 **Cachia PG**, Taylor C, Thompson PW, Tennant GB, Masters G, Pettersson T, Whittaker JA, Burnett AK, Jacobs A, Padua RA. Non-dysplastic myelodysplasia? *Leukemia* 1994; **8**: 677-681 [PMID: 8152265]
84 **Sorenson GD**, Pribish DM, Valone FH, Memoli VA, Bzik DJ, Yao SL. Soluble normal and mutated DNA sequences from single-copy genes in human blood. *Cancer Epidemiol Biomarkers Prev* 1994; **3**: 67-71 [PMID: 8118388]
85 **Kopreski MS**, Benko FA, Kwak LW, Gocke CD. Detection of tumor messenger RNA in the serum of patients with malignant melanoma. *Clin Cancer Res* 1999; **5**: 1961-1965 [PMID: 10473072]
86 **Lo KW**, Lo YM, Leung SF, Tsang YS, Chan LY, Johnson PJ, Hjelm NM, Lee JC, Huang DP. Analysis of cell-free Epstein-Barr virus associated RNA in the plasma of patients with nasopharyngeal carcinoma. *Clin Chem* 1999; **45**: 1292-1294 [PMID: 10430801]
87 **Dasí F**, Martínez-Rodes P, March JA, Santamaría J, Martínez-Javaloyas JM, Gil M, Aliño SF. Real-time quantification of human telomerase reverse transcriptase mRNA in the plasma of patients with prostate cancer. *Ann N Y Acad Sci* 2006; **1075**: 204-210 [PMID: 17108213 DOI: 10.1196/annals.1368.028]
88 **Chen XQ**, Bonnefoi H, Pelte MF, Lyautey J, Lederrey C, Movarekhi S, Schaeffer P, Mulcahy HE, Meyer P, Stroun M, Anker P. Telomerase RNA as a detection marker in the serum of breast cancer patients. *Clin Cancer Res* 2000; **6**: 3823-3826 [PMID: 11051224]
89 **Silva JM**, Rodriguez R, Garcia JM, Muñoz C, Silva J, Dominguez G, Provencio M, España P, Bonilla F. Detection of epithelial tumour RNA in the plasma of colon cancer patients is associated with advanced stages and circulating tumour cells. *Gut* 2002; **50**: 530-534 [PMID: 11889075]
90 **Mitchell PS**, Parkin RK, Kroh EM, Fritz BR, Wyman SK, Pogosova-Agadjanyan EL, Peterson A, Noteboom J, O'Briant KC, Allen A, Lin DW, Urban N, Drescher CW, Knudsen BS, Stirewalt DL, Gentleman R, Vessella RL, Nelson PS, Martin DB, Tewari M. Circulating microRNAs as stable blood-based markers for cancer detection. *Proc Natl Acad Sci USA* 2008; **105**: 10513-10518 [PMID: 18663219 DOI: 10.1073/pnas.0804549105]
91 **Liao W**, Mao Y, Ge P, Yang H, Xu H, Lu X, Sang X, Zhong S. Value of quantitative and qualitative analyses of circulating cell-free DNA as diagnostic tools for hepatocellular carcinoma: a meta-analysis. *Medicine* (Baltimore) 2015; **94**: e722 [PMID: 25860220 DOI: 10.1097/MD.0000000000000722]
92 **Diehl F**, Li M, Dressman D, He Y, Shen D, Szabo S, Diaz LA, Goodman SN, David KA, Juhl H, Kinzler KW, Vogelstein B. Detection and quantification of mutations in the plasma of patients with colorectal tumors. *Proc Natl Acad Sci USA* 2005; **102**: 16368-16373 [PMID: 16258065 DOI: 10.1073/pnas.0507904102]
93 **van 't Veer LJ**, Dai H, van de Vijver MJ, He YD, Hart AA, Mao M, Peterse HL, van der Kooy K, Marton MJ, Witteveen AT, Schreiber GJ, Kerkhoven RM, Roberts C, Linsley PS, Bernards R, Friend SH. Gene expression profiling predicts clinical outcome of breast cancer. *Nature* 2002; **415**: 530-536 [PMID: 11823860 DOI: 10.1038/415530a]
94 **Dawson SJ**, Tsui DW, Murtaza M, Biggs H, Rueda OM, Chin SF, Dunning MJ, Gale D, Forshew T, Mahler-Araujo B, Rajan S, Humphray S, Becq J, Halsall D, Wallis M, Bentley D, Caldas C, Rosenfeld N. Analysis of circulating tumor DNA to monitor metastatic breast cancer. *N Engl J Med* 2013; **368**: 1199-1209 [PMID: 23484797 DOI: 10.1056/NEJMoa1213261]
95 **Chan KC**, Jiang P, Zheng YW, Liao GJ, Sun H, Wong J, Siu SS, Chan WC, Chan SL, Chan AT, Lai PB, Chiu RW, Lo YM. Cancer genome scanning in plasma: detection of tumor-associated copy number aberrations, single-nucleotide variants, and tumoral heterogeneity by massively parallel sequencing.

Clin Chem 2013; **59**: 211-224 [PMID: 23065472 DOI: 10.1373/clinchem.2012.196014]

96 **Iizuka N**, Sakaida I, Moribe T, Fujita N, Miura T, Stark M, Tamatsukuri S, Ishitsuka H, Uchida K, Terai S, Sakamoto K, Tamesa T, Oka M. Elevated levels of circulating cell-free DNA in the blood of patients with hepatitis C virus-associated hepatocellular carcinoma. *Anticancer Res* 2006; **26**: 4713-4719 [PMID: 17214331]

97 **Ren N**, Qin LX, Tu H, Liu YK, Zhang BH, Tang ZY. The prognostic value of circulating plasma DNA level and its allelic imbalance on chromosome 8p in patients with hepatocellular carcinoma. *J Cancer Res Clin Oncol* 2006; **132**: 399-407 [PMID: 16502316 DOI: 10.1007/s00432-005-0049-5]

98 **Yang YJ**, Chen H, Huang P, Li CH, Dong ZH, Hou YL. Quantification of plasma hTERT DNA in hepatocellular carcinoma patients by quantitative fluorescent polymerase chain reaction. *Clin Invest Med* 2011; **34**: E238 [PMID: 21810382]

99 **Chen H**, Sun LY, Zheng HQ, Zhang QF, Jin XM. Total serum DNA and DNA integrity: diagnostic value in patients with hepatitis B virus-related hepatocellular carcinoma. *Pathology* 2012; **44**: 318-324 [PMID: 22531347 DOI: 10.1097/PAT.0b013e328353a24c]

100 **Huang Z**, Hua D, Hu Y, Cheng Z, Zhou X, Xie Q, Wang Q, Wang F, Du X, Zeng Y. Quantitation of plasma circulating DNA using quantitative PCR for the detection of hepatocellular carcinoma. *Pathol Oncol Res* 2012; **18**: 271-276 [PMID: 21779787 DOI: 10.1007/s12253-011-9438-z]

101 **Chen K**, Zhang H, Zhang LN, Ju SQ, Qi J, Huang DF, Li F, Wei Q, Zhang J. Value of circulating cell-free DNA in diagnosis of hepatocelluar carcinoma. *World J Gastroenterol* 2013; **19**: 3143-3149 [PMID: 23716996 DOI: 10.3748/wjg.v19.i20.3143]

102 **Piciocchi M**, Cardin R, Vitale A, Vanin V, Giacomin A, Pozzan C, Maddalo G, Cillo U, Guido M, Farinati F. Circulating free DNA in the progression of liver damage to hepatocellular carcinoma. *Hepatol Int* 2013; **7**: 1050-1057 [PMID: 26202034 DOI: 10.1007/s12072-013-9481-9]

103 **Szymańska K**, Chen JG, Cui Y, Gong YY, Turner PC, Villar S, Wild CP, Parkin DM, Hainaut P. TP53 R249S mutations, exposure to aflatoxin, and occurrence of hepatocellular carcinoma in a cohort of chronic hepatitis B virus carriers from Qidong, China. *Cancer Epidemiol Biomarkers Prev* 2009; **18**: 1638-1643 [PMID: 19366907 DOI: 10.1158/1055-9965.EPI-08-1102]

104 **Jiang P**, Chan CW, Chan KC, Cheng SH, Wong J, Wong VW, Wong GL, Chan SL, Mok TS, Chan HL, Lai PB, Chiu RW, Lo YM. Lengthening and shortening of plasma DNA in hepatocellular carcinoma patients. *Proc Natl Acad Sci USA* 2015; **112**: E1317-E1325 [PMID: 25646427 DOI: 10.1073/pnas.1500076112]

105 **Wong IH**, Lo YM, Yeo W, Lau WY, Johnson PJ. Frequent p15 promoter methylation in tumor and peripheral blood from hepatocellular carcinoma patients. *Clin Cancer Res* 2000; **6**: 3516-3521 [PMID: 10999738]

106 **Jones PA**, Baylin SB. The fundamental role of epigenetic events in cancer. *Nat Rev Genet* 2002; **3**: 415-428 [PMID: 12042769 DOI: 10.1038/nrg816]

107 **Jones PA**, Baylin SB. The epigenomics of cancer. *Cell* 2007; **128**: 683-692 [PMID: 17320506 DOI: 10.1016/j.cell.2007.01.029]

108 **Wong IH**, Zhang J, Lai PB, Lau WY, Lo YM. Quantitative analysis of tumor-derived methylated p16INK4a sequences in plasma, serum, and blood cells of hepatocellular carcinoma patients. *Clin Cancer Res* 2003; **9**: 1047-1052 [PMID: 12631605]

109 **Chu HJ**, Heo J, Seo SB, Kim GH, Kang DH, Song GA, Cho M, Yang US. Detection of aberrant p16INK4A methylation in sera of patients with liver cirrhosis and hepatocellular carcinoma. *J Korean Med Sci* 2004; **19**: 83-86 [PMID: 14966347 DOI: 10.3346/jkms.2004.19.1.83]

110 **Yeo W**, Wong N, Wong WL, Lai PB, Zhong S, Johnson PJ. High frequency of promoter hypermethylation of RASSF1A in tumor and plasma of patients with hepatocellular carcinoma. *Liver Int* 2005; **25**: 266-272 [PMID: 15780049 DOI: 10.1111/j.1478-3231.2005.01084.x]

111 **Tan SH**, Ida H, Lau QC, Goh BC, Chieng WS, Loh M, Ito Y. Detection of promoter hypermethylation in serum samples of cancer patients by methylation-specific polymerase chain reaction for tumour suppressor genes including RUNX3. *Oncol Rep* 2007; **18**: 1225-1230 [PMID: 17914577]

112 **Zhang YJ**, Wu HC, Shen J, Ahsan H, Tsai WY, Yang HI, Wang LY, Chen SY, Chen CJ, Santella RM. Predicting hepatocellular carcinoma by detection of aberrant promoter methylation in serum DNA. *Clin Cancer Res* 2007; **13**: 2378-2384 [PMID: 17438096 DOI: 10.1158/1078-0432.ccr-06-1900]

113 **Chan KC**, Lai PB, Mok TS, Chan HL, Ding C, Yeung SW, Lo YM. Quantitative analysis of circulating methylated DNA as a biomarker for hepatocellular carcinoma. *Clin Chem* 2008; **54**: 1528-1536 [PMID: 18653827 DOI: 10.1373/clinchem.2008.104653]

114 **Chang H**, Yi B, Li L, Zhang HY, Sun F, Dong SQ, Cao Y. Methylation of tumor associated genes in tissue and plasma samples from liver disease patients. *Exp Mol Pathol* 2008; **85**: 96-100 [PMID: 18691570 DOI: 10.1016/j.yexmp.2008.07.001]

115 **Iyer P**, Zekri AR, Hung CW, Schiefelbein E, Ismail K, Hablas A, Seifeldin IA, Soliman AS. Concordance of DNA methylation pattern in plasma and tumor DNA of Egyptian hepatocellular carcinoma patients. *Exp Mol Pathol* 2010; **88**: 107-111 [PMID: 19818350 DOI: 10.1016/j.yexmp.2009.09.012]

116 **Huang ZH**, Hu Y, Hua D, Wu YY, Song MX, Cheng ZH. Quantitative analysis of multiple methylated genes in plasma for the diagnosis and prognosis of hepatocellular carcinoma. *Exp Mol Pathol* 2011; **91**: 702-707 [PMID: 21884695 DOI: 10.1016/j.yexmp.2011.08.004]

117 **Iizuka N**, Oka M, Sakaida I, Moribe T, Miura T, Kimura N, Tamatsukuri S, Ishitsuka H, Uchida K, Terai S, Yamashita S, Okita K, Sakata K, Karino Y, Toyota J, Ando E, Ide T, Sata M, Tsunedomi R, Tsutsui M, Iida M, Tokuhisa Y, Sakamoto K, Tamesa T, Fujita Y, Hamamoto Y. Efficient detection of hepatocellular carcinoma by a hybrid blood test of epigenetic and classical protein markers. *Clin Chim Acta* 2011; **412**: 152-158 [PMID: 20883676 DOI: 10.1016/j.cca.2010.09.028]

118 **Mohamed NA**, Swify EM, Amin NF, Soliman MM, Tag-Eldin LM, Elsherbiny NM. Is serum level of methylated RASSF1A valuable in diagnosing hepatocellular carcinoma in patients with chronic viral hepatitis C? *Arab J Gastroenterol* 2012; **13**: 111-115 [PMID: 23122451 DOI: 10.1016/j.ajg.2012.06.009]

119 **Sun FK**, Fan YC, Zhao J, Zhang F, Gao S, Zhao ZH, Sun Q, Wang K. Detection of TFPI2 methylation in the serum of hepatocellular carcinoma patients. *Dig Dis Sci* 2013; **58**: 1010-1015 [PMID: 23108564 DOI: 10.1007/s10620-012-2462-3]

120 **Zhang P**, Wen X, Gu F, Deng X, Li J, Dong J, Jiao J, Tian Y. Methylation profiling of serum DNA from hepatocellular carcinoma patients using an Infinium Human Methylation 450 BeadChip. *Hepatol Int* 2013; **7**: 893-900 [PMID: 26201927 DOI: 10.1007/s12072-013-9437-0]

121 **Han LY**, Fan YC, Mu NN, Gao S, Li F, Ji XF, Dou CY, Wang K. Aberrant DNA methylation of G-protein-coupled bile acid receptor Gpbar1 (TGR5) is a potential biomarker for hepatitis B Virus associated hepatocellular carcinoma. *Int J Med Sci* 2014; **11**: 164-171 [PMID: 24465162 DOI: 10.7150/ijms.6745]

122 **Huang G**, Krocker JD, Kirk JL, Merwat SN, Ju H, Soloway RD, Wieck LR, Li A, Okorodudu AO, Petersen JR, Abdulla NE, Duchini A, Cicalese L, Rastellini C, Hu PC, Dong J. Evaluation of INK4A promoter methylation using pyrosequencing and circulating cell-free DNA from patients with hepatocellular carcinoma. *Clin Chem Lab Med* 2014; **52**: 899-909 [PMID: 24406287 DOI: 10.1515/cclm-2013-0885]

123 **Ji XF**, Fan YC, Gao S, Yang Y, Zhang JJ, Wang K. MT1M and MT1G promoter methylation as biomarkers for hepatocellular carcinoma. *World J Gastroenterol* 2014; **20**: 4723-4729 [PMID: 24782625 DOI: 10.3748/wjg.v20.i16.4723]

124 **Kuo CC**, Lin CY, Shih YL, Hsieh CB, Lin PY, Guan SB, Hsieh MS, Lai HC, Chen CJ, Lin YW. Frequent methylation of HOXA9 gene in tumor tissues and plasma samples from human hepatocellular carcinomas. *Clin Chem Lab Med* 2014; **52**: 1235-1245 [PMID: 24681432 DOI: 10.1515/cclm-2013-0780]

125 **Earl J**, Garcia-Nieto S, Martinez-Avila JC, Montans J, Sanjuanbenito A, Rodríguez-Garrote M, Lisa E, Mendía E, Lobo E, Malats N, Carrato A, Guillen-Ponce C. Circulating tumor cells (Ctc) and kras mutant circulating free Dna (cfdna) detection in peripheral blood as biomarkers in patients diagnosed with exocrine pancreatic cancer. *BMC Cancer* 2015; **15**: 797 [PMID: 26498594 DOI: 10.1186/s12885-015-1779-7]

126 **Kinugasa H**, Nouso K, Miyahara K, Morimoto Y, Dohi C, Tsutsumi K, Kato H, Matsubara T, Okada H, Yamamoto K. Detection of K-ras gene mutation by liquid biopsy in patients with pancreatic cancer. *Cancer* 2015; **121**: 2271-2280 [PMID: 25823825 DOI: 10.1002/cncr.29364]

127 **Sausen M**, Phallen J, Adleff V, Jones S, Leary RJ, Barrett MT, Anagnostou V, Parpart-Li S, Murphy D, Kay Li Q, Hruban CA, Scharpf R, White JR, O'Dwyer PJ, Allen PJ, Eshleman JR, Thompson CB, Klimstra DS, Linehan DC, Maitra A, Hruban RH, Diaz LA, Von Hoff DD, Johansen JS, Drebin JA, Velculescu VE. Clinical implications of genomic alterations in the tumour and circulation of pancreatic cancer patients. *Nat Commun* 2015; **6**: 7686 [PMID: 26154128 DOI: 10.1038/ncomms8686]

128 **Takai E**, Totoki Y, Nakamura H, Morizane C, Nara S, Hama N, Suzuki M, Furukawa E, Kato M, Hayashi H, Kohno T, Ueno H, Shimada K, Okusaka T, Nakagama H, Shibata T, Yachida S. Clinical utility of circulating tumor DNA for molecular assessment in pancreatic cancer. *Sci Rep* 2015; **5**: 18425 [PMID: 26669280 DOI: 10.1038/srep18425]

129 **Zill OA**, Greene C, Sebisanovic D, Siew LM, Leng J, Vu M, Hendifar AE, Wang Z, Atreya CE, Kelley RK, Van Loon K, Ko AH, Tempero MA, Bivona TG, Munster PN, Talasaz A, Collisson EA. Cell-Free DNA Next-Generation Sequencing in Pancreatobiliary Carcinomas. *Cancer Discov* 2015; **5**: 1040-1048 [PMID: 26109333 DOI: 10.1158/2159-8290.CD-15-0274]

130 **Diaz LA**, Williams RT, Wu J, Kinde I, Hecht JR, Berlin J, Allen B, Bozic I, Reiter JG, Nowak MA, Kinzler KW, Oliner KS, Vogelstein B. The molecular evolution of acquired resistance to targeted EGFR blockade in colorectal cancers. *Nature* 2012; **486**: 537-540 [PMID: 22722843 DOI: 10.1038/nature11219]

131 **Misale S**, Yaeger R, Hobor S, Scala E, Janakiraman M, Liska D, Valtorta E, Schiavo R, Buscarino M, Siravegna G, Bencardino K, Cercek A, Chen CT, Veronese S, Zanon C, Sartore-Bianchi A, Gambacorta M, Gallicchio M, Vakiani E, Boscaro V, Medico E, Weiser M, Siena S, Di Nicolantonio F, Solit D, Bardelli A. Emergence of KRAS mutations and acquired resistance to anti-EGFR therapy in colorectal cancer. *Nature* 2012; **486**: 532-536 [PMID: 22722830 DOI: 10.1038/nature11156]

132 **Murtaza M**, Dawson SJ, Tsui DW, Gale D, Forshew T, Piskorz AM, Parkinson C, Chin SF, Kingsbury Z, Wong AS, Marass F, Humphray S, Hadfield J, Bentley D, Chin TM, Brenton JD, Caldas C, Rosenfeld N. Non-invasive analysis of acquired resistance to cancer therapy by sequencing of plasma DNA. *Nature* 2013; **497**: 108-112 [PMID: 23563269 DOI: 10.1038/nature12065]

133 **Reddi KK**, Holland JF. Elevated serum ribonuclease in patients with pancreatic cancer. *Proc Natl Acad Sci USA* 1976; **73**: 2308-2310 [PMID: 1065880]

134 **Houseley J**, LaCava J, Tollervey D. RNA-quality control by the exosome. *Nat Rev Mol Cell Biol* 2006; **7**: 529-539 [PMID: 16829983 DOI: 10.1038/nrm1964]

135 **Silva JM**, Dominguez G, Silva J, Garcia JM, Sanchez A, Rodriguez O, Provencio M, España P, Bonilla F. Detection of epithelial messenger RNA in the plasma of breast cancer patients is associated with poor prognosis tumor characteristics. *Clin Cancer Res* 2001; **7**: 2821-2825 [PMID: 11555599]

136 **Wong SC**, Lo SF, Cheung MT, Ng KO, Tse CW, Lai BS, Lee KC, Lo YM. Quantification of plasma beta-catenin mRNA in colorectal cancer and adenoma patients. *Clin Cancer Res* 2004; **10**: 1613-1617 [PMID: 15014011]

137 **Garcia V**, García JM, Peña C, Silva J, Domínguez G, Hurtado A, Alonso I, Rodriguez R, Provencio M, Bonilla F. Thymidylate synthase messenger RNA expression in plasma from patients with colon cancer: prognostic potential. *Clin Cancer Res* 2006; **12**: 2095-2100 [PMID: 16609021 DOI: 10.1158/1078-0432.ccr-05-1644]

138 **ENCODE Project Consortium.** An integrated encyclopedia of DNA elements in the human genome. *Nature* 2012; **489**: 57-74 [PMID: 22955616 DOI: 10.1038/nature11247]

139 Lander ES, Linton LM, Birren B, Nusbaum C, Zody MC, Baldwin J, Devon K, Dewar K, Doyle M, FitzHugh W, Funke R, Gage D, Harris K, Heaford A, Howland J, Kann L, Lehoczky J, LeVine R, McEwan P, McKernan K, Meldrim J, Mesirov JP, Miranda C, Morris W, Naylor J, Raymond C, Rosetti M, Santos R, Sheridan A, Sougnez C, Stange-Thomann Y, Stojanovic N, Subramanian A, Wyman D, Rogers J, Sulston J, Ainscough R, Beck S, Bentley D, Burton J, Clee C, Carter N, Coulson A, Deadman R, Deloukas P, Dunham A, Dunham I, Durbin R, French L, Grafham D, Gregory S, Hubbard T, Humphray S, Hunt A, Jones M, Lloyd C, McMurray A, Matthews L, Mercer S, Milne S, Mullikin JC, Mungall A, Plumb R, Ross M, Shownkeen R, Sims S, Waterston RH, Wilson RK, Hillier LW, McPherson JD, Marra MA, Mardis ER, Fulton LA, Chinwalla AT, Pepin KH, Gish WR, Chissoe SL, Wendl MC, Delehaunty KD, Miner TL, Delehaunty A, Kramer JB, Cook LL, Fulton RS, Johnson DL, Minx PJ, Clifton SW, Hawkins T, Branscomb E, Predki P, Richardson P, Wenning S, Slezak T, Doggett N, Cheng JF, Olsen A, Lucas S, Elkin C, Uberbacher E, Frazier M, Gibbs RA, Muzny DM, Scherer SE, Bouck JB, Sodergren EJ, Worley KC, Rives CM, Gorrell JH, Metzker ML, Naylor SL, Kucherlapati RS, Nelson DL, Weinstock GM, Sakaki Y, Fujiyama A, Hattori M, Yada T, Toyoda A, Itoh T, Kawagoe C, Watanabe H, Totoki Y, Taylor T, Weissenbach J, Heilig R, Saurin W, Artiguenave F, Brottier P, Bruls T, Pelletier E, Robert C, Wincker P, Smith DR, Doucette-Stamm L, Rubenfield M, Weinstock K, Lee HM, Dubois J, Rosenthal A, Platzer M, Nyakatura G, Taudien S, Rump A, Yang H, Yu J, Wang J, Huang G, Gu J, Hood L, Rowen L, Madan A, Qin S, Davis RW, Federspiel NA, Abola AP, Proctor MJ, Myers RM, Schmutz J, Dickson M, Grimwood J, Cox DR, Olson MV, Kaul R, Raymond C, Shimizu N, Kawasaki K, Minoshima S, Evans GA, Athanasiou M, Schultz R, Roe BA, Chen F, Pan H, Ramser J, Lehrach H, Reinhardt R, McCombie WR, de la Bastide M, Dedhia N, Blöcker H, Hornischer K, Nordsiek G, Agarwala R, Aravind L, Bailey JA, Bateman A, Batzoglou S, Birney E, Bork P, Brown DG, Burge CB, Cerutti L, Chen HC, Church D, Clamp M, Copley RR, Doerks T, Eddy SR, Eichler EE, Furey TS, Galagan J, Gilbert JG, Harmon C, Hayashizaki Y, Haussler D, Hermjakob H, Hokamp K, Jang W, Johnson LS, Jones TA, Kasif S, Kaspryzk A, Kennedy S, Kent WJ, Kitts P, Koonin EV, Korf I, Kulp D, Lancet D, Lowe TM, McLysaght A, Mikkelsen T, Moran JV, Mulder N, Pollara VJ, Ponting CP, Schuler G, Schultz J, Slater G, Smit AF, Stupka E, Szustakowki J, Thierry-Mieg D, Thierry-Mieg J, Wagner L, Wallis J, Wheeler R, Williams A, Wolf YI, Wolfe KH, Yang SP, Yeh RF, Collins F, Guyer MS, Peterson J, Felsenfeld A, Wetterstrand KA, Patrinos A, Morgan MJ, de Jong P, Catanese JJ, Osoegawa K, Shizuya H, Choi S, Chen YJ, Szustakowki J; International Human Genome Sequencing Consortium. Initial sequencing and analysis of the human genome. *Nature* 2001; **409**: 860-921 [PMID: 11237011 DOI: 10.1038/35057062]

140 **Venter JC,** Adams MD, Myers EW, Li PW, Mural RJ, Sutton GG, Smith HO, Yandell M, Evans CA, Holt RA, Gocayne JD, Amanatides P, Ballew RM, Huson DH, Wortman JR, Zhang Q, Kodira CD, Zheng XH, Chen L, Skupski M, Subramanian G, Thomas PD, Zhang J, Gabor Miklos GL, Nelson C, Broder S, Clark AG, Nadeau J, McKusick VA, Zinder N, Levine AJ, Roberts RJ, Simon M, Slayman C, Hunkapiller M, Bolanos R, Delcher A, Dew I, Fasulo D, Flanigan M, Florea L, Halpern A, Hannenhalli S, Kravitz S, Levy S, Mobarry C, Reinert K, Remington K, Abu-Threideh J, Beasley E, Biddick K, Bonazzi V, Brandon R, Cargill M, Chandramouliswaran I, Charlab R, Chaturvedi K, Deng Z, Di Francesco V, Dunn P, Eilbeck K, Evangelista C, Gabrielian AE, Gan W, Ge W, Gong F, Gu Z, Guan P, Heiman TJ, Higgins ME, Ji RR, Ke Z, Ketchum KA, Lai Z, Lei Y, Li Z, Li J, Liang Y, Lin X, Lu F, Merkulov GV, Milshina N, Moore HM, Naik AK, Narayan VA, Neelam B, Nusskern D, Rusch DB, Salzberg S, Shao

W, Shue B, Sun J, Wang Z, Wang A, Wang X, Wang J, Wei M, Wides R, Xiao C, Yan C, Yao A, Ye J, Zhan M, Zhang W, Zhang H, Zhao Q, Zheng L, Zhong F, Zhong W, Zhu S, Zhao S, Gilbert D, Baumhueter S, Spier G, Carter C, Cravchik A, Woodage T, Ali F, An H, Awe A, Baldwin D, Baden H, Barnstead M, Barrow I, Beeson K, Busam D, Carver A, Center A, Cheng ML, Curry L, Danaher S, Davenport L, Desilets R, Dietz S, Dodson K, Doup L, Ferriera S, Garg N, Gluecksmann A, Hart B, Haynes J, Haynes C, Heiner C, Hladun S, Hostin D, Houck J, Howland T, Ibegwam C, Johnson J, Kalush F, Kline L, Koduru S, Love A, Mann F, May D, McCawley S, McIntosh T, McMullen I, Moy M, Moy L, Murphy B, Nelson K, Pfannkoch C, Pratts E, Puri V, Qureshi H, Reardon M, Rodriguez R, Rogers YH, Romblad D, Ruhfel B, Scott R, Sitter C, Smallwood M, Stewart E, Strong R, Suh E, Thomas R, Tint NN, Tse S, Vech C, Wang G, Wetter J, Williams S, Williams M, Windsor S, Winn-Deen E, Wolfe K, Zaveri J, Zaveri K, Abril JF, Guigó R, Campbell MJ, Sjolander KV, Karlak B, Kejariwal A, Mi H, Lazareva B, Hatton T, Narechania A, Diemer K, Muruganujan A, Guo N, Sato S, Bafna V, Istrail S, Lippert R, Schwartz R, Walenz B, Yooseph S, Allen D, Basu A, Baxendale J, Blick L, Caminha M, Carnes-Stine J, Caulk P, Chiang YH, Coyne M, Dahlke C, Mays A, Dombroski M, Donnelly M, Ely D, Esparham S, Fosler C, Gire H, Glanowski S, Glasser K, Glodek A, Gorokhov M, Graham K, Gropman B, Harris M, Heil J, Henderson S, Hoover J, Jennings D, Jordan C, Jordan J, Kasha J, Kagan L, Kraft C, Levitsky A, Lewis M, Liu X, Lopez J, Ma D, Majoros W, McDaniel J, Murphy S, Newman M, Nguyen T, Nguyen N, Nodell M, Pan S, Peck J, Peterson M, Rowe W, Sanders R, Scott J, Simpson M, Smith T, Sprague A, Stockwell T, Turner R, Venter E, Wang M, Wen M, Wu D, Wu M, Xia A, Zandieh A, Zhu X. The sequence of the human genome. *Science* 2001; **291**: 1304-1351 [PMID: 11181995 DOI: 10.1126/science.1058040]

141 **Szymanski M**, Barciszewska MZ, Erdmann VA, Barciszewski J. A new frontier for molecular medicine: noncoding RNAs. *Biochim Biophys Acta* 2005; **1756**: 65-75 [PMID: 16125325 DOI: 10.1016/j.bbcan.2005.07.005]

142 **Valadi H**, Ekström K, Bossios A, Sjöstrand M, Lee JJ, Lötvall JO. Exosome-mediated transfer of mRNAs and microRNAs is a novel mechanism of genetic exchange between cells. *Nat Cell Biol* 2007; **9**: 654-659 [PMID: 17486113 DOI: 10.1038/ncb1596]

143 **Kosaka N**, Iguchi H, Yoshioka Y, Takeshita F, Matsuki Y, Ochiya T. Secretory mechanisms and intercellular transfer of microRNAs in living cells. *J Biol Chem* 2010; **285**: 17442-17452 [PMID: 20353945 DOI: 10.1074/jbc.M110.107821]

144 **Arroyo JD**, Chevillet JR, Kroh EM, Ruf IK, Pritchard CC, Gibson DF, Mitchell PS, Bennett CF, Pogosova-Agadjanyan EL, Stirewalt DL, Tait JF, Tewari M. Argonaute2 complexes carry a population of circulating microRNAs independent of vesicles in human plasma. *Proc Natl Acad Sci USA* 2011; **108**: 5003-5008 [PMID: 21383194 DOI: 10.1073/pnas.1019055108]

145 **Li LM**, Hu ZB, Zhou ZX, Chen X, Liu FY, Zhang JF, Shen HB, Zhang CY, Zen K. Serum microRNA profiles serve as novel biomarkers for HBV infection and diagnosis of HBV-positive hepatocarcinoma. *Cancer Res* 2010; **70**: 9798-9807 [PMID: 21098710 DOI: 10.1158/0008-5472.can-10-1001]

146 **Gui J**, Tian Y, Wen X, Zhang W, Zhang P, Gao J, Run W, Tian L, Jia X, Gao Y. Serum microRNA characterization identifies miR-885-5p as a potential marker for detecting liver pathologies. *Clin Sci* (Lond) 2011; **120**: 183-193 [PMID: 20815808 DOI: 10.1042/cs20100297]

147 **Qi P**, Cheng SQ, Wang H, Li N, Chen YF, Gao CF. Serum microRNAs as biomarkers for hepatocellular carcinoma in Chinese patients with chronic hepatitis B virus infection. *PLoS One* 2011; **6**: e28486 [PMID: 22174818 DOI: 10.1371/journal.pone.0028486]

148 **Qu KZ**, Zhang K, Li H, Afdhal NH, Albitar M. Circulating microRNAs as biomarkers for hepatocellular carcinoma. *J Clin Gastroenterol* 2011; **45**: 355-360 [PMID: 21278583 DOI: 10.1097/MCG.0b013e3181f18ac2]

149 **Xu J**, Wu C, Che X, Wang L, Yu D, Zhang T, Huang L, Li H, Tan W, Wang C, Lin D. Circulating microRNAs, miR-21, miR-122, and miR-223, in patients with hepatocellular carcinoma or chronic hepatitis. *Mol Carcinog* 2011; **50**: 136-142 [PMID: 21229610 DOI: 10.1002/mc.20712]

150 **Zhou J**, Yu L, Gao X, Hu J, Wang J, Dai Z, Wang JF, Zhang Z, Lu S, Huang X, Wang Z, Qiu S, Wang X, Yang G, Sun H, Tang Z, Wu Y, Zhu H, Fan J. Plasma microRNA panel to diagnose hepatitis B virus-related hepatocellular carcinoma. *J Clin Oncol* 2011; **29**: 4781-4788 [PMID: 22105822 DOI: 10.1200/jco.2011.38.2697]

151 **Li L**, Guo Z, Wang J, Mao Y, Gao Q. Serum miR-18a: a potential marker for hepatitis B virus-related hepatocellular carcinoma screening. *Dig Dis Sci* 2012; **57**: 2910-2916 [PMID: 22865399 DOI: 10.1007/s10620-012-2317-y]

152 **Liu AM**, Yao TJ, Wang W, Wong KF, Lee NP, Fan ST, Poon RT, Gao C, Luk JM. Circulating miR-15b and miR-130b in serum as potential markers for detecting hepatocellular carcinoma: a retrospective cohort study. *BMJ Open* 2012; **2**: e000825 [PMID: 22403344 DOI: 10.1136/bmjopen-2012-000825]

153 **Tomimaru Y**, Eguchi H, Nagano H, Wada H, Kobayashi S, Marubashi S, Tanemura M, Tomokuni A, Takemasa I, Umeshita K, Kanto T, Doki Y, Mori M. Circulating microRNA-21 as a novel biomarker for hepatocellular carcinoma. *J Hepatol* 2012; **56**: 167-175 [PMID: 21749846 DOI: 10.1016/j.jhep.2011.04.026]

154 **Fu Y**, Wei X, Tang C, Li J, Liu R, Shen A, Wu Z. Circulating microRNA-101 as a potential biomarker for hepatitis B virus-related hepatocellular carcinoma. *Oncol Lett* 2013; **6**: 1811-1815 [PMID: 24260081 DOI: 10.3892/ol.2013.1638]

155 **Köberle V**, Kronenberger B, Pleli T, Trojan J, Imelmann E, Peveling-Oberhag J, Welker MW, Elhendawy M, Zeuzem S, Piiper A, Waidmann O. Serum microRNA-1 and microRNA-122 are prognostic markers in patients with hepatocellular carcinoma. *Eur J Cancer* 2013; **49**: 3442-3449 [PMID: 23810247 DOI: 10.1016/j.ejca.2013.06.002]

156 **Luo J**, Chen M, Huang H, Yuan T, Zhang M, Zhang K, Deng S. Circulating microRNA-122a as a diagnostic marker for hepatocellular carcinoma. *Onco Targets Ther* 2013; **6**: 577-583 [PMID: 23723713 DOI: 10.2147/ott.s44215]

157 **Shen J**, Wang A, Wang Q, Gurvich I, Siegel AB, Remotti H, Santella RM. Exploration of genome-wide circulating microRNA in hepatocellular carcinoma: MiR-483-5p as a potential biomarker. *Cancer Epidemiol Biomarkers Prev* 2013; **22**: 2364-2373 [PMID: 24127413 DOI: 10.1158/1055-9965.epi-13-0237]

158 **Zhang Z**, Ge S, Wang X, Yuan Q, Yan Q, Ye H, Che Y, Lin Y, Zhang J, Liu P. Serum miR-483-5p as a potential biomarker to detect hepatocellular carcinoma. *Hepatol Int* 2013; **7**: 199-207 [PMID: 26201634 DOI: 10.1007/s12072-012-9341-z]

159 **Zheng J**, Dong P, Gao S, Wang N, Yu F. High expression of serum miR-17-5p associated with poor prognosis in patients with hepatocellular carcinoma. *Hepatogastroenterology* 2013; **60**: 549-552 [PMID: 23108086 DOI: 10.5754/hge12754]

160 **El-Garem H**, Ammer A, Shehab H, Shaker O, Anwer M, El-Akel W, Omar H. Circulating microRNA, miR-122 and miR-221 signature in Egyptian patients with chronic hepatitis C related hepatocellular carcinoma. *World J Hepatol* 2014; **6**: 818-824 [PMID: 25429320 DOI: 10.4254/wjh.v6.i11.818]

161 **Ge W**, Yu DC, Li QG, Chen X, Zhang CY, Ding YT. Expression of serum miR-16, let-7f, and miR-21 in patients with hepatocellular carcinoma and their clinical significances. *Clin Lab* 2014; **60**: 427-434 [PMID: 24697119]

162 **Giray BG**, Emekdas G, Tezcan S, Ulger M, Serin MS, Sezgin O, Altintas E, Tiftik EN. Profiles of serum microRNAs; miR-125b-5p and miR223-3p serve as novel biomarkers for HBV-positive hepatocellular carcinoma. *Mol Biol Rep* 2014; **41**: 4513-4519 [PMID: 24595450 DOI: 10.1007/s11033-014-3322-3]

163 **Li T**, Yin J, Yuan L, Wang S, Yang L, Du X, Lu J. Downregulation of microRNA-139 is associated with hepatocellular carcinoma risk and short-term survival. *Oncol Rep* 2014; **31**: 1699-1706 [PMID: 24549282 DOI: 10.3892/or.2014.3032]

164 **Liu M**, Liu J, Wang L, Wu H, Zhou C, Zhu H, Xu N, Xie Y. Association of serum microRNA expression in hepatocellular carcinomas treated with transarterial chemoembolization and

patient survival. *PLoS One* 2014; **9**: e109347 [PMID: 25275448 DOI: 10.1371/journal.pone.0109347]
165 **Meng FL**, Wang W, Jia WD. Diagnostic and prognostic significance of serum miR-24-3p in HBV-related hepatocellular carcinoma. *Med Oncol* 2014; **31**: 177 [PMID: 25129312 DOI: 10.1007/s12032-014-0177-3]
166 **Tan Y**, Ge G, Pan T, Wen D, Chen L, Yu X, Zhou X, Gan J. A serum microRNA panel as potential biomarkers for hepatocellular carcinoma related with hepatitis B virus. *PLoS One* 2014; **9**: e107986 [PMID: 25238238 DOI: 10.1371/journal.pone.0107986]
167 **Xie Y**, Yao Q, Butt AM, Guo J, Tian Z, Bao X, Li H, Meng Q, Lu J. Expression profiling of serum microRNA-101 in HBV-associated chronic hepatitis, liver cirrhosis, and hepatocellular carcinoma. *Cancer Biol Ther* 2014; **15**: 1248-1255 [PMID: 24971953 DOI: 10.4161/cbt.29688]
168 **Zhang ZQ**, Meng H, Wang N, Liang LN, Liu LN, Lu SM, Luan Y. Serum microRNA 143 and microRNA 215 as potential biomarkers for the diagnosis of chronic hepatitis and hepatocellular carcinoma. *Diagn Pathol* 2014; **9**: 135 [PMID: 24993656 DOI: 10.1186/1746-1596-9-135]
169 **Chen L**, Chu F, Cao Y, Shao J, Wang F. Serum miR-182 and miR-331-3p as diagnostic and prognostic markers in patients with hepatocellular carcinoma. *Tumour Biol* 2015; **36**: 7439-7447 [PMID: 25903466 DOI: 10.1007/s13277-015-3430-2]
170 **Chen Y**, Chen J, Liu Y, Li S, Huang P. Plasma miR-15b-5p, miR-338-5p, and miR-764 as Biomarkers for Hepatocellular Carcinoma. *Med Sci Monit* 2015; **21**: 1864-1871 [PMID: 26119771 DOI: 10.12659/msm.893082]
171 **Chen Y**, Dong X, Yu D, Wang X. Serum miR-96 is a promising biomarker for hepatocellular carcinoma in patients with chronic hepatitis B virus infection. *Int J Clin Exp Med* 2015; **8**: 18462-18468 [PMID: 26770453]
172 **Cho HJ**, Kim JK, Nam JS, Wang HJ, Lee JH, Kim BW, Kim SS, Noh CK, Shin SJ, Lee KM, Cho SW, Cheong JY. High circulating microRNA-122 expression is a poor prognostic marker in patients with hepatitis B virus-related hepatocellular carcinoma who undergo radiofrequency ablation. *Clin Biochem* 2015; **48**: 1073-1078 [PMID: 26129878 DOI: 10.1016/j.clinbiochem.2015.06.019]
173 **Cui L**, Hu Y, Bai B, Zhang S. Serum miR-335 Level is Associated with the Treatment Response to Trans-Arterial Chemoembolization and Prognosis in Patients with Hepatocellular Carcinoma. *Cell Physiol Biochem* 2015; **37**: 276-283 [PMID: 26305026 DOI: 10.1159/000430352]
174 **El-Abd NE**, Fawzy NA, El-Sheikh SM, Soliman ME. Circulating miRNA-122, miRNA-199a, and miRNA-16 as Biomarkers for Early Detection of Hepatocellular Carcinoma in Egyptian Patients with Chronic Hepatitis C Virus Infection. *Mol Diagn Ther* 2015; **19**: 213-220 [PMID: 26133725 DOI: 10.1007/s40291-015-0148-1]
175 **Jiang L**, Cheng Q, Zhang BH, Zhang MZ. Circulating microRNAs as biomarkers in hepatocellular carcinoma screening: a validation set from China. *Medicine* (Baltimore) 2015; **94**: e603 [PMID: 25761179 DOI: 10.1097/md.0000000000000603]
176 **Liu D**, Wu J, Liu M, Yin H, He J, Zhang B. Downregulation of miRNA-30c and miR-203a is associated with hepatitis C virus core protein-induced epithelial-mesenchymal transition in normal hepatocytes and hepatocellular carcinoma cells. *Biochem Biophys Res Commun* 2015; **464**: 1215-1221 [PMID: 26210453 DOI: 10.1016/j.bbrc.2015.07.107]
177 **Motawi TK**, Shaker OG, El-Maraghy SA, Senousy MA. Serum MicroRNAs as Potential Biomarkers for Early Diagnosis of Hepatitis C Virus-Related Hepatocellular Carcinoma in Egyptian Patients. *PLoS One* 2015; **10**: e0137706 [PMID: 26352740 DOI: 10.1371/journal.pone.0137706]
178 **Oksuz Z**, Serin MS, Kaplan E, Dogen A, Tezcan S, Aslan G, Emekdas G, Sezgin O, Altintas E, Tiftik EN. Serum microRNAs; miR-30c-5p, miR-223-3p, miR-302c-3p and miR-17-5p could be used as novel non-invasive biomarkers for HCV-positive cirrhosis and hepatocellular carcinoma. *Mol Biol Rep* 2015; **42**: 713-720 [PMID: 25391771 DOI: 10.1007/s11033-014-3819-9]
179 **Sohn W**, Kim J, Kang SH, Yang SR, Cho JY, Cho HC, Shim SG, Paik YH. Serum exosomal microRNAs as novel biomarkers for hepatocellular carcinoma. *Exp Mol Med* 2015; **47**: e184 [PMID: 26380927 DOI: 10.1038/emm.2015.68]
180 **Wang X**, Zhang J, Zhou L, Lu P, Zheng ZG, Sun W, Wang JL, Yang XS, Li XL, Xia N, Zhang N, Dou KF. Significance of serum microRNA-21 in diagnosis of hepatocellular carcinoma (HCC): clinical analyses of patients and an HCC rat model. *Int J Clin Exp Pathol* 2015; **8**: 1466-1478 [PMID: 25973032]
181 **Xu Y**, Bu X, Dai C, Shang C. High serum microRNA-122 level is independently associated with higher overall survival rate in hepatocellular carcinoma patients. *Tumour Biol* 2015; **36**: 4773-4776 [PMID: 25636448 DOI: 10.1007/s13277-015-3128-5]
182 **Yin J**, Hou P, Wu Z, Wang T, Nie Y. Circulating miR-375 and miR-199a-3p as potential biomarkers for the diagnosis of hepatocellular carcinoma. *Tumour Biol* 2015; **36**: 4501-4507 [PMID: 25618599 DOI: 10.1007/s13277-015-3092-0]
183 **Yu F**, Lu Z, Chen B, Dong P, Zheng J. microRNA-150: a promising novel biomarker for hepatitis B virus-related hepatocellular carcinoma. *Diagn Pathol* 2015; **10**: 129 [PMID: 26215970 DOI: 10.1186/s13000-015-0369-y]
184 **Zhuang L**, Xu L, Wang P, Meng Z. Serum miR-128-2 serves as a prognostic marker for patients with hepatocellular carcinoma. *PLoS One* 2015; **10**: e0117274 [PMID: 25642945 DOI: 10.1371/journal.pone.0117274]
185 **Zhuang LP**, Meng ZQ. Serum miR-224 reflects stage of hepatocellular carcinoma and predicts survival. *Biomed Res Int* 2015; **2015**: 731781 [PMID: 25688365 DOI: 10.1155/2015/731781]
186 **Amr KS**, Ezzat WM, Elhosary YA, Hegazy AE, Fahim HH, Kamel RR. The potential role of miRNAs 21 and 199-a in early diagnosis of hepatocellular carcinoma. *Gene* 2016; **575**: 66-70 [PMID: 26302751 DOI: 10.1016/j.gene.2015.08.038]
187 **Chen S**, Chen H, Gao S, Qiu S, Zhou H, Yu M, Tu J. Differential expression of plasma microRNA-125b in hepatitis B virus-related liver diseases and diagnostic potential for hepatitis B virus-induced hepatocellular carcinoma. *Hepatol Res* 2017; **47**: 312-320 [PMID: 27152955 DOI: 10.1111/hepr.12739]
188 **Ghosh A**, Ghosh A, Datta S, Dasgupta D, Das S, Ray S, Gupta S, Datta S, Chowdhury A, Chatterjee R, Mohapatra SK, Banerjee S. Hepatic miR-126 is a potential plasma biomarker for detection of hepatitis B virus infected hepatocellular carcinoma. *Int J Cancer* 2016; **138**: 2732-2744 [PMID: 26756996 DOI: 10.1002/ijc.29999]
189 **Hung CH**, Hu TH, Lu SN, Kuo FY, Chen CH, Wang JH, Huang CM, Lee CM, Lin CY, Yen YH, Chiu YC. Circulating microRNAs as biomarkers for diagnosis of early hepatocellular carcinoma associated with hepatitis B virus. *Int J Cancer* 2016; **138**: 714-720 [PMID: 26264553 DOI: 10.1002/ijc.29802]
190 **Khairy A**, Hamza I, Shaker O, Yosry A. Serum miRNA Panel in Egyptian Patients with Chronic Hepatitis C Related Hepatocellular Carcinoma. *Asian Pac J Cancer Prev* 2016; **17**: 2699-2703 [PMID: 27268654]
191 **Lin L**, Lu B, Yu J, Liu W, Zhou A. Serum miR-224 as a biomarker for detection of hepatocellular carcinoma at early stage. *Clin Res Hepatol Gastroenterol* 2016; **40**: 397-404 [PMID: 26724963 DOI: 10.1016/j.clinre.2015.11.005]
192 **Okajima W**, Komatsu S, Ichikawa D, Miyamae M, Kawaguchi T, Hirajima S, Ohashi T, Imamura T, Kiuchi J, Arita T, Konishi H, Shiozaki A, Moriumura R, Ikoma H, Okamoto K, Taniguchi H, Itoh Y, Otsuji E. Circulating microRNA profiles in plasma: identification of miR-224 as a novel diagnostic biomarker in hepatocellular carcinoma independent of hepatic function. *Oncotarget* 2016; **7**: 53820-53836 [PMID: 27462777 DOI: 10.18632/oncotarget.10781]
193 **Yang L**, Xu Q, Xie H, Gu G, Jiang J. Expression of serum miR-218 in hepatocellular carcinoma and its prognostic significance. *Clin Transl Oncol* 2016; **18**: 841-847 [PMID: 26586116 DOI: 10.1007/s12094-015-1447-z]
194 **Zekri AN**, Youssef AS, El-Desouky ED, Ahmed OS, Lotfy MM, Nassar AA, Bahnassey AA. Serum microRNA panels as potential biomarkers for early detection of hepatocellular carcinoma on top

of HCV infection. *Tumour Biol* 2016; **37**: 12273-12286 [PMID: 27271989 DOI: 10.1007/s13277-016-5097-8]

195 **Zhuang C**, Jiang W, Huang D, Xu L, Yang Q, Zheng L, Wang X, Hu L. Serum miR-21, miR-26a and miR-101 as potential biomarkers of hepatocellular carcinoma. *Clin Res Hepatol Gastroenterol* 2016; **40**: 386-396 [PMID: 26669589 DOI: 10.1016/j.clinre.2015.11.002]

196 **Law WI**, Chu KW, Ho JW, Chan CW. Risk factors for anastomotic leakage after low anterior resection with total mesorectal excision. *Am J Surg* 2000; **179**: 92-96 [PMID: 10773140]

197 **Merkel S**, Wang WY, Schmidt O, Dworak O, Wittekind C, Hohenberger W, Hermanek P. Locoregional recurrence in patients with anastomotic leakage after anterior resection for rectal carcinoma. *Colorectal Dis* 2001; **3**: 154-160 [PMID: 12790981]

198 **Walker KG**, Bell SW, Rickard MJ, Mehanna D, Dent OF, Chapuis PH, Bokey EL. Anastomotic leakage is predictive of diminished survival after potentially curative resection for colorectal cancer. *Ann Surg* 2004; **240**: 255-259 [PMID: 15273549]

199 **Branagan G**, Finnis D; Wessex Colorectal Cancer Audit Working Group. Prognosis after anastomotic leakage in colorectal surgery. *Dis Colon Rectum* 2005; **48**: 1021-1026 [PMID: 15789125 DOI: 10.1007/s10350-004-0869-4]

200 **Peeters KC**, Tollenaar RA, Marijnen CA, Klein Kranenbarg E, Steup WH, Wiggers T, Rutten HJ, van de Velde CJ; Dutch Colorectal Cancer Group. Risk factors for anastomotic failure after total mesorectal excision of rectal cancer. *Br J Surg* 2005; **92**: 211-216 [PMID: 15584062 DOI: 10.1002/bjs.4806]

201 **Mirnezami A**, Mirnezami R, Chandrakumaran K, Sasapu K, Sagar P, Finan P. Increased local recurrence and reduced survival from colorectal cancer following anastomotic leak: systematic review and meta-analysis. *Ann Surg* 2011; **253**: 890-899 [PMID: 21394013 DOI: 10.1097/SLA.0b013e3182128929]

202 **Park JS**, Choi GS, Kim SH, Kim HR, Kim NK, Lee KY, Kang SB, Kim JY, Lee KY, Kim BC, Bae BN, Son GM, Lee SI, Kang H. Multicenter analysis of risk factors for anastomotic leakage after laparoscopic rectal cancer excision: the Korean laparoscopic colorectal surgery study group. *Ann Surg* 2013; **257**: 665-671 [PMID: 23333881 DOI: 10.1097/SLA.0b013e31827b8ed9]

203 **McDermott FD**, Heeney A, Kelly ME, Steele RJ, Carlson GL, Winter DC. Systematic review of preoperative, intraoperative and postoperative risk factors for colorectal anastomotic leaks. *Br J Surg* 2015; **102**: 462-479 [PMID: 25703524 DOI: 10.1002/bjs.9697]

204 **Siegel RL**, Miller KD, Jemal A. Cancer statistics, 2015. *CA Cancer J Clin* 2015; **65**: 5-29 [PMID: 25559415 DOI: 10.3322/caac.21254]

205 **Hain E**, Maggiori L, Manceau G, Mongin C, Prost À la Denise J, Panis Y. Oncological impact of anastomotic leakage after laparoscopic mesorectal excision. *Br J Surg* 2017; **104**: 288-295 [PMID: 27762432 DOI: 10.1002/bjs.10332]

206 **Shen S**, Lin Y, Yuan X, Shen L, Chen J, Chen L, Qin L, Shen B. Biomarker MicroRNAs for Diagnosis, Prognosis and Treatment of Hepatocellular Carcinoma: A Functional Survey and Comparison. *Sci Rep* 2016; **6**: 38311 [PMID: 27917899 DOI: 10.1038/srep38311]

207 **Zhang Y**, Zhang X, Zhang J, Sun B, Zheng L, Li J, Liu S, Sui G, Yin Z. Microfluidic chip for isolation of viable circulating tumor cells of hepatocellular carcinoma for their culture and drug sensitivity assay. *Cancer Biol Ther* 2016; **17**: 1177-1187 [PMID: 27662377 DOI: 10.1080/15384047.2016.1235665]

P- Reviewer: Lee HC, Yao DF, Lee HC **S- Editor**: Qi Y
L- Editor: A **E- Editor**: Li D

World Journal of Gastroenterology

Submit a Manuscript: http://www.f6publishing.com

World J Gastroenterol 2017 August 21; 23(31): 5669-5679

DOI: 10.3748/wjg.v23.i31.5669

ISSN 1007-9327 (print) ISSN 2219-2840 (online)

ORIGINAL ARTICLE

Basic Study

Fluctuation of zonulin levels in blood *vs* stability of antibodies

Aristo Vojdani, Elroy Vojdani, Datis Kharrazian

Aristo Vojdani, Department of Preventive Medicie, Loma Linda University, Evans Hall, Loma Linda, CA 92354, United States

Aristo Vojdani, Immunosciences Lab., Inc., Los Angeles, CA 90035, United States

Elroy Vojdani, Regenera Wellness, Los Angeles, CA 90025 United States

Datis Kharrazian, Harvard Medical School, Boston, MA 02115, United States

Datis Kharrazian, TRANSCEND Research, Department of Neurology, Massachusetts General Hospital, Charlestown, MA 02129, United States

Datis Kharrazian, Loma Linda University School of Medicine, Loma Linda, CA 92354, United States

Author contributions: Vojdani A designed and coordinated the research and drafted the manuscript; Vojdani E performed some of the assays; Kharrazian D provided statistical analysis and reviewed the manuscript; all of the authors have read and approved the final manuscript.

Institutional review board statement: The appropriate approvals were obtained from Western International Review Boards.

Conflict-of-interest statement: Dr. Aristo Vojdani is the CEO and technical director of Immunosciences Lab., Inc.

Data sharing statement: No additional data are available.

Manuscript source: Unsolicited manuscript

Correspondence to: Aristo Vojdani, PhD, MSc, CLS, Immunosciences Lab., Inc., 822 S. Robertson Blvd., Ste. 312, Los Angeles, CA 90035, United States. drari@msn.com
Telephone: +1-310-6571077
Fax: +1-310-6571053

Received: May 18, 2017
Peer-review started: May 19, 2017
First decision: June 22, 2017
Revised: June 30, 2017
Accepted: July 12, 2017
Article in press: July 12, 2017
Published online: August 21, 2017

Abstract

AIM

To evaluate the measurement of zonulin level and antibodies of zonulin and other tight junction proteins in the blood of controls and celiac disease patients.

METHODS

This study was conducted to assess the variability or stability of zonulin levels *vs* IgA and IgG antibodies against zonulin in blood samples from 18 controls at 0, 6, 24 and 30 h after blood draw. We also measured zonulin level as well as zonulin, occludin, vinculin, aquaporin 4 and glial fibrillary acidic protein antibodies in the sera of 30 patients with celiac disease and 30 controls using enzyme-linked immunosorbent assay methodology.

RESULTS

The serum zonulin level in 6 out of 18 subjects was low or < 2.8 ng/mL and was very close to the detection limit of the assay. The other 12 subjects had zonulin levels of > 2.8 ng/mL and showed significant fluctuation from sample to sample. Comparatively, zonulin

antibody measured in all samples was highly stable and reproducible from sample to sample. Celiac disease patients showed zonulin levels with a mean of 8.5 ng/mL compared to 3.7 ng/mL in controls ($P < 0.0001$). Elevation of zonulin level at 2SD above the mean was demonstrated in 37% of celiac disease patients, while antibodies against zonulin, occludin and other tight junction proteins was detected in up to 86% of patients with celiac disease.

CONCLUSION

Due to its fluctuation, a single measurement of zonulin level is not recommended for assessment of intestinal barrier integrity. Measurement of IgG and IgA antibodies against zonulin, occludin, and other tight junction proteins is proposed for the evaluation of the loss of intestinal barrier integrity.

Key words: Zonulin; Occludin; Tight junction protein; Intestinal barrier integrity; Celiac disease

Core tip: We studied possible variability in zonulin levels *vs* measuring antibodies against zonulin and other tight junction proteins in blood. We found that fluctuations in zonulin level from hour-to-hour and day-to-day were too great to recommend it for assessing intestinal permeability. Measurement of IgG and IgA antibodies against tight junction proteins in controls and in celiac disease patients proved to be very stable and reproducible, and we recommend this method for such an assessment in future studies.

Vojdani A, Vojdani E, Kharrazian D. Fluctuation of zonulin levels in blood vs stability of antibodies. *World J Gastroenterol* 2017; 23(31): 5669-5679 Available from: URL: http://www.wjgnet.com/1007-9327/full/v23/i31/5669.htm DOI: http://dx.doi.org/10.3748/wjg.v23.i31.5669

INTRODUCTION

The intestinal barrier is one of the most continuously challenged body barriers. Its importance for maintaining health cannot be overestimated. Protected by outer layers of gut microbiota and mucus, the intestinal epithelial layer is the last defensive barrier. This one-cell-thick, picket fence-like structure both absorbs nutrients and blocks the entry of immunogenic molecules from infiltrating the body. If the barrier is breached, inflammation, autoimmunity or even cancer may follow[1,2]. A broken barrier, therefore, is a serious matter and a therapeutic target for disease amelioration[3,4].

Intestinal barrier structures include epithelial cells and a system of junctions linking them together. This structure prevents pathogens, endotoxins and undigested dietary proteins from reaching the underlying lamina propria. Many factors can alter intestinal barrier structures, causing increased barrier permeability. These factors include physical and/or emotional stress[5], gut microbiota modifications[6-8], dust mite allergen[9], long-term use of non-steroidal anti-inflammatory drugs[10-12], diet[8,13], alcohol[14] and autoimmune reactivity against barrier structures[15-17].

Lacing the epithelial cells to one another are complex cellular junctions: tight junctions, gap junctions, adherens junctions and desmosomes[4]. Making up the tight junctions are occludins and claudins with zonulin anchoring them to the actomyosin network within the epithelial cells. Together these cells regulate the intestinal paracellular pathway.

Occludin and claudin are intra-membrane proteins, which regulate water ion flow and electrolyte loss[3]. Occludin has also been linked to the regulation of intermembrane and paracellular diffusion of small molecules[18].

Zonula occludens (ZO-1, ZO-2, ZO-3) are intracellular tight junction proteins that bind directly the C-terminal 146 amino acids of occludin to the cable cytoskeletal protein actomyosin[19]. Zonula occludens are members of a family of membrane-associated signaling proteins known as the membrane-associated guanylate kinase homologs (MAGUKs)[20]. MAGUKs are suggested to be involved in signal transduction pathways controlling growth and differentiation[21,22]. Zonulin modulates small-intestinal tight junction permeability through a protein kinase C-alpha-mediated actin polymerization[23].

Vinculin is a cytoskeletal protein that is found in both focal contacts and adherens junction[24,25], and contributes to the mechanical link of the contractile actomyosin cytoskeleton to the extracellular matrix through integrin receptors. Vinculin is capable of binding to alpha-actinin, actin, talin[26] and to itself[27-29]. Vinculin also plays a role in the establishment, or regulation, of cadherin-based cell adhesion[30,31].

Beneath the intestinal epithelial cells reside astrocyte-like cells, known as enteric glia cells (EGCs). The expression marker, glial fibrillary acidic protein (GFAP), of EGCs is identical to the astrocytes of the central nervous system[32,33]. GFAP is an intermediate filament that is closely related to its non-epithelial family members, vimentin, desmin, and peripherin, which are all involved in the structure and function of the cell's cytoskeleton. GFAP is thought to help to maintain astrocyte mechanical strength[34]. The mucosal EGC population are in close proximity to the epithelial cells of the colonic crypts and their terminal foot processes often extend to the epithelial basement membrane and blood capillaries in the intestinal mucosa[33,35]. EGCs are the major constituent of the enteric nervous system and outnumber enteric neurons by a factor of 4 to 10[35].

Aquaporin 4 (AQP4) is a class of water channels found in many cells of the body including the stomach,

brain, lung, and skeletal muscle. It is the predominant water channel in the central nervous system. In the brain, AQP4 is believed to have a role in maintaining and regulating the brain's functions. These same water channel cells are found in plants, which studies indicate may be involved in the development of some neural autoimmune diseases through molecular mimicry[36]. Other studies also suggest the involvement of intestinal aquaporins in early stage inflammatory bowel disease and intestinal barrier integrity impairment[37-39].

A variety of tests have been introduced for the assessment of intestinal epithelial cell damage, intestinal tight junction integrity and increased intestinal permeability to macromolecules. This includes the measurement of fatty acid binding proteins, glutathione S-transferase, claudins, the absorption of polyethylene glycols, circulating bacterial endotoxins, anti-endotoxin antibodies, zonulin level in blood, and others. These methods for the assessment of barrier integrity and function were reviewed by Grootjans *et al*[40].

During the past 3 years, a few published studies have shown elevations of zonulin levels in the blood of subgroups of patients with type 1 diabetes[41], metabolic syndrome[42], polycystic ovary syndrome[43], and type 2 diabetes[44]. Based on these publications, several clinical laboratories are now offering measurement of zonulin levels in blood as a biomarker of gut barrier assessment and autoimmunities.

This is despite indications that molecules such as zonulin and occludin have molecular sizes from 45000-65000 Da[45-47]. Molecules greater than 5000 Da in size are immunogenic and thus, incite immune cells into action. That is why levels of molecules such as zonulin and similar molecules, in a single individual, fluctuate from non-detectable to upregulated within minutes to hours[41,48-50]. When these immunogenic molecules enter the submucosa and then into circulation, immune system macrophages will take up the molecules, or they are processed by liver Kupffer cells. Because of this innate immune response, molecule levels will fluctuate in the blood stream. The half-life of these molecules, in the blood stream, ranges from 4 min to 4 h[48,50,51]. Indeed, this fluctuation in blood zonulin level was studied for a period of 6 d in ICU patients with sepsis, and values were varied by a factor of 2-10 from day to day[52].

The first goal of this study was to measure zonulin level at 0-, 6-, 24- and 30-h blood-draw intervals. On the other hand, because the half-life of antibodies is about 21 d, the assessment of antibodies against zonulin provides a better clinical picture with one blood draw. Consequently we decided to measure IgA and IgG antibodies against zonulin in the same blood specimens. Finally, zonulin levels in blood have not been measured in celiac disease (CD). We decided to measure both zonulin level and zonulin antibody as well as antibodies against other tight junction proteins in patients with CD.

MATERIALS AND METHODS

Antigens such as zonulin, occludin, vinculin, AQP4, and GFAP were purchased from Abcam (Abcam, Cambridge, MA, United States). A zonulin enzyme-linked immunosorbent assay (ELISA) kit was purchased from MyBioSource (MyBioSource, Inc., San Diego, CA, United States). Seventy-two blood samples were obtained from 18 volunteers at intervals of 0, 6, 24, and 30 h. We did not test the 18 volunteers for allergies, diabetes, CD, NCGS, other possible GI complaints, autoimmune disorders or any other general conditions. Blood samples were then centrifuged and the separated sera were kept at -20 ℃ for 48 h and then used for the measurement of zonulin concentration as well as IgG and IgA levels to zonulin and other tight junction proteins. Sera from 30 random human donors aged 18-65 were purchased from Innovative Research Inc. (Southfield, MI, United States). The samples were registered as healthy human subjects. Before shipping, each blood sample was tested according to FDA guidelines for the detection of hepatitis B surface antigen, antibodies to HIV, antibodies to hepatitis C, HIV-1 RNA, and syphilis. All units yielded non-reactive/negative results for each test performed. Additionally, commercially available sera from 30 patients with CD were purchased from the Binding Site (San Diego, CA, United States), Inova (San Diego, CA, United States), Diamedix (Miami Lakes, FL, United States), Innovative Research (Novi, MI, United States), and Trina International Nanikon (Switzerland). The samples from patients with CD were confirmed by degree of positivity for IgA against both deamidated alpha gliadin peptide as well as IgA to transglutaminase-2 antibody using kits purchased from Inova Diagnostics. Zonulin levels as well as levels of IgG and IgA antibodies to zonulin and other tight junction proteins were measured in these specimens.

Measurement of zonulin

Determination of zonulin levels in serum was done using sandwich ELISA technique. In this kit the precoated antibody is human zonulin monoclonal antibody, and the detecting antibody is polyclonal antibody labeled with biotin. The standard curve ranged from 1.5-100 ng/mL with a sensitivity starting at 3 ng/mL.

Measurement of IgG and IgA against tight junction proteins by ELISA

Zonulin, occludin, vinculin, AQP4, and GFAP at a concentration of 100 ng/mL were each dissolved in 0.01 mol/L phosphate buffer saline with a pH of 7.4. These proteins were then diluted 1:100 in 0.1 mol/L carbonate buffer, pH 9.5, and 100 μL were added to wells of microtiter plates and incubated for 8 hours at room temperature followed by incubation at 4 ℃ for 16 h. The plates were washed three times with 200 μL of Tris-buffered saline (TBS) containing 0.05% Tween 20 (pH 7.4). The non-specific binding of immunoglobulins

was prevented by adding 200 μL of 2% bovine serum albumin (BSA) in TBS, and incubated overnight at 4 ℃. Plates were washed as previously described and then serum samples (diluted 1:50 for IgA, 1:100 for IgG) in 1% BSA in TBS containing 0.05% Tween 20 (pH 7.4) were added to duplicate wells and incubated for 1 h at room temperature.

Plates were washed, and then alkaline phosphatase goat antihuman IgG or IgA F(ab)2 fragments (KPI, Gaithersburg, MD) optimal dilution of 1:400 for IgA and 1:800 for IgG in 1% BSA-TBS were added to each appropriate well; plates were incubated for an additional hour at room temperature. After washing five times with TBS-Tween buffer, the enzyme reaction was started by adding 100 μL of 1 mg/mL paranitrophenylphosphate in diethanolamine buffer containing 1 mmol/L $MgCl_2$ and sodium azide (pH 9.8). The reaction was stopped 45 mins later with 50 μL of 2 mol/L NaOH. The optical density (OD) was read at 405 nm by a microtiter plate reader. To exclude nonspecific binding, the ODs of the control wells coated with dry milk or human serum albumin were subtracted from all other wells. Sera from patients with CD with known high titers of IgG and IgA against various tight junction proteins were used as positive controls. Also assay normalizer positive and negative controls were used for additional levels of quality control and the calculation of the ELISA indices. For each assay the ELISA index was calculated using the following formula: ELISA index = (mean OD of sample - background)/(mean OD of serum normalizer - background)

Statistical analysis

Statistical analysis was performed to study the relationships of zonulin level, zonulin antibody, occludin antibody, vinculin antibody, AQP4 antibody, and glial fibrillary acid protein antibody. The determination of the presence of statistically significant correlative relationships was conducted with Pearson's correlation coefficients, Kendall's tau and Spearman's rho. These measures are invariant to any monotonic transformation. A standard *P*-value of 0.05 and a confidence interval of 95% were used. Correlative analysis and the magnitude of relationship were reported. STATA software package was used to conduct all inferential and descriptive analysis.

RESULTS

Serum zonulin level was measured in the sera of 18 control subjects at different intervals as well as in sera from 30 patients with known CD. The zonulin assay r^2 for the standard curve was 0.998, and the reproducibility of the duplicates varied less than 10% for samples with zonulin concentration of 2.8 ng/mL or greater. This indicated that the analytical sensitivity of the assay for serum zonulin levels was 2.8 ng/mL; for samples with zonulin levels < 2.8 the reproducibility of duplicates was not good. Of the 18 control subjects, 6 had serum zonulin levels measuring less than 2.8 ng/mL, and due to lack of sensitivity those levels did not significantly fluctuate, as shown in Figure 1. However, for the other 12 subjects who had serum zonulin levels measuring greater than 2.8 ng/mL at time 0 (Figure 2), significant fluctuation in zonulin levels was observed in almost all 12 of these subjects at the 6-, 24- or 30-h blood draws (Figure 2). Since zonulin is a relatively large molecule with the approximate size of 55000 Da, it may enter the systemic circulation after its release from the tight junctions where an immune response against it can result in the production of zonulin-specific antibodies. To demonstrate their stability, IgG and IgA antibodies to zonulin were measured in the same 18 subjects along the 30-h time course. Data presented in Figures 1B and C and 2B and C showed that both IgG and IgA antibody levels from blood obtained at 0, 6, 24, and 30 h were highly stable with variations of less than 10%.

Serum zonulin levels were then measured in 30 healthy controls along with 30 patients with known celiac disease. The CD patients showed statistically significant higher serum zonulin levels with a mean of 8.5 ng/mL compared to healthy control subjects with a mean of 3.7 ng/mL ($P < 0.0001$). At 2 standard deviations above the mean of control subjects, 10% or 33% of the 30 CD patients demonstrated elevation of serum zonulin levels (Figure 3A).

To establish whether serum zonulin levels correlate with zonulin and other tight junction protein antibodies, zonulin, occludin, vinculin, AQP4 and GFAP antibody levels were measured in the same 30 patients and 30 controls. The distribution of IgG and IgA antibodies against tight junction proteins in these patients is shown in Figure 3B-F. At three standard deviations above the mean of healthy controls, 63% and 67%, 87% and 77%, 70% and 57% respectively had serum IgG and IgA antibody reactivity against zonulin, occludin, and vinculin. The elevation of both IgG and IgA antibodies against AQP4 was 43%; against enteric glial cells expressing GFAP it was 23% for IgG and 53% for IgA (Figure 3). Statistical analysis was performed using Ecxel to compare controls and CD patients; for zonulin level *P* value $\leqslant 0.002$, while for tight junction proteins antibody levels *P* value $\leqslant 0.001$. Since not all patients with celiac disease had serum zonulin elevation, we examined the correlation between serum zonulin levels and tight junction protein antibodies. Overall, we found three subgroups. Subgroup 1 consists of 9% or 30% of the CD patients with significant elevations in both zonulin level and antibodies against zonulin and other tight junction proteins when compared to the mean control levels shown in Figure 3. Subgroup 2 consists of 13% or 43% of the CD patients with a normal serum zonulin level but a significant elevation in IgG or IgA antibodies against zonulin, occludin, and other tight junction proteins. Subgroup 3 is composed of 8% or 27% of the CD patients with low or normal serum zonulin levels and low or normal IgG and IgA

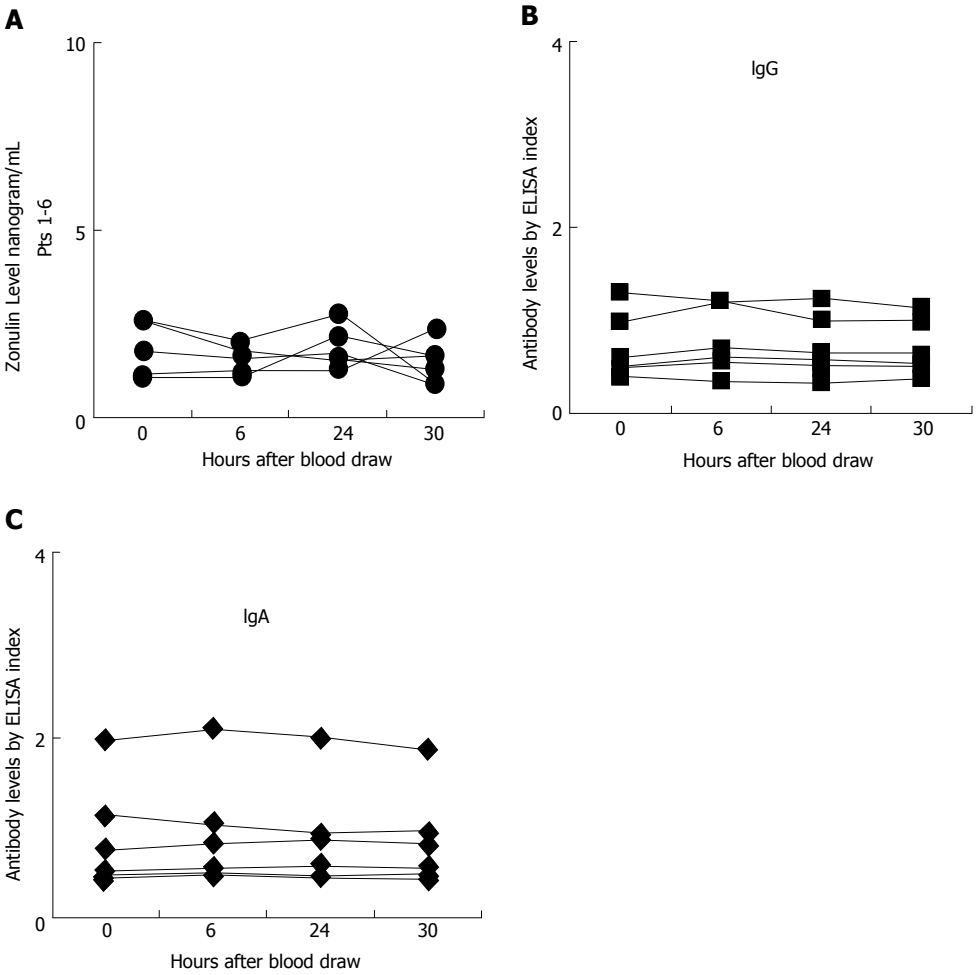

Figure 1 Minimal fluctuations in zonulin levels in individuals with low levels of zonulin (A), IgG antibody (B), and IgA antibody (C) in a subgroup of 6 out of 18 subjects.

Table 1 Correlation between serum zonulin level and different tight junction protein antibodies

Tight junction protein	IgG		IgA	
	r	*P* value	*r*	*P* value
Zonulin	0.34	0.064	0.55	0.002
Occludin	0.60	< 0.001	0.50	0.005
Vinculin	0.40	0.032	0.52	0.003
Aquaporin 4	0.42	0.020	0.24	0.197
Glial fibrillary acidic protein	0.55	0.002	0.60	< 0.001

antibody levels to tight junction proteins. This direct or indirect correlation between serum zonulin levels and various tight junction protein antibodies is shown in Table 1, where the "r" is the best indication of correlation between serum zonulin level and antibodies against zonulin and other tight junction proteins. This table summary of the two-way scatter plot evaluation for zonulin levels and antibody measurements of the tight junction proteins demonstrates a strong positive monotonic relationship for all correlations (Table 1). Statistical analysis using Pearson's correlations coefficient were statistically significant for 9 of the 10 correlations, showing a positive relationship, with the exceptions of zonulin level with AQP4 IgA (r = 0.24, P = 0.197).

Zonulin levels had statistically significant correlations with zonulin IgA and IgG antibodies; for IgG the relationship with zonulin levels and zonulin IgG was r = 0.34, P = 0.064, but the magnitude of the relationship was much stronger with zonulin IgA antibodies (r = 0.55, P = 0.002). Zonulin levels also had statistically significant correlations with vinculin IgA and IgG antibodies, and the magnitude of the relationship was likewise better with vinculin IgA antibodies (Table 1).

DISCUSSION

Due to the availability of methods for the measurement of serum zonulin levels, several laboratories in the United States have begun to offer zonulin level analysis for the detection of increased intestinal permeability in patients with autoimmune disease or other chronic inflammatory illnesses. The majority of these laboratories analyze serum zonulin levels from a single blood draw without consideration for the variability of serum zonulin levels during the time course of a single day or from day to day. The scientific basis for

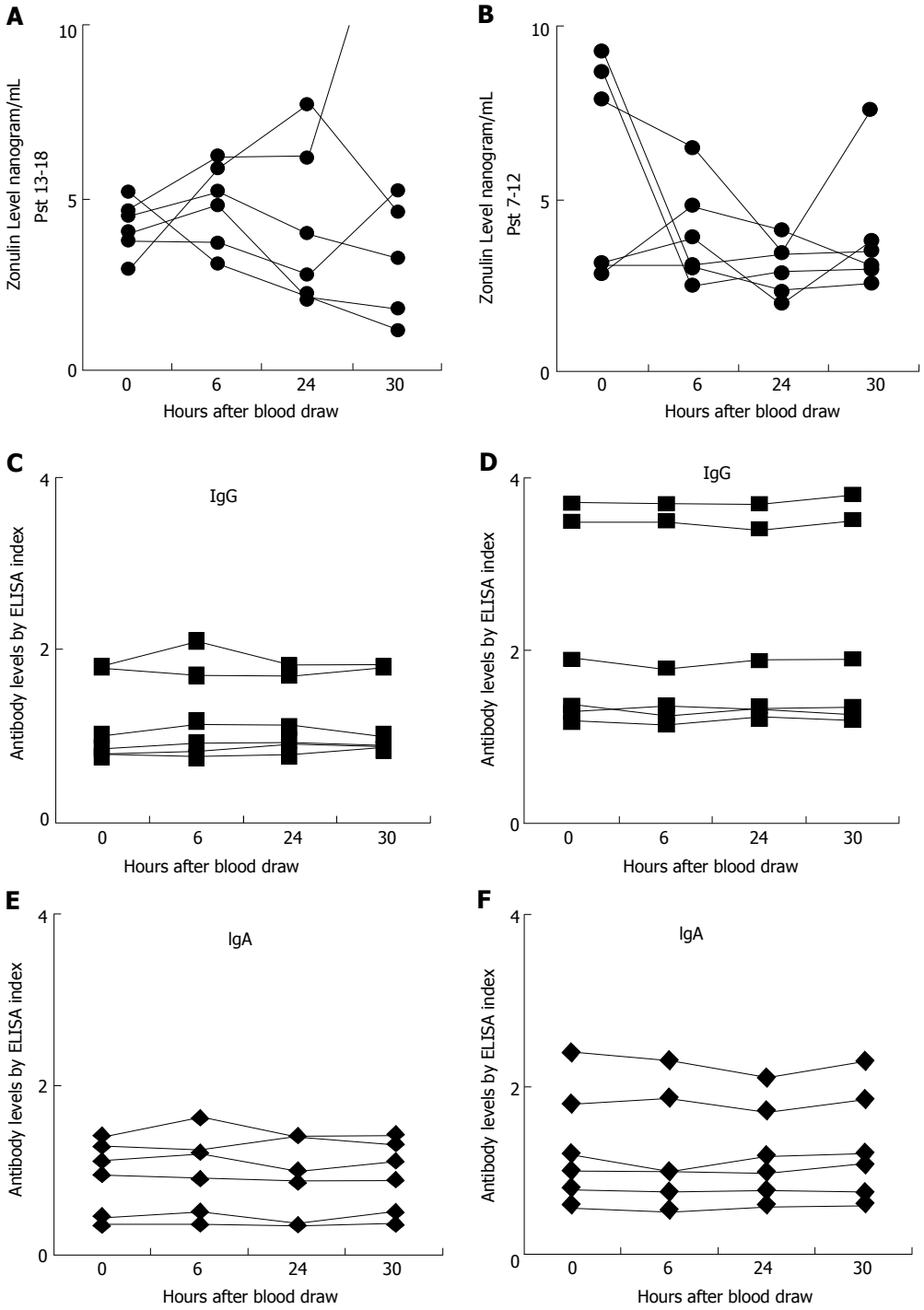

Figure 2 Fluctuation of serum level of zonulin in a subgroup of 12 out of 18 subjects with zonulin elevations (A, B) *vs* much more stable zonulin IgG (C, D) and zonulin IgA (E, F) antibodies.

offering serum zonulin levels as a diagnostic indicator mainly stems from a paper published by Sapone *et al*[41] in 2006 which demonstrated a correlation with zonulin upregulation and increased gut permeability in a subgroup of patients with type 1 diabetes. While this study contains several key and landmark discoveries with which we agree wholeheartedly, it is our opinion that the data on which the conclusions were drawn merit further analysis before they become the sole basis for future diagnostic utility.

One of the many points used by Sapone to demonstrate a correlation between zonulin upregulation and increased gut permeability in his study is an overall elevated serum zonulin level detected in a subgroup of patients with type 1 diabetes[41]. Careful examination of the data reveals that only 42% of the patients have an elevated serum zonulin level (defined by two standard deviations above the control group mean). Furthermore, in correlating serum zonulin levels and leaky gut, the data was plotted against lactulose/mannitol levels in the same patients. These revealed a correlation coefficient of 0.36, which is very weak. In

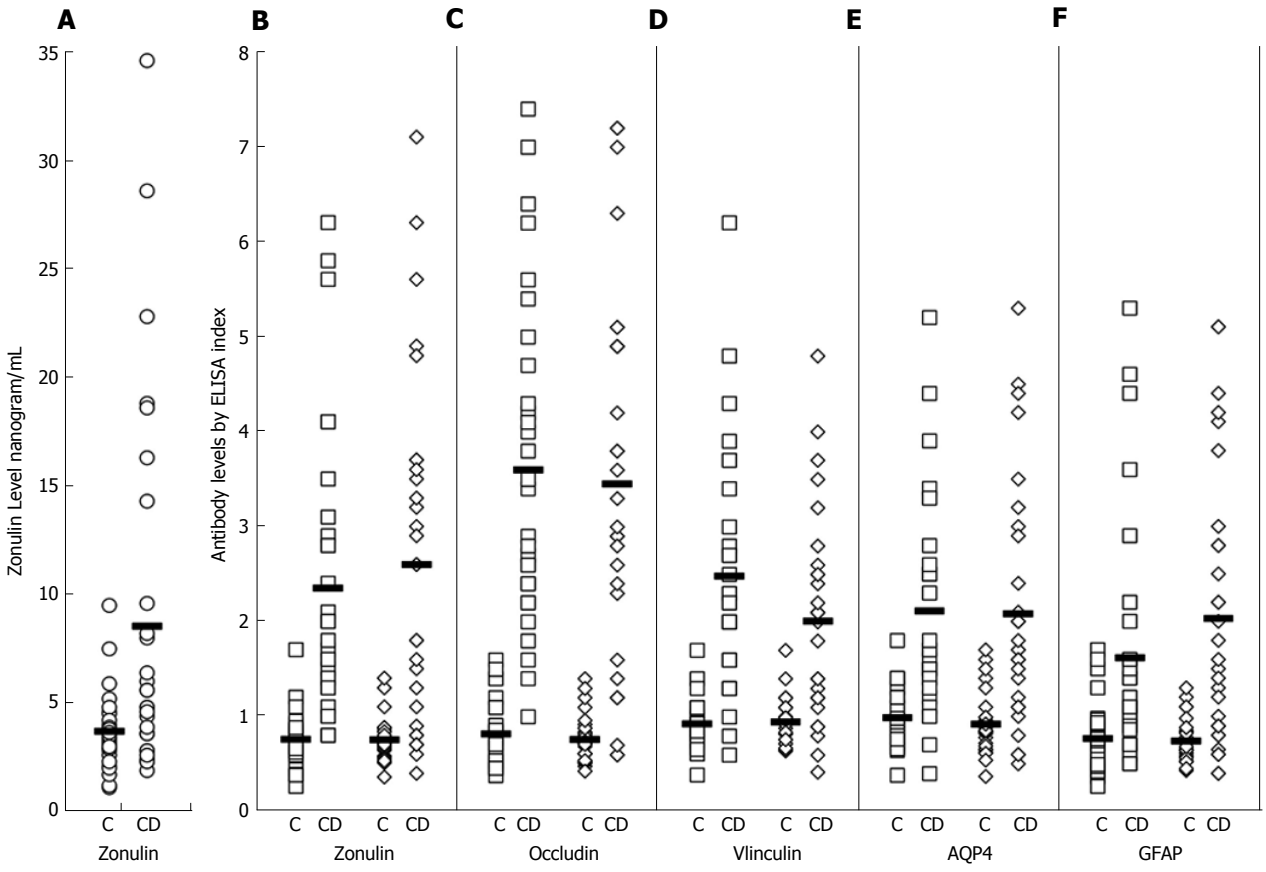

Figure 3 Differences in serum level of zonulin (A) and IgG (square markers) and IgA (diamond markers) tight junction proteins zonulin (B), occludin (C), vinculin (D), aquaporin 4 (E) and glial fibrillary acidic protein (F) in controls (C) and patients with celiac disease. CD: Celiac disease; GFAP: Glial fibrillary acidic protein; AQP4: Aquaporin 4.

fact, it was concluded by the authors that "While these numbers are very useful in the setting of research analysis, they are insufficiently correlated to be applied to diagnostic medical use[41]".

Another point of interest is the importance of intra-day or day-to-day variability of serum zonulin levels and their effect on use as a diagnostic marker. In an article published by Klaus *et al*[52] in 2013, plasma zonulin levels were measured and analyzed in ICU patients with sepsis and compared to healthy controls. Analysis of the day-to-day serum zonulin levels for septic patients presented a significant day-to-day fluctuation. In the present study we decided to extrapolate this idea further with a timed blood draw protocol in which serum was drawn at 0-, 6-, 24-, and 30-h intervals in 18 control volunteers to uncover any significant intra-day fluctuation of serum zonulin levels. Analysis of the data demonstrates significant variability of serum zonulin levels in 12 out of 18 controls with baseline zonulin level of > 2.8 ng/mL, but not in 6 samples with zonulin levels around the detection limit of the zonulin ELISA kit.

It is important to point out that our 18 volunteer subjects were controls in the sense that they had not been definitely confirmed to be positive for CD, unlike the 30 purchased samples. We did not test the 18 volunteers for allergies, diabetes, CD, NCGS, other possible GI complaints, autoimmune disorders or any other general conditions. In light of this, and given the plurality of the individual, it is not surprising that a subgroup of 6 of the 18 had lower levels than the other 12. In fact, the whole point of the study is to show the widely varying fluctuations in measuring zonulin levels, even among so-called controls.

Zonulin is a protein the size of 47000 Da. Due to many environmental factors, it is released from the lamina propria and is presented to the submucosal gut immune system, where an immune response against it results in the production of zonulin-specific antibodies[53]. This immune response against zonulin and other large molecules may be an explanation for zonulin fluctuation from sample to sample in the 12 control specimens with relatively elevated zonulin. Although the half-life in serum of zonulin has yet to be determined, it is reasonable to assume zonulin's half-life based on the known half-lives of other similarly-sized proteins. For example, LPS, which, along with zonulin, is involved in the induction of inflammation in type-2 diabetes, has a known half-life of 2-4 min in blood[50].

This fluctuation is not unique to zonulin. For example, the presence of circulating autoantibodies directed against U1 nuclear antigen and elevated blood levels of U1 antigen were shown to be the hallmark of systemic lupus erythematosus. While antibody levels against U1 antigens was demonstrated to be highly stable, the level of U1 antigens varied from day to

day[54]. This fluctuation in antigen level in the blood could be associated with antibody-antigen complex formation in the circulation, where it is expected to exit transiently[55].

Based on this mucosal and possible systemic immune response against zonulin, we measured both IgA and IgG antibodies to zonulin in the 72 specimens from the 18 control subjects. In contrast to zonulin level and its fluctuation, we observed a significant stability in antibody levels in all four blood specimens obtained at different intervals from each of the 18 subjects. The variability for both IgA and IgG antibodies against zonulin was 10% or less which is similar to inter-assay variation of the ELISA methodology used in this study (Figures 1A-C, 2A-F).

Celiac disease is an autoimmune disease in which exposure to dietary gluten peptides results in villous atrophy and crypt hypertrophy[56]. During the acute phase of CD when the tight junctions are open, zonulin expression in intestinal specimens was shown to be increased by three-fold[53]. The increased expression of zonulin due to tight junction breakdown allows zonulin presentation to the immune system and production of antibodies against zonulin in a subgroup of patients with CD[53]. In one study that followed 7 patients with CD longitudinally, the raised anti-zonulin IgA returned to normal after 3-6 mo on a gluten-free diet[57]. While zonulin upregulation in CD has been shown in several studies[48,53,57], to the best of our knowledge and throughout our literature search, zonulin elevation in the sera of patients with CD has not been examined. For this reason, we measured serum zonulin levels as well as serum antibody levels to several tight junction proteins in 30 patients with CD. At 2 standard deviations above the mean of control or a serum zonulin level of 7.1 ng/mL, 10 out of the 30, or 33% of the CD patients exhibited elevations in zonulin levels ($P < 0.0001$) as well as in zonulin IgA and IgG antibody levels. However, we found that an additional 10 CD patients or a total of 20 (67%) produced antibodies to zonulin without having a significant elevation in serum zonulin levels (Figure 3A and B). The detection of antibodies against zonulin in 67% of patients with CD while zonulin level elevations were detected in only 33% may be related to the zonulin fluctuation in the blood and its removal by the immune system.

Because intestinal tight junctions consist of several protein complexes including occludin, zonulin, vinculin, talin, claudin, actin, alpha-actinin, desmoglein, and others, we decided to test for antibody production to additional tight junction proteins including occludin and vinculin. We found a significant elevation in antibody production against both occludin and vinculin in addition to zonulin. In fact, levels of these antibodies were the highest against occludin. Further analysis of the data reveals that occludin IgG actually has a stronger positive correlation to serum zonulin levels ($r = 0.6$) than either zonulin or vinculin antibody measurement ($r = 0.34$-0.55 and $r = 0.40$-0.52 respectively). The reason for this is not immediately clear though it appears from our data that the inclusion of antibody measurement to other tight junction proteins such as occludin may enhance the diagnostic utility of these antibodies.

Recent research by Spadoni *et al*[58] has shed light on the existence and function of the gut vascular barrier, which in healthy individuals functions to protect the systemic blood from pathogenic microbiota. In their article they discuss the importance of the expression of intermediate GFAP by enteric glial cells in their formation and function of a gut vascular unit. In addition, AQP4 is a known component of the blood brain barrier, and is also a resident water channel in human stomach tissue, as published by Laforenza[38]. We therefore decided to measure for potential antibody formation against these two proteins in our CD group in an attempt to further understand the pathogenic process of inflammatory and autoimmune disease in the gastrointestinal (GI) tract. We were not surprised to detect elevated antibody levels to both AQP4 and GFAP in these patients because of their structural presence and utility in the gut. Antibody levels to both proteins (except AQP4 IgA) positively correlated with serum zonulin levels as demonstrated in Table 1 with "*r*" values ranging from 0.42-0.60. This indicates a promising area of future study into what appears to be a clear indicator that reactivity to proteins outside of the tight junction plays a role in inflammatory pathogenesis of CD and possibly other GI disorders.

Although this was a small study, the data shows significant hourly fluctuation of serum zonulin levels in control subjects, making its clinical utility questionable. In comparison, both IgG and IgA zonulin antibodies measured in the sera of the same individuals showed excellent stability over the course of the blood draw. Moreover, measuring antibodies to zonulin and other tight junction proteins revealed significant elevation in a large percentage of patients with CD, which suggests that they play a significant role in the pathogenesis of CD and possibly other autoimmune disorders. This indicates a need for further research about the role of antibodies against tight junction proteins in patients with inflammatory and autoimmune disorders.

ACKNOWLEDGMENTS

Acknowledgment is given to Joel Bautista for the preparation of this manuscript for publication as well as the creation of the figures.

COMMENTS

Background

In recent times newly available technology has led to laboratories offering testing for serum levels of zonulin, a gut barrier tight junction protein, for the detection of increased intestinal permeability in patients with autoimmune disease or other chronic inflammatory disorders. However, studies demonstrate that the testable half-life of zonulin and similar molecules is extremely brief,

so that the reliability of tests based just on zonulin levels is arguable. A more stable, more reliably accurate methodology is required.

Research frontiers

The scientific basis for offering serum zonulin levels as a diagnostic indicator comes mainly from a 2006 paper by Sapone *et al* which demonstrated a correlation between zonulin upregulation and increased gut permeability in a subgroup of patients with type 1 diabetes. However, Sapone *et al* themselves concluded that their numbers were "insufficiently correlated to be applied to diagnostic medical use."

Innovations and breakthroughs

This study shows that due to the size of zonulin and similar molecules, the normal functions of the immune system may cause zonulin levels in the blood to rise and fall from day to day, and even from hour to hour. This may cast doubt on their reliability as biomarkers, whereas the measurement of antibodies against zonulin and other tight junction proteins is comparatively much more stable, accurate and reliable. This was demonstrated in a large percentage of patients with celiac disease who showed significant elevations in antibodies against zonulin and other tight junction proteins as opposed to measurements of just zonulin level.

Applications

Measuring antibodies against zonulin and other tight junction proteins may be an important diagnostic tool in the detection of intestinal hyperpermeability in patients with inflammatory disorders and autoimmune disease.

Terminology

The intestinal or gut barrier is one of the body's most important defenses against the entry of disease-causing pathogens and food antigens. It is a complex wall of layered and inter-laced proteins. Zonulin is one of the foremost of these tight junction proteins.

Peer-review

Th paper is well done and helps to clarify some questions about zonulin and related molecules. It is practically very relevant.

REFERENCES

1 **Fasano A**. Zonulin and its regulation of intestinal barrier function: the biological door to inflammation, autoimmunity, and cancer. *Physiol Rev* 2011; **91**: 151-175 [PMID: 21248165 DOI: 10.1152/physrev.00003.2008]

2 **Tlaskalová-Hogenová H**, Stěpánková R, Kozáková H, Hudcovic T, Vannucci L, Tučková L, Rossmann P, Hrnčíř T, Kverka M, Zákostelská Z, Klimešová K, Přibylová J, Bártová J, Sanchez D, Fundová P, Borovská D, Srůtková D, Zídek Z, Schwarzer M, Drastich P, Funda DP. The role of gut microbiota (commensal bacteria) and the mucosal barrier in the pathogenesis of inflammatory and autoimmune diseases and cancer: contribution of germ-free and gnotobiotic animal models of human diseases. *Cell Mol Immunol* 2011; **8**: 110-120 [PMID: 21278760 DOI: 10.1038/cmi.2010.67]

3 **Bischoff SC**, Barbara G, Buurman W, Ockhuizen T, Schulzke JD, Serino M, Tilg H, Watson A, Wells JM. Intestinal permeability--a new target for disease prevention and therapy. *BMC Gastroenterol* 2014; **14**: 189 [PMID: 25407511 DOI: 10.1186/s12876-014-0189-7]

4 **Yu YB**, Li YQ. Enteric glial cells and their role in the intestinal epithelial barrier. *World J Gastroenterol* 2014; **20**: 11273-11280 [PMID: 25170211 DOI: 10.3748/wjg.v20.i32.11273]

5 **Saunders PR**, Kosecka U, McKay DM, Perdue MH. Acute stressors stimulate ion secretion and increase epithelial permeability in rat intestine. *Am J Physiol* 1994; **267**: G794-G799 [PMID: 7977741]

6 **Moreira AP**, Texeira TF, Ferreira AB, Peluzio Mdo C, Alfenas Rde C. Influence of a high-fat diet on gut microbiota, intestinal permeability and metabolic endotoxaemia. *Br J Nutr* 2012; **108**: 801-809 [PMID: 22717075 DOI: 10.1017/S0007114512001213]

7 **Wang W**, Uzzau S, Goldblum SE, Fasano A. Human zonulin, a potential modulator of intestinal tight junctions. *J Cell Sci* 2000; 113 Pt **24**: 4435-4440 [PMID: 11082037]

8 **Ulluwishewa D**, Anderson RC, McNabb WC, Moughan PJ, Wells JM, Roy NC. Regulation of tight junction permeability by intestinal bacteria and dietary components. *J Nutr* 2011; **141**: 769-776 [PMID: 21430248 DOI: 10.3945/jn.110.135657]

9 **Wan H**, Winton HL, Soeller C, Tovey ER, Gruenert DC, Thompson PJ, Stewart GA, Taylor GW, Garrod DR, Cannell MB, Robinson C. Der p 1 facilitates transepithelial allergen delivery by disruption of tight junctions. *J Clin Invest* 1999; **104**: 123-133 [PMID: 10393706 DOI: 10.1172/JCI5844]

10 **Bjarnason I**, Zanelli G, Smith T, Prouse P, Williams P, Smethurst P, Delacey G, Gumpel MJ, Levi AJ. Nonsteroidal antiinflammatory drug-induced intestinal inflammation in humans. *Gastroenterology* 1987; **93**: 480-489 [PMID: 3609658]

11 **Fries JF**, Miller SR, Spitz PW, Williams CA, Hubert HB, Bloch DA. Toward an epidemiology of gastropathy associated with nonsteroidal antiinflammatory drug use. *Gastroenterology* 1989; **96**: 647-655 [PMID: 2909442]

12 **Lanas A**, Serrano P, Bajador E, Esteva F, Benito R, Sáinz R. Evidence of aspirin use in both upper and lower gastrointestinal perforation. *Gastroenterology* 1997; **112**: 683-689 [PMID: 9041228]

13 **Pendyala S**, Walker JM, Holt PR. A high-fat diet is associated with endotoxemia that originates from the gut. *Gastroenterology* 2012; **142**: 1100-1101.e2 [PMID: 22326433 DOI: 10.1053/j.gastro.2012.01.034]

14 **Massey VL**, Arteel GE. Acute alcohol-induced liver injury. *Front Physiol* 2012; **3**: 193 [PMID: 22701432 DOI: 10.3389/fphys.2012.00193]

15 **Clemente MG**, Musu MP, Frau F, Brusco G, Sole G, Corazza GR, De Virgiliis S. Immune reaction against the cytoskeleton in coeliac disease. *Gut* 2000; **47**: 520-526 [PMID: 10986212]

16 **Pimentel M**, Morales W, Pokkunuri V, Brikos C, Kim SM, Kim SE, Triantafyllou K, Weitsman S, Marsh Z, Marsh E, Chua KS, Srinivasan S, Barlow GM, Chang C. Autoimmunity Links Vinculin to the Pathophysiology of Chronic Functional Bowel Changes Following Campylobacter jejuni Infection in a Rat Model. *Dig Dis Sci* 2015; **60**: 1195-1205 [PMID: 25424202 DOI: 10.1007/s10620-014-3435-5]

17 **Das KM**, Dasgupta A, Mandal A, Geng X. Autoimmunity to cytoskeletal protein tropomyosin. A clue to the pathogenetic mechanism for ulcerative colitis. *J Immunol* 1993; **150**: 2487-2493 [PMID: 8450225]

18 **Balda MS**, Whitney JA, Flores C, González S, Cereijido M, Matter K. Functional dissociation of paracellular permeability and transepithelial electrical resistance and disruption of the apical-basolateral intramembrane diffusion barrier by expression of a mutant tight junction membrane protein. *J Cell Biol* 1996; **134**: 1031-1049 [PMID: 8769425]

19 **Furuse M**, Itoh M, Hirase T, Nagafuchi A, Yonemura S, Tsukita S, Tsukita S. Direct association of occludin with ZO-1 and its possible involvement in the localization of occludin at tight junctions. *J Cell Biol* 1994; **127**: 1617-1626 [PMID: 7798316 DOI: 10.1083/jcb.127.6.1617]

20 **Fanning AS**, Jameson BJ, Jesaitis LA, Anderson JM. The tight junction protein ZO-1 establishes a link between the transmembrane protein occludin and the actin cytoskeleton. *J Biol Chem* 1998; **273**: 29745-29753 [PMID: 9792688]

21 **Fanning AS,** Lapierre LA, Brecher AR, Itallie CMV, Anderson JM. Protein interactions in the tight junction: the role of MAGUK proteins in regulating tight junction organization and function. *Curr Top Membr* 1996; **43**: 211-235 [DOI: 10.1016/S0070-2161(08)60391-3]

22 **Kornau HC**, Seeburg PH, Kennedy MB. Interaction of ion channels and receptors with PDZ domain proteins. *Curr Opin Neurobiol* 1997; **7**: 368-373 [PMID: 9232802 DOI: 10.1016/

S0959-4388(97)80064-5]
23 **Fasano A**, Fiorentini C, Donelli G, Uzzau S, Kaper JB, Margaretten K, Ding X, Guandalini S, Comstock L, Goldblum SE. Zonula occludens toxin modulates tight junctions through protein kinase C-dependent actin reorganization, in vitro. *J Clin Invest* 1995; **96**: 710-720 [PMID: 7635964 DOI: 10.1172/JCI118114]
24 **Otto JJ**. Vinculin. *Cell Motil Cytoskeleton* 1990; **16**: 1-6 [PMID: 2112986 DOI: 10.1002/cm.970160102]
25 **Geiger B**, Ginsberg D. The cytoplasmic domain of adherens-type junctions. *Cell Motil Cytoskeleton* 1991; **20**: 1-6 [PMID: 1756576 DOI: 10.1002/cm.970200102]
26 **Burridge K**, Mangeat P. An interaction between vinculin and talin. *Nature* 1984; **308**: 744-746 [PMID: 6425696 DOI: 10.1038/308744a0]
27 **Bendori R**, Salomon D, Geiger B. Identification of two distinct functional domains on vinculin involved in its association with focal contacts. *J Cell Biol* 1989; **108**: 2383-2393 [PMID: 2500446]
28 **Johnson RP**, Craig SW. An intramolecular association between the head and tail domains of vinculin modulates talin binding. *J Biol Chem* 1994; **269**: 12611-12619 [PMID: 8175670]
29 **Johnson RP**, Craig SW. F-actin binding site masked by the intramolecular association of vinculin head and tail domains. *Nature* 1995; **373**: 261-264 [PMID: 7816144 DOI: 10.1038/373261a0]
30 **Hazan RB**, Kang L, Roe S, Borgen PI, Rimm DL. Vinculin is associated with the E-cadherin adhesion complex. *J Biol Chem* 1997; **272**: 32448-32453 [PMID: 9405455]
31 **Mierke CT**, Kollmannsberger P, Zitterbart DP, Diez G, Koch TM, Marg S, Ziegler WH, Goldmann WH, Fabry B. Vinculin facilitates cell invasion into three-dimensional collagen matrices. *J Biol Chem* 2010; **285**: 13121-13130 [PMID: 20181946 DOI: 10.1074/jbc.M109.087171]
32 **Gershon MD**, Rothman TP. Enteric glia. *Glia* 1991; **4**: 195-204 [PMID: 1827778 DOI: 10.1002/glia.440040211]
33 **Cabarrocas J**, Savidge TC, Liblau RS. Role of enteric glial cells in inflammatory bowel disease. *Glia* 2003; **41**: 81-93 [PMID: 12465048 DOI: 10.1002/glia.10169]
34 **Cullen DK**, Simon CM, LaPlaca MC. Strain rate-dependent induction of reactive astrogliosis and cell death in three-dimensional neuronal-astrocytic co-cultures. *Brain Res* 2007; **1158**: 103-115 [PMID: 17555726 DOI: 10.1016/j.brainres.2007.04.070]
35 **Neunlist M**, Aubert P, Bonnaud S, Van Landeghem L, Coron E, Wedel T, Naveilhan P, Ruhl A, Lardeux B, Savidge T, Paris F, Galmiche JP. Enteric glia inhibit intestinal epithelial cell proliferation partly through a TGF-beta1-dependent pathway. *Am J Physiol Gastrointest Liver Physiol* 2007; **292**: G231-G241 [PMID: 16423922 DOI: 10.1152/ajpgi.00276.2005]
36 **Vojdani A**, Mukherjee PS, Berookhim J, Kharrazian D. Detection of Antibodies against Human and Plant Aquaporins in Patients with Multiple Sclerosis. *Autoimmune Dis* 2015; **2015**: 905208 [PMID: 26290755 DOI: 10.1155/2015/905208]
37 **Laforenza U**. Water channel proteins in the gastrointestinal tract. *Mol Aspects Med* 2012; **33**: 642-650 [PMID: 22465691 DOI: 10.1016/j.mam.2012.03.001.]
38 **Zhang W**, Xu Y, Chen Z, Xu Z, Xu H. Knockdown of aquaporin 3 is involved in intestinal barrier integrity impairment. *FEBS Lett* 2011; **585**: 3113-3119 [PMID: 21907710 DOI: 10.1016/j.febslet.2011.08.045]
39 **Morgan E**, Peplowski M, MacNaughton W. Aquaporin 3 promotes intestinal epithelial proliferation and inhibits cytokine-induced apoptosis. *FASEB* 2015; **29**: 766 [DOI: 10.1096/fj.1530-6860]
40 **Grootjans J**, Thuijls G, Verdam F, Derikx JPM, Lenaerts K, Buurman WA. Non-invasive assessment of barrier integrity and function of the human gut. *World J Gastrointest Surg* 2010; **2**: 61-69 [PMID: 2999221 DOI: 10.4240/wjgs.v2.i3.61]
41 **Sapone A**, de Magistris L, Pietzak M, Clemente MG, Tripathi A, Cucca F, Lampis R, Kryszak D, Cartenì M, Generoso M, Iafusco D, Prisco F, Laghi F, Riegler G, Carratu R, Counts D, Fasano A. Zonulin upregulation is associated with increased gut permeability in subjects with type 1 diabetes and their relatives. *Diabetes* 2006; **55**: 1443-1449 [PMID: 16644703 DOI: 10.2337/db05-1593]
42 **Moreno-Navarrete JM**, Sabater M, Ortega F, Ricart W, Fernández-Real JM. Circulating zonulin, a marker of intestinal permeability, is increased in association with obesity-associated insulin resistance. *PLoS One* 2012; **7**: e37160 [PMID: 22629362 DOI: 10.1371/journal.pone.0037160]
43 **Zhang D**, Zhang L, Yue F, Zheng Y, Russell R. Serum zonulin is elevated in women with polycystic ovary syndrome and correlates with insulin resistance and severity of anovulation. *Eur J Endocrinol* 2015; **172**: 29-36 [PMID: 25336505 DOI: 10.1530/EJE-14-0589]
44 **Jayashree B**, Bibin YS, Prabhu D, Shanthirani CS, Gokulakrishnan K, Lakshmi BS, Mohan V, Balasubramanyam M. Increased circulatory levels of lipopolysaccharide (LPS) and zonulin signify novel biomarkers of proinflammation in patients with type 2 diabetes. *Mol Cell Biochem* 2014; **388**: 203-210 [PMID: 24347174 DOI: 10.1007/s11010-013-1911-4]
45 **Vanuytsel T**, Vermeire S, Cleynen I. The role of Haptoglobin and its related protein, Zonulin, in inflammatory bowel disease. *Tissue Barriers* 2013; **1**: e27321 [PMID: 24868498 DOI: 10.4161/tisb.27321]
46 **Fasano A**. Intestinal zonulin: open sesame! *Gut* 2001; **49**: 159-162 [PMID: 11454785 DOI: 10.1136/gut.49.2.159]
47 **Furuse M**, Hirase T, Itoh M, Nagafuchi A, Yonemura S, Tsukita S, Tsukita S. Occludin: a novel integral membrane protein localizing at tight junctions. *J Cell Biol* 1993; **123**: 1777-1788 [PMID: 8276896]
48 **Drago S**, El Asmar R, Di Pierro M, Grazia Clemente M, Tripathi A, Sapone A, Thakar M, Iacono G, Carroccio A, D'Agate C, Not T, Zampini L, Catassi C, Fasano A. Gliadin, zonulin and gut permeability: Effects on celiac and non-celiac intestinal mucosa and intestinal cell lines. *Scand J Gastroenterol* 2006; **41**: 408-419 [PMID: 16635908 DOI: 10.1080/00365520500235334]
49 **Sapone A,** de Magistris L, Caravelli G, Familiar V, Riegler G, Zampini L, Catassi C, Fasano A. Serum zonulin and intestinal permeability before and after a gluten-containing meal in both type 1 diabetes and in their relatives. *Dig Liver Dis* 2006; **38**: S75 [DOI: 10.1016/S1590-8658(06)80197-0]
50 **Yao Z**, Mates JM, Cheplowitz AM, Hammer LP, Maiseyeu A, Phillips GS, Wewers MD, Rajaram MV, Robinson JM, Anderson CL, Ganesan LP. Blood-Borne Lipopolysaccharide Is Rapidly Eliminated by Liver Sinusoidal Endothelial Cells via High-Density Lipoprotein. *J Immunol* 2016; **197**: 2390-2399 [PMID: 27534554 DOI: 10.4049/jimmunol.1600702]
51 **Li C**, Gao M, Zhang W, Chen C, Zhou F, Hu Z, Zeng C. Zonulin Regulates Intestinal Permeability and Facilitates Enteric Bacteria Permeation in Coronary Artery Disease. *Sci Rep* 2016; **6**: 29142 [PMID: 27353603 DOI: 10.1038/srep29142]
52 **Klaus DA**, Motal MC, Burger-Klepp U, Marschalek C, Schmidt EM, Lebherz-Eichinger D, Krenn CG, Roth GA. Increased plasma zonulin in patients with sepsis. *Biochem Med* (Zagreb) 2013; **23**: 107-111 [PMID: 23457771 DOI: 10.11613/BM.2013.013]
53 **Fasano A,** Not T, Wang W, Uzzau S, Berti I, Tommasini A, Goldblum SE. Zonulin, a newly discovered modulator of intestinal permeability, and its expression in coeliac disease. *Lancet* 2000; **355**: 1518-1519 [PMID: 10801176 DOI: 10.1016/s0140-6736(00)02169-3]
54 **Doedens JR**, Jones WD, Hill K, Mason MJ, Gersuk VH, Mease PJ, Dall'Era M, Aranow C, Martin RW, Cohen SB, Fleischmann RM, Kivitz AJ, Burge DJ, Chaussabel D, Elkon KB, Posada JA. Blood-Borne RNA Correlates with Disease Activity and IFN-Stimulated Gene Expression in Systemic Lupus Erythematosus. *J Immunol* 2016; **197**: 2854-2863 [PMID: 27534558 DOI: 10.4049/jimmunol.1601142]
55 **Davies KA**, Peters AM, Beynon HL, Walport MJ. Immune complex processing in patients with systemic lupus erythematosus. In vivo imaging and clearance studies. *J Clin Invest* 1992; **90**: 2075-2083 [PMID: 1430231 DOI: 10.1172/jci116090]
56 **Green PH**, Cellier C. Celiac disease. *N Engl J Med* 2007; **357**: 1731-1743 [PMID: 17960014 DOI: 10.1056/nejmra071600]
57 **Duerksen DR**, Wilhelm-Boyles C, Parry DM. Intestinal

permeability in long-term follow-up of patients with celiac disease on a gluten-free diet. *Dig Dis Sci* 2005; **50**: 785-790 [PMID: 15844719 DOI: 10.1007/s10620-005-2574-0]

58 **Spadoni I**, Zagato E, Bertocchi A, Paolinelli R, Hot E, Di Sabatino A, Caprioli F, Bottiglieri L, Oldani A, Viale G, Penna G, Dejana E, Rescigno M. A gut-vascular barrier controls the systemic dissemination of bacteria. *Science* 2015; **350**: 830-834 [PMID: 26564856 DOI: 10.1126/science.aad0135]

P- Reviewer: Esposito O **S- Editor**: Ma YJ **L- Editor**: A
E- Editor: Huang Y

World Journal of Gastroenterology

Submit a Manuscript: http://www.f6publishing.com

World J Gastroenterol 2017 August 21; 23(31): 5680-5691

DOI: 10.3748/wjg.v23.i31.5680

ISSN 1007-9327 (print) ISSN 2219-2840 (online)

ORIGINAL ARTICLE

Basic Study

Effects of albumin/glutaraldehyde glue on healing of colonic anastomosis in rats

Kalliopi Despoudi, Ioannis Mantzoros, Orestis Ioannidis, Aggeliki Cheva, Nikolaos Antoniou, Dimitrios Konstantaras, Savvas Symeonidis, Manousos George Pramateftakis, Efstathios Kotidis, Stamatis Angelopoulos, Konstantinos Tsalis

Kalliopi Despoudi, Ioannis Mantzoros, Orestis Ioannidis, Nikolaos Antoniou, Dimitrios Konstantaras, Savvas Symeonidis, Manousos George Pramateftakis, Efstathios Kotidis, Stamatis Angelopoulos, Konstantinos Tsalis, Fourth Surgical Department, Medical School, Aristotle University of Thessaloniki, 57010 Thessaloniki, Greece

Aggeliki Cheva, Department of Pathology, General Hospital "G. Papanikolaou", 57010 Thessaloniki, Greece

Author contributions: Despoudi K, Mantzoros I and Ioannidis O contributed equally to this work; Despoudi K, Pramateftakis MG, Angelopoulos S and Tsalis K designed coordinated the research; Despoudi K, Mantzoros I, Antoniou N, Konstantaras D and Symeonidis S performed the experiments; Despoudi K, Antoniou N, Konstantaras D, Pramateftakis MG and Kotidis E participated equally in treatment of animals; Despoudi K, Ioannidis O and Cheva A analysed the data; Despoudi K, Mantzoros I, Ioannidis O and Cheva A wrote the paper; Despoudi K, Mantzoros I, Ioannidis O, Cheva A, Antoniou N, Konstantaras D, Pramateftakis MG, Kotidis E, Angelopoulos S and Tsalis K significantly contributed to the linguistic formatting and correction of the manuscript, revised it critically for important intellectual content, and were responsible for final proof reading of the article.

Institutional review board statement: The study was reviewed and approved by the Faculty of Surgery, Medical School, Aristotle University of Thessaloniki, Thessaloniki, Greece Institutional Review Board.

Institutional animal care and use committee statement: All procedures involving animals were reviewed and approved by the Institutional Animal Care and Use Committee of the Veterinary Manager of the Prefecture of Thessaloniki [IACUC protocol number: (S.N.: 13/11872/11-09-08)].

Conflict-of-interest statement: No conflict of interest.

Data sharing statement: No additional data are available.

Manuscript source: Invited manuscript

Correspondence to: Dr. Orestis Ioannidis, MD, MSc, PhD, Surgeon, Scientific Fellow, Fourth Surgical Department, Medical School, Aristotle University of Thessaloniki, Alexandrou Mihailidi 13, 54640 Thessaloniki, Greece. telonakos@hotmail.com
Telephone: +30-231-0814161
Fax: +30-231-0551301

Received: December 29, 2016
Peer-review started: December 30, 2016
First decision: February 13, 2017
Revised: June 8, 2017
Accepted: July 22, 2017
Article in press: July 24, 2017
Published online: August 21, 2017

Abstract

AIM

To evaluate the effect of local surgical adhesive glue (albumin/glutaraldehyde-Bioglue) on the healing of colonic anastomoses in rats.

METHODS

Forty Albino-Wistar male rats were randomly divided into two groups, with two subgroups of ten animals each. In the control group, an end-to-end colonic anastomosis was performed after segmental resection. In the Bioglue group, the anastomosis was protected with extraluminar application of adhesive glue containing albumin and glutaraldehyde. Half of the rats were

sacrificed on the fourth and the rest on the eighth postoperative day. Anastomoses were resected and macroscopically examined. Bursting pressures were calculated and histological features were graded. Other parameters of healing, such as hydroxyproline and collagenase concentrations, were evaluated. The experimental data were summarized and computed from the results of a one-way ANOVA. Fisher's exact test was applied to compare percentages.

RESULTS

Bursting pressures, adhesion formation, inflammatory cell infiltration, and collagen deposition were significantly higher on the fourth postoperative day in the albumin/glutaraldehyde group than in the control group. Furthermore, albumin/glutaraldehyde significantly increased adhesion formation, inflammatory cell infiltration, neoangiogenesis, and collagen deposition on the eighth postoperative day. There was no difference in fibroblast activity or hydroxyproline and collagenase concentrations.

CONCLUSION

Albumin/glutaraldehyde, when applied on colonic anastomoses, promotes their healing in rats. Therefore, the application of protective local agents in colonic anastomoses leads to better outcomes.

Key words: Adhesions; Bursting pressure; Bioglue™; Albumin/glutaraldehyde; Collagen; Colonic anastomosis

Core tip: The present study was designed to investigate the effect of local surgical adhesive glue composed of albumin/glutaraldehyde in the healing of colonic anastomoses in rats. The application of adhesive glue promotes the healing of colonic anastomoses in rats as it significantly increases the bursting pressure in the early period, but it also causes more adhesions and an enhanced inflammatory reaction.

Despoudi K, Mantzoros I, Ioannidis O, Cheva A, Antoniou N, Konstantaras D, Symeonidis S, Pramateftakis MG, Kotidis E, Angelopoulos S, Tsalis K. Effects of albumin/glutaraldehyde glue on healing of colonic anastomosis in rats. *World J Gastroenterol* 2017; 23(31): 5680-5691 Available from: URL: http://www.wjgnet.com/1007-9327/full/v23/i31/5680.htm DOI: http://dx.doi.org/10.3748/wjg.v23.i31.5680

INTRODUCTION

Anastomosis dehiscence is a serious postoperative complication, and the risk of anastomotic leakage is higher in large intestine surgery compared with other gastrointestinal anastomoses[1,2]. Different techniques of using additive materials such as omentum and several types of fibrin sealants to cover the anastomosis have been proposed[3,4], and in experimental studies, various protective methods such as endoluminar latex prostheses, stents, biofragmental rings, and local application of bioadhesives have been used, with promising results[5-9]. Tissue glues and fibrin adhesives, which are biodegradable and biocompatible, have been used to seal suture lines for haemostasis and/or to strengthen and reinforce fragile tissues by tissue adherence and replacement or support of sutures by biomaterial gluing[9,10]. The goal is to reduce the incidence of dehiscence by increasing the strength of anastomoses, covering the anastomotic line, and stimulating healing[11]. The possibility of direct influence of extraluminar contents and the substance's biological compatibility, as well as the adhesive and tension strength of the glue, has as a result in the critical healing phase: an increase in the force needed for anastomosis bursting[12].

Local application of albumin/glutaraldehyde (Bioglue™), a haemostatic and adhesive agent, has received approval for many vascular, pulmonary and soft tissue repairs, and its use is already established in cardiothoracic surgery[13,14]. So far, however, there have been no published experiments using this glue in colonic anastomosis. The aim of this experimental study was to investigate the effects of surgical adhesive glue during the healing process of colonic anastomosis in rats.

MATERIALS AND METHODS

Laboratory animals

The animal protocol was designed to minimize pain and discomfort to the animals. Forty male Wistar rats weighing 200-300 g were used in this study. The research protocol was approved by the Ethical Committee of the Department of Veterinary Services of the Prefecture of Thessaloniki (S.N.: 13/11872/11-09-08). Principles of laboratory animal care were followed. Animals were housed individually and had unrestricted access to the standard laboratory diet and water pre- and postoperatively. They were kept in our laboratory for seven-ten days before the experiment on a 12-h light and dark cycle and did not receive any course of chemoprophylaxis. At the sacrifice, all animals were euthanized by intracardiac administration of KCL 10% for tissue collection.

Anaesthesia, operative technique and experimental groups

The rats were weighed on the day of operation as well as before the sacrifice, and changes in weight were recorded. Operations were performed through a 3-cm midline incision under intraperitoneal thiopental anaesthesia (40 mg/kg bodyweight). After resection of a 1-cm segment of the colon and 5 cm from the rectum, an end-to-end anastomosis was created using a single layer of eight interrupted extramucosal 6-0 polypropylene sutures. Rats were randomly assigned

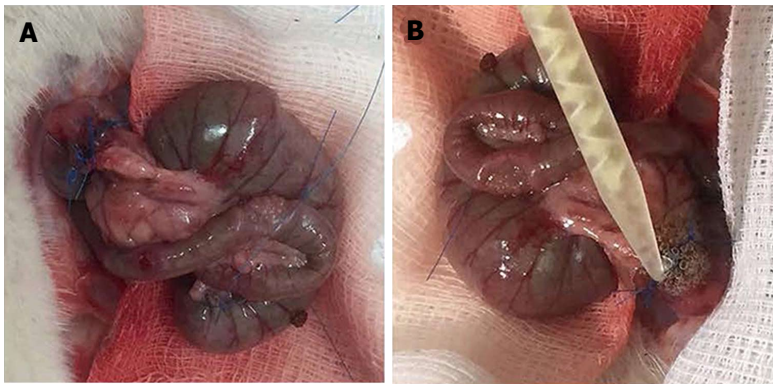

Figure 1 Control and Bioglue group. A: Creation of end-to-end anastomosis using a single layer of eight interrupted extramucosal 6-0 polypropylene sutures; B: Application of the Bioglue on the colon edges after taking precautions to avoid dispersion of the glue in the peritoneal cavity.

to two groups of 20 animals. In the CONTROL group, an end-to-end anastomosis was created (Figure 1A). In the BIOGLUE group, after creating the anastomosis, albumin/glutaraldehyde was applied around it (Figure 1B). The glue was applied on the colon's edges with an applicator. Holding the applicator was sufficient to place the liquid adhesive on the cut edges of the colon, taking precautions to avoid dispersion of the glue in the peritoneal cavity. The abdominal muscle layer and the skin were closed in one layer, using three sutures (3/0 silk). Each group was subdivided in two subgroups of ten animals each, with half of the animals being sacrificed on the fourth postoperative day (CONTROL4 and BIOGLUE4) and the other half being sacrificed on the eighth postoperative day (CONTROL8 and BIOGLUE8)

Macroscopic examination

On the day of sacrifice, the animals were anaesthetized again, and the anastomotic segments were isolated during relaparotomy. The anastomoses were examined macroscopically. Integrity of the anastomosis, existence of perianastomotic abscess or peritonitis, and adhesion formation were recorded. The evaluation was performed according to the scale of van der Ham *et al*[15], as has been described elsewhere. Briefly, anastomosis was given score 0 when no adhesions occurred; score 1 represented minimal adhesions mainly between the anastomosis and the omentum; score 2 corresponded to moderate adhesions, *i.e.*, between the omentum and the anastomotic site or between the anastomosis and a loop of small intestine; finally, score 3 represented severe and extensive adhesions, including abscess formation.

Bursting pressure

Bursting pressure was measured *ex vivo*. The anastomosis was removed along with a 2.5 cm segment of the colon on either side *en bloc* with the formed adhesions and cleared of stools. The proximal end was ligated using a 3/0 silk suture, and a catheter was secured into the distal end and fixed to the bursting pressure apparatus as described elsewhere[16-18]. Through this catheter, the bowel was infused with a continuous flow of physiological saline at a rate of 1 mL/min. The bursting pressure was defined as the pressure at which leakage of saline or gross rupture was noted and recorded in mmHg. The site of leakage during the bursting pressure measurement was also recorded, since in some rats, rupture occurred at the anastomotic site, and in others far from it.

Histological assessment

After the *ex vivo* measurement of bursting pressure, the anastomotic segment of the colon was cleared of the surrounding mesentery and fat and rinsed with saline. The anastomosis was resected along with a 0.5 cm segment of the colon on either side and divided into two parts vertically. The first segment was placed in 4% formaldehyde solution for histopathological examination and stained with haematoxylin and eosin. The anastomosis was examined under a light microscope and graded histologically in a blind fashion, using a 0-4 Ehrlich and Hunt numerical scale as modified by Phillips *et al*[19]. The evaluated parameters were inflammatory cell infiltration (white blood cell count), neoangiogenesis (new blood vessel formation), fibroblast activity, and collagen deposition[20]. Each studied parameter was evaluated individually using a numerical scale from 0 to 4 as follows: 0 (-) = no evidence; 1 (+) = occasional evidence; 2 (++) = light scattering; 3 (+++) = abundant evidence; and 4 (++++) = confluent fibres or cells.

Hydroxyproline

Quantification of collagen in colonic anastomosis is synonymous with quantification of hydroxyproline. The second segment of the anastomosis was weighed and then divided into two parts vertically and stored at -20 ℃. Determination of hydroxyproline tissue contents was performed as described in previous experiments, with some modifications[13,21]. Briefly, after the specimens were lyophilized, a polytron homogenizer was used to homogenize the tissue sample in distilled

water. The acid-soluble collagen was extracted from the tissue sample by overnight incubation with acetic acid 0.5 mol/L at 4 ℃. 70 μL of standard/test sample was hydrolysed in 30 μL NaOH 10.125 mol/L for 25 min at 120 ℃ by autoclaving. The hydrolysed sample was then mixed with a buffered (pH 7) chloramines-T reagent (0.056 mol/L), and at room temperature the oxidation was continued for 25 min. Following the development of chromophore was achieved with the addition of Ehrlich's reagent. The absorbance was measured at 550 nm using a Biotek μQuant™ spectrophotometer. Absorbance values were plotted against the concentration of standard hydroxyproline, and the presence of hydroxyproline in unknown tissue extracts was determined from the standard curve. The results were expressed in μg/g of tissue[21].

Collagenase I

The concentration of collagenase I was estimated in another segment of the anastomotic site by using a commercial ELISA kit (USCNLIFE, E0212r). The test sample was added to the appropriate plate well pre-coated with anti-collagenase I antibody-microtiter with a biotin-conjugated polyclonal antibody specific to collagenase I Then, avidin conjugated to HRP was added to the microplate well and incubated. The chromophore was then developed with the addition of TMB substrate solution, and the reaction stopped with sulphuric acid solution. The colour change was measured spectrophotometrically at 450 nm using a Stat Fax-210™ spectrophotometer (Awareness Technology Inc.). The concentration of collagenase I in unknown tissue samples was determined from the standard curve. The results were calculated as μg/g of wet tissue weight[22].

Statistical analysis

Using statistical descriptive indices of central tendency and dispersion the experimental data were summarized. Data are presented as mean ± SD. After performing a normality test, if the data presented a normal distribution we used ANOVA to compare all four groups and and the least significant difference criterion[23] as *post hoc* analysis to make comparisons between groups. If the data didn't have normal distribution we used the non-parametric Kruskal-Wallis test to compare all four groups and performed the Mann-Whitney test to make comparisons between groups, with the significance level for the certain test adjusted to $P = 0.0125$ (0.05/4). The significance level of statistical hypothesis testing procedures concerning comparisons of means was pre-set at $P < 0.05$. All the statistical analyses were performed using the SPSS version 15.0 statistical package (SPSS Inc., Chicago, IL, United States) enhanced with the module Exact Tests[24,25]. The statistical methods of this study were reviewed by Dr. Haidich AB, Assistant Professor in Hygiene-Medical Statistics, Aristotle University of Thessaloniki, Greece.

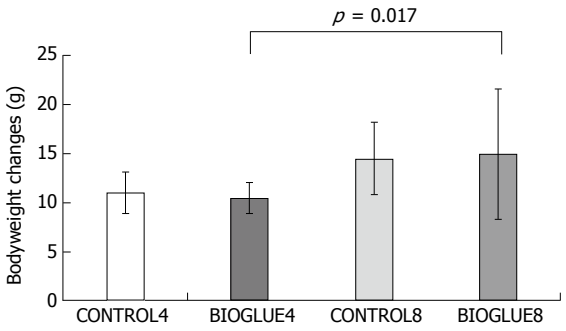

Figure 2 Bodyweight changes in grams in the two groups (mean ± SD). A statistically significant difference was found between subgroups BIOGLUE4 and BIOGLUE8.

RESULTS

Mortality, infection, and anastomotic dehiscence

No deaths or wound infections occurred, and no anastomotic dehiscence was noted before the day of sacrifice.

Bodyweight change

In all the experimental groups, the bodyweight decreased from the day of the experiment till the day of sacrifice. Bodyweight changes differed significantly among the subgroups ($P = 0.03$). In particular, the only significant difference in bodyweight change was between subgroups BIOGLUE4 and BIOGLUE8 ($P = 0.017$), but there were no other differences between subgroups. The bodyweight changes are presented in Figure 2.

Adhesion Formation

On the fourth postoperative day, in subgroup CONTROL4, 90% of animals had no adhesions, and only 10% presented with grade 1 adhesions, while in subgroup BIOGLUE4, all animals had adhesions, and the adhesion formation score was grade 2 in all animals. On the eighth postoperative day, in subgroup CONTROL8, 90% of animals had no adhesions, and only 10% presented with grade 1 adhesions, while in subgroup BIOGLUE8, all animals had adhesions, and the adhesion formation score was grade 2 in all animals (Figure 3).

The adhesion formation score differed significantly between groups ($P < 0.001$). It was significantly higher in both Bioglue subgroups than in the two control groups ($P < 0.001$ in both cases). The adhesion formation scores are presented in Figure 4.

Bursting Pressure measurement

There was a significant difference in bursting pressure among groups ($P < 0.001$). Bursting pressure was significantly increased in the Bioglue subgroup

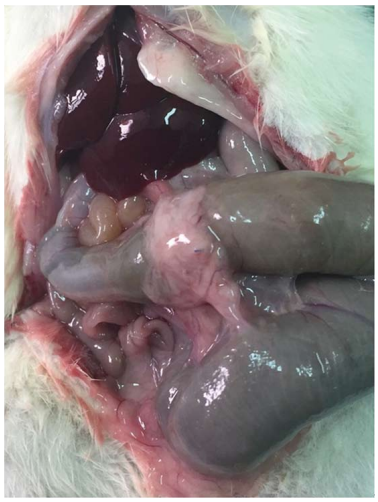

Figure 3 Moderate adhesion formation between the omentum and the anastomotic site in the Bioglue group.

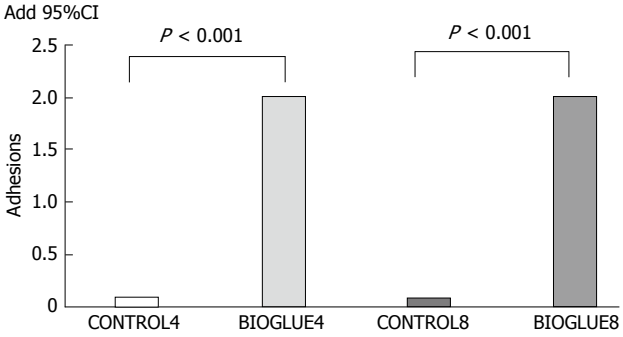

Figure 4 Comparative bar chart of adhesion formation (mean). The adhesion formation score was statistically significantly higher in both Bioglue subgroups compared to control.

compared to the control subgroup on the fourth postoperative day (P = 0.017) but not on the eighth postoperative day (P = 0.545). Furthermore, bursting pressure was statistically significantly higher on the eighth postoperative day in both the Bioglue and the control groups, with P < 0.001 in both cases. The differences in bursting pressures are presented in Figure 5.

Regarding the site of leakage during the measurement of bursting pressure, on the fourth postoperative day in both the control (CONTROL4) and the study (BIOGLUE4) groups, the rupture occurred in 50% of the animals at the anastomosis and in 50% far from it, while on the eighth postoperative day in both subgroups (CONTROL8 and BIOGLUE8), all ruptures occurred far from the anastomotic site.

Histological assessment

The histological assessment of the anastomotic healing included measurements of inflammatory cell infiltration, neoangiogenesis, fibroblast activity, and collagen deposition. In Figure 6, histology images of various degrees of inflammation, neoangiogenesis, fibroblast activity, and collagen deposition are presented,

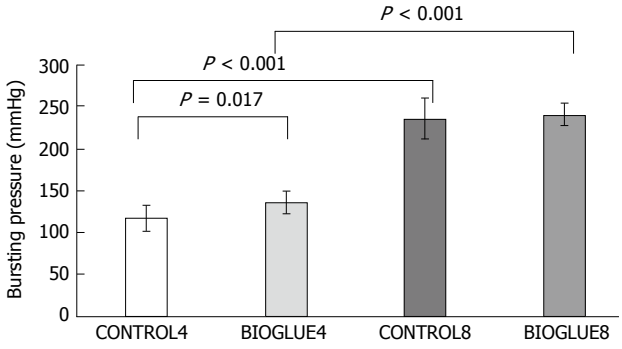

Figure 5 Comparative bar chart presenting bursting pressures (mmHg) (mean ± SD). A statistically significant increase in the bursting pressure was noted on the fourth postoperative day in the Bioglue subgroup compared to the control.

respectively.

Statistical analysis revealed significant changes in all histological parameters: inflammation (P < 0.001), neoangiogenesis (P < 0.001), fibroblast activity (P = 0.001), and collagen deposition (P < 0.001).

The average inflammatory cell infiltration was significantly higher in the Bioglue subgroups than in the controls for both postoperative days, with P < 0.001 in both cases. There was also a significant difference between subgroups CONTROL4 and CONTROL8 (P < 0.001) and between BIOGLUE4 and BIOGLUE8 (P = 0.001). The changes in inflammatory cell infiltration among groups are presented in a histogram in Figure 7A.

Regarding neoangiogenesis, in the Bioglue group, there was an increase on the fourth and eighth postoperative days compared to the control group, but this difference was significant only on the eighth postoperative day (CONTROL4 *vs* BIOGLUE4 with P = 0.2398 and CONTROL8 *vs* BIOGLUE8 with P = 0.039). Neoangiogenesis was also statistically significantly higher on the eighth postoperative day in both Bioglue and control groups (CONTROL4 *vs* CONTROL8 with P = 0.014 and BIOGLUE4 *vs* BIOGLUE8 with P = 0.002). Changes in neoangiogenesis between groups are plotted in Figure 7B.

The fibroblast activity was similar in the Bioglue subgroups and in the control subgroups on both postoperative days (CONTROL4 *vs* BIOGLUE4, P = 1, and CONTROL8 *vs* BIOGLUE8, P = 1). However, there was a significant difference between subgroups CONTROL4 and CONTROL8 (P = 0.002) and between BIOGLUE4 and BIOGLUE8 (P = 0.002). The changes in fibroblast activity among groups are presented in a histogram in Figure 7C.

Collagen deposition was statistically significantly lower in the control subgroups than in the Bioglue subgroups (CONTROL4 *vs* BIOGLUE4 and CONTROL8 *vs* BIOGLUE8 with P = 0.032 and P = 0.002, respectively). There was also a significant increase in collagen deposition between subgroups CONTROL4 and CONTROL8 (P < 0.001) and between BIOGLUE4 and BIOGLUE8 (P < 0.001). Changes in collagen deposition between groups are presented in Figure 7D.

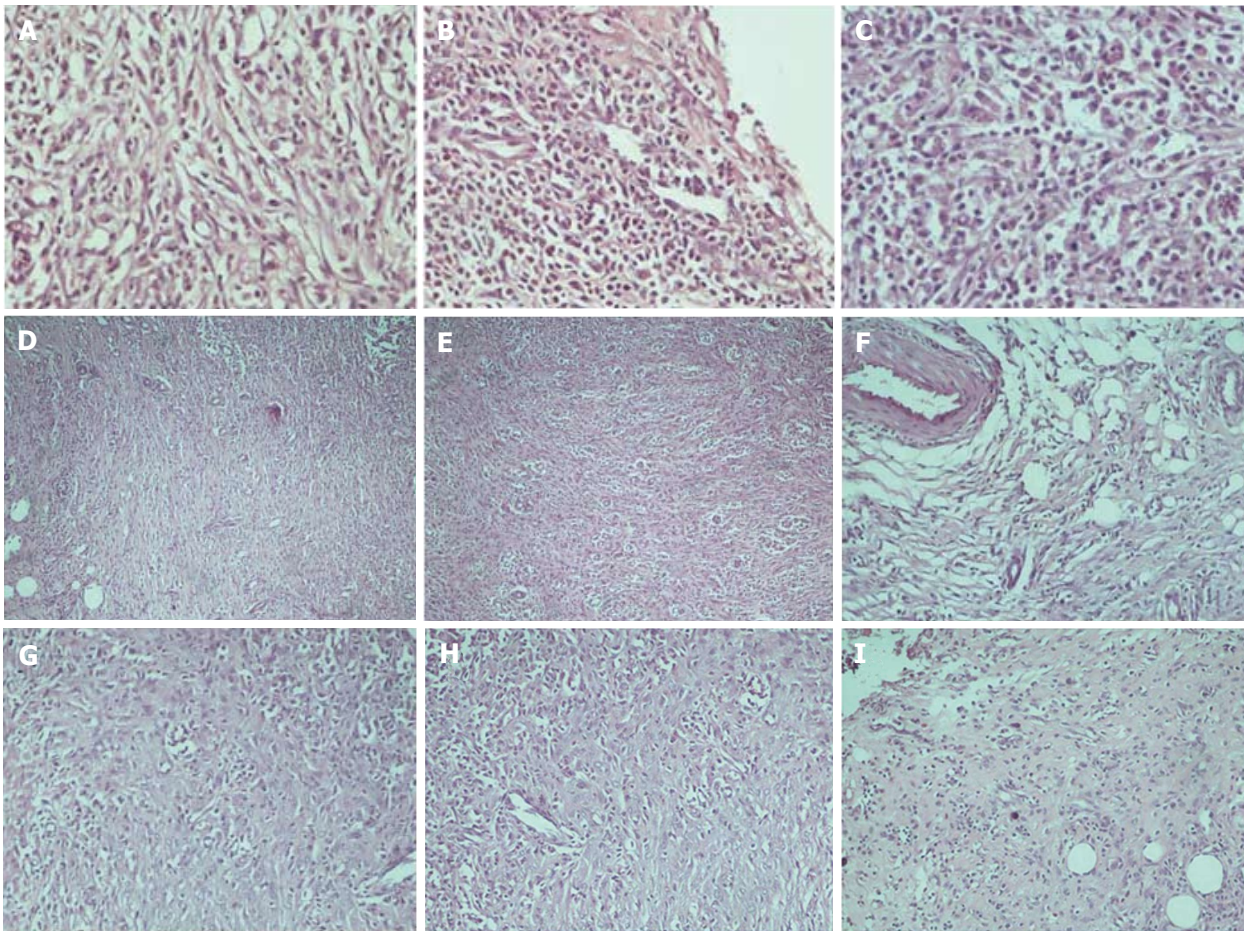

Figure 6 Representative haematoxylin-eosin histopathology images. A: Inflammatory cell infiltration revealing light scattering (× 400); B: Abundant evidence (× 400); C: Confluent cells (× 400); D: Neoangiogenesis revealing light scattering (A, × 100); E: Abundant evidence (× 100); F: Fibroblast activity revealing light scattering (× 100); G: Abundant evidence (× 200); H: Collagen deposition revealing light scattering (× 200); I: Abundant evidence (× 100).

Hydroxyproline and collagenase I concentration

Hydroxyproline concentration differed significantly between groups. Specifically, it was similar on the fourth and eighth postoperative days between the two groups (CONTROL4 *vs* BIOGLUE4 with $P = 0.656$ and CONTROL8 *vs* BIOGLUE8 with $P = 0.309$), but there was a significant increase in the hydroxyproline tissue content of both groups (control and Bioglue) on the eighth postoperative day compared to the fourth (BIOGLUE4 *vs* BIOGLUE8 and CONTROL4 *vs* CONTROL8, with $P < 0.001$ in both cases). The results are presented in Figure 8A.

Collagenase I concentration was similar between the two groups and subgroups on the fourth and eighth postoperative days ($P = 0.959$). Specifically, CONTROL4 *vs* BIOGLUE4 ($P = 0.912$) and CONTROL8 *vs* BIOGLUE8 ($P = 0.796$). CONTROL4 *vs* CONTROL8 ($P = 0.684$) and BIOGLUE4 *vs* BIOGLUE8: ($P = 0.912$). The results are presented in Figure 8B.

DISCUSSION

Anastomotic leakage remains the most important cause of postoperative mortality and morbidity in colorectal surgery[26,27]. Intestinal anastomoses are complicated by leakages, even in the most experienced of hands and despite the development of new surgical techniques, suture materials, and stapling devices[28,29].

Many factors affect the healing of anastomoses, divided into general and local ones[30]. General factors include the patient's age and diet, hypovolemia, malignancy, medications (*e.g.*, steroids, nonsteroidal anti-inflammatory drugs, and 5-FU), immunocompetence, blood transfusion, radiotherapy, diabetes, uraemia, anaemia, jaundice, and nutrient deficiencies (vitamin C, iron, zinc, methionine, cysteine, *etc.*)[16,31-34]. Local factors include ischaemia at the anastomotic site, anastomotic tension, surgical technique, peritonitis, pre-operative bowel preparation, infection, and emergency or elective surgery[34-36]

Bioglue surgical adhesive is a two-component surgical adhesive that confers enhanced bonding properties. It is composed of 45% purified bovine serum albumin and 10% glutaraldehyde. The advantage of Bioglue is that the bi-functional glutaraldehyde molecule covalently bonds the bovine serum albumin molecules to each other, as well as to lysine in proteins on the cell surface and in the extracellular matrix. This reaction is spontaneous, increasing tensile and shear strength. The albumin provides an extensive flexible network of bonds.

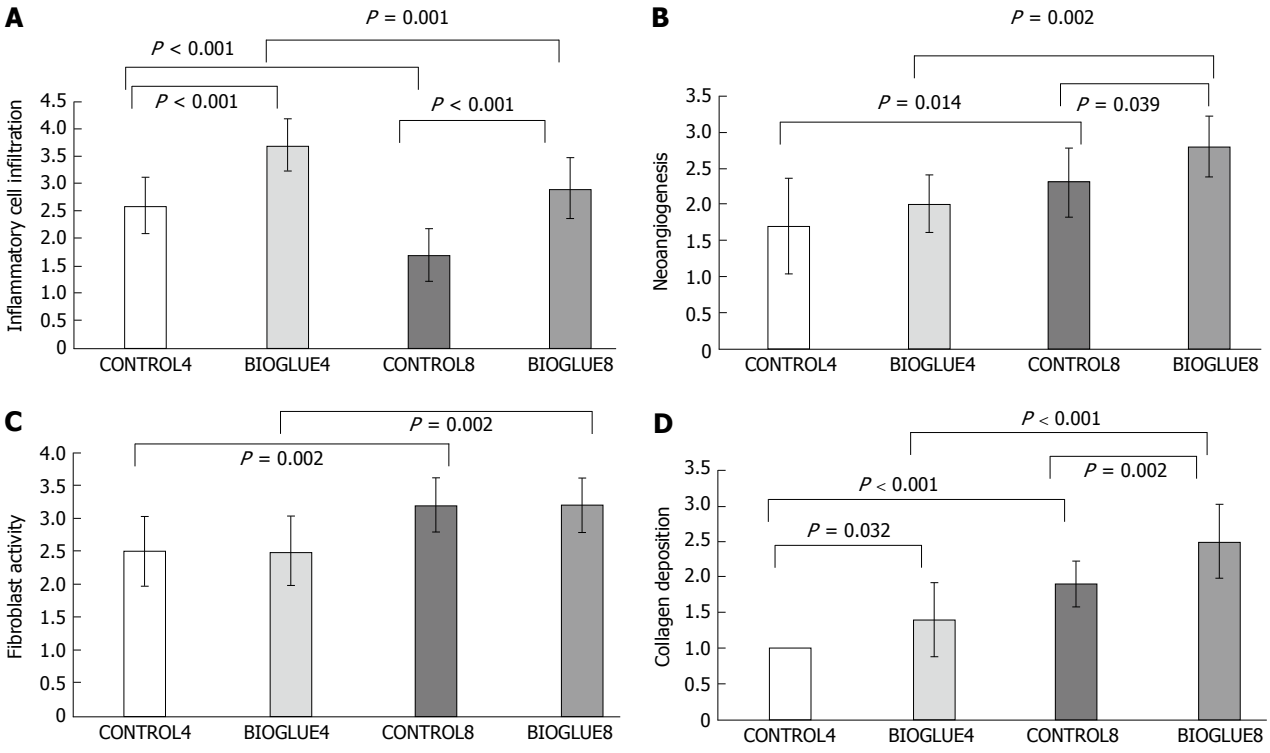

Figure 7 Comparative bar chart presenting the average inflammatory cell infiltration (A), new vessel formation (neoangiogenesis) (B), fibroblast activity (C) and collagen deposition (D), according to the scale of Ehrlich and Hunt, as modified by Phillips *et al*[19] (0-4) (mean ± SD). A: The average inflammatory cell infiltration was statistically significantly higher in the Bioglue subgroups on both the fourth and eighth days than in the controls. Also, in each subgroup, there was a statistically significant decrease in the average inflammatory cell infiltration from the fourth to the eighth day; B: The average neoangiogenesis was statistically significantly higher in the Bioglue subgroups on the eighth day than in the control. Also, in each subgroup, there was a statistically significant increase in neoangiogenesis from the fourth to the eighth day; C: The average fibroblast activity was statistically significantly higher in each subgroup from the fourth to the eighth day; D: The average collagen deposition was statistically significantly higher in the Bioglue subgroups on both the fourth and eighth days than in the control. Also, in each subgroup there was a statistically significant increase in collagen deposition from the fourth to the eighth day.

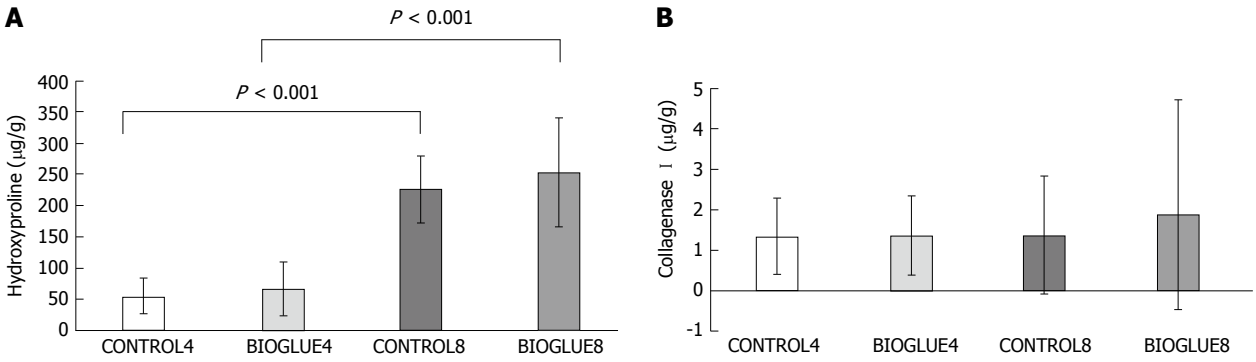

Figure 8 Comparative bar chart of hydroxyproline tissue contents (A), collagenase I tissue contents (B) (μg/g tissue) at the anastomotic site (mean ± SD). A: In each subgroup, there was a statistically significant increase in hydroxyproline tissue content from the fourth to the eighth day; B: No statistically significant difference was noted.

When applied to the repair site, it forms a watertight mechanical seal and holds sutures securely[13]. It is necessary to dry the completed anastomosis as much as possible and to protect the area surrounding the target tissue with moist sterile gauze pads[37]. Polymerisation commences rapidly within 20 to 30 s and reaches full bonding strength in two minutes[38].

Patients with colorectal cancer usually lose weight, and malnutrition accompanying loss of bodyweight decreases the deposition of collagen and the anastomotic strength[39]. As expected following surgery, in our study, the mean postoperative bodyweight was lower both on the fourth and the eighth postoperative days in all subgroups compared to the beginning of the experiment. However, a comparison of the control and Bioglue subgroups revealed that there wasn't any statistically significant difference between their mean bodyweights. The only significant difference was a greater decrease in bodyweight in the Bioglue group on the eighth day compared to the fourth day.

Adhesions are fibrous bands that connect the peritoneal organs to each other or the peritoneum and could possibly seal any potential micro-leakages from the anastomosis and simultaneously enhance the local blood supply[40,41]. The incidence of adhesion formation appears to be caused by many factors, such as sutures or staples that can potentially cause topical ischemia. The foreign material used can lead to an infected anastomosis followed by anastomotic leakage[42]. Furthermore, adhesion formation is dependent on the severity of the intestinal serosal trauma, fibroblast activation, metalloproteinase activity, and the efficiency of the fibrinolytic mechanism[43-45]. Adhesion formation is a serious problem to tackle when using glue for anastomosis. In the Bioglue group, there was an increase in the adhesion formation score that was statistically significant. Similar are the results of Ozel *et al*[46], who, in an experimental study in rats using a fibrin patch to support colonic anastomoses, found more adhesions of greater degree in the study group compared to the control. However, Kanellos *et al*[47] using a fibrin glue, didn't notice any difference in adhesion formation compared to the control group in rats with colonic anastomosis, while Haukipuro *et al*[48] demonstrated fewer adhesions using fibrin sealant. Detweiler *et al*[49] proposed the combination of absorbable stents and fibrin glue to avoid adhesion formation and intestinal obstruction.

The percentage of anastomotic leakage is the most important marker reflecting the efficacy of the healing mechanisms of intestinal anastomoses and ranges from 3% to 30%[1,2,50,51]. In the present study, no anastomotic leakage was noted in either subgroup on the fourth or the eighth postoperative day, reflecting the efficacy of healing mechanisms in both groups. The mechanical strength of the anastomosis is determined by its bursting pressure. It is therefore a useful parameter to measure the healing process in the first week after anastomotic formation[52]. Bursting pressure increases progressively after the formation of the anastomosis. In our study, the bursting pressures were significantly higher in both the control group and the Bioglue group on the eighth postoperative day than the fourth. Moreover, Bioglue significantly increased bursting pressures compared to the control on the fourth postoperative day but not on the eighth. Hjortrup *et al*[53] found that the bursting pressure of small bowel segments with fibrin anastomoses was similar to those with sutured anastomoses. Capitán Morales *et al*[54] compared three groups of rats: one with anastomoses sutured with silk 5/0, one with anastomoses sutured with polyglycolic acid 5/0, and one with suture-less fibrin adhesive anastomoses. They found that the greatest bursting pressure occurred in the last series. Additionally, Akgün *et al*[55] in an experimental study using a fibrin sealant to protect anastomoses in rats, demonstrated an increase in bursting pressure in the study group compared to the control.

A fundamental element in the assessment of bursting pressure and the efficacy of healing mechanisms is the part of the colon that ruptures during the measurement of bursting pressure[10,56,57]. Rupture at the anastomotic site happens in mechanically weaker anastomoses or anastomoses at the early healing phase, between the third and fifth days. In contrast, rupture far from an anastomosis presents in mechanically very strong anastomoses or in anastomoses in the late healing phase, specifically in the remodelling phase[2,28]. In the current study, there were no differences in the rupture sites among the subgroups.

Healing of anastomoses is a complicated process which is divided into four different phases: coagulation, inflammation, migration and proliferation, and remodelling. Inflammation is the second phase and is characterized by infiltration of the anastomosis by inflammatory cells, especially leukocytes[58-60]. Macrophages, lymphocytes and thrombocytes produce and secrete cytokines and growth factors that regulate neoangiogenesis and collagen synthesis[60-63] and have mitogenic, chemotactic, and cell movement stimulant functions[62]. The crucial role of neutrophils in the early postoperative weakening of the anastomosis due to activation of metalloproteinases and collagen degradation is well established[64-67]. The foreign bodies such as sutures, clips, and any biological substances (glues) which are used in the anastomosis are those that keep the anastomosis intact during the healing phase[1,3,10]. In our study, inflammatory cell infiltration was statistically significantly higher in the Bioglue subgroups than in the control subgroups on both postoperative days. Ozel *et al*[46] noticed a significant increase in the inflammatory reaction in the fibrin patch group compared to the control, which was attributed to the increased activity of the inflammatory cells and metalloproteinases between the third and seventh postoperative days due to the presence of the fibrin patch.

After inflammation comes the proliferative phase of healing, characterized by the production of collagen by fibroblasts, which increases the strength of the anastomosis[68-70]. The fibroblasts secrete hyaluronic acid and proteoglycans, which are important for cell movement, function, and tissue resilience, and collagen, promoting anastomotic healing[71]. According to the results of our experimental study, fibroblast activity was similar between the subgroups both on the fourth and the eighth postoperative days. This finding is in contrast with Akgün *et al*[55], who demonstrated an increase of fibroblasts in the fibrin sealant group compared to the control.

Neoangiogenesis is the formation of new blood vessels from the endothelium of pre-existing ones and takes place in the third phase of healing, the proliferative phase, leading to the formation of granular tissue[39,72-74]. It has been shown that this phase is affected by various angiogenic factors such as platelet derived growth factor, tumour necrosis factor-α, and

Vascular Endothelial Growth Factor family[61,75]. In our study, the degree of neoangiogenesis was affected by the presence of Bioglue: neoangiogenesis was statistically significantly higher in the Bioglue group only on the eighth postoperative day. Ozel *et al*[46] also found that neoangiogenesis was higher in the fibrin patch group than in the control.

The production and deposition of collagen, which takes place during the third (proliferation) and fourth (remodelling) phases, is a significant marker of the efficacy of the anastomotic healing process[45,65,68,76,77]. Collagen is mainly produced by fibroblasts and metabolized by certain metalloproteinases, called collagenases[68,78,79]. In our study, collagen deposition was significantly higher in the Bioglue group on both the fourth and the eighth days, a finding similar to Ozel *et al*[46] who noticed increased collagen production in the fibrin patch group compared to the control.

Histological analysis of anastomotic colon wall samples demonstrated the favourable influence of Bioglue on the complex process of colon anastomosis healing, reflected in the stimulation of the proliferative response, promotion of neoangiogenesis, more abundant young collagen synthesis, and reduction of the duration of the critical healing period.

The mechanical strength of healing wounds depends on fibroblast proliferation and the synthesis of collagen molecules. Collagen determines the mechanical stability and healing capacity of connective tissue. The quantitative measurement of collagen deposed in the anastomosis is accomplished by the measurement of hydroxyproline in the anastomotic tissue[45,80]. Hydroxyproline is one of the basic amino acids of collagen, and its presence is restricted exclusively to the collagen of connective tissue. Low hydroxyproline levels negatively affect the mechanism of colonic anastomosis healing[44,81]. We found that there was a statistically significant increase in hydroxyproline tissue content in both groups (control and Bioglue) on the eighth postoperative day compared to the fourth but no difference between the groups on either the fourth or the eighth day. Ozel *et al*[46] also demonstrated an increased hydroxyproline concentration in the fibrin patch group compared to the control.

In the third phase of healing, the collagen is synthesized and degraded by a variety of collagenase enzymes from granulocytes, macrophages, and fibroblasts. The concentration of mature collagen in the early phase of healing is decreased up to 40%, an event that correlates with a reduction in the mechanical strength of the anastomosis at this phase and with possible anastomotic dehiscence[45,77,80]. Many studies have shown that their activity is a major pathogenic factor in the postoperative decline of colonic anastomosis strength. Experimental studies have shown maximal collagenetic activity in the colon on the third postoperative day[82]. Collagenase is responsible for the degradation of mature collagen, and its concentration maximizes on the third postoperative day, when increased degradation of type Ⅲ collagen and synthesis of type Ⅰ collagen takes place[44,70,71,83].

Furthermore, immunohistochemical studies have shown that collagenase and other matrix metalloproteinases (MMPs) are in close vicinity to the suture line in uncomplicated anastomotic healing[71], so the measurement of collagenase concentration is a marker reflecting the balance of collagenogenesis and collagenolysis[43,84,85]. It has been previously demonstrated that the MMP levels in the anastomotic line are very different from those in adjacent tissue, where the level of MMPs was measured at up to 0.15-0.2 cm from the anastomotic line[86,87]. In the current experiment, collagenase was measured in a segment of 0.5 cm on both sides of the anastomosis in each animal. While the levels of collagenase vary at the anastomotic line and 0.5 cm from it, as tissue samples were the same in all animals, the measured collagenase activity in 1 cm of large intestine with the anastomosis in the middle reflects the total collagenase activity, which is comparable between groups. Collagenase Ⅰ concentration was similar between the two groups and subgroups on the fourth and on the eighth postoperative days.

In the early period of anastomotic healing, Bioglue seems to support anastomotic integrity in rats, since it increases the bursting pressure. This effect of Bioglue has also been demonstrated in *ex vivo* porcine gastrojejunal anastomosis[88]. However, it also causes an inflammatory reaction which may increase the time necessary for the healing process. This may represent a major disadvantage for this biomaterial. Regarding the safety of Bioglue, our study demonstrated that the application of Bioglue on the suture line is not associated with increased mortality or dehiscence, in contrast with the study of Slieker *et al*[89] where the application of Bioglue on sutured colonic anastomoses in mice caused a 100% mortality rate, compared with the 40% mortality rate in the control group. Further studies are most likely required in order to assess the effects of Bioglue on anastomotic healing after direct administration into the colon, as there is only one other study assessing Bioglue's effect in suture-less closure of colonic defects[90].

COMMENTS

Background

Anastomosis dehiscence is a serious postoperative complication in gastrointestinal surgery, and anastomotic leakage remains the most important cause of postoperative mortality and morbidity in colorectal surgery. The risk of anastomotic leakage is higher in large intestine surgery compared with other gastrointestinal anastomoses. Intestinal anastomoses are complicated by leakages, even in the best and most experienced of hands and despite the development of new surgical techniques, suture materials, and stapling devices. The efficacy of biomaterial over intestinal anastomoses is still controversial in clinical practice.

Research frontiers

The replacement or support of sutures by biomaterial gluing procedures has been investigated for many years. Different techniques using additive materials such as omentum and several types of fibrin sealants to cover the anastomosis have been proposed. Out of a large number of experimental studies, various

protective methods such as endoluminar latex prostheses, stents, biofragmental rings, and local application of bioadhesives have been used, with promising results. Tissue glues have been used to seal suture lines for haemostasis and to strengthen and reinforce fragile tissues by tissue adherence. The main idea was to reduce the incidence of dehiscence by increasing the strength of anastomoses, covering the anastomotic line and stimulating healing.

Innovations and breakthroughs

The current study demonstrated the safety and efficacy of Bioglue application on a colonic anastomosis, as it promotes the healing process, especially in the early stages, and increases the bursting pressure. The increase in the mechanical strength of the colonic anastomosis in the early stages is a result of increased adhesion formation and increased collagen deposition and takes place in spite of increased inflammatory cell infiltration.

Applications

The application of biological glue on colonic anastomosis in clinical practice may reduce anastomotic dehiscence and leakage and decrease the related morbidity and mortality

Terminology

Bioglue is a two-component surgical adhesive that confers enhanced bonding properties. It is composed of 45% purified BSA and 10% glutaraldehyde. The advantage of Bioglue is that the bi-functional glutaraldehyde molecule covalently bonds the bovine serum albumin molecules to each other, as well as to lysine in proteins on the cell surface in the extracellular matrix. This reaction is spontaneous, increasing tensile and shear strength independently of the coagulation status of the patient. The albumin provides an extensive flexible network of bonds. When applied to the repair site, it forms a mechanical watertight seal and holds sutures securely.

Peer-review

An interesting paper on sealment of experimental anastomoses in a rat model.

REFERENCES

1 **Buchs NC**, Gervaz P, Secic M, Bucher P, Mugnier-Konrad B, Morel P. Incidence, consequences, and risk factors for anastomotic dehiscence after colorectal surgery: a prospective monocentric study. *Int J Colorectal Dis* 2008; **23**: 265-270 [PMID: 18034250 DOI: 10.1007/s00384-007-0399-3]

2 **Rudinskaite G**, Tamelis A, Saladzinskas Z, Pavalkis D. Risk factors for clinical anastomotic leakage following the resection of sigmoid and rectal cancer. *Medicina* (Kaunas) 2005; **41**: 741-746 [PMID: 16227705]

3 **Kanellos I**. Progress in the treatment of colorectal cancer. *Tech Coloproctol* 2004; **8** Suppl 1: s1-s2 [PMID: 15655586 DOI: 10.1007/s10151-010-0619-7]

4 **Schrock TR**, Deveney CW, Dunphy JE. Factor contributing to leakage of colonic anastomoses. *Ann Surg* 1973; **177**: 513-518 [PMID: 4540874 DOI: 10.1097/00000658-197305000-00002]

5 **Fukunaga S**, Karck M, Harringer W, Cremer J, Rhein C, Haverich A. The use of gelatin-resorcin-formalin glue in acute aortic dissection type A. *Eur J Cardiothorac Surg* 1999; **15**: 564-569; discussion 570 [PMID: 10386398 DOI: 10.1016/s1010-7940(99)00084-6]

6 **Nomori H**, Horio H, Morinaga S, Suemasu K. Gelatin-resorcinol-formaldehyde-glutaraldehyde glue for sealing pulmonary air leaks during thoracoscopic operation. *Ann Thorac Surg* 1999; **67**: 212-216 [PMID: 10086552 DOI: 10.1016/s0003-4975(98)0184-9]

7 **Fleisher AG**, Evans KG, Nelems B, Finley RJ. Effect of routine fibrin glue use on the duration of air leaks after lobectomy. *Ann Thorac Surg* 1990; **49**: 133-134 [PMID: 2297261 DOI: 10.1016/0003-4975(90)90371-C]

8 **Luukkonen P**, Järvinen HJ, Haapiainen R. Early experience with biofragmentable anastomosis ring in colon surgery. *Acta Chir Scand* 1990; **156**: 795-799 [PMID: 2075777]

9 **Hardy TG Jr**, Pace WG, Maney JW, Katz AR, Kaganov AL. A biofragmentable ring for sutureless bowel anastomosis. An experimental study. *Dis Colon Rectum* 1985; **28**: 484-490 [PMID: 4017807 DOI: 10.1007/BF02554090]

10 **Uzunköy A**, Akinci OF, Coskun A, Aslan O, Kocyigit A. Effects of antiadhesive agents on the healing of intestinal anastomosis. *Dis Colon Rectum* 2000; **43**: 370-375 [PMID: 10733119 DOI: 10.1007/BF02258304]

11 **Fini M,** Giardino R, Giavaresi G, Rocca M, Aldini N. Tissue Adhesives in Experimental Intestinal Anastomoses. Fibrin Sealing in Surgical and Nonsurgical Fields. *Gen Abdominal Surg Pediatr Surg* 1994; **2**: 136-141 [DOI: 10.1007/978-3-642-85101-8_17]

12 **Coselli JS,** Bavaria JE, Fehrenbacher J, Stowe CL, Macheers SK, Gundry SR. Prospective randomised study of a protein-based tissue adhesive used as a haemostatic and structural adjunct in cardiac and vascular anastomotic repair procedures. *J Am Coll Surg* 2003; **197**: 243-253 [DOI: 10.1016/S1072-7515(03)00376-4]

13 **Hewitt CW,** Mara S, Chrzanowski ANFJ. A novel tissue bioadhesive (BioGlue®) for thoracic aorta repair in coagulopathic sheep. 34th Congress of the European Society for Surgical Research; 1999 April; Bern, Switzerland

14 **Raanani E**, Latter DA, Errett LE, Bonneau DB, Leclerc Y, Salasidis GC. Use of "BioGlue" in aortic surgical repair. *Ann Thorac Surg* 2001; **72**: 638-640 [PMID: 11515926 DOI: 10.1016/S0003-4975(01)02663-7]

15 **van der Ham AC**, Kort WJ, Weijma IM, van den Ingh HF, Jeekel H. Effect of antibiotics in fibrin sealant on healing colonic anastomoses in the rat. *Br J Surg* 1992; **79**: 525-528 [PMID: 1611443 DOI: 10.1002/bjs.1800790617]

16 **Sapidis N**, Tziouvaras C, Ioannidis O, Kalaitsidou I, Botsios D. The effect of glutamine and synbiotics on the healing of colonic anastomosis. *Rev Esp Enferm Dig* 2014; **106**: 255-262 [PMID: 25075656]

17 **Galanopoulos G**, Pramateftakis MG, Raptis D, Mantzoros I, Kanellos D, Angelopoulos S, Koliakos G, Zaraboukas T, Lazaridis C. The effects of iloprost on colonic anastomotic healing in rats. *Tech Coloproctol* 2011; **15** Suppl 1: S117-S120 [PMID: 21956403 DOI: 10.1007/s10151-011-0758-5.]

18 **Galanopoulos G**, Raptis D, Pramateftakis MG, Mantzoros I, Kanellos I, Lazarides C. The effects of iloprost on colonic anastomotic healing in rats under obstructive ileus conditions. *J Surg Res* 2014; **189**: 22-31 [PMID: 24582070 DOI: 10.1016/j.jss.2014.01.052.]

19 **Phillips JD**, Kim CS, Fonkalsrud EW, Zeng H, Dindar H. Effects of chronic corticosteroids and vitamin A on the healing of intestinal anastomoses. *Am J Surg* 1992; **163**: 71-77 [PMID: 1733376 DOI: 10.1016/0002-9610(92)90255-P]

20 **Shomaf M**. Histopathology of human intestinal anastomosis. *East Mediterr Health J* 2003; **9**: 413-421 [PMID: 15751935]

21 **Reddy GK**, Enwemeka CS. A simplified method for the analysis of hydroxyproline in biological tissues. *Clin Biochem* 1996; **29**: 225-229 [PMID: 8740508 DOI: 10.1016/0009-9120(96)00003-6]

22 **Raptis D**, Mantzoros I, Pramateftakis MG, Despoudi K, Zaraboukas T, Koliakos G, Kanellos I, Lazarides Ch. The effects of tacrolimus on colonic anastomotic healing in rats. *Int J Colorectal Dis* 2012; **27**: 299-308 [PMID: 22065109 DOI: 10.1007/s00384-011-1337-y.]

23 **Toothaker L**. Multiple Comparison Procedures. Newbury Park: Sage Publications, Inc., 1993

24 **Mehta C**, Patel R. SPSS Exact Tests 7.0 for Windows. Chicago 1996: SPSS Inc.

25 **Fleis JL**. Statistical methods for rates and proportions. 2nd ed. New York: John Wiley and Sons, 1981

26 **Platell C**, Barwood N, Dorfmann G, Makin G. The incidence of anastomotic leaks in patients undergoing colorectal surgery. *Colorectal Dis* 2007; **9**: 71-79 [PMID: 17181849 DOI: 10.1111/j.1463-1318.2006.01002.x]

27 **Zacharakis E,** Demetriades H, Kanellos D, Sapidis N, Zacharakis E, Mantzoros I, Kanellos I, Koliakos G, Zaraboukas T, Topouridou K, Betsis D. Contribution of insulin-like growth factor I to the healing of colonic anastomoses in rats. *J Invest Surg* 2007; **20**: 9-14

[PMID: 17365402 DOI: 10.1080/08941930601126074]
28 **Willis S**, Stumpf M. [Leakages after surgery of the lower gastrointestinal tract]. *Chirurg* 2004; **75**: 1071-1078 [PMID: 15316639 DOI: 10.1007/s00104-004-0895-8]
29 **Kanellos I**, Mantzoros I, Demetriades H, Kalfadis S, Sakkas L, Kelpis T, Betsis D. Sutureless colonic anastomosis in the rat: a randomized controlled study. *Tech Coloproctol* 2002; **6**: 143-146 [PMID: 12525906 DOI: 10.1007/s101510200033]
30 **Kingham TP**, Pachter HL. Colonic anastomotic leak: risk factors, diagnosis, and treatment. *J Am Coll Surg* 2009; **208**: 269-278 [PMID: 19228539 DOI: 10.1016/j.jamcollsurg.2008.10.015]
31 **Kanellos D**, Pramateftakis MG, Mantzoros I, Zacharakis E, Raptis D, Despoudi K, Zaraboukas T, Koliakos G, Lazaridis H. The effects of the intraperitoneal administration of oxaliplatin and 5-FU on the healing of colonic anastomoses: an experimental study. *Tech Coloproctol* 2011; **15** Suppl 1: S111-S115 [PMID: 21953242 DOI: 10.1007/s10151-011-0754-9.]
32 **Pramateftakis MG**, Kanellos D, Mantzoros I, Despoudi K, Raptis D, Angelopoulos S, Koliakos G, Zaraboukas T, Lazaridis C. Intraperitoneally administered irinotecan with 5-fluorouracil impair wound healing of colonic anastomoses in a rat model: an experimental study. *Tech Coloproctol* 2011; **15** Suppl 1: S121-S125 [PMID: 21887556 DOI: 10.1007/s10151-011-0755-8]
33 **Mantzoros I**, Kanellos I, Demetriades H, Christoforidis E, Kanellos D, Pramateftakis MG, Zaraboukas T, Betsis D. Effects of steroid on the healing of colonic anastomoses in the rat. *Tech Coloproctol* 2004; **8** Suppl 1: s180-s183 [PMID: 15655615 DOI: 10.1007/s10151-004-0150-9]
34 **Goulder F**. Bowel anastomoses: The theory, the practice and the evidence base. *World J Gastrointest Surg* 2012; **4**: 208-213 [PMID: 23293735 DOI: 10.4240/wjgs.v4.i9.208]
35 **Rygl M**, Novotna J, Herget J, Skaba R, Snajdauf J. Parameters of healing in approximative intestinal anastomosis. *Eur J Pediatr Surg* 2009; **19**: 25-29 [PMID: 19221949 DOI: 10.1055/s-2008-1039010]
36 **Kanellos D**, Pramateftakis MG, Demetriades H, Zacharakis E, Angelopoulos S, Mantzoros I, Kanellos I, Despoudi K, Zaraboukas T, Koliakos G, Galovatsea K, Lazaridis H. Healing of colonic anastomoses after immediate postoperative intraperitoneal administration of oxaliplatin. *Int J Colorectal Dis* 2008; **23**: 1185-1191 [PMID: 18677490 DOI: 10.1007/s00384-008-0538-5]
37 **Downing SW**. What are the risks of using biologic glues? *Ann Thorac Surg* 2003; **75**: 1063; author reply 1063-1063; author reply 1064 [PMID: 12645755 DOI: 10.1016/S0003-4975(02)03473-2]
38 **Hewitt CW**, Marra SW, Kann BR, Tran HS, Puc MM, Chrzanowski FA Jr, Tran JL, Lenz SD, Cilley JH Jr, Simonetti VA, DelRossi AJ. BioGlue surgical adhesive for thoracic aortic repair during coagulopathy: efficacy and histopathology. *Ann Thorac Surg* 2001; **71**: 1609-1612 [PMID: 11383808 DOI: 10.1016/S0003-4975(01)02424-9]
39 **Demling RH**. Nutrition, anabolism, and the wound healing process: an overview. *Eplasty* 2009; **9**: e9 [PMID: 19274069]
40 **Wasserberg N**, Nunoo-Mensah JW, Ruiz P, Tzakis AG. The effect of immunosuppression on peritoneal adhesions formation after small bowel transplantation in rats. *J Surg Res* 2007; **141**: 294-298 [PMID: 17543342 DOI: 10.1016/j.jss.2006.12.541]
41 **Hoffmann NE**, Siddiqui SA, Agarwal S, McKellar SH, Kurtz HJ, Gettman MT, Ereth MH. Choice of hemostatic agent influences adhesion formation in a rat cecal adhesion model. *J Surg Res* 2009; **155**: 77-81 [PMID: 19181342 DOI: 10.1016/j.jss.2008.08.008]
42 **Kanellos I**, Blouhos K, Demetriades H, Pramateftakis MG, Mantzoros I, Zacharakis E, Betsis D. The failed intraperitoneal colon anastomosis after colon resection. *Tech Coloproctol* 2004; **8** Suppl **1**: s53-s55 [PMID: 15655643 DOI: 10.1007/s10151-004-0111-3]
43 **Steffensen B**, Häkkinen L, Larjava H. Proteolytic events of wound-healing--coordinated interactions among matrix metalloproteinases (MMPs), integrins, and extracellular matrix molecules. *Crit Rev Oral Biol Med* 2001; **12**: 373-398 [PMID: 12002821 DOI: 10.1177/10454411010120050201]
44 **Desmoulière A**, Chaponnier C, Gabbiani G. Tissue repair, contraction, and the myofibroblast. *Wound Repair Regen* 2005; **13**: 7-12 [PMID: 15659031 DOI: 10.1111/j.1067-1927.2005.130102.x]
45 **Stumpf M**, Cao W, Klinge U, Klosterhalfen B, Kasperk R, Schumpelick V. Collagen distribution and expression of matrix metalloproteinases 1 and 13 in patients with anastomotic leakage after large-bowel surgery. *Langenbecks Arch Surg* 2002; **386**: 502-506 [PMID: 11819107 DOI: 10.1007/s00423-001-0255-9]
46 **Ozel SK**, Kazez A, Akpolat N. Does a fibrin-collagen patch support early anastomotic healing in the colon? An experimental study. *Tech Coloproctol* 2006; **10**: 233-236 [PMID: 16969611 DOI: 10.1007/s10151-006-0285-y]
47 **Kanellos I**, Mantzoros I, Goulimaris I, Zacharakis E, Zavitsanakis A, Betsis D. Effects of the use of fibrin glue around the colonic anastomosis of the rat. *Tech Coloproctol* 2003; **7**: 82-84 [PMID: 14605925 DOI: 10.1007/s10151-003-0014-8]
48 **Haukipuro KA**, Hulkko OA, Alavaikko MJ, Laitinen ST. Sutureless colon anastomosis with fibrin glue in the rat. *Dis Colon Rectum* 1988; **31**: 601-604 [PMID: 2456902 DOI: 10.1007/BF02556795]
49 **Detweiler MB**, Kobos JW, Fenton J. Gastrointestinal sutureless anastomosis in pigs using absorbable intraluminal stents, stent placement devices, and fibrin glue - a summary. *Langenbecks Arch Surg* 1999; **384**: 445-452 [PMID: 10552290 DOI: 10.1007/s004230050229]
50 **Moran B**, Heald R. Anastomotic leakage after colorectal anastomosis. *Semin Surg Oncol* 2000; **18**: 244-248 [PMID: 10757890 DOI: 10.1002/(SICI)1098-2388(200004/05)18]
51 **Gainant A**. [Prevention of anastomotic dehiscence in colorectal surgery]. *J Chir (Paris)* 2000; **137**: 45-50 [PMID: 10790619]
52 **Ekmektzoglou KA**, Zografos GC, Kourkoulis SK, Dontas IA, Giannopoulos PK, Marinou KA, Poulakou MV, Perrea DN. Mechanical behavior of colonic anastomosis in experimental settings as a measure of wound repair and tissue integrity. *World J Gastroenterol* 2006; **12**: 5668-5673 [PMID: 17007020 DOI: 10.3748/wjg.v12.i35.5668]
53 **Hjortrup A**, Nordkild P, Kiaergaard J, Sjøntoft E, Olesen HP. Fibrin adhesive versus sutured anastomosis: a comparative intraindividual study in the small intestine of pigs. *Br J Surg* 1986; **73**: 760-761 [PMID: 3756445 DOI: 10.1002/bjs.1800730928]
54 **Capitán Morales LC**, Rodríguez Nuñez E, Morales Conde S, Sanchez Ganfornina F, Del Rio Lafuente FD, Cabot Ostos E, Ortega Beviá JM, Loscertales Abril J, Cantillana Martínez J. Experimental study of sutureless colorectal anastomosis. *Hepatogastroenterology* 2000; **47**: 1284-1290 [PMID: 11100334]
55 **Akgün A**, Kuru S, Uraldi C, Tekin O, Karip B, Tug T, Ongören AU. Early effects of fibrin sealant on colonic anastomosis in rats: an experimental and case-control study. *Tech Coloproctol* 2006; **10**: 208-214 [PMID: 16969615 DOI: 10.1007/s10151-006-0281-2]
56 **Walker KG**, Bell SW, Rickard MJ, Mehanna D, Dent OF, Chapuis PH, Bokey EL. Anastomotic leakage is predictive of diminished survival after potentially curative resection for colorectal cancer. *Ann Surg* 2004; **240**: 255-259 [PMID: 15273549 DOI: 10.1097/01.sla.0000133186.81222.0]
57 **Izbicki JR**, Kreusser T, Meier M, Prenzel KL, Knoefel WT, Passlick B, Kuntz G, Schiele U, Thetter O. Fibrin-glue-coated collagen fleece in lung surgery--experimental comparison with infrared coagulation and clinical experience. *Thorac Cardiovasc Surg* 1994; **42**: 306-309 [PMID: 7863495 DOI: 10.1055/s-2007-1016510]
58 **Yol S**, Tekin A, Yilmaz H, Küçükkartallar T, Esen H, Caglayan O, Tatkan Y. Effects of platelet rich plasma on colonic anastomosis. *J Surg Res* 2008; **146**: 190-194 [PMID: 18028949 DOI: 10.1016/j.jss.2007.05.015]
59 **Cicha I**, Garlichs CD, Daniel WG, Goppelt-Struebe M. Activated human platelets release connective tissue growth factor. *Thromb Haemost* 2004; **91**: 755-760 [PMID: 15045137 DOI: 10.1160/TH03-09-0602]
60 **Crowther M**, Brown NJ, Bishop ET, Lewis CE. Microenvironmental influence on macrophage regulation of angiogenesis in wounds and malignant tumors. *J Leukoc Biol* 2001; **70**: 478-490 [PMID: 11590184]

61 Softova EB. Examining cellular communication and role of growth factors during wound healing. *J Wound Cage* 2005; **14**: 172 [DOI: 10.12968/jowc.2005.14.4.26755]

62 **Park JE**, Barbul A. Understanding the role of immune regulation in wound healing. *Am J Surg* 2004; **187**: 11S-16S [PMID: 15147986 DOI: 10.1016/S0002-9610(03)00296-4]

63 **Weisel JW**. Fibrinogen and fibrin. *Adv Protein Chem* 2005; **70**: 247-299 [PMID: 15837518 DOI: 10.1016/S0065-3233(05)70008-5]

64 **Wilson DA**. Principles of early wound management. *Vet Clin North Am Equine Pract* 2005; **21**: 45-62, vi [PMID: 15691599 DOI: 10.1016/j.cveq.2004.11.005]

65 **Tidball JG**. Inflammatory processes in muscle injury and repair. *Am J Physiol Regul Integr Comp Physiol* 2005; **288**: R345-R353 [PMID: 15637171 DOI: 10.1152/ajpregu.00454.2004]

66 **Salmela MT**, Pender SL, Karjalainen-Lindsberg ML, Puolakkainen P, Macdonald TT, Saarialho-Kere U. Collagenase-1 (MMP-1), matrilysin-1 (MMP-7), and stromelysin-2 (MMP-10) are expressed by migrating enterocytes during intestinal wound healing. *Scand J Gastroenterol* 2004; **39**: 1095-1104 [PMID: 15545168 DOI: 10.1080/00365520410003470]

67 **Toy LW**. Matrix metalloproteinases: their function in tissue repair. *J Wound Care* 2005; **14**: 20-22 [PMID: 15656460 DOI: 10.12968/jowc.2005.14.1.26720]

68 **Tettamanti G**, Grimaldi A, Congiu T, Perletti G, Raspanti M, Valvassori R, de Eguileor M. Collagen reorganization in leech wound healing. *Biol Cell* 2005; **97**: 557-568 [PMID: 15898949 DOI: 10.1042/BC20040085]

69 **Clark RA**, An JQ, Greiling D, Khan A, Schwarzbauer JE. Fibroblast migration on fibronectin requires three distinct functional domains. *J Invest Dermatol* 2003; **121**: 695-705 [PMID: 14632184 DOI: 10.1046/j.1523-1747.2003.12484.x]

70 **Ottani V**, Martini D, Franchi M, Ruggeri A, Raspanti M. Hierarchical structures in fibrillar collagens. *Micron* 2002; **33**: 587-596 [PMID: 12475555 DOI: 10.1016/S0968-4328(02)00033-1]

71 **Steffensen B**, Xu X, Martin PA, Zardeneta G. Human fibronectin and MMP-2 collagen binding domains compete for collagen binding sites and modify cellular activation of MMP-2. *Matrix Biol* 2002; **21**: 399-414 [PMID: 12225805 DOI: 10.1016/S0945-053X(02)00032-X]

72 **Otrock ZK**, Mahfouz RA, Makarem JA, Shamseddine AI. Understanding the biology of angiogenesis: review of the most important molecular mechanisms. *Blood Cells Mol Dis* 2007; **39**: 212-220 [PMID: 17553709 DOI: 10.1016/j.bcmd.2007.04.001]

73 **Murray B**, Wilson DJ. A study of metabolites as intermediate effectors in angiogenesis. *Angiogenesis* 2001; **4**: 71-77 [PMID: 11824381 DOI: 10.1023/A:1016792319207]

74 **Srivastava K**, Dash D. Changes in membrane microenvironment and signal transduction in platelets from NIDDM patients-a pilot study. *Clin Chim Acta* 2002; **317**: 213-220 [PMID: 11814478 DOI: 10.1016/S0009-8981(01)00794-X]

75 **Rabinovsky ED**, Draghia-Akli R. Insulin-like growth factor I plasmid therapy promotes in vivo angiogenesis. *Mol Ther* 2004; **9**: 46-55 [PMID: 14741777 DOI: 10.1016/j.ymthe.2003.10.003]

76 **Lygoe KA**, Norman JT, Marshall JF, Lewis MP. AlphaV integrins play an important role in myofibroblast differentiation. *Wound Repair Regen* 2004; **12**: 461-470 [PMID: 15260812 DOI: 10.1111/j.1067-1927.2004.12402.x]

77 **Oxlund H**, Christensen H, Seyer-Hansen M, Andreassen TT. Collagen deposition and mechanical strength of colon anastomoses and skin incisional wounds of rats. *J Surg Res* 1996; **66**: 25-30 [PMID: 8954827 DOI: 10.1006/jsre.1996.0367]

78 **Carlson MA**, Longaker MT. The fibroblast-populated collagen matrix as a model of wound healing: a review of the evidence. *Wound Repair Regen* 2004; **12**: 134-147 [PMID: 15086764 DOI: 10.1111/j.1067-1927.2004.012208.x]

79 **Kobayashi T**, Inoue T, Okada H, Kikuta T, Kanno Y, Nishida T, Takigawa M, Sugaya T, Suzuki H. Connective tissue growth factor mediates the profibrotic effects of transforming growth factor-beta produced by tubular epithelial cells in response to high glucose. *Clin Exp Nephrol* 2005; **9**: 114-121 [PMID: 15980944 DOI: 10.1007/s10157-005-0347-x]

80 **Syk I**, Agren MS, Adawi D, Jeppsson B. Inhibition of matrix metalloproteinases enhances breaking strength of colonic anastomoses in an experimental model. *Br J Surg* 2001; **88**: 228-234 [PMID: 11167872 DOI: 10.1046/j.1365-2168.2001.01649.x]

81 **Hendriks T**, Hesp WL, Klompmakers AA, Lubbers EJ, de Boer HH. Solubility of tissue hydroxyproline in experimental intestinal anastomoses. *Exp Mol Pathol* 1985; **43**: 253-259 [PMID: 4043344 DOI: 10.1016/0014-4800(85)90045-0]

82 **Sottile J**, Hocking DC. Fibronectin polymerization regulates the composition and stability of extracellular matrix fibrils and cell-matrix adhesions. *Mol Biol Cell* 2002; **13**: 3546-3559 [PMID: 12388756 DOI: 10.1091/mbc.E02-01-0048]

83 **Hall MC**, Young DA, Waters JG, Rowan AD, Chantry A, Edwards DR, Clark IM. The comparative role of activator protein 1 and Smad factors in the regulation of Timp-1 and MMP-1 gene expression by transforming growth factor-beta 1. *J Biol Chem* 2003; **278**: 10304-10313 [PMID: 12525489 DOI: 10.1074/jbc.M212334200]

84 **Dabareiner RM**, Sullins KE, White NA, Snyder JR. Serosal injury in the equine jejunum and ascending colon after ischemia-reperfusion or intraluminal distention and decompression. *Vet Surg* 2001; **30**: 114-125 [PMID: 11230765 DOI: 10.1053/jvet.2001.21393]

85 **Madl C**, Druml W. Gastrointestinal disorders of the critically ill. Systemic consequences of ileus. *Best Pract Res Clin Gastroenterol* 2003; **17**: 445-456 [PMID: 12763506 DOI: 10.1016/S1521-6918(03)00022-2]

86 **Agren MS**, Andersen TL, Mirastschijski U, Syk I, Schiødt CB, Surve V, Lindebjerg J, Delaissé JM. Action of matrix metalloproteinases at restricted sites in colon anastomosis repair: an immunohistochemical and biochemical study. *Surgery* 2006; **140**: 72-82 [PMID: 16857445 DOI: 10.1016/j.surg.2005.12.013]

87 **Krarup PM**, Eld M, Heinemeier K, Jorgensen LN, Hansen MB, Ågren MS. Expression and inhibition of matrix metalloproteinase (MMP)-8, MMP-9 and MMP-12 in early colonic anastomotic repair. *Int J Colorectal Dis* 2013; **28**: 1151-1159 [PMID: 23619615 DOI: 10.1007/s00384-013-1697-6]

88 **Nandakumar G**, Richards BG, Trencheva K, Dakin G. Surgical adhesive increases burst pressure and seals leaks in stapled gastrojejunostomy. *Surg Obes Relat Dis* 2010; **6**: 498-501 [PMID: 20176513 DOI: 10.1016/j.soard.2009.11.016]

89 **Slieker JC**, Vakalopoulos KA, Komen NA, Jeekel J, Lange JF. Prevention of leakage by sealing colon anastomosis: experimental study in a mouse model. *J Surg Res* 2013; **184**: 819-824 [PMID: 23764314 DOI: 10.1016/j.jss.2013.04.015]

90 **Vakalopoulos KA**, Wu Z, Kroese LF, Jeekel J, Kleinrensink GJ, Dodou D, Lam KH, Lange JF. Sutureless closure of colonic defects with tissue adhesives: an in vivo study in the rat. *Am J Surg* 2017; **213**: 151-158 [PMID: 27474497 DOI: 10.1016/j.amjsurg.2016.05.009]

P- Reviewer: Krarup PM, Liu L, Nagata J **S- Editor**: Qi Y
L- Editor: A **E- Editor**: Huang Y

World Journal of Gastroenterology

Submit a Manuscript: http://www.f6publishing.com

World J Gastroenterol 2017 August 21; 23(31): 5692-5699

DOI: 10.3748/wjg.v23.i31.5692

ISSN 1007-9327 (print) ISSN 2219-2840 (online)

ORIGINAL ARTICLE

Basic Study

Cytoplasmic domain of tissue factor promotes liver fibrosis in mice

Virginia Knight, Dinushka Lourensz, Jorge Tchongue, Jeanne Correia, Peter Tipping, William Sievert

Virginia Knight, Dinushka Lourensz, Jorge Tchongue, Jeanne Correia, Peter Tipping, William Sievert, Centre for Inflammatory Diseases, Department of Medicine, School of Clinical Sciences, Monash University, Melbourne, Victoria 3168, Australia

Virginia Knight, William Sievert, Gastroenterology and Hepatology Unit, Monash Health, Melbourne, Victoria 3168, Australia

Author contributions: Knight V, Lourensz D, Tchongue J and Correia J acquired and analysed data; Knight V, Sievert W and Tipping P designed the study, interpreted the data and contributed to writing of the article, editing, and reviewing; all authors approved the final version of the article.

Institutional animal care and use committee statement: All procedures involving animals were reviewed and approved by the Monash University Animal Ethics Committee (MMCB 2004/10).

Conflict-of-interest statement: The authors have no conflicts of interest to report.

Data sharing statement: All available data can be obtained by contacting the corresponding author.

Manuscript source: Invited manuscript

Correspondence to: William Sievert, MD, FRACP, Professor, Director, Gastroenterology and Hepatology Unit, Monash Health, 246 Clayton Road, Melbourne, Victoria 3168, Australia. william.sievert@monash.edu
Telephone: +61-95943177
Fax: +61-95946250

Received: January 6, 2017
Peer-review started: January 9, 2017
First decision: March 16, 2017
Revised: May 9, 2017
Accepted: July 4, 2017
Article in press: July 4, 2017
Published online: August 21, 2017

Abstract

AIM

To evaluate the role of tissue factor (TF) and protease activated receptor (PAR)-2 in liver fibrosis.

METHODS

Using CCl_4 administration for eight weeks, we induced hepatic fibrosis in wild-type C57BL/6 mice and in mice with deletion of the cytoplasmic signalling domain of TF ($TF^{\S CT/\S CT}$), deletion of PAR-2 ($PAR\text{-}2^{-/-}$) and combined deletion of TF signalling domain and PAR-2 ($TF^{\S CT/\S CT}$/$PAR\text{-}2^{-/-}$). Hepatic fibrosis area was assessed by quantitative imaging of picrosirius red staining. Hepatic collagen content was assessed by hydroxyproline levels. Hepatic stellate cells (αSMA positive) and hepatic macrophages (CD68 positive) were identified by immunohistochemistry. Hepatic gene expression was determined by PCR and liver TGFβ1 content by ELISA.

RESULTS

CCl_4 treated mice with deletion of the *PAR-2* gene ($PAR\text{-}2^{-/-}$) and the cytoplasmic domain of TF ($TF^{\S CT/\S CT}$) developed significantly less hepatic fibrosis, characterised by reduced liver fibrosis area and hydroxyproline content, compared to control wildtype mice treated with CCl_4. The observed reduction in histological fibrosis was accompanied by a significant decrease in the hepatic content of TGFβ, the prototypic fibrogenic cytokine, as well as fewer activated hepatic stellate cells and hepatic macrophages. Deletion of the TF cytoplasmic signalling domain reduced hepatic fibrosis to levels similar to those

observed in mice lacking PAR-2 signalling but combined deletion provided no added protection against fibrosis indicating a lack of mutual modulating effects that have been observed in other contexts such as angiogenic responses.

CONCLUSION

Tissue factor cytoplasmic domain is involved in TF-PAR-2 signalling initiating hepatic fibrosis and is a potential therapeutic target, as its deletion would not impact coagulation.

Key words: Tissue factor; Protease activated receptor; Hepatic stellate cell; Liver fibrosis; Macrophage

Core tip: No effective anti-fibrotic therapies are available for patients with cirrhosis. PAR-2, a receptor that activates coagulation and inflammation, promotes hepatic fibrosis; whether tissue factor (TF), the primary initiator of the coagulation cascade, affects hepatic fibrosis is unknown. We found that deletion of the TF cytoplasmic domain reduces fibrosis through an effect on hepatic stellate cell activation, possibly mediated through reduced hepatic macrophage activation. Currently available direct thrombin inhibitors may be useful in preventing hepatic fibrosis while therapeutic targeting of the cytoplasmic domain of TF may be useful in patients with advanced liver disease, as its deletion does not alter coagulation.

Knight V, Lourensz D, Tchongue J, Correia J, Tipping P, Sievert W. Cytoplasmic domain of tissue factor promotes liver fibrosis in mice. *World J Gastroenterol* 2017; 23(31): 5692-5699 Available from: URL: http://www.wjgnet.com/1007-9327/full/v23/i31/5692.htm DOI: http://dx.doi.org/10.3748/wjg.v23.i31.5692

INTRODUCTION

Chronic hepatocyte injury leads to a wound healing response that can result in excessive inflammation, collagen deposition and advanced hepatic fibrosis. The coagulation system is involved in the acute response to injury with formation of a fibrin clot, but also plays an important role in the inflammatory signalling that perpetuates wound healing and tissue remodelling. The links between inflammation and coagulation occur through tissue factor (TF) and through protease activated receptors (PAR) although the relative contributions of each to inflammatory and fibrotic outcomes are unclear. TF is a transmembrane glycoprotein receptor with a pivotal role in hemostasis initiated by binding FⅦa, its principal ligand. Clot formation following TF ligation is well known, however downstream events also include expression of pro-inflammatory cytokines such as interleukin (IL)-6. Evidence for this relationship is seen in healthy human subjects who demonstrate IL6 and IL8 induction following exposure to recombinant FVIIa and in mice expressing low TF levels (< 1% of wildtype) which show reduced inflammatory cytokine expression and mortality following lipopolysaccharide (LPS) exposure[1,2].

The TF molecule has three domains; binding of the extracellular domain to Factor Ⅶ/Ⅶa initiates coagulation, the transmembrane domain has anchoring properties necessary for normal coagulation and the cytoplasmic domain, which is not required for coagulant activity, plays a role in intracellular signalling. For example, binding of FⅦa to macrophage TF leads to phospholipase C-dependent intracellular calcium fluxes and reactive oxygen species production that requires an intact TF cytoplasmic domain[3]. In the liver, hepatocytes are the primary source of Factor Ⅶ/Ⅶa. Constitutive hepatocyte expression of TF mRNA is low but can be upregulated in circulating monocytes by LPS[4], monocyte chemotactic protein-1 and platelet derived growth factor as well as by direct contact with platelets[4,5].

The TF cytoplasmic domain also plays a regulatory role in PAR-2 signalling. Mice with deletion of the cytoplasmic domain ($TF^{\S CT/\S CT}$) demonstrate enhanced PAR-2 dependent angiogenesis suggesting that the TF cytoplasmic domain acts as a negative regulator of PAR-2 signalling[6]. Context may be important, however, as others have shown that the TF cytoplasmic domain is necessary for PAR-2 regulated inflammation[7]. A role for TF-PAR-2 signalling in the development of obesity and insulin resistance has recently been demonstrated. TF-Ⅶa-PAR-2 signalling in adipocytes regulates weight gain and in macrophages promotes inflammation and insulin resistance[8]. Such pathways may play a role in the development of non-alcoholic fatty liver disease (NAFLD) as direct thrombin inhibition has been shown to reduce hepatic inflammation in murine NAFLD[9].

The aim of our study was to evaluate the role of the TF cytoplasmic domain in the hepatic inflammatory response and liver fibrogenesis following chronic injury. We have previously shown that PAR-2 deficiency ameliorates experimental liver fibrosis[10]. Given the observed interactions between TF cytoplasmic domain and PAR-2 in angiogenesis and inflammation, we explored a possible relationship between the TF cytoplasmic domain and the PAR-2 receptor in the development of liver fibrosis in mice with deletion of the TF cytoplasmic domain, deletion of PAR-2 and deletion of both the TF cytoplasmic domain and PAR-2.

MATERIALS AND METHODS

Animals

Mice on a 25%Swiss/25%129S/50% MF-1 background with deletion of 18 of the 20 amino acids of the TF cytoplasmic domain ($TF^{\S CT/\S CT}$) were generated by Cre-lox recombination as previously described and backcrossed 9 generations onto a C57BL6 background[11]. $TF^{\S CT/\S CT}$

mice have normal development, coagulation and fertility. PAR-2 knockout mice were generated as previously described[10]. Mice with deletion of both the TF cytoplasmic domain and PAR 2 ($TF^{\S CT/\S CT}$/PAR-$2^{-/-}$) were generated; these mice have normal development, coagulation and fertility. Mice were allowed food and water *ad libitum* and were housed at a constant temperature in 12:12 hour light-dark cycle. Experimental protocols were approved by the Monash University Animal Ethics Committee and mice received humane care as specified under the Australian code of practice for the care and use of animals for scientific purposes.

Induction of hepatic fibrosis

Liver fibrosis was induced in male mice by twice-weekly intraperitoneal injections of 1 μL/g body weight CCl_4 mixed with olive oil (1:10). Starting between 8-10 wk of age, four groups of mice were studied. $TF^{\S CT/\S CT}$ (n = 9), $TF^{\S CT/\S CT}$/PAR-$2^{-/-}$ (n = 6) and wild type (WT) C57BL/6 (n = 10) all received CCl_4 for 8 wk. A control group of WT C57BL/6 mice (n = 8) received olive oil alone for 8 wk as a vehicle control.

Hepatic fibrosis assessment

Liver fibrosis area: Four micron thick sections of paraffin embedded liver tissue were deparaffinised and stained with picrosirius red (Sirius red F3BA 0.1% wt/vol in saturated picric acid) for 90 min, washed in acetic acid and water (5:1000), dehydrated in ethanol and mounted in neutral DPX. Fifteen consecutive non-overlapping fields were acquired for each mouse liver, the image digitised and fibrosis area analysed by Scion Image for Windows (vAlpha 4.0.3.2, Scion Corporation, Frederick, MD, United States).

Hepatic collagen content: Hydroxyproline is an amino acid that stabilises collagen deposited in the liver and is exclusively associated with collagenous connective tissue and therefore is a good surrogate for quantification of collagen deposition[12]. Hepatic hydroxyproline content was quantified using liver tissue frozen in liquid nitrogen as previously described with minor modification[13]. Briefly, liver samples were weighed and hydrolysed in 2.5 mL of 6 N HCl at 110 ℃ for 18 h in Teflon coated tubes. The hydrolysate was centrifuged at 3000 rpm for 10 min; the pH of the resulting supernatant was adjusted to 7.4 and absorbance measured at 558 nm. Total hydroxyproline content was measured against a standard curve prepared with trans-4-hydroxy-L-proline (Sigma-Aldrich, St Louis, MO, United States) preparations in the range of 0.156 to 5.0 μg/mL and expressed per milligram of wet tissue weight.

Hepatic stellate cell and macrophage immunohistochemistry: To identify activated hepatic stellate cells (myofibroblasts) and hepatic macrophages, paraformaldehyde fixed 4 micron thick liver tissue sections were stained with primary antibody for αSMA (monoclonal mouse anti-mouse α-smooth muscle actin, Sigma, St Louis, MO, United States) and CD68 (rat anti mouse CD68, FA11 a gift of Dr G Koch, Cambridge United Kingdom, 1:100). The following secondary antibodies were used: αSMA biotinylated rabbit anti-mouse IgG2a antibody (Invitrogen, Camarillo, CA, United States, 1:300) and CD68 polyclonal rabbit anti rat IgG (DAKO #E0468 1:150). In brief sections were dewaxed, rehydrated and then blocked with 0.6% hydrogen peroxide and cellular apoptosis susceptibility protein blocking solution (Invitrogen, Camarillo, CA, United States). Primary antibody incubations for 30 min at room temperature (αSMA) and overnight at 4 ℃ (CD68) were followed by application of secondary antibody. Staining was amplified using avidin-biotin complex kit (Vector Laboratories, Burlingame, CA, United States) and detected with 3,3′ diaminobenzidine (Dako, Carpentaria, CA, United States). Slides were counterstained with Harris hematoxylin. For quantification of immunoreactivity, 15 consecutive non-overlapping fields at 250 × magnification (αSMA, CD68) were scored using a graticule eyepiece in a blinded fashion. Negative controls consisted of a mouse IgG1 isotype control antibody (Dako, Glostrup, Denmark) and water substituting for the primary antibody.

Gene expression studies

Mouse RNA was extracted using the Qiagen RNeasy mini kit according to the manufacturer's instructions (Qiagen Pty Ltd, Hilden, Germany). Briefly, 0.02 to 0.03 g of liver was placed in RNAse free tube. 600 μL of RLT was added to each sample which was then vortexed for 15 min. The resultant lysate was pipetted into a QIA shredder spin column and centrifuged initially at full speed for 2 min, then the column was removed and the lysate was centrifuged for a further 3 min. The resultant supernatant was removed and added to equal volume of 50% ethanol, transferred to an RNeasy spin column, centrifuged for 15 s and the flow through discarded. Seven hundred microliter Buffer RW1 was added and the column was centrifuged for 15 s and followed by the addition of two aliquots of 500 μL of RPE, centrifuging in between for 15 s and 2 min respectively. The RNeasy spin column was placed in a new collection tube, centrifuged for 1 min and then 30 μL of RNase-free water was added directly to the spin column membrane, centrifuged and then a further 30 μL of RNase-free water was added. Four microliter of RNa was added to 76 μL of RNase free water. The RNA concentration was measured with a Nanodrop ND-100 spectrophotometer (Thermo Scientific, Waltham, MA, United States). RNA was used to generate cDNA using the High-Capacity cDNA Reverse Transcription Kit (Applied Biosystems, Foster City, CA, United States) as per manufacturer's instructions. Briefly, 2 × RT

Table 1 Primer sequences used in gene expression studies

Target gene	Primer sequence (5′-3′)
18s	Forward: 5′-GTAACCCGTTGAACCCCATTC-3′ Reverse: 5′-GCCTCACTAAACCATCCAATC G-3′
TGFβ	Forward: 5′-TGCCCTCTACAACCAACACA-3′ Reverse: 5′-GTTGGACAACTGCTCCACCT-3
MMP-2	Forward: 5′-ACCCAGATGTGGCCAACTAC-3′ Reverse: 5′-TCATTTTAAGGCCCGAGCAA-3′
TIMP-1	Forward: 5′-ACGAGACCACCTTATACCAGCCG-3′ Reverse: 5′-GCGGTTCTGGGACTTGTGGGC-3′
PAR-1	Forward: 5′-CTCCTCAAGGAGCAGACCCAC-3′ Reverse: 5′-AGACCGTGGAAACGATCAAC-3′
PAR-2	Mm00433160_m1, using TaqMan Gene Expression Master Mix (Applied Biosystems)
18S	Hs03003631_g1 using TaqMan Gene Expression Master Mix (Applied Biosystems)

master mix was prepared from supplied components as follows: 2.0 μL 10 × RT buffer, 0.8 μL 25 × dNTP mix (100 mmol/L), 10 × RT Random Primers, 1.0 μL Multiscribe™ Reverse Transcriptase, 1.0 μL RNase Inhibitor and 3.2 μL of Nuclease free water. Nineteen microliter of 2 × RT master mix was combined with 10 μL of RNA containing 1 μg RNA. The tubes were centrifuged. The PCR program involved Step 1: 25 ℃ for 10 min, Step 2: 37 ℃ for 120 min, Step 3: 85 ℃ for 5 s, and Step 4: 4 ℃ for 10 min and then samples were collected and stored at -80 ℃.

Real time PCR analysis was performed (Power Sybr Green, Roche, Manheim, Germany) using a Rotor Gene 3000 light cycler (Qiagen Pty Ltd, Sydney, Australia) and the specific target mRNA of interest quantified as a ratio relative to 18S RNA content of the sample. 200 ng of cDNA was used per reaction. The primer sequences used in analysis are found in Table 1.

Protein expression studies

Extracts were prepared from snap frozen liver by homogenisation in lysis buffer (Tris-HCl 50 mmol/L, NaCl 150 mmol/L, EDTA 1 mmol/L, 1% Triton X-100, 0.5% Tween-20, 0.1% SDS) containing a protease inhibitor cocktail (#11836170, Roche Diagnostics, Mannheim, Germany) followed by centrifugation at 14000 × *g* for 15 min at 4 ℃. Supernatants were collected and activated with acetic acid/urea prior to analysis. TGFβ1 content of liver protein extracts were measured using a mouse TGFβ1 ELISA kit (R and D Systems Inc, Minneapolis, MN, United States). Plates were read using the Bio-Rad microplate reader at 450 nm and TGFβ1 concentrations were calculated from the standard curve by the plate reader software.

Statistical analysis

Data are expressed as mean ± SEM. Statistical significance was determined by one-way ANOVA with Newman-Keuls post-test for multiple comparisons or Student's *t*-test for comparisons between two groups as appropriate, using GraphPad Prism 5.03 for Windows (GraphPad Software, Inc, La Jolla, United States). A P value < 0.05 was considered significant.

RESULTS

Hepatic fibrosis

Quantitative analysis of histological fibrosis by computer-assisted morphometry in CCl_4-treated WT mice showed a marked increase in liver fibrosis area (LFA) at 8 wk (3.39% ± 0.26%) compared to vehicle controls (LFA 0.7% ± 014%) (P < 0.0001). CCl_4 administration induced similar levels of fibrosis in $TF^{\S CT/\S CT}$ and $TF^{\S CT/\S CT}$/PAR-$2^{-/-}$ mice (1.76% ± 0.17% and 1.94% ± 0.11% respectively), which were similar to that seen with PAR-$2^{-/-}$ mice (LFA 2.09% ± 0.28%). Compared to WT mice, at 8 wk LFA was significantly lower in the PAR-$2^{-/-}$ (P < 0.001), $TF^{\S CT/\S CT}$ (P < 0.0001) and $TF^{\S CT/\S CT}$/PAR-$2^{-/-}$ mice (P < 0.01) (Figure 1A-F).

Hepatic hydroxyproline content

Histological assessment of fibrosis area correlated with the amount of liver hydroxyproline, a surrogate marker for collagen content. $TF^{\S CT/\S CT}$ and $TF^{\S CT/\S CT}$/PAR-$2^{-/-}$ mice showed significantly less hepatic hydroxyproline content (0.37 ± 0.017 μg/mg and 0.37 ± 0.02 μg/mg) compared to WT mice (0.61 ± 0.03 μg/mg) at 8 wk (P < 0.05). Hydroxyproline content in $TF^{\S CT/\S CT}$ and $TF^{\S CT\ \S CT}$/PAR-$2^{-/-}$ mice were similar to that seen in the PAR-$2^{-/-}$ mice (0.39 ± 0.02 μg/mg) (Figure 2).

Reduced hepatic stellate cell activation in $TF^{\S CT/\S CT}$ and $TF^{\S CT/\S CT}$/PAR-$2^{-/-}$ mice

We identified αSMA positive cells as a marker of HSC activation and myofibroblast differentiation. There were significantly fewer αSMA positive cells seen histologically in the $TF^{\S CT/\S CT}$ and $TF^{\S CT/\S CT}$/PAR-$2^{-/-}$ groups compared to WT (19.99, 19.96 and 30.09 mean αSMA positive cells/hpf respectively, P < 0.0001) (Figure 3). The reduction observed in αSMA positive cells in the $TF^{\S CT/\S CT}$ and $TF^{\S CT/\S CT}$/PAR-$2^{-/-}$ groups was similar to that observed in PAR-$2^{-/-}$ alone.

$TF^{\S CT/\S CT}$ and $TF^{\S CT/\S CT}$/PAR-2 deficiency reduces hepatic TGFβ expression

CCl_4 induced hepatic fibrosis was associated with upregulation of TGFβ mRNA (3.57 fold greater than control) and protein (11.41 ± 0.98 pg/mg liver *vs* control 7.01 ± 0.01 pg/mg in WT mice) at 8 wk. In $TF^{\S CT/\S CT}$ mice, TGFβ mRNA expression was significantly reduced (0.22 ± 0.05 fold greater than control, P < 0.0001). In $TF^{\S CT/\S CT}$/PAR-$2^{-/-}$ mice there was a trend towards TGFβ mRNA reduction (1.21 ± 0.14 fold greater than control, P = NS) (Figure 4A). In both the $TF^{\S CT/\S CT}$ and $TF^{\S CT/\S CT}$/PAR-$2^{-/-}$ mice, TGFβ protein was similar to controls (6.14 ± 0.33, 6.45 ± 0.84 and 7.01 ± 0.18 pg/mg wet liver weight respectively) and significantly lower than the TGFβ protein level in wildtype mice (P < 0.0001) (Figure 4B).

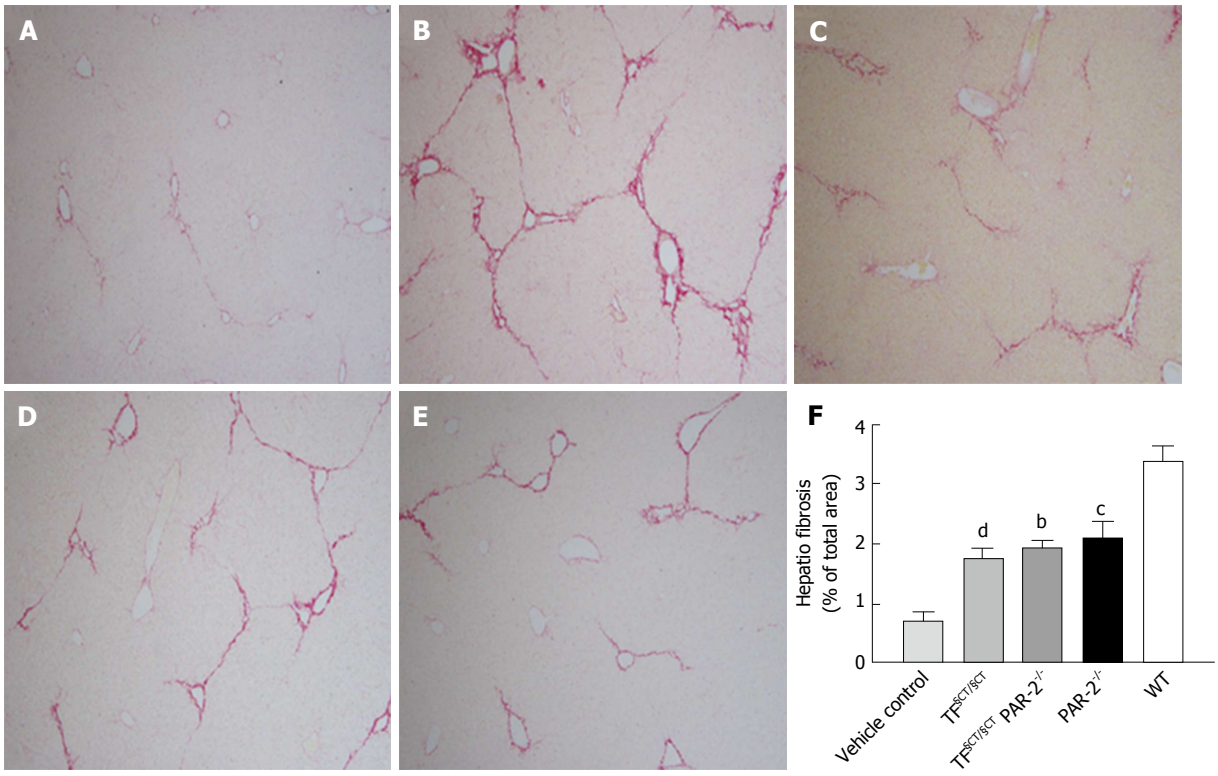

Figure 1 Hepatic fibrosis area. Wildtype control mice administered vehicle alone showed minimal fibrosis (A). Compared to CCl_4 treated wild-type mice (B), hepatic fibrosis area was significantly lower in the PAR-2$^{-/-}$ (C), TF$^{\S CT/\S CT}$ (D) and TF$^{\S CT/\S CT}$/PAR-2$^{-/-}$ (E) mice after CCl_4 exposure for 8 wk. ($^{b}P < 0.01$, $^{c}P < 0.001$ $^{d}P < 0.0001$).

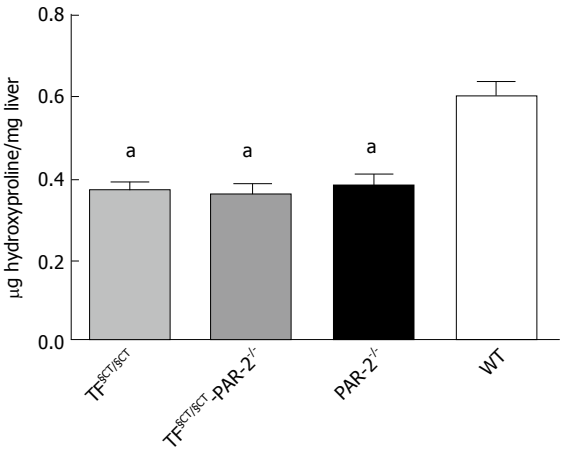

Figure 2 Hepatic hydroxyproline content. Hydroxyproline content, a surrogate marker for collagen, was significantly less in the PAR-2$^{-/-}$, TF$^{\S CT/\S CT}$ and TF$^{\S CT/\S CT}$-PAR-2 KO mice compared to wildtype mice ($^{a}P < 0.05$).

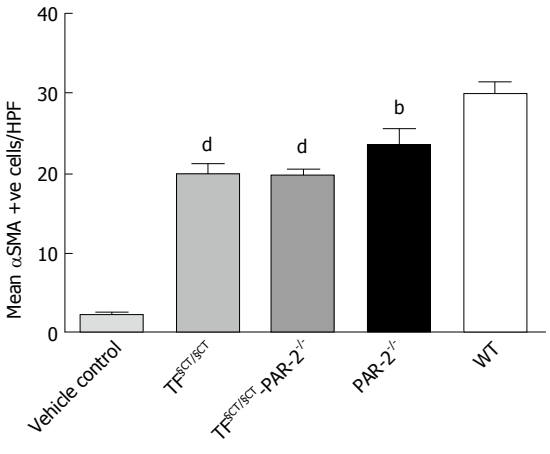

Figure 3 Hepatic stellate cell activation (smooth muscle actin expression). The number of αSMA positive cells was significantly lower in the TF$^{\S CT/\S CT}$ and TF$^{\S CT/\S CT}$/PAR-2$^{-/-}$ mice compared to wildtype and was similar to PAR-2 KO mice ($^{b}P < 0.01$, $^{d}P < 0.0001$).

TF$^{\S CT/\S CT}$ and TF$^{\S CT/\S CT}$/PAR-2 deficiency decreases MMP2 mRNA

Matrix metalloproteinases (MMP) regulate matrix composition and turnover and in turn are regulated by specific tissue inhibitors, TIMPs. The balance of the expression of different MMPs changes throughout the development of liver injury, but in general there is upregulation of the basement membrane-like MMPs, such as MMP2 and 9 and down regulation of interstitial type MMPs such as MMP1 (MMP13 in mice). In WT mice treated with CCl_4 for 8 wk, MMP2 mRNA increased (6.29 ± 1.45 fold greater than control), consistent with active ECM remodelling during development of hepatic fibrosis (Figure 5). MMP-2 mRNA expression was significantly lower in TF$^{\S CT/\S CT}$ and TF$^{\S CT/\S CT}$/PAR-2$^{-/-}$ mice compared to WT mice ($P < 0.0001$ and $P < 0.01$ respectively), suggesting ECM remodelling is reduced in association with the lower levels of fibrosis seen at 8 wk in these mice.

Activated hepatic macrophages are decreased in TF$^{\S CT/\S CT}$ and TF $^{\S CT/\S CT}$/PAR-2 deficient mice

We used CD68 (macrosialin) to identify activated macro-

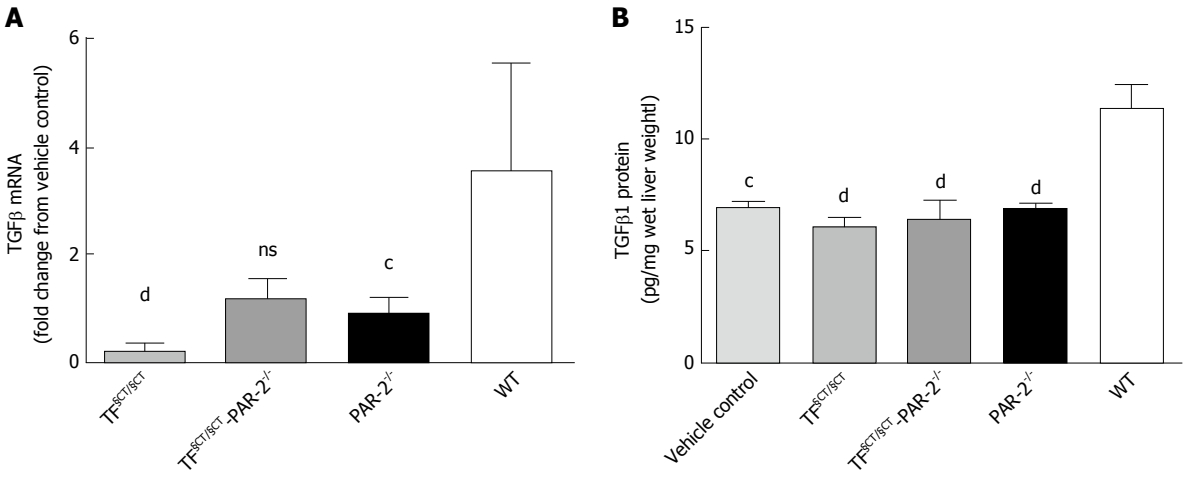

Figure 4 TGFβ mRNA and protein expression. A: TGFβ mRNA expression was significantly lower in the TF§$^{CT/§CT}$ group with a similar but non-significant trend in TF$^{§CT/§CT}$/PAR-2$^{-/-}$ mice compared to wildtype. Levels were similar to PAR-2 KO mice, which were also significantly lower than WT; B: TGFβ protein was significantly lower in TF$^{§CT/§CT}$, TF$^{§CT/§CT}$/PAR-2$^{-/-}$ and PAR-2$^{-/-}$ mice compared to wildtype with levels similar to vehicle controls. $^{c}P < 0.001$, $^{d}P < 0.0001$. ns: Not significant.

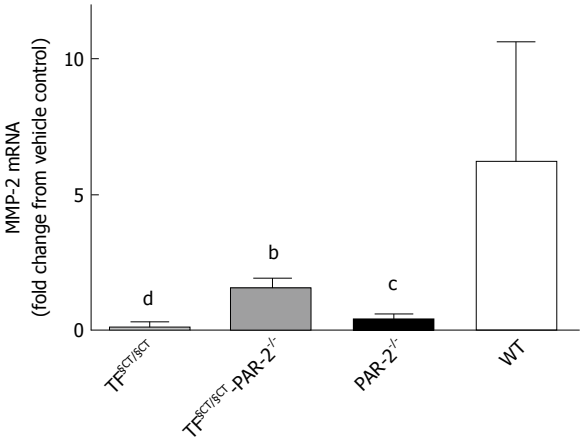

Figure 5 Matrix metalloproteinase expression. MMP-2 mRNA expression was significantly lower in TF$^{§CT/§CT}$, TF$^{§CT/§CT}$/PAR-2$^{-/-}$ and PAR-2$^{-/-}$ mice compared to wildtype. $^{b}P < 0.01$, $^{c}P < 0.001$, $^{d}P < 0.0001$.

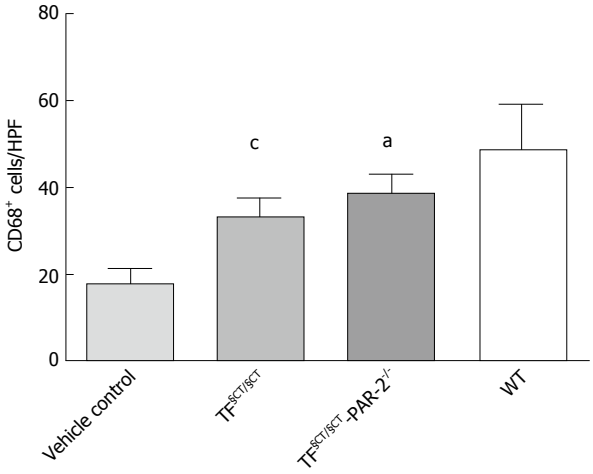

Figure 6 Hepatic macrophage expression. There were significantly fewer activated CD68^{+} macrophages in both TF$^{§CT/§CT}$ and TF$^{§CT/§CT}$/PAR-2$^{-/-}$ mice compared with WT mice. $^{a}P < 0.05$, $^{c}P < 0.001$.

phages. There were significantly fewer CD68^{+} hepatic macrophages in both the TF$^{§CT/§CT}$ and TF$^{§CT\ §CT}$/PAR-2$^{-/-}$ mice compared to WT mice (33.24 ± 1.47, 38.70 ± 1.78, 48.75 ± 2.87 positive cells/hpf; $P < 0.001$, $P < 0.05$ respectively) (Figure 6). We observed similar findings in PAR-2$^{-/-}$ mice suggesting a role for PAR-2 in macrophage recruitment and activation[9]. The current findings suggest that the TF cytoplasmic domain, as well as PAR-2, may be involved in this process.

DISCUSSION

There is growing evidence in animal models and in humans that injury-related signalling through the pivotal coagulation receptors, TF and PAR, can drive hepatic fibrogenesis. A recent study of acute injury in mice given a single injection of CCl_4 demonstrated elevated hepatocyte TF levels and tissue injury that were blocked by specific TF antisense oligonucleotide therapy[14]. In man, TF levels have been found to be over 100 fold higher in patients with cirrhosis compared to non-cirrhotic patients[15]. PAR-1 polymorphisms were shown to influence the hepatic fibrosis rate in Brazilian and European patients with chronic hepatitis C infection[16]. Resistance to activated protein C occurs in patients heterozygous for the factor V Leiden mutation leading to increased thrombin activity, which is a mitogen for hepatic stellate cells. Factor V Leiden heterozygosity has been associated with rapid fibrosis progression in hepatitis C patients[17]. Given our previous study showing that PAR-2 deletion decreased hepatic fibrosis in mice and data showing that the TF cytoplasmic domain induces proinflammatory effects in macrophages we examined the relative contributions of TF and PAR-2 in the development of toxin-induced liver fibrosis.

We found that mice with deletion of the TF cytoplasmic domain had lower hepatic collagen content and less histological fibrosis than wild type mice following 8 wk of

CCL_4 exposure. This was accompanied by fewer αSMA positive cells histologically suggesting reduced hepatic stellate cell activation. There was significantly lower gene and protein expression of the key profibrogenic cytokine TGFβ and a reduction in MMP2 expression in $TF^{\S CT/\S CT}$ mice. These data suggest that activation of the cytoplasmic domain of TF promotes hepatic fibrosis by inducing a profibrogenic phenotype in hepatic stellate cells. In angiogenesis, the cytoplasmic domain of TF acts as a negative regulator of PAR-2. If that were true in this model of liver fibrosis, then loss of the cytoplasmic domain and thus loss of negative regulation of PAR-2, should lead to increased fibrosis through increased PAR-2 activation. However this was not observed in our study. In fact, the protection from experimentally induced liver fibrosis that the $TF^{\S CT/\S CT}$ mice were afforded was similar to that which we previously observed in mice with PAR 2 deficiency[10]. This observation is consistent with the observation in other studies that TF may be necessary for PAR-2 mediated inflammation[7].

We found that mice with dual receptor deletion ($TF^{\S CT/\S CT}$/PAR-$2^{-/-}$) in this experimental model also exhibited reduced fibrosis, reduced stellate cell activation and reduced expression of TGFβ. If the mechanisms underlying fibrogenesis through the TF cytoplasmic domain and PAR-2 were independent, an additive effect and thus greater reduction in fibrosis would potentially have been observed in these mice. However, the extent of fibrosis reduction seen in the $TF^{\S CT/\S CT}$/PAR-$2^{-/-}$ mice was similar to that seen in $TF^{\S CT/\S CT}$ mice and PAR-$2^{-/-}$ mice, suggesting that the TF cytoplasmic domain and PAR-2 may signal through a common downstream pathway to promote fibrosis.

Our studies in $TF^{\S CT/\S CT}$ mice demonstrated significantly fewer $CD68^+$ activated macrophages supporting the view that TF cytoplasmic domain signalling is important for macrophage activation. Hepatic macrophages (Kupffer cells) play a pivotal role in both fibrogenesis and fibrolysis. Macrophages constitutively express TF, which is upregulated during macrophage maturation. Activated macrophages release TGFβ1, which activates HSC, in addition to mitogenic and chemotactic factors for activated HSC[18]. At 8 wk we observed a reduction in the number of activated macrophages ($CD68^+$) in both $TF^{\S CT/\S CT}$ mice and $TF^{\S CT/\S CT}$/PAR-$2^{-/-}$ compared to WT. This may be because the cytoplasmic domain of tissue factor is essential for Factor Ⅶa induced calcium fluxes in macrophages *in vitro*. *In vivo* studies in which TF/Factor Ⅶa interactions were blocked using a TF antibody led to reduced expression of MHC class Ⅱ and β2 integrin leucocyte adhesion molecules which are markers of macrophage activation[3].

There is increasing interest in macrophage phenotypes in liver disease as classically activated M1 macrophages are proinflammatory and alternatively activated M2 macrophages are anti-inflammatory. A recent study has shown that $TF^{\S CT/\S CT}$ mice fed a high fat diet demonstrated reduced inflammatory macrophages in adipose tissue with reduced proinflammatory cytokine production, suggesting that TF signalling is directly involved in regulating macrophage inflammation and may sustain M1 polarisation. Interestingly, there was no additive effect of double deletion of TF and PAR-2 on diet induced obesity, similar to the outcomes we have observed in hepatic fibrosis[8].

In conclusion we have established, for the first time to our knowledge, that deletion of the TF cytoplasmic domain significantly reduces experimental hepatic fibrosis. Furthermore we have shown that deletion of the cytoplasmic domain in addition to PAR-2 deficiency does not lead to more profound protection from fibrosis and in fact that mice lacking the tissue factor cytoplasmic domain phenocopy PAR-2 deficiency. This demonstrates that the tissue factor cytoplasmic domain is involved in pathological TF-PAR-2 signalling. The potential to intervene in this process by inhibiting thrombin or FXa is relevant given the widespread clinical availability of direct inhibitors. For example, administration of argatroban, a direct thrombin inhibitor, to mice fed a Western diet significantly reduced hepatic macrophage accumulation, pro-fibrogenic gene expression and hepatic steatosis suggesting that thrombin inhibition could reduce the risk of fibrosis development in NAFLD patients[9]. It would be prudent to limit therapeutic coagulation inhibition to non-cirrhotic patients at risk of fibrosis progression in order to avoid the risk of bleeding events in cirrhotic patients. This makes the cytoplasmic domain of TF an attractive therapeutic target, as its deletion would not impact on coagulation and thus could be a potentially beneficial anti-fibrotic strategy in patients with advanced liver disease.

COMMENTS

Background

Globally, liver cirrhosis is the sixth most common cause of life-years lost to premature mortality. Cirrhosis represents a "wound healing" response to persistent inflammatory injury (commonly due to fat, alcohol or hepatitis viruses) that can lead to excessive collagen deposition and disruption of normal liver architecture. The coagulation system is active in both the acute response to organ injury as well as in inflammatory signaling that perpetuates the wound healing response. The molecular link between inflammation and coagulation occurs through tissue factor (TF) and protease activated receptors (PARs) although the relative contribution of each remains unclear.

Research frontiers

Currently no anti-fibrotic agents are available for patients with cirrhosis. Liver transplantation may be the only effective treatment for those who progress to hepatic decompensation or develop hepatocellular carcinoma. In order to develop therapeutic anti-fibrotic agents, the authors must understand the cellular and molecular pathways that cause inflammation and fibrosis.

Innovations and breakthroughs

The authors previously showed that PAR-2 was involved in hepatic fibrosis, since deletion of the *PAR-2* gene resulted in decreased fibrosis in mice. Since the TF cytoplasmic domain is a negative regulator of PAR-2 in angiogenesis, they explored this relationship in a model of liver fibrosis. They found that mice with low levels of the cytoplasmic domain of TF had less fibrosis than control mice with fewer activated hepatic stellate cells, the principal liver cells that

produce collagen, and fewer activated macrophages, which express cytokines that drive HSC activation.

Applications

Inhibition of coagulation, for example, by direct thrombin inhibitors, could prevent fibrosis progression in cirrhotic patients but would increase the risk of bleeding events in a patient group at high risk for such events. However, direct targeting of the cytoplasmic domain of TF, which is involved in intracellular signalling but not in coagulation, could be a potentially beneficial anti-fibrotic strategy in cirrhotic patients.

Peer-review

The paper by Knight *et al* describes that genetic ablation of the intracellular portion of TF or of PAR2 downstream to TF both reduce in a non-additive fashion fibrosis in the liver induced by treating mice with CCl_4. Some insights in the mechanism of action of the two manipulations were provided by histological data indicating that they both reduce the frequency of activated smooth muscle cells and activated macrophages and the levels of TGF-β, a known profibrotic factor, in the liver. The results are interesting in view of the fact that liver fibrosis is an unmet clinical need which involves a large number of patients and that drugs targeting TF have been developed and are currently in clinical trials for treatment of thrombosis.

REFERENCES

1 **de Jonge E**, Friederich PW, Vlasuk GP, Rote WE, Vroom MB, Levi M, van der Poll T. Activation of coagulation by administration of recombinant factor VIIa elicits interleukin 6 (IL-6) and IL-8 release in healthy human subjects. *Clin Diagn Lab Immunol* 2003; **10**: 495-497 [PMID: 12738659 DOI: 10.1128/CDLI.10.3.495-497.2003]

2 **Pawlinski R**, Fernandes A, Kehrle B, Pedersen B, Parry G, Erlich J, Pyo R, Gutstein D, Zhang J, Castellino F, Melis E, Carmeliet P, Baretton G, Luther T, Taubman M, Rosen E, Mackman N. Tissue factor deficiency causes cardiac fibrosis and left ventricular dysfunction. *Proc Natl Acad Sci USA* 2002; **99**: 15333-15338 [PMID: 12426405 DOI: 10.1073/pnas.242501899]

3 **Cunningham MA**, Romas P, Hutchinson P, Holdsworth SR, Tipping PG. Tissue factor and factor VIIa receptor/ligand interactions induce proinflammatory effects in macrophages. *Blood* 1999; **94**: 3413-3420 [PMID: 10552951]

4 **Rivers RP**, Hathaway WE, Weston WL. The endotoxin-induced coagulant activity of human monocytes. *Br J Haematol* 1975; **30**: 311-316 [PMID: 1201214 DOI: 10.1111/j.1365-2141.1975.tb00547.x]

5 **Ernofsson M**, Siegbahn A. Platelet-derived growth factor-BB and monocyte chemotactic protein-1 induce human peripheral blood monocytes to express tissue factor. *Thromb Res* 1996; **83**: 307-320 [PMID: 8870175 DOI: 10.1016/0049-3848(96)00139-9]

6 **Belting M**, Dorrell MI, Sandgren S, Aguilar E, Ahamed J, Dorfleutner A, Carmeliet P, Mueller BM, Friedlander M, Ruf W. Regulation of angiogenesis by tissue factor cytoplasmic domain signaling. *Nat Med* 2004; **10**: 502-509 [PMID: 15098027 DOI: 10.1038/nm1037]

7 **Redecha P**, Franzke CW, Ruf W, Mackman N, Girardi G. Neutrophil activation by the tissue factor/Factor VIIa/PAR2 axis mediates fetal death in a mouse model of antiphospholipid syndrome. *J Clin Invest* 2008; **118**: 3453-3461 [PMID: 18802482 DOI: 10.1172/JCI36089]

8 **Badeanlou L**, Furlan-Freguia C, Yang G, Ruf W, Samad F. Tissue factor-protease-activated receptor 2 signaling promotes diet-induced obesity and adipose inflammation. *Nat Med* 2011; **17**: 1490-1497 [PMID: 22019885 DOI: 10.1038/nm.2461]

9 **Kassel KM**, Sullivan BP, Cui W, Copple BL, Luyendyk JP. Therapeutic administration of the direct thrombin inhibitor argatroban reduces hepatic inflammation in mice with established fatty liver disease. *Am J Pathol* 2012; **181**: 1287-1295 [PMID: 22841818 DOI: 10.1016/j.ajpath.2012.06.011]

10 **Knight V**, Tchongue J, Lourensz D, Tipping P, Sievert W. Protease-activated receptor 2 promotes experimental liver fibrosis in mice and activates human hepatic stellate cells. *Hepatology* 2012; **55**: 879-887 [PMID: 22095855 DOI: 10.1002/hep.24784]

11 **Melis E**, Moons L, De Mol M, Herbert JM, Mackman N, Collen D, Carmeliet P, Dewerchin M. Targeted deletion of the cytosolic domain of tissue factor in mice does not affect development. *Biochem Biophys Res Commun* 2001; **286**: 580-586 [PMID: 11511099 DOI: 10.1006/bbrc.2001.5425]

12 **Lee HS**, Shun CT, Chiou LL, Chen CH, Huang GT, Sheu JC. Hydroxyproline content of needle biopsies as an objective measure of liver fibrosis: Emphasis on sampling variability. *J Gastroenterol Hepatol* 2005; **20**: 1109-1114 [PMID: 15955222 DOI: 10.1111/j.1440-1746.2005.03901.x]

13 **Patella S**, Phillips DJ, Tchongue J, de Kretser DM, Sievert W. Follistatin attenuates early liver fibrosis: effects on hepatic stellate cell activation and hepatocyte apoptosis. *Am J Physiol Gastrointest Liver Physiol* 2006; **290**: G137-G144 [PMID: 16123203 DOI: 10.1152/ajpgi.00080.2005]

14 **Abdel-Bakky MS**, Helal GK, El-Sayed EM, Saad AS. Carbon tetrachloride-induced liver injury in mice is tissue factor dependent. *Environ Toxicol Pharmacol* 2015; **39**: 1199-1205 [PMID: 25982951 DOI: 10.1016/j.etap.2015.02.012]

15 **Van Thiel DH**, Farr DE, Mindikoglu AL, Todo A, George MM. Recombinant human factor VIIa-induced alterations in tissue factor and thrombomodulin in patients with advanced liver cirrhosis. *J Gastroenterol Hepatol* 2005; **20**: 882-889 [PMID: 15946135 DOI: 10.1111/j.1440-1746.2005.03761.x]

16 **Martinelli A**, Knapp S, Anstee Q, Worku M, Tommasi A, Zucoloto S, Goldin R, Thursz M. Effect of a thrombin receptor (protease-activated receptor 1, PAR-1) gene polymorphism in chronic hepatitis C liver fibrosis. *J Gastroenterol Hepatol* 2008; **23**: 1403-1409 [PMID: 18005014 DOI: 10.1111/j.1440-1746.2007.05220.x]

17 **Wright M**, Goldin R, Hellier S, Knapp S, Frodsham A, Hennig B, Hill A, Apple R, Cheng S, Thomas H, Thursz M. Factor V Leiden polymorphism and the rate of fibrosis development in chronic hepatitis C virus infection. *Gut* 2003; **52**: 1206-1210 [PMID: 12865283 DOI: 10.1136/gut.52.8.1206]

18 **Marra F**, Aleffi S, Galastri S, Provenzano A. Mononuclear cells in liver fibrosis. *Semin Immunopathol* 2009; **31**: 345-358 [PMID: 19533130 DOI: 10.1007/s00281-009-0169-0]

P- Reviewer: Lee HC, Migliaccio AR **S- Editor**: Gong ZM
L- Editor: A **E- Editor**: Li D

World Journal of Gastroenterology

Submit a Manuscript: http://www.f6publishing.com

World J Gastroenterol 2017 August 21; 23(31): 5700-5712

DOI: 10.3748/wjg.v23.i31.5700

ISSN 1007-9327 (print) ISSN 2219-2840 (online)

ORIGINAL ARTICLE

Basic Study

Schistosoma japonicum attenuates dextran sodium sulfate-induced colitis in mice *via* reduction of endoplasmic reticulum stress

Ya Liu, Qing Ye, Yu-Lan Liu, Jian Kang, Yan Chen, Wei-Guo Dong

Ya Liu, Jian Kang, Yan Chen, Wei-Guo Dong, Department of Gastroenterology, Key Laboratory of Hubei Province for Digestive System Disease, Renmin Hospital of Wuhan University, Wuhan 430060, Hubei Province, China

Qing Ye, Department of Hospital Infection, Renmin Hospital of Wuhan University, Wuhan 430060, Hubei Province, China

Yu-Lan Liu, Departments of Critical Care Medicine, Renmin Hospital of Wuhan University, Wuhan 430060, Hubei Province, China

Author contributions: Liu Y and Ye Q contributed equally to this work; Liu Y, Ye Q, Liu YL, Chen Y and Kang J performed the experiments and analysed the data; Liu Y wrote the manuscript; Ye Q revised the manuscript; all authors have read and approved this manuscript.

Institutional review board statement: This study was reviewed and approved by Wuhan University Institutional Review Board.

Institutional animal care and use committee statement: All procedures involving animals were reviewed and approved by the Institutional Animal Care and Use Committee of the Wuhan University.

Conflict-of-interest statement: To the best of our knowledge, no conflict of interest exists.

Data sharing statement: No additional data are available.

Manuscript source: Unsolicited manuscript

Correspondence to: Wei-Guo Dong, MD, PhD, Department of Gastroenterology, Key Laboratory of Hubei Province for Digestive System Disease, Renmin Hospital of Wuhan University, 238 Jiefang Road, Wuhan 430060, Hubei Province, China. dwg@whu.edu.cn
Telephone: +86-27-88041911
Fax: +86-27-88042292

Received: February 16, 2017
Peer-review started: February 22, 2017
First decision: March 3, 2017
Revised: March 30, 2017
Accepted: April 21, 2017
Article in press: April 21, 2017
Published online: August 21, 2017

Abstract

AIM

To elucidate the impact of *Schistosoma* (*S.*) *japonicum* infection on inflammatory bowel disease by studying the effects of exposure to *S. japonicum* cercariae on dextran sodium sulfate (DSS)-induced colitis.

METHODS

Infection was percutaneously established with 20 ± 2 cercariae of *S. japonicum*, and colitis was induced by administration of 3% DSS at 4 wk post infection. Weight change, colon length, histological score (HS) and disease activity index (DAI) were evaluated. Inflammatory cytokines, such as IL-2, IL-10 and IFN-γ, were tested by a cytometric bead array and real-time quantitative polymerase chain reaction (RT-PCR). Protein and mRNA levels of IRE1α, IRE1β, GRP78, CHOP, P65, P-P65, P-IκBα and IκBα in colon tissues were examined by Western blot and RT-PCR, respectively. Terminal deoxynucleotidyl transferase-mediated dUTP nick-end labeling positive cells, cleaved-caspase 3 expression and

Bcl2/Bax were investigated to assess the apoptosis in colon tissues.

RESULTS

Mice infected with *S. japonicum* cercariae were less susceptible to DSS. Mice infected with *S. japonicum* cercariae and treated with DSS showed decreased weight loss, longer colon, and lower HS and DAI compared with mice treated with DSS alone. A substantial decrease in Th1/Th2/Th17 response was observed after infection with *S. japonicum*. Endoplasmic reticulum (ER) stress and the nuclear factor-kappa B (NF-κB) pathway were reduced in mice infected with *S. japonicum* cercariae and treated with DSS, along with ameliorated celluar apoptosis, in contrast to mice treated with DSS alone.

CONCLUSION

Exposure to *S. japonicum* attenuated inflammatory response in a DSS-induced colitis model. In addition to the Th1/Th2/Th17 pathway and NF-κB pathway, ER stress was shown to be involved in mitigating inflammation and decreasing apoptosis. Thus, ER stress is a new aspect in elucidating the relationship between helminth infection and inflammatory bowel disease (IBD), which may offer new therapeutic methods for IBD.

Key words: Endoplasmic reticulum stress; *Schistosoma japonicum*; Colitis

Core tip: *Schistosoma* (*S.*) *japonicum* has been demonstrated to participate in the development of colitis in animal experiments as well as clinical trials. However, the effects of *Schistosoma* infection on colitis and the underlying mechanism are still elusive. Here, we studied the effects of exposure to *S. japonicum* cercariae on dextran sodium sulfate (DSS)-induced colitis. We found that *S. japonicum* attenuated DSS-induced colitis in mice by reducing inflammatory response and apoptosis in colon tissues. Besides Th1/Th2/Th17 pathway and nuclear factor-kappa B pathway, endoplasmic reticulum stress played an important role in the preventive effects of parasite infection on DSS-induced colitis.

Liu Y, Ye Q, Liu YL, Kang J, Chen Y, Dong WG. *Schistosoma japonicum* attenuates dextran sodium sulfate-induced colitis in mice *via* reduction of endoplasmic reticulum stress. *World J Gastroenterol* 2017; 23(31): 5700-5712 Available from: URL: http://www.wjgnet.com/1007-9327/full/v23/i31/5700.htm DOI: http://dx.doi.org/10.3748/wjg.v23.i31.5700

INTRODUCTION

Inflammatory bowel disease (IBD), which involves chronic and complicated inflammatory lesions of the intestinal tract, includes ulcerative colitis (UC) and Crohn's disease (CD)[1,2]. Epidemiological investigations have shown that the incidence and morbidity of IBD are increasing worldwide[3,4]. However, the mechanism of IBD is still unclear, and the environment, individual genetics, infection and host immunity are involved[1,5]. Elucidating the exact mechanism of IBD and developing effective treatments will be valuable for ameliorating patients' quality of life.

Exposures to infectious agents (such as parasites) are suggested to have fundamental effects on the development and behavior of the immune system, which may decrease the incidence of both allergic and autoimmune diseases[6]. Thus, several studies were performed to investigate the effects of helminth infections on IBD. Patients with UC or CD showed significant disease remission after administration of viable and embryonated eggs of *T. suis* (the porcine whipworm), suggesting the therapeutic effects of parasites on IBD[7,8]. Seven of nine Crohn's patients infected with larvae of *Necator*, the human hookworm, showed an improved disease score, and their inflammatory cytokine (IFN-γ and IL-17) responses in duodenal biopsies were reduced compared to those of placebo-treated patients[9,10]. In addition, a mouse model of experimental colitis induced with trinitrobenzene sulfonic acid (TNBS) or dextran sodium sulfate (DSS) also showed decreased susceptibility to IBD or attenuated symptoms after treatment with eggs or larvae of *Schistosoma* (*S.*)[11-13]. However, infection with *S. mansoni* soluble egg antigen had no effect on mice with DSS–induced colitis[14]. Moreover, Smith *et al*[15] demonstrated that mice with colitis induced with DSS displayed worsening results after injection of *S. mansoni* eggs. These dissimilar outcomes of the impact of *Schistosoma* on IBD have yet to be investigated since the underlying mechanism is still unclear.

Here, we infected mice with *S. japonicum* cercariae *via* contact with the abdomen skin, which is a classical and natural method to infect hosts, such as mice[16]. Then, we investigated the effects of *S. japonicum* infection on the relatively simple and replicable DSS-induced colitis model due to the limitations of human clinical trials. DSS-induced colitis has been widely used as an animal model of experimental IBD, especially UC, due to its similarities to IBD characteristics, such as diarrhea, mucosal ulceration, rectal bleeding and body weight loss[17-19]. In the present study, we aimed to explore the effects of exposure to *S. japonicum* cercariae on DSS-induced colitis and identify the underlying pathogenesis of IBD.

MATERIALS AND METHODS

Ethics statement

All animal experiments during this research were performed in accordance with the recommendations in

Table 1 Disease activity index score parameters

Score	Body weight loss	Stool consistency	Rectal bleeding
0	0%-1%	Normal	None
1	1%-5%	Soft and shaped	Between
2	5%-10%	Loose	Slight
3	10%-15%	Between	Between
4	> 15%	Diarrhea	Gross bleeding

the Guide for the Care and Use of Laboratory Animals of Wuhan University.

Materials and grouping

Oncomelania hupensis snails infected with *S. japonicum* were obtained from the Institute of Parasitic Disease Control and Prevention, Jiangsu Province, China. Male Kunming mice, weighing 14-16 g, were purchased from the Hubei Provincial Center for Disease Control.

DSS for inducing acute colitis was purchased from MP Biochemicals (Solon, OH, United States). Antibodies for immunofluorescence, Western blot and cytokine tests were purchased from Abcam (Cambridge, MA, United States), Bioworld Technology (Minneapolis, MN, United States), Millipore (Billerica, MA, United States), Santa Cruz Biotechnology (Santa Cruz, CA, United States) and Cell Signaling Technology (Danvers, MA, United States).

Forty mice were randomly divided into four groups with ten mice in each group. The mice only treated with DSS were termed the DSS group, and those only infected with cercariae were called the CER group. The mice in the CER + DSS group were infected with cercariae and subsequently treated with DSS. In the control group, the mice were treated with saline instead.

Infection with S. japonicum

The infected snails were illuminated to induce cercarial shedding. The mice from the CER group and CER + DSS group were percutaneously infected with 20 ± 2 cercariae of *S. japonicum*, while those in the control group and DSS group were treated with saline by dermal contact.

Induction and evaluation of colitis

After 4 wk of the infection, the mice in the CER + DSS group and DSS group were fed 3% (wt/vol) DSS freely to induce acute colitis. The status of each mouse, including weight, morbidity, stool properties, and bleeding, was recorded daily. Disease activity index (DAI) was assessed as described in Table 1[20].

All mice were sacrificed on day 7 after DSS feeding. Blood samples were collected and centrifuged to isolate serum, which was subsequently stored at -80 ℃. The entire colon was cut away and gently washed with saline precooled to 4 ℃, most of which was dried and frozen in liquid nitrogen immediately for subsequent Western blot or RT-PCR analysis. The distal segment of the colon (approximately 0.5 cm) was fixed in 10% buffered formalin for histological observation.

Histological observation

To assess colon inflammation, the formalin-treated colon was embedded into paraffin. Serial sections with 5 mm thickness were cut and stained with hematoxylin and eosin (H and E, Richard Allen Scientific, Kalamazoo, MI, United States). Histological score (HS) was calculated in a blinded manner three times as shown in Table 2[21]. CD3 and Ly6G monoclonal antibodies were used to assess the infiltration of inflammatory cells. Cleaved caspase 3 (C-C3) was tested to identify the cellular apoptosis in colon tissues. All digital images were taken using a fluorescence microscope (Olympus DX51, Olympus, Tokyo, Japan) and processed with a digital image analysis system (Image-Pro Plus version 6.0, Media Cybernetics, Bethesda, MD, United States). Then the original pictures were merged and the positive cells were quantified. Data were obtained from 3 or more mice per group.

Detection of inflammatory cytokines

Cytometric bead array (CBA) was used to detect the expression of several inflammatory cytokines (IL-2, IL-4, IL-6, IL-10, IL-17A, TNFα and IFN-γ) in the serum of different groups. Serum samples were assayed with a mouse Th1/Th2/Th17 Cytokine Kit (560484, BD), which included seven specific capture beads. After reacting with the bead mixture for 3 h in a dark environment at room temperature, blood samples were analyzed by flow cytometry (Aira Ⅲ, BD) to identify the numbers of different positive beads. FCAP Array v3 version 3.0.1 from BD Biosciences was employed to translate the images into data.

Western blot analysis

The proteins extracted from colon tissues of the mice in different groups were boiled with loading buffer and subjected to SDS-PAGE. Then, they were blotted onto polyvinylidene fluoride membranes (IPVH00010, Millipore), which were then washed and blocked with Tris-buffered saline containing 5% milk and 0.1% Tween-20 for 2 h. The treated membranes were incubated with particular antibodies overnight at 4 ℃. An enhanced chemiluminescence reagent (LiDE110, Canon) was used to detect the expression of proteins according to the protocol. All images were analyzed with AlphaEaseFC software, and GAPDH was used as the reference.

Real-time PCR

Total RNA was obtained from 1 mg of colon tissue using TRIzol reagent (15596-026, Invitrogen) and converted into cDNA using a PrimeScript™ RT reagent Kit with gDNA eraser (RR047A, TaKaRa). The parameters for RT-PCR amplification were as follows: 95 ℃ for 1 min,

Table 2 Histological scoring system used in this study

Score	Damaged area	Mucodepletion of glands	Tissue damage	Inflammatory cell infiltration
0	N/A	None	No mucosal damage	Occasional inflammatory cells in the lamina propria
1	≤ 25%	Mild	Discrete epithelial lesions	Increased numbers of inflammatory cells in the lamina propria
2	≤ 50%	Moderate	Surface mucosal erosion or focal ulceration	Confluence inflammatory cells, extending into the submucosa
3	≤ 75%	Moderate	Extensive mucosal damage and extension into deeper structures of the bowel wall	Transmural extension of the infiltrate
4	≤ 100%	Severe		

Table 3 Gene-specific primer pairs used in the study

Primer name		Primer sequence	Product length (bp)
M-GAPDH	Forward	5′-TGAAGGGTGGAGCCAAAAG-3′	227
	Reverse	5′-AGTCTTCTGGGTGGCAGTGAT-3′	
M-IL-6	Forward	5′-CTTCTTGGGACTGATGCTGGT-3′	171
	Reverse	5′-CACAACTCTTTTCTCATTTCCACG-3′	
M-IL-10	Forward	5′-TACAGCCGGGAAGACAATAACT-3′	142
	Reverse	5′-AGGAGTCGGTTAGCAGTATGTTG-3′	
M-TNF-α	Forward	5`-TCCCCAAAGGGATGAGAAGTT-3′	298
	Reverse	5′-GAGGAGGTTGACTTTCTCCTGG-3′	
M-TGF-β	Forward	5′-AGAGCCCTGGATACCAACTATTG-3′	286
	Reverse	5′-TGCGACCCACGTAGTAGACG-3′	
M-IFN-γ	Forward	5′-CTCAAGTGGCATAGATGTGGAAG-′	250
	Reverse	5′-GACCTCAAACTTGGCAATACTCA-3′	
M-IL-1b	Forward	5′-GGGCCTCAAAGGAAAGAATCT-3′	195
	Reverse	5′-GAGGTGCTGATGTACCAGTTGG-3′	
M-IL-17a	Forward	5′-GTCTTTAACTCCCTTGGCGC-3′	136
	Reverse	5′-GGCACTGAGCTTCCCAGATC-3′	
M-IRE1a	Forward	5′-ACACACCGACCACCGTATCTC-3′	157
	Reverse	5′-GGGTAAGTGATGATGAACGCC-3′	
M-IRE1b	Forward	5′-TGGACGGTCCCACAACAGAT-3′	140
	Reverse	5′-GGGAGGTTCGTGGTATCCAA-3′	
M-GRP78	Forward	5′-GATGAAATTGTTCTGGTTGGTGG-3′	203
	Reverse	5′-AGTGTAAGGGGACAAACATCAAG-3′	
M-CHOP	Forward	5′-GGAGCTGGAAGCCTGGTATG-3′	285
	Reverse	5′-GGGCACTGACCACTCTGTTTC-3′	

followed by 40 cycles of 95 ℃ for 15 s, 58 ℃ for 20 s and 72 ℃ for 45 s. Primers for RT-PCR are listed in Table 3, and GAPDH was used as the housekeeping gene.

Terminal deoxynucleotidyl transferase-mediated dUTP nick-end labeling assay

Transferase-mediated dUTP nick-end labeling (TUNEL) (ApopTag Plus In Situ Apoptosis Fluorescein Detection Kit, Millipore) assay was performed to assess cellular apoptosis. Paraffin-embedded tissue sections were treated with protease K solution for 15-30 min at 37 ℃ after dewaxing and rehydrating. Sections were washed and incubated with TUNEL reaction mixture for 60 min at 37 ℃ in a moist chamber. Addition of converter-POD for 30 min at 37 ℃ and substrate solution for 30 min at room temperature was performed sequentially. Fluorescence microscopy was used to analyze the sections, and Image-Pro Plus version 6.0 was adopted to process the digital images. Then the original pictures were merged and the positive cells were quantified. Data obtained from 3 or more mice per group were calculated in a blinded manner.

Statistical analysis

One-way analysis of variance or Kruskal-Wallis *H* test was performed to analyze all the data (SPSS 20.0 software). $P < 0.05$ was considered statistically significant.

RESULTS

Effect of S. japonicum infection on the development of colitis

To evaluate the effect of exposure to *S. japonicum* cercariae on the development of colitis, a chemical model of mucosal inflammation induced by oral administration of 3% DSS was established in mice infected with cercariae for 4 wk. Various indexes, including body weight, DAI, colon length, histological observation and HS, were used to assess the severity of acute colitis in mice.

On the 7th day of DSS treatment, three mice from the DSS group had died due to substantial weight

loss (15.4%-19.3%). One of ten mice in the CER + DSS group died on the 5th day due to collision with the cage, and another died for unclear reasons before DSS treatment. From the 5th day, the body weights of mice in both the CER + DSS and DSS groups began to decline, while those in the control and CER groups remained stable. On the 7th day, the mice in the DSS group presented a more significant weight loss than those in the CER + DSS group (Figure 1A; $P < 0.0001$). In addition, the DAI scores of the mice in the CER + DSS group were lower than those in the DSS group (Figure 1B, $P = 0.005$). Among the mice in the four groups, the colon length was shortest in DSS mice and shorter in CER + DSS mice (Figure 1C and D; $P < 0.001$ DSS *vs* control, $P = 0.004$ DSS *vs* CER + DSS). There was no significant difference between control mice and CER mice with regard to colon length. Although evident colon hyperemia and edema were observed in both colon tissues of DSS mice and CER + DSS mice, reduced architecture loss, goblet damage and inflammatory cell infiltration were observed in colon tissues of CER + DSS mice compared to those of DSS mice under a microscope (Figure 1E). No pathological lesions were found in the control and CER groups. According to blind assessments from three independent experimenters, the HS of DSS mice was much larger than that of CER + DSS mice (Figure 1F; $P = 0.004$).

Detection of inflammatory cell infiltration by immunofluorescence

CD3 (indicates lymphocytes) and Ly6G (indicates neutrophils) were detected to assess the infiltration of inflammatory cells in colon tissues. CD3 and Ly6G were both labeled red, and nuclei were stained with 4′, 6-diamidino-2-phenylindole (DAPI). CD3 positive cells were more abundant in DSS mice than those in control mice after merging CD3 with nuclei using Image-Pro Plus (Figure 2A and B; $P < 0.001$). Mice in the CER + DSS group presented fewer CD3 positive cells compared to those of mice in the DSS group (Figure 2A and B; $P < 0.05$). As for Ly6G, there were differences among the four groups (Figure 2C; $P = 0.019$). The number of Ly6G positive cells was larger in the DSS group than that in mice of the CER+DSS group (Figure 2C). Nevertheless, mice in the control group and CER group showed no difference in the abundance of CD3 positive cells and Ly6G positive cells.

Expression of inflammatory cytokines in serum samples and colon tissues of treated mice

The expression levels of IL-2, IFN-γ and TNFα were detected to assess the Th1 response in mice of each group, and IL-4, IL-6 and IL-10 were examined to evaluate the Th2 response. In addition, IL-17A was tested to assess the Th17 response. CBA tests indicated that the mice in the CER + DSS and DSS groups showed higher levels of inflammatory cytokines compared with control and CER mice (Figure 3). The expression levels of IL-2, IFN-γ, TNFα, IL-6, IL-10 and IL-17a in CER + DSS mice were much lower than those in DSS mice, especially for IL-6, IL-10 and IFN-γ (Figure 3A, $P < 0.001$ for IL-6, IL-10 and IFN-γ). However, there were no significant differences between control and CER mice. IL-4 was hardly detected in any samples. Higher mRNA levels of IL-1β, IL-6, IL-10, IL-17a, IFN-γ, TNFα and TGFβ were observed in colon tissues of CER + DSS and DSS mice compared to control mice (Figure 3B). Among the four groups, mice in the DSS group displayed the highest expression of IL-6, while mice in the CER + DSS group presented much lower expression of IL-6 compared with that in mice of the DSS group (Figure 3B; $P < 0.001$). Additionally, IL-10 and IFN-γ were lower in the CER+DSS group than in the DSS group (Figure 3B; $P < 0.001$ for IL-10; $P < 0.05$ for IFN-γ). No significant difference was observed between mice of the control group and CER group.

Expression of proteins involved in the NF-κB signaling pathway and endoplasmic reticulum stress pathway in inflamed colitis

The expression level of phosphorylated-p65 (P-p65) in colon tissues of DSS mice was the highest among the four groups (Figure 4A and B). Mice in the CER + DSS group presented lower P-p65 expression than mice in the DSS group (Figure 4A and B; $P < 0.05$). Consistent with the P-p65 results, mice in the DSS group showed much higher expression of phosphorylated-IκBα (P-IκBα) compared with the control group (Figure 4A and D; $P < 0.05$). The expression level of P-IκBα in CER + DSS mice was lower than that in mice of the DSS group (Figure 4A and D). There were no differences in expression levels of P-p65, P65, P-IκBα and IκBα between mice of the control group and CER group.

For endoplasmic reticulum (ER) stress markers, the expression levels of IRE1α, IRE1β and CHOP were significantly higher in DSS mice than in control mice as revealed by both Western blot (Figure 5A-D, $P < 0.0001$ for IRE1α and IRE1β, $P < 0.01$ for CHOP) and RT-PCR (Supplementary Figure 1). Compared with mice in the DSS group, mice in the CER + DSS group presented much lower expression levels of IRE1α and IRE1β (Figure 5A and B; $P < 0.01$; Figure 5A and C; $P < 0.05$). Furthermore, there were clear differences in the expression levels of GRP78 among the four groups (Figure 5A and E; $P = 0.0006$ for 4 groups). The expression levels of GRP78 and CHOP in mice of the CER + DSS group were lower than those in mice of the DSS group (Figure 5A, D and E). Mice in the control group and CER group showed no difference in ER stress markers.

Observation of cellular apoptosis in colon tissues

To estimate celluar apoptosis in colon tissues, TUNEL and C-C3 positive cells were investigated. C-C3 and TUNEL positive cells were labeled red and green, respectively. Nuclei were stained with DAPI. There

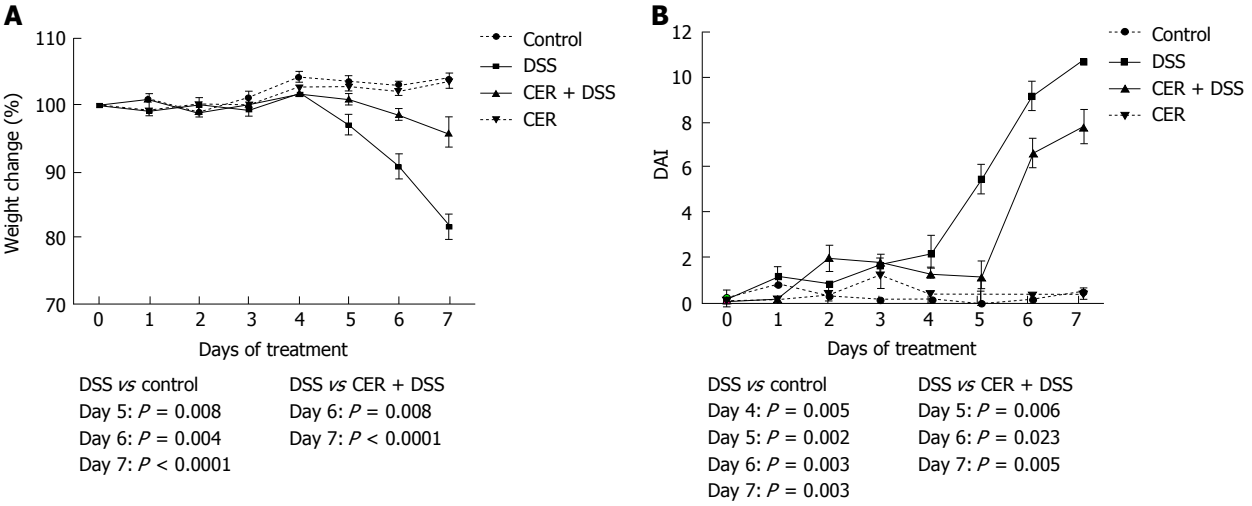

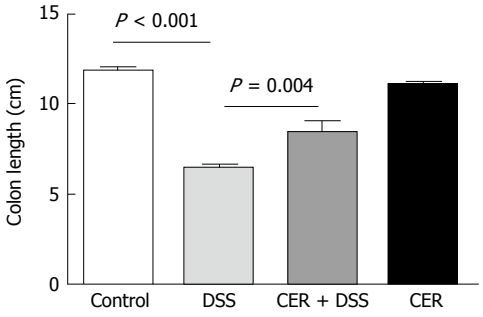

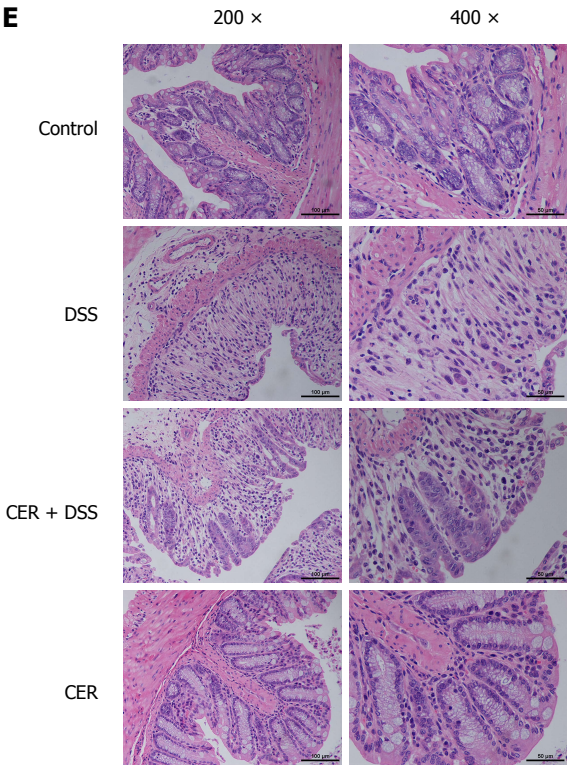

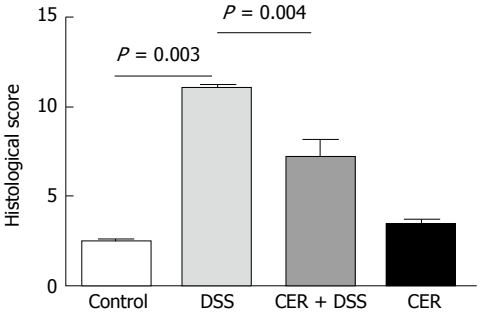

Figure 1 Treatment with *S. japonicum* cercariae results in reduced susceptibility to dextran sodium sulfate-induced colitis in mice. Mice were infected with 20 ± 2 *S. japonicum* cercariae percutaneously, and experimental colitis was induced by administration of 3% DSS at 4 wk post infection. A: Weight change in percent; B: DAI based on weight change, stool characteristics and bleeding; C and D: Colon length; E: H and E staining was performed in colonic sections (original magnification, × 200 and × 400); F: HS was scored as described in Materials and Methods. $n = 6$. The mice infected with *S. japonicum* cercariae presented longer colons, decreased weight loss and lower DAI and HS after being induced with DSS compared to those without parasite infection. DSS: Dextran sodium sulfate treatment alone; CER + DSS: Infection with *S. japonicum* before DSS treatment; CER: *S. japonicum* infection alone.

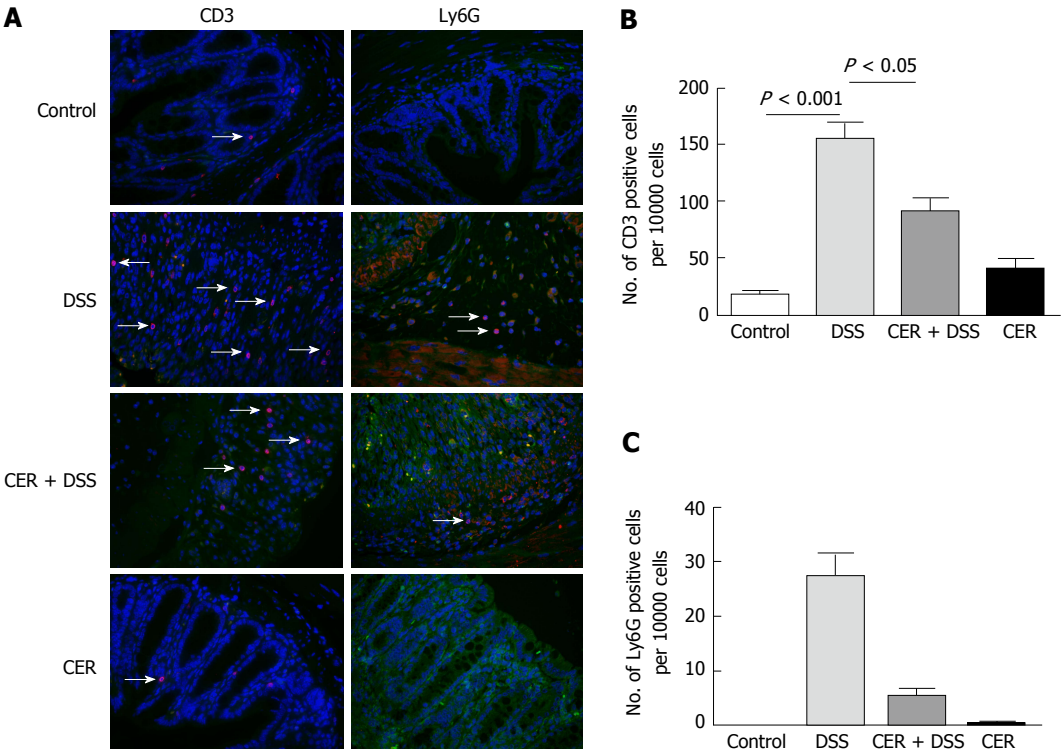

Figure 2 Infection with *S. japonicum* decreases infiltration of inflammatory cells in colon tissues. A: Immunofluorescence staining of CD3 and Ly6G in the colon sections; B and C: Respective quantification of CD3 and Ly6G positive cells. *n* = 3. DSS: Dextran sodium sulfate treatment alone; CER + DSS: Infection with *S. japonicum* before DSS treatment; CER: *S. japonicum* infection alone.

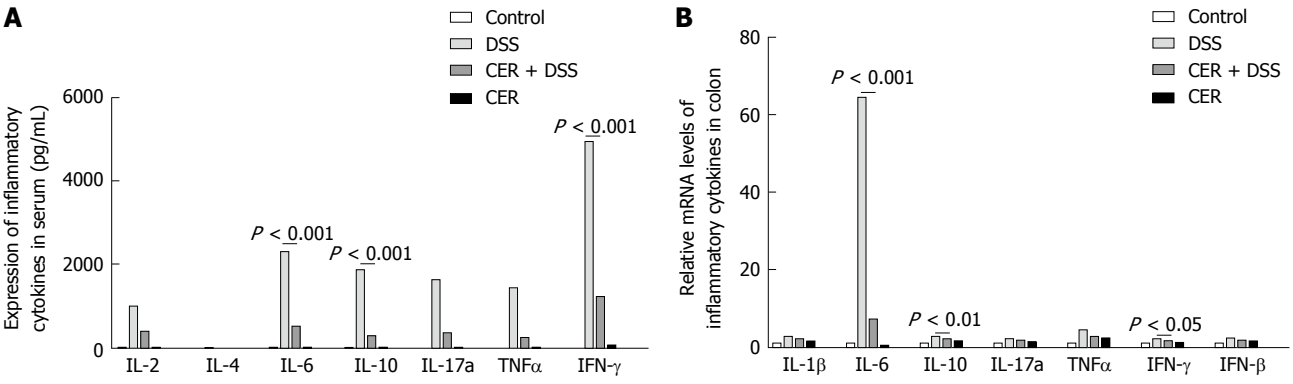

Figure 3 Administration of *S. japonicum* leads to lowered inflammatory cytokines in dextran sodium sulfate-induced colitis mice. A: The production of IL-2, IL-6, IL-10, IL-17A, TNFα and IFN-γ in blood samples was detected by CBA and flow cytometry; B: IL-1β, IL-6, IL-10, IL-17a, IFN-γ, TNFα and TGFβ levels in colon tissues were tested by RT-PCR. *n* = 3 or 4. Exposure to *S. japonicum* protected mice from DSS-induced colitis with down-regulation of the Th1/Th2/Th17 pathway. DSS: Dextran sodium sulfate treatment alone; CER + DSS: Infection with *S. japonicum* before DSS treatment; CER: *S. japonicum* infection alone.

were significant difference in the numbers of C-C3 positive cells and TUNEL positive cells among the mice of the four groups (Figure 6A-C, $P = 0.015$ for the four groups). Mice of the DSS group presented a dramatically larger number of C-C3 positive cells than mice of the control group as well as the CER group (Figure 6A and B). Large numbers of TUNEL positive cells were observed in colon tissues of DSS mice (Figure 6A and C). There were fewer C-C3 positive cells and TUNEL positive cells in CER+DSS mice compared with DSS mice (Figure 6A-C). Hardly any difference in the abundance of C-C3 positive cells and TUNEL positive cells was observed between mice in the control group and CER group.

In addition, mice in the DSS group showed distinctly lower Bcl-2 expression than mice in the control group (Figure 6D and F; $P < 0.0001$). The expression level of Bcl-2 was much higher in mice of the CER + DSS group than in mice of the DSS group (Figure 6D and F; $P < 0.05$). Additionally, there was a difference in Bax levels among the four groups (Figure 6D and E; $P = 0.015$ for 4 groups). Mice of the CER + DSS group had much lower Bax expression than mice of the DSS group (Figure 6D and E). Mice in the control group and

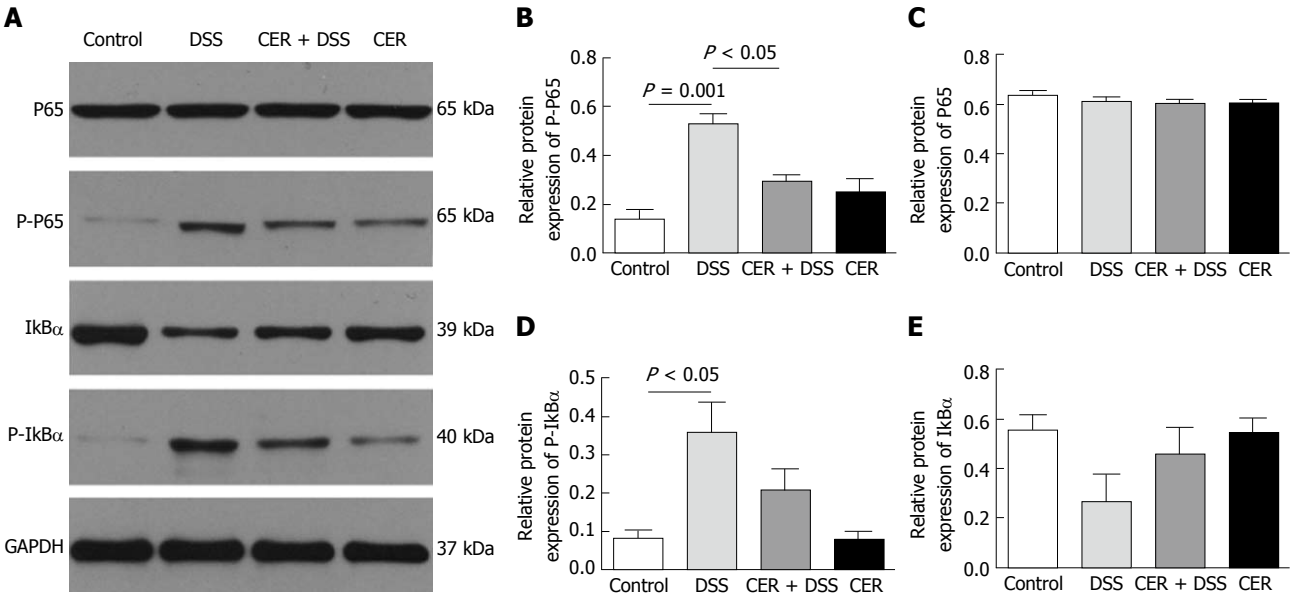

Figure 4 Infection with *S. japonicum* decreases the expression of phosphorylated-p65 in mice treated with dextran sodium sulfate. A: The expression of P-P65 and P65 in colon tissues was examined by Western blot; B and C: Respective quantification of P-P65 and P65; D and E: Respective quantification of P-IKBα and IKBα. *n* = 3. DSS: Dextran sodium sulfate treatment alone; CER + DSS: Infection with *S. japonicum* before DSS treatment; CER: *S. japonicum* infection alone.

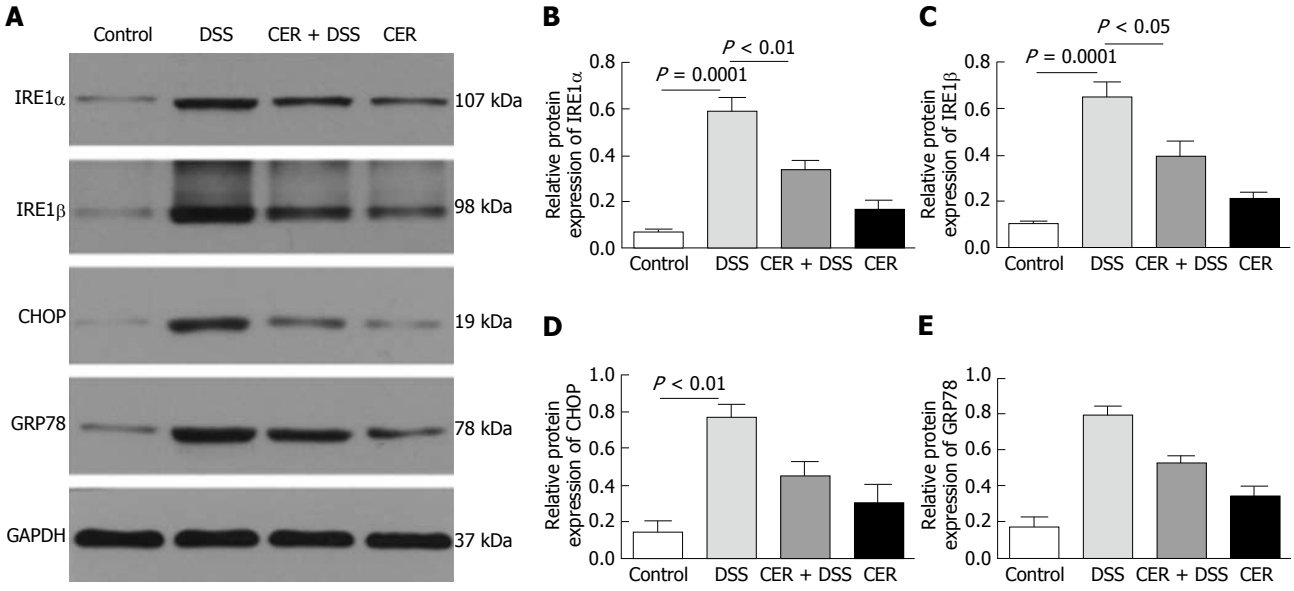

Figure 5 Endoplasmic reticulum stress markers are downregulated in mice induced with dextran sodium sulfate after infection. A: The expression of IRE1α, IRE1β, GRP78 and CHOP in colon tissues was examined by Western blot; B-E: Respective quantification of IRE1α, IRE1β, GRP78 and CHOP. *n* = 4. DSS: Dextran sodium sulfate treatment alone; CER + DSS: Infection with *S. japonicum* before DSS treatment; CER: *S. japonicum* infection alone.

CER group displayed no difference in the expression levels of Bcl-2 and Bax.

DISCUSSION

According to the "hygiene hypothesis", which was first proposed by Strachan[22] in 1958, early childhood infections were associated with decreased atopy in children. Although the concept began with allergic disorders, it has been extended and is currently related to autoimmunity, neuroinflammatory disorders, atherosclerosis, and some cancers[23]. In the 1990s, the "inflammatory bowel disease hygiene hypothesis" was first proposed, which stated that children in extremely hygienic environments that might impede the proper maturation of their immune system were predisposed to IBD later in life[11]. According to epidemiological investigations, helminth infection was suggested to decrease the susceptibility to or prevent the development of IBD[11]. Here, we investigated the effects of *S. japonicum* infection on a DSS-induced colitis model, and we found that *S. japonicum* infection reduced the

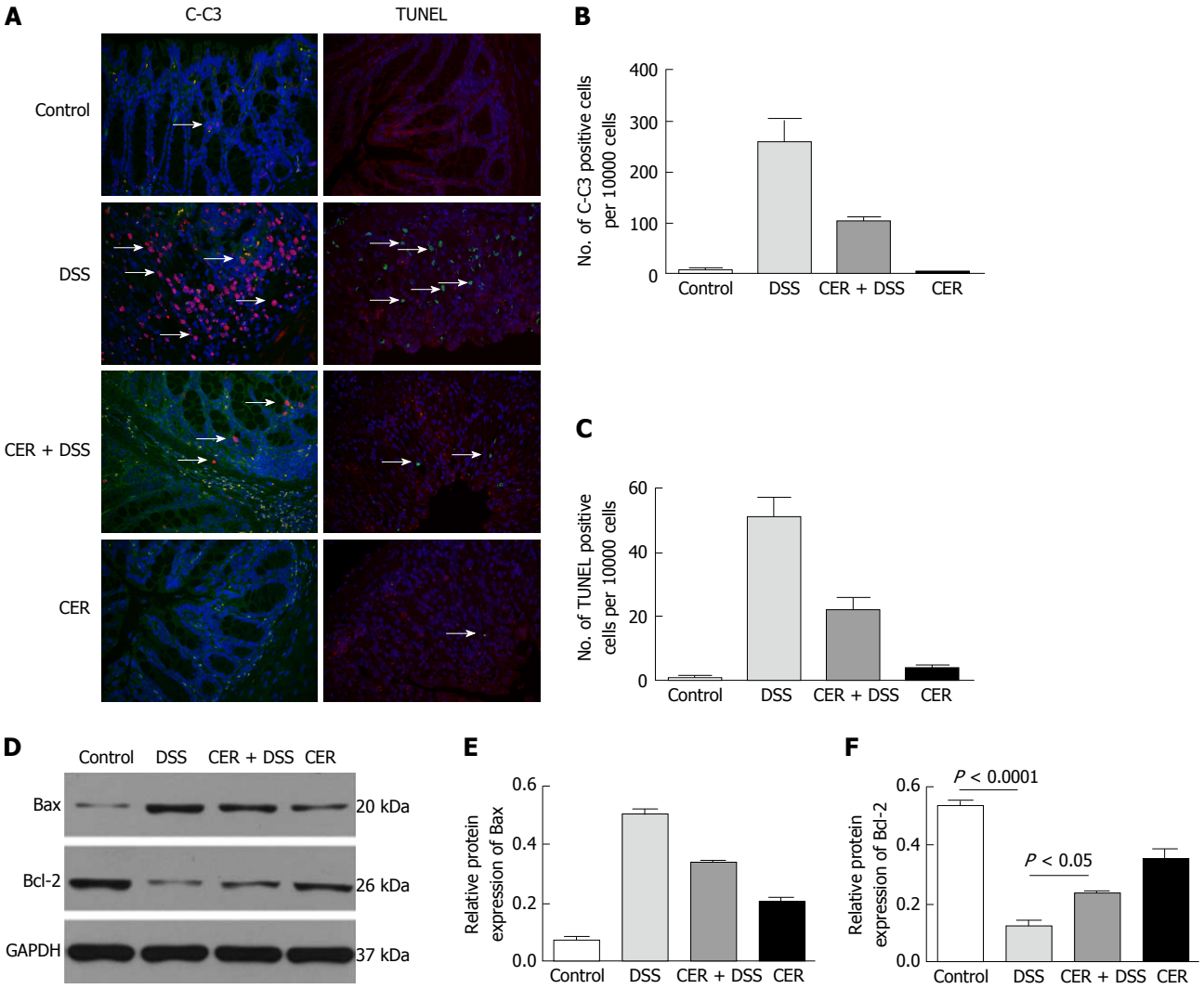

Figure 6 Apoptosis in colitic mice after infection with *S. japonicum*. A: Immunofluorescence staining of cleaved-caspase3 (C-C3) and TUNEL staining; B and C: Respective quantification of C-C3 and TUNEL positive cells; D: Bax and Bal-2 were tested by Western blot; E and F: Respective quantification of Bax and Bal-2. *n* = 3. DSS: Dextran sodium sulfate treatment alone; CER + DSS: Infection with *S. japonicum* before DSS treatment; CER: *S. japonicum* infection alone.

susceptibility to DSS and decreased the infiltration of inflammatory cells, ER stress and the NF-κB pathway.

There were no significant differences in colon length, weight loss, DAI and HS between the mice in the control and CER groups. The colon length of mice in the DSS group was not only shorter than that of control mice but also shorter than that of mice in the CER + DSS group. The weights of the mice in the DSS group decreased significantly from the 5th day of DSS treatment, while the mice in the CER + DSS group showed a slower decrease from the 6th day of DSS treatment. Both DAI and HS were highest in the DSS group mice and were significantly higher than those of mice infected with *S. japonicum* cercariae prior to DSS treatment (CER + DSS mice). In addition, less lymphocyte and neutrophil infiltration was observed in colon tissues of CER + DSS mice compared with DSS mice. All results indicated that exposure to *S. japonicum* contributed to preventing the development of colitis induced with DSS.

Although the mechanism underlying IBD is complicated, the influence of *Schistosoma* or its molecules on animal colitis was predominantly suggested to be related to the balance between Th1 response and Th2 response[12,14,24,25]. Research by Elliott *et al*[12] illustrated that infection with eggs of *S. mansoni* attenuated TNBS-induced colitis by reducing Th1 response and increasing Th2 response. However, DSS-induced colitis mice presented diminished expression levels of TNFα, IL-2 and IL-4 mRNA after exposure to *S. mansoni* larvae[14]. Recombinant cystatin from *S. japonicum* showed a therapeutic effect on mice with TNBS-induced colitis by suppressing IFN-γ and IL-17a and enhancing IL-4 and IL-13[24]. In addition, Ruyssers *et al*[25] reported augmented IL-10 mRNA expression and diminished IFN-γ mRNA and IL-17 mRNA expression. In our study, compared with DSS mice, significant decreases in IL-6, IL-2, IL-10, IL-17, IFN-γ and TNFα were observed in CER + DSS mice as revealed by the CBA technique, which are consistent with the

diminished levels of inflammatory cytokines and transcription factors detected by RT-PCR, especially for IL-10, IL-6 and IFN-γ. In other words, we observed that *S. japonicum* infection ameliorated DSS-induced colitis with decreased Th1, Th2 and Th17 responses. Thus, we hypothesize that the Th1/Th2/Th17 pathway may not be the dominant mediator during colitis following exposure to *S. japonicum*. Additionally, these results might be caused by the different time points we chose to induce colitis, diverse infection methods, disparate animal models and other factors compared to those of other studies. For example, Elliott *et al*[12] and Xia *et al*[26] adopted TNBS-induced colitis and Bodammer *et al*[14] used *S. mansoni* larvae to infect mice.

Oh *et al*[27] identified an important effect of NF-κB in regulating differentiation and maturation of Th cells. Furthermore, connections between the NF-κB pathway and IBD have been reported in previous studies[28,29]. In our previous study, CARD3 deficiency alleviated the infiltration of inflammatory cells and cellular apoptosis during DSS-induced colitis followed by decreased NF-κB activation[21]. Hence, we examined the protein levels of P65, P-P65, IκBα and P-IκBα in colon tissues of mice. The results showed high expression of P-P65 and P-IκBα in DSS mice. Consistent with the cytokine results of serum samples and colon tissues, CER + DSS mice displayed lower P-P65 and P-IκBα levels compared to DSS mice. It was reported that NF-κB was essential for the production of IL-2[27], and the absence of P65 could impair IFN-γ production in Th1 cells[30]. Additionally, NF-κB activation played an important role in regulating the expression of the GATA3 and RORγt genes, which are transcription factors of Th2 cells and Th17 cells, respectively[31,32]. Thus, the attenuation of the DSS-induced colitis in mice *via* exposure to *S. japonicum* as well as the change in cytokines related to Th1, Th2 and Th17 responses was probably due NF-κB activation.

ER stress participates in many inflammatory diseases, such as CD and T2DM, and has shown great potential in regulating inflammatory responses through the unfolded protein response (UPR) pathway[33,34]. Increased expression of ER stress markers was observed in ileal and/or colonic epithelial tissues of active IBD patients[34,35]. Adolph *et al*[36] also demonstrated spontaneous transmural ileitis similar to CD accompanied by activated IRE1α in intestinal epithelial cells of mice with *Xbp1* and *Atg1611* deletions. However, addition of ER stress inhibitors, such as tauroursodeoxycholate and 4-phenylbutyrate, mitigated intestinal inflammation in *IL-10*$^{-/-}$ and *Tnf*$^{\Delta ARE}$ mice induced with DSS[37]. In addition, taurine supplement attenuated hepatic granuloma and fibrosis in *S. japonicum*-infected mice, with a significant decrease in ER stress[38]. In our study, the expression levels of IRE1α, IRE1β, GRP78 and CHOP and their coding genes were notably highest in DSS mice among the four groups. Although the expression levels of these molecules were still higher in CER + DSS mice compared with those in control mice, they were much lower than those in DSS mice. Coupling of the UPR in cells triggered inflammation and played an important role in the pathogenesis of inflammatory diseases[39]. Additionally, IRE1α activation by binding with TNFα receptor-associated factor 2 (TRAF2) may affect TRAF2 and subsequently activate the NF-κB pathway[40,41]. Inflammation induced by *Brucella abortus* accompanied by high expression levels of IL-6 and ER stress in an NOD1/NOD2-dependent manner was suppressed by IRE1α kinase inhibitor[42]. Hence, we hypothesized that the decrease in NF-κB activation detected in the CER + DSS group might be influenced by ER stress. Two hypotheses were proposed here: first, the damage in enterocytes caused by DSS treatment triggered inflammation and ER stress/UPR, and UPR probably aggravated inflammation *via* the NF-κB pathway simultaneously; second, *S. japonicum* infection regulated the activation of ER stress or UPR directly.

Moreover, colon inflammation was reported to lead to dysfunction in epithelial barrier and apoptosis of intestinal epithelial cells[43]. In this study, we tested the expression of C-C3, TUNEL, Bcl-2 and Bax to assess the apoptosis in colon tissues of the treated mice. DSS mice showed more C-C3 positive cells and TUNEL positive cells compared with control mice. However, fewer C-C3 positive cells and TUNEL positive cells were observed in CER + DSS mice than in DSS mice. DSS mice displayed the highest expression level of Bax and the lowest expression level of Bcl-2 among the mice in the four groups. CER + DSS mice exhibited significantly lower Bax levels and higher Bcl-2 levels than DSS mice. On one hand, this remissive apoptosis in colon tissues might be caused by the attenuation of colon inflammation in DSS-induced colitis mice infected with *S. japonicum*. On the other hand, Chen *et al*[44] showed that activation of the NF-κB signaling pathway enhanced the apoptosis of dental epithelial cells *in vitro*; thus, the high apoptosis level in DSS-treated intestinal cells might be affected by the strong response of NF-κB, which is consistent with our previous research showing that diminished NF-κB activation accompanied by decreased apoptosis in colon tissues, especially enterocytes in CARD3$^{-/-}$ mice induced with DSS.

Additionally, ER stress also exhibited a connection with apoptosis through multiple mechanisms. Wang *et al*[45] found that overexpression of IRE1 could promote apoptosis of HEK193 human embryonic kidney cells. Under ER stress, IRE1α could not only prevent cell apoptosis caused by sustained ER stress *via* activation of Xbp1[36] but also promote mitochondrion-dependent cell death by binding to Bax on the outer membrane of mitochondria[46,47]. When IRE1 associates with TRAF2 and Aask1 to form the IRE1-TRAF2-ASK1 complex, it can play a pro-apoptotic role by enhancing the JNK pathway. Additionally, enhanced expression of CHOP might lead to apoptosis by reducing expression of Bcl-2, decreasing endocellular glutathione and increasing

generation of reactive oxygen intermediates[48]. By forming a dimer with cAMP response element binding protein, CHOP could also promote apoptosis by inhibiting the expression of Bcl-2 and enhancing the mitochondria sensitivity to pro-apoptotic factors[49]. Thus, we propose that the less severe apoptosis in CER + DSS mice was associated with a lower level of ER stress in contrast to DSS mice.

In conclusion, exposure to *S. japonicum* cercariae can prevent inflammation progression and apoptosis in colon tissues of DSS-induced experimental colitis. In addition to the Th1/Th2/Th17 pathway and NF-κB pathway, ER stress was also shown to be involved in attenuating the inflammatory response by parasite infection in DSS-induced colitis. Further investigations are needed to determine the exact mechanism of its action for further development as a therapeutic strategy for IBD treatment.

ACKNOWLEDGMENTS

The authors thank Professor Hui-Fen Dong at Department of Medical Parasitology and Research Laboratory of Schistosomiasis, Wuhan University School of Medicine for experimental guidance.

COMMENTS

Background

Schistosoma (*S.*) and its protein extracts have shown therapeutic effects in ameliorating colitis. It was supposed that the Th1/Th2/Th17 pathway might be involved in the induction of remission while the outcomes were dissimilar and the underlying mechanism is still unclear. To further elucidate the role and mechanism of *S. japonicum* infection on inflammatory bowel disease (IBD), the authors studied the effects of exposure to *S. japonicum* cercariae on dextran sodium sulfate (DSS)-induced colitis.

Research frontiers

Nuclear factor-kappa B (NF-κB) has been reported to play an important role in regulating differentiation and maturation of Th cells. In previous studies, NF-κB also showed a pro-inflammation and pro-apoptosis effect on DSS-induced colitis. In addition, endoplasmic reticulum (ER) stress, which has a close relationship with inflammation and apoptosis, takes a significant part in the development of IBD.

Innovations and breakthroughs

This is the first time to elucidate the effect of *S. japonicum* infection on IBD from the aspect of considering NF-κB pathway, ER stress pathway and apoptosis together.

Applications

S. japonicum attenuates DSS-induced colitis in mice and decreases the cellular apoptosis in colon tissues accompanied by reduced expression of NF-κB and ER stress proteins, especially ER stress proteins. Therefore, ER stress-related proteins might be potential therapeutic targets for IBD.

Terminology

ER stress is a cellular stress response related to the endoplasmic reticulum, which has been found to be conserved between all mammalian species, as well as yeast and worm organisms. Unfolded protein response is activated by the accumulation of unfolded or misfolded proteins in the lumen of the ER.

Peer-review

Authors demonstrated down-regulated expression of cytokines and transcriptional factors such as IL-6, IL-10 and IFN-γ as well as phosphorylated-P65 and ER stress-related proteins after exposure to *S. japonicum* in DSS-induced colitis mice. Besides, ER stress probably contributed to the cellular apoptosis in colon tissues during *S. japonicum* infection in colitis mice.

REFERENCES

1 **Kaser A**, Zeissig S, Blumberg RS. Inflammatory bowel disease. *Annu Rev Immunol* 2010; **28**: 573-621 [PMID: 20192811 DOI: 10.1146/annurev-immunol-030409-101225]
2 **Xavier RJ**, Podolsky DK. Unravelling the pathogenesis of inflammatory bowel disease. *Nature* 2007; **448**: 427-434 [PMID: 17653185 DOI: 10.1038/nature06005]
3 **Molodecky NA**, Soon IS, Rabi DM, Ghali WA, Ferris M, Chernoff G, Benchimol EI, Panaccione R, Ghosh S, Barkema HW, Kaplan GG. Increasing incidence and prevalence of the inflammatory bowel diseases with time, based on systematic review. *Gastroenterology* 2012; **142**: 46-54.e42; quiz e30 [PMID: 22001864 DOI: 10.1053/j.gastro.2011.10.001]
4 **Prideaux L**, Kamm MA, De Cruz PP, Chan FK, Ng SC. Inflammatory bowel disease in Asia: a systematic review. *J Gastroenterol Hepatol* 2012; **27**: 1266-1280 [PMID: 22497584 DOI: 10.1111/j.1440-1746.2012.07150.x]
5 **Cho JH**, Brant SR. Recent insights into the genetics of inflammatory bowel disease. *Gastroenterology* 2011; **140**: 1704-1712 [PMID: 21530736 DOI: 10.1053/j.gastro.2011.02.046]
6 **Briggs N**, Weatherhead J, Sastry KJ, Hotez PJ. The Hygiene Hypothesis and Its Inconvenient Truths about Helminth Infections. *PLoS Negl Trop Dis* 2016; **10**: e0004944 [PMID: 27632204 DOI: 10.1371/journal.pntd.0004944]
7 **Summers RW**, Elliott DE, Qadir K, Urban JF, Thompson R, Weinstock JV. Trichuris suis seems to be safe and possibly effective in the treatment of inflammatory bowel disease. *Am J Gastroenterol* 2003; **98**: 2034-2041 [PMID: 14499784 DOI: 10.1111/j.1572-0241.2003.07660.x]
8 **Summers RW**, Elliott DE, Urban JF, Thompson R, Weinstock JV. Trichuris suis therapy in Crohn's disease. *Gut* 2005; **54**: 87-90 [PMID: 15591509 DOI: 10.1136/gut.2004.041749]
9 **Croese J**, O'neil J, Masson J, Cooke S, Melrose W, Pritchard D, Speare R. A proof of concept study establishing Necator americanus in Crohn's patients and reservoir donors. *Gut* 2006; **55**: 136-137 [PMID: 16344586 DOI: 10.1136/gut.2005.079129]
10 **McSorley HJ**, Gaze S, Daveson J, Jones D, Anderson RP, Clouston A, Ruyssers NE, Speare R, McCarthy JS, Engwerda CR, Croese J, Loukas A. Suppression of inflammatory immune responses in celiac disease by experimental hookworm infection. *PLoS One* 2011; **6**: e24092 [PMID: 21949691 DOI: 10.1371/journal.pone.0024092]
11 **Elliott DE**, Urban JF JR, Argo CK, Weinstock JV. Does the failure to acquire helminthic parasites predispose to Crohn's disease? *FASEB J* 2000; **14**: 1848-1855 [PMID: 10973934]
12 **Elliott DE**, Li J, Blum A, Metwali A, Qadir K, Urban JF, Weinstock JV. Exposure to schistosome eggs protects mice from TNBS-induced colitis. *Am J Physiol Gastrointest Liver Physiol* 2003; **284**: G385-G391 [PMID: 12431903 DOI: 10.1152/ajpgi.00049.2002]
13 **Zhao Y**, Zhang S, Jiang L, Jiang J, Liu H. Preventive effects of Schistosoma japonicum ova on trinitrobenzenesulfonic acid-induced colitis and bacterial translocation in mice. *J Gastroenterol Hepatol* 2009; **24**: 1775-1780 [PMID: 20136961 DOI: 10.1111/j.1440-1746.2009.05986.x]
14 **Bodammer P**, Waitz G, Loebermann M, Holtfreter MC, Maletzki C, Krueger MR, Nizze H, Emmrich J, Reisinger EC. Schistosoma mansoni infection but not egg antigen promotes recovery from colitis in outbred NMRI mice. *Dig Dis Sci* 2011; **56**: 70-78 [PMID: 20428947 DOI: 10.1007/s10620-010-1237-y]
15 **Smith P**, Mangan NE, Walsh CM, Fallon RE, McKenzie AN, van Rooijen N, Fallon PG. Infection with a helminth parasite prevents experimental colitis via a macrophage-mediated mechanism. *J*

Immunol 2007; **178**: 4557-4566 [PMID: 17372014]
16 **Wu J**, Xu W, Ming Z, Dong H, Tang H, Wang Y. Metabolic changes reveal the development of schistosomiasis in mice. *PLoS Negl Trop Dis* 2010; **4**: pii: e807 [PMID: 20824219 DOI: 10.1371/journal.pntd.0000807]
17 **Arseneau KO**, Pizarro TT, Cominelli F. Discovering the cause of inflammatory bowel disease: lessons from animal models. *Curr Opin Gastroenterol* 2000; **16**: 310-317 [PMID: 17031094]
18 **Shang J**, Li L, Wang X, Pan H, Liu S, He R, Li J, Zhao Q. Disruption of Tumor Necrosis Factor Receptor-Associated Factor 5 Exacerbates Murine Experimental Colitis via Regulating T Helper Cell-Mediated Inflammation. *Mediators Inflamm* 2016; **2016**: 9453745 [PMID: 27110068 DOI: 10.1155/2016/9453745]
19 **Yu SJ**, Liu Y, Deng Y, Zhu XY, Zhan N, Dong WG. CARD3 deficiency protects against colitis through reduced epithelial cell apoptosis. *Inflamm Bowel Dis* 2015; **21**: 862-869 [PMID: 25742400 DOI: 10.1097/MIB.0000000000000322]
20 **Alex P**, Zachos NC, Nguyen T, Gonzales L, Chen TE, Conklin LS, Centola M, Li X. Distinct cytokine patterns identified from multiplex profiles of murine DSS and TNBS-induced colitis. *Inflamm Bowel Dis* 2009; **15**: 341-352 [PMID: 18942757 DOI: 10.1002/ibd.20753]
21 **Ohya S**, Fukuyo Y, Kito H, Shibaoka R, Matsui M, Niguma H, Maeda Y, Yamamura H, Fujii M, Kimura K, Imaizumi Y. Upregulation of KCa3.1 K(+) channel in mesenteric lymph node CD4(+) T lymphocytes from a mouse model of dextran sodium sulfate-induced inflammatory bowel disease. *Am J Physiol Gastrointest Liver Physiol* 2014; **306**: G873-G885 [PMID: 24674776 DOI: 10.1152/ajpgi.00156.2013]
22 **Strachan DP**. Hay fever, hygiene, and household size. *BMJ* 1989; **299**: 1259-1260 [PMID: 2513902]
23 **Ben-Ami Shor D**, Harel M, Eliakim R, Shoenfeld Y. The hygiene theory harnessing helminths and their ova to treat autoimmunity. *Clin Rev Allergy Immunol* 2013; **45**: 211-216 [PMID: 23325330 DOI: 10.1007/s12016-012-8352-9]
24 **Wang S**, Xie Y, Yang X, Wang X, Yan K, Zhong Z, Wang X, Xu Y, Zhang Y, Liu F, Shen J. Therapeutic potential of recombinant cystatin from Schistosoma japonicum in TNBS-induced experimental colitis of mice. *Parasit Vectors* 2016; **9**: 6 [PMID: 26728323 DOI: 10.1186/s13071-015-1288-1]
25 **Ruyssers NE**, De Winter BY, De Man JG, Loukas A, Pearson MS, Weinstock JV, Van den Bossche RM, Martinet W, Pelckmans PA, Moreels TG. Therapeutic potential of helminth soluble proteins in TNBS-induced colitis in mice. *Inflamm Bowel Dis* 2009; **15**: 491-500 [PMID: 19023900 DOI: 10.1002/ibd.20787]
26 **Xia CM**, Zhao Y, Jiang L, Jiang J, Zhang SC. Schistosoma japonicum ova maintains epithelial barrier function during experimental colitis. *World J Gastroenterol* 2011; **17**: 4810-4816 [PMID: 22147983 DOI: 10.3748/wjg.v17.i43.4810]
27 **Oh H**, Ghosh S. NF-κB: roles and regulation in different CD4(+) T-cell subsets. *Immunol Rev* 2013; **252**: 41-51 [PMID: 23405894 DOI: 10.1111/imr.12033]
28 **Hollenbach E**, Vieth M, Roessner A, Neumann M, Malfertheiner P, Naumann M. Inhibition of RICK/nuclear factor-kappaB and p38 signaling attenuates the inflammatory response in a murine model of Crohn disease. *J Biol Chem* 2005; **280**: 14981-14988 [PMID: 15691843 DOI: 10.1074/jbc.M500966200]
29 **Atreya I**, Atreya R, Neurath MF. NF-kappaB in inflammatory bowel disease. *J Intern Med* 2008; **263**: 591-596 [PMID: 18479258 DOI: 10.1111/j.1365-2796.2008.01953.x]
30 **Balasubramani A**, Shibata Y, Crawford GE, Baldwin AS, Hatton RD, Weaver CT. Modular utilization of distal cis-regulatory elements controls Ifng gene expression in T cells activated by distinct stimuli. *Immunity* 2010; **33**: 35-47 [PMID: 20643337 DOI: 10.1016/j.immuni.2010.07.004]
31 **Das J**, Chen CH, Yang L, Cohn L, Ray P, Ray A. A critical role for NF-kappa B in GATA3 expression and TH2 differentiation in allergic airway inflammation. *Nat Immunol* 2001; **2**: 45-50 [PMID: 11135577]
32 **Ruan Q**, Kameswaran V, Zhang Y, Zheng S, Sun J, Wang J, DeVirgiliis J, Liou HC, Beg AA, Chen YH. The Th17 immune response is controlled by the Rel-RORγ-RORγ T transcriptional axis. *J Exp Med* 2011; **208**: 2321-2333 [PMID: 22006976 DOI: 10.1084/jem.20110462]
33 **Montane J**, Cadavez L, Novials A. Stress and the inflammatory process: a major cause of pancreatic cell death in type 2 diabetes. *Diabetes Metab Syndr Obes* 2014; **7**: 25-34 [PMID: 24520198 DOI: 10.2147/DMSO.S37649]
34 **Kaser A**, Lee AH, Franke A, Glickman JN, Zeissig S, Tilg H, Nieuwenhuis EE, Higgins DE, Schreiber S, Glimcher LH, Blumberg RS. XBP1 links ER stress to intestinal inflammation and confers genetic risk for human inflammatory bowel disease. *Cell* 2008; **134**: 743-756 [PMID: 18775308 DOI: 10.1016/j.cell.2008.07.021]
35 **Hu S**, Ciancio MJ, Lahav M, Fujiya M, Lichtenstein L, Anant S, Musch MW, Chang EB. Translational inhibition of colonic epithelial heat shock proteins by IFN-gamma and TNF-alpha in intestinal inflammation. *Gastroenterology* 2007; **133**: 1893-1904 [PMID: 18054561 DOI: 10.1053/j.gastro.2007.09.026]
36 **Adolph TE**, Tomczak MF, Niederreiter L, Ko HJ, Böck J, Martinez-Naves E, Glickman JN, Tschurtschenthaler M, Hartwig J, Hosomi S, Flak MB, Cusick JL, Kohno K, Iwawaki T, Billmann-Born S, Raine T, Bharti R, Lucius R, Kweon MN, Marciniak SJ, Choi A, Hagen SJ, Schreiber S, Rosenstiel P, Kaser A, Blumberg RS. Paneth cells as a site of origin for intestinal inflammation. *Nature* 2013; **503**: 272-276 [PMID: 24089213 DOI: 10.1038/nature12599]
37 **Cao SS**, Zimmermann EM, Chuang BM, Song B, Nwokoye A, Wilkinson JE, Eaton KA, Kaufman RJ. The unfolded protein response and chemical chaperones reduce protein misfolding and colitis in mice. *Gastroenterology* 2013; **144**: 989-1000.e6 [PMID: 23336977 DOI: 10.1053/j.gastro.2013.01.023]
38 **Yu YR**, Ni XQ, Huang J, Zhu YH, Qi YF. Taurine drinking ameliorates hepatic granuloma and fibrosis in mice infected with Schistosoma japonicum. *Int J Parasitol Drugs Drug Resist* 2016; **6**: 35-43 [PMID: 27054062 DOI: 10.1016/j.ijpddr.2016.01.003]
39 **Zhang K**, Kaufman RJ. From endoplasmic-reticulum stress to the inflammatory response. *Nature* 2008; **454**: 455-462 [PMID: 18650916 DOI: 10.1038/nature07203]
40 **Urano F**, Wang X, Bertolotti A, Zhang Y, Chung P, Harding HP, Ron D. Coupling of stress in the ER to activation of JNK protein kinases by transmembrane protein kinase IRE1. *Science* 2000; **287**: 664-666 [PMID: 10650002]
41 **Walter P**, Ron D. The unfolded protein response: from stress pathway to homeostatic regulation. *Science* 2011; **334**: 1081-1086 [PMID: 22116877 DOI: 10.1126/science.1209038]
42 **Keestra-Gounder AM**, Byndloss MX, Seyffert N, Young BM, Chávez-Arroyo A, Tsai AY, Cevallos SA, Winter MG, Pham OH, Tiffany CR, de Jong MF, Kerrinnes T, Ravindran R, Luciw PA, McSorley SJ, Bäumler AJ, Tsolis RM. NOD1 and NOD2 signalling links ER stress with inflammation. *Nature* 2016; **532**: 394-397 [PMID: 27007849 DOI: 10.1038/nature17631]
43 **Cummins EP**, Seeballuck F, Keely SJ, Mangan NE, Callanan JJ, Fallon PG, Taylor CT. The hydroxylase inhibitor dimethyloxalylglycine is protective in a murine model of colitis. *Gastroenterology* 2008; **134**: 156-165 [PMID: 18166353 DOI: 10.1053/j.gastro.2007.10.012]
44 **Chen G**, Sun W, Liang Y, Chen T, Guo W, Tian W. Maternal diabetes modulates offspring cell proliferation and apoptosis during odontogenesis via the TLR4/NF-κB signalling pathway. *Cell Prolif* 2016; Epub ahead of print [PMID: 27981756 DOI: 10.1111/cpr.12324]
45 **Wang XZ**, Harding HP, Zhang Y, Jolicoeur EM, Kuroda M, Ron D. Cloning of mammalian Ire1 reveals diversity in the ER stress responses. *EMBO J* 1998; **17**: 5708-5717 [PMID: 9755171 DOI: 10.1093/emboj/17.19.5708]
46 **Iwakoshi NN**, Pypaert M, Glimcher LH. The transcription factor XBP-1 is essential for the development and survival of dendritic cells. *J Exp Med* 2007; **204**: 2267-2275 [PMID: 17875675 DOI: 10.1084/jem.20070525]

47 **Tabas I**, Ron D. Integrating the mechanisms of apoptosis induced by endoplasmic reticulum stress. *Nat Cell Biol* 2011; **13**: 184-190 [PMID: 21364565 DOI: 10.1038/ncb0311-184]
48 **McCullough KD**, Martindale JL, Klotz LO, Aw TY, Holbrook NJ. Gadd153 sensitizes cells to endoplasmic reticulum stress by down-regulating Bcl2 and perturbing the cellular redox state. *Mol Cell Biol* 2001; **21**: 1249-1259 [PMID: 11158311 DOI: 10.1128/MCB.21.4.1249-1259.2001]
49 **Gachon F**, Gaudray G, Thébault S, Basbous J, Koffi JA, Devaux C, Mesnard J. The cAMP response element binding protein-2 (CREB-2) can interact with the C/EBP-homologous protein (CHOP). *FEBS Lett* 2001; **502**: 57-62 [PMID: 11478948]

P- Reviewer: Hashimoto N, Tomizawa M **S- Editor**: Qi Y
L- Editor: Wang TQ **E- Editor**: Li D

World Journal of Gastroenterology

Submit a Manuscript: http://www.f6publishing.com

World J Gastroenterol 2017 August 21; 23(31): 5713-5721

DOI: 10.3748/wjg.v23.i31.5713

ISSN 1007-9327 (print) ISSN 2219-2840 (online)

ORIGINAL ARTICLE

Basic Study

Metabolomic profiling for identification of metabolites and relevant pathways for taurine in hepatic stellate cells

Xin Deng, Xing-Qiu Liang, Fei-Guo Lu, Xiao-Fang Zhao, Lei Fu, Jian Liang

Xin Deng, Xing-Qiu Liang, Fei-Guo Lu, Xiao-Fang Zhao, Lei Fu, Jian Liang, Department of Infectious Diseases, Ruikang Hospital Affiliated to Guangxi University of Chinese Medicine, Nanning 541100, Guangxi Zhuang Autonomous Region, China

Author contributions: Deng X performed the majority of experiments and analyzed the data; Liang XQ wrote the paper; Lu FG, Zhao XF and Fu L participated equally in the culture and treatment of hepatic stellate cells; Liang J designed and coordinated the research.

Supported by National Natural Science Foundation of China, No. 81360595 and No. 81360532; Guangxi Natural Science Foundation Program, No. 2014GXNSFDA118027; Bagui Scholars Foundation Program of Guangxi; and Special-term Experts Foundation Program of Guangxi.

Institutional review board statement: The study was approved by the Institutional Review Board of Ruikang Hospital Affiliated to Guangxi University of Chinese Medicine.

Conflict-of-interest statement: To the best of our knowledge, no conflict of interest exists.

Data sharing statement: No additional data are available.

Manuscript source: Unsolicited manuscript

Correspondence to: Jian Liang, MD, Professor, Department of Infectious Diseases, Ruikang Hospital Affiliated to Guangxi University of Chinese Medicine, No. 10 Huadong Road, Nanning 541100, Guangxi Zhuang Autonomous Region, China. dr_jianliang@163.com

Telephone: +86-771-2639080
Fax: +86-771-2639080

Received: March 6, 2017
Peer-review started: March 7, 2017
First decision: April 17, 2017
Revised: June 11, 2017
Accepted: June 19, 2017
Article in press: June 19, 2017
Published online: August 21, 2017

Abstract

AIM

To develop a reliable and simple method to identify important biological metabolites and relevant pathways for taurine in hepatic stellate cells (HSCs), in order to provide more data for taurine therapy.

METHODS

All the biological samples were analyzed by using high-performance liquid chromatography-time electrospray ionization/quadrupole-time of flight mass spectrometry. Principal component analysis and partial least squares discriminant analysis were used to identify statistically different metabolites for taurine in HSCs, and metabolomic pathway analysis was used to do pathway analysis for taurine in HSCs. The chemical structure of the related metabolites and pathways was identified by comparing the m/z ratio and ion mode with the data obtained from free online databases.

RESULTS

A total of 32 significant differential endogenous metabolites were identified, which may be related to the mechanism of action of taurine in HSCs. Among the seven relevant pathways identified, sphingolipid metabolism pathway, glutathione metabolism pathway and thiamine metabolism pathway were found to be

the most important metabolic pathways for taurine in HSCs.

CONCLUSION

This study showed that there were distinct changes in biological metabolites of taurine in HSCs and three differential metabolic pathways including sphingolipid pathway, glutathione pathway and thiamine metabolism pathway might be of key importance in mediating the mechanism of action of taurine in HSCs.

Key words: Natural taurine; Hepatic stellate cells; Pathway; High performance liquid chromatography-time electrospray ionization/quadrupole-time of flight mass spectrometry; Metabolomics

Core tip: At the cellular level, it is reported that the activation of hepatic stellate cells (HSCs) in the subendothelial space may result in hepatic fibrosis. Although taurine was found to increase HSC apoptosis significantly, its molecular mechanisms are still unknown. This study developed a reliable and simple method to identify important biological metabolites and relevant pathways for taurine in HSCs, in order to provide more data for taurine therapy. We found that there were distinct changes in the biological metabolites of taurine in HSCs, and identified three differential metabolic pathways that might be of key importance in mediating the mechanism of action of taurine in HSCs.

Deng X, Liang XQ, Lu FG, Zhao XF, Fu L, Liang J. Metabolomic profiling for identification of metabolites and relevant pathways for taurine in hepatic stellate cells. *World J Gastroenterol* 2017; 23(31): 5713-5721 Available from: URL: http://www.wjgnet.com/1007-9327/full/v23/i31/5713.htm DOI: http://dx.doi.org/10.3748/wjg.v23.i31.5713

INTRODUCTION

Hepatic fibrosis (HF) is a scarring process in which the liver forms scar tissue due to an abnormal deposition of extracellular matrix (ECM)[1]. Recently, more and more attention has been paid to the molecular mechanisms of hepatic fibrosis. At the cellular level, it is reported that the activation of hepatic stellate cells (HSCs) in the subendothelial space may result in hepatic fibrosis[2]. Moreover, reversal or apoptosis of activated HSCs has been proven to be beneficial for the treatment or regression of hepatic fibrosis[3].

Metabolomics methods can be used to characterize the metabolic profiles of a biological system. As metabolites with relatively low molecular weight are downstream products of biological processes, their identity and concentrations in a living biological system can provide biochemical signatures for globally tracking the physiological effects and exploring the drug effects[4-6]. A previous study[7] systematically analyzed the protective effects of traditional Chinese medicine Hongshan Capsules, and identified the potential target biomarkers through the metabonomic approach of ultra-performance liquid chromatography coupled to mass spectrometry. Therefore, metabolomics methods can be used to identify biomarkers for clinical drug therapy, especially in cancer research[8,9].

Taurine, a beta-amino acid with a simple structure that is extracted from animal tissue, has been investigated as a promising drug for the treatment of many hepatic injuries[10-13]. In previous studies, taurine was showed to significantly increase the apoptosis of HSCs and raise the levels of 19 proteins related to cellular apoptosis or oxidation in HSCs[14,15]. However, the exact metabolic pathways and molecules involved in the mechanisms of action of taurine are still unknown. Therefore, this study aimed at developing a reliable and simple method to find important biological metabolites and pathways that are related to taurine in HSCs, in order to provide more data for taurine therapy.

MATERIALS AND METHODS

Cell culture and cell viability assay

Human HSCs (LX-2) were obtained from Xiangya Central Experiment Laboratory of Central South University (Changsha, China) and were incubated in DMEM (Thermo Scientific Hyclone, Logan, UT, United States) containing 100 U/mL penicillin (North China Pharmaceutical, China), 100 μg/mL streptomycin (North China Pharmaceutical, China) and 10% fetal bovine serum (Biochrom AG, Berlin, Germany) at room temperature in an incubator with 50 mL/L CO_2 and saturated humidity. The culture medium was replaced every two days. Trypsin (0.25%) was added for digestion when the confluence of HSCs reached 80%-90% and the supernatant was discarded after centrifugation at 1000 r/min for 5 min. Then, the cells were resuspended to a density of 5×10^5/mL.

MTT method was used to determine the optimum drug concentration of taurine for the subsequent study. Briefly, HSCs were added into a 96-well plate at a density of 5×10^4 cells per well. Natural taurine (Yuanlong Pearl Co. Ltd., Beihai, China) was dissolved in dimethyl sulphoxide (DMSO) at a concentration of 8 mol/L, and then diluted with 2% DMEM to 10, 20, 40, 60, 80 and 100 mmol/L. Six replicates were applied for each concentration of taurine and the whole reaction system was maintained for 48 h. Cells treated with DMSO alone were used as controls. Subsequently, 10 μL of MTT solution (5 mg/mL in PBS) was added and the cells were further incubated for 4 h at 37 ℃. Then, the reaction was terminated by the addition of 100 μL DMSO and absorbance was measured at 495 nm using

Table 1 Gradient elution program of the mobile phase

Time (min)	Flow rate (mL/min)	Solution B (%)
0	0.35	5
1	0.35	5
6	0.35	20
9	0.35	50
13	0.35	95
15	0.35	95

a microplate reader (Molecular Devices, United States). Based on the results, the concentration of 40 mmol/L was chosen as the optimum drug concentration of taurine for the following study.

Sample preparation

For the following metabolomic study, HSCs were incubated in 10-cm culture dishes until approximately 70% confluence and then treated with celastrol and other control drugs for 12 h. Each dish was washed twice at 37 ℃ with PBS after removing the culture medium, and dried in the vacuum. Then, the cells were quenched by adding 1.5 mL HPLC-grade methanol at -80 ℃ and were separated from the culture dish with a cell lifter (Fisher Scientific, United States). The cell solution was subsequently transferred to a 2 mL centrifuge tube and frozen in liquid nitrogen until liquid-liquid extraction. Six replicates were applied for 40 μmol/L of natural taurine for 48 h as the test group and the same concentration of DMSO was used as the control group. To avoid cell cytotoxicity, the final concentration of DMSO must be less than 0.1% for both the taurine group and the control group. Additionally, five parallel blank culture dishes were trypsinized and counted for the normalizing the subsequent analysis.

After incubation, the culture medium was removed generally and the residual medium was removed by using 2 mL 0.9% [w/v] ice-cold isotonic saline (NaCl) to arrest cellular metabolism. Subsequently, the cells were added with 1 mL cold methanol/water (4:1) to quench cells and then collected in 2 mL centrifuge tubes. Then, the cells were ultrasonicated for 5 min (5 s ultrasonication at a 10-s interval) in an ice bath and centrifuged at 13000 *g* for 10 min at 4 ℃. Finally, the supernatant was dried with nitrogen and stored at -80 ℃ before detection.

Chromatography and spectrometry conditions

Samples were resolved with acetonitrile/water (1:1, v/v) mixture according to the cell number counted in advance and detected by high performance liquid chromatography-electrosprayionization/quadrupole-time-of-flight mass spectrometry (HPLC ESI/Q-TOF MS) (Agilent Technologies, United States). All the samples were separated on an Agilent C18 column (2.1 mm × 100 mm, 1.8 μm, Agilent Technologies, United States) with the following parameters: injection volume, 4 μL; flow rate, 0.35 mL/min; column temperature, 40 ℃. The mobile phase was composed of (A) 0.1% formic acid water solution and (B) 0.1% formic acid acetonitrile solution. The gradient elution program (Table 1) was linearly increased from 5% to 20% B (0-6 min), stable at 50% B (6-8 min), linearly increased to 95% B (8-12 min) and maintained for 3 min. The quality control (QC) was prepared and injected before the injection of test samples.

Both ESI^+ and ESI^- ionization modes were used to find the potential specific metabolites of taurine in HSCs. The ionization mode was set at a capillary voltage of 4.0 kV (ESI^+) or 3.5 kV (ESI^-), cone voltage of 35V (ESI^+) and 50V (ESI^-), source temperature of 100 ℃, cone gas flow of 50 L/h, desolvation gas flow, desolvation gas flow of 600 L/h, and desolvation gas temperature of 350 ℃. Data were collected in the centroid mode with the mass range (m/z) of 50-1000, scan time of 0.03 s and inter-scan delay of 0.02 s. To lock the mass system, 100 pg/μL leucine-enkephalin (m/z 556.2771 in ESI^+ mode or m/z 554.2615 in ESI^- mode) at 0.05 mL/min with the frequency of 10 s was used.

Data processing and statistical analysis

After excluding the noise and background interference, raw mass spectral data of both ESI^+ and ESI^- modes were analyzed by using Mass Profiler (Agilent Technologies, United States) to generate data, including retention time, signal intensity and m/z ratio for peak identification. Subsequently, SIMCA-P 13.0 software (Umetric AB, CA, United States) was applied to do principal component analysis (PCA) to distinguish different scatters of the biological metabolites for taurine in HSCs, partial least squares discriminant analysis (PLS-DA) to find statistically different metabolites. Variable importance in the projection (VIP) plots (VIP > 1) of the PLS-DA was used to find the exact potential biomarkers. Finally, the structure of the related metabolites and pathways was identified by comparing the m/z ratio and ion mode with the data obtained from free online databases including Human Metabolome Database (HMDB) (www.hmdb.ca), Metlin metabolomics database (http://metlin.scripps.edu/) and Kyoto Encyclopedia of Genes and Genomes (KEGG) pathway database (www.genome.jp/kegg/pathway.html). MetPA network software[16] (http://metpa.metabolomics.ca/Met PA/faces/Home.jsp) was used to do pathway analysis for taurine in HSCs.

RESULTS

Total ion current spectra of taurine in HSCs

In the current study, all the biological metabolites of taurine in HSCs were detected by HPLC-ESI/Q-TOFMS, which might provide useful information for unveiling the underlying molecular mechanisms of taurine in HSCs. The total ion current spectra of the samples

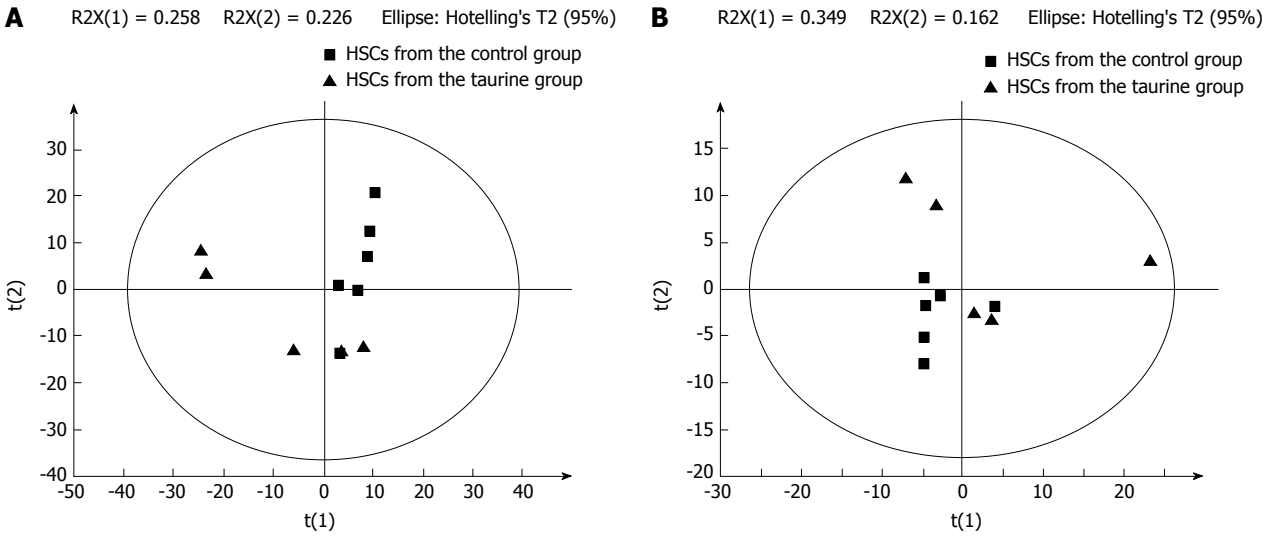

Figure 1 Principal component analysis plots of biological metabolites for taurine in hepatic stellate cells in electrosprayionization$^+$ mode (A) and in electrosprayionization$^-$ mode (B). HSCs: Hepatic stellate cells; ESI: Electrosprayionization.

between the control and taurine-treated HSCs differed greatly, suggesting that there might be some metabolic changes for taurine in HSCs.

PCA

PCA statistically divided all the detected metabolites into smaller clusters as principal components (PCs) to find the potential biomarkers. In this study, all the samples were classified into two small clusters between the control and taurine-treated cells in the PCA score plots (Figure 1), demonstrating that there were significant metabolic differences between the control and taurine-treated HSCs.

PLS-DA

Then, the potential important metabolites were further analyzed by using PLS-DA. Consistent with the results of PCA, PLS-DA plots showed two clear groups between the control and taurine-treated cells (Figure 2). Moreover, a total of 27 metabolites in ESI$^+$ mode and five metabolites in ESI$^-$ mode were found to be the significant metabolites between the control and taurine-treated cells (VIP > 1) (P < 0.05) (Table 2).

Structure identifications and pathway identification

The definite identity of the significant metabolites in the biological samples and their contributions to the biological processes are important for the current metabolomics study. Therefore, the structure of the related metabolites and pathways was identified by comparing the m/z ratio and ion mode with the data obtained from on-line free databases including HMDB (www.hmdb.ca), Metlin metabolomics database (http://metlin.scripps.edu/) and KEGG pathway database (www.genome.jp/kegg/pathway.html).

Additionally, 16 potential metabolic pathways were analyzed by MetPA network software and three significant metabolic pathways (sphingolipid metabolism, glutathione metabolism and thiamine metabolism) were found to be the most important metabolic pathways for taurine in HSCs (Table 3 and Figure 3).

DISCUSSION

In this study, a simple chromatography method coupled with pathway analysis by using high-performance liquid chromatography-time electrospray ionization/quadrupole-time of flight mass spectrometry (HPLC-ESI/Q-TOF-MS) was successfully performed for analyzing the mechanism of taurine in HSCs. A total of 32 significant differential endogenous metabolites were identified. Among the seven relevant pathways for taurine, sphingolipid metabolism pathway (Figure 4), glutathione metabolism pathway (Figure 5) and thiamine metabolism pathway were found to be the most important metabolic pathways for taurine in HSCs.

The sphingolipid metabolism pathway contributes greatly to structural functions and cellular signaling. For example, membrane sphingolipids can regulate cell proliferation, differentiation and death[17-19]. Increasing evidence shows that sphingolipids are important in stress and ligand-induced hepatocellular death, which can cause several liver diseases like steatohepatitis, ischaemia-reperfusion hepatic damage or hepatic cancer[20]. Additionally, increased levels of sphingolipids in specific cell subcompartments can cause liver dysfunctions and some inherited diseases. Tumour necrosis factor (TNF) is an important death receptor, and abnormal expression of TNF can cause many liver diseases[21]. Thus, TNF becomes an important target for liver disease. In this study, taurine was found to be able to regulate sphingolipid metabolism. Therefore, we hypothesize that taurine might be able to intervene the activation of HSCs and regulate TNF expression.

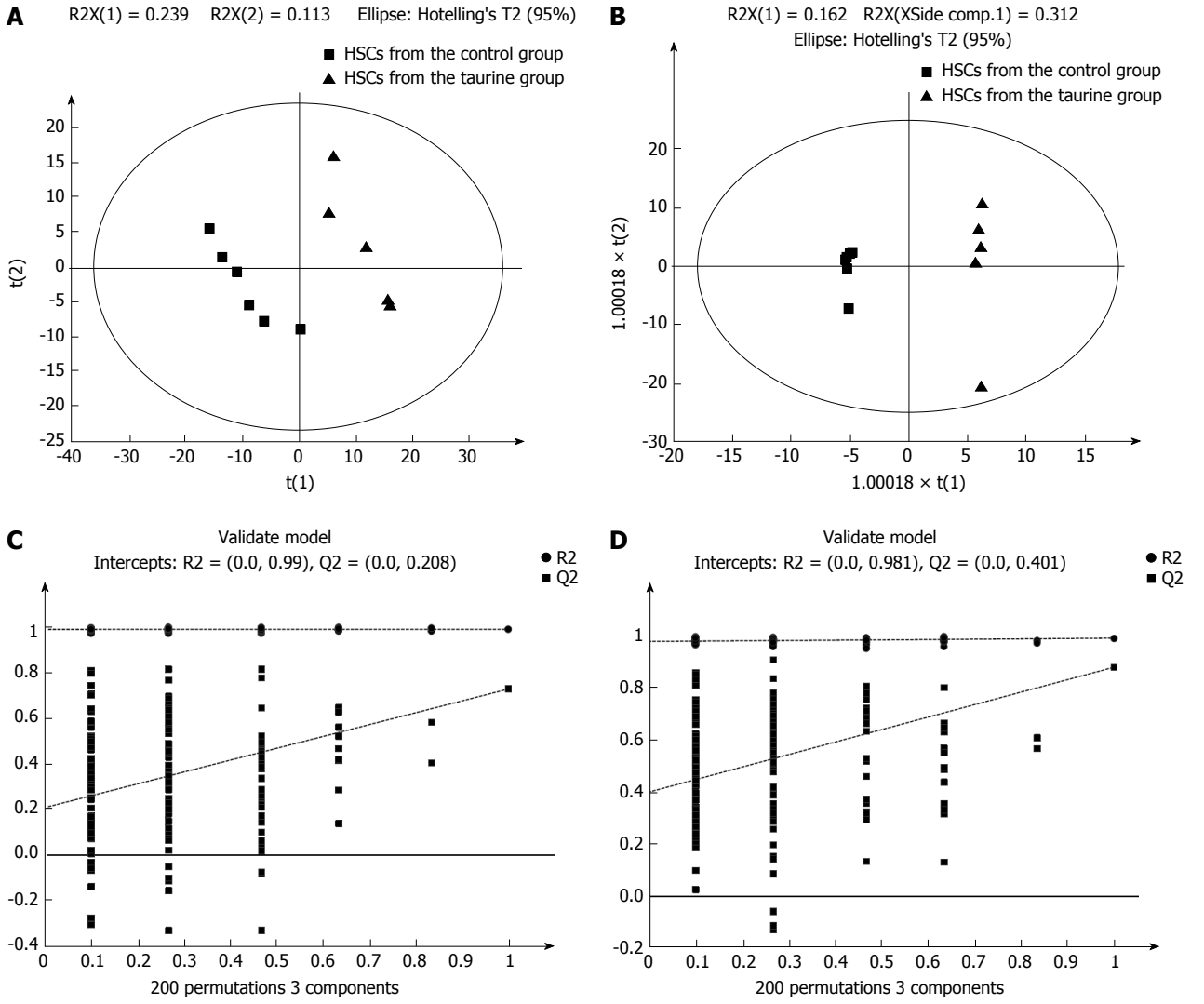

Figure 2 Partial least square discriminant analysis and validation of biological metabolites for taurine in hepatic stellate cells in electrosprayionization$^+$ mode and in electrosprayionization$^-$ mode. A: Partial least square discriminant analysis (PLS-DA) plots of biological metabolites for taurine in hepatic stellate cells (HSCs) in ESI$^+$ mode; B: PLS-DA plots of biological metabolites for taurine in HSCs in ESI$^-$ mode; C: Validation of biological metabolites for taurine in HSCs in ESI$^+$ mode; D: Validation of biological metabolites for taurine in HSCs in ESI$^-$ mode. ESI: Electrosprayionization; HSCs: Hepatic stellate cells.

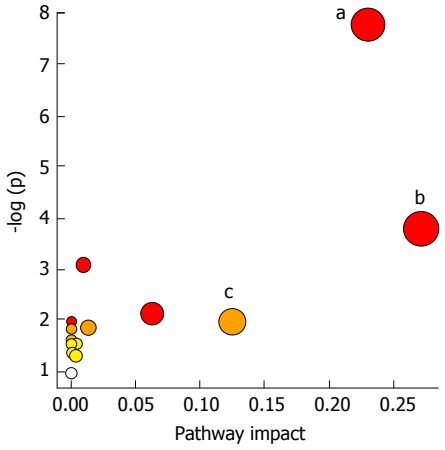

Figure 3 Potential pathways for taurine in hepatic stellate cells identified by using MetPA pathway analysis. [a]Sphingolipid metabolism pathway; [b]Glutathione metabolism pathway; [c]Thiamine metabolism pathway.

However, the exact mechanism of the action of taurine in the HSCs needs further investigation.

Besides, lysophosphatidylcholine (LysoPC) can affect HSCs through several mechanisms. First, LysoPC can inhibit proliferation of endothelial cells and increase their apoptosis, thereby affecting the molecular structure of the endothelium and the proliferation of vascular smooth muscle cells[22,23]. Second, LysoPC can downregulate endothelium-derived NO and activate the LOX-1 receptor to desensitize eNOS, thus causing endothelial dysfunction[24]. Furthermore, activation of HSCs can lead to increased expression of genes relevant to lipid accumulation and increased levels of intracellular lipids. In this study, LysoPC was found as the significantly different metabolite between the control and taurine-treated groups. LysoPC is an important plasma lipid cell signaling molecule for LDL oxidization and can be generated by phospholipase A2 hydrolysis or phosphatidylcholine (PC) oxidation[25]. Thus, we hypothesize that the interventional effect of taurine on HSCs is related with lipid metabolism. This

Table 2 Potential important biological metabolites in ESI$^+$ and ESI$^-$ modes for taurine in hepatic stellate cells

Number	Mode	VIP	RT (min)	m/z ratio	Compound name	Fold change (B/A)	*P* value
1	ESI$^+$	1.312	11.16	495.3338	PC (16:0)	-0.758↓	0.037
2	ESI$^+$	1.973	14.02	148.0160	2-oxo-4-methylthiobutanoic acid	-3.094↓	0.001
3	ESI$^+$	1.326	7.51	215.1890	Amino-dodecanoic acid	1.249↑	0.043
4	ESI$^+$	1.316	3.89	231.1475	Butyryl-L-carnitine	-1.711↓	0.041
5	ESI$^+$	1.644	8.87	273.2679	C16 Sphinganine	-0.837↓	0.034
6	ESI$^+$	1.329	0.74	161.1047	Carnitine	2.324↑	0.049
7	ESI$^+$	1.570	13.27	375.3125	Docosatetraenoyl Ethanolamide	2.200↑	0.017
8	ESI$^+$	1.706	11.46	399.3362	Palmitoylcarnitine	-1.419	0.005
9	ESI$^+$	1.484	11.01	199.1943	Dodecanamide	1.521↑	0.022
10	ESI$^+$	1.590	1.09	307.0848	Glutathione	-1.372↓	0.019
11	ESI$^+$	1.268	6.03	259.1792	Hexanoylcarnitine	-1.216↓	0.046
12	ESI$^+$	1.565	4.59	282.1684	Hydroxydesipramine	2.210↑↓	0.013
13	ESI$^+$	1.601	11.01	569.3486	LysoPC(22:5)	17.551↑	0.048
14	ESI$^+$	1.483	1.01	175.0482	N-acetylaspartate	-1.160↓	0.018
15	ESI$^+$	1.495	12.63	369.3254	N-palmitoyl isoleucine	1.375↑	0.017
16	ESI$^+$	1.557	12.15	369.3254	N-palmitoyl isoleucine	2.683↑	0.039
17	ESI$^+$	1.245	10.48	371.3045	N-stearoyl serine	-1.027↓	0.048
18	ESI$^+$	1.312	13.05	281.2728	Oleamide	-0.852↓	0.036
19	ESI$^+$	1.469	10.13	212.1417	Oxo-dodecenoic acid	1.750↑	0.019
20	ESI$^+$	1.595	11.24	479.3025	PC (15:1)/PE (18:1)	-1.141↓	0.018
21	ESI$^+$	1.284	11.30	521.3494	PC (18:1)	-0.727↓	0.048
22	ESI$^+$	2.021	8.93	317.2939	Phytosphingosine	-1.274↓	0.001
23	ESI$^+$	1.290	0.65	202.2163	Spermine	-0.874↓	0.039
24	ESI$^+$	1.443	9.90	301.2992	Sphinganine	-0.807↓	0.040
25	ESI$^+$	1.394	11.60	299.2835	Sphingosine	-0.949↓	0.026
26	ESI$^+$	1.430	12.34	427.3675	Stearoylcarnitine	-1.006↓	0.026
27	ESI$^+$	1.818	0.80	117.0791	Valine	-0.681↓	0.037
28	ESI$^-$	2.017	1.13	192.0270	Citric acid	-0.870↓	0.001
29	ESI$^-$	1.678	11.11	453.2859	Glycerophospho-N-Palmitoyl Ethanolamine	-1.125↓	0.011
30	ESI$^-$	2.076	11.46	479.3016	PC (15:1)	-1.697↓	0.000
31	ESI$^-$	1.648	0.69	264.1045	Thiamine	0.394↑	0.040
32	ESI$^-$	1.448	9.25	250.1204	Ubiquinone-1	1.538↑	0.031

Comparisons were done by two-sample *t*-test. A total of 27 metabolites in ESI$^+$ mode and 5 metabolites in ESI$^-$ mode were found to be the significant metabolites between the control and taurine-treated cells (VIP > 1) ($P < 0.05$). PC: Phosphatidylcholine; VIP: Variable importance in the projection; (↑): Up-regulated; (↓): Down-regulated.

Table 3 Results of MetPA pathway analysis

Pathway name	Compounds[1]	Expected[2]	Hits	Raw *P*[3]	FDR *P*[4]	Impact
Glutathione metabolism	38	0.23681	2	0.022	0.896	0.272
Sphingolipid metabolism	25	0.1558	3	0.000	0.033	0.231
Thiamine metabolism	24	0.14956	1	0.140	1	0.125
Citrate cycle (TCA cycle)	20	0.12464	1	0.118	1	0.063
Valine, leucine and isoleucine biosynthesis	27	0.16826	1	0.156	1	0.013
Cysteine and methionine metabolism	56	0.34898	2	0.046	1	0.009
Glyoxylate and dicarboxylate metabolism	50	0.31159	1	0.271	1	0.003
Glycerophospholipid metabolism	39	0.24304	1	0.218	1	0.003

[1]The total number of metabolites in each pathway; [2]The actually matched number according to the uploaded data; [3]The original *P*-value using enrichment analysis; [4]The adjusted *P*-value using false discovery rate. The table shows the detailed results from the pathway analysis. Since we tested many pathways at the same time, the *P*-values from enrichment analysis are further adjusted for multiple tests. In particular, the Hits is the actually matched number from the user uploaded data; the Raw *P* is the original *P*-value calculated from the enrichment analysis; the FDR *P* is the *P*-value adjusted using false discovery rate; the Impact is the pathway impact value calculated from pathway topology analysis. Sixteen potential metabolic pathways were analyzed by MetPA network software and three significant metabolic pathways (Sphingolipid metabolism, glutathione metabolism and thiamine metabolism) were found to be the most important metabolic pathways for taurine in HSCs; HSCs: Hepatic stellate cells.

was consistent with the finding of a previous study which showed that taurine can obviously decrease LDL-C level[26].

Moreover, amino-dodecanoic acid, 2-oxo-4-methylthiobutanoic acid, oxo-dodecenoic acid, valine, citric acid, thiamine, and N-acetylaspartate were also identified in the current study. It is therefore proposed that taurine may intervene HSCs through the valine, leucine and isoleucine biosynthesis pathway, cysteine and methionine metabolism pathway, citrate cycle (TCA cycle) pathway, alanine, aspartate and glutamate metabolism pathway, lysine degradation pathway, glyo-

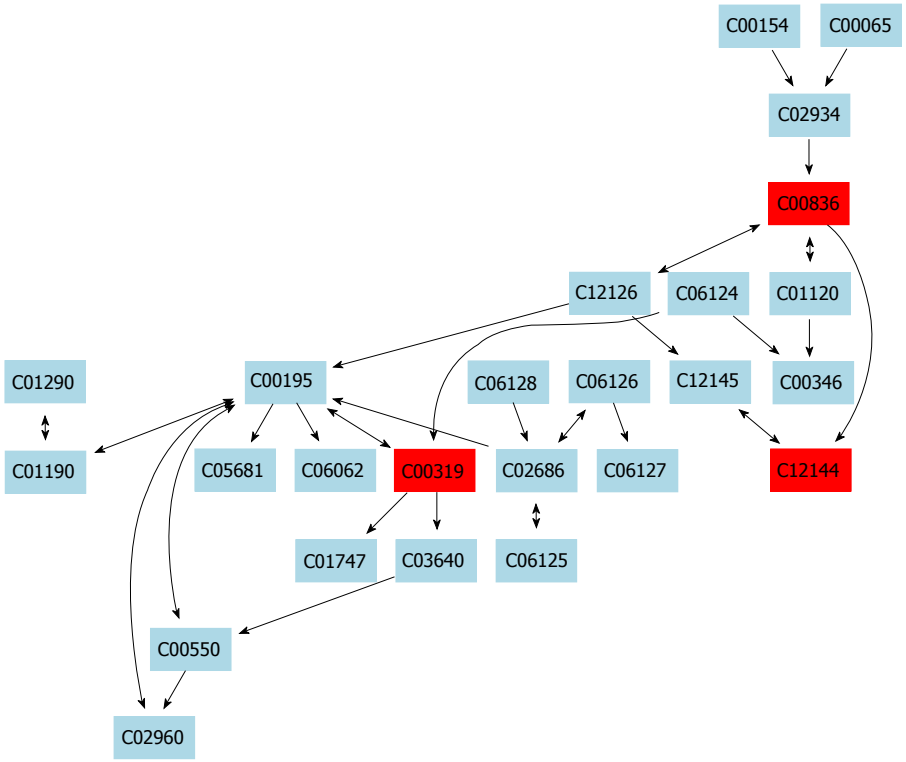

Figure 4 Sphingolipid metabolism pathway.

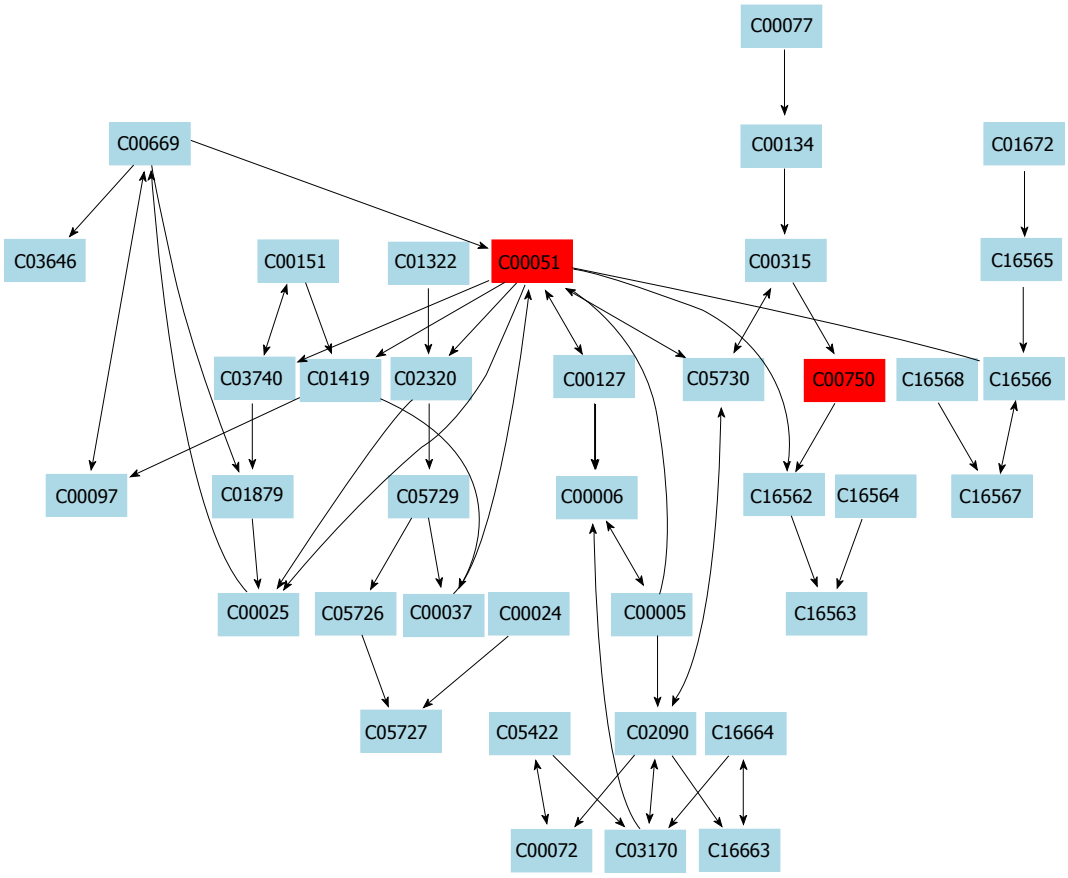

Figure 5 Glutathione metabolism pathway.

xylate and dicarboxylate metabolism pathway, arginine and proline metabolism pathway and aminoacyl-tRNA

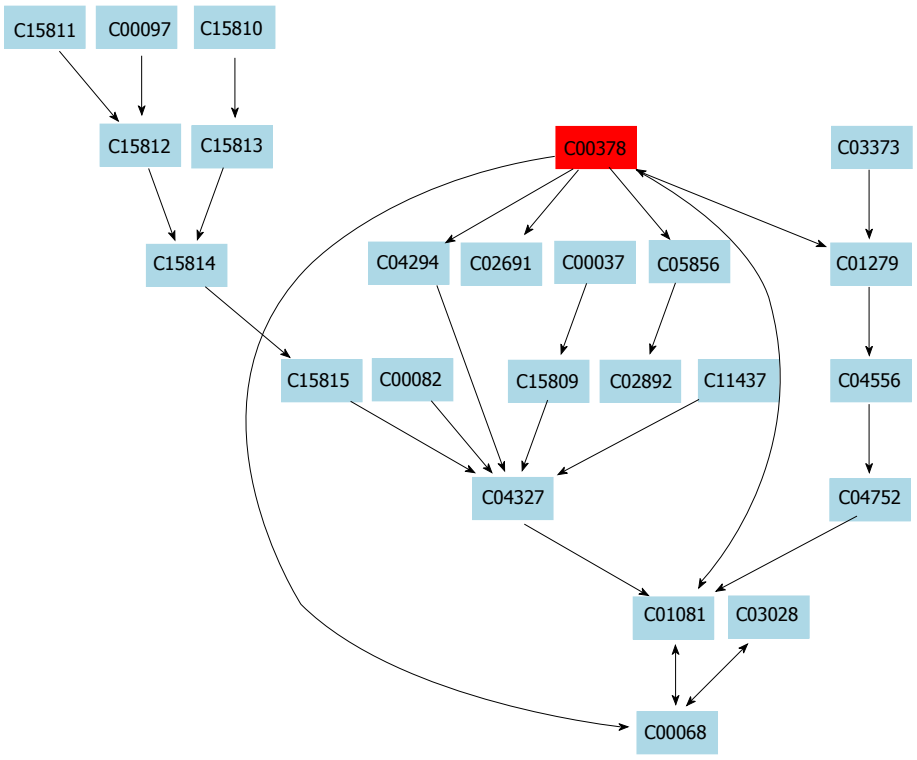

Figure 6 Thiamine metabolism pathway.

biosynthesis pathway.

This study has several limitations. Validation of this current chromatography method using targeted metabolomics and application of this current chromatography method on other cell lines or *in vivo* models need to be studied in the future. In addition, dose-dependence of taurine should be clarified in the future.

To conclude, this study has found that there were distinct changes in the biological metabolites of taurine in HSCs by using HPLC-ESI/Q-TOF-MS. A total of 32 significant differential endogenous metabolites and 3 differential metabolic pathways including sphingolipid pathway, glutathione pathway and thiamine metabolism pathway (Figure 6) were identified, which might be of key importance in mediating the mechanism of action of taurine in HSCs.

COMMENTS

Background

It is well-known that quiescent hepatic stellate cells (HSC) may become matrix-secreting myofibroblasts upon activation and are the primary sources of extracellular matrix (ECM) during liver fibrogenesis. Thus, a novel therapeutic method for hepatic fibrosis can rely on the inhibition of activated HSCs. Taurine, a beta-amino acid with a simple structure that is extracted from animal tissue, has been investigated as a promising drug for the treatment of many hepatic injuries. In previous studies, taurine was found to significantly increase the apoptosis of HSCs and raise the concentrations of 19 proteins related to cellular apoptosis or oxidation in HSCs. However, the exact metabolic pathways and molecular mechanisms for taurine are still unknown.

Research frontiers

Metabolomics methods can be used to characterize the metabolic profiles of a biological system. Since metabolites with relatively low molecular weight are downstream products of biological processes, their identity and concentrations in a living biological system can provide biochemical signatures for globally tracking the physiological effects and exploring the drug effects. Therefore, metabolomics methods can be used to identify biomarkers for clinical drug therapy, especially in cancer research.

Innovations and breakthroughs

In this study, a simple chromatography method coupled with pathway analysis by using high-performance liquid chromatography-time electrospray ionization/quadrupole-time of flight mass spectrometry was successfully performed for analyzing the mechanism of action of taurine in HSCs. A total of 32 significantly differential endogenous metabolites were identified, which may mediate the mechanism of action of taurine in HSCs. Among the seven relevant pathways identified for taurine, sphingolipid metabolism pathway, glutathione metabolism pathway and thiamine metabolism pathway were found to be the most important metabolic pathways for taurine in HSCs.

Applications

Taurine, a beta-amino acid with a simple structure that is extracted from animal tissue, has been investigated as a promising drug for the treatment of many hepatic injuries. In previous studies, taurine was found to significantly increase the apoptosis of HSCs and raise the concentrations of 19 proteins related to cellular apoptosis or oxidation in HSCs. However, the exact metabolic pathways and molecular mechanisms for taurine are still unknown. Therefore, this study aimed at developing a reliable and simple method to identify important biological metabolites and relevant pathways for taurine in HSCs, in order to provide more data for taurine therapy.

Terminology

Hepatic fibrosis is a pathological condition characterized by excessive deposition of ECM proteins, which may led to the development of liver cirrhosis or even hepatocellular carcinoma in the absence of effective treatment.

Peer-review

This is an interesting paper looking to identify biological pathways and meta-

bolites for taurine in hepatocytes.

REFERENCES

1 **Roderburg C**, Luedde M, Vargas Cardenas D, Vucur M, Mollnow T, Zimmermann HW, Koch A, Hellerbrand C, Weiskirchen R, Frey N, Tacke F, Trautwein C, Luedde T. miR-133a mediates TGF-β-dependent derepression of collagen synthesis in hepatic stellate cells during liver fibrosis. *J Hepatol* 2013; **58**: 736-742 [PMID: 23183523 DOI: 10.1016/j.jhep.2012.11.022]

2 **Zhang CY**, Yuan WG, He P, Lei JH, Wang CX. Liver fibrosis and hepatic stellate cells: Etiology, pathological hallmarks and therapeutic targets. *World J Gastroenterol* 2016; **22**: 10512-10522 [PMID: 28082803 DOI: 10.3748/wjg.v22.i48.10512]

3 **Jung YK**, Yim HJ. Reversal of liver cirrhosis: current evidence and expectations. *Korean J Intern Med* 2017; **32**: 213-228 [PMID: 28171717 DOI: 10.3904/kjim.2016.268]

4 **Li JP**, Guo JM, Shang EX, Zhu ZH, Liu Y, Zhao BC, Zhao J, Tang ZS, Duan JA. Quantitative determination of five metabolites of aspirin by UHPLC-MS/MS coupled with enzymatic reaction and its application to evaluate the effects of aspirin dosage on the metabolic profile. *J Pharm Biomed Anal* 2017; **138**: 109-117 [PMID: 28192718 DOI: 10.1016/j.jpba.2016.12.038]

5 **Ilievski V**, Kinchen JM, Prabhu R, Rim F, Leoni L, Unterman TG, Watanabe K. Experimental Periodontitis Results in Prediabetes and Metabolic Alterations in Brain, Liver and Heart: Global Untargeted Metabolomic Analyses. *J Oral Biol* (Northborough) 2016; **3** [PMID: 27390783 DOI: 10.13188/2377-987X.1000020]

6 **Tang Z**, Liu L, Li Y, Dong J, Li M, Huang J, Lin S, Cai Z. Urinary Metabolomics Reveals Alterations of Aromatic Amino Acid Metabolism of Alzheimer's Disease in the Transgenic CRND8 Mice. *Curr Alzheimer Res* 2016; **13**: 764-776 [PMID: 26825095 DOI: 10.2174/1567205013666160129095340]

7 **Liu Y,** Lin ZB, Tan GG, Chu ZY, Lou ZY, Zhang JP, Hong ZY, Chai YF. Metabonomic studies on potential plasma biomarkers in rats exposed to ionizing radiation and the protective effects of hong shan, capsule. *Metabolomics* 2013; **9**: 1082-1095 [DOI: 10.1007/s11306-013-0529-6]

8 **Maertens A**, Bouhifd M, Zhao L, Odwin-DaCosta S, Kleensang A, Yager JD, Hartung T. Metabolomic network analysis of estrogen-stimulated MCF-7 cells: a comparison of overrepresentation analysis, quantitative enrichment analysis and pathway analysis versus metabolite network analysis. *Arch Toxicol* 2017; **91**: 217-230 [PMID: 27039105 DOI: 10.1007/s00204-016-1695-x]

9 **Ganti S**, Weiss RH. Urine metabolomics for kidney cancer detection and biomarker discovery. *Urol Oncol* 2011; **29**: 551-557 [PMID: 21930086 DOI: 10.1016/j.urolonc.2011.05.013]

10 **Zhao XF,** Liang XQ, Zhu CY, Liang J, Fu L, Deng X. Effect of natural taurine combine with traditional Chinese medicine on hepatic fibrosis in rats. *Internal Medicine* 2016; (**6**): 819-822

11 **Zhao XF,** Liang J, Zhu CY, Liang XQ, Wen B, Deng X. Effects of natural taurine combined with Chinese medicine on hepatic stellate cells. *Zhongguo Yixue Gongcheng* 2016; **24**: 5-9

12 **Deng X,** Liang J, Li YZ, Huang B, Zhang XL. Protective effect of natural taurine on mitochondria of hepatic fibrosis in rats. *Xi'an Jiaotong Daxue Xuebao* 2007; **28**: 648-703

13 **Miyazaki T**, Matsuzaki Y. Taurine and liver diseases: a focus on the heterogeneous protective properties of taurine. *Amino Acids* 2014; **46**: 101-110 [PMID: 22918604 DOI: 10.1007/s00726-012-1381-0]

14 **Liang J,** Deng X, Wu JY, Yang GY, Huang RB. The effect of natural taurine on hepatic stellate cell of rat. *Guangxi Yixue* 2006; **1**: 35-37

15 **Deng X**, Liang J, Lin ZX, Wu FS, Zhang YP, Zhang ZW. Natural taurine promotes apoptosis of human hepatic stellate cells in proteomics analysis. *World J Gastroenterol* 2010; **16**: 1916-1923 [PMID: 20397272 DOI: 10.3748/wjg.v16.i15.1916]

16 **Xia J**, Wishart DS. MetPA: a web-based metabolomics tool for pathway analysis and visualization. *Bioinformatics* 2010; **26**: 2342-2344 [PMID: 20628077 DOI: 10.1093/bioinformatics/btq418]

17 **Green CL**, Mitchell SE, Derous D, Wang Y, Chen L, Han JJ, Promislow DEL, Lusseau D, Douglas A, Speakman JR. The effects of graded levels of calorie restriction: IX. Global metabolomic screen reveals modulation of carnitines, sphingolipids and bile acids in the liver of C57BL/6 mice. *Aging Cell* 2017; **16**: 529-540 [PMID: 28139067 DOI: 10.1111/acel.12570]

18 **Bilal F**, Pérès M, Le Faouder P, Dupuy A, Bertrand-Michel J, Andrieu-Abadie N, Levade T, Badran B, Daher A, Ségui B. Liquid Chromatography-High Resolution Mass Spectrometry Method to Study Sphingolipid Metabolism Changes in Response to CD95L. *Methods Mol Biol* 2017; **1557**: 213-217 [PMID: 28078596 DOI: 10.1007/978-1-4939-6780-3_20]

19 **Ozbayraktar FB**, Ulgen KO. Molecular facets of sphingolipids: mediators of diseases. *Biotechnol J* 2009; **4**: 1028-1041 [PMID: 19579220 DOI: 10.1002/biot.200800322]

20 **Wang SY**, Zhang JL, Zhang D, Bao XQ, Sun H. [Recent advances in study of sphingolipids on liver diseases]. *Yao Xue Xue Bao* 2015; **50**: 1551-1558 [PMID: 27169276]

21 **Kiraz Y**, Adan A, Kartal Yandim M, Baran Y. Major apoptotic mechanisms and genes involved in apoptosis. *Tumour Biol* 2016; **37**: 8471-8486 [PMID: 27059734 DOI: 10.1007/s13277-016-5035-9]

22 **Takahashi M**, Okazaki H, Ogata Y, Takeuchi K, Ikeda U, Shimada K. Lysophosphatidylcholine induces apoptosis in human endothelial cells through a p38-mitogen-activated protein kinase-dependent mechanism. *Atherosclerosis* 2002; **161**: 387-394 [PMID: 11888522 DOI: 10.1016/S0021-9150(01)00674-8]

23 **Hirsova P**, Ibrahim SH, Krishnan A, Verma VK, Bronk SF, Werneburg NW, Charlton MR, Shah VH, Malhi H, Gores GJ. Lipid-Induced Signaling Causes Release of Inflammatory Extracellular Vesicles From Hepatocytes. *Gastroenterology* 2016; **150**: 956-967 [PMID: 26764184 DOI: 10.1053/j.gastro.2015.12.037]

24 **Campos-Mota GP**, Navia-Pelaez JM, Araujo-Souza JC, Stergiopulos N, Capettini LSA. Role of ERK1/2 activation and nNOS uncoupling on endothelial dysfunction induced by lysophosphatidylcholine. *Atherosclerosis* 2017; **258**: 108-118 [PMID: 28235709 DOI: 10.1016/j.atherosclerosis.2016.11.022]

25 **Kume N**, Gimbrone MA Jr. Lysophosphatidylcholine transcriptionally induces growth factor gene expression in cultured human endothelial cells. *J Clin Invest* 1994; **93**: 907-911 [PMID: 7509351 DOI: 10.1172/JCI117047]

26 **Dan H**, Wu J, Peng M, Hu X, Song C, Zhou Z, Yu S, Fang N. Hypolipidemic effects of Alismatis rhizome on lipid profile in mice fed high-fat diet. *Saudi Med J* 2011; **32**: 701-707 [PMID: 21748207]

P- Reviewer: Tsoulfas G **S- Editor**: Ma YJ **L- Editor**: Wang TQ **E- Editor**: Li D

World Journal of Gastroenterology

Submit a Manuscript: http://www.f6publishing.com

World J Gastroenterol 2017 August 21; 23(31): 5722-5731

DOI: 10.3748/wjg.v23.i31.5722

ISSN 1007-9327 (print) ISSN 2219-2840 (online)

ORIGINAL ARTICLE

Basic Study

Protective effects of *Foeniculum vulgare* root bark extract against carbon tetrachloride-induced hepatic fibrosis in mice

Cai Zhang, Xing Tian, Ke Zhang, Guo-Yu Li, Hang-Yu Wang, Jin-Hui Wang

Cai Zhang, Xing Tian, Ke Zhang, Guo-Yu Li, Hang-Yu Wang, Jin-Hui Wang, School of Pharmacy, Shihezi University, Shihezi 832002, Xinjiang Uygur Autonomous Region, China

Author contributions: Zhang C performed the majority of experiments; Tian X made contributions to data interpretation and wrote the manuscript; Zhang K participated in the establishment of the animal model; Li GY and Wang HY performed data analysis; Wang JH designed the study and revised the manuscript.

Supported by National Key Technology R&D Program, No. 2012BAI30B02.

Institutional review board statement: All experiments were reviewed and approved by the Institute Ethnics Committee of Shihezi University and the methods were carried out in accordance with the Animal Management Rules of the Chinese Ministry of Health.

Institutional animal care and use committee statement: The protocol on animal use was approved by the Institute Ethnics Committee of Shihezi University.

Conflict-of-interest statement: No potential conflicts of interest relevant to this article are reported.

Data sharing statement: No additional data are available.

Manuscript source: Unsolicited manuscript

Correspondence to: Xing Tian, PhD, School of Pharmacy, Shihezi University, North Road 4, Shihezi 832002, Xinjiang Uygur Autonomous Region, China. tianxing2017@shzu.edu.cn
Telephone: +86-993-2310715

Received: February 13, 2017
Peer-review started: February 14, 2017
First decision: April 7, 2017
Revised: May 14, 2017
Accepted: June 9, 2017
Article in press: June 12, 2017
Published online: August 21, 2017

Abstract

AIM

To investigate the protective effects of *Foeniculum vulgare* root bark (FVRB), a traditional Uyghur medicine, against carbon tetrachloride (CCl_4)-induced hepatic fibrosis in mice.

METHODS

Mice were randomly divided into eight groups (n = 20 each). Except for the normal control group, mice in the rest groups were intraperitoneally injected (i.p.) with 0.1% CCl_4-olive oil mixture at 10 mL/kg twice a week to induce liver fibrosis. After 4 wk, mice were treated concurrently with the 70% ethanol extract of FVRB (88, 176, 352 and 704 mg/kg, respectively) daily by oral gavage for 4 wk to evaluate its protective effects. Serum aspartate aminotransferase (AST), alanine aminotransferase (ALT), triglyceride (TG), hexadecenoic acid (HA), laminin (LN), glutathione (GSH), superoxide dismutase (SOD), and malondialdehyde (MDA) in liver tissues were measured. Hematoxylin-eosin (H and E) staining and Masson trichrome (MT) staining were performed to assess histopathological changes in the liver. The expression of transforming growth factor β_1 (TGF-β_1), matrix metalloprotein 9 (MMP-9) and metallopeptidase inhibitor 1 (TIMP-1) was detected by immunohistochemical analysis. Additionally, TGF-β_1 and alpha-smooth muscle actin (α-SMA) protein expression was measured by Western blot.

RESULTS

A significant reduction in serum levels of AST, ALT, TG, HA and LN was observed in the FVRB-treated groups, suggesting that FVRB displayed hepatoprotective effects. Also, the depletion of GSH, SOD, and MDA accumulation in liver tissues was suppressed by FVRB. The expression of TGF-β_1, MMP-9 and TIMP-1 determined by immunohistochemistry was markedly reduced in a dose-dependent manner by FVRB treatment. Furthermore, protective effects of FVRB against CCl_4-induced liver injury were confirmed by histopathological studies. Protein expression of TGF-β_1 and α-SMA detected by Western blot was decreased by FVRB treatment.

CONCLUSION

Our results indicate that FVRB may be a promising agent against hepatic fibrosis and its possible mechanisms are inhibiting lipid peroxidation and reducing collagen formation in liver tissue of liver fibrosis mice.

Key words: Hepatic fibrosis; *Foeniculum vulgare* root bark; Histopathology; Carbon tetrachloride; TGF-β1

Core tip: Hepatic fibrosis is a wound-healing pathological process resulting from chronic hepatic injuries. In the present study, hepatoprotective effects of *Foeniculum vulgare* root bark (FVRB), a traditional Uyghur medicine, against carbon tetrachloride (CCl_4)-induced hepatic fibrosis in mice were investigated. FVRB reduced serum levels of aspartate aminotransferase, alanine aminotransferase, triglyceride, hexadecenoic acid and laminin. Furthermore, FVRB inhibited CCl_4-induced TGF-β_1, MMP-9, TIMP-1 expression and histopathological changes. Our study indicated that the protective effects of FVRB are through inhibiting lipid peroxidation and collagen formation in liver tissue of liver fibrosis mice.

Zhang C, Tian X, Zhang K, Li GY, Wang HY, Wang JH. Protective effects of *Foeniculum vulgare* root bark extract against carbon tetrachloride-induced hepatic fibrosis in mice. *World J Gastroenterol* 2017; 23(31): 5722-5731 Available from: URL: http://www.wjgnet.com/1007-9327/full/v23/i31/5722.htm DOI: http://dx.doi.org/10.3748/wjg.v23.i31.5722

INTRODUCTION

Hepatic fibrosis is a wound-healing pathological process resulting from chronic hepatic injuries, which is characterized by the accumulation of extracellular matrix (ECM)[1]. It occurs during most continuous and chronic liver diseases, driven by inflammatory responses to tissue injury, which ultimately lead to liver cirrhosis. Previous studies indicated that activation of hepatic stellate cells (HSCs) plays an important role in the progress of hepatic fibrosis[2,3]. Activation of HSCs increases cell proliferation, producing large amounts of ECM components including hexadecenoic acid (HA) and laminin (LN)[4,5]. In addition, aberrant activity of transforming growth factor β_1 (TGF-β_1) or members of the platelet derived growth factor family are also the most prominent drivers to activate and transdifferent HSCs into myofibroblast[6,7]. Further, several chemokines that modulate the inflammatory reaction are involved in the progression of HSC activation and the fibrotic insult[8,9]. Many studies have demonstrated that the reversion of fibrosis can be achieved, particularly in the early course of the disease. Currently, treatment of liver damage mainly consists of inhibiting early activation and proliferation of HSCs and collagen fiber growth, and promoting HSC apoptosis and collagen degradation.

Many studies indicated that *Foeniculum vulgare* root bark (FVRB), a traditional Uyghur medicine, contains many chemical constituents, such as saccharides, glycosides, lactone compounds, phenols, tannins, flavonoids, alkaloids, volatile oil, grease, triterpenes and sterols[10,11]. In addition, FVRB has been traditionally used for the treatment of several pathophysiological conditions in China, exhibiting the activity of dispelling coldness, warming kidney and stomach, removing dampness, and alleviating swelling and pain[12-15]. For the first time, the present study was aimed to investigate the protective effects of FVRB against CCl_4-induced liver injury *in vivo* and the possible mechanisms involved.

MATERIALS AND METHODS

Animals

Male Kunming mice weighing 20 ± 2 g were supplied by the Experimental Animal Center of Urumqi (Urumqi, China). Mice were housed at room temperature under a 12 h light/dark cycle (lights on at 08:00 h) and were fed a standard diet *ad libitum*. All animal care and experimental procedures were approved by the Institute Ethnics Committee of Shihezi University.

Drug material

FVRB was obtained from Uygur Pharmaceutical Company (Uygur, China). FVRB was extracted with 70% ethanol by using the method of heating reflux and steam drying. A voucher specimen (No. 20070820) has been deposited in School of Pharmacy, Shihezi University.

Reagents

CCl_4 was obtained from Tianjin Guangfu Science and Technology Development Co. (Tianjin, China). Yiganling Pian (batch number 150102044) containing 38.5 mg of *Silybum marianum* each piece was purchased from Shanxi Lijun Chinese Medicine Co. (Shanxi,

China). Alanine aminotransferase (ALT), aspartate aminotransferase (AST), triglyceride, malondialdehyde (MDA), reduced glutathione hormone (GSH), and superoxide dismutase (SOD) assay kits were all purchased from Nanjing Jiancheng (Nanjing, China). Hyaluronic acid (HA) and laminin (LN) assay kits were obtained from Xitang Co. (Shanghai, China). Rabbit primary antibodies against TGF-β_1, alpha-smooth muscle actin (α-SMA), matrix metalloprotein 9 (MMP-9), and metallopeptidase inhibitor 1 (TIMP-1), and horseradish peroxidase labeled secondary antibody were purchased from BOSTER (Wuhan, China).

Experimental protocol

Mice were randomly divided into eight groups (n = 20 each): A-H. Group A (normal control group) was allowed free access to water and food. In the other seven experimental groups (B-H), the mice were treated with CCl_4 (10 mL/kg, i.p.) in olive oil (1:1000, v/v), twice a week for eight weeks. Group B served as a solvent control group, in which mice were given olive oil at 10 mL/kg at the fifth week. Group C was a model group, in which mice were given water at 10 mL/kg at the fifth week. Groups D, E, F, and G were orally administered with FVRB (88, 176, 352 and 704 mg/kg, respectively) once daily from the fifth week for four weeks. Group H was a positive control group, in which mice were treated with Yiganling Pian (200 mg/kg).

Mice were anesthetized with ethyl ether and blood samples were harvested. The blood was centrifuged at 3500 rpm for 10 min at 4 ℃ to obtain the supernatant serum, which was stored at 80 ℃ until further use for biochemical analysis. Liver, spleen and kidney were dissected out and washed immediately with ice cold saline to weigh.

Biochemical analysis

Serum was collected as mentioned above. ALT, AST and TG were determined according to the manufacturer's protocols using a Microplate Reader Thermo 3001. The absorbance of ALT and AST reactions was read at 505 nm and the absorbance of TG reaction was read at 546 nm. The enzyme activity is calculated as U/L. HA and LN levels were determined by enzyme-linked immunosorbent assay using the commercial kits. The absorbance of the reaction was read at 450 nm.

Measurement of MDA, GSH and SOD activities

Liver tissues samples were homogenized in physiological saline to give a 10% (w/v) liver homogenate, which was then centrifuged at 2500 rpm for 15 min at 4 ℃. The supernatant was used for the measurement of MDA, GSH and SOD activities with the commercial kits following the manufacture's protocols. Data are expressed as U/mg of protein.

Histopathological evaluation

Liver specimens were fixed in 10% formalin and then embedded in paraffin. Four-micrometer-thick sections were obtained from paraffin blocks and stained with hematoxylin and eosin (H and E) and Masson's trichrome (MT) before they were examined under a light microscope. The images were randomly taken from ten fields under a light microscope (200 × magnification).

Immunohistochemistry

TGF-β_1, MMP-9 and TIMP-1 expression levels in the liver were measured by immunohistochemistry. The liver tissues were sectioned and incubated with rabbit anti-TGF-β_1 antibody (1:100), rabbit anti-MMP-9 antibody (1:100), and rabbit anti-TIMP-1 antibody (1:100). Then the slides were processed using an immunohistochemical staining kit. After that, the slides were counterstained with hematoxylin and mounted with a glycerin gel. In the negative control groups, the primary antibodies were replaced with PBS. The sections were observed under a microscope (Nikon 80i).

Western blot analysis

Total protein was extracted from the liver tissue and the protein concentration was determination by BCA method. The protein was separated by SDS-polyacrylamide gel electrophoresis, followed by transfer to PVDF membrane. The membranes were blocked with 5% nonfat milk in TBST buffer for 1 h. Then target proteins were incubated overnight at 4 ℃ with TGF-β_1 and α-SMA primary antibodies (1:1000). After washing four times with TBST, the membranes were incubated with HRP-conjugated secondary antibody (1:10000) for 1 h at room temperature. Then the membranes were immersed in an enhanced chemiluminescence detection solution. Protein was analyzed by the gray value of the band, which is expressed as the ratio of the target protein and the β-actin protein.

Statistical analysis

All quantitative data are expressed as mean ± SE. Data were analyzed with SPSS 13.0 software. Statistical significance between groups was determined by one-way analysis of variance (ANOVA) followed by Tukey's multiple range post hoc test. $P < 0.05$ was considered statistically significant.

RESULTS

Effect of FVRB on organ index increase induced by CCl_4 treatment

As demonstrated in Figure 1, organ indexes including liver, spleen and kidney coefficients were measured in mice. Similar to previous studies[16], liver and spleen indexes were significantly increased in mice treated with CCl_4. Compared with the model group, the increase of liver index and spleen index in CCl_4-treated group was reduced by FVRB and Yiganling Pian treatment. However, there were no significant

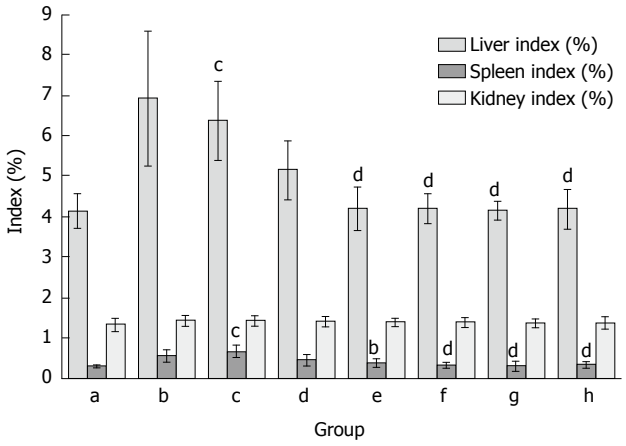

Figure 1 Effect of *Foeniculum vulgare* root bark extract on organ indexes in hepatic fibrosis mice. Data are expressed as the mean ± SD (n = 20). ^{b}P < 0.01 *vs* the normal control group; ^{c}P < 0.05 *vs* the CCl_4-treated group; ^{d}P < 0.01 *vs* the CCl_4-treated group. a: Normal group; b: Solvent group + CCl_4; c: CCl_4-treated group; d, e, f and g: FVRB treatment groups (88, 176, 352 and 704 mg/kg, respectively); h: Yiganling Pian + CCl_4.

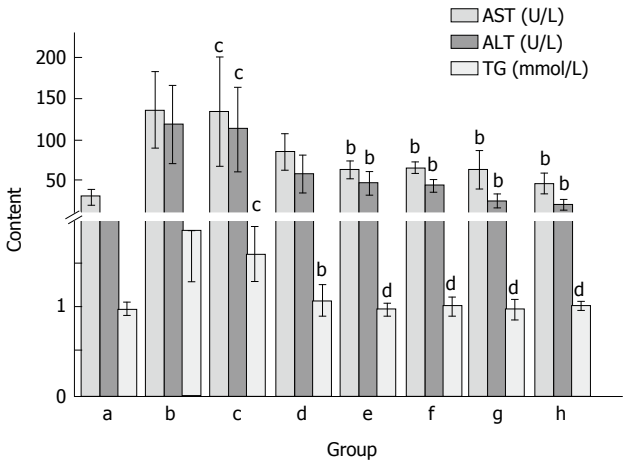

Figure 2 Effect of *Foeniculum vulgare* root bark extract on alanine aminotransferase, aspartate aminotransferase and triglyceride activities in CCl_4-treated mice. Data are expressed as the mean ± SD (n = 20). ^{b}P < 0.01 *vs* the normal control group; ^{c}P < 0.05 *vs* the CCl_4-treated group; ^{d}P < 0.01 *vs* the CCl_4-treated group. a: Normal group; b: Solvent group + CCl_4; c: CCl_4-treated group; d, e, f and g: FVRB treatment groups (88, 176, 352 and 704 mg/kg, respectively); h: Yiganling Pian + CCl_4.

differences in the kidney coefficient between the groups.

Effect of FVRB on serum AST, ALT and TG activities in mice

As shown in Figure 2, CCl_4 treatment markedly elevated serum AST, ALT and TG activities as compared with the normal control group. The AST and ALT activities after CCl_4 treatment were about 5 and 4 times higher than that of the normal group, respectively. However, Yiganling Pian treatment markedly inhibited the increase of serum AST, ALT and TG after long-term CCl_4 injection in mice (P < 0.05; Figure 2). Similarly, the administration of FVRB at different dosages significantly decreased AST, and ALT and TG activities (P < 0.05 or P < 0.01; Figure 2).

Effect of FVRB on MDA, GSH and SOD levels in CCl_4-treated mice

Lipid peroxidation was evaluated by measuring MDA content in liver tissue. In the CCl_4 treatment group, the content of MDA was elevated as compared with the normal control group. The administration of FVRB significantly decreased MDA content in a dose-dependent manner. Also, as compared with the normal control group, CCl_4 treatment markedly decreased the GSH level and SOD activity in liver tissue. However, treatment with the extract of FVRB (352 and 704 mg/kg) markedly recovered the CCl_4-induced GSH depletion (P < 0.01; Figure 3). In addition, FVRB treatment (88, 176, 352 and 704 mg/kg) significantly restored the depletion of SOD activity in a dose-dependent manner (Figure 3). Similarly, Yiganling Pian treatment (200 mg/kg) increased the GSH content and SOD activity as compared with the CCl_4 group (P < 0.01; Figure 3). Further, there was no significant difference in the levels of MDA, GSH and SOD between the CCl_4 group and the solvent control group.

Effect of FVRB on serum HA and LN in mice

After CCl_4 administration, the levels of serum HA and LN were significantly increased as compared with the normal control group (P < 0.05; Figure 4). Treatment with Yiganling Pian (200 mg/kg) significantly decreased the levels of serum HA and LN (P < 0.05; Figure 4). Meanwhile, FVRB treatment markedly decreased the elevation of serum HA and LN in a dose-dependent manner after long-term CCl_4 injection in mice (P < 0.05; Figure 4).

Effect of FVRB on histopathological alterations

As shown in Figure 5A, the liver sections of the normal control group exhibited the normal cellular structure with well-preserved cytoplasm, prominent nucleolus and central vein. In contrast, the liver sections of the CCl_4-treated group and solvent control group exhibited significant pathological changes, such as fibrosis, ballooning degeneration, steatosis, disseminated macrovesicular and microvesicular changes (Figure 5B and C). There was focal necrosis as well as piecemeal necrosis and fibrosis of portal areas. However, the FVRB and Yiganling Pian treatment groups showed a few to milder degree of leukocytes infiltration and necrosis (Figure 5E-H). In addition, as compared to the normal control group, the livers of mice treated with CCl_4 and the solvent exhibited extensive accumulation of connective tissue, leading to the formation of continuous fibrotic septa, nodules of regeneration, and noticeable alterations in the central vein (Figure 6A-C). However, treatment with FVRB and Yiganling Pian significantly attenuated CCl_4-induced alterations (Figure 6E-H). The severe hepatic fibrosis was reduced by treatment with FVRB, which was in good correlation with the results of hepatic antioxidant enzyme activities and serum aminotransferase activities.

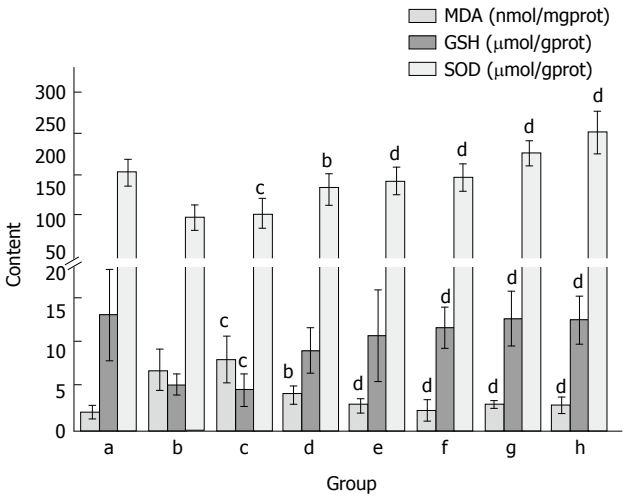

Figure 3 Effect of *Foeniculum vulgare* root bark extract on malondialdehyde, glutathione and superoxide dismutase levels in CCl_4-treated mice. Data are expressed as the mean ± SD (n = 20). $^bP < 0.01$ *vs* the normal control group; $^cP < 0.05$ *vs* the CCl_4-treated group; $^dP < 0.01$ *vs* the CCl_4-treated group. a: Normal group; b: Solvent group + CCl_4; c: CCl_4-treated group; d, e, f and g: FVRB treatment groups (88, 176, 352 and 704 mg/kg, respectively); h: Yiganling Pian + CCl_4.

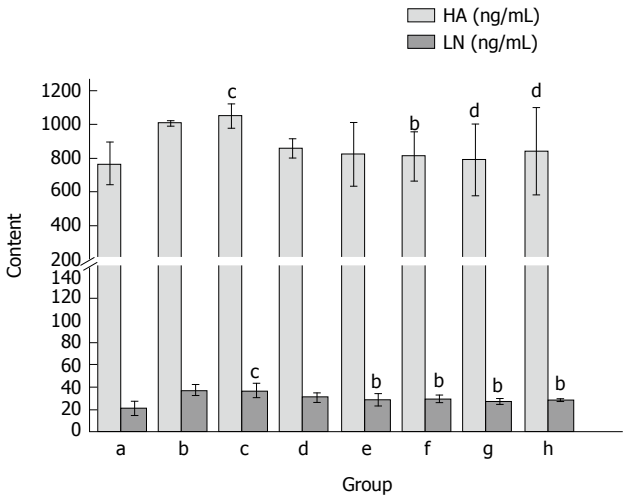

Figure 4 Effect of *Foeniculum vulgare* root bark extract on serum hexadecenoic acid and laminin levels in mice. Data are expressed as the mean ± SD (n = 20). $^bP < 0.01$ *vs* the normal control group; $^cP < 0.05$ *vs* the CCl_4-treated group; $^dP < 0.01$ *vs* the CCl_4-treated group. a: Normal group; b: Solvent group + CCl_4; c: CCl_4-treated group; d, e, f and g: *Foeniculum vulgare* root bark (FVRB) treatment groups (88, 176, 352 and 704 mg/kg, respectively); h: Yiganling Pian + CCl_4.

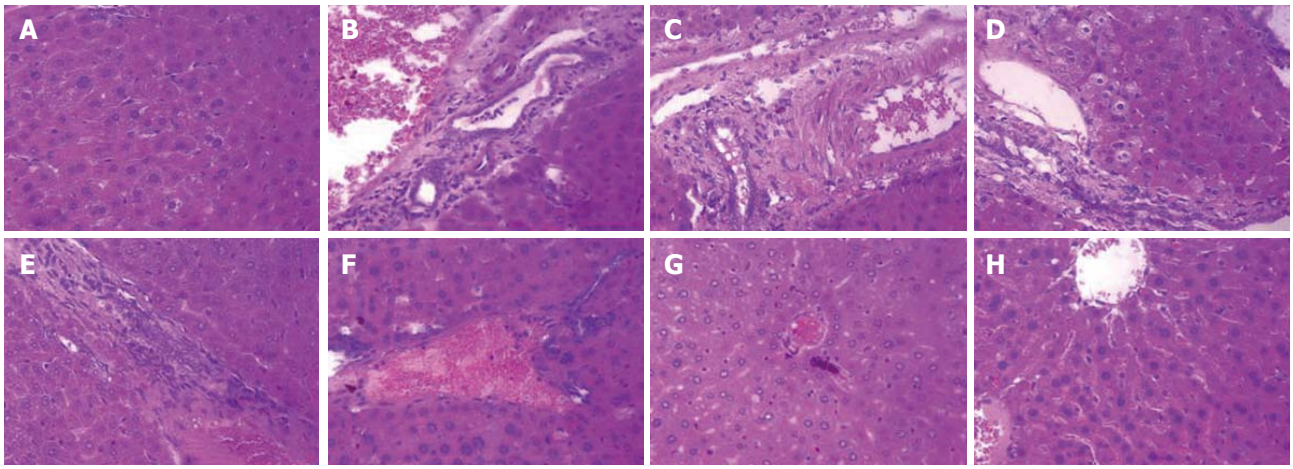

Figure 5 H and E staining (× 400) of the liver sections of mice. A: Normal control group; B: Solvent group + CCl_4; C: CCl_4-treated group; D-G: *Foeniculum vulgare* root bark (FVRB) treatment groups (88, 176, 352 and 704 mg/kg, respectively); H: Yiganling Pian + CCl_4.

Effect of FVRB on immunohistochemical staining for TGF-β1, MMP-9 and TIMP-1

As shown in Figure 7A, the expression of TGF-β1 in the normal control group was only observed in the portal area and central vein, with a relatively shallow, narrow range. In Figure 7B and C, the expression of TGF-β1 in the model group was mainly distributed in the portal area and central vein, with brown granules showing a wide distribution. However, the positive expression of TGF-β1 was significantly decreased in the FVRB treatment group (Figure 7D-G). The positive control group also showed a good reduction in the expression of TGF-β1 (Figure 7H).

Immunohistochemical expression of MMP-9 protein is shown in Figure 8. Positive MMP-9 staining appeased as brown granules in the cytoplasm and membrane. The overall color of the normal group was light brown, while the model group was significantly different. Compared with the model group, the positive expression in the treatment group was decreased, especially in the dose group of 704 mg/kg.

The results of TIMP-1 protein expression are shown in Figure 9. In the normal control group, there was positive expression of TIMP-1 in peripheral blood vessels and bile duct wall of the portal area (Figure 9A). In the solvent group and the model group, the positive staining of TIMP-1 was distributed in the fiber spacing and the central vein, and the brown yellow was obviously visible (Figure 9B and C). Compared with the model group, the positive expression of TIMP-1 in the FVRB treatment groups was markedly decreased (Figure 9 D-G). Further, there was a small amount of

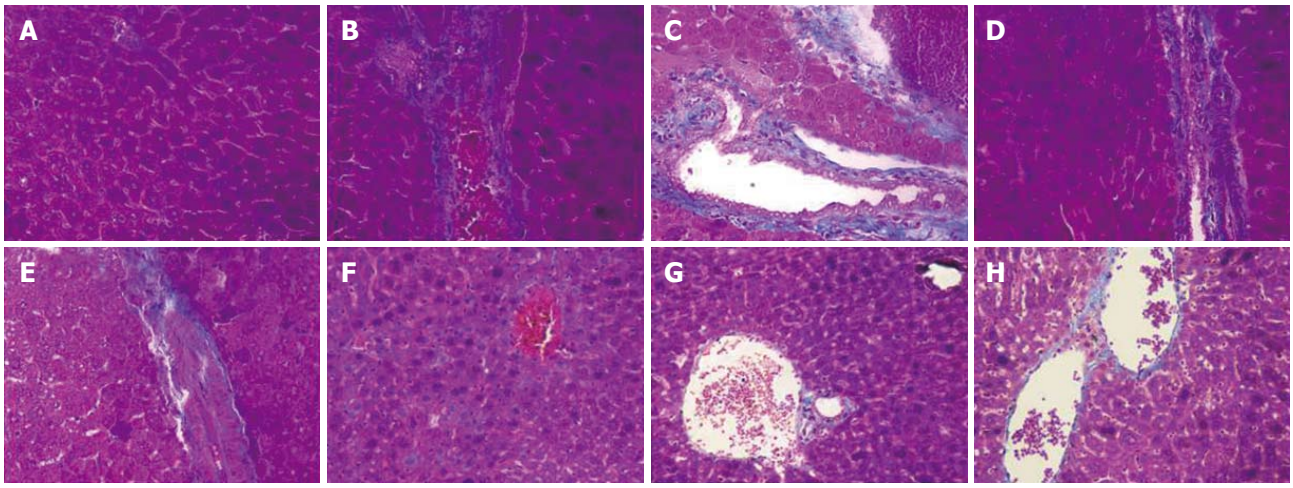

Figure 6 Masson trichrome staining (× 400) of the liver sections of mice. A: Normal control group; B: Solvent group + CCl_4; C: CCl_4-treated group; D-G: FVRB treatment groups (88, 176, 352and 704 mg/kg, respectively); H: Yiganling Pian + CCl_4.

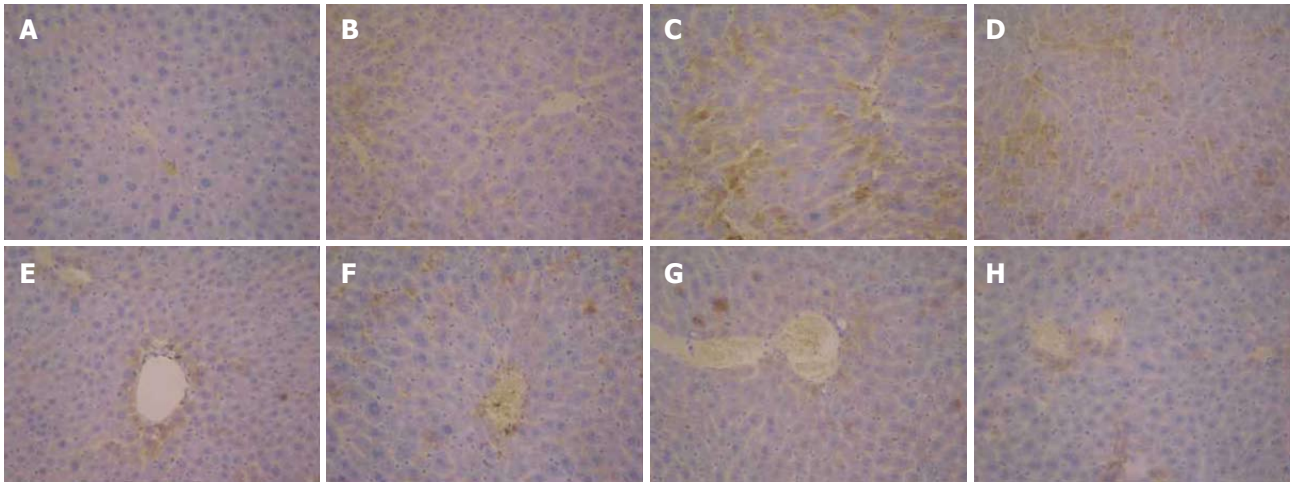

Figure 7 Immunohistochemical examination (× 400) of transforming growth factor β1 expression in liver tissues of mice. A: Normal group; B: Solvent group + CCl_4; c: CCl_4-treated group; D-G: *Foeniculum vulgare* root barks (FVRB) treatment groups (88, 176, 352 and 704 mg/kg, respectively); H: Yiganling Pian + CCl_4.

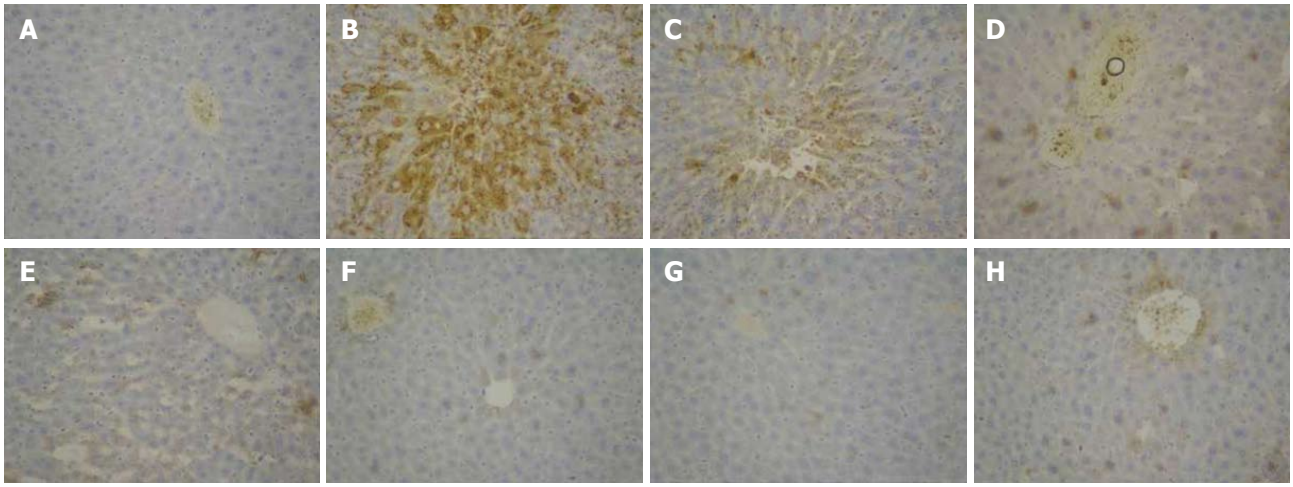

Figure 8 Immunohistochemical examination (× 400) of matrix metalloprotein 9 expression in liver tissues of mice. A: Normal control group; B: Solvent group + CCl_4; C: CCl_4-treated group; D-G: *Foeniculum vulgare* root bark (FVRB) treatment groups (88, 176, 352 and 704 mg/kg, respectively); H: Yiganling Pian + CCl_4.

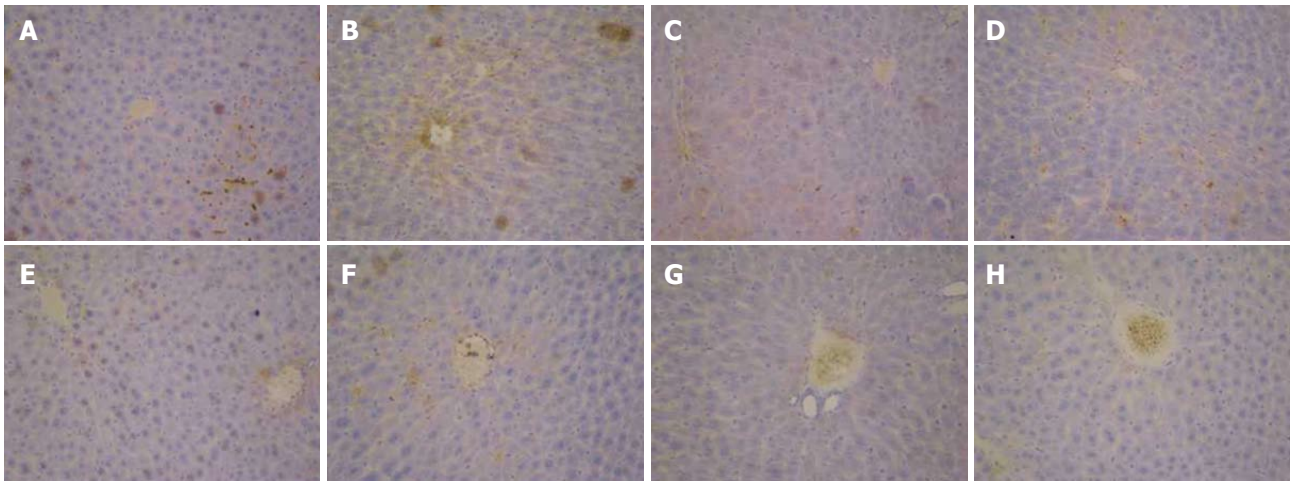

Figure 9 Immunohistochemical examination (× 400) of metallopeptidase inhibitor 1 expression in liver tissues of mice. A: Normal control group; B: Solvent group + CCl_4; C: CCl_4-treated group; D-G: *Foeniculum vulgare* root bark (FVRB) treatment groups (88, 176, 352 and 704 mg/kg, respectively); H: Yiganling Pian + CCl_4.

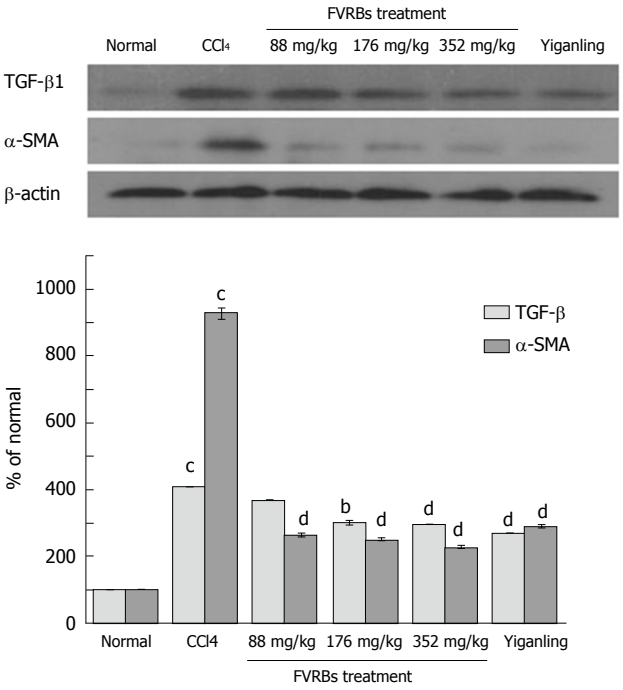

Figure 10 Effect of *Foeniculum vulgare* root bark extract on the expression of transforming growth factor-β1 and α-SMA proteins. $^{b}P < 0.01$ *vs* the normal control group; $^{c}P < 0.05$ *vs* the CCl_4-treated group; $^{d}P < 0.01$ *vs* the CCl_4-treated group. TGF-β: Transforming growth factor β; α-SMA: Alpha-smooth muscle actin.

positive TIMP-1 staining in the Yiganling Pian positive control group (Figure 9H).

Effect of FVRB on TGF-β1 and α-SMA protein expression

As illustrated in Figure 10, compared to the normal control group, the expression of TGF-β1 and α-SMA in the CCl_4 treatment group was significantly increased ($P < 0.01$). However, FVRB treatment markedly decreased TGF-β1 and α-SMA expression as compared with the CCl_4 treatment group ($P < 0.05$ or $P < 0.01$). Meanwhile, treatment with Yiganling Pian also significantly attenuated TGF-β1 and α-SMA expression ($P < 0.01$).

DISCUSSION

Liver fibrosis is usually regarded as an outcome of chronic liver injury in the process of long-term wound healing[17-19]. In the present study, CCl_4-induced liver injury, the most commonly used model for hepatic fibrosis[20,21], was induced. We detected the levels of ALT, AST, TG, HA and LN to assess liver function and the degree of liver fibrosis. There is evidence that natural substances may have a protective role against CCl_4-induced liver injury[22,23]. Considerable efforts have been made in the study of natural products with hepatoprotective activities[24,25]. Our study showed that CCl_4 caused a significant increase in serum levels of ALT, AST, TG, HA and LN in mice. However, FVRB treatment significantly altered these trends. Its hepatoprotective effect was further confirmed by histopathological observation that FVRB attenuated CCl_4-induced necro-inflammatory and fibrogenic effects.

There is growing evidence that oxidative stress contributes to the development of liver fibrosis by activating various signaling pathways involved in fibrogenesis[26,27]. The tissue concentration of MDA, a product of lipid peroxidation during liver fibrogenesis, was assayed. Also, the SOD and GSH activities were measured. In the present study, in the CCl_4-treated mice, the MDA level in liver tissue was elevated and the activities of SOD and GSH were decreased. Reversal of these trends by FVRB treatment suggests that FVRB prevented the progression of liver fibrosis by inhibiting oxidative stress in the liver.

The histopathological studies are a direct means for assessing the protective effect of FVRB. HE and Masson staining results showed that FVRB could reduce liver necrosis, significantly inhibit collagen fiber hyperplasia, improve liver tissue structure and reduce

fiber tissue. These results further confirmed that FVRB dose-dependently decreased hepatic histopathological changes.

The activation of HSCs is the central event in the pathogenesis of liver fibrosis[28-30]. In recent years, many studies found that TGF-β1 is the strongest factor inducing fibrosis, and it is also an important factor to promote the activation of HSCs[28,31]. Our result confirmed that administration of FVRB reduced the expression of TGF-β1 protein. Therefore, the anti-fibrotic effect of FVRB may be mediated by its inhibitory effect on TGF-β1. In addition, α-SMA expression also increases the generation and proliferation of chemotactic factors that are capable of recruiting inflammatory cells[32,33]. From the results we know that expression of α-SMA was enhanced by CCl_4 treatment, while the administration of FVRB prevented the development of fibrosis perhaps through the inhibition of α-SMA.

The major pathological change of liver fibrosis is the excessive accumulation of collagen and other extracellular matrixes[34]. Under normal circumstances, the synthesis and decomposition of collagen is balanced. Once the synthesis is over than decomposition, it will cause the accumulation of collagen in the liver, leading to the formation of liver fibrosis[35]. Matrix metalloproteinases (MMPs) can promote the degradation of extracellular matrix, which is consistent with the previous finding that the tissue inhibitors of metalloproteinase (TIMPs) can reduce liver fibrosis severity[36,37]. Among the MMP family members, MMP-9 plays an essential role in fibrosis formation. Many studies have shown that MMP-9 is elevated in patients with liver fibrosis. TIMP-1 can inhibit MMP-9[38], preventing the degradation of ECM and thereby promoting liver fibrosis. In the present study, the expression of MMP-9 and TIMP-1 proteins showed significant differences between CCl_4 and FVRB treatment groups, which suggests that MMP-9 and TIMP-1 are related to the protective effects of FVRB against the formation of liver fibrosis.

In conclusion, FVRB dose-dependently ameliorated hepatic oxidative stress and suppressed inflammation in CCl_4-injured liver fibrosis, and its mechanisms against liver fibrosis may be related with inhibiting lipid peroxidation formation in liver tissue of liver fibrosis mice and reducing the collagen formation by suppressing protein expression of TGF-β1, α-SMA, MMP-9 and TIMP-1. Thus, FVRB may have potential therapeutic utilities for protecting against liver fibrosis. Further experimental studies are necessary to determine the effective constituents of FVRB.

COMMENTS

Background

Hepatic fibrosis is a wound-healing pathological process resulting from chronic hepatic injuries, which is characterized by the accumulation of extracellular matrix. It occurs during most continuous and chronic liver diseases, driven by inflammatory responses to injury tissues, which ultimately lead to liver cirrhosis.

Research frontiers

Currently, treatment of liver damage mainly consists of inhibiting early activation and proliferation of hepatic stellate cells (HSCs) and collagen fiber growth, and promoting HSC apoptosis and collagen degradation. *Foeniculum vulgare* root bark (FVRB), a traditional Uyghur medicine, has been used for the treatment of several pathophysiological conditions in China, exhibiting the activity of dispelling coldness, warming kidney and stomach, removing dampness, and alleviating swelling and pain.

Innovations and breakthroughs

For the first time, the present study was aimed to investigate the protective effects of FVRB against CCl_4-induced liver injury *in vivo*. And its mechanisms against liver fibrosis may be related with inhibiting lipid peroxidation in liver tissue of liver fibrosis mice and inhibiting the collagen formation by suppressing protein expression of transforming growth factor-β1, alpha-smooth muscle actin, matrix metalloprotein 9 and metallopeptidase inhibitor 1.

Applications

FVRB dose-dependently ameliorated hepatic oxidative stress and suppressed inflammation in CCl_4-injured liver injury. Thus, FVRB may have potential therapeutic utilities for protecting against liver fibrosis.

Terminology

Liver fibrosis is usually regarded as an outcome of chronic liver injury in the process of long-term wound healing.

Peer-review

The authors' aim was to investigate the protective effects of FVRB extract against carbon tetrachloride-induced hepatic fibrosis in mice. The methods are appropriate, and the results are moderate.

REFERENCES

1 **Iwakiri Y**, Shah V, Rockey DC. Vascular pathobiology in chronic liver disease and cirrhosis - current status and future directions. *J Hepatol* 2014; **61**: 912-924 [PMID: 24911462 DOI: 10.1016/j.jhep.2014.05.047]

2 **Tai CJ**, Choong CY, Lin YC, Shi YC, Tai CJ. The anti-hepatic fibrosis activity of ergosterol depended on upregulation of PPARgamma in HSC-T6 cells. *Food Funct* 2016; **7**: 1915-1923 [PMID: 27040153 DOI: 10.1039/c6fo00117c]

3 **Zhao J**, Tang N, Wu K, Dai W, Ye C, Shi J, Zhang J, Ning B, Zeng X, Lin Y. MiR-21 simultaneously regulates ERK1 signaling in HSC activation and hepatocyte EMT in hepatic fibrosis. *PLoS One* 2014; **9**: e108005 [PMID: 25303175 DOI: 10.1371/journal.pone.0108005]

4 **Mòdol T**, Brice N, Ruiz de Galarreta M, García Garzón A, Iraburu MJ, Martínez-Irujo JJ, López-Zabalza MJ. Fibronectin peptides as potential regulators of hepatic fibrosis through apoptosis of hepatic stellate cells. *J Cell Physiol* 2015; **230**: 546-553 [PMID: 24976518 DOI: 10.1002/jcp.24714]

5 **Thomas RG**, Moon MJ, Kim JH, Lee JH, Jeong YY. Effectiveness of Losartan-Loaded Hyaluronic Acid (HA) Micelles for the Reduction of Advanced Hepatic Fibrosis in C3H/HeN Mice Model. *PLoS One* 2015; **10**: e0145512 [PMID: 26714035 DOI: 10.1371/journal.pone.0145512]

6 **Peng J**, Li X, Feng Q, Chen L, Xu L, Hu Y. Anti-fibrotic effect of Cordyceps sinensis polysaccharide: Inhibiting HSC activation, TGF-β1/Smad signalling, MMPs and TIMPs. *Exp Biol Med* (Maywood) 2013; **238**: 668-677 [PMID: 23918878 DOI: 10.1177/1535370213480741]

7 **He Y**, Huang C, Sun X, Long XR, Lv XW, Li J. MicroRNA-146a modulates TGF-beta1-induced hepatic stellate cell proliferation by targeting SMAD4. *Cell Signal* 2012; **24**: 1923-1930 [PMID: 22735812 DOI: 10.1016/j.cellsig.2012.06.003]

8 **Wasmuth HE**, Weiskirchen R. [Pathogenesis of liver fibrosis:

modulation of stellate cells by chemokines]. *Z Gastroenterol* 2010; **48**: 38-45 [PMID: 20072995 DOI: 10.1055/s-0028-1109933]
9 **Wasmuth HE**, Tacke F, Trautwein C. Chemokines in liver inflammation and fibrosis. *Semin Liver Dis* 2010; **30**: 215-225 [PMID: 20665374 DOI: 10.1055/s-0030-1255351]
10 **Parejo I**, Jauregui O, Sánchez-Rabaneda F, Viladomat F, Bastida J, Codina C. Separation and characterization of phenolic compounds in fennel (Foeniculum vulgare) using liquid chromatography-negative electrospray ionization tandem mass spectrometry. *J Agric Food Chem* 2004; **52**: 3679-3687 [PMID: 15186082 DOI: 10.1021/jf030813h]
11 **Badgujar SB**, Patel VV, Bandivdekar AH. Foeniculum vulgare Mill: a review of its botany, phytochemistry, pharmacology, contemporary application, and toxicology. *Biomed Res Int* 2014; **2014**: 842674 [PMID: 25162032 DOI: 10.1155/2014/842674]
12 **Tripathi P**, Tripathi R, Patel RK, Pancholi SS. Investigation of antimutagenic potential of Foeniculum vulgare essential oil on cyclophosphamide induced genotoxicity and oxidative stress in mice. *Drug Chem Toxicol* 2013; **36**: 35-41 [PMID: 22264205 DOI: 10.3109/01480545.2011.648328]
13 **Berrington D**, Lall N. Anticancer Activity of Certain Herbs and Spices on the Cervical Epithelial Carcinoma (HeLa) Cell Line. *Evid Based Complement Alternat Med* 2012; **2012**: 564927 [PMID: 22649474 DOI: 10.1155/2012/564927]
14 **Bogucka-Kocka A**, Smolarz HD, Kocki J. Apoptotic activities of ethanol extracts from some Apiaceae on human leukaemia cell lines. *Fitoterapia* 2008; **79**: 487-497 [PMID: 18672039 DOI: 10.1016/j.fitote.2008.07.002]
15 **Singh B**, Kale RK. Chemomodulatory action of Foeniculum vulgare (Fennel) on skin and forestomach papillomagenesis, enzymes associated with xenobiotic metabolism and antioxidant status in murine model system. *Food Chem Toxicol* 2008; **46**: 3842-3850 [PMID: 18976688 DOI: 10.1016/j.fct.2008.10.008]
16 **Tsai CF**, Hsu YW, Chen WK, Chang WH, Yen CC, Ho YC, Lu FJ. Hepatoprotective effect of electrolyzed reduced water against carbon tetrachloride-induced liver damage in mice. *Food Chem Toxicol* 2009; **47**: 2031-2036 [PMID: 19477216 DOI: 10.1016/j.fct.2009.05.021]
17 **Elpek GÖ**. Cellular and molecular mechanisms in the pathogenesis of liver fibrosis: An update. *World J Gastroenterol* 2014; **20**: 7260-7276 [PMID: 24966597 DOI: 10.3748/wjg.v20.i23.7260]
18 **Getachew Y**, Cusimano FA, Gopal P, Reisman SA, Shay JW. The Synthetic Triterpenoid RTA 405 (CDDO-EA) Halts Progression of Liver Fibrosis and Reduces Hepatocellular Carcinoma Size Resulting in Increased Survival in an Experimental Model of Chronic Liver Injury. *Toxicol Sci* 2016; **149**: 111-120 [PMID: 26443840 DOI: 10.1093/toxsci/kfv213]
19 **Melino M**, Gadd VL, Alexander KA, Beattie L, Lineburg KE, Martinez M, Teal B, Le Texier L, Irvine KM, Miller GC, Boyle GM, Hill GR, Clouston AD, Powell EE, MacDonald KP. Spatiotemporal Characterization of the Cellular and Molecular Contributors to Liver Fibrosis in a Murine Hepatotoxic-Injury Model. *Am J Pathol* 2016; **186**: 524-538 [PMID: 26762581 DOI: 10.1016/j.ajpath.2015.10.029]
20 **Huang SS**, Chen DZ, Wu H, Chen RC, Du SJ, Dong JJ, Liang G, Xu LM, Wang XD, Yang YP, Yu ZP, Feng WK, Chen YP. Cannabinoid receptors are involved in the protective effect of a novel curcumin derivative C66 against CCl4-induced liver fibrosis. *Eur J Pharmacol* 2016; **779**: 22-30 [PMID: 26945822 DOI: 10.1016/j.ejphar.2016.02.067]
21 **Hafez MM**, Hamed SS, El-Khadragy MF, Hassan ZK, Al Rejaie SS, Sayed-Ahmed MM, Al-Harbi NO, Al-Hosaini KA, Al-Harbi MM, Alhoshani AR, Al-Shabanah OA, Alsharari SD. Effect of ginseng extract on the TGF-β1 signaling pathway in CCl4-induced liver fibrosis in rats. *BMC Complement Altern Med* 2017; **17**: 45 [PMID: 28086769 DOI: 10.1186/s12906-016-1507-0]
22 **Sun Y**, Jia L, Huang Z, Wang J, Lu J, Li J. Hepatoprotective effect against CCl4-induced acute liver damage in mice and High-performance liquid chromatography mass spectrometric method for analysis of the constituents of extract of Rubus crataegifolius. *Nat Prod Res* 2017; Epub ahead of print [PMID: 28322066 DOI: 10.1080/14786419.2017.1292264]
23 **Pareek A**, Godavarthi A, Issarani R, Nagori BP. Antioxidant and hepatoprotective activity of Fagonia schweinfurthii (Hadidi) Hadidi extract in carbon tetrachloride induced hepatotoxicity in HepG2 cell line and rats. *J Ethnopharmacol* 2013; **150**: 973-981 [PMID: 24140589 DOI: 10.1016/j.jep.2013.09.048]
24 **Vladimir-Knežević S**, Cvijanović O, Blažeković B, Kindl M, Štefan MB, Domitrović R. Hepatoprotective effects of Micromeria croatica ethanolic extract against CCl4-induced liver injury in mice. *BMC Complement Altern Med* 2015; **15**: 233 [PMID: 26174335 DOI: 10.1186/s12906-015-0763-8]
25 **Wahid A**, Hamed AN, Eltahir HM, Abouzied MM. Hepatoprotective activity of ethanolic extract of Salix subserrata against CCl4-induced chronic hepatotoxicity in rats. *BMC Complement Altern Med* 2016; **16**: 263 [PMID: 27473536 DOI: 10.1186/s12906-016-1238-2]
26 **Heeba GH**, Mahmoud ME. Therapeutic potential of morin against liver fibrosis in rats: modulation of oxidative stress, cytokine production and nuclear factor kappa B. *Environ Toxicol Pharmacol* 2014; **37**: 662-671 [PMID: 24583409 DOI: 10.1016/j.etap.2014.01.026]
27 **Domitrović R**, Jakovac H, Marchesi VV, Blažeković B. Resolution of liver fibrosis by isoquinoline alkaloid berberine in CCl_4-intoxicated mice is mediated by suppression of oxidative stress and upregulation of MMP-2 expression. *J Med Food* 2013; **16**: 518-528 [PMID: 23734997 DOI: 10.1089/jmf.2012.0175]
28 **He YH**, Li Z, Ni MM, Zhang XY, Li MF, Meng XM, Huang C, Li J. Cryptolepine derivative-6h inhibits liver fibrosis in TGF-β1-induced HSC-T6 cells by targeting the Shh pathway. *Can J Physiol Pharmacol* 2016; **94**: 987-995 [PMID: 27295431 DOI: 10.1139/cjpp-2016-0157]
29 **Wang Q**, Dai X, Yang W, Wang H, Zhao H, Yang F, Yang Y, Li J, Lv X. Caffeine protects against alcohol-induced liver fibrosis by dampening the cAMP/PKA/CREB pathway in rat hepatic stellate cells. *Int Immunopharmacol* 2015; **25**: 340-352 [PMID: 25701503 DOI: 10.1016/j.intimp.2015.02.012]
30 **Wu T**, Chen JM, Xiao TG, Shu XB, Xu HC, Yang LL, Xing LJ, Zheng PY, Ji G. Qinggan Huoxue Recipe suppresses epithelial-to-mesenchymal transition in alcoholic liver fibrosis through TGF-β1/Smad signaling pathway. *World J Gastroenterol* 2016; **22**: 4695-4706 [PMID: 27217701 DOI: 10.3748/wjg.v22.i19.4695]
31 **Tang LX**, He RH, Yang G, Tan JJ, Zhou L, Meng XM, Huang XR, Lan HY. Asiatic acid inhibits liver fibrosis by blocking TGF-beta/Smad signaling in vivo and in vitro. *PLoS One* 2012; **7**: e31350 [PMID: 22363627 DOI: 10.1371/journal.pone.0031350]
32 **Zhou DJ**, Mu D, Jiang MD, Zheng SM, Zhang Y, He S, Weng M, Zeng WZ. Hepatoprotective effect of juglone on dimethylnitrosamine-induced liver fibrosis and its effect on hepatic antioxidant defence and the expression levels of α-SMA and collagen III. *Mol Med Rep* 2015; **12**: 4095-4102 [PMID: 26126609 DOI: 10.3892/mmr.2015.3992]
33 **Zakaria S**, Youssef M, Moussa M, Akl M, El-Ahwany E, El-Raziky M, Mostafa O, Helmy AH, El-Hindawi A. Value of α-smooth muscle actin and glial fibrillary acidic protein in predicting early hepatic fibrosis in chronic hepatitis C virus infection. *Arch Med Sci* 2010; **6**: 356-365 [PMID: 22371771 DOI: 10.5114/aoms.2010.14255]
34 **Wu K**, Huang R, Wu H, Liu Y, Yang C, Cao S, Hou X, Chen B, DaI J, Wu C. Collagen-binding vascular endothelial growth factor attenuates CCl4-induced liver fibrosis in mice. *Mol Med Rep* 2016; **14**: 4680-4686 [PMID: 27748931 DOI: 10.3892/mmr.2016.5826]
35 **Fuchs BC**, Wang H, Yang Y, Wei L, Polasek M, Schühle DT, Lauwers GY, Parkar A, Sinskey AJ, Tanabe KK, Caravan P. Molecular MRI of collagen to diagnose and stage liver fibrosis. *J Hepatol* 2013; **59**: 992-998 [PMID: 23838178 DOI: 10.1016/j.jhep.2013.06.026]
36 **Cong M**, Liu T, Wang P, Fan X, Yang A, Bai Y, Peng Z, Wu P, Tong X, Chen J, Li H, Cong R, Tang S, Wang B, Jia J, You H. Antifibrotic effects of a recombinant adeno-associated virus

carrying small interfering RNA targeting TIMP-1 in rat liver fibrosis. *Am J Pathol* 2013; **182**: 1607-1616 [PMID: 23474083 DOI: 10.1016/j.ajpath.2013.01.036]

37 **Peng WH**, Tien YC, Huang CY, Huang TH, Liao JC, Kuo CL, Lin YC. Fraxinus rhynchophylla ethanol extract attenuates carbon tetrachloride-induced liver fibrosis in rats via down-regulating the expressions of uPA, MMP-2, MMP-9 and TIMP-1. *J Ethnopharmacol* 2010; **127**: 606-613 [PMID: 20035854 DOI: 10.1016/j.jep.2009.12.016]

38 **Latronico T**, Mascia C, Pati I, Zuccala P, Mengoni F, Marocco R, Tieghi T, Belvisi V, Lichtner M, Vullo V, Mastroianni CM, Liuzzi GM. Liver Fibrosis in HCV Monoinfected and HIV/HCV Coinfected Patients: Dysregulation of Matrix Metalloproteinases (MMPs) and Their Tissue Inhibitors TIMPs and Effect of HCV Protease Inhibitors. *Int J Mol Sci* 2016; **17**: 455 [PMID: 27023536 DOI: 10.3390/ijms17040455]

P- Reviewer: Bacskay I, Lee HC **S- Editor**: Qi Y
L- Editor: Wang TQ **E- Editor**: Li D

World Journal of Gastroenterology

Submit a Manuscript: http://www.f6publishing.com

World J Gastroenterol 2017 August 21; 23(31): 5732-5738

DOI: 10.3748/wjg.v23.i31.5732

ISSN 1007-9327 (print) ISSN 2219-2840 (online)

ORIGINAL ARTICLE

Retrospective Cohort Study

Hypothesized summative anal physiology score correlates but poorly predicts incontinence severity

Christopher J Young, Assad Zahid, Cherry E Koh, Jane M Young

Christopher J Young, Assad Zahid, Cherry E Koh, Department of Colorectal Surgery, University of Sydney, Sydney, NSW 2042, Australia

Christopher J Young, RPAH Medical Centre, Sydney, NSW 2042, Australia

Cherry E Koh, Jane M Young, Surgical Outcome Research Centre (SOuRCe), Royal Prince Alfred Hospital, University of Sydney, Sydney, NSW 2042, Australia

Christopher J Young, Assad Zahid, Discipline of Surgery, University of Sydney, Sydney, NSW 2042, Australia

Jane M Young, School of Public health, University of Sydney, Sydney, NSW 2006, Australia

Author contributions: Young CJ, Koh CE and Young JM designed the research; Young CJ, Zahid A, Koh CE and Young JM performed the research; Young CJ and Zahid A contributed new ideas to the manuscript publications; Koh CE and Young JM analyzed the data; Young CJ, Zahid A, Koh CE and Young JM wrote the paper.

Institutional review board statement: This study proves by University of Sydney Institutional Review Board.

Informed consent statement: Patients were not required to give informed consent to the study because the analysis used anonymous clinical data that were obtained after each patient agreed to treatment by written consent.

Conflict-of-interest statement: None of them has received fees for serving as a speaker, or been a consultant and/or an advisory board member for any organization(s). None has received research funding for this project. None owns stocks and/or shares relevant to this research. None owns any patents

Data sharing statement: No additional data are available.

Manuscript source: Unsolicited manuscript

Correspondence to: Dr. Christopher J Young, Professor, RPAH Medical Centre, Suite 415, 100 Carillon Avenue, Sydney, NSW 2042, Australia. cyoungnsw@aol.com
Telephone: +61-2-95197576
Fax: +61-2-95191806

Received: March 13, 2017
Peer-review started: March 14, 2017
First decision: May 16, 2017
Revised: June 14, 2017
Accepted: July 12, 2017
Article in press: July 12, 2017
Published online: August 21, 2017

Abstract

AIM

To explore the relationship between such a construct and an existing continence score.

METHODS

A retrospective study of incontinent patients who underwent anal physiology (AP) was performed. AP results and Cleveland Clinic Continence Scores (CCCS) were extracted. An anal physiology score (APS) was developed using maximum resting pressures (MRP), anal canal length (ACL), internal and external sphincter defects and pudendal terminal motor latency. Univariate associations between each variable, APS and CCCS were assessed. Multiple regression analyses were performed.

RESULTS

Of 508 (419 women) patients, 311 had both APS and CCCS measured. Average MRP was 51 mmHg (SD

23.2 mmHg) for men and 39 mmHg (19.2 mmHg) for women. Functional ACL was 1.7 cm for men and 0.7 cm for women. Univariate analyses demonstrated significant associations between CCCS and MRP (P = 0.0002), ACL (P = 0.0006) and pudendal neuropathy (P < 0.0001). The association between APS and CCCS was significant (P < 0.0001) but accounted for only 9.2% of the variability in CCCS. Multiple regression showed that the variables most useful in predicting CCCS were external sphincter defect, pudendal neuropathy and previous pelvic surgery, but only improving the scores predictive ability to 12.5%.

CONCLUSION

This study shows that the ability of AP tests to predict continence scores improves when considered collectively, but that a constructed summation model before and after multiple regression is poor at predicting the variability in continence scores.

Key words: Incontinence; Anal physiology; Anal canal; Anal ultrasound; Manometry; Electromyography

Core tip: This study explored the relationship between a hypothesized anal physiology score combining rankings from maximal manometric resting pressures and anal canal length, ultrasound proportions of anal canal length of internal and external anal sphincters which were intact, and bilateral pudendal nerve terminal motor latencies; with the Cleveland Clinic Continence Score. The association between physiology and continence scores was significant but accounted for only 9.2% of the variability. The most useful variables predicting continence score were proportion of external sphincter intact, pudendal neuropathy and previous pelvic surgery. This study shows anal physiology tests predict continence scores better when considered collectively.

Young CJ, Zahid A, Koh CE, Young JM. Hypothesized summative anal physiology score correlates but poorly predicts incontinence severity. *World J Gastroenterol* 2017; 23(31): 5732-5738 Available from: URL: http://www.wjgnet.com/1007-9327/full/v23/i31/5732.htm DOI: http://dx.doi.org/10.3748/wjg.v23.i31.5732

INTRODUCTION

The extent of anal incontinence often determines the most appropriate treatment and facilitates monitoring treatment response[1]. Measuring anal incontinence severity is complex and requires considering the separate elements of gas, liquid, and solid, the frequency, the circumstances (*e.g.,* diarrhea), and impact on lifestyle and pad use[2-4]. Since the first grading system described by Browning and Parks, numerous grading scores have been developed, each with varying utility[5,6]. The importance of subjective assessments in a symptom-based condition such as incontinence is well established[1,6].

The preponderance of available continence scores indicates that none is perfect. Incontinence is a heterogeneous condition including groups of patients with soiling rather than frank liquid stool incontinence, yet few continence scores make that distinction between the two[6,7]. Though continence scores are often taken as surrogate measures of anorectal function with higher continence scores associated with worse anorectal function, they usually correlate poorly with anorectal physiology[6,8]. Continence scores reflect patient perception of the severity and burden of incontinence, but are often unhelpful in guiding treatment choice[8].

An objective measure that quantifies anal function and could be extrapolated to incontinence was considered as being desirable in providing clinicians with an alternative grading scale, which could also be useful in guiding treatment selection or predicting treatment response. Since no single anal physiology (AP) test is capable of thoroughly assessing anorectal function, such a measure could be derived using several different anal physiology tests. It is important to note that such a measure does not replace continence scores but serves to complement in the assessment of incontinence.

It was hypothesized that a summation measure that considered anal physiology tests collectively would correlate with continence scores better than when they were considered individually.

MATERIALS AND METHODS

Study design

A retrospective study of consecutive patients presenting for anal physiology with a single colorectal surgeon for anal incontinence at the Royal Prince Alfred Hospital between 1999 and 2006 was carried out. All patients routinely underwent anorectal manometry, endoanal ultrasound (EUS) and pudendal terminal motor latency (PNTML).

Anal physiology study results and continence scores were extracted from a prospectively maintained electronic database and medical records. Data collection began after written approval from the local human research and ethics committee was obtained.

Anorectal manometry

Anorectal manometry was performed using a Stryker manometer (Stryker Corp, San Jose, CA, United States) with a station pull-through technique. After a thorough inspection of perineum for surgical scars or asymmetry in skin corrugations, the catheter is gently introduced into the anal canal before digital examination to avoid pressure artifacts. Six resting pressures were measured at 1 cm intervals in a craniocaudal direction. The point with the highest resting pressure was taken

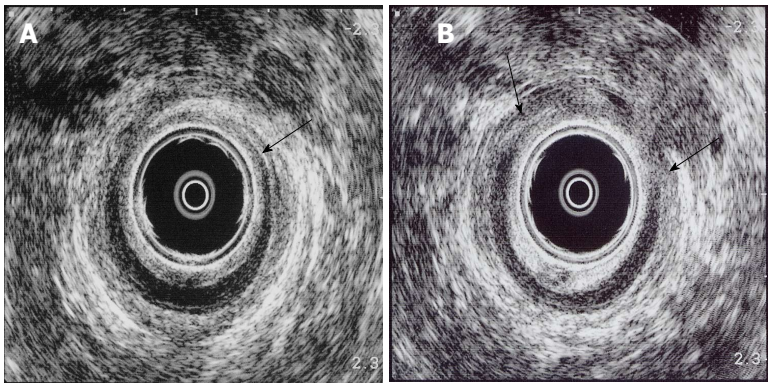

Figure 1 All internal and external anal sphincter lengths found on endoanal ultrasound. A: Internal anal sphincter defect (arrowed) of the mid anal canal on endoanal ultrasound; B: External anal sphincter defect (arrowed) of the mid anal canal on endoanal ultrasound.

Table 1 Hypothesized anal physiology score

	Maximum resting pressure (mmHg)	Anal canal length (cm)	Internal sphincter defect	External sphincter defect	PNTML
0	> 40	> 3	Intact	Intact	Normal
1	> 30, ⩽ 40	> 2, ⩽ 3	⩽ ¼ defect	⩽ ¼ defect	-
2	> 20, ⩽ 30	> 1, ⩽ 2	> ¼, ⩽ ½	> ¼, ⩽ ½	Unilateral neuropathy
3	> 10, ⩽ 20	> ½, ⩽ 1	> ½, ⩽ ¾	> ½, ⩽ ¾	-
4	⩽ 10	⩽ ½	> ¾	> ¾	Bilateral neuropathy

PNTML: Pudendal terminal motor latency.

as the site of the high-pressure zone and this was the position at which squeeze pressures were measured.

Endoanal ultrasound

EUS was performed using a 10 MHz Bruel and Kjaer rotating endoprobe with the patient in left lateral position. Sphincter defects were graded according to the longitudinal extent of sphincter defect. Sphincter quality is graded as either homogeneous or heterogeneous. Hard copies of sonographic images at the level of puborectalis, upper anal canal, mid anal canal and lower anal canal were also obtained so that sphincter thickness could be measured.

Pudendal nerve terminal motor latency

PNTML was measured using a glove mounted St. Mark's electrode with the patient in left lateral position. Three readings on each side with a satisfactory electrical tracing were taken with the shortest latency being recorded as the PNTML. Prolonged latency was defined as PNTML ⩾ 2.2 ms.

Anal physiology score

The hypothesized anal physiology score (APS) consisted of variables derived from manometry, EUS and PNTML. Manometry, EUS, and PNTML were chosen because these are the most commonly used anorectal physiology tests for incontinence investigation and the most likely to be informative and incorporated into clinical practice[8,9].

The five variables in the hypothesized APS were maximum resting pressure, anal canal length, internal sphincter defects, external sphincter defects and PNTML (Table 1). Individual variables were rated from zero to four; giving a possible APS value that ranged from zero to twenty where zero was hypothesized as associated with continence and twenty with incontinence. The worse the resting pressure, the shorter the anal canal length, the worse the sphincter defects and the worse the neuropathy, the higher the APS and therefore the worse the incontinence was anticipated to be.

Anal canal length was calculated using the technique described by Hool *et al*[10] using 30 mmHg as a cutoff. Although a study by Morgado *et al*[11] found mean pressures to be a better measure than maximum pressures, using mean resting pressures and anal canal length as variables would have led to repeated use of the same measurements. Choices of variables with EUS were sphincter defects, sphincter thickness, and sphincter morphology. Internal and external sphincter defects were chosen as the third and fourth variables because the main strength of EUS is its ability to detect sphincter defects[3,12]. All internal and external anal sphincter lengths found on EUS, specifically designation as fully intact or the proportion intact and proportion non-intact due to defects, were recorded by Author (Young CJ) at the time of EUS (Figure 1). This was measured relative to the length of anal canal found at EUS, whether intact or not, from the lower anal canal to puborectalis, allowing for rank classification of 0-4 as shown in Table 1. External anal sphincter thickness was explored as a potential variable but was considered difficult because the outer boundary of the external sphincter is often difficult to discern as it merges with surrounding fibro-fatty tissue. Its utility remains controversial[13-17]. Sphincter morphology was not chosen because the value of sphincter morphology remains to be determined in the available literature[18]. Finally, PNTML was included to complement manometry and EUS in the global assessment of anal function.

Table 2 Cleveland Clinic Continence Score[4]

	Never	Rarely < 1/mo	Sometimes ⩾ 1/mo	Usually ⩾ 1/wk	Always ⩾ 1/d
Gas	0	1	2	3	4
Liquid	0	1	2	3	4
Solids	0	1	2	3	4
Pads	0	1	2	3	4
Lifestyle	0	1	2	3	4

Table 3 Patient demographics for 508 patients presenting with faecal incontinence *n* (%)

	Men	Women
n	89 (17.5)	419 (82.5)
mean Age	57.8 (SD 15.1)	60.3 (SD 14.1)
Diabetes		
Yes	10 (11.2)	17 (4.1)
No	72 (80.9)	362 (86.4)
Irritable bowel syndrome		
Yes	9 (10.1)	16 (3.8)
No	73 (82.0)	363 (86.6)
Urinary incontinence		
Yes	9 (10.1)	42 (10.0)
No	73 (82.0)	365 (87.0)
Previous pelvic surgery		
Yes	13 (14.6)	197 (47.0)
No	70 (78.7)	184 (43.9)
Hysterectomy	-	148 (35.3)
Anterior resection	8 (9.0)	11 (2.6)
Rectopexy	3 (3.4)	15 (3.6)
Zaccharin's procedure	-	45 (10.7)
Bladder procedure	-	45 (10.7)
Previous OSR	-	12 (2.9)
Other gynae surgery	-	48 (11.5)
Prostatectomy	6 (6.7)	-
Anorectal surgery		
Yes	37 (41.6)	85 (20.3)
No	45 (50.6)	373 (89.0)
Hemorrhoidectomy	17 (19.1)	34 (8.1)
Sphincterotomy	4 (4.5)	9 (2.1)
Anal dilatation	0 (0)	6 (1.4)
Fistulotomy	8 (9.0)	13 (3.1)

Total percentages may not add up to 100% because of missing data, other categories which have not been included in this table for simplicity or because patients might have had more than one procedure.

Continence scores

Cleveland Clinic Continence Scores (CCCS) were also collected (Table 2)[3].

Statistical analysis

The analysis was performed using SAS (SAS Instutitute Inc, 2005). APS variables were expressed as means with standard deviations and medians with inter-quartile ranges. Univariate associations between individual APS variables and CCCS were first analyzed using an ANOVA procedure. The association between APS and CCCS was assessed next. In order to determine whether different combinations of variables could provide a more predictive model and to adjust for potential confounding variables, multiple regression was undertaken. All variables (including clinical information) that were significant or near significant ($P < 0.1$) in univariate analyses were included in the full base model. A manual backwards stepwise approach was then used to eliminate variables from the model in order of least significance. R^2 values were used to calculate the proportion of variability in CCCS that was explained by the model. Gender differences were analyzed using Wilcoxon rank sum test for the continuous variables and chi-square tests for categorical variables.

RESULTS

Patients

There were 508 (419 females) patients over the eight-year study period with a mean age of 57.8 for men and 60.3 for women (Table 3). The prevalence of urinary incontinence was similar between men and women in our cohort and was 10%. Women were much more likely to have had pelvic surgery with the most common procedure being hysterectomy followed by a range of gynecological procedures mainly for pelvic prolapse. Men were much more likely to have had anorectal surgery with hemorrhoidectomy being the most common procedure (Table 3).

Manometry and EUS results were available in all 508 patients. PNTML was unavailable in 34 patients due to faulty software resulting in PNTML being available in 474 patients. CCCS was available in 397 patients. Of 508 patients, 311 patients had adequate data to derive both APS and CCCS. The distribution for each APS variable is shown in Table 4. All APS variables were significantly different between men and women, except for internal sphincter defect. Almost 80% of men had normal pudendal nerve function while only 46% of women did. Women were at least four times more likely than men to have unilateral or bilateral neuropathy.

Univariate associations

Univariate associations between each APS variable and CCCS is shown in Table 5. Maximum resting pressures, anal canal length, and pudendal neuropathy were all significantly associated with CCCS but the associations between internal or external sphincter defects and CCCS were not statistically significant.

The mean APS value was 7.2 (SD 4.1). The association between the derived APS and CCCS was also highly significant ($P < 0.0001$) with a Pearson correlation coefficient of 0.3. However, the R^2 was 0.092 meaning that APS was only able to explain 9.2% of the variability in CCCS.

Multiple regressions

Following multiple regression modeling, only external sphincter defect, pudendal neuropathy and previous pelvic surgery were significant and independent predictors of CCCS (Table 6). After adjusting for the other variables in the model maximum resting pressure and anal canal length were not significantly associated with CCCS, whereas external sphincter became significant.

Table 4 Distribution of anal physiology score variables by gender

	Men	Women	*P* value	Mean reference range
Maximum RP (mmHg)				Men: 50-80
Mean	51.0 (SD 23.2)	38.8 (SD 15.6)	< 0.0001	Women: 30-60
Median	52.0 (IQR 33.5)	38.0 (IQR 22.5)		
ACL (cm)				Men: 2.5-3.5
Mean	1.7 (SD 1.4)	0.7 (SD 0.8)	< 0.0001	Women: 2.0-3.0
Median	2.0 (IQR 2.8)	0.5 (IQR 1.0)		
IAS defect				
Intact	61 (68.5)	286 (68.3)	0.7	-
⩽ ¼ defect	0 (0.0)	4 (1)	(c2 = 2.4, df = 4)	
> ¼, ⩽ ½	12 (13.5)	49 (11.7)		
> ½, ⩽ ¾	2 (2.2)	21 (5.0)		
> ¾	14 (15.7)	59 (14.1)		
EAS defect				
Intact	85 (95.5)	305 (73.0)	< 0.0001	-
⩽ ¼ defect	0 (0.0)	2 (0.5)	(c2 = 21.7, df = 4)	
> ¼, ⩽ ½	2 (2.2)	62 (14.8)		
> ½, ⩽ ¾	1 (1.1)	36 (8.6)		
> ¾	1 (1.1)	13 (3.1)		
Pudendal Neuropathy				
Normal	70 (78.7)	191 (45.6)	< 0.0001	
Unilateral	3 (3.4)	67 (16.0)	(c2 = 43.1, df=2)	2.20 ms
Bilateral	6 (6.7)	137 (32.7)		
Mean CCCS	5.9	8	0.001	-

CCCS: Cleveland Clinic Continence Scores; ACL: Anal canal length.

Table 5 Univariate associations between individual anal physiology score variables and Cleveland Clinic continence scores

	F value	df	*P*[1] value	Proportion variability in CCCS explained
Maximum RP (mmHg)	13.8	1, 395	0.0002	3.10%
ACL	12.1	1, 395	0.0006	2.70%
IAS defect	2.2	4, 392	0.07	1.20%
EAS defect	2.3	4, 392	0.06	1.30%
Pudendal neuropathy	11.7	2, 394	< 0.0001	5.10%

[1]Based on ANOVA procedure. CCCS: Cleveland Clinic Continence Scores; ACL: Anal canal length.

Table 6 Multiple regression analyses

Variable	Classification	Change in CCCS	*P* value
EAS defect	Intact	-	0.01
	¼	4	
	½	0.3	
	¾	1.5	
	> ¾	5.1	
PNTML	Normal	-	< 0.0001
	Unilateral neuropathy	1.2	
	Bilateral neuropathy	2.6	
Previous pelvic surgery	Yes	-	0.0007
	No	-1.6	

CCCS: Cleveland Clinic Continence Scores; PNTML: Pudendal terminal motor latency.

In combination, external sphincter defect, pudendal neuropathy and previous pelvic surgery accounted for 12.5% of the variability in CCCS.

DISCUSSION

This study shows that anal physiology tests can predict continence scores better when considered collectively rather than individually. While aiming to develop an objective score quantifying anal function and thereby incontinence, we showed that the APS only accounted for 9.2% of the variability in CCCS. The remaining variability suggests that there are many other factors in the anal incontinent population to account for it.

The five APS variables were chosen based on our understanding of the strengths and weaknesses of each variable, and because they are the most commonly used tests in our unit. Anal manometry squeeze pressures rely on patient effort and the ability of patients to squeeze their sphincters and pelvic floor. Many were found to adjunct this with "buttock squeeze", and potentially the measurement obtained may not be adequately representative of the actual sphincter function. The large overlap in squeeze pressures between incontinent and healthy individuals also means that squeeze pressures were inadequately discriminatory and therefore not chosen as a variable[19]. Maximum resting pressure reflects pressure generated by the high-pressure zone, and has been shown to be significantly different between incontinent and continent subjects[20]. Functional anal canal length was chosen due to its importance as a marker of continence[10,11].

Normal continence is a complex interaction of several factors including the rectum, pelvic nerves, pelvic floor, anal sphincters, colonic motility and stool consistency[1]. Anorectal function and incontinence can only be fully assessed when each of these elements has been evaluated and included within the APS model respective to their importance to continence. The APS model may then appear very sphincter-centric because manometry, EUS, and PNTML each assess a separate aspect of the sphincter. If APS is found to be helpful in guiding treatment selection or predicting treatment outcome, it is more likely to be incorporated into routine clinical practice as the tests are commonly performed. Further, it is fruitless to subject patients to time-consuming and potentially uncomfortable or embarrassing and costly investigations (such as defecography, colonic transit study) if clinical assessment can provide the required answer and when their relative importance to sphincter function is unknown. The role of stool consistency in aggravating incontinence or causing incontinence in an individual with compromised

anorectal function is well known[21]. While information on stool consistency using the Bristol chart was collected, this data was only available for 20% of the subjects and could not be included for analysis[22]. Because each physiology parameter has contributed less than 5% each to the predictive ability of CCCS, we doubt that inclusion of stool consistency to the APS would have made a dramatic difference to the predictive ability of the APS.

Because of the poor predictive ability of APS, analysis of variables that may influence continence was carried out using multiple regression. These included gender, age, parity and previous pelvic surgery[23-25]. Using multiple regression, we found that external sphincter defect, pudendal neuropathy, and previous pelvic surgery were most useful in predicting CCCS. Although external sphincter defect was not found to be significantly associated with continence scores on univariate associations, it was significant using multiple regression. This apparent initial lack of association between external sphincter defect and continence scores is assumed to be due to masking by other variables. Conversely, maximum resting pressures and anal canal length were significantly associated with continence scores on univariate associations but not multiple regression. This apparent effect was the result of confounding due to the differences in the distribution of external sphincter defect, pudendal neuropathy and previous pelvic surgery between men and women. Similarly, the strong apparent gender influence was also a confounder due to the much higher prevalence of external sphincter defect, pelvic surgery and pudendal neuropathy amongst females. The predictive ability of this new model improved marginally to account for 12.5% of the variability in CCCS.

The association between bilateral pudendal neuropathy and continence scores has previously been shown by Ricciardi *et al*[26] but not the relationship between unilateral neuropathy and continence score. This study demonstrated an almost linear relationship between neuropathy and continence scores. The same could not be demonstrated for external sphincter defect and is likely related to the small sample size in this study, and the results should be confirmed using a larger sample size. The role of pelvic surgery in incontinence had been controversial. Hysterectomy was the most widely studied pelvic procedure, and conflicting results have been reported[27,28]. Due to the relatively small numbers of each procedure except hysterectomy, all those involving pelvic viscera (uterus, rectum) and the pelvic floor were classified as pelvic surgery. The results of this study indicate that previous pelvic surgery was associated with greater incontinence.

In this study, the gender difference in CCCS was highly significant suggesting that women had more severe incontinence than men. A meta-analysis by Pretlove *et al*[23] reported that more women experienced severe incontinence than men because of the higher prevalence of solid and liquid incontinence among women. All APS variables were significantly different between men and women, except for internal sphincter defect, and this may be a clue as to why there is a gender difference in CCCS.

Given that the majority of CCCS is unexplained by clinical or anal physiology data, we believe that although continence scores and anorectal physiology are both used in incontinence, they measure different aspects of incontinence. The clinical utility of this newly developed measure in guiding treatment selection or predicting treatment response needs to be determined in a prospective clinical study.

In conclusion, anal physiology tests correlate better with continence scores when considered collectively rather than individually. Our APS model was only able to predict 9.2% of the variability in CCCS, suggesting that continence scores and physiology measure different aspects of incontinence. These aspects are likely to be complementary in the assessment of incontinence, with the clinical utility of the APS derived using multiple regression requiring prospective assessment in a clinical setting.

COMMENTS

Background

Anal physiology tests involving manometry, ultrasound and electromyography are routine in the investigation of fecal incontinence. Continence scores are also routinely assessed. This study aimed to research the connection between anal physiology and continence score as a means of correlating and subsequently applying the findings to the diagnosis, management and understanding of fecal incontinence.

Research frontiers

The ongoing relevance of anal physiology tests and their role in the diagnosis and management of fecal incontinence continues to require clarification and validation, to bring a clearer understanding of when and why they are beneficial.

Innovations and breakthroughs

The innovation of this study is the way the anal physiology data has been combined to create a summative anal physiology score, much in the same vain as a continence score, which can shed new insights into the diagnosis and management of fecal incontinence.

Applications

The novel summative anal physiology score presented and studied in this research can be used for future research projects involving the diagnosis and management of fecal incontinence. That will potentially open an entire new field of assessment of fecal incontinence in line with quality of life measures also.

Terminology

There are no terms that the authors do not believe are unfamiliar to most readers.

Peer-review

Authors established the anal physiology score model and it is helpful to assess the incontinence.

REFERENCES

1 **Saldana Ruiz N**, Kaiser AM. Fecal incontinence - Challenges and solutions. *World J Gastroenterol* 2017; **23**: 11-24 [PMID: 28104977 DOI: 10.3748/wjg.v23.i1.11]

2 **Stanley TH**, Webster LR. Anesthetic requirements and car-

diovascular effects of fentanyl-oxygen and fentanyl-diazepam-oxygen anesthesia in man. *Anesth Analg* 1978; **57**: 411-416 [PMID: 568401 DOI: 10.1007/BF02049407]
3 **Jorge JM**, Wexner SD. Etiology and management of fecal incontinence. *Dis Colon Rectum* 1993; **36**: 77-97 [PMID: 8416784 DOI: 10.1007/BF02050307]
4 **de la Portilla F**, Calero-Lillo A, Jiménez-Rodríguez RM, Reyes ML, Segovia-González M, Maestre MV, García-Cabrera AM. Validation of a new scoring system: Rapid assessment faecal incontinence score. *World J Gastrointest Surg* 2015; **7**: 203-207 [PMID: 26425269 DOI: 10.4240/wjgs.v7.i9.203]
5 **Parks AG**. Royal Society of Medicine, Section of Proctology; Meeting 27 November 1974. President's Address. Anorectal incontinence. *Proc R Soc Med* 1975; **68**: 681-690 [PMID: 1197295]
6 **Takács L**, Debreczeni LA. Circulatory regulation in pregnant rats: pregnancy and haemorrhagic hypotension. *Acta Physiol Acad Sci Hung* 1972; **42**: 345-365 [PMID: 4668583]
7 **O'Brien PE**, Skinner S. Restoring control: the Acticon Neosphincter artificial bowel sphincter in the treatment of anal incontinence. *Dis Colon Rectum* 2000; **43**: 1213-1216 [PMID: 11005485 DOI: 10.1007/BF02237423]
8 **Whitehead WE**, Wald A, Norton NJ. Treatment options for fecal incontinence. *Dis Colon Rectum* 2001; **44**: 131-142; discussion 142-144 [PMID: 11805574 DOI: 10.1007/BF02234835]
9 **Terra MP**, Deutekom M, Dobben AC, Baeten CG, Janssen LW, Boeckxstaens GE, Engel AF, Felt-Bersma RJ, Slors JF, Gerhards MF, Bijnen AB, Everhardt E, Schouten WR, Berghmans B, Bossuyt PM, Stoker J. Can the outcome of pelvic-floor rehabilitation in patients with fecal incontinence be predicted? *Int J Colorectal Dis* 2008; **23**: 503-511 [PMID: 18228027 DOI: 10.1007/s00384-008-0438-8]
10 **Hool GR**, Lieber ML, Church JM. Postoperative anal canal length predicts outcome in patients having sphincter repair for fecal incontinence. *Dis Colon Rectum* 1999; **42**: 313-318 [PMID: 10223749 DOI: 10.1007/BF02236345]
11 **Morgado PJ Jr**, Wexner SD, Jorge JM. Discrepancies in anal manometric pressure measurement--important or inconsequential? *Dis Colon Rectum* 1994; **37**: 820-823 [PMID: 8055728 DOI: 10.1007/BF02050148]
12 **Andromanakos N**, Filippou D, Skandalakis P, Papadopoulos V, Rizos S, Simopoulos K. Anorectal incontinence. pathogenesis and choice of treatment. *J Gastrointestin Liver Dis* 2006; **15**: 41-49 [PMID: 16680232]
13 **Gantke B**, Schäfer A, Enck P, Lübke HJ. Sonographic, manometric, and myographic evaluation of the anal sphincters morphology and function. *Dis Colon Rectum* 1993; **36**: 1037-1041 [PMID: 8223056 DOI: 10.1007/BF02047296]
14 **Schäfer R**, Heyer T, Gantke B, Schäfer A, Frieling T, Häussinger D, Enck P. Anal endosonography and manometry: comparison in patients with defecation problems. *Dis Colon Rectum* 1997; **40**: 293-297 [PMID: 9118743 DOI: 10.1007/BF02050418]
15 **Voyvodic F**, Rieger NA, Skinner S, Schloithe AC, Saccone GT, Sage MR, Wattchow DA. Endosonographic imaging of anal sphincter injury: does the size of the tear correlate with the degree of dysfunction? *Dis Colon Rectum* 2003; **46**: 735-741 [PMID: 12794574 DOI: 10.1007/s10350-004-6650-x]
16 **Prichard D**, Harvey DM, Fletcher JG, Zinsmeister AR, Bharucha AE. Relationship Among Anal Sphincter Injury, Patulous Anal Canal, and Anal Pressures in Patients With Anorectal Disorders. *Clin Gastroenterol Hepatol* 2015; **13**: 1793-1800.e1 [PMID: 25869638 DOI: 10.1016/j.cgh.2015.03.033]
17 **Gurland B**, Hull T. Transrectal ultrasound, manometry, and pudendal nerve terminal latency studies in the evaluation of sphincter injuries. *Clin Colon Rectal Surg* 2008; **21**: 157-166 [PMID: 20011414 DOI: 10.1055/s-2008-1080995]
18 **Lam TJ**, Kuik DJ, Felt-Bersma RJ. Anorectal function evaluation and predictive factors for faecal incontinence in 600 patients. *Colorectal Dis* 2012; **14**: 214-223 [PMID: 21689265 DOI: 10.1111/j.1463-1318.2011.02548.x]
19 **McHugh SM**, Diamant NE. Effect of age, gender, and parity on anal canal pressures. Contribution of impaired anal sphincter function to fecal incontinence. *Dig Dis Sci* 1987; **32**: 726-736 [PMID: 3595385 DOI: 10.1007/BF01296139]
20 **Osterberg A**, Graf W, Påhlman L. The longitudinal high-pressure zone profile in patients with fecal incontinence. *Am J Gastroenterol* 1999; **94**: 2966-2971 [PMID: 10520853 DOI: 10.1016/S0002-9270(99)00429-3]
21 **Read NW**, Bartolo DC, Read MG. Differences in anal function in patients with incontinence to solids and in patients with incontinence to liquids. *Br J Surg* 1984; **71**: 39-42 [PMID: 6689968 DOI: 10.1002/bjs.1800710112]
22 **Lewis SJ**, Heaton KW. Stool form scale as a useful guide to intestinal transit time. *Scand J Gastroenterol* 1997; **32**: 920-924 [PMID: 9299672 DOI: 10.3109/00365529709011203]
23 **Pretlove SJ**, Radley S, Toozs-Hobson PM, Thompson PJ, Coomarasamy A, Khan KS. Prevalence of anal incontinence according to age and gender: A systematic review and meta-regression analysis. *Int Urogynecol J Pelvic Floor Dysfunct* 2006; **17**: 407-417 [PMID: 16572280 DOI: 10.1007/s00192-005-0014-5]
24 **Bharucha AE**, Zinsmeister AR, Locke GR, Seide BM, McKeon K, Schleck CD, Melton LJ 3rd. Risk factors for fecal incontinence: a population-based study in women. *Am J Gastroenterol* 2006; **101**: 1305-1312 [PMID: 16771954 DOI: 10.1111/j.1572-0241.2006.00553.x]
25 **Lunniss PJ**, Gladman MA, Hetzer FH, Williams NS, Scott SM. Risk factors in acquired faecal incontinence. *J R Soc Med* 2004; **97**: 111-116 [PMID: 14996955 DOI: 10.1258/jrsm.97.3.111]
26 **Ricciardi R**, Mellgren AF, Madoff RD, Baxter NN, Karulf RE, Parker SC. The utility of pudendal nerve terminal motor latencies in idiopathic incontinence. *Dis Colon Rectum* 2006; **49**: 852-857 [PMID: 16598403 DOI: 10.1007/s10350-006-0529-y]
27 **Forsgren C**, Zetterström J, Lopez A, Nordenstam J, Anzen B, Altman D. Effects of hysterectomy on bowel function: a three-year, prospective cohort study. *Dis Colon Rectum* 2007; **50**: 1139-1145 [PMID: 17587089 DOI: 10.1007/s10350-007-0224-7]
28 **Altman D**, Zetterström J, López A, Pollack J, Nordenstam J, Mellgren A. Effect of hysterectomy on bowel function. *Dis Colon Rectum* 2004; **47**: 502-508; discussion 508-509 [PMID: 14994113 DOI: 10.1007/s10350-003-0087-5]

P- Reviewer: Yu CG **S- Editor**: Qi Y **L- Editor**: A
E- Editor: Xu XR

World Journal of Gastroenterology

Submit a Manuscript: http://www.f6publishing.com

World J Gastroenterol 2017 August 21; 23(31): 5739-5745

DOI: 10.3748/wjg.v23.i31.5739

ISSN 1007-9327 (print) ISSN 2219-2840 (online)

ORIGINAL ARTICLE

Retrospective Cohort Study

Minor endoscopic sphincterotomy followed by large balloon dilation for large choledocholith treatment

Xiao-Dan Xu, Bo Chen, Jian-Jun Dai, Jian-Qing Qian, Chun-Fang Xu

Xiao-Dan Xu, Bo Chen, Jian-Jun Dai, Jian-Qing Qian, Department of Gastroenterology, Changshu Affiliated Hospital of Soochow University, Changshu 215500, Jiangsu Province, China

Chun-Fang Xu, Department of Gastroenterology, the First Affiliated Hospital of Soochow University, Soozhou 215000, Jiangsu Province, China

Author contributions: Chen B, Dai JJ and Qian JQ performed the majority of experiments; Xu XD and Qian JQ contributed analytic tools and analyzed the data; Xu CF designed the research and Xu XD wrote the paper.

Supported by Project of Jiangsu Provincial Medical Youth Talent, No. QNRC2016213; Soochow Special Project for Major Clinical Diseases, No. LCZX201319; and Science and Technology Bureau of Changshu, No. CS201501.

Institutional review board statement: This study was reviewed and approved by the Institutional Review Board of Changshu Hospital Affiliated to Soochow University, Changshu, China.

Informed consent statement: All study participants or their legal guardian provided informed written consent about personal and medical data collection prior to study enrollment.

Conflict-of-interest statement: The authors declare no conflict of interest.

Data sharing statement: Technical appendix, statistical code and dataset available from the corresponding author at xxd20@163.com. Participants gave informed consent for data sharing.

Manuscript source: Unsolicited manuscript

Correspondence to: Xiao-Dan Xu, MD, Department of Gastroenterology, Changshu Affiliated Hospital of Soochow University, No. 1, Shuyuan Street, Changshu 215500, Jiangsu Province, China. xuxiaodan@jscsyy.cn
Telephone: +86-189-13631835
Fax: +86-512-52160115

Received: April 10, 2017
Peer-review started: April 12, 2017
First decision: May 12, 2017
Revised: May 29, 2017
Accepted: July 12, 2017
Article in press: July 12, 2017
Published online: August 21, 2017

Abstract

AIM

To evaluate early and late outcomes of endoscopic papillary large balloon dilation (EPLBD) with minor endoscopic sphincterotomy (mEST) for stone removal.

METHODS

A total of 149 consecutive patients with difficult common bile duct (CBD) stones (diameter ⩾ 10 mm or ⩾ 3 stones) underwent conventional endoscopic sphincterotomy (EST) or mEST plus EPLBD from May 2012 to April 2016. Their demographic, laboratory and procedural data were collected, and pancreaticobiliary complications were recorded.

RESULTS

Sixty-nine (94.5%) of the patients in the EPLBD + mEST group and 64 (84.2%) in the conventional EST group achieved stone clearance following the first session (P = 0.0421). The procedure time for EPLBD + mEST was shorter than for EST alone (42.1 ± 13.6 min *vs* 47.3 ± 11.8 min, P = 0.0128). The overall rate of

early complications in the EPLBD + mEST group (11%) was lower than in the EST group (21.1%); however, the difference was not significant (P = 0.0938). The cumulative recurrence rate of cholangitis and CBD stones between the two groups was also similar. The procedure time was independently associated with post-endoscopic retrograde cholangiopancreatography pancreatitis (OR = 6.374, 95%CI: 1.193-22.624, P = 0.023), CBD stone diameter ⩾ 16 mm (OR = 7.463, 95%CI: 2.705-21.246, P = 0.0452) and use of mechanical lithotripsy (OR = 9.913, 95%CI: 3.446-23.154, P = 0.0133) were independent risk factors for stone recurrence.

CONCLUSION

EPLBD with mEST is more effective than EST alone for difficult CBD stone removal, with shorter procedure time and fewer early complications.

Key words: Endoscopic papillary balloon dilation; Pancreatitis; Endoscopic sphincterotomy; Common bile duct stones

Core tip: This is a retrospective comparative study to investigate the efficacy and safety of endoscopic papillary large balloon dilation (EPLBD) with minor endoscopic sphincterotomy (mEST) for the removal of difficult common bile duct stones. EPLBD + mEST was found to be more effective than conventional endoscopic sphincterotomy alone for difficult stone removal, with shorter procedure time and potentially fewer early complications.

Xu XD, Chen B, Dai JJ, Qian JQ, Xu CF. Minor endoscopic sphincterotomy followed by large balloon dilation for large choledocholith treatment. *World J Gastroenterol* 2017; 23(31): 5739-5745 Available from: URL: http://www.wjgnet.com/1007-9327/full/v23/i31/5739.htm DOI: http://dx.doi.org/10.3748/wjg.v23.i31.5739

INTRODUCTION

Endoscopic retrograde cholangiopancreatography (ERCP) combined with endoscopic sphincterotomy (EST) is now widely accepted as the first-line procedure for treatment of choledocholithiasis[1]. Stone extraction with EST is successful in > 90% of cases, but adverse events such as bleeding, perforation, pancreatitis and cholangitis occur in 5%-10% of patients, with a mortality rate of < 1%[2,3]. Endoscopic papillary balloon dilation (EPBD; with a 6-mm to 10-mm dilating balloon) with conventional EST, was regarded as a safer and easier option than EST alone in patients with coagulopathy, Billroth Ⅱ anastomosis, or periampullary diverticulum because of the lower risk of bleeding and perforation, as well as preservation of sphincter of Oddi function[4-8].

In patients with difficult common bile duct (CBD) stones (diameter ⩾ 10 mm or ⩾ 3 stones), EPBD limits the extent of orifice dilation to a diameter of ⩽ 10 mm; as such, mechanical lithotripsy (MLT) is more frequently required to facilitate stone extraction, and this adjunct procedure is associated with a higher risk of post-ERCP pancreatitis (PEP)[9-12]. Recent studies have reported that endoscopic papillary large balloon dilation (EPLBD), as an extension of EPBD, might be effective for removal of difficult stones[13-16]. However, these studies were based on different definitions and few have focused on late outcomes.

Thus, we carried out a retrospective comparative study to investigate the efficacy and safety of EPLBD with minor (m)EST for the removal of difficult CBD stones.

MATERIALS AND METHODS

Patients

Patients receiving ERCP for the removal of CBD stones at our hospital between May 2012 and April 2016 were included in this study. Inclusion criteria were as follows: (1) age ⩾ 18 years; (2) maximum stone diameter ⩾ 10 mm or ⩾ 3 stones; and (3) diameter of the distal common bile duct ⩾ 12 mm. Exclusion criteria were: (1) pre-existing acute pancreatitis; (2) previous ERCP-related procedures; (3) presence of intrahepatic duct stones, distal bile duct strictures or malignant biliary obstruction; and (4) coagulopathy with platelet count < 50000/mL or anticoagulation therapy within 1 wk. Patients' medical records, laboratory tests, imaging findings, and records of ERCP were reviewed.

Endoscopic procedures

All ERCP-related procedures were performed according to a standardized protocol by three endoscopy specialists, each with > 15 years of ERCP experience, using a side-viewing duodenoscope (TJF-260; Olympus, Tokyo, Japan) with a large accessory channel. Local anesthesia of the pharynx was required using 10% xylocaine and intramuscular injection of 40 mg hyoscine butylbromide, and 50-100 mg meperidine was administered as premedication. EST or EPLBD + mEST were chosen at the discretion of the endoscopists for stone removal.

EST was performed according to the conventional method. mEST was performed proximally from the orifice of the papilla, but did not extend beyond the horizontal fold or the transverse fold of the papilla. EPLBD was performed following mEST and using a dilating balloon (CRE balloon 5.5 cm long, 12-20 mm diameter; Boston Scientific, Boston, MA, United States). The diameter of the balloons was set at 12-20 mm based on the size of the stones and distal bile duct. The balloon was then filled gradually with diluted contrast medium under endoscopic and fluoroscopic

Table 1 Baseline characteristics of patients

Variable	EPLBD + mEST *n* = 73	EST *n* = 76	*P* value
Age in yr	59.7 ± 12.4	62.1 ± 13.7	0.2647
Sex, male/female	47/26	45/31	0.5160
Cholecystolithiasis	22 (30.1)	19 (25)	0.4828
Cirrhosis	5 (6.8)	6 (7.9)	0.8073
History of cholecystectomy	7 (9.6)	7 (9.2)	0.9369
Periampullary diverticulum	9 (12.3)	11 (14.5)	0.7010
Billroth Ⅱ gastrectomy	2 (2.7)	3 (3.9)	0.9635
AMY in U/L	84.1 ± 21.9	90.1 ± 24.3	0.1160
TB in mg/dL	4.9 ± 2.1	5.3 ± 2.6	0.3007
ALT in IU/L	121.8 ± 27.6	117.3 ± 37.2	0.4005
AST in IU/L	91.1 ± 27.7	95.6 ± 31.3	0.3550
PT in s	11.2 ± 2.1	11.7 ± 2.3	0.1684
PC as $\times 10^6$/L	157.2 ± 31.3	158.1 ± 31.2	0.8896
Maximum CBD diameter in mm	17.5 ± 4.6	18.1 ± 5.7	0.4817
Maximum stone diameter in mm	16.9 ± 4.1	16.5 ± 4.7	0.5813
CBD stones	2.9 ± 1.1	2.3 ± 1.9	0.4354

Data are presented as *n* (%) or mean ± SD. ALT: Alanine aminotransferase; AMY: Serum amylase level; AST: Aspartate aminotransferase; CBD: Common bile duct; EPLBD: Endoscopic papillary large balloon dilation; EST: Endoscopic sphincterotomy; LC: Leukocyte count; mEST: EST: Endoscopic sphincterotomy; PC: Platelet count; PT: Prothrombin time; TB: Total serum bilirubin.

guidance, to observe the gradual disappearance of the waist in the balloon. Once the waist disappeared, the balloon remained inflated for 60 s before stone extraction.

Complete stone removal was determined by final cholangiography. An endoscopic nasobiliary drainage catheter (7.5 Fr; Boston Scientific) was inserted routinely following endoscopic clearance of the CBD stones. It was withdrawn at 48 h after ERCP if no remnant stones were visualized by magnetic resonance cholangiopancreatography after improvement of symptoms and abnormal laboratory values. Initial success was defined as complete CBD stone removal when only one session of the stone removal procedure was performed independent of MLT use; otherwise, a second session of ERCP was performed to retrieve the remnant stones. All patients enrolled were hospitalized and received antibiotics routinely following ERCP.

Definition of post-ERCP complications

Complications were evaluated according to the 1991 consensus guidelines[17]. PEP was defined as abdominal pain with at least a 3-fold elevation of serum amylase > 24 h after the procedure that required treatment for > 2 d. Post-ERCP cholangitis was defined as a fever higher than 38 ℃ lasting > 48 h due to biliary causes. Post-ERCP hemorrhage was defined as mild when there was a decrease in hemoglobin level, moderate when transfusion was required (< 4 U) and severe when > 5 U was needed or when intervention was required.

Late outcomes

Each patient who received ERCP procedures in our hospital was followed up routinely. They were interviewed by telephone or advised to visit our outpatient clinic after discharge. If there was any suspicion of recurrence during follow-up, liver function tests and imaging studies were performed. Patients with recurrent pancreaticobiliary complications treated with or without ERCP-related procedures, patients with gallstones undergoing cholecystectomy, or patients who had died were all recorded in our database with SPSS software (SPSS Inc., Chicago, IL, United States).

Statistical analysis

Statistical analysis was performed on an intention-to-treat basis with SPSS version 20.0. For analysis of categorical data, a χ^2 test with a Yates correction, or Fisher's exact test was used. A normality test was applied for continuous data, which were then analyzed with Student's *t* or Mann-Whitney *U* test. Patient characteristics are expressed as mean ± SD or as percentages. All statistical tests were two-tailed and the threshold for statistical significance was set at $P < 0.05$. It was assumed that 90% of cases would achieve stone clearance, and a 20% decrease in clearance rate was considered to be clinically significant. Fisher's exact two-sided test was performed to detect a significant difference ($\alpha = 0.05$) for a sample of 126 patients (63 in each group) with 80% power.

RESULTS

From May 2012 to April 2016, 879 consecutive patients who underwent ERCP procedures in our hospital were reviewed and 149 fulfilled the inclusion criteria of the current study. Of these, 73 patients were treated with EPLBD + mEST for CBD stone removal, while the other 76 were treated with EST alone. The mean diameter of CBD stones was 15.7 mm (range: 10.0-21.1 mm).

The two groups showed no significant difference in baseline characteristics. Laboratory and imaging findings were also similar between the two groups (Table 1). CBD stone clearance was successfully performed in all patients (Table 2). Sixty-eight (93.2%) of the patients in the EPLBD + mEST group achieved stone clearance without MLT, as well as 62 (81.6%) in the EST group ($P = 0.0343$). Sixty-nine (94.5%) of the patients in the EPLBD + mEST group and 64 (84.2%) in the EST group achieved stone clearance following the first session ($P = 0.0421$) and the procedure time of EPLBD + mEST was shorter than EST alone (42.1 ± 13.6 min *vs* 47.3 ± 11.8 min, $P = 0.0128$). Duration of hospital stay following ERCP was similar between the two groups (5.1 ± 2.2 d *vs* 5.7 ± 1.9 d, $P = 0.0753$). Early and late complications are listed in Table 2, and there were no differences between the two groups (11.0% *vs* 21.1%, $P = 0.0938$) in early complications. Six (8.2%) of the patients in the EPLBD + mEST group and 7 (9.2%) in the control group had PEP ($P = 0.8303$). All cases of PEP were mild and recovered

Table 2 Outcomes of endoscopic papillary large balloon dilation + minor endoscopic sphincterotomy for stone removal compared with endoscopic sphincterotomy alone

Outcome	EPLBD + mEST *n* = 73	EST *n* = 76	*P* value
Stone removal succeeded without MLT	68 (93.2)	62 (81.6)	0.0343
Procedure time in min	42.1 ± 13.6	47.3 ± 11.8	0.0128
Initial success	69 (94.5)	64 (84.2)	0.0421
Overall success	73 (100)	76 (100)	-
ENBD placement time in d	2.6 ± 0.7	2.5 ± 0.6	0.3990
Duration of hospital stay in d	5.1 ± 2.2	5.7 ± 1.9	0.0753
Early complications	8 (11.0)	16 (21.1)	0.0938
PEP	6 (8.2)	7 (9.2)	0.8303
Mild	6	7	0.8303
Moderate	0	0	-
Severe	0	0	-
Cholangitis	1 (1.4)	3 (4.0)	0.6411
Hemorrhage		0	-
Intraprocedural	1 (1.4)	6 (7.9)	0.1351
Post-procedural	0	0	-
Perforation	0	0	-
Late complications	4 (5.5)	4 (5.2)	0.7604
Recurrence of cholangitis	0	1 (1.3)	1.0000
Recurrence of CBD stones	4 (5.5)	3 (3.9)	0.9565
CBD stricture	0	0	-
Duration of follow-up in mo	14.1 ± 5.5	12.9 ± 5.5	0.2140
Cholecystectomy	5 (6.8)	7 (9.2)	0.5965
Loss to follow-up	0	0	-
Death	0	0	-

Data are presented as *n* (%) or mean ± SD. CBD: Common bile duct; ENBD: Endoscopic nasobiliary drainage; EPLBD: Endoscopic papillary large balloon dilation; EST: Endoscopic sphincterotomy; mEST: Minor endoscopic sphincterotomy; MLT: Mechanical lithotripsy; PEP: Post-endoscopic retrograde cholangiopancreatography pancreatitis.

after conservative treatment. More patients had intraprocedural hemorrhage in the EST (7.9%) group than in the EPLBD + mEST group (1.4%), although there was no significant difference (P = 0.1351). Additionally, serious complications such as perforation, post-procedural hemorrhage, or severe pancreatitis were not observed in any patient.

The median follow-up duration was 13.5 mo (range: 3-26 mo) for all patients, and there was no significant difference between the two groups (Table 2). There was no death or loss to follow-up. Cholecystectomy was performed in 5 (6.8%) patients in the EPLBD + mEST group and 7 (9.2%) in the EST group (P = 0.5965). The overall rate of late complications was similar between the two groups (5.5% *vs* 5.2%, P = 0.7604). There was only 1 patient in the EST group (1.3%) who experienced recurrence of cholangitis during follow-up. A total of 7 patients, 4 (5.5%) in the EPLBD + mEST group and 3 (3.9%) in the EST group (P = 0.9565), had CBD stone recurrence and were treated again by ERCP. The cumulative recurrence rate of cholangitis and CBD stones between the two groups did not differ significantly (log rank, P = 0.859; Figure 1).

According to PEP and stone recurrence, which comprised the majority of early and late complications, patients were divided into two subgroups: those who

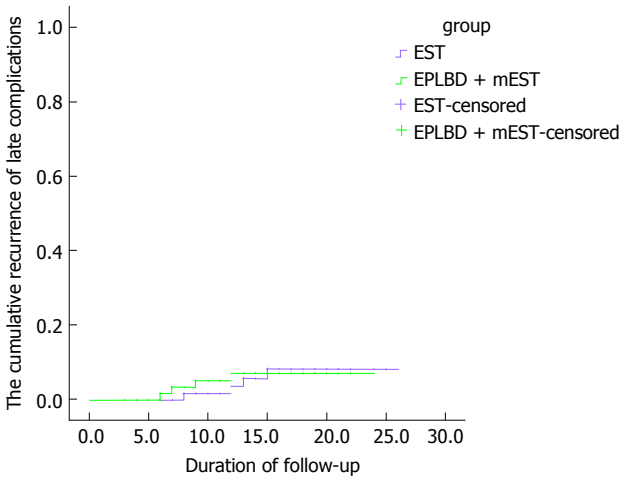

Figure 1 Estimated cholangitis and common bile duct stone recurrence rates. Kaplan-Meier analysis showed no significant difference between the EPLBD + mEST group and the EST group (P = 0.859). EST: Endoscopic sphincterotomy; EPLBD: Endoscopic papillary large balloon dilation; mEST: Minor endoscopic sphincterotomy.

developed PEP (PEP group, n = 13; No-PEP group, n = 136) or recurrence of CBD stones (Stone recurrence group, n = 7; No-stone recurrence group, n = 142). Univariate and multivariate logistic regression analyses were performed to identify independent risk factors. Compared to the No-PEP group, significantly longer procedure times (51.3 ± 11.7 min *vs* 43.6 ± 12.5 min, P = 0.0346) and CBD stone diameters ⩾ 16 mm (53.8% *vs* 16.9%, P = 0.0049) were observed in the PEP group (Table 3). Further analysis with multivariate logistic regression indicated that the procedure time was independently associated with PEP (OR = 6.374, 95%CI: 1.193-22.624, P = 0.023). For stone recurrence, maximum stone diameter (19.9 ± 7.7 mm *vs* 15.3 ± 5.1 mm, P = 0.0246), patients whose CBD stone diameter was ⩾ 16 mm (57.1% *vs* 18.3%, P = 0.0435) and use of MLT (57.1% *vs* 10.6%, P = 0.0053) were significantly different between the two subgroups. CBD stone diameter ⩾ 16 mm (OR = 7.463, 95%CI: 2.705-21.246, P = 0.0452) (Table 3) and MLT (OR = 9.913, 95%CI: 3.446-23.154, P = 0.0133) were independent risk factors for stone recurrence.

DISCUSSION

Since 2003, there have been a series of studies demonstrating the safety and efficacy of EPLBD with a preceding EST, for removal of CBD stones[10,18,19]. However, it is difficult to make an accurate judgment because some technical criteria mentioned in these studies differed, such as the extent of EST, balloon dilation protocol and CBD stone size. Additionally, most of the studies only focused on early complications of these procedures, but not on the late complications.

In the current study, stone clearance was performed successfully in all patients and the results were similar to those in a recent review[20]. That review showed that

Table 3 Univariate analysis of risk factors for post-endoscopic retrograde cholangiopancreatography pancreatitis and stone recurrence

Variable	PEP n = 13	No-PEP n = 136	P value	Stone recurrence n = 7	No-stone recurrence n = 142	P value
Age in yr	60.3 ± 10.7	61.1 ± 11.3	0.8069	59.6 ± 11.4	60.7 ± 9.9	0.7760
Sex, male/female	8/5	84/52	0.7775	5/2	87/55	0.8873
Cholecystolithiasis	2 (15.4)	39 (28.7)	0.4838	1 (14.3)	40 (28.2)	0.7118
History of cholecystectomy	1 (7.7)	13 (9.6)	0.7817	1 (14.3)	14 (9.9)	0.5319
Periampullary diverticulum	0	20 (14.7)	0.2891	2 (28.6)	18 (12.7)	0.2378
Billroth Ⅱ gastrectomy	1 (7.7)	4 (2.9)	0.3706	0	5 (3.5)	1.0000
Procedure time in min	51.3 ± 11.7	43.6 ± 12.5	0.0346	50.1 ± 10.8	48.1 ± 11.1	0.6420
Maximum CBD diameter in mm	17.1 ± 5.3	16.7 ± 4.9	0.7804	18.7 ± 8.1	16.7 ± 7.7	0.5043
Maximum stone diameter in mm	17.3 ± 5.1	16.9 ± 6.1	0.8194	19.9 ± 7.7	15.3 ± 5.1	0.0246
⩾ 16	7 (53.8)	23 (16.9)	0.0049	4 (57.1)	26 (18.3)	0.0435
⩾ 22	2	3	0.0607	1 (14.3)	4 (2.8)	0.2165
No. of CBD stones	2.4 ± 1.2	2.2 ± 1.0	0.4995	2.1 ± 1.1	1.9 ± 1.0	0.6071
MLT performed	3 (23.1)	16 (11.7)	0.4635	4 (57.1)	15 (10.6)	0.0053
Dilating procedure performed	6 (46.2)	67 (49.3)	0.8303	4 (57.1)	69 (48.6)	0.6586
ENBD placement time in d	2.3 ± 0.5	2.6 ± 0.7	0.0960	2.8 ± 0.7	2.6 ± 0.7	0.5010

Data are presented as n (%) or mean ± SD. CBD: Common bile duct; ENBD: Endoscopic nasobiliary drainage; EPLBD: Endoscopic papillary large balloon dilation; mEST: Minor endoscopic sphincterotomy; MLT: Mechanical lithotripsy; PEP: Post-endoscopic retrograde cholangiopancreatography pancreatitis.

the initial success rate was also similar between the two groups; however, that was not confirmed by the current study, which showed a higher initial success rate in the EPLBD + mEST group compared with the EST group. Also, the initial success rates of both groups were higher than that reported by the review (EPLBD + EST group: 87% *vs* EST group: 79%). It is hard to explain this discrepancy because success rates of stone removal are usually associated with the experience of the endoscopist, condition of the patient, shape and size of the CBD stones, time and size of the dilating balloon, and extent of the EST.

Nevertheless, according to our study, large balloon dilation along with mEST facilitated difficult CBD stone removal and could significantly shorten the procedure time (EPLBD + mEST group: 42.1 ± 13.6 min *vs* EST group: 47.3 ± 11.8 min). A total of 19 patients who failed stone clearance using a Dormia basket or balloon catheter had to undergo MLT. In this study, we also found a significantly lower rate of MLT usage when comparing the EPLBD + mEST group with the control group (EPLBD + EST group: 6.8% *vs* EST group: 18.4%), and the results were similar to those in the previous review[20]. MLT has proven to be a time-consuming and a challenging technique with related adverse events, such as basket impaction and bile duct injury. The extended ampullary orifice made by EPLBD facilitates difficult CBD stone extraction and it might reduce the need for MLT if EPLBD was used after EST, as compared to EST alone. We found a significantly shorter procedure time in the EPLBD + mEST group than in the EST group. Decreased procedure time indicates a decrease in radiation exposure, which is associated with a reduction in the risk of post-ERCP complications[21].

In the current study, the overall rate of early complications in the EPLBD + mEST group (11%) was lower than that in the EST group (21.1%), although the difference was not significant. PEP, which is the major early complication of ERCP, is closely related to the EPBD procedure[11]. However, it was not confirmed in the current study, in which PEP occurred in 8.2% patients in the EPLBD + mEST group and 9.2% in the EST group, and both the incidence and severity were similar. Further analysis demonstrated that the procedure time and CBD stone diameter ⩾ 16 mm were associated with PEP. In the current study, balloon dilation of the orifice failed to demonstrate an increased incidence of PEP, as had been noted previously[22-24]. It appears that, with a preceding EST, the dilating force of the balloon is more accurate in the direction of the sphincterotomy, away from the pancreatic duct orifice, and this reduces the likelihood of PEP.

Previous studies have shown a high incidence of hemorrhage (8.3%-9%) during full EST before EPLBD[10,12]. One of the key purposes for developing EPBD was to minimize the risk of hemorrhage by avoiding sphincterotomy. In the current study, the incidence of hemorrhage was controlled to a low level (1.4%) with limited sphincterotomy followed by EPLBD, which was lower than 7.9 in the EST group. However, the difference was not significant. All bleeding complications in this study were mild and easily controlled using argon-plasma coagulation, epinephrine spray, or compression by the balloon. The incidence of cholangitis (1.4% *vs* 4%) was also comparable and there was no perforation in any patient.

To date, few studies have looked beyond the early complications of EPLBD + EST, paying attention to either mid- or long-term outcomes. Recently, a Greek research team prospectively evaluated the 4-year outcomes of a multicenter randomized trial of EPLBD + EST and found an overall low risk (7.5%)

of recurrent CBD stones[25]. They reported that most stone recurrence occurred within the first 2.5 or 3.5 year following stone removal, and the mean interval between ERCP and recurrence of CBD stones was 37.5 ± 5.7 mo (range: 28-42 mo). In our study, 7 patients, 4 (5.5%) in the EPLBD + mEST group and 3 (3.9%) in the EST group, had CBD stone recurrence during follow-up. The incidence was lower than that of the Greek study, which could be because of the short follow-up period in the current study. CBD stone diameter ⩾ 16 mm and MLT were found to be independent risk factors for stone recurrence. This explained why MLT was more frequently used with larger stones and increased the risk of recurrence because even a few missed tiny stone fragments may act as a nidus for stone reaggregation[26].

Nevertheless, all the patients enrolled were in a single center and the retrospective nature of the study could bring potential biases in the selection of patients and procedures. Furthermore, large, prospective randomized comparative studies are necessary to evaluate the significant differences between EPLBD + mEST and EST for difficult CBD stone removal.

In conclusion, EPLBD with mEST was more effective than EST alone for difficult CBD stone removal, with a shorter procedure time, reduced use of MLT, and the potential to reduce early complications.

COMMENTS

Background

Endoscopic sphincterotomy (EST) is the standard method for enlarging the bile duct opening in the duodenum before stone removal during endoscopic retrograde cholangiopancreatography (ERCP). Although EST is effective, it permanently destroys the biliary sphincter. Endoscopic papillary balloon dilation (EPBD; with a 6-mm to 10-mm dilating balloon) is an alternative technique to enlarge the papillary orifice for stone retrieval, with the potential advantage of biliary sphincter function preservation. However, in patients with difficult common bile duct (CBD) stones (diameter ⩾ 10 mm or ⩾ 3 stones), EPBD limits the extent of orifice dilation to a diameter of ⩽ 10 mm. Thus, mechanical lithotripsy is more frequently required and it is believed to be associated with a higher risk of post-ERCP pancreatitis (PEP).

Research frontiers

Minor (m)EST followed by endoscopic papillary large balloon dilation (EPLBD) might be more effective for removal of difficult CBD stones. However, previous studies were ambiguous in their definitions and tended to neglect long-term outcomes, and the conclusions were inconsistent. In the current study, technical criteria, such as the extent of EST and balloon dilation protocol were all precisely defined and both early and late outcomes were observed.

Innovations and breakthroughs

In the current study, more patients in the EPLBD + mEST group achieved stone clearance following the first session and the procedure time was shorter than for EST alone. The procedure time was independently associated with PEP. The cumulative recurrence rate of cholangitis and CBD stones was similar between the two groups. CBD stone diameter ⩾ 16 mm and use of mechanical lithotripsy were independent risk factors for stone recurrence.

Applications

This study suggests that the EPLBD + mEST combination was a better choice for difficult CBD stone removal, having shorter procedure time and the potential to reduce development of early complications.

Terminology

PEP is defined as abdominal pain with at least a 3-fold elevation of serum amylase > 24 h after the procedure that requires treatment for > 2 d. Post-ERCP hemorrhage was defined as mild when there was a decrease in hemoglobin level, moderate when transfusion was required (< 4 U), and severe when > 5 U blood transfusion was needed or when intervention was required.

Peer-review

This is an interesting paper. It would be interesting to know how much time the effects of sphincter dilatation persist. This could be evaluated with imaging controls.

REFERENCES

1 **Adler DG**, Baron TH, Davila RE, Egan J, Hirota WK, Leighton JA, Qureshi W, Rajan E, Zuckerman MJ, Fanelli R, Wheeler-Harbaugh J, Faigel DO; Standards of Practice Committee of American Society for Gastrointestinal Endoscopy. ASGE guideline: the role of ERCP in diseases of the biliary tract and the pancreas. *Gastrointest Endosc* 2005; **62**: 1-8 [PMID: 15990812 DOI: 10.1016/j.gie.2005.04.015]

2 **Kim TH**, Kim JH, Seo DW, Lee DK, Reddy ND, Rerknimitr R, Ratanachu-Ek T, Khor CJ, Itoi T, Yasuda I, Isayama H, Lau JY, Wang HP, Chan HH, Hu B, Kozarek RA, Baron TH. International consensus guidelines for endoscopic papillary large-balloon dilation. *Gastrointest Endosc* 2016; **83**: 37-47 [PMID: 26232360 DOI: 10.1016/j.gie.2015.06.016]

3 **Carr-Locke DL.** Therapeutic role of ERCP in the management of suspected common bile duct stones. *Gastrointest Endosc* 2002; **56**: S170-174 [DOI: 10.1016/S0016-5107(02)70006]

4 **Kawabe T**, Komatsu Y, Tada M, Toda N, Ohashi M, Shiratori Y, Omata M. Endoscopic papillary balloon dilation in cirrhotic patients: removal of common bile duct stones without sphincterotomy. *Endoscopy* 1996; **28**: 694-698 [PMID: 8934088 DOI: 10.1055/s-2007-1005579]

5 **Bergman JJ**, van Berkel AM, Bruno MJ, Fockens P, Rauws EA, Tijssen JG, Tytgat GN, Huibregtse K. A randomized trial of endoscopic balloon dilation and endoscopic sphincterotomy for removal of bile duct stones in patients with a prior Billroth II gastrecyomy. *Gastrointest Endosc* 2001; **53**: 19-26 [DOI:10.1067/mge.2001.110454]

6 **Lin CK**, Lai KH, Chan HH, Tsai WL, Wang EM, Wei MC, Fu MT, Lo CC, Hsu PI, Lo GH. Endoscopic balloon dilatation is a safe method in the management of common bile duct stones. *Dig Liver Dis* 2004; **36**: 68-72 [PMID: 14971818 DOI: 10.1016/j.dld.2003.09.014]

7 **Yasuda I**, Tomita E, Enya M, Kato T, Moriwaki H. Can endoscopic papillary balloon dilation really preserve sphincter of Oddi function? *Gut* 2001; **49**: 686-691 [PMID: 11600473 DOI: 10.1136/gut.49.5.686]

8 **Takezawa M**, Kida Y, Kida M, Saigenji K. Influence of endoscopic papillary balloon dilation and endoscopic sphincterotomy on sphincter of oddi function: a randomized controlled trial. *Endoscopy* 2004; **36**: 631-637 [PMID: 15243887 DOI: 10.1055/s-2004-814538]

9 **Mac Mathuna P**, White P, Clarke E, Lennon J, Crowe J. Endoscopic sphincteroplasty: a novel and safe alternative to papillotomy in the management of bile duct stones. *Gut* 1994; **35**: 127-129 [PMID: 8307433 DOI: 10.1136/gut.35.1.127]

10 **Maydeo A**, Bhandari S. Balloon sphincteroplasty for removing difficult bile duct stones. *Endoscopy* 2007; **39**: 958-961 [PMID: 17701853 DOI: 10.1055/s-2007-966784]

11 **Baron TH**, Harewood GC. Endoscopic balloon dilation of the biliary sphincter compared to endoscopic biliary sphincterotomy for removal of common bile duct stones during ERCP: a metaanalysis of

randomized, controlled trials. *Am J Gastroenterol* 2004; **99**: 1455-1460 [PMID: 15307859 DOI: 10.1111/j.1572-0241.2004.30151.x]
12 **Ersoz G**, Tekesin O, Ozutemiz AO, Gunsar F. Biliary sphincterotomy plus dilation with a large balloon for bile duct stones that are difficult to extract. *Gastrointest Endosc* 2003; **57**: 156-159 [PMID: 12556775 DOI: 10.1067/mge.2003.52]
13 **Heo JH**, Kang DH, Jung HJ, Kwon DS, An JK, Kim BS, Suh KD, Lee SY, Lee JH, Kim GH, Kim TO, Heo J, Song GA, Cho M. Endoscopic sphincterotomy plus large-balloon dilation versus endoscopic sphincterotomy for removal of bile-duct stones. *Gastrointest Endosc* 2007; **66**: 720-726; quiz 768, 771 [PMID: 17905013]
14 **Stefanidis G**, Viazis N, Pleskow D, Manolakopoulos S, Theocharis L, Christodoulou C, Kotsikoros N, Giannousis J, Sgouros S, Rodias M, Katsikani A, Chuttani R. Large balloon dilation vs. mechanical lithotripsy for the management of large bile duct stones: a prospective randomized study. *Am J Gastroenterol* 2011; **106**: 278-285 [PMID: 21045816 DOI: 10.1038/ajg.2010.421]
15 **Kim HG**, Cheon YK, Cho YD, Moon JH, Park DH, Lee TH, Choi HJ, Park SH, Lee JS, Lee MS. Small sphincterotomy combined with endoscopic papillary large balloon dilation versus sphincterotomy. *World J Gastroenterol* 2009; **15**: 4298-4304 [PMID: 19750573 DOI: 10.3748/wjg.15.4298]
16 **Teoh AY**, Cheung FK, Hu B, Pan YM, Lai LH, Chiu PW, Wong SK, Chan FK, Lau JY. Randomized trial of endoscopic sphincterotomy with balloon dilation versus endoscopic sphincterotomy alone for removal of bile duct stones. *Gastroenterology* 2013; **144**: 341-345. e1 [PMID: 23085096 DOI: 10.1053/j.gastro.2012.10.027]
17 **Cotton PB**, Lehman G, Vennes J, Geenen JE, Russell RC, Meyers WC, Liguory C, Nickl N. Endoscopic sphincterotomy complications and their management: an attempt at consensus. *Gastrointest Endosc* 1991; **37**: 383-393 [PMID: 2070995 DOI: 10.1016/S0016-5107(91)70740-2]
18 **Kim TH**, Oh HJ, Lee JY, Sohn YW. Can a small endoscopic sphincterotomy plus a large-balloon dilation reduce the use of mechanical lithotripsy in patients with large bile duct stones? *Surg Endosc* 2011; **25**: 3330-3337 [PMID: 21533521 DOI: 10.1007/s00464-011-1720-3]
19 **Attasaranya S**, Cheon YK, Vittal H, Howell DA, Wakelin DE, Cunningham JT, Ajmere N, Ste Marie RW Jr, Bhattacharya K, Gupta K, Freeman ML, Sherman S, McHenry L, Watkins JL, Fogel EL, Schmidt S, Lehman GA. Large-diameter biliary orifice balloon dilation to aid in endoscopic bile duct stone removal: a multicenter series. *Gastrointest Endosc* 2008; **67**: 1046-1052 [PMID: 18178208 DOI: 10.1016/j.gie.2007.08.047]
20 **Madhoun MF**, Wani S, Hong S, Tierney WM, Maple JT. Endoscopic papillary large balloon dilation reduces the need for mechanical lithotripsy in patients with large bile duct stones: a systematic review and meta-analysis. *Diagn Ther Endosc* 2014; **2014**: 309618 [PMID: 24729674 DOI: 10.1155/2014/309618]
21 **Meine GC,** Baron TH. Endoscopic papillary large-balloon dilation combined with endoscopic biliary sphincterotomy for the removal of bile duct stones (with video). *Gastrointest Endosc* 2011; **74**: 1119-1126; quiz 1115.e1-5 [PMID: 21944309 DOI: 10.1016/j.gie.2011.06.042]
22 **Misra SP**, Dwivedi M. Endoscopic papillary balloon dilation for choledocholithiasis: does it have a future? *Endoscopy* 1999; **31**: 211-212 [PMID: 10223375]
23 **Vlavianos P**, Chopra K, Mandalia S, Anderson M, Thompson J, Westaby D. Endoscopic balloon dilatation versus endoscopic sphincterotomy for the removal of bile duct stones: a prospective randomised trial. *Gut* 2003; **52**: 1165-1169 [PMID: 12865276 DOI: 10.1136/gut.52.8.1165]
24 **Disario JA**, Freeman ML, Bjorkman DJ, Macmathuna P, Petersen BT, Jaffe PE, Morales TG, Hixson LJ, Sherman S, Lehman GA, Jamal MM, Al-Kawas FH, Khandelwal M, Moore JP, Derfus GA, Jamidar PA, Ramirez FC, Ryan ME, Woods KL, Carr-Locke DL, Alder SC. Endoscopic balloon dilation compared with sphincterotomy for extraction of bile duct stones. *Gastroenterology* 2004; **127**: 1291-1299 [PMID: 15520997 DOI: 10.1053/j.gastro.2004.07.017]
25 **Paspatis GA**, Paraskeva K, Vardas E, Papastergiou V, Tavernaraki A, Fragaki M, Theodoropoulou A, Chlouverakis G. Long-term recurrence of bile duct stones after endoscopic papillary large balloon dilation with sphincterotomy: 4-year extended follow-up of a randomized trial. *Surg Endosc* 2017; **31**: 650-655 [PMID: 27317037 DOI: 10.1007/s00464-016-5012-9]
26 **Sugiyama M**, Atomi Y. Risk factors predictive of late complications after endoscopic sphincterotomy for bile duct stones: long-term (more than 10 years) follow-up study. *Am J Gastroenterol* 2002; **97**: 2763-2767 [PMID: 12425545 DOI: 10.1111/j.1572-0241.2002.07019.x]

P- Reviewer: Manenti A **S- Editor**: Qi Y **L- Editor**: Filipodia
E- Editor: Huang Y

World Journal of Gastroenterology

Submit a Manuscript: http://www.f6publishing.com

World J Gastroenterol 2017 August 21; 23(31): 5746-5754

DOI: 10.3748/wjg.v23.i31.5746

ISSN 1007-9327 (print) ISSN 2219-2840 (online)

ORIGINAL ARTICLE

Retrospective Cohort Study

Diagnostic value of FIB-4, aspartate aminotransferase-to-platelet ratio index and liver stiffness measurement in hepatitis B virus-infected patients with persistently normal alanine aminotransferase

You-Wen Tan, Xing-Bei Zhou, Yun Ye, Cong He, Guo-Hong Ge

You-Wen Tan, Xing-Bei Zhou, Yun Ye, Cong He, Guo-Hong Ge, Department of Hepatology, the Third Hospital of Zhenjiang Affiliated Jiangsu University, Zhenjiang 212001, Jiangsu Province, China

Author contributions: Tan YW and Zhou XB contributed equally to this work; Tan YW designed the research; Ye Y, He C and Ge GH collected and analysed the data, and drafted the manuscript; Zhou XB performed the research; Ye Y and He C interpreted the data and performed the statistical analysis; Tan YW revised the article; all authors have read and approved the final version to be published.

Institutional review board statement: The study was approved by the Medical Ethics Committee of the Third Hospital of Zhenjiang Affiliated Jiangsu University (No. 2013011).

Informed consent statement: All study participants or their legal guardian provided informed written consent about personal and medical data collection prior to study enrolment.

Conflict-of-interest statement: All the authors have no conflict of interest related to the manuscript.

Data sharing statement: The original anonymous dataset is available on request from the corresponding author at tyw915@sina.com.

Manuscript source: Unsolicited manuscript

Correspondence to: Dr. You-Wen Tan, Department of Hepatology, the Third Hospital of Zhenjiang Affiliated Jiangsu University, 300 Daijiamen, Zhenjiang 212001, Jiangsu Province, China. tyw915@sina.com
Telephone: +86-511-88614915
Fax: +86-511-88970796

Received: May 2, 2017
Peer-review started: May 4, 2017
First decision: June 6, 2017
Revised: June 10, 2017
Accepted: July 12, 2017
Article in press: July 12, 2017
Published online: August 21, 2017

Abstract

AIM

To assess the diagnostic value of FIB-4, aspartate aminotransferase-to-platelet ratio index (APRI), and liver stiffness measurement (LSM) in patients with hepatitis B virus infection who have persistently normal alanine transaminase (PNALT).

METHODS

We enrolled 245 patients with chronic hepatitis B: 95 in PNALT group, 86 in intermittently elevated alanine transaminase (PIALT1) group [alanine transaminase (ALT) within 1-2 × upper limit of normal value (ULN)], and 64 in PIALT2 group (ALT > 2 × ULN). All the patients received a percutaneous liver biopsy guided by ultrasonography. LSM, biochemical tests, and complete blood cell counts were performed.

RESULTS

The pathological examination revealed moderate inflammatory necrosis ratios of 16.81% (16/95), 32.56% (28/86), and 45.31% (28/64), and moderate liver

fibrosis of 24.2% (23/95), 33.72% (29/86), and 43.75% (28/64) in the PNALT, PIALT1, and PIALT2 groups, respectively. The degrees of inflammation and liver fibrosis were significantly higher in the PIALT groups than in the PNALT group ($P < 0.05$). No significant difference was found in the areas under the curve (AUCs) between APRI and FIB-4 in the PNALT group; however, significant differences were found between APRI and LSM, and between FIB-4 and LSM in the PNALT group ($P < 0.05$ for both). In the PIALT1 and PIALT2 groups, no significant difference ($P > 0.05$) was found in AUCs for all comparisons ($P > 0.05$ for all). In the overall patients, a significant difference in the AUCs was found only between LSM and APRI ($P < 0.05$).

CONCLUSION

APRI and FIB-4 are not the ideal noninvasive hepatic fibrosis markers for PNALT patients. LSM is superior to APRI and FIB-4 in PNALT patients because of the influence of liver inflammation and necrosis.

Key words: Liver stiffness measurement; Hepatitis B virus; FIB-4; Aspartate aminotransferase-to-platelet ratio index; Normal; Alanine aminotransferase

Core tip: To assess the diagnostic value of FIB-4, aspartate aminotransferase-to-platelet ratio index (APRI), and liver stiffness measurement (LSM) in patients with hepatitis B virus infection who have persistently normal alanine transaminase (PNALT), we enrolled 245 patients with chronic hepatitis B: 95 in PNALT group, 86 in intermittently elevated alanine transaminase (PIALT1) group [alanine transaminase (ALT) within 1-2 × upper limit of normal value (ULN)], and 64 in PIALT2 group (ALT > 2 × ULN). The results showed that APRI and FIB-4 are not the ideal noninvasive hepatic fibrosis markers for PNALT patients. LSM is superior to APRI and FIB-4 in PNALT patients because of the influence of liver inflammation and necrosis.

Tan YW, Zhou XB, Ye Y, He C, Ge GH. Diagnostic value of FIB-4, aspartate aminotransferase-to-platelet ratio index and liver stiffness measurement in hepatitis B virus-infected patients with persistently normal alanine aminotransferase. *World J Gastroenterol* 2017; 23(31): 5746-5754 Available from: URL: http://www.wjgnet.com/1007-9327/full/v23/i31/5746.htm DOI: http://dx.doi.org/10.3748/wjg.v23.i31.5746

INTRODUCTION

Approximately a third of the world's population have serological evidence of past or present hepatitis B virus (HBV) infection, and 350-400 million people are known to be chronic HBV surface antigen (HBsAg) carriers. The disease spectrum and natural history of chronic HBV infection are diverse and varied, ranging from an inactive carrier state to progressive chronic hepatitis B (CHB), which may progress to cirrhosis and hepatocellular carcinoma (HCC)[1,2]. Chronic HBV infection is a dynamic process, and its natural history was schematically divided into five phases by the European Association for the Study of the Liver Clinical Practice Guidelines (2012) as follows[1]: (1) the "immune tolerant" phase; (2) the "immune reactive HBeAg-positive phase"; (3) the "inactive HBV carrier phase"; (4) "HBeAg-negative CHB" phase; and (5) the "HBeAg-negative CHB" or "HBsAg-negative" phase.

Although serum levels of alanine transaminase (ALT), an enzyme released from hepatocytes during liver injury, should reflect the degree of liver damage[3], not all patients with chronic HBV infection have persistently elevated ALT levels. Patients in the immune-tolerant phase and inactive carriers have persistently normal ALT (PNALT) levels[4,5], while a proportion of patients with HBeAg-negative CHB may have intermittently normal ALT levels. Histological injury in patients with normal ALT levels has also been reported[5-10]. Furthermore, some large cohort studies have shown that patients with CHB who have normal serum ALT levels were also at risk for the development of cirrhosis and HCC[11,12]. Liver biopsy (LB) is the current gold standard for assessing hepatic inflammation and fibrosis in patients with chronic HBV infection who have PNALT[7]. The invasiveness of liver puncture, the limitation of the specimen, and the poor patient compliance have restricted the application of LB, which has led to the development of noninvasive methods such as FIB-4[13] and aspartate amino-transferase (AST)-to-platelet ratio index (APRI)[14] for evaluating fibrosis in patients with chronic HBV infection. Liver stiffness measurement (LSM) using transient elastography (FibroScan) has been widely used in the diagnosis of chronic liver fibrosis[15,16]. However, the diagnostic value of FIB-4, APRI, and LSM in patients with HBV infection with PNALT is not clear.

In this study, we comprehensively evaluated the characteristics of histological abnormalities in a large population of Chinese CHB patients with PNALT, with an aim to analyze the diagnostic value of FIB-4, APRI, and LSM in patients with HBV who have PNALT.

MATERIALS AND METHODS

Ethics statement

The study was approved by the Medical Ethics Committee of The Third Hospital of Zhenjiang Affiliated Jiangsu University (No. 2013011), and written informed consent was obtained from each patient prior to participation. The study was conducted in accordance with the Declaration of Helsinki.

Patients

This was a retrospective cohort study of patients with CHB diagnosed between January 2011 and June 2016 at the Department of Hepatology, The Third Hospital

of Zhenjiang Affiliated Jiangsu University. The patients were examined every 3 to 6 mo, or more often if clinically indicated. At each visit, liver biochemistry and HBV serology, including HBsAg, HBeAg, anti-HBe, and HBV DNA levels, and HBV genotype, were evaluated. The inclusion criteria were as follows[17]: (1) being HBsAg positive for at least 6 mo; (2) HBV DNA level > 1000 copies/mL; and (3) patients with PNALT levels who had at least three ALT values taken in the year prior to baseline LB, with all values > 40 IU/L and remaining so until the start of treatment or the last follow-up if not treated. Patients were categorized as having PIALT levels if they had at least three ALT values taken, and at least one measurement of > 40 IU/L in the year prior to the baseline LB, or any time until the start of treatment or the last follow-up if not treated (intermittently elevated)[6-8,10,18,19]. The exclusion criteria were as follows: (1) hepatitis A, C, or D, or human immunodeficiency virus coinfection; (2) evidence of liver disease with another etiology; (3) use of hepatotoxic drugs or regular consumption of alcohol; (4) previous antiviral (HBV) therapy or any liver functional protection therapy to alleviate hepatic inflammation; and (5) less than three normal ALT values taken prior to the biopsy. The clinical data from these participants were given new numbers and anonymized before analysis. All data were provided separately as Supporting Information.

Biochemical and serologic tests

Biochemical tests and complete blood cell counts were performed using routine automated analyzers. The upper limit of normal value (ULN) of ALT level was 40 IU/L. HBsAg, HBeAg, and anti-HBe levels were assayed with commercially available enzyme-linked immunosorbent assay (ELISA) kits. HBV DNA level was measured using real-time polymerase chain reaction (PCR), with a lower detection limit of 1000 copies/mL (DaAn Gene Co, China).

Genotyping by multiplex PCR

Genotyping was performed using multiplex PCR with specific primers for each genotype (A-F) of HBV[20].

LB and histological assessment

Liver biopsies were obtained using a 16-G core aspiration needle, a biopsy length of at least 1.5 cm, and six portal tracts or more. Biopsies were fixed, paraffin-embedded, and stained with hematoxylin and eosin for morphological evaluation and Masson's trichrome stain for the assessment of fibrosis. The pathologist who reviewed all biopsy specimens was blinded to the biochemical and virological results of the patients, the amount of necrosis and inflammation, and the degree of fibrosis according to the Knodell scoring system[21]. Knodell necroinflammatory scores were classified into four categories as follows: Minimal (0-3), mild (4-6), moderate (7-9), and severe (10-14)[22]. Minimal and mild necroinflammatory scores were considered insignificant, while moderate and severe scores were considered significant. Knodell fibrosis scores were also classified into four categories as follows: Minimal (0), mild (1), moderate (2), and severe (3). Minimal and mild fibrosis scores were considered insignificant, while moderate and severe scores were considered significant.

LSM

LSM was assessed using transient elastography (FibroScan502, Echosens, Paris, France) with the 3.5-MHz standard probe by the same operator (experience, > 10000 measurements) who was blinded to the other parameters of the patients, as previously described. The examination was performed with the patient lying in the dorsal decubitus position, with the right arm in maximal abduction. The tip of the probe transducer was placed on the skin, between the ribs at the level of the right lobe of the liver. The results are expressed in kPa, and each LSM corresponded to the median of 10 validated measurements.

Statistical analysis

Results are presented as median (range) or mean ± SD as appropriate. Data on demographic and clinical features of the CHB patients were analyzed using Statistical Package for the Social Sciences (SPSS) version 21.0 (SPSS Inc, Chicago, IL, United States). Statistical analyses were performed using χ^2 and Fisher exact tests for categorical variables. The Student's *t*-test or one-way analysis of variance was used for group comparisons of parametric quantitative data. The equations for the two noninvasive markers analyzed were as follows: FIB-4 = (Age × AST)/(PLT × ALT1/2) and APRI = (AST/ULN) × 100/PLT. The receiver-operating characteristic (ROC) curves were used to calculate the cutoff values of FIB-4, APRI, and LSM. The ROC analysis was performed using MedCalc software version 10.4.7.0 (MedCalc, Mariakerke, Belgium). All *P*-values were two-sided.

RESULTS

Clinical and pathological characteristics of CHB patients with different levels of ALT

Table 1 shows that among 245 cases of CHB, 95 were in the PNALT group, 86 in the PIALT1 group (ALT within 1-2 × ULN), and 64 in the PIALT2 group (ALT > 2 × ULN). Body mass index (BMI), platelet count (PLT), prothrombin activity (PTA), ALT and AST (aspiration aminotransferase), serum albumin, E antigen status (positive or negative), HBsAg level, and HBV DNA expression level (⩾ 3, < 5 and ⩾ 5) were analyzed. We found that the differences in age, ALT, AST, PLT, and other factors were statistically significant ($P < 0.05$) between the PNALT and PIALT groups. No significant differences were found in E antigen status, HBsAg level, and HBV DNA. The pathological examination revealed moderate inflammatory necrosis ratios of

Table 1 Demographic and clinical characteristics of chronic hepatitis B patients *n* (%)

Characteristic	PNALT (*n* = 95)	PIALT1 (*n* = 86)	PIALT2 (*n* = 64)	Statistic	*P* value
Age (yr)	34.5 ± 11.2	34.2 ± 12.5	36.5 ± 13.5	5.423	0.021[1]
Sex					
Male	70 (73.7)	58 (67.4)	46 (71.9)	0.885	0.642[2]
Female	25 (26.3)	28 (32.6)	18 (28.1)		
BMI	23.4 ± 2.65	24.0 ± 3.6	24.25 ± 3.37	1.231	0.543[1]
PLT (× 10^9/L)	200.1 ± 60.3	196.8 ± 65.4	186.5 ± 74.5	6.364	0.018[1]
PTA (%)	99.6 ± 6.7	99.6 ± 8.7	102.3 ± 10.3	0.674	0.774[1]
ALB (g/L)	41.3 ± 3.4	41.6 ± 3.7	42.4 ± 4.1	1.536	0.543[1]
ALT (U/L)	21.4 ± 4.3	56.2 ± 19.4	113.6 ± 55.3	25.754	< 0.001[1]
AST (U/L)	22.6 ±6.8	55.4 ± 16.6	124.5 ± 57.6	31.644	< 0.001[1]
APRI	0.32 ± 0.14	0.61 ± 0.44	1.25 ± 0.62	284.92	< 0.001[1]
FIB-4	0.72 ± 0.36	1.12 ± 0.53	1.67 ± 0.84	56.37	< 0.001[1]
FibroScan (kPa)	5.33± 2.45	7.36 ± 3.14	10.22 ± 5.53	46.34	< 0.001[1]
HBsAg [lg (IU/L)]	4.41 ± 0.73	4.53 ± 0.88	4.38 ± 0.64	0.743	0.437
HBV DNA [lg (IU/mL)]	6.78 ± 2.13	6.53 ± 2.43	6.42 ± 2.54	0.864	0.254[1]
⩾ 3, < 5	15 (15.8)	11 (12.8)	10 (15.6)	0.384	0.825[2]
⩾ 5	80 (84.2)	75 (87.2)	54 (84.4)		
E antigen					
Positive	42 (44.2)	31 (36)	29 (45.3)	1.78	0.411[2]
Negative	53 (55.8)	55 (64)	35 (54.7)		
Necroinflammatory score	2.21 ± 2.14	3.47 ± 3.64	4.74 ± 3.65	23.43	0.001
Minimal	35 (32.4)	20 (23.3)	8 (12.5)	18.69	0.005
Mild	44 (38)	38 (44.2)	27 (42.4)		
Moderate	15 (15.8)	26 (30.2)	22 (34.4)		
Severe	1 (0.9)	2 (2.3)	7 (10.9)		
Fibrosis score	1.53 ± 0.46	2.38 ± 1.27	2.85 ± 1.75	15.237	0.005[1]
Minimal	32 (33.7)	18 (20.9)	13 (20.3)	13.275	0.035[2]
Mild	40 (42.1)	40 (51.2)	23 (35.9)		
Moderate	21 (22.1)	24 (27.9)	21 (32.8)		
Severe	2 (2.1)	5 (5.8)	7 (10.9)		

[1]One-way analysis of variance; [2]Pearson χ^2. APRI = [AST (U/L)/ULN × 100/PLT (10^9/L)]; FIB-4 = [age (yr) × AST (U/L)]/[PLT (10^9/L) × (ALT U/L)$^{1/2}$].

16.81% (16/95), 32.56% (28/86), and 45.31% (28/64), and moderate liver fibrosis of 24.2% (23/95), 33.72% (29/86), and 43.75% (28/64) in the PNALT, PIALT1, and PIALT2 groups, respectively. The degrees of inflammation and liver fibrosis in the PIALT groups were significantly higher than those in the PNALT group ($P < 0.05$).

Diagnostic value of APRI in the three groups of CHB

We considered hepatic fibrosis (insignificant/significant) as a categorical variable and APRI as a variable to test the AUC of APRI in the PNALT, PIALT1, and PIALT2 groups and in all the patients. The AUC of APRI was 0.518 in the PNALT group (95%CI: 0.414-0.622; specificity, 43.1%; sensitivity, 69.6%; cutoff value, 0.202; $P = 0.7852$), 0.659 in the PNALT1 group (95%CI: 0.548-0.757; specificity, 34.5%; sensitivity, 82.4%; cutoff value, 0.524; $P = 0.011$), 0.735 in the PNALT2 group (95%CI: 0.609-0.837; specificity, 83.7%; sensitivity, 85.7%; cutoff value, 1.26; $P < 0.001$), and 0.65 for all the patients (95%CI: 0.587-0.710; specificity, 88.5%; sensitivity, 54.4%; cutoff value, 1.15; $P < 0.001$). APRI showed a high diagnostic value for hepatic fibrosis in CHB patients with abnormal ALT levels in comparison with those with normal ALT levels (Figure 1).

Diagnostic value of FIB-4 in the three groups of CHB

We considered hepatic fibrosis (insignificant/significant) as a categorical variable and FIB-4 as a variable to test the AUC of FIB-4 in the PNALT, PIALT1, and PIALT2 groups and in all the patients. The AUC of FIB-4 was 0.597 in the PNALT group (95%CI: 0.492-0.697; specificity, 68.1%; sensitivity, 52.2%; cutoff value, 0.698; $P = 0.152$), 0.642 in the PNALT1 group (95%CI: 0.531-0.742; specificity, 67.9%; sensitivity, 56.9%; cutoff value, 1.174; $P = 0.021$), 0.667 in the PNALT2 group (95%CI: 0.538-0.780; specificity, 52.8%; sensitivity, 78.7%; cutoff value, 1.46; $P = 0.015$), and 0.659 for all the patients (95%CI: 0.596-0.718; specificity, 66.8%; sensitivity, 74.2%; cutoff value, 0.96; $P < 0.001$). FIB-4 showed a high diagnostic value for hepatic fibrosis in CHB patients with abnormal ALT levels in comparison with those with normal ALT levels (Figure 2).

Diagnostic value of LSM in the three groups of CHB

We considered hepatic fibrosis (insignificant/significant) as a categorical variable and LSM as a variable to test the AUC of LSM in the PNALT, PIALT1, and PIALT2 groups and in all the patients. The AUC of LSM was 0.769 in the PNALT group (95%CI: 0.009-0.879; 95%CI: 0.709-0.850; specificity, 79.2%; sensitivity,

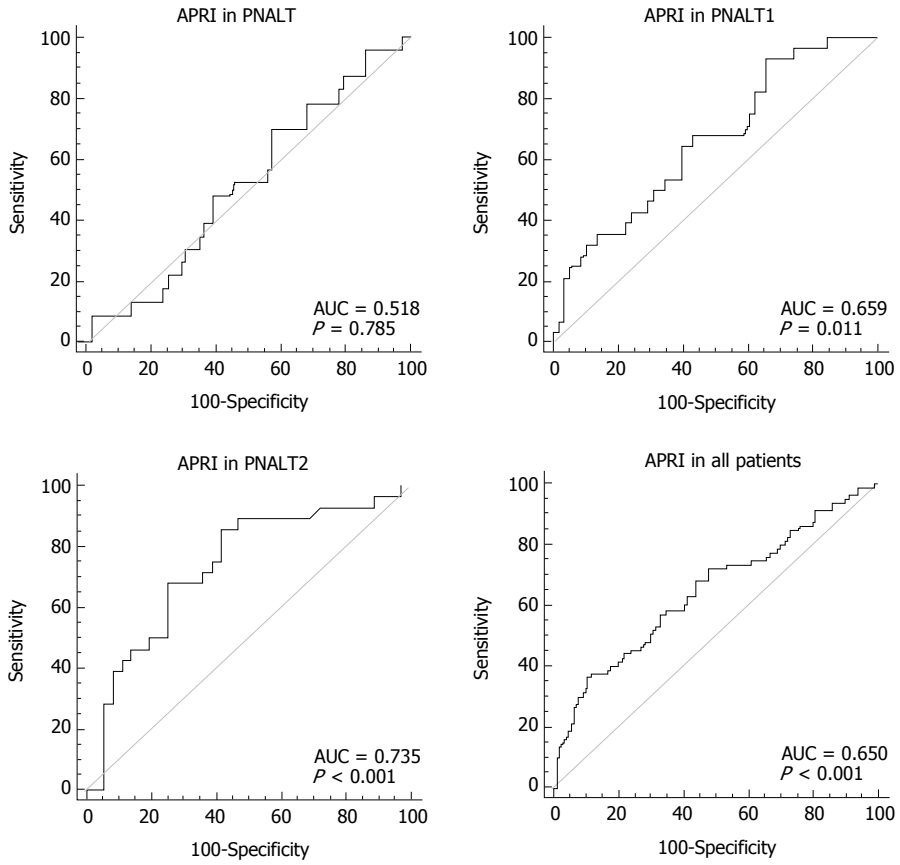

Figure 1 Diagnostic value of aspartate aminotransferase-to-platelet ratio index in different groups of chronic hepatitis B patients. PNALT: Persistently normal alanine transaminase; APRI: Aspartate aminotransferase-to-platelet ratio index; AUC: Areas under the curve.

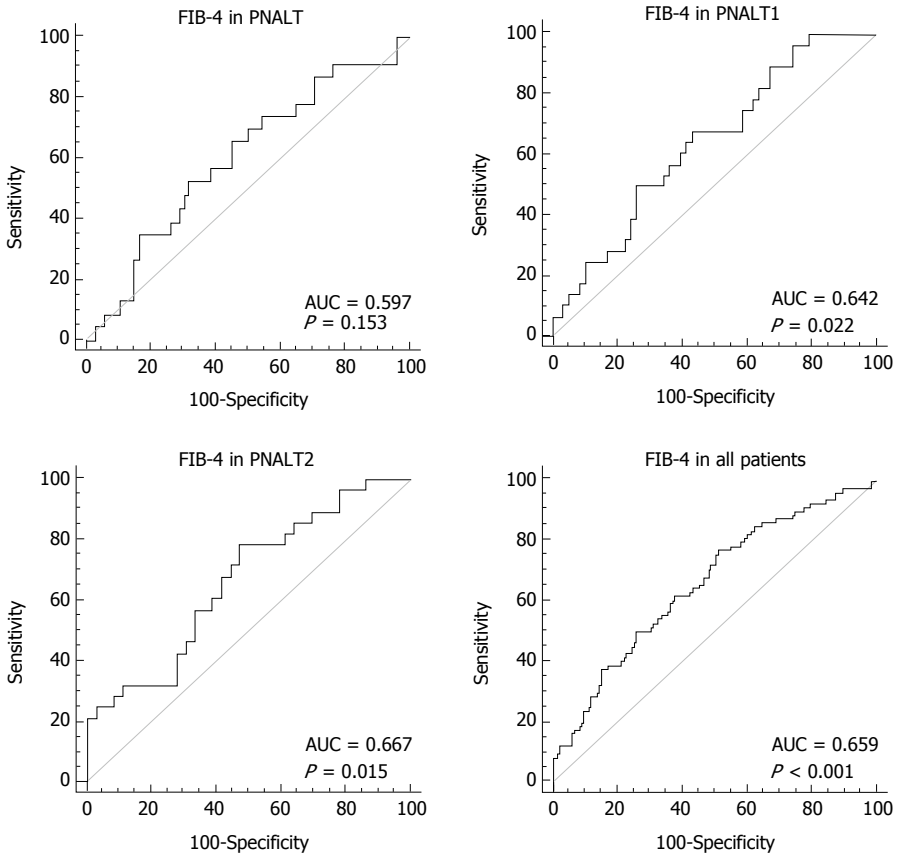

Figure 2 Diagnostic value of FIB-4 in different groups of chronic hepatitis B patients. PNALT: Persistently normal alanine transaminase; AUC: Areas under the curve.

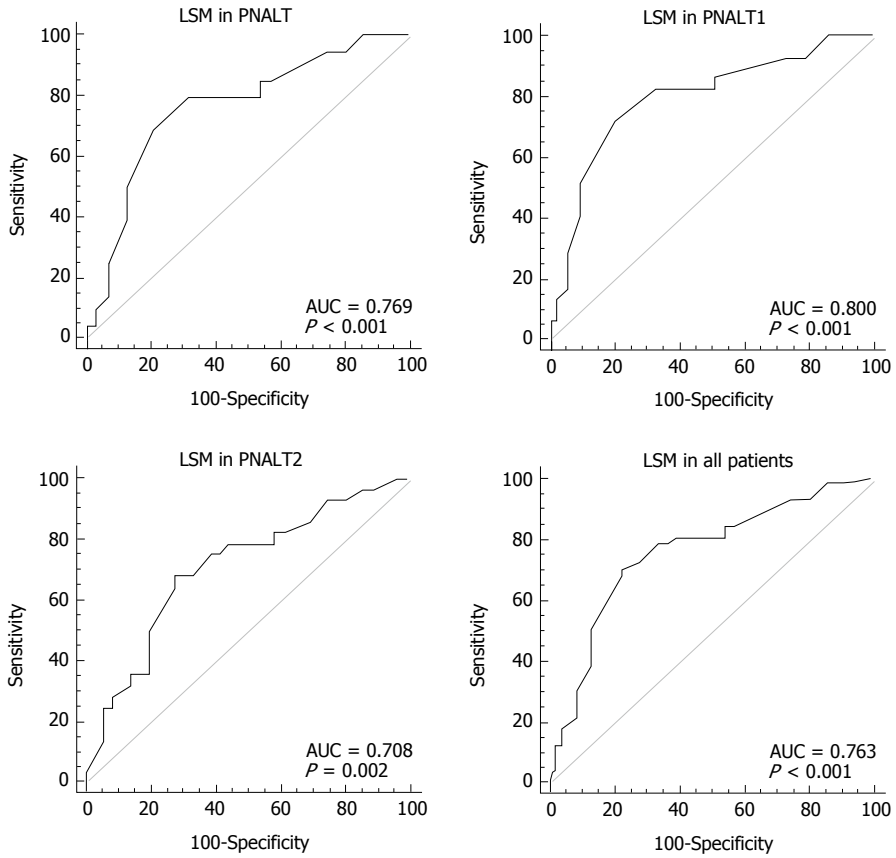

Figure 3 Diagnostic value of liver stiffness measurement in different groups of chronic hepatitis B patients. PNALT: Persistently normal alanine transaminase; LSM: Liver stiffness measurement; AUC: Areas under the curve.

Table 2 Pairwise comparisons of receiver-operating characteristic curves

	PNALT	PIALT1	PIALT2	All patients
APRI *vs* FIB-4				
Difference between areas	0.0628	0.0169	0.068	0.00904
Standard error	0.0557	0.0699	0.0738	0.0245
95%CI	-0.046 to 0.172	-0.120 to 0.154	-0.077 to 0.213	-0.039 to 0.057
z statistic	1.129	0.242	0.921	0.369
P value	0.2588	0.8087	0.3569	0.712
APRI *vs* LSM				
Difference between areas	0.256	0.124	0.0263	0.111
Standard error	0.104	0.0896	0.0882	0.0518
95%CI	0.0525-0.459	-0.0511 to 0.30	-0.147 to 0.19	0.00909-0.212
z statistic	2.465	1.389	0.298	2.135
P value	0.0137	0.1649	0.7655	0.0327
FIB 4 *vs* LSM				
Difference between areas	0.193	0.141	0.0417	0.102
Standard error	0.106	0.0938	0.0957	0.0531
95%CI	-0.014 to 0.400	-0.0425 to 0.325	-0.146 to 0.229	-0.00246 to 0.206
z statistic	1.829	1.507	0.435	1.914
P value	0.0374	0.1318	0.663	0.0557

70.1%; cutoff value, 7.3; $P < 0.001$), 0.800 in the PNALT1 group (95%CI: 0.700-0.879; specificity, 72.4%; sensitivity, 82.7%; cutoff value, 7.5; $P < 0.001$), 0.708 in the PNALT2 group (95%CI: 0.581-0.815; specificity, 72.7%; sensitivity, 67.9%; cutoff value, 8.5; $P = 0.017$), and 0.763 for all the patients (95%CI: 0.596-0.718; specificity, 78.2%; sensitivity, 70.1%; cutoff value, 7.5; $P < 0.001$). LSM showed a high diagnostic value for the three groups of CHB, although the sensitivity and specificity in the PNALT2 showed a downward trend (Figure 3).

Comparison of the diagnostic value of the three noninvasive liver fibrosis markers in CHB

As shown in Table 2 and Figure 4, there was no significant difference in the AUCs between APRI and FIB-4 in the

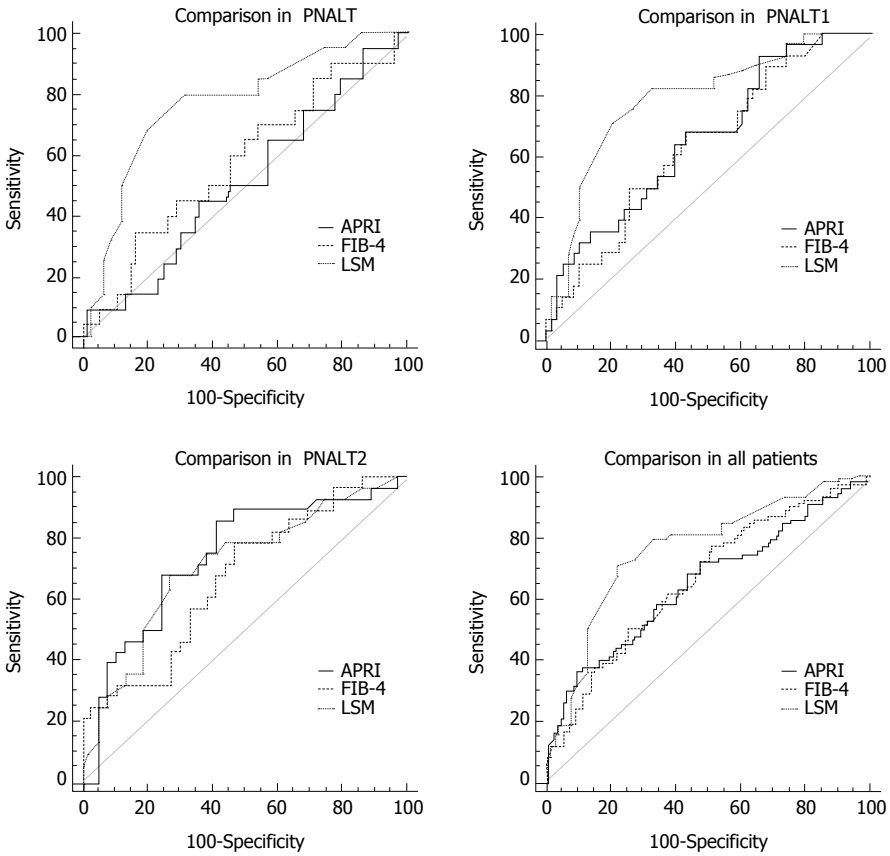

Figure 4 Comparison of the diagnostic value of the three noninvasive liver fibrosis markers in different groups of chronic hepatitis B patients. APRI: Aspartate aminotransferase-to-platelet ratio index; FIB-4: Fibrosis-4; LSM: Liver stiffness measurement.

PNALT group; however, significant differences were found between APRI and LSM, and between FIB-4 and LSM in the PNALT group ($P < 0.05$ for both). In the PIALT1 and PIALT2 groups, no significant difference ($P > 0.05$) was found in AUCs for all comparisons ($P > 0.05$ for all). In the overall patients, a significant difference in the AUCs was found only between LSM and APRI ($P < 0.05$).

DISCUSSION

Hepatic fibrosis is a compensatory repair process associated with inflammation and necrosis of the liver. Therefore, 25% to 40% of liver fibrosis cases will eventually progress to cirrhosis and even liver cancer. Early liver fibrosis can be reversed after correct treatment; thus, early diagnosis of liver fibrosis will be beneficial to the treatment of CHB.

LB is still the gold standard for assessment of liver fibrosis in CHB, although it is invasive, expensive, and associated with risk of complications and poor patient compliance, and of subjective differences in pathologists. The accuracy of the pathological diagnosis of liver fibrosis can only be approximately 90% and even reported to be < 80%[23]. Therefore, noninvasive diagnostic markers for liver fibrosis have been developed, such as serum markers and models, imaging, transient liver hardness, and other noninvasive techniques. Although these noninvasive diagnostic methods have their own advantages and disadvantages, they have not completely replaced LB. However, new techniques and methods have become greatly improved. Among the noninvasive tests developed are FIB-4, APRI, and LSM; previous studies have shown these noninvasive markers and techniques to be strong predictors of liver fibrosis.

A multicenter, retrospective study reported that the AUCs of APRI were 0.72, 0.812, and 0.707 in CHB patients with F2, F3, and F4 fibrosis, respectively[24]. The AUCs of APRI were 0.65, 0.659, and 0.735 in our PNALT, PIALT1, and PIALT2 CHB patients, respectively. These results showed that the diagnostic value of APRI in the CHB patients with elevated ALT levels was better than that in the CHB patients with normal ALT. APRI is the ratio of AST to PLT, and elevated AST levels has a higher APRI value and thus is more likely to distinguish patient groups with different AST levels.

In a study of 388 cases of cirrhosis of varied severity assessed using APRI and FIB-4, the AUCs were 0.68 (95%CI: 0.63-0.74) and 0.73 (95%CI: 0.68-0.78)[25], respectively. In our study, the AUC of FIB-4 was 0.597 for PNALT, 0.642 for PNALT1, and 0.667 for PNALT2. The diagnostic value of FIB-4 in the CHB patients with elevated ALT levels was better than that in the CHB patients with normal ALT levels and APRI.

We detected LSM by FibroScan in the CHB patients, with an AUC of 0.769 for PNALT, 0.800 for PIALT1, 0.708 for PIALT2, and 0.763 for all the patients. LSM showed

a good diagnostic value for the three groups of CHB patients. Furthermore, the diagnostic value of LSM in the high ALT group was not as good as that in the PNALT group, and the sensitivity and specificity in the PNALT2 group even had a downward trend. In a report on FibroScan in China[26], the AUCs were 0.916 and 0.971 for the diagnosis of ⩾ F2 liver fibrosis (F0-1 *vs* F2-4) and cirrhosis (F = 4, F0-3 *vs* F4), and the sensitivity and accuracy in the ALT level ⩾ 2 × ULN group were significantly lower than those in the other lower-level ALT groups. The reason is that LSM is susceptible to liver inflammation[27,28] and cholestasis[29,30].

We compared the three noninvasive methods for the diagnosis of hepatic fibrosis. The results showed that the AUC differences between LSM and APRI, and between LSM and FIB-4 were statistically significant in the PNALT group ($P < 0.05$ for both), but not in the PIALT1 and PIALT2 groups ($P > 0.05$ for all). For all the patients, we found that the AUC difference was statistically significant only between LSM and APRI ($P < 0.05$).

In a previous report from South Korea, the diagnostic value of LSM for hepatic fibrosis was compared with that of APRI. The results suggested that LSM is superior to APRI in 916 patients with CHB (AUC: 0.774 *vs* 0.72 for ⩾ F2, 0.849 *vs* 0.812 for ⩾ F3, and 0.902 *vs* 0.707 for F4; all $P < 0.05$)[24]. Another report revealed that LSM was better than APRI and FIB-4 when the LSM cutoff value was > 13.6 kPa for the diagnosis of portal hypertension in cirrhosis patients[31].

In conclusion, we evaluated three common noninvasive hepatic fibrosis techniques in CHB patients with different ALT levels. The results showed that APRI and FIB-4 are not the ideal noninvasive hepatic fibrosis markers in the PNALT patients and that APRI and FIB-4 established according to the common blood biochemical indicators are more suitable for active CHB. LSM, which determines liver hardness for assessment of the degree of liver fibrosis, is superior to APRI and FIB-4 in patients with PNALT because of the influence of liver inflammation and necrosis.

COMMENTS

Background

Although serum levels of alanine transaminase (ALT), an enzyme released from hepatocytes during liver injury, should reflect the degree of liver damage, not all patients with chronic HBV infection have persistently elevated ALT levels. Furthermore, some large cohort studies have shown that patients with chronic hepatitis B (CHB) who have normal serum ALT levels are also at risk for the development of cirrhosis and hepatocellular carcinoma. Liver biopsy is the current gold standard for assessing hepatic inflammation and fibrosis in patients with chronic hepatitis B virus (HBV) who have persistently normal alanine transaminase (PNALT). The invasiveness of liver puncture, the limitation of the specimen, and the poor patient compliance have restricted the application of liver biopsy.

Research frontiers

The limitation of liver biopsy has led to the development of noninvasive methods such as FIB-4 and aspartate aminotransferase-to-platelet ratio index (APRI) for evaluating fibrosis in patients with chronic HBV infection. Liver stiffness measurement (LSM) using transient elastography (FibroScan) has been widely used in the diagnosis of chronic liver fibrosis. However, the diagnostic value of FIB-4, APRI, and LSM in patients with HBV infection with PNALT is not clear.

Innovations and breakthroughs

The authors evaluated three common noninvasive hepatic fibrosis markers in CHB patients with different ALT levels. The results showed that APRI and FIB-4 are not the ideal noninvasive hepatic fibrosis markers for PNALT patients. LSM is superior to APRI and FIB-4 in PNALT patients because of the influence of liver inflammation and necrosis.

Applications

Noninvasive markers such as FIB-4, APRI and liver stiffness measurement for evaluating fibrosis in patients with chronic HBV infection.

Terminology

PNALT means patients with hepatitis B virus infection who have persistently normal alanine transaminase.

Peer-review

The manuscript is well written and the numerical simulations are well performed.

REFERENCES

1 **Yan H**, Zhong G, Xu G, He W, Jing Z, Gao Z, Huang Y, Qi Y, Peng B, Wang H, Fu L, Song M, Chen P, Gao W, Ren B, Sun Y, Cai T, Feng X, Sui J, Li W. Sodium taurocholate cotransporting polypeptide is a functional receptor for human hepatitis B and D virus. *Elife* 2012; **1**: e00049 [PMID: 23150796 DOI: 10.7554/eLife.00049]

2 **McMahon BJ**. The natural history of chronic hepatitis B virus infection. *Semin Liver Dis* 2004; **24** Suppl 1: 17-21 [PMID: 15192797 DOI: 10.1055/s-2004-828674]

3 **Kim WR**, Flamm SL, Di Bisceglie AM, Bodenheimer HC; Public Policy Committee of the American Association for the Study of Liver Disease. Serum activity of alanine aminotransferase (ALT) as an indicator of health and disease. *Hepatology* 2008; **47**: 1363-1370 [PMID: 18366115 DOI: 10.1002/hep.22109]

4 **Nunnari G**, Pinzone MR, Cacopardo B. Lack of clinical and histological progression of chronic hepatitis C in individuals with true persistently normal ALT: the result of a 17-year follow-up. *J Viral Hepat* 2013; **20**: e131-e137 [PMID: 23490382 DOI: 10.1111/jvh.12029]

5 **Lai M**, Hyatt BJ, Nasser I, Curry M, Afdhal NH. The clinical significance of persistently normal ALT in chronic hepatitis B infection. *J Hepatol* 2007; **47**: 760-767 [PMID: 17928090 DOI: 10.1016/j.jhep.2007.07.022]

6 **Wang H**, Xue L, Yan R, Zhou Y, Wang MS, Cheng MJ, Hai-Jun Huang. Comparison of histologic characteristics of Chinese chronic hepatitis B patients with persistently normal or mildly elevated ALT. *PLoS One* 2013; **8**: e80585 [PMID: 24260428 DOI: 10.1371/journal.pone.0080585]

7 **Papatheodoridis GV**, Manolakopoulos S, Liaw YF, Lok A. Follow-up and indications for liver biopsy in HBeAg-negative chronic hepatitis B virus infection with persistently normal ALT: a systematic review. *J Hepatol* 2012; **57**: 196-202 [PMID: 22450396 DOI: 10.1016/j.jhep.2011.11.030]

8 **Kumar M**, Sarin SK, Hissar S, Pande C, Sakhuja P, Sharma BC, Chauhan R, Bose S. Virologic and histologic features of chronic hepatitis B virus-infected asymptomatic patients with persistently normal ALT. *Gastroenterology* 2008; **134**: 1376-1384 [PMID: 18471514 DOI: 10.1053/j.gastro.2008.02.075]

9 **Lin CL**, Liao LY, Liu CJ, Yu MW, Chen PJ, Lai MY, Chen DS, Kao JH. Hepatitis B viral factors in HBeAg-negative carriers with persistently normal serum alanine aminotransferase levels. *Hepatology* 2007; **45**: 1193-1198 [PMID: 17464993 DOI: 10.1002/hep.21585]

10 **Dai CY**, Chuang WL, Huang JF, Yu ML. Hepatitis B e antigen-negative patients with persistently normal alanine aminotransferase levels and hepatitis B virus DNA > 2000 IU/mL. *Hepatology* 2009;

49: 704-705; author reply 705-706 [PMID: 19177587 DOI: 10.1002/hep.22723]
11 **Yuen MF**, Yuan HJ, Wong DK, Yuen JC, Wong WM, Chan AO, Wong BC, Lai KC, Lai CL. Prognostic determinants for chronic hepatitis B in Asians: therapeutic implications. *Gut* 2005; **54**: 1610-1614 [PMID: 15871997 DOI: 10.1136/gut.2005.065136]
12 **Chen CJ**, Yang HI, Su J, Jen CL, You SL, Lu SN, Huang GT, Iloeje UH; REVEAL-HBV Study Group. Risk of hepatocellular carcinoma across a biological gradient of serum hepatitis B virus DNA level. *JAMA* 2006; **295**: 65-73 [PMID: 16391218 DOI: 10.1001/jama.295.1.65]
13 **Sterling RK**, Lissen E, Clumeck N, Sola R, Correa MC, Montaner J, S Sulkowski M, Torriani FJ, Dieterich DT, Thomas DL, Messinger D, Nelson M; APRICOT Clinical Investigators. Development of a simple noninvasive index to predict significant fibrosis in patients with HIV/HCV coinfection. *Hepatology* 2006; **43**: 1317-1325 [PMID: 16729309 DOI: 10.1002/hep.21178]
14 **Wai CT**, Greenson JK, Fontana RJ, Kalbfleisch JD, Marrero JA, Conjeevaram HS, Lok AS. A simple noninvasive index can predict both significant fibrosis and cirrhosis in patients with chronic hepatitis C. *Hepatology* 2003; **38**: 518-526 [PMID: 12883497 DOI: 10.1053/jhep.2003.50346]
15 **Huang R**, Jiang N, Yang R, Geng X, Lin J, Xu G, Liu D, Chen J, Zhou G, Wang S, Luo T, Wu J, Liu X, Xu K, Yang X. Fibroscan improves the diagnosis sensitivity of liver fibrosis in patients with chronic hepatitis B. *Exp Ther Med* 2016; **11**: 1673-1677 [PMID: 27168788 DOI: 10.3892/etm.2016.3135]
16 **Mikolasevic I**, Orlic L, Franjic N, Hauser G, Stimac D, Milic S. Transient elastography (FibroScan(®)) with controlled attenuation parameter in the assessment of liver steatosis and fibrosis in patients with nonalcoholic fatty liver disease - Where do we stand? *World J Gastroenterol* 2016; **22**: 7236-7251 [PMID: 27621571 DOI: 10.3748/wjg.v22.i32.7236]
17 **Liao B**, Wang Z, Lin S, Xu Y, Yi J, Xu M, Huang Z, Zhou Y, Zhang F, Hou J. Significant fibrosis is not rare in Chinese chronic hepatitis B patients with persistent normal ALT. *PLoS One* 2013; **8**: e78672 [PMID: 24205292 DOI: 10.1371/journal.pone.0078672]
18 **Wang H**, Xue L, Yan R, Zhou Y, Wang MS, Cheng MJ, Huang HJ. Comparison of FIB-4 and APRI in Chinese HBV-infected patients with persistently normal ALT and mildly elevated ALT. *J Viral Hepat* 2013; **20**: e3-e10 [PMID: 23490387 DOI: 10.1111/jvh.12010]
19 **Arora S**, O'Brien C, Zeuzem S, Shiffman ML, Diago M, Tran A, Pockros PJ, Reindollar RW, Gane E, Patel K, Wintfeld N, Green J. Treatment of chronic hepatitis C patients with persistently normal alanine aminotransferase levels with the combination of peginterferon alpha-2a (40 kDa) plus ribavirin: impact on health-related quality of life. *J Gastroenterol Hepatol* 2006; **21**: 406-412 [PMID: 16509866 DOI: 10.1111/j.1440-1746.2005.04059.x]
20 **Kirschberg O**, Schüttler C, Repp R, Schaefer S. A multiplex-PCR to identify hepatitis B virus--enotypes A-F. *J Clin Virol* 2004; **29**: 39-43 [PMID: 14675868]
21 **Knodell RG**, Ishak KG, Black WC, Chen TS, Craig R, Kaplowitz N, Kiernan TW, Wollman J. Formulation and application of a numerical scoring system for assessing histological activity in asymptomatic chronic active hepatitis. *Hepatology* 1981; **1**: 431-435 [PMID: 7308988]
22 **Marcellin P**, Gane E, Buti M, Afdhal N, Sievert W, Jacobson IM, Washington MK, Germanidis G, Flaherty JF, Aguilar Schall R, Bornstein JD, Kitrinos KM, Subramanian GM, McHutchison JG, Heathcote EJ. Regression of cirrhosis during treatment with tenofovir disoproxil fumarate for chronic hepatitis B: a 5-year open-label follow-up study. *Lancet* 2013; **381**: 468-475 [PMID: 23234725 DOI: 10.1016/S0140-6736(12)61425-1]
23 **Jin SY**. [Role of liver biopsy in the assessment of hepatic fibrosis--its utility and limitations]. *Korean J Hepatol* 2007; **13**: 138-145 [PMID: 17585187]
24 **Seo YS**, Kim MY, Kim SU, Hyun BS, Jang JY, Lee JW, Lee JI, Suh SJ, Park SY, Park H, Jung EU, Kim BS, Kim IH, Lee TH, Um SH, Han KH, Kim SG, Paik SK, Choi JY, Jeong SW, Jin YJ, Lee KS, Yim HJ, Tak WY, Hwang SG, Lee YJ, Lee CH, Kim DG, Kang YW, Kim YS; Korean Transient Elastography Study Group. Accuracy of transient elastography in assessing liver fibrosis in chronic viral hepatitis: A multicentre, retrospective study. *Liver Int* 2015; **35**: 2246-2255 [PMID: 25682719 DOI: 10.1111/liv.12808]
25 **Martin J**, Khatri G, Gopal P, Singal AG. Accuracy of ultrasound and noninvasive markers of fibrosis to identify patients with cirrhosis. *Dig Dis Sci* 2015; **60**: 1841-1847 [PMID: 25586089 DOI: 10.1007/s10620-015-3531-1]
26 **Chen XB**, Zhu X, Chen LY, Chen EQ, Tang H. [Accuracy of FibroScan for the diagnosis of liver fibrosis influenced by serum alanine aminotransferase levels in patients with chronic hepatitis B]. *Zhonghua Gan Zang Bing Za Zhi* 2011; **19**: 286-290 [PMID: 21586228 DOI: 10.3760/cma.j.issn.1007-3418.2011.04.013]
27 **Liang XE**, Chen YP, Zhang Q, Dai L, Zhu YF, Hou JL. Dynamic evaluation of liver stiffness measurement to improve diagnostic accuracy of liver cirrhosis in patients with chronic hepatitis B acute exacerbation. *J Viral Hepat* 2011; **18**: 884-891 [PMID: 21062388 DOI: 10.1111/j.1365-2893.2010.01389.x]
28 **Wong GL**, Wong VW, Choi PC, Chan AW, Chim AM, Yiu KK, Chan FK, Sung JJ, Chan HL. Increased liver stiffness measurement by transient elastography in severe acute exacerbation of chronic hepatitis B. *J Gastroenterol Hepatol* 2009; **24**: 1002-1007 [PMID: 19457152 DOI: 10.1111/j.1440-1746.2009.05779.x]
29 **Harata M**, Hashimoto S, Kawabe N, Nitta Y, Murao M, Nakano T, Arima Y, Shimazaki H, Ishikawa T, Okumura A, Ichino N, Osakabe K, Nishikawa T, Yoshioka K. Liver stiffness in extrahepatic cholestasis correlates positively with bilirubin and negatively with alanine aminotransferase. *Hepatol Res* 2011; **41**: 423-429 [PMID: 21435129 DOI: 10.1111/j.1872-034X.2011.00797.x]
30 **Millonig G**, Reimann FM, Friedrich S, Fonouni H, Mehrabi A, Büchler MW, Seitz HK, Mueller S. Extrahepatic cholestasis increases liver stiffness (FibroScan) irrespective of fibrosis. *Hepatology* 2008; **48**: 1718-1723 [PMID: 18836992 DOI: 10.1002/hep.22577]
31 **Zhang W**, Wang L, Wang L, Li G, Huang A, Yin P, Yang Z, Ling C, Wang L. Liver stiffness measurement, better than APRI, Fibroindex, Fib-4, and NBI gastroscopy, predicts portal hypertension in patients with cirrhosis. *Cell Biochem Biophys* 2015; **71**: 865-873 [PMID: 25417057 DOI: 10.1007/s12013-014-0275-z]

P- Reviewer: Nakao T **S- Editor**: Qi Y **L- Editor**: Wang TQ
E- Editor: Xu XR

World Journal of Gastroenterology

Submit a Manuscript: http://www.f6publishing.com

World J Gastroenterol 2017 August 21; 23(31): 5755-5763

DOI: 10.3748/wjg.v23.i31.5755

ISSN 1007-9327 (print) ISSN 2219-2840 (online)

ORIGINAL ARTICLE

Retrospective Study

Accuracy of endoscopic ultrasound-guided tissue acquisition in the evaluation of lymph nodes enlargement in the absence of on-site pathologist

Yung Ka Chin, Julio Iglesias-Garcia, Daniel de la Iglesia, Jose Lariño-Noia, Ihab Abdulkader-Nallib, Hector Lázare, Susana Rebolledo Olmedo, J Enrique Dominguez-Muñoz

Yung Ka Chin, Julio Iglesias-Garcia, Daniel de la Iglesia, Jose Lariño-Noia, Susana Rebolledo Olmedo, J Enrique Dominguez-Muñoz, Department of Gastroenterology and Hepatology, University Hospital of Santiago de Compostela, 15706 Santiago de Compostela, Spain

Julio Iglesias-Garcia, Daniel de la Iglesia, Jose Lariño-Noia, Susana Rebolledo Olmedo, J Enrique Dominguez-Muñoz, Health Research Institute of Santiago de Compostela (IDIS), University Hospital of Santiago de Compostela, 15706 Santiago de Compostela, Spain

Ihab Abdulkader-Nallib, Hector Lázare, Department of Pathology, University Hospital of Santiago de Compostela, 15706 Santiago de Compostela, Spain

Author contributions: Chin YK designed and performed the research and wrote the manuscript; Iglesias-Garcia J designed the research and supervised the report; de la Iglesia D, Lariño-Noia J and Abdulkader-Nallib I contributed to the analysis and supervised the report; Lázare H and Rebolledo Olmedo S assisted with data acquisition; and Dominguez-Muñoz JE supervised the report and overall study supervision.

Institutional review board statement: This study was reviewed and approved by the Institutional Review Board of University Hospital of Santiago de Compostela, Santiago de Compostela, Spain.

Informed consent statement: The authors of this paper guarantee that all study participants or their legal guardian provided informed written consent regarding personal and medical data collection prior to study enrollment.

Conflict-of-interest statement: We have no financial relationships to disclose.

Data sharing statement: There are no additional data available.

Manuscript source: Unsolicited manuscript

Correspondence to: Julio Iglesias-Garcia, MD, PhD, Department of Gastroenterology and Hepatology, University Hospital of Santiago de Compostela, 15706 Santiago de Compostela, Spain. julio.iglesias.garcia@sergas.es
Telephone: +34-98-1951364
Fax: +34-98-1955100

Received: April 9, 2017
Peer-review started: April 10, 2017
First decision: June 1, 2017
Revised: June 15, 2017
Accepted: June 18, 2017
Article in press: June 19, 2017
Published online: August 21, 2017

Abstract

AIM

To evaluate factors that influence the diagnostic accuracy of endoscopic ultrasound (EUS)-guided tissue acquisition for lymph node enlargement in the absence of an on-site pathologist.

METHODS

A retrospective analysis of patients who underwent EUS-guided tissue acquisition for the pathological diagnosis of lymph node enlargement between April

2012 and June 2015 is reported. Tissue acquisition was performed with both cytology and biopsy needles of different calibers. The variables evaluated were lymph node location and size, number of passes and type of needle used. Final diagnosis was based on surgical histopathology or, in non-operated cases, on EUS-guided tissue acquisition and imaging assessment with a minimum clinical follow-up of 6 mo.

RESULTS

During the study period, 168 lymph nodes with a median size of 20.3 mm (range 12.5-27) were sampled from 152 patients. Ninety lymph nodes (53.6%) were located at mediastinum, and 105 (62.5%) were acquired with biopsy needles. The final diagnosis was benign/reactive origin in 87 cases (51.8%), malignant in 65 cases (38.7%), and lymphoma in 16 cases (9.5%). The sensitivity, specificity, positive predictive value and negative predictive value for the detection of malignancy were 74.1%, 100%, 100% and 80.6%, respectively. The overall accuracy was 87.5% (95%CI: 81.7-91.7). No variables were independently associated with a correct final diagnosis according to the multivariate analysis.

CONCLUSION

EUS-guided tissue acquisition is a highly accurate technique for assessing lymph node enlargement. None of the variables evaluated were associated with diagnostic accuracy.

Key words: Lymph node; Endoscopic ultrasound; Fine-needle aspiration; Fine-needle biopsy; Accuracy

Core tip: This study shows that the accuracy of endoscopic ultrasound-guided tissue acquisition in enlarged lymph nodes is not affected by the type of needle used, the number of needle passes, or the location or characteristics of the enlarged lymph nodes. Histological specimens are essential for establishing the diagnosis of lymphoproliferative disease. Employing complementary imaging techniques, such as contrast enhancement and elastography, might help improve the diagnostic yield.

Chin YK, Iglesias-Garcia J, de la Iglesia D, Lariño-Noia J, Abdulkader-Nallib I, Lázare H, Rebolledo Olmedo S, Dominguez-Muñoz JE. Accuracy of endoscopic ultrasound-guided tissue acquisition in the evaluation of lymph node enlargement in the absence of an on-site pathologist. *World J Gastroenterol* 2017; 23(31): 5755-5763 Available from: URL: http://www.wjgnet.com/1007-9327/full/v23/i31/5755.htm DOI: http://dx.doi.org/10.3748/wjg.v23.i31.5755

INTRODUCTION

The advent of advanced diagnostic imaging modalities, such as computer-aided tomography (CT) scanning and magnetic resonance imaging (MRI), has led to increased detection rates of enlarged mediastinal and intra-abdominal lymph nodes. When no primary malignant lesion is evident, the differential diagnosis of these enlarged lymph nodes can be difficult. Open thoracic surgery, laparotomy or other surgical procedures such as mediastinoscopy or laparoscopy are often required in this setting. However, these procedures are invasive and not cost-effective[1].

Endoscopic ultrasound (EUS)-guided tissue acquisition with either fine-needle aspiration (FNA) or fine-needle biopsy (FNB) is an essential tool used to facilitate the diagnosis of periluminal lymphadenopathy adjacent to the gastrointestinal tract, particularly around the esophagus, stomach, and duodenum[2,3]. This is pivotal in patient care because malignant nodal disease will alter prognosis and overall disease management, requiring neoadjuvant therapy or a shift from futile curative treatment to palliative treatment[4]. In contrast, the diagnosis of non-malignant conditions, such as tuberculosis (TB) or sarcoidosis, not only guides the appropriate treatment but also reduces patient anxiety[5-8].

In the context of EUS-guided FNA and/or FNB, the presence of an on-site pathological evaluation during the procedure is very useful. Several studies have demonstrated the positive impact of such evaluations on the diagnostic yield of EUS-guided tissue acquisition[9-12], although not all centers are able to perform on-site evaluations due to costs and/or logistic issues. However, other factors have been identified to influence the accuracy of EUS-guided tissue acquisition, such the characteristics of the target lesion, the number of needle passes and the needle size[13]. In this retrospective analysis, we aimed to evaluate the factors that might influence the diagnostic accuracy of EUS-guided tissue acquisition of lymph node enlargement in the absence of an on-site cytopathological evaluation.

MATERIALS AND METHODS

Design

We conducted a retrospective analysis of a prospectively maintained endoscopy database with a specific EUS registry of a single tertiary referral hospital. The study was approved by the local ethics committee and was conducted in accordance with the Declaration of Helsinki and its amendments as well as Good Clinical Practice guidelines.

Patient characteristics

Consecutive patients who were referred for EUS-guided tissue acquisition of enlarged lymph nodes between April 2012 and June 2015 and who required a cytopathological evaluation were included in the analysis. We excluded patients whose information regarding the procedure was not complete or only partially available and those who were lost to follow-

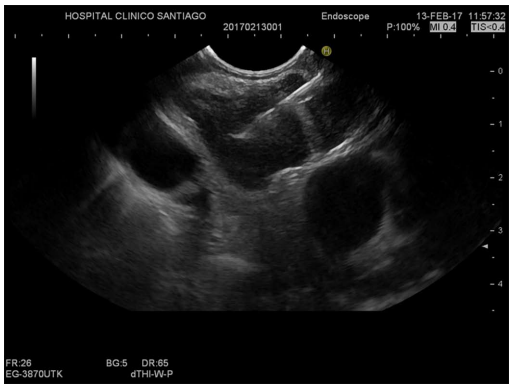

Figure 1 Endoscopic ultrasound-guided fine-needle biopsy of an intra-abdominal lymph node. The needle and needle tip are clearly visible inside the targeted lymph node.

Figure 2 Example of a core sample obtained with endoscopic ultrasound-guided tissue acquisition using a biopsy needle.

up and for whom sufficient information to establish the final diagnosis of the lymph nodes was unavailable.

Technical procedures

All EUS-guided tissue acquisition procedures were performed by two experienced operators (Iglesias-Garcia J and Lariño-Noia J), each of whom had performed more than 1000 EUS-guided tissue acquisitions. All patients received conscious sedation. The procedures were performed using Pentax curvilinear array echoendoscopes (EG-3870UTK and EG-3270UK) and a HITACHI ultrasound device. The needles used included 19-G, 22-G and 25-G cytology and histology needles (Echotip Ultra and Echotip Procore™; Cook-Medical, Winston-Salem, NC, United States, and Expect™ Slimline, Boston Scientific) and 20-G Procore™ histology needles (Cook-Medical, Winston-Salem). The selection of the needle was at the endosonographer's discretion. All procedures were performed by first localizing the lymph node using an electronic curvilinear array echoendoscope and confirming the absence of intervening vessels via color flow and/or fine flow Doppler. A stylet was routinely used when puncturing the lymph node. Prior to puncturing the lymph node, the stylet was withdrawn 1 cm when using cytology needles; no adjustment of the stylet was required when using Procore™ needles. Once the needle was within the lesion (Figure 1), the stylet was advanced to the tip of the needle to expel any mucosal tissue from the gut wall and then removed. A 10-mL syringe was attached to the hub of the needle, and negative suction was then applied. Five to 10 to-and-fro movements were made within the lymph node in a fanning approach. Finally, the needle was withdrawn into the sheath, and the entire system was then withdrawn from the biopsy channel. The specimen was expelled into a tube containing a cytological solution (ThinPrep®; Cytyc Co., Marlborough, MA, United States) (Figure 2). Further needle passes were performed at the discretion of the endosonographer after gross visual assessment of the initial specimen. The puncture procedure was repeated until whitish material became macroscopically visible but was limited to a maximum of five passes if no material was obtained. All procedures were performed in the absence of an on-site pathologist. After the samples were processed, they were embedded in paraffin. Tissue sections of 3 to 4 μm were stained with hematoxylin-eosin for morphological evaluation and/or different immunohistochemical analysis (Figure 3). If the pathologists were unable to obtain a core for histological evaluation, they processed the same material as a cell block for cytological evaluation.

The procedure was performed on an outpatient basis, unless the patient had been hospitalized for other medical conditions. The outpatients were observed for immediate adverse events in the recovery room for 2 h before being discharged from the unit. Outpatients were also ambulatorily monitored for a minimum of 48 h for the detection of further complications. All adverse events were documented.

Gold standard

The final diagnosis was made according to one of the following reference methods: (1) definite benign or malignant histological diagnosis based on surgical resection of specimens from operated patients; (2) cytology or histology findings with definite proof of malignancy in patients with unresectable lesions according to EUS, multidetector CT scan and/or PET scan findings and compatible clinical follow-up; or (3) cytology or histology findings without proof of malignancy and compatible imaging evaluation, including EUS multidetector CT scan and/or PET scan and a minimum clinical follow-up time of 12 mo.

In patients with a high probability of an inflammatory disorder (such as sarcoidosis), the detection of specific types of granulomas was considered diagnostic of benign disease, but in patients suspected of disseminated malignancy, the detection of granulomas was considered a true negative for malignancy. Inconclusive or benign cytology was considered a false negative if further diagnostic workup or clinical follow-up showed signs positive for malignancy. Negative cytology was

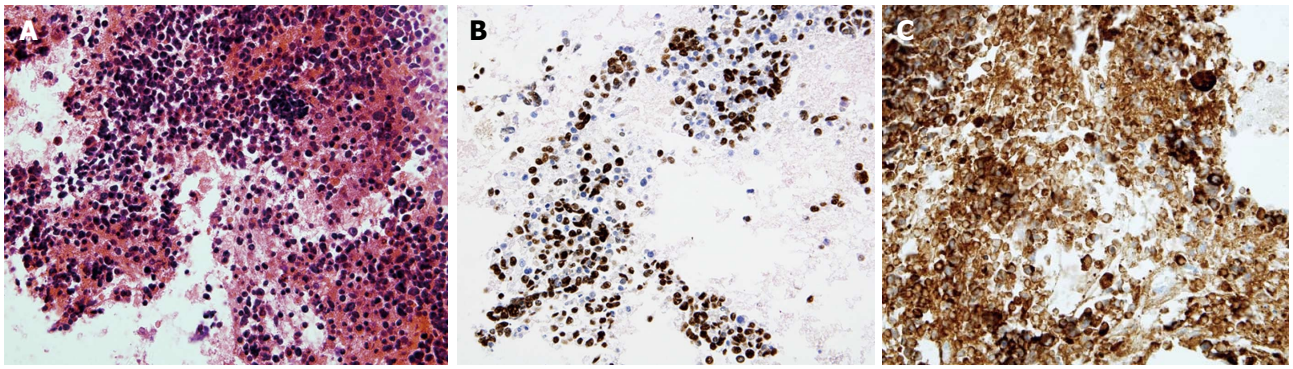

Figure 3 Small cell carcinoma from an fine-needle aspiration subcarinal lymph node (cell block). A: Note the small cell neoplastic population with hyperchromatic nuclei, scant cytoplasm and absent nucleoli; B: Nuclear positivity for TTF-1; C: Cytoplasmic positivity for synaptophysin.

Table 1 Demographics and lymph node characteristics by location *n* (%)

Characteristics	Total (*n* = 168)	Abdominal (*n* = 78)	Mediastinal (*n* = 90)	*P* value
Size (mm), mean ± SD	20.3 ± 9.9	19.3 ± 9.0	21.4 ± 18.4	0.280
Histology needle	105 (61.3)	48 (61.5)	57 (61.1)	0.955
19-G	17 (10.1)	5 (6.4)	12 (13.3)	
20-G	7 (4.2)	3 (3.9)	4 (4.4)	
22-G	48 (28.6)	23 (29.5)	25 (27.8)	
25-G	33 (19.6)	17 (21.8)	16 (17.8)	
Cytology needle	63 (38.7)	30 (38.5)	33 (38.9)	0.955
19-G	4 (2.4)	-	4 (5.6)	
22-G	30 (17.9)	14 (18.0)	16 (17.8)	
25-G	29 (17.3)	16 (20.5)	13 (14.4)	
No. of passes (median, range)	214	99 (11, 4)	115 (1, 1-3)	

considered a true negative when histology did not show any abnormality or when imaging studies during follow-up showed spontaneous resolution or lack of progression of the lymph nodes under evaluation.

Statistical analysis

The statistical analysis was performed with SATA version 13. Categorical variables are presented as numbers (percentages). Continuous variables are presented as the means ± SDs. The number of needle passes is presented as the median (range). A multivariate logistic regression analysis was performed to identify the variables (lymph node location and size, needle type and number of needle passes) that affect the diagnostic yield. Performance characteristics of the EUS-guided tissue acquisition, including the sensitivity, specificity, positive predictive value (PPV), negative predictive value (NPV), and diagnostic accuracy, were calculated. These values were determined by comparing the EUS-guided tissue acquisition results with the final diagnosis of the lesions based on the abovementioned criteria. Accuracy was defined as the ratio of the sum of true positive and true negative values divided by the number of lesions. $P < 0.05$ was considered statistically significant.

RESULTS

A total of 5184 EUS examinations were performed during the study period. Of these, 152 patients fulfilled the inclusion and exclusion criteria. A total of 168 EUS-guided tissue acquisitions of lymph nodes were performed (Figure 4), and 117 (69.6%) and 35 (30.4%) of these were males and females, respectively. Eight patients had two lymph nodes sampled from different sites. The mean age of the patients was 63.8 ± 15 years. Ninety (53.6%) cases presented enlarged mediastinal lymph nodes, and in 78 cases (46.4%), the enlarged lymph nodes were located in the intra-abdominal region. The mean size of the enlarged lymph nodes was 20.3 ± 9.9 mm.

EUS biopsy needles were used in 105 (62.5%) of the procedures, whereas cytology needles were used in only 63 cases (37.5%). The distribution of the needles used is shown in Table 1. A total of 214 needle passes were performed, with a median number of 1 (range of 1 to 4). Of these, 115 were performed on mediastinal lymph nodes, and 99 were performed on intra-abdominal lymph nodes (Table 1). There were no adverse events reported (0%).

The final diagnosis was established based on surgical specimen evaluations for three cases (1.8%) and on the results of EUS-guided tissue acquisition and follow-up for the remaining 165 cases (98.2%). According to the defined gold standard, 87 (51.8%) cases were benign, and 81 (48.2%) were malignant. According to the EUS-guided tissue acquisition pathological results, 108 lymph nodes were considered

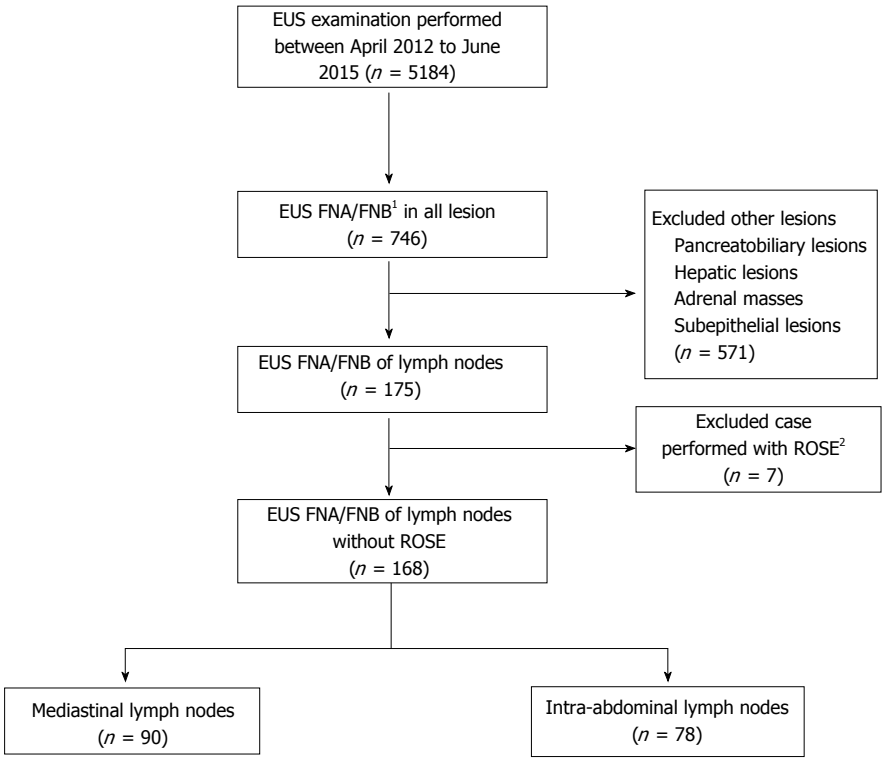

Figure 4 Flow chart of the selection of endoscopic ultrasound-guided tissue acquisition cases. [1]Fine-needle aspiration/biopsy; [2]Rapid on-site evaluation. EUS: endoscopic ultrasound; FNA: Fine-needle aspiration; FNB: Fine-needle biopsy.

Table 2 Endoscopic ultrasound fine-needle aspiration/fine-needle biopsy diagnoses and final diagnoses in 168 lymph nodes *n* (%)

	EUS FNA/FNB diagnoses	Final diagnoses
Metastasis		
Carcinoma	51 (30.3)	62 (36.9)
Neuroendocrine	2 (1.2)	2 (1.2)
Melanoma	1 (0.6)	1 (0.6)
Benign/reactive		
Granulomatous	8 (4.8)	21 (12.5)
Unspecific reactive	100 (59.5)	66 (39.3)
Lymphoma	6 (3.6)	16 (9.5)

EUS: Endoscopic ultrasound; FNA: Fine-needle aspiration; FNB: Fine-needle biopsy.

Table 3 Accuracy of endoscopic ultrasound fine-needle aspiration/fine-needle biopsy for diagnosis of malignancy

Overall (*n* = 168)	Estimate (%)	95%CI
Sensitivity	74.1%	63.6-82.4
Specificity	100%	95.8-100
Positive predictive value	100%	94.0-100
Negative predictive value	80.6%	72.1-86.9
Accuracy	87.5%	81.7-91.7

benign (inflammatory, granulomatous), and 60 were considered malignant (carcinoma, neuroendocrine tumor (NET), melanoma and lymphoma) (Table 2). The sensitivity, specificity, PPV and NPV for the detection of malignancy were 74.1%, 100%, 100% and 80.6%, respectively. The overall accuracy was 87.5% (95%CI: 81.7-91.7) (Table 3).

The analysis of factors that might influence the diagnostic outcome of EUS-guided tissue acquisition techniques revealed that none of these factors demonstrated a significant effect. There was no correlation between the number of needle passes and the diagnostic accuracy. Only one case required four passes to procure sufficient material for pathological assessment. There was also no significant association between lymph node size and diagnostic accuracy. The presence of larger lymph nodes was not associated with better accuracy. The subgroup analysis of the needles used for the procedure also revealed no significant correlation with diagnostic accuracy (Table 4).

DISCUSSION

The results of this study demonstrate that EUS-guided tissue acquisition has a high rate of clinical success and diagnostic accuracy in sampling tissue from enlarged mediastinal and intra-abdominal lymph nodes. EUS has the ability to identify and sample even small lymph nodes just a few millimeters in size. We did not identify any specific factor related to the procedure that affected the final diagnostic accuracy of the procedure (lymph node size and location, number of passes and/or needle type and size). In this large series of cases, no adverse events were reported, highlighting the safety of this technique.

When enlarged lymph nodes are detected based on

Table 4 Analysis of factors associated with the diagnostic accuracy of endoscopic ultrasound fine-needle aspiration/fine-needle biopsy

Variable	OR (95%CI)	*P* value	OR (95%CI)	*P* value
Mediastinal location	1.05 (0.42-2.64)	0.907	0.93 (0.30-2.92)	0.900
Histology needle	1.02 (0.40-2.64)	0.952	1.01 (0.31-3.31)	0.993
No. of passes	0.58 (0.27-1.24)	0.161	1.54 (0.41-5.80)	0.522
Size	0.98 (0.93-1.03)	0.383	0.98 (0.93-1.03)	0.411

different imaging techniques, such as MRI, CT scan or even EUS, there is often a need for these lesions to be further characterized to facilitate patient management. Malignant morphological predictors on EUS for lymph nodes include a rounded shape, size greater than 10 mm, hypoechoic echotexture and well-defined margins. If a lymph node exhibits all four features, the accuracy of malignant diagnosis ranges from 80% to 100%[14,15]. However, only 25% of malignant lymph nodes present all four features[16], and benign lymph nodes can also fulfill these criteria. Hence, tissue sampling from enlarged lymph nodes is important for obtaining a pathological diagnosis, thus optimizing and determining patient treatment. Previous studies have shown that the use of EUS-guided tissue acquisition greatly increases the diagnostic yield and accuracy with a good safety profile[2,3,14,17,18]. In fact, no adverse events were observed in our study. This low rate of complications could be related to the high spatial resolution of EUS and the short needle tract used to access the target lesions. EUS allows the presence of interposed vessels to be identified, allowing them to be avoided during the process of tissue acquisition. Since the first report of EUS-FNA in 1992[19], there have been significant advances in both the techniques and equipment used for tissue sampling.

Another important finding of our study was that few needle passes (1-2) were needed to obtain sufficient material for the pathological assessment in the absence of on-site pathological evaluation. This observation could be related to needle selection because the majority of the samples included in our study were acquired with biopsy needles (61.3%), although the choice of needle was not significant. A plausible explanation is the ability of biopsy needles to procure a larger amount of specimen with preserved cellular architecture, which is crucial for certain diagnoses, such as lymphoproliferative diseases and some inflammatory conditions[20]. Our findings are in agreement with previous studies that achieved adequate specimens in one to two needle passes[21,22]. In contrast to our study, LeBlanc *et al*[23] suggested a maximum of five needle passes for achieving sufficient sample because further needle passes did not increase the diagnostic sensitivity. Despite the preferential use of biopsy needles, the diagnostic accuracy for lymphoproliferative disease in our study cohort was suboptimal. This result could have been related to the procurement of a non-diagnostic part of the lymph node, *e.g.*, the necrotic portion. Evidence suggests that employing complementary tools, such as contrast-enhanced EUS or EUS elastography, might help in guiding to the area for tissue procurement, thus improving the diagnostic yield[24,25]. However, further studies are required to validate the benefits of these advanced imaging techniques associated with EUS. In our series, suction was used as a standard in all cases. Whether the application of suction during EUS-guided tissue acquisition could have contributed to the overall results was not evaluated in the current study. However, previous studies published in the literature have shown that the application of suction does not affect the diagnostic accuracy but is associated with bloody contamination of the specimens[26-29].

In our study, intrinsic (size and location of the enlarged lymph nodes) and extrinsic factors (type or size of the needle and number of needle passes) had no bearing on the diagnostic yield of EUS-guided tissue acquisition. A possible explanation for these findings could be that the procedure is highly dependent on the operator. The endosonographers (Iglesias-Garcia J and Lariño-Noia J) who performed the procedures in this study were very experienced operators, and their technique could have contributed to the diagnostic yield. In addition, a high level of expertise in the interpretation of the acquired specimens is a key element in the diagnostic success of EUS-guided tissue acquisition. In our center, a dedicated cytopathologist examined all specimens from the EUS-guided tissue acquisition, which were dispatched to the ThinPrep laboratory (Cytyc Co, Marlborough, MA, United States). Liquid-based cytology has the advantage of a monolayer cell dispersion, avoiding the contamination of samples by mucus and blood and ensuring consistent cell preparation without artifacts. Whether the methods used for processing the specimens could have influenced the diagnostic yield remains to be determined.

There were 21 (19.4%) false-negative results. Sampling error might explain the relatively low sensitivity (74.1%). This was especially true for the presence of multiple enlarged lymph nodes; even given the efforts that were taken to target the most "malignant appearing" lymph node based on EUS features, the diagnostic yield was still suboptimal. This finding is in accordance with previous studies published in the literature. There are no reliable endosonographic features that indicate the malignant potential of enlarged lymph nodes[16,30]; hence, EUS-guided tissue acquisition will remain an important tool

for discerning the nature of enlarged lymph nodes. According to recent reports, techniques such as EUS elastography, which helps distinguish between benign and malignant lesions, have gained much attention over the last decade[31,32]. Malignant lesions tend to be solid due to pathologic processes that decrease tissue elasticity and hence increase tissue stiffness, resulting in a blue pattern on qualitative EUS elastography[25]. Targeting the needle to the "solid area" during the tissue acquisition process could potentially improve the diagnostic yield of malignant lesions. Another factor that might have influenced these results, as previously mentioned, is the low number of needle passes performed, which was based on gross visual inspection by the endosonographers. Although we did not evaluate this specific variable in the present study, gross visual inspection might have hindered the procurement of better results. Performing another session of EUS-guided tissue acquisition may improve the diagnostic yield in situations where there is high clinical suspicion[33].

This study has certain limitations. It was a single-center study, and the results might not reflect practices or technologies used at other institutions. The lack of an on-site pathologist evaluation may influence the final results. Previous studies have established that on-site pathological evaluation improves the diagnostic yield by 10%-15%[9,34]. However, in many occasions and in many centers, on-site pathological evaluation is not possible due to manpower and cost limitations. The type of needle used was based on the endosonographer's preference and was not randomized; however, there was a tendency toward the use of smaller and more flexible needles for lesions that pose technical difficulties or a high risk of bleeding. We did not include data corresponding to the gold standard analysis, which is considered the analysis of the surgical specimen. In fact, this was available in only three cases. However, this reflects the real clinical practice in the evaluation of enlarged lymph nodes. It is logical that lymph node enlargement in almost any disease is indicative of an advanced condition that does not merit surgical management. In addition, the presence of benign lymph nodes precludes the need for surgery. However, to overcome this limitation, we included a robust clinical follow-up protocol over a minimum of 12 mo, coupled with advanced imaging studies (MRI, CT scan and PET). The duration of follow-up was deemed sufficient because any malignancy with significant nodal involvement would be at least stage Ⅱ disease[35-37]. The primary malignancy would be clearly evident or the patient could have succumbed to the disease within the follow-up period; hence, a 12-mo follow-up period was deemed appropriate in our study cohort.

In conclusion, EUS-guided tissue acquisition is a highly accurate technique for the evaluation of enlarged lymph nodes. No factor was found to affect the operating characteristics or accuracy of this technique. Increasing the number of needle passes could be an option to improve the diagnostic yield but might be associated with a theoretically increased risk of adverse events. Whether the results of the present study can be replicated in other centers remains questionable because the level of expertise of the endosonographer and cytopathologist could be crucial for the high diagnostic yield of this technique. Future studies should include multicenter approaches with different operators to draw firmer conclusions.

COMMENTS

Background

Lymph node enlargement is increasingly detected on various imaging modalities. In the absence of primary malignancy, it is difficult to establish a diagnosis for lymph node enlargement. Previously, a surgical approach was the main diagnostic tool in such circumstances despite its disadvantages. Recently, endoscopic ultrasound-fine-needle aspiration/biopsy (EUS-FNA/B) has become a pivotal diagnostic tool to guide appropriate treatment. In this study, we evaluated factors that might influence the diagnostic accuracy of EUS-guided tissue acquisition of lymph node enlargement in the absence of on-site cytopathological evaluation.

Research frontiers

EUS-FNA/B is important for determining the nature of lymph node enlargement in the absence of an on-site pathologist. The results of this study contribute to the clarification that there are no factors associated with the diagnostic accuracy of this technique.

Innovations and breakthroughs

The results of this study showed that no factor appeared to affect the operating characteristics and accuracy of EUS-FNA/B. This finding raises the question of the possible role of complementary techniques, such as EUS-elastography and contrast-enhanced EUS, to help improve the accuracy of this technique. This issue requires further study.

Applications

This study suggests that EUS-guided tissue acquisition is a highly accurate technique for the evaluation of enlarged lymph nodes. No factors were identified to be associated with the operating characteristics or accuracy of this technique.

Peer-review

The author of this paper evaluated the accuracy of EUS-guided tissue acquisition of lymph node enlargement in the absence of an on-site pathologist. None of the variables evaluated were associated with the diagnostic accuracy of this technique. Further studies to assess the role of EUS elastography and contrast-enhanced EUS in this context might be valuable.

REFERENCES

1 **Yasuda I**, Tsurumi H, Omar S, Iwashita T, Kojima Y, Yamada T, Sawada M, Takami T, Moriwaki H, Soehendra N. Endoscopic ultrasound-guided fine-needle aspiration biopsy for lymphadenopathy of unknown origin. *Endoscopy* 2006; **38**: 919-924 [PMID: 16981110 DOI: 10.1055/s-2006-944665]

2 **Bardales RH**, Stelow EB, Mallery S, Lai R, Stanley MW. Review of endoscopic ultrasound-guided fine-needle aspiration cytology. *Diagn Cytopathol* 2006; **34**: 140-175 [PMID: 16511852 DOI: 10.1002/dc.20300]

3 **Mohammad Alizadeh AH**, Shahrokh S, Hadizadeh M, Padashi M, Zali MR. Diagnostic potency of EUS-guided FNA for the evaluation of pancreatic mass lesions. *Endosc Ultrasound* 2016; **5**:

30-34 [PMID: 26879164 DOI: 10.4103/2303-9027.175879]
4 **Gheonea DI**, Săftoiu A, Popescu C, Ciurea T, Iordache S, Filip M, Maloş A. EUS and cytological EUS-FNA prognostic factors in patients with unresectable pancreatic cancer receiving chemotherapy. *Hepatogastroenterology* 2010; **57**: 155-161 [PMID: 20422893]
5 **Puri R**, Vilmann P, Sud R, Kumar M, Taneja S, Verma K, Kaushik N. Endoscopic ultrasound-guided fine-needle aspiration cytology in the evaluation of suspected tuberculosis in patients with isolated mediastinal lymphadenopathy. *Endoscopy* 2010; **42**: 462-467 [PMID: 20432206 DOI: 10.1055/s-0029-1244133]
6 **Berzosa M**, Tsukayama DT, Davies SF, Debol SM, Cen YY, Li R, Mallery S. Endoscopic ultrasound-guided fine-needle aspiration for the diagnosis of extra-pulmonary tuberculosis. *Int J Tuberc Lung Dis* 2010; **14**: 578-584 [PMID: 20392350]
7 **Sharma M**, Rafiq A, Kirnake V. Dysphagia due to tubercular mediastinal lymphadenitis diagnosed by endoscopic ultrasound fine-needle aspiration. *Endosc Ultrasound* 2015; **4**: 348-350 [PMID: 26643706 DOI: 10.4103/2303-9027.170447]
8 **Rana SS**, Chaudhary V, Sharma V, Sharma R, Gupta N, Sampath S, Mittal BR, Gupta R, Dutta U, Bhasin DK. Unusual cause of obstructive jaundice revealed by endoscopic ultrasound guided fine-needle aspiration of mediastinal lymph node. *Endosc Ultrasound* 2015; **4**: 73-75 [PMID: 25789290 DOI: 10.4103/2303-9027.151370]
9 **Klapman JB**, Logrono R, Dye CE, Waxman I. Clinical impact of on-site cytopathology interpretation on endoscopic ultrasound-guided fine needle aspiration. *Am J Gastroenterol* 2003; **98**: 1289-1294 [PMID: 12818271 DOI: 10.1111/j.1572-0241.2003.07472.x]
10 **Cleveland P**, Gill KR, Coe SG, Woodward TA, Raimondo M, Jamil L, Gross SA, Heckman MG, Crook JE, Wallace MB. An evaluation of risk factors for inadequate cytology in EUS-guided FNA of pancreatic tumors and lymph nodes. *Gastrointest Endosc* 2010; **71**: 1194-1199 [PMID: 20598246 DOI: 10.1016/j.gie.2010.01.029]
11 **Alsohaibani F**, Girgis S, Sandha GS. Does onsite cytotechnology evaluation improve the accuracy of endoscopic ultrasound-guided fine-needle aspiration biopsy? *Can J Gastroenterol* 2009; **23**: 26-30 [PMID: 19172205]
12 **Iglesias-Garcia J**, Lariño-Noia J, Abdulkader I, Domínguez-Muñoz JE. Rapid on-site evaluation of endoscopic-ultrasound-guided fine-needle aspiration diagnosis of pancreatic masses. *World J Gastroenterol* 2014; **20**: 9451-9457 [PMID: 25071339 DOI: 10.3748/wjg.v20.i28.9451]
13 **Savides TJ**. Tricks for improving EUS-FNA accuracy and maximizing cellular yield. *Gastrointest Endosc* 2009; **69**: S130-S133 [PMID: 19179138 DOI: 10.1016/j.gie.2008.12.018]
14 **Catalano MF**, Sivak MV Jr, Rice T, Gragg LA, Van Dam J. Endosonographic features predictive of lymph node metastasis. *Gastrointest Endosc* 1994; **40**: 442-446 [PMID: 7926534]
15 **Wiersema MJ**, Hassig WM, Hawes RH, Wonn MJ. Mediastinal lymph node detection with endosonography. *Gastrointest Endosc* 1993; **39**: 788-793 [PMID: 8293902]
16 **Bhutani MS**, Hawes RH, Hoffman BJ. A comparison of the accuracy of echo features during endoscopic ultrasound (EUS) and EUS-guided fine-needle aspiration for diagnosis of malignant lymph node invasion. *Gastrointest Endosc* 1997; **45**: 474-479 [PMID: 9199903]
17 **Williams DB**, Sahai AV, Aabakken L, Penman ID, van Velse A, Webb J, Wilson M, Hoffman BJ, Hawes RH. Endoscopic ultrasound guided fine needle aspiration biopsy: a large single centre experience. *Gut* 1999; **44**: 720-726 [PMID: 10205212]
18 **Fisher L**, Segarajasingam DS, Stewart C, Deboer WB, Yusoff IF. Endoscopic ultrasound guided fine needle aspiration of solid pancreatic lesions: Performance and outcomes. *J Gastroenterol Hepatol* 2009; **24**: 90-96 [PMID: 19196396 DOI: 10.1111/j.1440-1746.2008.05569.x]
19 **Wiersema MJ**, Hawes RH, Tao LC, Wiersema LM, Kopecky KK, Rex DK, Kumar S, Lehman GA. Endoscopic ultrasonography as an adjunct to fine needle aspiration cytology of the upper and lower gastrointestinal tract. *Gastrointest Endosc* 1992; **38**: 35-39 [PMID: 1612376]
20 **Guo J**, Sun B, Wang S, Ge N, Wang G, Wu W, Liu X, Sun S. Diagnosis of lymphoma by endoscopic ultrasound-assisted transendoscopic direct retroperitoneal lymph node biopsy: A case report (with video). *Endosc Ultrasound* 2015; **4**: 69-72 [PMID: 25789289 DOI: 10.4103/2303-9027.151368]
21 **Erickson RA**, Sayage-Rabie L, Beissner RS. Factors predicting the number of EUS-guided fine-needle passes for diagnosis of pancreatic malignancies. *Gastrointest Endosc* 2000; **51**: 184-190 [PMID: 10650262]
22 **Berzosa M**, Villa N, El-Serag HB, Sejpal DV, Patel KK. Comparison of endoscopic ultrasound guided 22-gauge core needle with standard 25-gauge fine-needle aspiration for diagnosing solid pancreatic lesions. *Endosc Ultrasound* 2015; **4**: 28-33 [PMID: 25789281 DOI: 10.4103/2303-9027.151320]
23 **LeBlanc JK**, Ciaccia D, Al-Assi MT, McGrath K, Imperiale T, Tao LC, Vallery S, DeWitt J, Sherman S, Collins E. Optimal number of EUS-guided fine needle passes needed to obtain a correct diagnosis. *Gastrointest Endosc* 2004; **59**: 475-481 [PMID: 15044881]
24 **Dietrich CF**, Sharma M, Hocke M. Contrast-enhanced endoscopic ultrasound. *Endosc Ultrasound* 2012; **1**: 130-136 [PMID: 24949350 DOI: 10.7178/eus.03.003]
25 **Iglesias-Garcia J**, Lindkvist B, Lariño-Noia J, Domínguez-Muñoz JE. Endoscopic ultrasound elastography. *Endosc Ultrasound* 2012; **1**: 8-16 [PMID: 24949330 DOI: 10.7178/eus.01.003]
26 **Wallace MB**, Kennedy T, Durkalski V, Eloubeidi MA, Etamad R, Matsuda K, Lewin D, Van Velse A, Hennesey W, Hawes RH, Hoffman BJ. Randomized controlled trial of EUS-guided fine needle aspiration techniques for the detection of malignant lymphadenopathy. *Gastrointest Endosc* 2001; **54**: 441-447 [PMID: 11577304]
27 **Puri R**, Vilmann P, Săftoiu A, Skov BG, Linnemann D, Hassan H, Garcia ES, Gorunescu F. Randomized controlled trial of endoscopic ultrasound-guided fine-needle sampling with or without suction for better cytological diagnosis. *Scand J Gastroenterol* 2009; **44**: 499-504 [PMID: 19117242 DOI: 10.1080/00365520802647392]
28 **Nakai Y**, Isayama H, Chang KJ, Yamamoto N, Hamada T, Uchino R, Mizuno S, Miyabayashi K, Yamamoto K, Kawakubo K, Kogure H, Sasaki T, Hirano K, Tanaka M, Tada M, Fukayama M, Koike K. Slow pull versus suction in endoscopic ultrasound-guided fine-needle aspiration of pancreatic solid masses. *Dig Dis Sci* 2014; **59**: 1578-1585 [PMID: 24429514 DOI: 10.1007/s10620-013-3019-9]
29 **Villa NA**, Berzosa M, Wallace MB, Raijman I. Endoscopic ultrasound-guided fine needle aspiration: The wet suction technique. *Endosc Ultrasound* 2016; **5**: 17-20 [PMID: 26879162 DOI: 10.4103/2303-9027.175877]
30 **Song HJ**, Kim JO, Eun SH, Cho YD, Jung IS, Cheon YK, Moon JH, Lee JS, Lee MS, Shim CS, Kim BS, Jin SY. Endoscopic Ultrasonograpic Findings of Benign Mediastinal and Abdominal Lymphadenopathy Confirmed by EUS-guided Fine Needle Aspiration. *Gut Liver* 2007; **1**: 68-73 [PMID: 20485661 DOI: 10.5009/gnl.2007.1.1.68]
31 **Săftoiu A**, Vilmann P, Ciurea T, Popescu GL, Iordache A, Hassan H, Gorunescu F, Iordache S. Dynamic analysis of EUS used for the differentiation of benign and malignant lymph nodes. *Gastrointest Endosc* 2007; **66**: 291-300 [PMID: 17643702]
32 **Giovannini M**, Thomas B, Erwan B, Christian P, Fabrice C, Benjamin E, Geneviève M, Paolo A, Pierre D, Robert Y, Walter S, Hanz S, Carl S, Christoph D, Pierre E, Jean-Luc VL, Jacques D, Peter V, Andrian S. Endoscopic ultrasound elastography for evaluation of lymph nodes and pancreatic masses: a multicenter study. *World J Gastroenterol* 2009; **15**: 1587-1593 [PMID: 19340900 DOI: 10.3748/wjg.15.1587]
33 **Téllez-Ávila FI**, Martínez-Lozano JA, Rosales-Salinas A, Bernal-Méndez AR, Guerrero-Velásquez C, Ramírez-Luna MÁ, Valdovinos-Andraca F. Repeat endoscopic ultrasound fine needle aspiration after a first negative procedure is useful in pancreatic

lesions. *Endosc Ultrasound* 2016; **5**: 258-262 [PMID: 27503159 DOI: 10.4103/2303-9027.187889]

34 **Jhala NC**, Jhala D, Eltoum I, Vickers SM, Wilcox CM, Chhieng DC, Eloubeidi MA. Endoscopic ultrasound-guided fine-needle aspiration biopsy: a powerful tool to obtain samples from small lesions. *Cancer* 2004; **102**: 239-246 [PMID: 15368316 DOI: 10.1002/cncr.20451]

35 **Waddell T**, Verheij M, Allum W, Cunningham D, Cervantes A, Arnold D; European Society for Medical Oncology (ESMO); European Society of Surgical Oncology (ESSO); European Society of Radiotherapy and Oncology (ESTRO). Gastric cancer: ESMO-ESSO-ESTRO Clinical Practice Guidelines for diagnosis, treatment and follow-up. *Ann Oncol* 2013; **24** Suppl 6: vi57-vi63 [PMID: 24078663 DOI: 10.1093/annonc/mdt344]

36 **Stahl M**, Mariette C, Haustermans K, Cervantes A, Arnold D; ESMO Guidelines Working Group. Oesophageal cancer: ESMO Clinical Practice Guidelines for diagnosis, treatment and follow-up. *Ann Oncol* 2013; **24** Suppl 6: vi51-vi56 [PMID: 24078662 DOI: 10.1093/annonc/mdt342]

37 **Ducreux M,** Cuhna AS, Caramella C, Hollebecque A, Burtin P, Goere D, Seufferlein T, Haustremans K, Van Laethem JL, Conroy T, Arnold D. Cancer of the pancreas: ESMO Clinical Practice Guidelines for diagnosis, treatment and follow-up. *Ann Oncol* 2015; **26**: v56-v68 [PMID: 26314780 DOI: 10.1093/annonc/mdv295]

P- Reviewer: McHenry L, Schmidt J **S- Editor**: Wang JL
L- Editor: A **E- Editor**: Li D

World Journal of Gastroenterology

Submit a Manuscript: http://www.f6publishing.com

World J Gastroenterol 2017 August 21; 23(31): 5764-5772

DOI: 10.3748/wjg.v23.i31.5764

ISSN 1007-9327 (print) ISSN 2219-2840 (online)

ORIGINAL ARTICLE

Retrospective Study

Doublecortin and CaM kinase-like-1 as an independent prognostic factor in patients with resected pancreatic carcinoma

Kohei Nishio, Kenjiro Kimura, Ryosuke Amano, Bunzo Nakata, Sadaaki Yamazoe, Go Ohira, Kotaro Miura, Naoki Kametani, Hiroaki Tanaka, Kazuya Muguruma, Kosei Hirakawa, Masaichi Ohira

Kohei Nishio, Kenjiro Kimura, Ryosuke Amano, Sadaaki Yamazoe, Go Ohira, Kotaro Miura, Naoki Kametani, Hiroaki Tanaka, Kazuya Muguruma, Kosei Hirakawa, Masaichi Ohira, Department of Surgical Oncology, Osaka City University Graduate School of Medicine, Abeno-ku, Osaka 545-8585, Japan

Bunzo Nakata, Department of Surgery, Kashiwara Municipal Hospital, Kashiwara City, Osaka 582-0005, Japan

Author contributions: Kimura K designed the studies; Nishio K drafted the manuscript; Amano R, Muguruma K, Tanaka H, Yamazoe S, Ohira G, Miura K, Kametani N and Hirakawa K provided support in design and interpretation of the study; Nishio K and Kimura K performed the statistical analyses; Hirakawa K and Nakata B helped in drafting of the manuscript; Ohira M provided overall supervision of the manuscript; all authors read and approved the final manuscript.

Institutional review board statement: The study was reviewed and approved by the Osaka City University Institutional Review Board.

Informed consent statement: Written informed consent was obtained from all patients.

Conflict-of-interest statement: The authors declare that they have no competing interests.

Data sharing statement: No additional data are available.

Manuscript source: Unsolicited manuscript

Correspondence to: Kenjiro Kimura, MD, PhD, Senior Lecturer, Department of Surgical Oncology, Osaka City University Graduate School of Medicine, 1-4-3 Asahimachi, Abeno-ku, Osaka 545-8585, Japan. kenjiro@med.osaka-cu.ac.jp
Telephone: +81-6-66453838
Fax: +81-6-66466450

Received: March 31, 2017
Peer-review started: April 8, 2017
First decision: April 26, 2017
Revised: May 11, 2017
Accepted: July 22, 2017
Article in press: July 24, 2017
Published online: August 21, 2017

Abstract

AIM

To elucidate the effect of expression of doublecortin and CaM kinase-like-1 (DCLK1) in patients with pancreatic ductal adenocarcinoma (PDAC).

METHODS

Tumor specimens were obtained from 136 patients with pancreatic cancer who had undergone resection without preoperative therapy between January 2000 and December 2013 at the Department of Surgical Oncology, Osaka City University. The resected specimens were analyzed for associations with clinicopathological data, including DCLK1 expression, epithelial mesenchymal transition (EMT) marker expression, and cancer stem cell (CSC) marker expression. Univariate and multivariate survival analyses were performed and we assessed the association between DCLK1 expression and clinicopathological factors, including the EMT marker and CSC marker.

RESULTS

In total, 48.5% (66/136) of the pancreatic cancer samples were positive for DCLK1. Patients with DCLK1-positive tumors had significantly shorter survival times than those with DCLK1-negative tumors (median, 18.7 mo *vs* 49.5 mo, respectively; $P < 0.0001$). Positive DCLK1 expression correlated with histological grade ($P = 0.0290$), preoperative CA19-9 level ($P = 0.0060$), epithelial cell adhesion molecule (EpCAM) expression ($P = 0.0235$), and the triple-positive expression of CD44/CD24/EpCAM ($P = 0.0139$). On univariate survival analysis, five factors were significantly associated with worse overall survival: histological grade of G2 to G4 ($P = 0.0091$), high preoperative serum SPan-1 level ($P = 0.0034$), R1/2 ($P < 0.0001$), positive expression of DCLK1 ($P < 0.0001$) or CD44 ($P = 0.0245$). On multivariate survival analysis, R1/2 [odds ratio (OR) = 2.019, 95% confidence interval (CI): 1.380-2.933; $P = 0.0004$] and positive DCLK1 expression (OR = 1.848, 95%CI: 1.2854-2.661; $P = 0.0009$) were independent prognostic factors.

CONCLUSION

DCLK1 expression was found to be an independent prognostic factor and it may play a crucial prognostic role by promoting acquisition of stemness.

Key words: Doublecortin and CaM kinase-like-1; Pancreatic cancer; Epithelial mesenchymal transition; Cancer stem cell; Prognostic factor

Core tip: Doublecortin and CaM kinase-like-1 (DCLK1) is a microtubule - associated kinase and has recently attracted much attention as an important cancer stem cell marker. DCLK1 expression is correlated with aggressiveness in various cancers. However, there have been few investigations correlating DCLK1 expression with survival in pancreatic ductal adenocarcinoma (PDAC). PDAC patients with DCLK1-positive tumors had significantly shorter survival times than those with DCLK1-negative tumors. DCLK1 expression was an independent prognostic factor by multivariate survival analysis. Furthermore, DCLK1-positive expression was correlated to EpCAM expression and triple-positive expression of CD44/CD24/EpCAM. These findings suggest DCLK1 may have a crucial prognostic role in acquisition of stemness.

Nishio K, Kimura K, Amano R, Nakata B, Yamazoe S, Ohira G, Miura K, Kametani N, Tanaka H, Muguruma K, Hirakawa K, Ohira M. Doublecortin and CaM kinase-like-1 as an independent poor prognostic factor for resected pancreatic carcinoma. *World J Gastroenterol* 2017; 23(31): 5764-5772 Available from: URL: http://www.wjgnet.com/1007-9327/full/v23/i31/5764.htm DOI: http://dx.doi.org/10.3748/wjg.v23.i31.5764

INTRODUCTION

Although the number of treatment strategies has increased for pancreatic ductal adenocarcinoma (PDAC), the disease still has a poor prognosis. Malignancy of PDAC is devastating, with a 5-year overall survival rate of approximately 5%[1]. The high mortality rate associated with PDAC is known to be due to extensive invasion into the surrounding tissues and early metastasis to distant organs; however, the molecular mechanisms of the highly aggressive nature of PDAC remain unclear.

Doublecortin and CaM kinase-like-1 (DCLK1) is a microtubule-associated kinase that has recently attracted much attention as an important cancer stem cell (CSC) marker. DCLK1 contains two doublecortin domains in the N terminus, which are involved in the regulation of microtubule polymerization, and a serine/threonine protein kinase domain in the C terminus. Between the N and C termini, there is a serine/proline-rich domain that mediates multiple protein-protein interactions[2]. DCLK1 is predominantly expressed in the low two-thirds of the intestinal crypt epithelium and occasionally in crypt-based columnar cells[3]. Originally, DLCK1 was reported as a putative intestinal and pancreatic stem cell marker[4,5]. More recently, however, DCLK1 has been demonstrated as expressed in CSCs but to be undetectable in normal stem cells[6]. Knockdown of DCLK1 in pancreatic cancer cells resulted in tumor growth arrest and the downregulation of Snail, Slug and Twist, which inhibit epithelial mesenchymal transition (EMT)[7-9]. As such, DCLK1 has become the focus of research into its potential as a candidate therapeutic target for various cancers.

Several studies have demonstrated that DCLK1 expression is correlated with cancer aggressiveness in colorectal[10], esophageal[11], breast[12], and renal cell[9] carcinomas. However, only few studies have investigated the correlation of DCLK1 expression with survival in PDAC. The aim of this study was to elucidate the effect of DCLK1 expression on the survival of patients with PDAC. Moreover, the correlations of clinicopathological features, including expression of EMT and CSC markers, with DCLK1 expression were investigated.

MATERIALS AND METHODS

Patients

The current study used tissue samples from 136 patients who underwent pancreatic resection for PDAC at our institution. All patients were histologically confirmed to have a common type of invasive ductal carcinoma of the pancreas. Patients with neuroendocrine carcinomas, mucinous cystic carcinomas, or intraductal papillary mucinous carcinomas were excluded. Moreover, we excluded patients who had undergone neoadjuvant therapy. Clinical records were reviewed to

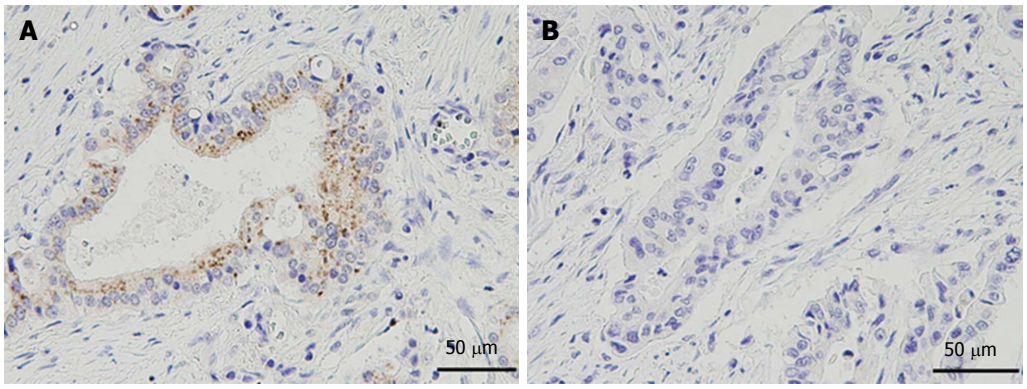

Figure 1 Immunohistochemical analysis of doublecortin and CaM kinase-like-1 expression. A: Positive expression; B: Negative expression. DCLK1: Doublecortin and CaM kinase-like-1.

examine clinical features, including demographic data (age and sex) and therapeutic data (chemotherapy performed after surgery, and interval from surgical resection to death). This study was approved by the ethics committee of Osaka City University and was in compliance with the Declaration of Helsinki. Each patient provided informed consent before tissue samples were obtained.

Surgery and pathology

Surgery involved standard or subtotal stomach-preserving pancreaticoduodenectomy in 76 (55.9%) patients, distal pancreatectomy in 54 (39.7%) patients, and total pancreatectomy in 6 (4.4%) patients. Regional lymph node dissection was performed in all patients. The resected specimens were fixed in 10% formalin at room temperature, and the size and gross appearance of each tumor were recorded. The pathologic stage of all tumor specimens was determined using the staging system of the American Joint Committee on Cancer (AJCC), 7th edition[13]. Tumor differentiation was classified according to the classification of tumors of the World Health Organization as well-differentiated (G1), moderately differentiated (G2), poorly differentiated (G3), or undifferentiated (G4)[14].

Immunohistochemistry

Formalin-fixed, paraffin-embedded tumor tissue was cut into 4-μm thick sections and immunohistochemistry was performed using a protocol previously reported by our group but with some modifications[15]. The most representative section of tumor for each case was selected for analysis. We analyzed not only DCLK1 expression, but also the expression of E-cadherin, N-cadherin, vimentin, and Snail as EMT markers, and CD24, CD44, CD133, and epithelial cell adhesion molecule (EpCAM) as CSC markers. The primary antibodies used for immunohistochemistry were: rabbit polyclonal anti-DCLK1 antibody (1:80 dilution; Abcam, Cambridge, MA, United States); rabbit polyclonal anti-Snail antibody (1:80 dilution; Abcam); mouse monoclonal anti-E-cadherin antibody (1:50 dilution; Dako Co., Carpinteria, CA, United States); rabbit monoclonal anti-vimentin antibody (1:100 dilution; Cell Signaling, Danvers, MA, United States); rabbit polyclonal anti-N-cadherin antibody (1:100 dilution; Abcam); goat polyclonal anti-CD24 antibody (1:20 dilution; Santa Cruz Biotechnology, Dallas, TX, United States); mouse monoclonal anti-CD44 antibody (1:50 dilution; Dako Co); mouse monoclonal anti-CD133 antibody (1:10 dilution; Miltenyi Biotec, Gladbach, Germany); and mouse monoclonal anti-EpCAM antibody (1:500 dilution; Cell Signaling).

Evaluation of staining

Intensity of the immunohistochemical staining (staining score) of each marker in a cancerous lesion of each sample was determined using a scoring system that ranged from 0 to 3 (0, no staining; 1, weak staining; 2, moderate staining; and 3, strong staining). Cytoplasmic staining was estimated for the analysis of DCLK1 and vimentin expression. Nuclear staining was estimated for the analysis of Snail expression. Membranous staining was estimated for the analysis of E-cadherin, N-cadherin, CD24, CD44, CD133 and EpCAM expression.

An example of the expression of each marker is shown in Figures 1 and 2. The staining score of each sample represents the average score of five randomly selected fields in the cancerous lesion. As there are no definitive standards that could be used to define positive and negative staining in this study, we defined a score of more than 2 as "positive staining" to roughly divide the samples into positive- and negative-staining groups. The scoring was performed by two surgeons (Nishio K, Kimura K) in a blinded fashion. Differences in scoring were resolved by validation of the two surgeons.

Outcome measures

The demographic and clinical variables included age, sex, tumor location, tumor size, surgery, histological grade, AJCC classification, lymph node metastasis, adjuvant therapy, resection margin status, preoperative serum CA19-9 level, preoperative serum SPan-1

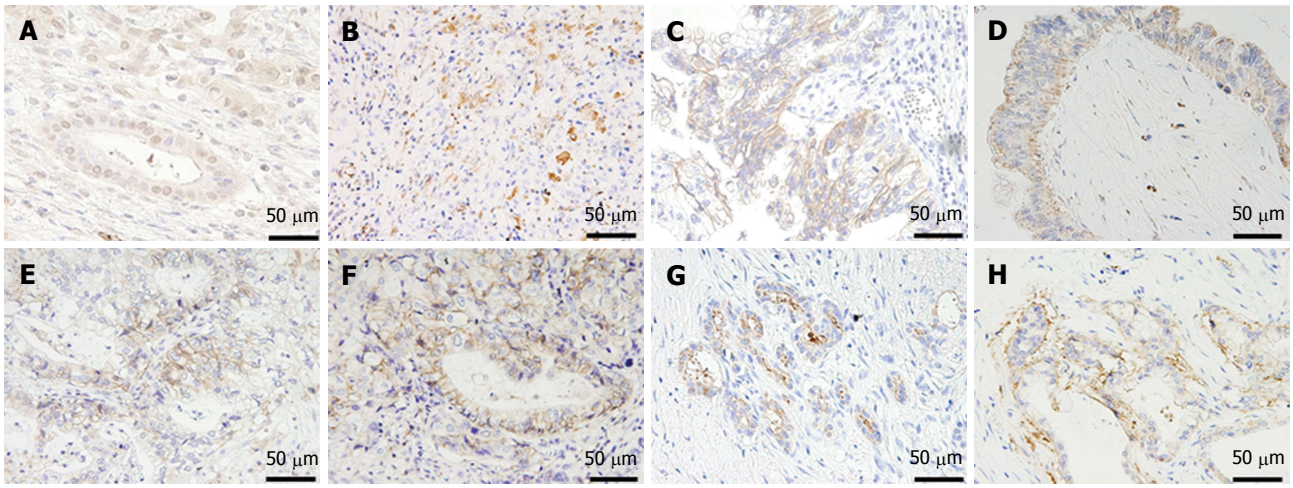

Figure 2 Immunohistochemical analysis of doublecortin and CaM kinase-like-1 expression, and epithelial mesenchymal transition and stem cell markers in pancreatic cancer. All pictures show positive expression for each marker (× 200). A: Snail; B: Vimentin; C: E-cadherin; D: N-cadherin; E: CD24; F: CD44; G: CD133; H: EpCAM. DCLK1: Doublecortin and CaM kinase-like-1; EpCAM: Epithelial cell adhesion molecule.

Table 1 Clinicopathological characteristics of the patients

Characteristic	*n*
Age	
Median (range)	70 (34-85)
Sex	
Male	66
Female	70
Location	
Head	80
Body-tail	56
Tumor size in cm	
Median (range)	3 (1-18)
Surgery	
Pancreaticoduodenectomy	76
Distal pancreatectomy	54
Total pancreatectomy	6
Histological differentiation	
G1	20
G2	89
G3	17
G4	10
AJCC staging system	
Ⅰ A	5
Ⅰ B	15
Ⅱ A	46
Ⅱ B	56
Ⅲ	3
Ⅳ	11
Lymph node	
N0	70
N1	66
Adjuvant therapy	
Yes	96
No	40
Resection margin status	
R0	86
R1	35
R2	15

AJCC: American Joint Committee on Cancer.

level, and expression of DCLK-1, Snail, E-cadherin, N-cadherin, vimentin, CD24, CD44, CD133 and EpCAM. For patients with preoperative jaundice, we used the preoperative serum CA19-9 data that were obtained after the jaundice had been reduced. At our medical center, endoscopic or percutaneous bile duct drainage is usually performed in patients with jaundice. For all patients, the CA19-9 level that was used in the analysis was measured when the total bilirubin level was < 5 mg/dL.

Statistical analysis

Categorical variables were compared using the χ^2 test or Fisher's exact test. Survival was calculated using the Kaplan-Meier method, and comparisons between groups were carried out by the log-rank test. *P* values < 0.05 were considered to be statistically significant. Variables with a significance of $P < 0.05$ on univariate analysis were included in the multivariate regression analysis to identify factors associated with survival after surgery. Statistical analyses were performed using SAS version 11.0 software (SAS Institute, Inc., Cary, NC, United States).

RESULTS

Characteristics of patients with resected PDAC

Characteristics of the patients who underwent surgery for PDAC are shown in Table 1. All patients were followed for survival, and the median follow-up period was 21.0 mo (range, 2.3-175.2 mo). The median overall survival time (MST) was 27.1 mo. The actuarial 3- and 5-year survival rates were 39.9% and 26.6%, respectively. Of the 136 total patients, 96 underwent adjuvant chemotherapy (5-fluorouracil: *n* = 1; tegafur-uracil: *n* = 28; gemcitabine: *n* = 46; S-1: *n* = 21).

Expression of DCLK1 and its effect on survival

Of the 136 total patients, 66 (48.5%) were positive for DCLK1 expression and 70 (51.5%) were negative for DCLK1 expression. The MST of the DCLK1-positive patients was 18.7 mo, while that of that DCLK1-negative patients was 49.5 mo. The MST of the DCLK1-

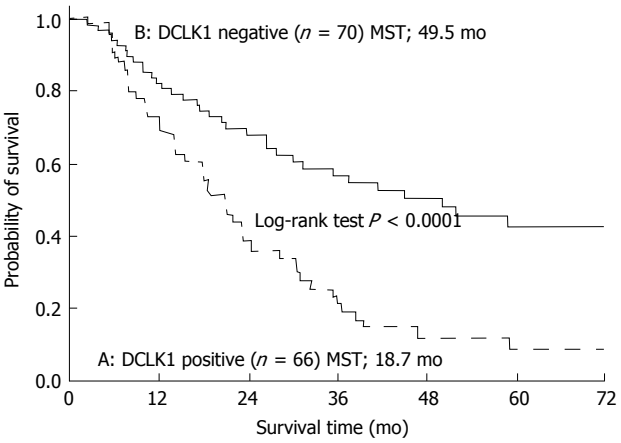

Figure 3 Overall survival of patients according to doublecortin and CaM kinase-like-1 expression. A: The MST of patients with DCLK1-positive tumors was 18.7 mo; B: That of patients with DLCK1-negative tumors was 49.5 mo. The MST of patients with DCLK1 positivity was significantly shorter than that of patients with DCLK1 negativity ($P < 0.0001$). DCLK1: Doublecortin and CaM kinase-like-1; MST: Median overall survival time.

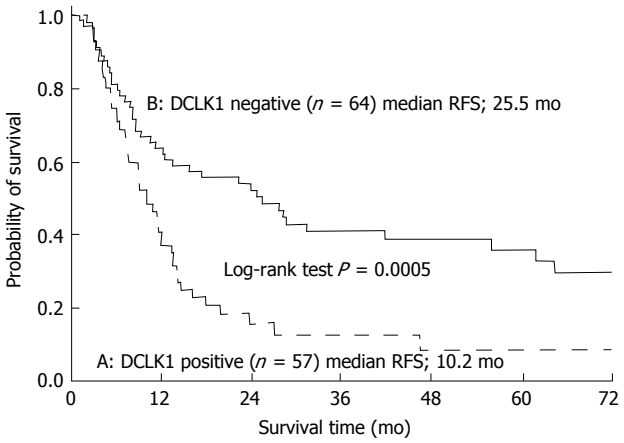

Figure 4 Relapse-free survival of patients according to doublecortin and CaM kinase-like-1 expression, excluding patients with macroscopic residual tumor. A: RFS of patients with DCLK1 positivity was 10.2 mo; B: That of patients with DCLK1 negativity was 25.5 mo. Relapse of patients with DCLK1 positivity was significantly shorter than that of patients with DCLK1 negativity ($P = 0.0005$). DCLK1: Doublecortin and CaM kinase-like-1; RFS: Relapse-free survival.

positive patients was significantly shorter than that of the DCLK1 -negative patients ($P < 0.0001$; Figure 3).

We examined relapse-free survival (RFS) and recurrent patterns of 121 patients, excluding patients with macroscopic residual tumor. Among these 121 patients, 57 were positive for DCLK1 expression and 64 patients were negative for DCLK1 expression. The DCLK1-positive patients relapsed more frequently, with 46 (80.7%) compared to the 40 (62.5%) DCLK1-negative patients who relapsed ($P = 0.0438$). The DCLK1-positive patients also had significantly shorter RFS than the DCLK-negative patients ($P = 0.0005$; Figure 4). Furthermore, of the 46 recurrent patients with DCLK1-positive tumors, 17 (37.0%) had local recurrence and 29 (63.0%) had distant metastasis. Of the 40 recurrent patients with DCLK1-negative tumors, 16 (40.0%) had local recurrence and 24 (60.0%) had distant metastasis. These results did not show significant difference for the recurrent pattern ($P = 0.82$).

Association of DCLK1 expression with clinicopathological factors

Table 2 shows the association of DCLK1 expression with clinicopathological factors, including EMT and CSC markers. The factors showing a significant correlation with positive DCLK1 expression were histological grade ($P = 0.0290$), high preoperative serum CA19-9 level ($P = 0.0060$), and EpCAM expression ($P = 0.0235$). Furthermore, referring to past literature[16], we examined the combination of CSC markers and found that triple-positive CD44/CD24/EpCAM expression was significantly correlated with DCLK1 expression ($P = 0.0139$).

Survival analysis of clinicopathological factors, including EMT and CSC markers, in resected PDAC

Table 3 shows the results of the univariate and multivariate survival analyses. Tumor size, histological grade, tumor grade (T) category, node (N) category, preoperative serum CA19-9 level, preoperative serum SPan-1 level, adjuvant therapy, resection margin status, and the expression of DCLK1, Snail, E-cadherin, N-cadherin, vimentin, CD24, CD44, CD133, and EpCAM were evaluated. On univariate analysis, five factors were significantly associated with worse overall survival: histological grade of G2 to G4 ($P = 0.0091$), high preoperative serum SPan-1 level ($P = 0.0034$), R1/2 factor ($P < 0.0001$), positive expression of DCLK1 ($P < 0.0001$) or CD44 ($P = 0.0245$). On multivariate analysis, R1/2 (OR = 2.019, 95%CI: 1.380-2.933; $P = 0.0004$) and positive DCLK1 expression (OR = 1.848; 95%CI: 1.2854-2.661; $P = 0.0009$) were independent factors of poor prognosis.

DISCUSSION

In the present study, we performed immunohistochemistry to analyze the expression of DCLK1 and clinicopathological variables, including EMT and CSC markers, to determine their correlation with survival in 136 patients with PDAC. DCLK1 expression was found to be significantly associated with the expression of EpCAM and the triple-positive expression of CD44/CD24/EpCAM. Moreover, DCLK1 expression was identified as an independent prognostic factor in resected PDAC. These findings suggest that DCLK1 may have a crucial prognostic role in the acquisition of stemness.

DCLK1, a putative marker of intestinal and pancreatic stem cells, is upregulated in various solid tumors, including colorectal, pancreatic, breast and prostate cancers, when compared to paired normal tissues[8-17]. Furthermore, recent reports indicated that DCLK1 can be used as a prognostic factor in colorectal

Table 2 Association between doublecortin and CaM kinase-like-1 expression and clinicopathological factors in resected pancreatic ductal adenocarcinoma *n* (%)

Characteristic	DCLK-1, *n* = 136		*P* value
	Positive, *n* = 66	Negative, *n* = 70	
Tumor size in cm			0.2962
< 2	11 (16.7)	17 (24.3)	
⩾ 2	55 (83.3)	53 (75.7)	
Histological grade			0.0290
G1	5 (7.6)	15 (21.4)	
G2-4	61 (92.4)	55 (78.6)	
T category			0.4326
T1/T2	14 (21.2)	19 (27.1)	
T3/T4	52 (78.8)	51 (72.9)	
N category			1.00
N0	34 (51.5)	37 (52.9)	
N1	32 (48.5)	33 (47.1)	
Serum CA19-9 level			0.0060
Normal	14 (21.2)	31 (44.3)	
Elevated	52 (78.8)	39 (55.7)	
Serum SPan-1 level			
Normal	23 (34.8)	34 (48.6)	0.1198
Elevated	43 (65.2)	36 (51.4)	
Residual tumor			0.2148
R0	38 (57.6)	48 (68.6)	
R1/2	28 (42.4)	22 (31.4)	
Snail			0.1237
Positive	41 (62.1)	34 (48.6)	
Negative	25 (37.9)	36 (51.4)	
E-cadherin			0.1151
Positive	31 (47.0)	23 (32.9)	
Negative	35 (53.0)	47 (67.1)	
N-cadherin			0.5967
Positive	23 (34.8)	28 (40.0)	
Negative	43 (65.2)	42 (60.0)	
Vimentin			0.5232
Positive	6 (9.1)	4 (5.7)	
Negative	60 (90.9)	66 (94.3)	
CD24			0.3758
Positive	27 (40.9)	23 (32.9)	
Negative	39 (59.1)	47 (67.1)	
CD44			1.00
Positive	49 (74.2)	52 (74.3)	
Negative	17 (25.8)	18 (25.7)	
EpCAM			0.0235
Positive	46 (69.7)	35 (50.0)	
Negative	20 (30.3)	35 (50.0)	
CD133			0.8301
Positive	12 (18.2)	14 (20.0)	
Negative	54 (81.8)	56 (80.0)	
CD24+CD44+EpCAM+			0.0139
Positive	18 (27.3)	7 (10.0)	
Negative	48 (72.7)	63 (90.0)	

DCLK1: Doublecortin and CaM kinase-like-1; EpCAM; Epithelial cell adhesion molecule; PDAC: Pancreatic ductal adenocarcinoma.

cancer[18,19]. However, no reports have yet indicated a correlation between DCLK1 expression and the prognosis of patients with PDAC.

Cells with positive DCLK1 expression showed CSC properties in pre-invasive pancreatic cancer[20]. In addition, small interfering (si)RNA-mediated knockdown of DCLK1 resulted in the upregulation of microRNA (miR)-200a, an inhibitor of EMT, and the corresponding upregulation of E-cadherin following the downregulation of ZEB1 and ZEB2 in both human pancreatic and colorectal cancer cells[7-17]. Weygant *et al*[9] demonstrated that siRNA-mediated knockdown of DCLK1 in clear cell renal carcinoma cells results in decreased expression of EMT and pluripotency factors, and significantly reduces the invasion, migration, focal adhesion, drug-resistance and clonogenic capacities of cells. Chandrakesan *et al*[10] reported that DCLK1 is critically involved in facilitating intestinal tumorigenesis by enhancing pluripotency and EMT factors in adenomatous polyposis coli (APC) mutant intestinal tumors. Sureban *et al*[21] indicated that XMD8-92 treatment of pancreatic tumors resulted in the inhibition of DCLK1 and downstream oncogenic pathways (*i.e.*, EMT, pluripotency, angiogenesis and anti-apoptotic pathways). These findings suggest that DCLK1 expression in human pancreatic cancer might directly regulate EMT, pluripotency and angiogenesis, and is significantly associated with survival. Although the abovementioned investigations on the molecular mechanisms of DCLK1 are all very important, we felt that there was a lack of reports on DCLK1 expression and its prognostic value in clinical samples of PDAC. As such, we investigated this topic, and found that DCLK1 over-expression had a significant impact on survival.

The results of the current study also indicated that the expression of EMT markers, such as E-cadherin, N-cadherin, vimentin and Snail, was not associated with poor prognosis. Cates *et al*[22] reported that the expression of EMT markers in PDAC was not associated with the duration of survival. In contrast, Yamada *et al*[23] reported that EMT markers predicted the prognosis of pancreatic cancer and that the EMT markers were associated with portal vein invasion and lymph node metastasis. Other researchers have also indicated that the expression of ZEB1 in pancreatic cancer is associated with poor prognosis[24,25].

Furthermore, we investigated stem cell markers, such as CD24, CD44, CD133 and EpCAM, to see whether they were associated with poor prognosis. Only the expression of CD44 showed an association with worse prognosis in the univariate analysis, but this association was not seen in the multivariate analysis. Pancreatic CSCs were first described by Li *et al*[5] in 2007. In our study, pancreatic cancer cells with triple-positive expression of CD44/CD24/EpCAM comprised only 0.2% to 0.8% of all the pancreatic cancer cells, but they had a 100-fold higher tumorigenic potential than the non-tumorigenic cancer cells[5]. In addition, Ohara *et al*[16] reported that triple-positive CD44/CD24/EpCAM expression was not correlated with poor prognosis, but overlapped with poorly differentiated cells and possessed high proliferative potential in clinical pancreatic cancer. Furthermore, they showed that the presence of double-positive CD44/CD24 expression appeared to be correlated with poor prognosis[16]. Finally, Akita *et al*[26] reported that EpCAM was a significant prognostic factor in pancreatic cancer.

To elucidate the role of DCLK1, we also analyzed the association between DCLK1 expression and clinicopathological factors, including EMT and CSC

Table 3 Univariate and multivariate survival analyses in resected pancreatic ductal adenocarcinoma

Variable	Comparison	Univariate analysis			Multivariate analysis		
		n	MST in mo	*P* value	Hazard ratio	95%CI	*P* value
Tumor size in cm	< 2	28	36.6	0.0735			
	⩾ 2	108	23.8				
Histological grade	G1	20	Not reached	0.0091	1.362	0.844-2.318	0.2130
	G2-4	116	23.8				
T category	T1/T2	33	30.3	0.7279			
	T3/T4	103	28.27				
N category	N0	71	35.4	0.0505			
	N1	65	21.2				
Serum CA19-9	Normal	45	31.37	0.2057			
	Elevated	91	24.43				
Serum SPan-1	Normal	57	36.6	0.0034	1.286	0.905-1.840	0.1608
	Elevated	79	21.2				
Adjuvant therapy	No	30	23.3	0.21			
	Yes	96	30.3				
Resection margin status	R0	86	36.6	< 0.0001	2.019	1.380-2.933	0.0004
	R1/2	50	17.9				
DCLK1	Negative	70	50.1	< 0.0001	1.848	1.2854-2.661	0.0009
	Positive	66	21.0				
Snail	Negative	61	30.3	0.2377			
	Positive	75	26.57				
E-cadherin	Negative	82	26.57	0.5448			
	Positive	54	30.3				
N-cadherin	Negative	85	26.57	0.4568			
	Positive	51	36.03				
Vimentin	Negative	126	30.07	0.0659			
	Positive	10	17.9				
CD24	Negative	86	24.43	0.6359			
	Positive	50	30.3				
CD44	Negative	35	45.1	0.0245	1.267	0.855-1.919	0.2414
	Positive	101	24.43				
CD133	Negative	110	23.37	0.1485			
	Positive	26	36.6				
EpCAM	Negative	55	23.37	0.6580			
	Positive	81	30.07				

DCLK1: Doublecortin and CaM kinase-like-1; EpCAM: Epithelial cell adhesion molecule; MST: Median overall survival time; N: Node; PDAC: Pancreatic ductal adenocarcinoma; T: Tumor.

markers. Our results showed that positive EpCAM expression was significantly correlated with positive DCLK1 expression. Furthermore, examination of the combination of stem cell markers showed that the triple-positive expression of CD44/CD24/EpCAM was significantly correlated with positive DCLK1 expression in PDAC. In contrast, positive EMT marker expression was not associated with positive DCLK1 expression. These results suggest that PDAC with DCLK1 expression may gain biological malignant potential by acquiring stemness. Some investigators have demonstrated DCLK1 expression on tumor stem cells that continuously produce tumor progeny in the polyps of $APC^{Min/+}$ mice, with ablation of these DCLK1-positive tumor stem cells resulting in a marked regression of polyps without any apparent damage to the normal intestine[6]. These findings suggest that DCLK1 exists in pancreatic tumor cells with stemness and that targeting DCLK1-positive cells may be a very effective advanced therapy. Recently, Westphalen *et al*[27] reported that there is a possibility of DCLK1 positive cells being the origin of PDAC. Accordingly, it has been postulated that DCLK1 is not only associated with stemness but also with carcinogenesis. Further studies are needed to fully elucidate the role of DCLK1 in PDAC.

There are some limitations to the present study which must be considered when interpreting the findings. This study was conducted at a single institution, and it had a small sample size. Moreover, it was a retrospective evaluation. A prospective investigation with a larger sample size is needed to confirm the significance of DCLK1 expression.

In conclusion, positive DCLK1 expression was identified as an independent prognostic factor in PDAC. The expression of DCLK1 was found to be associated with the triple-positive expression of CD44/CD24/EpCAM as well as EpCAM expression. Collectively, these findings indicate that DCLK1 may play a crucial prognostic role in the acquisition of stemness.

COMMENTS

Background

Doublecortin and CaM kinase-like-1 (DCLK1) is a microtubule-associated kinase and has recently attracted much attention due to its recognized

importance as a cancer stem cell (CSC) marker. Several studies have demonstrated that DCLK1 expression is correlated with aggressiveness in various cancers. However, only few studies have investigated the correlation of DCLK1 expression with survival in pancreatic ductal adenocarcinoma (PDAC). It is therefore worthwhile to elucidate the effect of DCLK1 expression on the survival of patients with PDAC.

Research frontiers

It has been reported that knockdown of DCLK1 in pancreatic cancer cells resulted in tumor growth arrest and the downregulation of epithelial mesenchymal transition (EMT), pluripotency and angiogenesis. Furthermore, several studies have demonstrated that DCLK1 expression is correlated with aggressiveness in various cancers. By using this marker in clinical samples of PDAC, the authors were able to identify DCLK1 expression as an independent prognostic factor in resected PDAC.

Innovations and breakthroughs

The authors found that DCLK1 over-expression had a significant impact on survival in resected PDAC, using clinical samples of PDAC. Furthermore, their findings suggest the possibility that PDAC with DCLK1 expression may gain biological malignant potential by acquiring stemness.

Applications

The results of the present study suggest that DCLK1 exists in pancreatic tumor cells with stemness, and that targeting DCLK1-positive cells may be very effective advanced therapy.

Terminology

DCLK1 is a microtubule-associated kinase and has recently attracted much attention as an important CSC marker, and has been reported as a putative intestinal and pancreatic stem cell marker. Recently, it has been reported that DCLK1 expression in human pancreatic cancer might directly regulate EMT, pluripotency, and angiogenesis.

Peer-review

Although this study is retrospective in design, it is well structured and the subject is very interesting. The manuscript is correctly written and the conclusions are justified by the data.

REFERENCES

1 **Siegel R**, Naishadham D, Jemal A. Cancer statistics, 2012. *CA Cancer J Clin* 2012; **62**: 10-29 [PMID: 22237781 DOI: 10.3322/caac.20138]

2 **Ohmae S**, Takemoto-Kimura S, Okamura M, Adachi-Morishima A, Nonaka M, Fuse T, Kida S, Tanji M, Furuyashiki T, Arakawa Y, Narumiya S, Okuno H, Bito H. Molecular identification and characterization of a family of kinases with homology to Ca2+/calmodulin-dependent protein kinases I/IV. *J Biol Chem* 2006; **281**: 20427-20439 [PMID: 16684769 DOI: 10.1074/jbc.M513212200]

3 **May R**, Sureban SM, Hoang N, Riehl TE, Lightfoot SA, Ramanujam R, Wyche JH, Anant S, Houchen CW. Doublecortin and CaM kinase-like-1 and leucine-rich-repeat-containing G-protein-coupled receptor mark quiescent and cycling intestinal stem cells, respectively. *Stem Cells* 2009; **27**: 2571-2579 [PMID: 19676123 DOI: 10.1002/stem.193]

4 **May R**, Riehl TE, Hunt C, Sureban SM, Anant S, Houchen CW. Identification of a novel putative gastrointestinal stem cell and adenoma stem cell marker, doublecortin and CaM kinase-like-1, following radiation injury and in adenomatous polyposis coli/multiple intestinal neoplasia mice. *Stem Cells* 2008; **26**: 630-637 [PMID: 18055444 DOI: 10.1634/stemcells.2007-0621]

5 **Li C**, Heidt DG, Dalerba P, Burant CF, Zhang L, Adsay V, Wicha M, Clarke MF, Simeone DM. Identification of pancreatic cancer stem cells. *Cancer Res* 2007; **67**: 1030-1037 [PMID: 17283135 DOI: 10.1158/0008-5472.CAN-06-2030]

6 **Nakanishi Y**, Seno H, Fukuoka A, Ueo T, Yamaga Y, Maruno T, Nakanishi N, Kanda K, Komekado H, Kawada M, Isomura A, Kawada K, Sakai Y, Yanagita M, Kageyama R, Kawaguchi Y, Taketo MM, Yonehara S, Chiba T. Dclk1 distinguishes between tumor and normal stem cells in the intestine. *Nat Genet* 2013; **45**: 98-103 [PMID: 23202126 DOI: 10.1038/ng.2481]

7 **Sureban SM**, May R, Qu D, Weygant N, Chandrakesan P, Ali N, Lightfoot SA, Pantazis P, Rao CV, Postier RG, Houchen CW. DCLK1 regulates pluripotency and angiogenic factors via microRNA-dependent mechanisms in pancreatic cancer. *PLoS One* 2013; **8**: e73940 [PMID: 24040120 DOI: 10.1371/journal.pone.0073940]

8 **Sureban SM**, May R, Lightfoot SA, Hoskins AB, Lerner M, Brackett DJ, Postier RG, Ramanujam R, Mohammed A, Rao CV, Wyche JH, Anant S, Houchen CW. DCAMKL-1 regulates epithelial-mesenchymal transition in human pancreatic cells through a miR-200a-dependent mechanism. *Cancer Res* 2011; **71**: 2328-2338 [PMID: 21285251 DOI: 10.1158/0008-5472.CAN-10-2738]

9 **Weygant N**, Qu D, May R, Tierney RM, Berry WL, Zhao L, Agarwal S, Chandrakesan P, Chinthalapally HR, Murphy NT, Li JD, Sureban SM, Schlosser MJ, Tomasek JJ, Houchen CW. DCLK1 is a broadly dysregulated target against epithelial-mesenchymal transition, focal adhesion, and stemness in clear cell renal carcinoma. *Oncotarget* 2015; **6**: 2193-2205 [PMID: 25605241 DOI: 10.18632/oncotarget.3059]

10 **Chandrakesan P**, Weygant N, May R, Qu D, Chinthalapally HR, Sureban SM, Ali N, Lightfoot SA, Umar S, Houchen CW. DCLK1 facilitates intestinal tumor growth via enhancing pluripotency and epithelial mesenchymal transition. *Oncotarget* 2014; **5**: 9269-9280 [PMID: 25211188 DOI: 10.18632/oncotarget.2393]

11 **Vega KJ**, May R, Sureban SM, Lightfoot SA, Qu D, Reed A, Weygant N, Ramanujam R, Souza R, Madhoun M, Whorton J, Anant S, Meltzer SJ, Houchen CW. Identification of the putative intestinal stem cell marker doublecortin and CaM kinase-like-1 in Barrett's esophagus and esophageal adenocarcinoma. *J Gastroenterol Hepatol* 2012; **27**: 773-780 [PMID: 21916995 DOI: 10.1111/j.1440-1746.2011.06928.x]

12 **Liu YH**, Tsang JY, Ni YB, Hlaing T, Chan SK, Chan KF, Ko CW, Mujtaba SS, Tse GM. Doublecortin-like kinase 1 expression associates with breast cancer with neuroendocrine differentiation. *Oncotarget* 2016; **7**: 1464-1476 [PMID: 26621833 DOI: 10.18632/oncotarget.6386]

13 **Edge SB,** Byrd DR, Compton CC, Fritz AG, Greene FL, Trotti A, editors. AJCC cancer staging manual (7th ed). New York, NY: Springer; 2010

14 **Fred T,** Bosman ES, Sunil R, Ohgaki H. WHO Classification of Tumours of the Digestive System. International Agency for Research on Cancer 2010

15 **Murata A**, Amano R, Yamada N, Kimura K, Yashiro M, Nakata B, Hirakawa K. Prognostic predictive values of gemcitabine sensitivity-related gene products for unresectable or recurrent biliary tract cancer treated with gemcitabine alone. *World J Surg Oncol* 2013; **11**: 117 [PMID: 23710668 DOI: 10.1186/1477-7819-11-117]

16 **Ohara Y**, Oda T, Sugano M, Hashimoto S, Enomoto T, Yamada K, Akashi Y, Miyamoto R, Kobayashi A, Fukunaga K, Morishita Y, Ohkohchi N. Histological and prognostic importance of CD44(+)/CD24(+)/EpCAM(+) expression in clinical pancreatic cancer. *Cancer Sci* 2013; **104**: 1127-1134 [PMID: 23679813 DOI: 10.1111/cas.12198]

17 **Sureban SM**, May R, Mondalek FG, Qu D, Ponnurangam S, Pantazis P, Anant S, Ramanujam RP, Houchen CW. Nanoparticle-based delivery of siDCAMKL-1 increases microRNA-144 and inhibits colorectal cancer tumor growth via a Notch-1 dependent mechanism. *J Nanobiotechnology* 2011; **9**: 40 [PMID: 21929751 DOI: 10.1186/1477-3155-9-40]

18 **Gagliardi G**, Goswami M, Passera R, Bellows CF. DCLK1 immunoreactivity in colorectal neoplasia. *Clin Exp Gastroenterol* 2012; **5**: 35-42 [PMID: 22557932 DOI: 10.2147/CEG.S30281]

19 **Gao T**, Wang M, Xu L, Wen T, Liu J, An G. DCLK1 is up-regulated and associated with metastasis and prognosis in colorectal cancer.

J Cancer Res Clin Oncol 2016; **142**: 2131-2140 [PMID: 27520310 DOI: 10.1007/s00432-016-2218-0]

20 **Bailey JM**, Alsina J, Rasheed ZA, McAllister FM, Fu YY, Plentz R, Zhang H, Pasricha PJ, Bardeesy N, Matsui W, Maitra A, Leach SD. DCLK1 marks a morphologically distinct subpopulation of cells with stem cell properties in preinvasive pancreatic cancer. *Gastroenterology* 2014; **146**: 245-256 [PMID: 24096005 DOI: 10.1053/j.gastro.2013.09.050]

21 **Sureban SM**, May R, Weygant N, Qu D, Chandrakesan P, Bannerman-Menson E, Ali N, Pantazis P, Westphalen CB, Wang TC, Houchen CW. XMD8-92 inhibits pancreatic tumor xenograft growth via a DCLK1-dependent mechanism. *Cancer Lett* 2014; **351**: 151-161 [PMID: 24880079 DOI: 10.1016/j.canlet.2014.05.011]

22 **Cates JM**, Byrd RH, Fohn LE, Tatsas AD, Washington MK, Black CC. Epithelial-mesenchymal transition markers in pancreatic ductal adenocarcinoma. *Pancreas* 2009; **38**: e1-e6 [PMID: 18766116 DOI: 10.1097/MPA.0b013e3181878b7f]

23 **Yamada S**, Fuchs BC, Fujii T, Shimoyama Y, Sugimoto H, Nomoto S, Takeda S, Tanabe KK, Kodera Y, Nakao A. Epithelial-to-mesenchymal transition predicts prognosis of pancreatic cancer. *Surgery* 2013; **154**: 946-954 [PMID: 24075276 DOI: 10.1016/j.surg.2013.05.004]

24 **Bronsert P**, Kohler I, Timme S, Kiefer S, Werner M, Schilling O, Vashist Y, Makowiec F, Brabletz T, Hopt UT, Bausch D, Kulemann B, Keck T, Wellner UF. Prognostic significance of Zinc finger E-box binding homeobox 1 (ZEB1) expression in cancer cells and cancer-associated fibroblasts in pancreatic head cancer. *Surgery* 2014; **156**: 97-108 [PMID: 24929761 DOI: 10.1016/j.surg.2014.02.018]

25 **Kurahara H**, Takao S, Maemura K, Mataki Y, Kuwahata T, Maeda K, Ding Q, Sakoda M, Iino S, Ishigami S, Ueno S, Shinchi H, Natsugoe S. Epithelial-mesenchymal transition and mesenchymal-epithelial transition via regulation of ZEB-1 and ZEB-2 expression in pancreatic cancer. *J Surg Oncol* 2012; **105**: 655-661 [PMID: 22213144 DOI: 10.1002/jso.23020]

26 **Akita H**, Nagano H, Takeda Y, Eguchi H, Wada H, Kobayashi S, Marubashi S, Tanemura M, Takahashi H, Ohigashi H, Tomita Y, Ishikawa O, Mori M, Doki Y. Ep-CAM is a significant prognostic factor in pancreatic cancer patients by suppressing cell activity. *Oncogene* 2011; **30**: 3468-3476 [PMID: 21399662 DOI: 10.1038/onc.2011.59]

27 **Westphalen CB**, Takemoto Y, Tanaka T, Macchini M, Jiang Z, Renz BW, Chen X, Ormanns S, Nagar K, Tailor Y, May R, Cho Y, Asfaha S, Worthley DL, Hayakawa Y, Urbanska AM, Quante M, Reichert M, Broyde J, Subramaniam PS, Remotti H, Su GH, Rustgi AK, Friedman RA, Honig B, Califano A, Houchen CW, Olive KP, Wang TC. Dclk1 Defines Quiescent Pancreatic Progenitors that Promote Injury-Induced Regeneration and Tumorigenesis. *Cell Stem Cell* 2016; **18**: 441-455 [PMID: 27058937 DOI: 10.1016/j.stem.2016.03.016]

P- Reviewer: Huan C, Kang KM **S- Editor**: Gong ZM **L- Editor**: A **E- Editor**: Li D

World Journal of Gastroenterology

Submit a Manuscript: http://www.f6publishing.com

World J Gastroenterol 2017 August 21; 23(31): 5773-5779

DOI: 10.3748/wjg.v23.i31.5773

ISSN 1007-9327 (print) ISSN 2219-2840 (online)

ORIGINAL ARTICLE

Retrospective Study

Study to determine guidelines for pediatric colonoscopy

Shinichiro Yoshioka, Hidetoshi Takedatsu, Shuhei Fukunaga, Kotaro Kuwaki, Hiroshi Yamasaki, Ryosuke Yamauchi, Atsushi Mori, Hiroshi Kawano, Tadahiro Yanagi, Tatsuki Mizuochi, Kosuke Ushijima, Keiichi Mitsuyama, Osamu Tsuruta, Takuji Torimura

Shinichiro Yoshioka, Shuhei Fukunaga, Kotaro Kuwaki, Hiroshi Yamasaki, Ryosuke Yamauchi, Atsushi Mori, Hiroshi Kawano, Keiichi Mitsuyama, Osamu Tsuruta, Takuji Torimura, Division of Gastroenterology, Department of Medicine, Kurume University School of Medicine, Asahi-machi Kurume, Fukuoka 830-0011, Japan

Hidetoshi Takedatsu, Department of Gastroenterology and Medicine, Fukuoka University Faculty of Medicine, Jonan-ku, Fukuoka 814-0180, Japan

Tadahiro Yanagi, Tatsuki Mizuochi, Kosuke Ushijima, Department of Pediatrics and Child Health Kurume University School of Medicine, Asahi-machi Kurume, Fukuoka 830-0011, Japan

Author contributions: Yoshioka S and Takedatsu H contributed equally to this work; Yoshioka S, Takedatsu H, Mitsuyama K and Torimura T designed the research; Yoshioka S, Takedatsu H, Fukunaga S, Kuwaki K, Yamasaki H, Yamauchi R, Mori A, Kawano H, Tsuruta O, Yanagi T, Mizuochi T and Ushijima K performed the research; Yoshioka S and Takedatsu H analyzed the data; Yoshioka S and Takedatsu H wrote the paper.

Institutional review board statement: The study was reviewed and approved by The Ethical Committee of Kurume University.

Informed consent statement: Patients were not required to give informed consent to the study because the analysis used anonymous clinical data that were obtained after each patient agreed to treatment by written consent. For full disclosure, the details of the study are published on the home page of Kurume University.

Conflict-of-interest statement: None of the authors have any conflict of interest disclosures to make.

Data sharing statement: No additional data are available.

Manuscript source: Unsolicited manuscript

Correspondence to: Hidetoshi Takedatsu, MD, PhD, Department of Gastroenterology and Medicine, Fukuoka University Faculty of Medicine, 7-45-1 Nanakuma, Jonan-ku, Fukuoka 814-0180, Japan. takedatsu@fukuoka-u.ac.jp
Telephone: +81-92-8011011
Fax: +81-92-8742663

Received: April 27, 2017
Peer-review started: April 27, 2017
First decision: June 8, 2017
Revised: June 23, 2017
Accepted: July 12, 2017
Article in press: July 12, 2017
Published online: August 21, 2017

Abstract

AIM

To investigated characteristics, diagnosis, bowel-cleansing preparation, sedation, and colonoscope length and diameter in Japanese pediatric patients receiving total colonoscopy.

METHODS

The present study evaluated consecutive patients aged ⩽ 15 years who had undergone their first colonoscopy in Kurume University between January 2007 and February 2015. Data were retrospectively analyzed. We identified 110 pediatric patients who had undergone colonoscopy that had reached the cecum, allowing the observation of the total colon.

RESULTS
Hematochezia, abdominal pain, and diarrhea were the most common symptoms. For bowel-cleansing preparation, pediatric patients aged ⩽ 12 years were treated with magnesium citrate, and patients aged 13-15 years were treated with polyethylene glycol 4000. For sedation, thiamylal with pentazocine, which has an analgesic effect, was used in patients aged ⩽ 6 years, and midazolam with pentazocine was used in patients aged ⩾ 7 years. Regarding the choice of endoscope, short and thin endoscopes were selected for younger patients, particularly patients aged ⩽ 3 years. Positive diagnoses were made in 78 patients (70.9%). Inflammatory bowel disease (n = 49, 44.5%), including ulcerative colitis (n = 37, 33.6%) and Crohn's disease (n = 12, 10.9%), was the most common diagnosis.

CONCLUSION
Colonoscopy offers a high diagnostic capability for pediatric patients with gastrointestinal symptoms. The selection of appropriate management the performance of colonoscopy is important in pediatric patients.

Key words: Pediatric endoscopy; Sedation; Bowel cleansing preparation; Inflammatory bowel disease; Complication

Core tip: A guideline for pediatric colonoscopy management have yet to be established in Japan. We investigated clinical characteristics, diagnostic utility, bowel cleansing preparation, sedation, and colonoscope length and diameter under 15 years of age who had undergone their first colonoscopy in our institution. Our results revealed that the symptoms associated with the indication of pediatric colonoscopy were hematochezia, abdominal pain, and diarrhea. Positive diagnoses were obtained in a majority of pediatric patients. More than 40% of patients were diagnosed with inflammatory bowel disease. Thus, our findings demonstrate the utility of colonoscopy as a diagnostic tool in pediatric patients with gastrointestinal symptoms.

Yoshioka S, Takedatsu H, Fukunaga S, Kuwaki K, Yamasaki H, Yamauchi R, Mori A, Kawano H, Yanagi T, Mizuochi T, Ushijima K, Mitsuyama K, Tsuruta O, Torimura T. Study to determine guidelines for pediatric colonoscopy. *World J Gastroenterol* 2017; 23(31): 5773-5779 Available from: URL: http://www.wjgnet.com/1007-9327/full/v23/i31/5773.htm DOI: http://dx.doi.org/10.3748/wjg.v23.i31.5773

INTRODUCTION

Colonoscopy is routinely performed in infants and children for the evaluation and treatment of diarrhea, weight loss, abdominal pain, unexplained iron deficiency anemia, abdominal pain, or rectal bleeding[1]. Colonoscopy has utility as a diagnostic and therapeutic tool for pediatric patients[2]. Recently, the American Society for Gastrointestinal Endoscopy (ASGE) and the North American Society for Pediatric Gastroenterology, Hepatology and Nutrition published modifications of their guidelines for pediatric patients, in which clear indications for colonoscopy in children were recommended[2]. As the diagnosis of bowel diseases, including inflammatory bowel disease (IBD) and polyposis syndrome, is important in children as well as adults, it has become increasingly necessary to perform total colonoscopy in pediatric patients[3,4].

There are limited pediatric data regarding the complication rates of pediatric colonoscopy. Thakkar *et al*[5] reported a complication rate of 1.1%, which was higher than that of adult colonoscopy (0.4%), in a multi-center retrospective study[6]. Furthermore, pediatric colonoscopy is associated with a greater risk of serious complications compared with that in adults, due to the high level of technical difficulty, low compliance with bowel cleansing, and uncooperativeness during the procedure. The success of total colonoscopy relies on suitable bowel-cleansing preparation, appropriate sedation for painless and safe colonoscopy, and the choice of an appropriate endoscope.

Bowel preparation regimens for pediatric colonoscopy have yet to be standardized and vary among medical centers. Propofol is commonly used for sedation during pediatric endoscopy[7]. The use of midazolam, fentanyl, meperidine, ketamine, and ketofol in pediatric colonoscopy have also been reported[8]. The dosing of sedative drugs is based on patient weight and is titrated by response, allowing adequate time between doses to assess the effects and the need for additional medication. Furthermore, there are few published data to support the choice of colonoscope in Japanese pediatric patients. Recommendations based on clinical experience suggest the use of a standard or pediatric colonoscope in patients weighing 12-15 kg, the use of infant or standard adult gastroscopes in patients weighing 5-12 kg, and the use of ultra-thin gastroscopes in patients weighing < 5 kg[9].

Here we conducted a retrospective study of medical records to assess the appropriate management for performing colonoscopy in pediatric patients at our hospital. The aims of the present study were to assess the following: (1) patient clinical characteristics; (2) bowel-cleansing preparation; (3) sedation; (4) the choice of endoscope; and (5) the diagnostic utility of colonoscopy in pediatric patients.

MATERIALS AND METHODS

Study protocol and data collection

Colonoscopies were performed in children after clinical evaluation by pediatric gastroenterologists at Kurume University School of Medicine. In the present study, we retrospectively reviewed the medical records of

Table 1 Characteristics of pediatric patients

Total number of patients		*n* = 110
Age (yr)	0	3
	1–3	14
	4–6	11
	7–9	19
	10–12	32
	13–15	31
Gender	Male	61
	Female	49
Reason for endoscopy	Hematochezia	62
	Abdominal pain	20
	Diarrhea	19
	Anemia	2
	Anal fistula	2
	Genital ulcer	2
	Other	2
Diagnosis	Ulcerative colitis	37
	Crohn's disease	12
	No specific colitis	13
	Juvenile polyp	7
	Normal	32
	Other	9

pediatric patients aged ⩽ 15 years who had undergone their first diagnostic total colonoscopy between January 1, 2007 and February 28, 2015. Endoscopic procedures were performed by two advanced experienced endoscopists. The present study protocol was approved by the Human Ethics Committee of Kurume University School of Medicine.

Bowel-cleansing preparation

Magnesium citrate (Magcorol), polyethylene glycol (PEG) 4000, and glycerin enema (GE), which are licensed for bowel-cleansing preparation in Japan, were used. Bowel-cleansing preparation protocols for colonoscopy in pediatric patients were selected depending on patient age, body weight, and clinical state by pediatric gastroenterologists.

Sedation

Sedation methods were selected at the discretion of pediatric gastroenterologists. Thiamylal, the combination of thiamylal and pentazocine, midazolam, and the combination of midazolam and pentazocine were used for sedation in pediatric patients. Continuous pulse oximetry and heart rate monitoring were performed throughout sedation to monitor patient vital signs. The initial intravenous dose of thiamylal was 20-30 mg/kg, with an additional 10 mg depending on patient condition. The initial intravenous dose of midazolam was 0.025-0.1 mg/kg, with an additional 1 mg depending on patient condition. Pentazocine was intravenously administered at a dose of 0.5 mg/kg in combination with thiamylal or midazolam.

Endoscopes

Endoscopes were selected based on patient age and body size by endoscopists. Carbon dioxide was used as much as possible during colonoscopy. Mucosal biopsies were not routinely performed and were performed based on the presence of macroscopic abnormalities and endoscopist experience.

RESULTS

Characteristics of pediatric patients who underwent colonoscopy

Children aged ⩽ 15 years who were referred for gastrointestinal symptoms with an indication for diagnostic colonoscopy were recruited between January 1, 2007 and February 28, 2015 (Table 1). A total of 110 individual pediatric patients, including patients aged < 1 year (*n* = 3, 2.7%), 1-3 years (*n* = 14, 12.7%), 4-6 years (*n* = 11, 10.0%), 7-9 years (*n* = 19, 17.3%), 10-12 years (*n* = 32, 29.1%), and 13-15 years (*n* = 31, 28.2%), were prepared for total colonoscopy by pediatric gastroenterologists. All 110 patients (100%) in whom colonoscopy reached the cecum, allowing the evaluation of the total colon from the cecum to the rectum, were included in the present study to evaluate factors related to total colonoscopy success. No complications were reported in any of the included cases. The terminal ileum was observed for diagnostic purposes in the majority of patients (105/110, 95.5%).

In the present study, 61 boys (55.5%) and 49 girls (44.5%) were included, with a male-to-female ratio of 1.2:1. Hematochezia, abdominal pain, and diarrhea were the most common indications for pediatric endoscopy, accounting for 62 (56.4%), 20 (18.1%), and 19 (17.3%) patients, respectively. Other presentations were anemia (*n* = 2, 1.8%), anal fistula (*n* = 2, 1.8%), genital ulcer (*n* = 2, 1.8%), and others (*n* = 2, 1.8%). Final diagnoses included IBD, comprising ulcerative colitis (UC; *n* = 37, 33.6%) and Crohn's disease (CD; *n* = 12, 10.9%), non-specific colitis (NSC; *n* = 13, 11.8%), juvenile polyp (JP; *n* = 7, 6.4%), and normal (*n* = 32, 29.1%). Of the 49 patients with IBD, UC (*n* = 37, 75.5%) was more common than CD (*n* = 12, 24.5%). Other diagnoses (*n* = 9, 8.2%) included Peutz-Jeghers syndrome (*n* = 3, 2.7%), familial adenomatous polyposis (*n* = 2, 1.8%), Behçet's disease (*n* = 1, 0.9%), diverticulitis (*n* = 1, 0.9%), internal hemorrhoids (*n* = 1, 0.9%), and venous angioma syndrome (*n* = 1, 0.9%).

Use of bowel-cleansing preparation and sedation

Table 2 shows the preparation methods used for bowel cleansing. Bowel-cleansing preparation protocols for colonoscopy in pediatric patients were selected by pediatric gastroenterologists. In all cases, bowel-cleansing preparation was effective and satisfactory. A total of 74 patients (67%) used Magcorol as a preparation. The remaining 27 patients (24.5%) used PEG-4000. GE alone was used in five patients (4.6%), all of whom had chronic diarrhea. The method of bowel preparation used was not recorded in four patients (3.6%). The majority of patients aged ⩽ 12 years (63/79, 84.0%) were treated with Magcorol, and the

Table 2 Bowel cleansing preparation *n* (%)

Age	*n*	Magcorol	PEG	GE	Unknown
0	3	2 (66.7)	0 (0.0)	1 (33.3)	0 (0.0)
1-3	14	10 (71.4)	1 (7.1)	1 (7.1)	2 (14.3)
4-6	11	9 (81.8)	0 (0.0)	1 (9.1)	1 (9.1)
7-9	19	15 (78.9)	2 (10.5)	1 (5.3)	1 (5.3)
10-12	32	27 (84.4)	4 (12.5)	1 (3.1)	0 (0.0)
13-15	31	11 (35.5)	20 (64.5)	0 (0.0)	0 (0.0)
Total	110	74 (67.3)	27 (24.5)	5 (4.6)	4 (3.6)

Magcorol: Magnesium citrate; PEG: Polyethylene glycol; GE: Glycerin enema.

majority of patients aged 13-15 years were treated with PEG-4000.

Sedation was used in 85 patients (77.3%) for colonoscopy (Table 3). Thiamylal, the combination of thiamylal and pentazocine, midazolam, and the combination of midazolam and pentazocine were predominantly used for sedation at our hospital. More than half of the patients aged ⩽ 6 years (15/28, 53.6%) were sedated with thiamylal, and the majority of patients aged ⩾ 7 years (52/82, 63.4%) were sedated with midazolam. Pentazocine in combination with thiamylal or midazolam was used for analgesia in 78 patients (70.9%). Sedation and analgesia were not required in 20 patients aged ⩾ 10 years (20/110, 18.2%). All patients were monitored by pediatric gastroenterologists and recovered after the procedure. No complications such as hypoxia or allergy occurred during the sedation.

Characteristics of colonoscopes used in pediatric patients

Two types of colonoscope, 1030 mm and 1330 mm, are used at our university. Endoscopes with a length of 1030 mm, typically used for upper endoscopy, were used for colonoscopy in 16 patients (14.5%; Table 4). In detail, all patients aged < 1 year (3/3, 100%) and the majority of patients aged 1-3 years (11/14, 78.6%) underwent colonoscopy using a 1030-mm endoscope due to their small body size. The majority of patients aged 4-6 years (9/11, 81.8%) and all patients aged ⩾ 7 years (82/82, 100%) underwent colonoscopy with a 1330-mm endoscope. Furthermore, endoscopes with six different shaft diameters were used in the present study (Table 5). We selected endoscopes with diameters of 11.7 mm (*n* = 26, 23.6%), 11.3 mm (*n* = 59, 53.6%), 9.2 mm (*n* = 9, 8.2%), 5.4 mm (*n* = 8, 7.3%), 10.5 mm (*n* = 5, 4.5%), and 9.8 mm (*n* = 3, 2.7%), according to patient age and clinical status. Endoscopes with a diameter of 5.4 mm, considered ultra-thin and typically used for nasal endoscopy, were used in all patients aged < 1 year (3/3, 100%) and in one-third of patients aged 1-3 years (5/14, 35.7%). The majority of patients aged ⩾ 7 years (total 82 patients) underwent colonoscopy using endoscopes with a diameter of 11.3 mm (53/82, 64.6%) or 11.7 mm (25/82, 30.5%). No serious complications such as bleeding or perforation occurred during colonoscopy in any patient. Thus, endoscopes matched according to patient body size and age were appropriately selected by endoscopists in the present study.

Association between presenting symptoms and final diagnoses

A total of 78 patients (78/110, 70.9%) had a positive diagnosis following colonoscopy, whereas no abnormalities were observed in 32 patients (29.1%). IBD, comprising UC (37/110, 33.6%) and CD (12/110, 10.9%), was the most common diagnosis. Additional findings included JP (7/110, 9.0%) and others (18/110, 23.1%). Hematochezia, which was the most common indication for pediatric colonoscopy (63/110, 57.3%), demonstrated a high positive diagnosis rate (54/63, 85.7%), particularly for UC (34/63, 54.0%). Abdominal pain and diarrhea were predominantly present in normal cases (50.0% and 52.6%, respectively) and CD (30.0% and 21.1%, respectively). These results demonstrate that hematochezia, abdominal pain, and diarrhea as important indications for total colonoscopy in pediatric patients. Further studies of pediatric colonoscopy are required to validate these findings regarding the associated between symptoms and final diagnoses (Table 6).

DISCUSSION

PEG is the most commonly used bowel-cleansing agent for bowel preparation regimens in children. Previous reports have demonstrated that PEG-3350 with simethicon has greater efficacy than other methods of pediatric bowel cleansing[10]. However, a proportion of pediatric patients are unlikely to ingest sufficient volumes due to its noxious taste[11]. The majority of prospective and comparative studies of bowel preparation for pediatric colonoscopy have been performed at single centers[11-13]. Recently, a randomized, blinded trial was conducted for bowel-cleansing preparation in pediatric patients who were randomly assigned to receive PEG 4000 with simethicon (PEG-S group), PEG-4000 with citrates and simethicone plus bisacodyl (PEG-CS + Bisacodyl group), PEG-3350 with ascorbic acid (PEG-Asc group), or sodium picosulfate plus magnesium oxide and citric acid (NaPico + MgCit group)[14]. In this study, PEG-CS + Bisacodyl, PEG-Asc, and NaPico + MgCit were all found to be non-inferior to PEG-S with respect to bowel-cleansing efficacy. NaPico + MgCit was reported as the most appropriate regimen for bowel preparation in children due to higher tolerability and a greater acceptability profile. PEG-4000 is the most commonly used agent in bowel-cleansing preparations for adult colonoscopy in Japan[15]. Only two kinds of bowel-cleansing preparation, PEG-4000 and Magcorol, are routinely used for children in Japan. The results of the present study demonstrated that the use of Magcorol with magnesium citrate has efficacy in bowel cleansing

Table 3 Sedation *n* (%)

Age	*n*	Thiamylal	Thiamylal + Pentazocine	Midazolam	Midazolam + Pentazocine	None	Unknown
0	3	0 (0.0)	1 (33.3)	0 (0.0)	2 (66.7)	0 (0.0)	0 (0.0)
1-3	14	1 (7.1)	7 (50.0)	1 (7.1)	3 (21.4)	0 (0.0)	2 (14.3)
4-6	11	1 (9.1)	5 (45.5)	0 (0.0)	4 (36.4)	0 (0.0)	1 (9.1)
7-9	19	0 (0.0)	2 (10.5)	0 (0.0)	15 (78.9)	0 (0.0)	2 (10.5)
10-12	32	1 (3.1)	4 (12.5)	2 (6.3)	21 (65.6)	4 (12.5)	0 (0.0)
13-15	31	0 (0.0)	1 (3.2)	1 (3.2)	13 (41.9)	16 (38.7)	0 (0.0)
Total	110	3 (2.7)	20 (18.2)	4 (3.6)	58 (52.7)	20 (18.2)	5 (4.5)

Table 4 Length of endoscope *n* (%)

Age	*n*	1030 mm	1330 mm
0	3	3 (100.0)	0 (0.0)
1-3	14	11 (78.6)	3 (21.4)
4-6	11	2 (18.2)	9 (81.8)
7-9	19	0 (0.0)	19 (100.0)
10-12	32	0 (0.0)	32 (100.0)
13-15	31	0 (0.0)	31 (100.0)
Total	110	16 (14.5)	94 (85.5)

and has greater tolerability in children aged ⩽ 12 years (63/79, 79.7%).

The purpose of sedation is to reduce patient anxiety and discomfort and the risk of injury during the procedure. The level of sedation targeted and the sedative agents chosen depend on the characteristics of the endoscopic procedure, including the type and length of procedure, degree of invasiveness, and endoscopist experience. Physiological differences between pediatric and adult patients alter the risks of potentially serious complications during sedation. Propofol, a phenol derivative with sedative, hypnotic, and anesthetic properties without analgesic effects, is routinely used for pediatric sedation[7]. The major disadvantage of propofol is its narrow therapeutic range and the risk of inadvertent anesthesia. Therefore, although, propofol is routinely administered by anesthesiologists, its use by non-anesthesiologists remains controversial[16,17]. In fact, propofol is rarely used in Japan because pediatric colonoscopy is performed without the presence of an anesthesiologist. Thiamylal, which has sedative, anticonvulsant, and hypnotic effects, is a barbiturate derivative invented in the 1950s. Thiamylal has been used for the induction of surgical anesthesia[18] and as an anticonvulsant to counteract the side-effects of other anesthetic agents[19]. We used thiamylal in more than half of the pediatric patients aged ⩽ 6 years (15/28, 53.6%) because it has a strong sedative effect while also being short-acting. Midazolam is a small, water-soluble benzodiazepine with anxiolytic, amnestic, sedative, muscle-relaxant, and anticonvulsant properties, which is widely used for sedation but generally considered to be insufficient as a monotherapy. Pentazocine is a synthetically prepared prototypical mixed agonist-antagonist narcotic drug of the benzomorphan class of opioids used to treat moderate-to-moderately severe pain. Pentazocine was used in our series as an analgesic agent, in combination with thiamylal (20/23, 87.0%) and midazolam (58/62, 93.5%). Although colonoscopy in adults has been performed without sedation at our hospital, no patient aged ⩽ 9 years and only 20 patients aged 10-15 years (20/63, 31.7%) received colonoscopy without sedation. The use of adequate sedation in pediatric patients is necessary to safely perform total colonoscopy.

The technical aspects of colonoscopy are similar between adults and children. However, adequate knowledge and good endoscopic technique are required due to a high rate of complications, the small body size of pediatric patients, and the excessive stretching of splenic and hepatic flexures associated with the use of thin endoscopes. Obvious differences between pediatric and adult colons are their length and diameter. The length of the colon is approximately 600 mm in patients aged 1 year, which increases to 1000 mm at 3 years, 1200 mm at 5 years, and finally reaches a length of 1500 mm in adults[20,21]. Variable insertion tube lengths (1030-1330 mm) and shaft diameters (5.6-11.8 mm) were used for pediatric colonoscopy. There are no published data to support colonoscope choice in children. Recommendations based on body weight have been published by the ASGE[9]. In general, the use of adult colonoscopes is acceptable in teenage patients. Smaller, more flexible colonoscopes are suitable for the majority of average-sized preschool- and elementary school-age children[22]. However, pediatric colonoscopes may be too large for children aged < 4 years[23]. In the present study, we recommended the use of a standard colonoscope in patients aged ⩾ 4 years, a standard adult gastroscope in patients aged 1-3 years, and an ultra-thin gastroscope in patients aged < 1 year. As data regarding body weight was not available for all patients, body weight-based analyses should be performed in future studies.

Common inductions for pediatric colonoscopy include chronic diarrhea, hematochezia, unexplained anemia, polyposis syndrome, and failure to thrive/weight loss[2]. In the present study, hematochezia, abdominal pain, and diarrhea were the most common presentations for pediatric colonoscopy referrals, corroborating the findings of a previous study[24]. Hematochezia was the most common symptom in patients with UC, whereas abdominal pain and diarrhea were the most common symptoms in CD patients. Compared with adults, pediatric patients are reported

Table 5 Shaft diameter of endoscope *n* (%)

Age	*n*	5.4 mm	9.2 mm	9.8 mm	10.5 mm	11.3 mm	11.7 mm
0	3	3 (100.0)	0 (0.0)	0 (0.0)	0 (0.0)	0 (0.0)	0 (0.0)
1-3	14	5 (35.7)	4 (28.6)	2 (14.3)	1 (7.1)	1 (7.1)	0 (0.0)
4-6	11	0 (0.0)	3 (27.3)	1 (9.1)	1 (9.1)	5 (45.5)	1 (9.1)
7-9	19	0 (0.0)	1 (5.3)	0 (0.0)	1 (5.3)	14 (73.7)	3 (15.8)
10-12	32	0 (0.0)	0 (0.0)	0 (0.0)	2 (6.3)	22 (68.8)	9 (28.1)
13-15	31	0 (0.0)	1 (3.2)	0 (0.0)	0 (0.0)	17 (54.8)	13 (41.9)
Total	110	8 (7.3)	9 (8.2)	3 (2.7)	5 (4.5)	59 (53.6)	26 (23.6)

Table 6 Symptoms and final diagnosis *n* (%)

	n	UC	CD	NSC	JP	Normal	Other
Hematochezia	63	34 (54.0)	1 (1.5)	6 (9.5)	7 (11.1)	9 (14.3)	6 (9.5)
Abdominal pain	20	1 (0.5)	6 (30.0)	2 (10.0)	0 (0.0)	10 (50.0)	1 (0.5)
Diarrhea	19	1 (5.3)	4 (21.1)	3 (15.7)	0 (0.0)	10 (52.6)	1 (5.3)
Anemia	2	1 (50.0)	0 (0.0)	0 (0.0)	0 (0.0)	1 (50.0)	0 (0.0)
Anal fistula	2	0 (0.0)	1 (50.0)	1 (50.0)	0 (0.0)	0 (0.0)	0 (0.0)
Genital ulcer	2	0 (0.0)	0 (0.0)	0 (0.0)	0 (0.0)	0 (0.0)	2 (100.0)
Other	2	0 (0.0)	0 (0.0)	0 (0.0)	0 (0.0)	2 (100.0)	0 (0.0)
Total	110	37 (33.6)	12 (10.9)	12 (10.9)	7 (6.4)	32 (29.1)	10 (9.1)

UC: Ulcerative colitis; CD: Crohn's disease; NSC: Non-specific colitis; JP: Juvenile polyp.

to have a higher frequency of positive findings resulting from colonoscopy[24-26]. In the present study, 71.9% (78/110) of patients had a positive diagnosis, including UC, CD, non-specific colitis, and JP. IBD consists of two major distinct disorders, CD and UC, and is characterized by chronic inflammation of the intestine as a result of undefined pathogenic mechanisms. In the present study, IBD (49/110, 44.5%) was the most common positive finding in pediatric colonoscopy patients. Community-based epidemiological studies have demonstrated a markedly higher incidence of IBD in Japanese and other Asian adults[27,28]. In pediatric patients, several studies have reported an increasing incidence of pediatric IBD[3,4]. In the present study, there were more UC patients than CD patients. IBD patients consistently presented with abdominal pain, hematochezia, or non-infected diarrhea. Therefore, the results of the present study indicate that colonoscopy has utility as a diagnostic tool for pediatric patients presenting with hematochezia, abdominal pain, or diarrhea. In addition, our finding suggests that the observation of terminal ileum is needed to diagnose IBD, especially CD.

In conclusion, the selection of appropriate management approaches before and during the performance of colonoscopy is important in pediatric patients. Colonoscopy has utility as a diagnostic tool for pediatric patients with gastrointestinal symptoms and may represent an important component of treatment strategies for early and appropriate treatment of pediatric patients.

COMMENTS

Background

Colonoscopy has utility as a diagnostic and therapeutic tool in both adults and pediatric patients. However, specific guidelines for the management of pediatric colonoscopy are not well established. They investigated clinical characteristics, diagnostic utility, bowel-cleansing preparation, sedation, and colonoscope length and diameter in pediatric patients receiving total colonoscopy.

Research frontiers

Although colonoscopy is commonly used as a diagnostic and therapeutic tool for adults and children. However, a guideline for pediatric colonoscopy management have yet to be established in Japan.

Innovations and breakthroughs

In this study, the authors investigated 110 patients under 15 years of age who had undergone their first colonoscopy in our institution between January 2007 and February 2015. These results showed the appropriate management of pediatric colonoscopy in bowel cleansing preparation, sedation, and the selection of colonoscopy. The authors also revealed that the symptoms associated with the indication of pediatric colonoscopy were hematochezia, abdominal pain, and diarrhea. Positive diagnoses were obtained in a majority of pediatric patients. More than 40% of patients were diagnosed with inflammatory bowel disease. Thus, our findings demonstrate the utility of colonoscopy as a diagnostic tool in pediatric patients with gastrointestinal symptoms.

Applications

This study suggests that colonoscopy has utility as a diagnostic tool for pediatric patients with gastrointestinal symptoms and may represent an important component of treatment strategies for early and appropriate treatment of pediatric patients.

Peer-review

The author mentioned the management and diagnosis of pediatric colonoscopy in many cases. This is a very important report.

REFERENCES

1 **Friedt M**, Welsch S. An update on pediatric endoscopy. *Eur J Med Res* 2013; **18**: 24 [PMID: 23885793 DOI: 10.1186/2047-783X-18-24]

2 **ASGE Standards of Practice Committee**, Lightdale JR, Acosta R, Shergill AK, Chandrasekhara V, Chathadi K, Early

D, Evans JA, Fanelli RD, Fisher DA, Fonkalsrud L, Hwang JH, Kashab M, Muthusamy VR, Pasha S, Saltzman JR, Cash BD; American Society for Gastrointestinal Endoscopy. Modifications in endoscopic practice for pediatric patients. *Gastrointest Endosc* 2014; **79**: 699-710 [PMID: 24593951 DOI: 10.1016/j.gie.2013.08.014]

3 **Ishige T,** Tomomasa T, Takebayashi T, Asakura K, Watanabe M, Suzuki T, Miyazawa R, Arakawa H. Inflammatory bowel disease in children: epidemiological analysis of the nationwide IBD registry in Japan. *J Gastroenterol* 2010; 45: 911-917 [DOI: 10.1007/s00535-010-0223-7]

4 **Wang XQ**, Zhang Y, Xu CD, Jiang LR, Huang Y, Du HM, Wang XJ. Inflammatory bowel disease in Chinese children: a multicenter analysis over a decade from Shanghai. *Inflamm Bowel Dis* 2013; **19**: 423-428 [PMID: 23340680 DOI: 10.1097/MIB.0b013e318286f9f2]

5 **Thakkar K**, El-Serag HB, Mattek N, Gilger M. Complications of pediatric colonoscopy: a five-year multicenter experience. *Clin Gastroenterol Hepatol* 2008; **6**: 515-520 [PMID: 18356115 DOI: 10.1016/j.cgh.2008.01.007]

6 **Jentschura D**, Raute M, Winter J, Henkel T, Kraus M, Manegold BC. Complications in endoscopy of the lower gastrointestinal tract. Therapy and prognosis. *Surg Endosc* 1994; **8**: 672-676 [PMID: 8059305]

7 **Cohen S**, Glatstein MM, Scolnik D, Rom L, Yaron A, Otremski S, Ben-Tov A, Reif S. Propofol for pediatric colonoscopy: the experience of a large, tertiary care pediatric hospital. *Am J Ther* 2014; **21**: 509-511 [PMID: 23567786 DOI: 10.1097/MJT.0b013 e31826a94e9]

8 **Amornyotin S**, Aanpreung P, Prakarnrattana U, Chalayonnavin W, Chatchawankitkul S, Srikureja W. Experience of intravenous sedation for pediatric gastrointestinal endoscopy in a large tertiary referral center in a developing country. *Paediatr Anaesth* 2009; **19**: 784-791 [PMID: 19624366 DOI: 10.1111/j.1460-9592.2009.03063.x]

9 **ASGE Technology Committee**, Barth BA, Banerjee S, Bhat YM, Desilets DJ, Gottlieb KT, Maple JT, Pfau PR, Pleskow DK, Siddiqui UD, Tokar JL, Wang A, Song LM, Rodriguez SA. Equipment for pediatric endoscopy. *Gastrointest Endosc* 2012; **76**: 8-17 [PMID: 22579260 DOI: 10.1016/j.gie.2012.02.023]

10 **Dahshan A**, Lin CH, Peters J, Thomas R, Tolia V. A randomized, prospective study to evaluate the efficacy and acceptance of three bowel preparations for colonoscopy in children. *Am J Gastroenterol* 1999; **94**: 3497-3501 [PMID: 10606310 DOI: 10.1111/j.1572-0241.1999.01613.x]

11 **Turner D**, Benchimol EI, Dunn H, Griffiths AM, Frost K, Scaini V, Avolio J, Ling SC. Pico-Salax versus polyethylene glycol for bowel cleanout before colonoscopy in children: a randomized controlled trial. *Endoscopy* 2009; **41**: 1038-1045 [PMID: 19967619 DOI: 10.1055/s-0029-1215333]

12 **Terry NA**, Chen-Lim ML, Ely E, Jatla M, Ciavardone D, Esch S, Farace L, Jannelli F, Puma A, Carlow D, Mamula P. Polyethylene glycol powder solution versus senna for bowel preparation for colonoscopy in children. *J Pediatr Gastroenterol Nutr* 2013; **56**: 215-219 [PMID: 22699838 DOI: 10.1097/MPG.0b013e3182633d0a]

13 **Abbas MI**, Nylund CM, Bruch CJ, Nazareno LG, Rogers PL. Prospective evaluation of 1-day polyethylene glycol-3350 bowel preparation regimen in children. *J Pediatr Gastroenterol Nutr* 2013; **56**: 220-224 [PMID: 22744195 DOI: 10.1097/MPG.0b013e31826630fc]

14 **Di Nardo G**, Aloi M, Cucchiara S, Spada C, Hassan C, Civitelli F, Nuti F, Ziparo C, Pession A, Lima M, La Torre G, Oliva S. Bowel preparations for colonoscopy: an RCT. *Pediatrics* 2014; **134**: 249-256 [PMID: 25002661 DOI: 10.1542/peds.2014-0131]

15 **Nagata K**, Endo S, Ichikawa T, Dasai K, Moriya K, Kushihashi T, Kudo SE. Polyethylene glycol solution (PEG) plus contrast medium vs PEG alone preparation for CT colonography and conventional colonoscopy in preoperative colorectal cancer staging. *Int J Colorectal Dis* 2007; **22**: 69-76 [PMID: 16583194 DOI: 10.1007/s00384-006-0113-x]

16 **Tan G**, Irwin MG. Recent advances in using propofol by non-anesthesiologists. *F1000 Med Rep* 2010; **2**: 79 [PMID: 21170368 DOI: 10.3410/M2-79]

17 **Vargo JJ**, Cohen LB, Rex DK, Kwo PY. Position statement: nonanesthesiologist administration of propofol for GI endoscopy. *Gastrointest Endosc* 2009; **70**: 1053-1059 [PMID: 19962497 DOI: 10.1016/j.gie.2009.07.020]

18 **Hsieh MY**, Hung GY, Hsieh YL, Chang CY, Hwang B. Deep sedation with methohexital or thiamylal with midazolam for invasive procedures in children with acute lymphoblastic leukemia. *Acta Paediatr Taiwan* 2005; **46**: 294-300 [PMID: 16640004]

19 **Tsai CJ**, Wang HM, Lu IC, Tai CF, Wang LF, Soo LY, Lu DV. Seizure after local anesthesia for nasopharyngeal angiofibroma. *Kaohsiung J Med Sci* 2007; **23**: 97-100 [PMID: 17339174 DOI: 10.1016/S1607-551X(09)70383-3]

20 **Struijs MC**, Diamond IR, de Silva N, Wales PW. Establishing norms for intestinal length in children. *J Pediatr Surg* 2009; **44**: 933-938 [PMID: 19433173 DOI: 10.1016/j.jpedsurg.2009.01.031]

21 **Hounnou G**, Destrieux C, Desmé J, Bertrand P, Velut S. Anatomical study of the length of the human intestine. *Surg Radiol Anat* 2002; **24**: 290-294 [PMID: 12497219 DOI: 10.1007/s00276-002-0057-y]

22 **Wyllie R**, Kay MH. Colonoscopy and therapeutic intervention in infants and children. *Gastrointest Endosc Clin N Am* 1994; **4**: 143-160 [PMID: 8137012]

23 **Thomson M**. Colonoscopy and enteroscopy. *Gastrointest Endosc Clin N Am* 2001; **11**: 603-639, vi [PMID: 11689359]

24 **Lei P**, Gu F, Hong L, Sun Y, Li M, Wang H, Zhong B, Chen M, Cui Y, Zhang S. Pediatric colonoscopy in South China: a 12-year experience in a tertiary center. *PLoS One* 2014; **9**: e95933 [PMID: 24759776 DOI: 10.1371/journal.pone.0095933]

25 **Tam YH**, Lee KH, Chan KW, Sihoe JD, Cheung ST, Mou JW. Colonoscopy in Hong Kong Chinese children. *World J Gastroenterol* 2010; **16**: 1119-1122 [PMID: 20205284 DOI: 10.3748/wjg.v16.i9.1119]

26 **Thakkar K**, Alsarraj A, Fong E, Holub JL, Gilger MA, El Serag HB. Prevalence of colorectal polyps in pediatric colonoscopy. *Dig Dis Sci* 2012; **57**: 1050-1055 [PMID: 22147243 DOI: 10.1007/s10620-011-1972-8]

27 **Asakura K**, Nishiwaki Y, Inoue N, Hibi T, Watanabe M, Takebayashi T. Prevalence of ulcerative colitis and Crohn's disease in Japan. *J Gastroenterol* 2009; **44**: 659-665 [PMID: 19424654 DOI: 10.1007/s00535-009-0057-3]

28 **Ng SC**, Tang W, Ching JY, Wong M, Chow CM, Hui AJ, Wong TC, Leung VK, Tsang SW, Yu HH, Li MF, Ng KK, Kamm MA, Studd C, Bell S, Leong R, de Silva HJ, Kasturiratne A, Mufeena MN, Ling KL, Ooi CJ, Tan PS, Ong D, Goh KL, Hilmi I, Pisespongsa P, Manatsathit S, Rerknimitr R, Aniwan S, Wang YF, Ouyang Q, Zeng Z, Zhu Z, Chen MH, Hu PJ, Wu K, Wang X, Simadibrata M, Abdullah M, Wu JC, Sung JJ, Chan FK; Asia-Pacific Crohn's and Colitis Epidemiologic Study (ACCESS) Study Group. Incidence and phenotype of inflammatory bowel disease based on results from the Asia-pacific Crohn's and colitis epidemiology study. *Gastroenterology* 2013; **145**: 158-165.e2 [PMID: 23583432 DOI: 10.1053/j.gastro.2013.04.007]

P- Reviewer: De Silva AP, Ikematsu H **S- Editor**: Ma YJ
L- Editor: A **E- Editor**: Li D

World Journal of Gastroenterology

Submit a Manuscript: http://www.f6publishing.com

World J Gastroenterol 2017 August 21; 23(31): 5780-5786

DOI: 10.3748/wjg.v23.i31.5780

ISSN 1007-9327 (print) ISSN 2219-2840 (online)

ORIGINAL ARTICLE

Retrospective Study

Postoperative changes of manometry after restorative proctocolectomy in Korean ulcerative colitis patients

Se Heon Oh, Yong Sik Yoon, Jong Lyul Lee, Chan Wook Kim, In Ja Park, Seok-Byung Lim, Chang Sik Yu, Jin Cheon Kim

Se Heon Oh, Yong Sik Yoon, Jong Lyul Lee, Chan Wook Kim, In Ja Park, Seok-Byung Lim, Chang Sik Yu, Jin Cheon Kim, Department of Surgery, Division of Colon and Rectal Surgery, University of Ulsan College of Medicine, Asan Medical Center, Seoul 05505, South Korea

Author contributions: Oh SH and Yoon YS designed the research and collected, and analyzed the data, and drafted the manuscript; Lee JL, Kim CW, Park IJ, Lim SB, Yu CS and Kim JC supervised the study; all authors have read and approved the final version to be published.

Institutional review board statement: The study was reviewed and approved by the Institutional Review Board of Asan Medical Center (IRB No. 2017-0088).

Informed consent statement: Because this was a retrospective study with minimal risk to patients, it was exempted from obtaining informed consent by the IRB.

Conflict-of-interest statement: No conflict.

Data sharing statement: No additional data are available.

Manuscript source: Unsolicited manuscript

Correspondence to: Yong Sik Yoon, MD, PhD, Department of Surgery, Division of Colon and Rectal Surgery, University of Ulsan College of Medicine, 88, Olympic-ro 43-gil, Songpa-gu, Seoul 05505, South Korea. yoonys@amc.seoul.kr
Telephone: +82-2-30105318
Fax: +82-2-30106701

Received: April 1, 2017
Peer-review started: April 9, 2017
First decision: April 26, 2017
Revised: May 7, 2017
Accepted: July 22, 2017
Article in press: July 24, 2017
Published online: August 21, 2017

Abstract

AIM

To investigate the changes of postoperative anal sphincter function and bowel frequency in Korean patients with ulcerative colitis (UC).

METHODS

A total of 127 patients with UC who underwent restorative proctocolectomy (RPC) during 20 years were retrospectively analyzed. The parameters of anal manometry and bowel frequency were compared according to the 6-mo intervals until 24 mo postoperatively. Manometry was used to measure the maximal squeezing pressure (MSP) and maximal resting pressure (MRP).

RESULTS

MSP decreased after surgery until 6 mo (157 to 142 mmHg); thereafter, it improved and was recovered to and maintained at the preoperative value at 12 mo postoperatively (142-170 mmHg, $P < 0.001$). Although the decreased MRP (65 to 56 mmHg) improved after 18 mo (62 mmHg), it did not completely recover to the preoperative value. The decreased rectal capacity after surgery (90 to 82 mL) gradually increased up to 150 mL at 24 mo. Although bowel frequency showed significant gradual decreases at each interval, it was stabilized after 12 mo postoperatively (6.5 times/d).

CONCLUSION
Postoperative changes of manometry and bowel frequency after restorative proctocolectomy in Korean patients with UC were not different from those in Western patients with UC.

Key words: Ulcerative colitis; Surgery; Treatment outcome; Manometry**;** Bowel frequency; Restorative proctocolectomy

Core tip: Although there has been an increase in the prevalence of ulcerative colitis (UC) and the numbers of UC surgery in Asian countries, studies on the functional outcomes of restorative proctocolectomy (RPC) or the quality of life in Asians are still deficient. Most UC studies on functional outcomes were done in Westerners. The authors found that maximal squeezing pressure, rectal capacity, and bowel frequency were stabilized at 12 mo after RPC. Although the decreased MRP was improved after 18 mo, it did not completely recover to the preoperative value. These findings in Korean patients with UC were not different from those in Western patients with UC.

Oh SH, Yoon YS, Lee JL, Kim CW, Park IJ, Lim SB, Yu CS, Kim JC. Postoperative changes of manometry after restorative proctocolectomy in Korean ulcerative colitis patients. *World J Gastroenterol* 2017; 23(31): 5780-5786 Available from: URL: http://www.wjgnet.com/1007-9327/full/v23/i31/5780.htm DOI: http://dx.doi.org/10.3748/wjg.v23.i31.5780

INTRODUCTION

Ulcerative colitis (UC) is a chronic inflammatory bowel disorder that is characterized by a relapsing and remitting course. The common surgical indications for UC are complications (such as severe UC) that are unresponsive to treatment, dysplasia or malignancy, bleeding, perforation, and a toxic megacolon. Restorative proctocolectomy (RPC) with ileal pouch-anal anastomosis (IPAA) was first introduced in 1978 and is still used as the standard surgery[1]. However, RPC causes decreased rectal reservoir, loss of anorectal sensation, and anal sphincter injury from surgical manipulation, resulting in functional derangement of bowel movement in patients postoperatively[2-4]. The frequency of postoperative defecation ranges between 6 and 8 times/day, and more than one-third of patients experience anal incontinence[5].

The incidence and prevalence of UC in South Korea are still lower than those in Western countries but have been rapidly increasing during the last decades[6]. The mean annual incidence rate of UC in Koreans increased by 9-fold from 0.34 per 100000 in 1986-1990 to 3.08 per 100000 in 2001-2005[7]. This recent change in the incidence and prevalence of UC is attributable to environmental factors, such as Westernized lifestyles featuring antibiotic use and improved hygiene[7]. Moreover, differences between Asian and Western countries are also found in the family history and genetics of UC[6]. A family history of UC among Asian cohorts was previously noted to be uncommon, with a frequency ranging from 0.0% to 3.4%[8], considerably lower than the reported rates in Western series (range, 10%-25%)[9]. The genetic susceptibilities of Asian patients with inflammatory bowel disease (IBD) differ from those of whites, as they are not associated with *NOD2/CARD15* mutations[10].

Although there has been an increase in the prevalence of UC and the numbers of UC surgery in Asian countries, studies on the functional outcomes of RPC or the quality of life in Asians are still deficient. Most UC studies on functional outcomes were done in Westerners. The purpose of the present study was to investigate the changes of postoperative anal sphincter function and bowel frequency in Korean patients with UC. Furthermore, we attempted to find the difference in functional outcomes between Western and Korean patients.

MATERIALS AND METHODS

Patient selection

The clinical data of patients with UC who underwent laparotomy between October 1994 and June 2013 were collected retrospectively. During the study period, a total of 192 patients with clinically diagnosed UC underwent abdominal surgery. Of them, 41 patients who did not undergo RPC and 2 patients proven to have indeterminate colitis on pathology were excluded. One of the two patients with indeterminate colitis was included in the 41 patients who did not undergo RPC. Among 150 patients with RPC, 23 patients who did not undergo any preoperative or postoperative manometry were also excluded. Finally, 127 patients were analyzed. The clinical variables were sex, age at diagnosis, age at surgery, duration from diagnosis to surgery, indication for surgery, emergency operation, type of surgery, anastomotic configuration, presence of mucosectomy, and postoperative bowel frequency. Any complication that occurred within 90 d after RPC was defined as early complication. The mean follow-up duration was 71.5 mo (range, 3-192 mo). The study protocol was approved by the institutional review board of Asan Medical Center (registration No. 2017-0088).

Operation

Most of the RPCs were performed by experienced, IBD-specialized surgeons (Yu CS and Yoon YS) at our institution. The decision of performing surgery was made by gastroenterologists and IBD surgeons. The type of operation was decided by IBD surgeons,

considering the severity of disease, patient's condition, and presence of malignancy. IPAA included a 12-15-cm-long ileal J-pouch that was constructed by using linear staples and pouch-anal anastomosis through a double-stapling technique. If malignancy was suspected, cancer was present in the rectum, or removal of the remaining rectal mucosa was needed for any cause, mucosectomy was performed. Mucosectomy and hand-sewn anastomosis were performed from the perineal side of patients. Then, diverting ileostomy was constructed in most cases. Usually, at least 2 mo later, the diverting ileostomy was closed after checking the anastomosis and the integrity of pouch through radiological evaluation with a water-soluble, double-contrast dye. Most RPCs were performed as two-stage procedures by using a double-stapling method.

Manometry and bowel frequency

Anorectal manometry was performed through water perfusion by using an eight-channel flexible catheter with side holes connected to a perfusion pump and a stationary manometry system (Polygraf ID; Medtronics, Copenhagen, Denmark). Anal manometry was performed with the continuous pull-through method (1 mm/s), starting 6 cm from the anal verge, by using a thin polyethylene (diameter: 5.5 mm, length: 150 cm). The catheter was constantly perfused with saline at a rate of 0.5 mL·channel^{-1}·min^{-1}, and was connected to a water-filled pressure transducer linked to multichannel recorder. A latex balloon at the tip of the perfused catheter (eight channels) was positioned in the ileal pouch or rectum so that the distal end of the balloon was 6 cm above the anal verge. Manometry was initially performed preoperatively. Secondary manometry was checked just before ileostomy closure. Thereafter, manometry was irregularly followed at 6-12-mo intervals without a protocol. The parameters of manometry, known to be indicators of anatomical and physiological changes, included the maximal squeezing pressure (MSP), maximal resting pressure (MRP), rectoanal inhibitory reflex (RAIR), and rectal capacity. The normal range is 100-180 mmHg for MSP, 40-70 mmHg for MRP, and 100-300 mL for rectal capacity. The presence of RAIR is the normal condition. Bowel frequency was retrospectively reviewed by using electronical medical records. Most patients were followed at 6-mo intervals until the postoperative first year; thereafter, they were followed at 1-year intervals. No questionnaires were used, and the degree of continence, night soiling, and whether gas could be discriminated from stool were not checked regularly. Therefore, only bowel frequency per day was evaluated during the postoperative period.

Statistical analysis

Because of our irregular check-up of manometry and records of bowel frequency, we arbitrary grouped the findings according to the 6-mo intervals until 24 mo after surgery. A linear mixed model was constructed to evaluate the differences between manometric measurements at 0-6, 6-12, 12-18, and 18-24 mo after and before the operation. The significance level for multiple comparisons was adjusted with Bonferroni's method. The dependent variables at various times from before the operation to 24 mo after the operation were suspected to have a nonlinear relation with time. Thus, we fitted piecewise linear mixed models by assuming a series of linear segments and accompanying breakpoints. *P*-values of 0.05 were considered statistically significant. For piecewise linear mixed models, results are presented as β coefficients with SE. For linear mixed models, results are presented as least-square means with SE. SAS version 9.3 was used for statistical analyses.

RESULTS

Patients' characteristics and operation

Among 127 patients with RPC, 74 (58.3%) were men. The median ages at diagnosis and surgery of UC were 35.5 years (range, 14-65 years; SE, 12.4 years) and 39.6 years (range, 16-65 years; SE, 12.4 years), respectively. The mean interval from diagnosis to surgery was 50.3 mo (range, 0-279 mo; SE, 59.6 mo). Emergency operation was performed in four patients (3.1%). The most common indication for surgery was medical intractability, followed by malignancy (Table 1). A laparoscopic two-stage procedure of RPC with diverting ileostomy was performed in only one patient. The mean interval to ileostomy take down was 3.4 mo (range, 2.1-12 mo).

Two-stage procedures of RPC with diverting ileostomy were performed in 109 patients (85.8%). Single procedures of RPC without diversion were done in 11 patients (8.7%). Three-stage procedures of total colectomy with end ileostomy, followed by completion proctectomy with IPAA construction and closure of ileostomy were performed in seven patients (5.5%). Double-stapling anastomoses were performed in 100 patients (78.7%), and hand-sewn anastomoses were done in 27 patients (21.3%). Complications occurred in 49 patients (39.2%). Anastomotic leakage was the most common early complication, and pouchitis was the most common late complication (Table 2).

Manometry and bowel frequency

Preoperative manometries were possible in 94 of 127 patients, and follow-up manometries were performed in 74, 45, 12 and 9 patients at each 6-mo interval, consecutively. MSP immediately decreased after surgery until 6 mo but recovered at 12 mo postoperatively. A significant increase of MSP was found between 0-6 and 6-12 mo (142.4-169.7 mmHg, $P = 0.0007$; Figure 1). MRP significantly decreased after surgery from 64.6 to 56.4 mmHg ($P = 0.0045$). Despite a slight elevation (to 61.8 mmHg) after 12 mo,

Table 1 Indications for surgery

Indication	*n* (%)
Medical intractability	100 (78.7)
Malignancy	10 (7.9)
Bleeding	8 (6.3)
Perforation	4 (3.1)
Toxic megacolon	3 (2.4)
Fistula	2 (1.6)
Total	127 (100)

Table 2 Postoperative complications

Variable	*n* (%)
Early complication	19 (15.2)
Leakage	5 (4.0)
Wound infection	5 (4.0)
Bleeding	2 (1.6)
Rectovaginal fistula	2 (1.6)
Thrombosis	2 (1.6)
Others	3 (2.4)
Late complication	30 (24.0)
Pouchitis	17 (13.6)
Ileus	5 (4.0)
Pouch failure	3 (2.4)
Others	5 (4.0)

MRP was not recovered to the preoperative value. After 12 mo, MRP was maintained steadily (Figure 2). Rectal capacity slightly decreased at 6 mo (90.1 to 82.3 mL), but exceeded the initial volume up to 132.5 mL at 6-12 mo ($P < 0.0001$). Until 24 mo, rectal capacity gradually increased up to 150.3 mL (Figure 3). RAIR was identified in 20 patients (26.3%) and 5 patients (11.1%) at 0-6 and 6-12 mo, respectively.

Bowel frequency was studied in 80, 62, 37 and 11 patients at each 6-mo interval, consecutively. Although bowel frequency showed significant gradual decreases at each interval, it was stabilized after 6-12 mo postoperatively (Figure 4). The parameters of MSP, MRP, rectal capacity, and bowel frequency were compared between the double-stapling and hand-sewn anastomosis groups. However, there was no significant difference between the two groups.

DISCUSSION

RPC contributes to the enhancement of the quality of life of patients with UC by avoiding permanent ileostomy and maintaining intestinal continuity[11]. However, defecatory dysfunction after surgery exists in many forms, such as anal sphincter injury and sensory loss of the anal transition zone (ATZ) from mucosectomy, and has a relatively long recovery of 6-12 mo[12,13]. The external sphincter, which surrounds the internal sphincter and is innervated by somatic nerves, generates the voluntary anal squeeze and is also considered to be unaffected during mucosal proctectomy[14]. This implies that the operation disturbs the function of the internal sphincter but does not affect that of the external sphincter[15]. On the other hand, some studies insisted that weeks of non-use of the sphincter muscle might be the reason for the decrease in sphincter pressure. In fact, continuous mucous discharge from the pouch occurs during fecal diversion, implying that it is not in a totally resting state. After loop ileostomy closure, the external sphincter strength quickly improves owing to advanced exercise caused by loose stool. It thus compensates for the relatively low resting pressure values in these patients[16]. A previous study reported that MSP decreased from 87.1 mmHg preoperatively to 68.1 mmHg at 8 wk postoperatively; however, at 1 year, it increased to 72.3 mmHg[17]. Others showed no significant difference between preoperative values and those obtained 1 year after surgery when the mean and maximal squeezing pressures were compared[18]. In addition, another study reported that the MSP was 88.5 mmHg preoperatively and decreased by 12% to 68.0 mmHg before ileostomy closure. One year after ileostomy closure, the MSP was 96.5 mmHg, 8% higher than before surgery[16]. In this study, MSP decreased at 6 mo and stabilized after 12 mo (8-9 mo after ileostomy closure). The result of our study was not different from those of previous Western studies.

Around 60%-80% of MRP originates from the internal anal sphincter. This muscle, which is responsible for the maintenance of resting anal tone, is innervated by the autonomic nervous system and is under involuntary control[14]. It has also been observed that 84% of rectal mucosal tissue is composed of smooth muscle cell originating from internal sphincter muscle fiber, and the amount of smooth muscle has a significant relationship with the decrease of MRP that is associated with the bowel habit change of patients[19]. Injury to the internal sphincter muscle can directly result from operative trauma, or secondarily result from denervation or ischemia. Injury to the autonomic nerve of the internal sphincter muscle during rectal dissection results in decreased MRP[20]. Therefore, maintaining the integrity of the internal sphincter is responsible for preserving the MRP. The internal sphincter muscle is partially resected during mucosal proctectomy, and this loss of the muscle or the scar formation from the proctectomy contributes to the dysfunction of internal anal sphincter[21]. In previous studies, early postoperative anal manometry revealed a significantly lower MRP (42 ± 4 mmHg) than the preoperative value (65 ± 4 mmHg). During the follow-up, MRP increased but remained within the lower limits late postoperatively (49 ± 5 mmHg)[15]. Another study showed that preoperative MRP was 60.2 mmHg and the immediate postoperative MRP was 33.2 mmHg, a decrease of 45%. One year after ileostomy closure, the MRP was 46.2 mmHg, which was 23% lower than preoperatively[16]. In this study, MRP decreased until 6 mo postoperatively and then

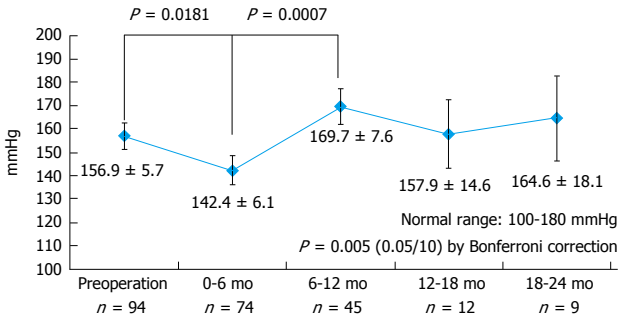

Figure 1 Maximal squeezing pressure. MSP immediately decreased after surgery until 6 mo; however, it was recovered after 12 mo postoperatively. MSP: Maximal squeezing pressure.

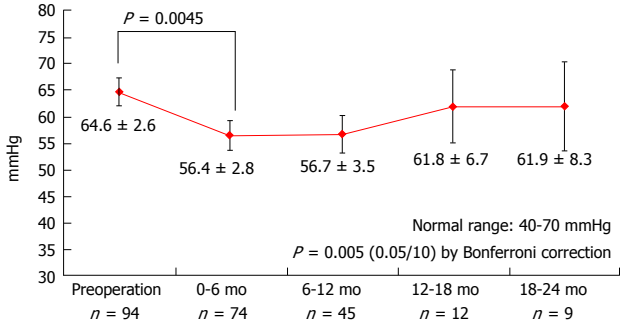

Figure 2 Maximal resting pressure. The decreased MRP after surgery increased slightly after 12 mo; however, it did not recover to the preoperative value. MRP: Maximal resting pressure.

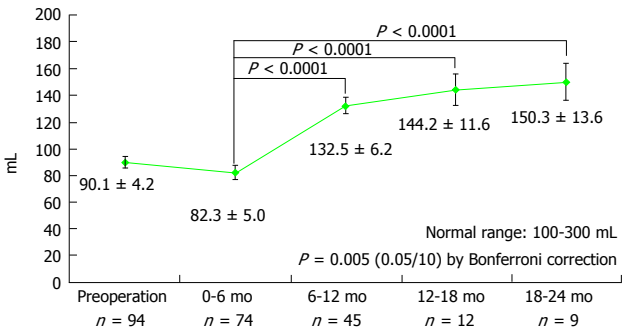

Figure 3 Rectal capacity. The decreased rectal capacity after surgery exceeded the initial volume up to 132.2 mL at 6-12 mo and increased up to 150 mL at 24 mo.

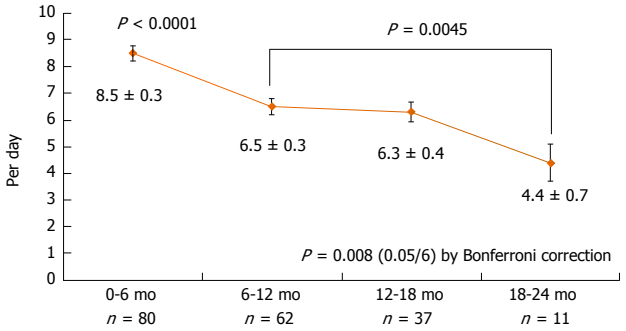

Figure 4 Bowel frequency. Bowel frequency gradually decreased at each interval and stabilized after 6-12 mo postoperatively.

gradually increased, but recovered to some extent at 2 years postoperatively. That the internal anal sphincter is sensitive to even minor degrees of dilatation is evident from the decrease in MRP. Although there were reports of slight improvements in MRP with time after RPC, other studies did not find any improvement after 1 year[20]. In some studies, the postoperative change of MRP resulting from injury of the internal anal sphincter during IPAA may seem permanent[20]. Although it is difficult, avoiding injury to the internal anal sphincter during RPC is the key to preserving structural integrity, improving continence, and preventing the decrease of MRP[22].

Many studies reported that the use of stapler reduces the injury to internal sphincter and has a small effect of decreasing MRP, resulting in superior defecatory function[1,20,23,24]. In contrast, surgeons who advocate mucosal proctectomy emphasize that the complete removal of all rectal mucosa not only confers the highest likelihood of complete surgical cure but, more importantly, removes all future risk of malignant transformation[14]. However, a long-term follow-up study of dysplasia within the ATZ showed the incidence of dysplasia in the ATZ to be 4.5%, with significant correlation to prepouch risk factors, including colorectal cancer or dysplasia[23]. Other contrasting studies argued that the sphincter complex could be easily damaged and functionally compromised[25]. In addition, hand-sewn anastomosis was reported to entail prolonged operative time and frequent manipulation, resulting in decreased functional outcome and increased complications[20,23]. On the other hand, some studies suggest that there is no significant difference in complications and bowel frequencies between double-stapling and hand-sewn anastomosis, which was consistent with our study[14,23,26]. In this study, manometric findings and bowel frequencies were not different between the two anastomosis types.

RAIR is recognized as an important contributor to fecal continence through sampling and discrimination of contents. Preservation of the RAIR has been shown to correlate with a decreased incidence of nocturnal soiling after RPC[27]. RAIR decreases up to 75%-100% in the immediate postoperative period, but is known to recover over time[28]. A recent study claims that RAIR, which was identified in only 18% of patients after low anterior resection, was checked in 21% after 1 year and in 85% after 2 years, denoting that it has a significant meaning in the recovery of defecatory function[29]. In our study, recovery was seen in 20 patients (26.3%) and 5 patients (11.1%) after 6 and 12 postoperative months; however, additional information was not obtained owing to follow-up loss and inaccurate data.

Rectal capacity is known to be an important factor in stool frequency and improves with time for 1-2 years after surgery[12,13,30]. In addition, rectal capacity is a good index of the volume of the reservoir and can

play an important role in the storing of stool[31]. This is increased compared with before surgery owing to the spontaneous adaptation of the ileal pouch and anal sphincter after ileostomy closure[31]. In some studies, the rectal capacity was 140-142 mL before ileostomy closure, 235-279 mL at 3-6 mo, and 338-344 mL at 12 mo[16]. In this study, rectal capacity also decreased in the immediate postoperative period, gradually increased after 6 mo, and showed marked improvement after 1 year, which seemed to contribute to the recovery of defecatory function.

The functional parameters of bowel frequency, which improved early after the operation, reached a plateau by 2 years and remained stable thereafter[32]. Defecatory function recovers over time after ileostomy take down and stabilizes to 6 to 7 per day at 1 postoperative year[32]. In a previous study, at 5 years after ileostomy closure, the average minimum and maximum 24-h frequency was 3.6 and 4.7, respectively[33]. In another study, a bowel frequency of 6 times/d was identified 3 years later[34]. In another report, the median bowel frequency per day was 6 at a mean follow-up of 40 mo[2]. A study of 100 J-pouch procedures reported that the bowel frequency at 1, 3, 6, 12, and 24 mo was 7.5, 6.5, 6.2, 5.4 and 5.4, respectively[35]. These results were similar to that of our study, which showed that the frequency decreased to 6.5 at 12 mo and 4.4 at 24 mo.

This study is limited by its retrospective design. Mainly, we did not use any questionnaire along with protocol. Major bias could result from the irregular check-up and follow-up of manometry. However, we attempted to minimize the bias of our study through specialized statistics. We expected to show the functional outcomes after RPC through our study. However, owing to the limited parameters, our study could show only a small part of the functional outcomes and quality of life after RPC.

In conclusion, the manometric findings of MSP and the rectal capacity and bowel frequency were stabilized at 12 mo after RPC. Although the decreased MRP was improved after 18 mo, it did not completely recover to the preoperative value. These findings in Korean patients with UC were not different from those of Western patients with UC.

COMMENTS

Background

Ulcerative colitis (UC) is a chronic inflammatory bowel disorder that is characterized by a relapsing and remitting course. The incidence and prevalence of UC in South Korea are still lower than those in Western countries but have been rapidly increasing during the last decades. Although there has been an increase in the prevalence of UC and the numbers of UC surgery in Asian countries, studies on the functional outcomes of restorative proctocolectomy (RPC) or the quality of life in Asians are still deficient. The purpose of the present study was to investigate the changes of postoperative anal sphincter function and bowel frequency in Korean patients with UC.

Research frontiers

The manometric findings of maximal squeezing pressure (MSP), rectal capacity and bowel frequency were stabilized at 12 mo after RPC. Although the decreased maximal resting pressure (MRP) was improved after 18 mo, it did not completely recover to the preoperative value.

Innovations and breakthroughs

This study identified that the manometric findings and bowel frequency after RPC in Korean patients with UC were not different from those of Western patients with UC.

Applications

The presented research could be useful in studying the manometric functional outcomes and bowel frequency of UC patients in Asia and South Koera.

Terminology

RPC: most RPCs were performed as two-stage procedures by using a double-stapling method. Ileal pouch-anal anastomosis (IPAA): included a 12-15-cm-long ileal J-pouch that was constructed by using linear staples and pouch-anal anastomosis through a double-stapling technique.

Peer-review

The authors retrospectively reviewed the data of patients who underwent RPC in a single institute and attempted to find the difference in functional outcomes between Western and Korean patients. This study could show only a small part of the functional outcomes and quality of life after RPC but the results were very interesting.

REFERENCES

1 **Parks AG**, Nicholls RJ. Proctocolectomy without ileostomy for ulcerative colitis. *Br Med J* 1978; **2**: 85-88 [PMID: 667572 DOI: 10.1136/bmj.2.6130.85]

2 **Fazio VW**, Ziv Y, Church JM, Oakley JR, Lavery IC, Milsom JW, Schroeder TK. Ileal pouch-anal anastomoses complications and function in 1005 patients. *Ann Surg* 1995; **222**: 120-127 [PMID: 7639579 DOI: 10.1097/00000658-199508000-00003]

3 **Meagher AP**, Farouk R, Dozois RR, Kelly KA, Pemberton JH. J ileal pouch-anal anastomosis for chronic ulcerative colitis: complications and long-term outcome in 1310 patients. *Br J Surg* 1998; **85**: 800-803 [PMID: 9667712 DOI: 10.1046/j.1365-2168.1998.00689.x]

4 **Park KJ,** Park G. Analysis of the Results of Surgical Treatment Options for Ulcerative Colitis. *J Korean Soc Coloproctol* 1997; **13**: 77-96

5 **Rink AD**, Nagelschmidt M, Radinski I, Vestweber KH. Evaluation of vector manometry for characterization of functional outcome after restorative proctocolectomy. *Int J Colorectal Dis* 2008; **23**: 807-815 [PMID: 18438676 DOI: 10.1007/s00384-008-0473-5]

6 **Park SJ**, Kim WH, Cheon JH. Clinical characteristics and treatment of inflammatory bowel disease: a comparison of Eastern and Western perspectives. *World J Gastroenterol* 2014; **20**: 11525-11537 [PMID: 25206259 DOI: 10.3748/wjg.v20.i33.11525]

7 **Lee HS**, Park SH, Yang SK, Lee J, Soh JS, Lee S, Bae JH, Lee HJ, Yang DH, Kim KJ, Yea BD, Byeon JS, Myung SJ, Yoon YS, Yu CS, Kim JH. Long-term prognosis of ulcerative colitis and its temporal change between 1977 and 2013: a hospital-based cohort study from Korea. *J Crohns Colitis* 2015; **9**: 147-155 [PMID: 25518059 DOI: 10.1093/ecco-jcc/jju017]

8 **Wang Y**, Ouyang Q; APDW 2004 Chinese IBD working group. Ulcerative colitis in China: retrospective analysis of 3100 hospitalized patients. *J Gastroenterol Hepatol* 2007; **22**: 1450-1455 [PMID: 17716349 DOI: 10.1111/j.1440-1746.2007.04873.x]

9 **Orholm M**, Munkholm P, Langholz E, Nielsen OH, Sørensen TI, Binder V. Familial occurrence of inflammatory bowel disease. *N Engl J Med* 1991; **324**: 84-88 [PMID: 1984188 DOI: 10.1056/NEJM199101103240203]

10 **Ng SC**, Tsoi KK, Kamm MA, Xia B, Wu J, Chan FK, Sung JJ. Genetics of inflammatory bowel disease in Asia: systematic review and meta-analysis. *Inflamm Bowel Dis* 2012; **18**: 1164-1176 [PMID: 21887729 DOI: 10.1002/ibd.21845]

11 **Silvestri MT**, Hurst RD, Rubin MA, Michelassi F, Fichera A. Chronic inflammatory changes in the anal transition zone after stapled ileal pouch-anal anastomosis: is mucosectomy a superior alternative? *Surgery* 2008; **144**: 533-537; discussion 537-539 [PMID: 18847636 DOI: 10.1016/j.surg.2008.06.003]

12 **Goes R**, Beart RW Jr. Physiology of ileal pouch-anal anastomosis. Current concepts. *Dis Colon Rectum* 1995; **38**: 996-1005 [PMID: 7656753 DOI: 10.1007/BF02049741]

13 **Yu CS,** Kim HC, Park SG, Kim SY, Cho YG, Hong HK, Kim JC. Manometric assessment after ileal pouch anal anastomosis. *J Korean Soc Coloproctol* 2001; **17**: 187-192

14 **Litzendorf ME**, Stucchi AF, Wishnia S, Lightner A, Becker JM. Completion mucosectomy for retained rectal mucosa following restorative proctocolectomy with double-stapled ileal pouch-anal anastomosis. *J Gastrointest Surg* 2010; **14**: 562-569 [PMID: 19937191 DOI: 10.1007/s11605-009-1099-9]

15 **Braun J**, Treutner KH, Harder M, Lerch MM, Töns C, Schumpelick V. Anal sphincter function after intersphincteric resection and stapled ileal pouch-anal anastomosis. *Dis Colon Rectum* 1991; **34**: 8-16 [PMID: 1846800 DOI: 10.1007/BF02050200]

16 **Luukkonen P**. Manometric follow-up of anal sphincter function after an ileo-anal pouch procedure. *Int J Colorectal Dis* 1988; **3**: 43-46 [PMID: 3361223 DOI: 10.1007/BF01649683]

17 **Becker JM**, Hillard AE, Mann FA, Kestenberg A, Nelson JA. Functional assessment after colectomy, mucosal proctectomy, and endorectal ileoanal pull-through. *World J Surg* 1985; **9**: 598-605 [PMID: 4036152 DOI: 10.1007/BF01656061]

18 **Wexner SD**, James K, Jagelman DG. The double-stapled ileal reservoir and ileoanal anastomosis. A prospective review of sphincter function and clinical outcome. *Dis Colon Rectum* 1991; **34**: 487-494 [PMID: 1645246 DOI: 10.1007/BF02049935]

19 **Becker JM**, LaMorte W, St Marie G, Ferzoco S. Extent of smooth muscle resection during mucosectomy and ileal pouch-anal anastomosis affects anorectal physiology and functional outcome. *Dis Colon Rectum* 1997; **40**: 653-660 [PMID: 9194458 DOI: 10.1007/BF02140893]

20 **Tuckson W**, Lavery I, Fazio V, Oakley J, Church J, Milsom J. Manometric and functional comparison of ileal pouch anal anastomosis with and without anal manipulation. *Am J Surg* 1991; **161**: 90-95; discussion 95-96 [PMID: 1987862 DOI: 10.1016/0002-9610(91)90366-L]

21 **Sharp FR**, Bell GA, Seal AM, Atkinson KG. Investigations of the anal sphincter before and after restorative proctocolectomy. *Am J Surg* 1987; **153**: 469-472 [PMID: 3578668 DOI: 10.1016/0002-9610(87)90795-1]

22 **Kroesen AJ**, Runkel N, Buhr HJ. Manometric analysis of anal sphincter damage after ileal pouch-anal anastomosis. *Int J Colorectal Dis* 1999; **14**: 114-118 [PMID: 10367257 DOI: 10.1007/s003840050195]

23 **Lovegrove RE**, Constantinides VA, Heriot AG, Athanasiou T, Darzi A, Remzi FH, Nicholls RJ, Fazio VW, Tekkis PP. A comparison of hand-sewn versus stapled ileal pouch anal anastomosis (IPAA) following proctocolectomy: a meta-analysis of 4183 patients. *Ann Surg* 2006; **244**: 18-26 [PMID: 16794385 DOI: 10.1097/01.sla.0000225031.15405.a3]

24 **Williams NS**, Marzouk DE, Hallan RI, Waldron DJ. Function after ileal pouch and stapled pouch-anal anastomosis for ulcerative colitis. *Br J Surg* 1989; **76**: 1168-1171 [PMID: 2597975 DOI: 10.1002/bjs.1800761119]

25 **Holder-Murray J**, Fichera A. Anal transition zone in the surgical management of ulcerative colitis. *World J Gastroenterol* 2009; **15**: 769-773 [PMID: 19230038 DOI: 10.3748/wjg.15.769]

26 **Gozzetti G**, Poggioli G, Marchetti F, Laureti S, Grazi GL, Mastrorilli M, Selleri S, Stocchi L, Di Simone M. Functional outcome in handsewn versus stapled ileal pouch-anal anastomosis. *Am J Surg* 1994; **168**: 325-329 [PMID: 7943588 DOI: 10.1016/S0002-9610(05)80158-8]

27 **Saigusa N**, Belin BM, Choi HJ, Gervaz P, Efron JE, Weiss EG, Nogueras JJ, Wexner SD. Recovery of the rectoanal inhibitory reflex after restorative proctocolectomy: does it correlate with nocturnal continence? *Dis Colon Rectum* 2003; **46**: 168-172 [PMID: 12576889 DOI: 10.1097/01.DCR.0000049345.21202.99]

28 **Annibali R**, Oresland T, Hultén L. Does the level of stapled ileoanal anastomosis influence physiologic and functional outcome? *Dis Colon Rectum* 1994; **37**: 321-329 [PMID: 8168410 DOI: 10.1007/BF02053591]

29 **O'Riordain MG**, Molloy RG, Gillen P, Horgan A, Kirwan WO. Rectoanal inhibitory reflex following low stapled anterior resection of the rectum. *Dis Colon Rectum* 1992; **35**: 874-878 [PMID: 1511649 DOI: 10.1007/BF02047876]

30 **Oresland T**, Fasth S, Nordgren S, Akervall S, Hultén L. Pouch size: the important functional determinant after restorative proctocolectomy. *Br J Surg* 1990; **77**: 265-269 [PMID: 2322787 DOI: 10.1002/bjs.1800770310]

31 **Chaussade S**, Michopoulos S, Hautefeuille M, Valleur P, Hautefeuille P, Guerre J, Couturier D. Clinical and physiological study of anal sphincter and ileal J pouch before preileostomy closure and 6 and 12 months after closure of loop ileostomy. *Dig Dis Sci* 1991; **36**: 161-167 [PMID: 1988259 DOI: 10.1007/BF01300750]

32 **Pemberton JH**, Kelly KA, Beart RW Jr, Dozois RR, Wolff BG, Ilstrup DM. Ileal pouch-anal anastomosis for chronic ulcerative colitis. Long-term results. *Ann Surg* 1987; **206**: 504-513 [PMID: 3662660 DOI: 10.1097/00000658-198710000-00011]

33 **Setti-Carraro P**, Ritchie JK, Wilkinson KH, Nicholls RJ, Hawley PR. The first 10 years' experience of restorative proctocolectomy for ulcerative colitis. *Gut* 1994; **35**: 1070-1075 [PMID: 7926908 DOI: 10.1136/gut.35.8.1070]

34 **McIntyre PB**, Pemberton JH, Wolff BG, Beart RW, Dozois RR. Comparing functional results one year and ten years after ileal pouch-anal anastomosis for chronic ulcerative colitis. *Dis Colon Rectum* 1994; **37**: 303-307 [PMID: 8168407DOI: 10.1007/BF02053588]

35 **Becker JM**, Raymond JL. Ileal pouch-anal anastomosis. A single surgeon's experience with 100 consecutive cases. *Ann Surg* 1986; **204**: 375-383 [PMID: 3767475 DOI: 10.1097/00000658-198610000-00005]

P- Reviewer: Ladic A, Lakatos, PL, M'Koma AE
S- Editor: Gong ZM **L- Editor**: A **E- Editor**: Li D

World Journal of Gastroenterology

Submit a Manuscript: http://www.f6publishing.com

World J Gastroenterol 2017 August 21; 23(31): 5787-5797

DOI: 10.3748/wjg.v23.i31.5787

ISSN 1007-9327 (print) ISSN 2219-2840 (online)

ORIGINAL ARTICLE

Retrospective Study

Threonine and tyrosine kinase may serve as a prognostic biomarker for gallbladder cancer

Yuan Xie, Jian-Zhen Lin, An-Qiang Wang, Wei-Yu Xu, Jun-Yu Long, Yu-Feng Luo, Jie Shi, Zhi-Yong Liang, Xin-Ting Sang, Hai-Tao Zhao

Yuan Xie, Jian-Zhen Lin, An-Qiang Wang, Wei-Yu Xu, Jun-Yu Long, Xin-Ting Sang, Hai-Tao Zhao, Department of Liver Surgery, Peking Union Medical College Hospital, Chinese Academy of Medical Sciences and Peking Union Medical College, Beijing 100730, China

Yu-Feng Luo, Jie Shi, Zhi-Yong Liang, Department of Pathology, Peking Union Medical College Hospital, Chinese Academy of Medical Sciences and Peking Union Medical College, Beijing 100730, China.

Author contributions: Xie Y designed the research, collected the clinical data and wrote the manuscript; Lin JZ and Shi J helped to analyze the data; Wang AQ, Xu WY and Long JY followed the patients; Luo YF helped to perform the experiments; Liang ZY provided paraffin-embedded tissues for the experiments; Sang XT and Zhao HT provided financial support for this work; Shi J, Liang ZY, Sang XT and Zhao HT are co-corresponding authors, and they contributed equally to this work; all authors read and approved the final manuscript.

Supported by International Science and Technology Cooperation Projects, No. 2015DFA30650 and No. 2016YFE0107100; The Capital Special Research Project for Clinical Application, No. Z151100004015170; Capital Special Research Project for Health Development, No. 2014-2-4012; and Beijing Nature Science Foundation for Young Scholars, No. 7164293.

Institutional review board statement: The publication of this manuscript has been reviewed and approved by the PUMCH Institutional Review Board.

Informed consent statement: All patients or their families signed informed consent statements before surgery, and surgical procedures were performed according to the approved guidelines.

Conflict-of-interest statement: We declare that the authors have no conflict of interest.

Data sharing statement: No additional data are available.

Manuscript source: Unsolicited manuscript

Correspondence to: Hai-Tao Zhao, MD, Department of Liver Surgery, Peking Union Medical College Hospital, Chinese Academy of Medical Sciences and Peking Union Medical College, 1 Shuaifuyuan, Wangfujing, Beijing 100730, China. zhaoht@pumch.cn
Telephone: +86-10-69156042
Fax: +86-10-69156042

Received: May 30, 2017
Peer-review started: May 31, 2017
First decision: June 22, 2017
Revised: July 3, 2017
Accepted: July 12, 2017
Article in press: July 12, 2017
Published online: August 21, 2017

Abstract

AIM

To detect the expression of threonine and tyrosine kinase (TTK) in gallbladder cancer (GBC) specimens and analyze the associations between TTK expression and clinicopathological parameters and clinical prognosis.

METHODS

A total of 68 patients with GBC who underwent surgical resection were enrolled in this study. The expression of TTK in GBC tissues was detected by immunohistochemistry. The assessment of TTK

expression was conducted using the H-scoring system. H-score was calculated by the multiplication of the overall staining intensity with the percentage of positive cells. The expression of TTK in the cytoplasm and nucleus was scored separately to achieve respective H-score values. The correlations between TTK expression and clinicopathological parameters and clinical prognosis were analyzed using Chi-square test, Kaplan-Meier method and Cox regression.

RESULTS

In both the nucleus and cytoplasm, the expression of TTK in tumor tissues was significantly lower than that in normal tissues ($P < 0.001$ and $P = 0.026$, respectively). Using the median H-score as the cutoff value, it was discovered that, GBC patients with higher levels of TTK expression in the nucleus, but not the cytoplasm, had favorable overall survival ($P < 0.001$), and it was still statistically meaningful in Cox regression analysis. Further investigation indicated that there were close negative correlations between TTK expression and tumor differentiation ($P = 0.041$), CA 19-9 levels ($P = 0.016$), T stage ($P < 0.001$), nodal involvement ($P < 0.001$), distant metastasis ($P = 0.024$) and TNM stage ($P < 0.001$).

CONCLUSION

The expression of TTK in GBC is lower than that in normal tissues. Higher levels of TTK expression in GBC are concomitant with longer overall survival. TTK is a favorable prognostic biomarker for patients with GBC.

Key words: Threonine and tyrosine kinase; Biomarker; Prognosis; Gallbladder cancer

Core tip: Numerous studies demonstrate that high levels of threonine and tyrosine kinase (TTK) are present in many types of human malignancies, and its overexpression closely correlates with early recurrence and poor survival. However, no prior studies have attempted to concentrate on the expression of TTK in patients with gallbladder cancer (GBC). In this study, we detected the expression of TTK in GBC specimens and analyzed the associations between TTK expression and clinicopathological parameters and clinical prognosis.

Xie Y, Lin JZ, Wang AQ, Xu WY, Long JY, Luo YF, Shi J, Liang ZY, Sang XT, Zhao HT. Threonine and tyrosine kinase may serve as a prognostic biomarker for gallbladder cancer. *World J Gastroenterol* 2017; 23(31): 5787-5797 Available from: URL: http://www.wjgnet.com/1007-9327/full/v23/i31/5787.htm DOI: http://dx.doi.org/10.3748/wjg.v23.i31.5787

INTRODUCTION

Gallbladder cancer (GBC) is the most common malignancy of the biliary tract. As a potentially lethal disease, GBC has a dismal prognosis, with a median survival of 3-11 mo and a 5-year survival of 3%-13%[1]. Prolonged survival and better prognosis could be primarily seen in a small group of patients with incidental gallbladder cancer (IGBC), but this fortunate scenario exists in only 0.3%-2% of all performed cholecystectomies due to benign conditions or after cholecystectomy[2,3]. The incidence of GBC is characterized by remarkable geographical variations and ethnic disparities, with an extraordinarily high occurrence in Chile, Japan, and northern India[4]. The incidence of GBC is quite low in most Western countries and thus it is referred to as an orphan disease in the United States[5]. However, with increasing global migration, the incidence of GBC in the West is on the rise, making it a global disease and afflicting thousands of individuals worldwide. Currently, radical surgical resection remains to be the mainstay treatment to extend the life expectancy for eligible patients. There are few chemotherapeutic agents for patients with GBC and there are low response rates to adjuvant treatments.

The spindle assembly checkpoint (SAC) is a safeguard mechanism that functions to monitor improperly oriented chromosomes, generate correct bipolar attachments to the spindle and minimize chromosome missegregation errors prior to anaphase onset[6,7]. Threonine and tyrosine kinase (TTK) is a dual-specificity protein kinase capable of phosphorylating threonines/serines and tyrosines[8]. It is the core component and major regulator of the SAC, which is able to recruit and orchestrate other SAC protein kinases to the kinetochore, thereby ensuring faithful chromosome segregation and maintaining genome stability[9,10]. Increased TTK levels are readily discovered in many types of human tumors, including glioblastoma, thyroid carcinoma, breast cancer, hepatocellular carcinoma, pancreatic cancer as well as prostate cancer, and TTK overexpression closely correlates with early recurrence and poor survival[11-23]. We reviewed the relevant clinical research and trials concerning TTK in several human cancers[24], however, no prior studies were found regarding the expression of TTK in patients with GBC. In this study, we detected the expression of TTK in GBC specimens and analyzed the associations between TTK expression and clinicopathological parameters and clinical prognosis.

MATERIALS AND METHODS

Patients and tissue specimens

Sixty-eight cases were selected retrospectively from patients with GBC who underwent surgical resection at the Department of Liver Surgery of Peking Union Medical College Hospital (PUMCH) between June 2004 and January 2014 (Figure 1). Sixty-eight pairs of GBC specimens and adjacent normal tissue specimens were acquired from these patients. Written informed consent

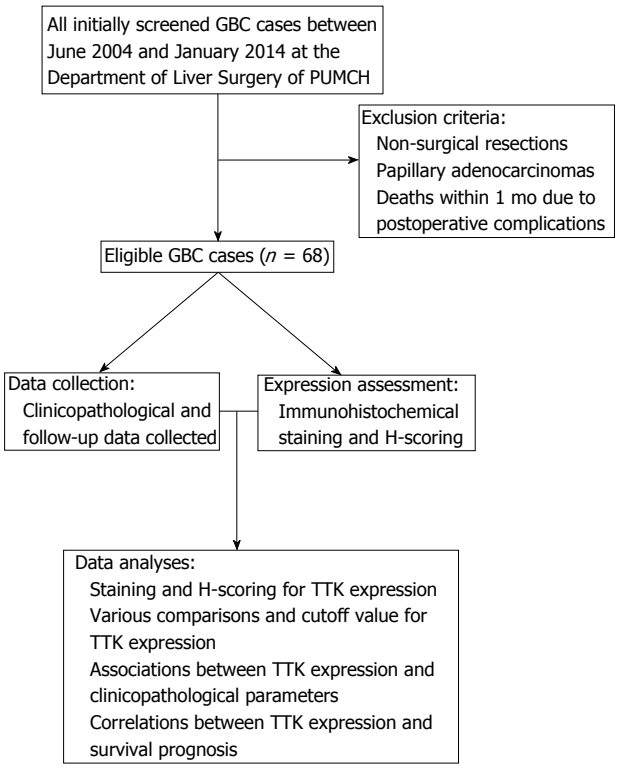

Figure 1 Flow diagram of the study. A total of 68 cases were enrolled in the study, with explicit exclusion criteria. After collecting clinicopathological and follow-up data and conducting immunohistochemistry staining, correlations between TTK expression and clinicopathological parameters and survival prognosis were analyzed. GBC: Gallbladder cancer; PUMCH: Peking Union Medical College Hospital; TTK: Threonine and tyrosine kinase.

was obtained from each patient before surgery, and surgical procedures were performed according to the approved guidelines. Surgical types were categorized as curative and noncurative resections. Curative resection (R0) referred to *en bloc* resection with a negative surgical margin, while the presence of microscopic (R1) or macroscopic (R2) residual cancer was considered noncurative. The clinicopathological data were collected from the medical records and the patients were followed from the date of surgery till October 2016. Patients with GBC were staged according to the 7th edition of American Joint Committee on Cancer system. The assays for liver function and serum tumor marker were considered positive when concentrations were beyond the normal upper limits. The follow-up data were obtained *via* outpatient records, phone visits and personal emails. The endpoint was overall survival (OS), defined as the time interval from the date of surgery to the cancer-related death. The study above was approved by the Ethics Committee of PUMCH.

Immunohistochemistry and H-scoring for TTK

All fresh tissue specimens were collected and immersed into 10% neutral-buffered formalin solution after immediate surgical resection and then embedded in paraffin. The paraffin-embedded tissues were sectioned at a thickness of 5 μm and stained immunohistochemically. Immunohistochemical staining was conducted manually and each slide was strictly processed in accordance with the immunohistochemical protocol. TTK polyclonal antibody (HPA016834, Sigma, the United States, 1:100), produced in rabbit, was used for biomarker expression analysis. High pressure induced antigen retrieval was performed in the PBS buffer solution (pH 7.3), and subsequent TTK staining was carried out for 90 min at the room temperature. Small intestinal tissue was recommended by the manufacturer as a positive control, and staining without the primary antibody was used as a negative control.

The immunohistochemical slides were evaluated independently by two experienced pathologists in a blinded fashion. The assessment of TTK staining was conducted using the H-scoring system[25-28], and H-score was calculated by the multiplication of the overall staining intensity with the percentage of positive cells. The staining intensity was graded from 0 to 3 (0 = negative, 1 = weak, 2 = medium, 3 = strong) and the positive percentage increased from 0 to 100. Theoretically, the final H-score values were obtained with a range from 0 to 300. TTK staining in the cytoplasm and nucleus was scored separately to achieve respective values.

Statistical analysis

Statistical analyses were performed using SPSS 17.0 software (Chicago, IL, United States). Kolmogorov-Smirnov test was used to assess the distribution of the data and to decide the selection of statistical method. Chi-square test was used to compare qualitative variables and Mann-Whitney *U* test was used to compare the abnormally distributed variables. Kaplan-Meier method and log-rank test were used to compare OS. All potential prognostic factors on univariate analyses were entered into the Cox regression model. Cox regression multivariate analysis was performed further to identify the independent prognostic factors. All *P*-values were two sided and considered statistically significant when less than 0.05.

RESULTS

Clinicopathological characteristics and survival data

The mean and median ages of patients at surgery were 65 and 66 years (range, 35-79 years), separately. The majority (57.4%) of patients were female and the female:male ratio was 1.3:1. Gallstones were present in 60.3% of cases. Slightly more than half (51.5%) of patients underwent curative resection and moderately to well-differentiated adenocarcinomas were found in 77.9% of cases. Nodal involvement and distant metastasis occurred in 44.1% and 11.8% of patients, respectively. Three cases were completely lost to follow-up after surgery. The median overall follow-up period was 55 mo (range, 27-159 mo). The 1-year and

Table 1 Clinicopathological characteristics of the cohort

Characteristic	*n* (%)
Age (yr)	
≤ 65	33 (48.5)
> 65	35 (51.5)
Gender	
Female	39 (57.4)
Male	29 (42.6)
Cholecystolithiasis	
Yes	41 (60.3)
No	27 (39.7)
Diabetes	
Yes	17 (25.0)
No	51 (75.0)
Fever	
Yes	9 (13.2)
No	59 (86.8)
Jaundice	
Yes	15 (22.1)
No	53 (77.9)
ALT	
Normal	53 (77.9)
Elevated	15 (22.1)
AST	
Normal	50 (75.8)
Elevated	16 (24.2)
TBil	
Normal	49 (72.1)
Elevated	19 (27.9)
DBil	
Normal	50 (73.5)
Elevated	18 (26.5)
GGT	
Normal	43 (69.4)
Elevated	19 (30.6)
ALP	
Normal	45 (72.6)
Elevated	17 (27.4)
CEA	
Normal	42 (72.4)
Elevated	16 (27.6)
CA 19-9	
Normal	26 (44.1)
Elevated	33 (55.9)
Surgical type	
Curative	35 (51.5)
Noncurative	33 (48.5)
Tumor size (cm)	
≤ 3	43 (63.2)
> 3	25 (36.8)
Differentiation	
Lowly-undifferentiated	15 (22.1)
Moderately-well	53 (77.9)
T stage	
Tis	1 (1.5)
T1	3 (4.4)
T2	29 (42.6)
T3	35 (51.5)
N stage	
N0	38 (55.9)
N1	22 (32.4)
N2	8 (11.7)
M stage	
M0	60 (88.2%)
M1	8 (11.8%)
TNM stage	
Ⅰ	4 (5.9)
Ⅱ	24 (35.3)
ⅢA	9 (13.2)
ⅢB	17 (25.0)
ⅣA	0 (0)
ⅣB	14 (20.6)

ALT: Alanine aminotransferase; AST: Aspartate aminotransferase; TBil: Total bilirubin; DBil: Direct bilirubin; GGT: Gamma-glutamyl transpeptidase; ALP: Alkaline phosphatase; CEA: Carcinoembryonic antigen; CA 19-9: Carbohydrate antigen 19-9.

Table 2 Threonine and tyrosine kinase staining results in tumor and normal tissues

Localization	Positive cell rate (%) Median (range)		*n* (%)	
	Tumor tissues	Normal tissues	Tumor tissues	Normal tissues
Cytoplasmic staining				
Negative	-	-	0	0
Positive	100 (10-100)	99 (40-100)	68 (100)	68 (100)
1+	55 (10-100)	85 (18-100)	41 (60.3)	14 (20.6)
2+	90 (5-100)	100 (80-100)	49 (72.1)	54 (79.4)
3+	20	90	1 (1.5)	1 (1.5)
Nuclear staining				
Negative	-	-	8 (11.8)	2 (2.9)
Positive	15 (1-98)	60 (1-90)	60 (88.2)	66 (97.1)
1+	15 (1-85)	60 (1-90)	57 (83.8)	59 (86.8)
2+	45 (5-98)	90 (60-90)	8 (11.8)	7 (10.3)
3+	-	-	0	0

2-year survival rates were 66.2% and 41.2%, separately. More information about the cohort is listed in Table 1.

Staining and H-scoring for TTK expression

TTK staining was counted and analyzed in the patients (Table 2 and Figure 2). In tumor tissues, all specimens displayed cytoplasmic staining, of which one case was strongly positive (3+); most specimens (88.2%, 60/68) displayed nuclear staining, eight cases exhibited negative nuclear staining, and no strongly positive cases were found among the specimens. While in normal tissues, overall specimens displayed cytoplasmic staining, of which one case was strongly positive (3+); nearly all specimens (97.1%, 66/68) displayed nuclear staining, two cases exhibited negative nuclear staining, and no strong positive cases were found within the specimens.

We calculated the H-score in both tumor and normal tissues (Table 3 and Figure 3), and it was found that, in tumor tissues, TTK exhibited a median H-score of 170 (range, 10-220) and 12.5 (range, 0-196) in the cytoplasm and nucleus, separately. While in normal tissues, the median H-scores observed for TTK were 190 (range, 40-270) and 60 (range, 0-180), respectively.

Various comparisons and cutoff value for TTK expression

Indicated by Kolmogorov-Smirnov test, the values of H-score were distributed abnormally. Therefore, Mann-Whitney *U* test was selected to make comparisons for

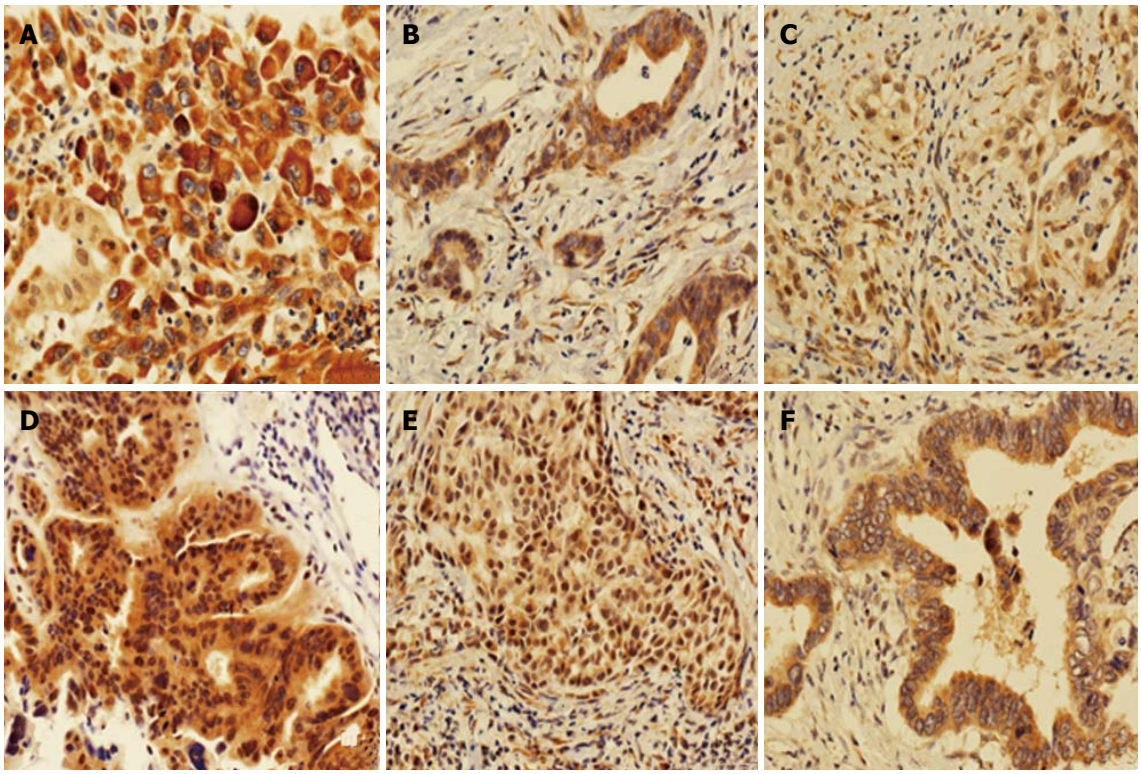

Figure 2 Immunohistochemical staining of tumor tissues (magnification, × 200). A-C: Cytoplasm staining with 3+, 2+ and 1+ intensity, respectively; D-F: Nuclear staining with 2+, 1+ and 0+ intensity, respectively.

Table 3 H-score values in tumor and normal tissues

Group	*n*	Localization	Minimum	Maximum	Median
Tumor	68	Nucleus	0	196	12.5
	68	Cytoplasm	10	220	170
Normal	68	Nucleus	0	180	60
	68	Cytoplasm	40	270	190

Table 4 Various comparisons in tumor and normal tissues for threonine and tyrosine kinase expression

Group	*n*	Minimum	Maximum	Median	Mean rank	*P* value
Comparison between nucleus and cytoplasm in normal tissues						
Nucleus	68	0	180	60	39.65	<0.001[1]
Cytoplasm	68	40	270	190	97.35	
Comparison between nucleus and cytoplasm in tumor tissues						
Nucleus	68	0	196	12.5	38.98	<0.001[1]
Cytoplasm	68	10	220	170	98.02	
Comparison between tumor and normal tissues in nucleus						
Tumor	68	0	196	12.5	49.54	<0.001[1]
Normal	68	0	180	60	87.46	
Comparison between tumor and normal tissues in cytoplasm						
Tumor	68	10	220	170	61.19	0.026[1]
Normal	68	40	270	190	75.81	

[1]Statistically significant.

them (Table 4). In both tumor and normal tissues, the expression of TTK in the nucleus was significantly lower than that in the cytoplasm ($P < 0.001$ for both). Moreover, we found that, in both the nucleus and cytoplasm, there was significantly lower expression of

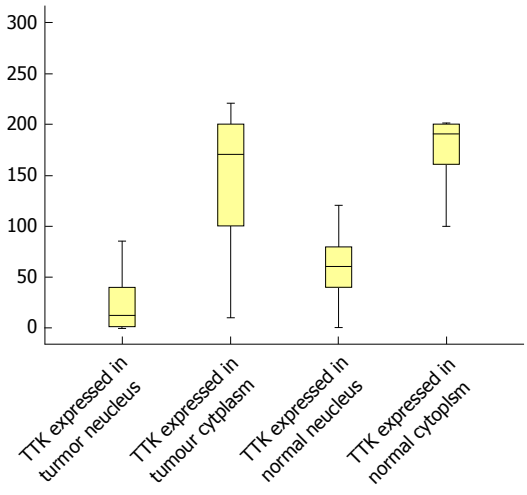

Figure 3 Boxplot for H-scores in tumor and normal tissues. TTK: Threonine and tyrosine kinase.

TTK in tumor tissues, compared with normal tissues ($P < 0.001$ and $P = 0.026$, respectively).

For patients with GBC, the population was divided into two groups according to the median H-score values of the nuclear and cytoplasmic staining. Surprisingly, we found that, patients with higher H-score values in the nucleus, but not the cytoplasm, had favorable OS (Figure 4A), and it was still statistically meaningful in Cox regression multivariate analysis (Table 5). Thus, the median nuclear H-score was used as the discriminating threshold[29] and the cutoff value was set at 12.5.

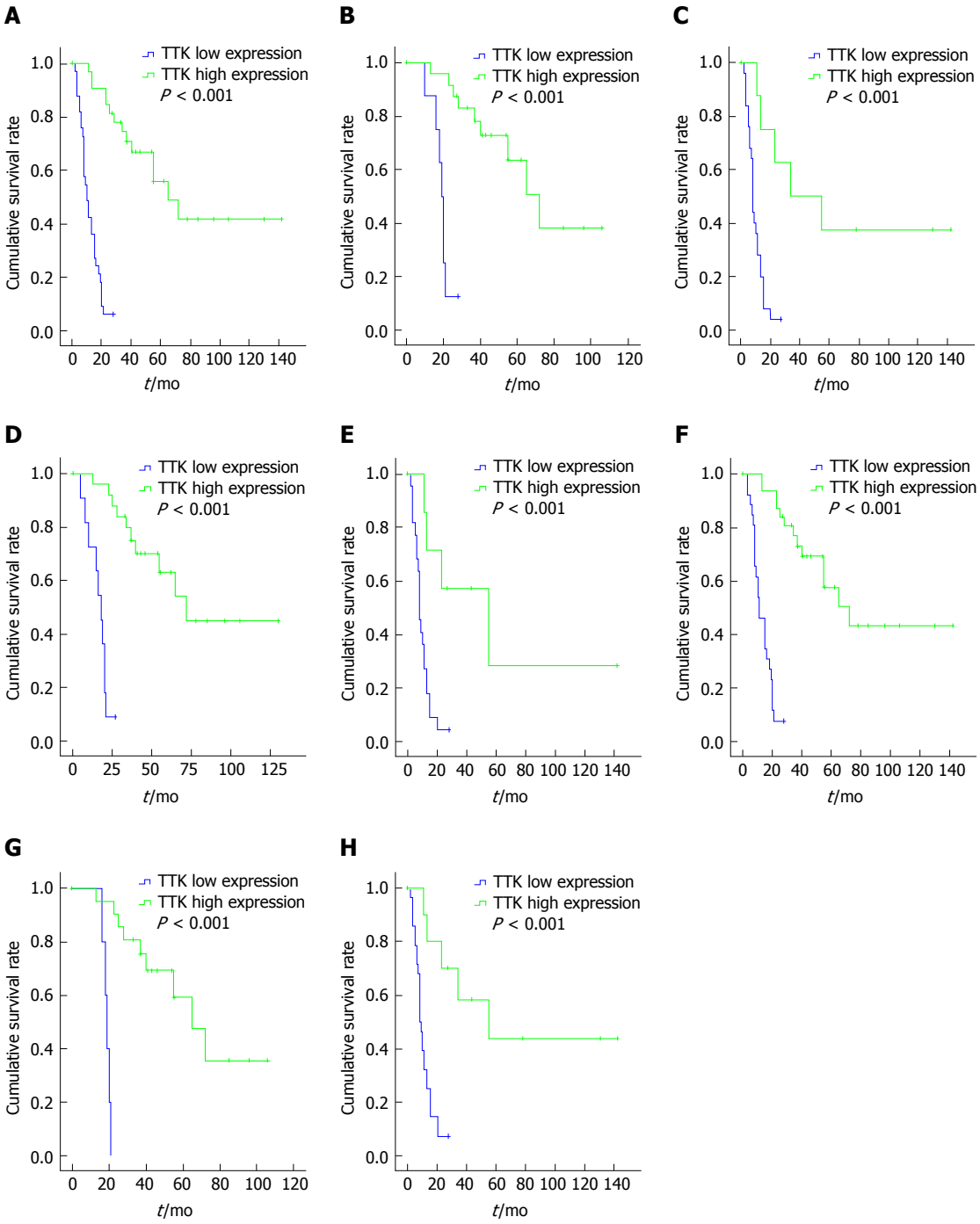

Figure 4 Kaplan-Meier survival analyses in different subgroups, according to threonine and tyrosine kinase expression. A: The whole cohort; B: T1 + 2 group; C: T3 group; D: Negative nodal involvement group; E: Positive nodal involvement group; F: Free distant metastasis group; G: Stage Ⅰ + Ⅱ group; H: Stage Ⅲ + Ⅳ group. TTK: Threonine and tyrosine kinase.

Correlations between TTK expression and clinicopathological parameters

The correlations between TTK expression and clinicopathological parameters are detailed in Table 6. There were no significant associations between TTK expressions and age, gender, tumor size or CEA levels. However, TTK expression exhibited significant negative correlations with tumor differentiation (P = 0.041), CA 19-9 levels (P = 0.016), T stage (P < 0.001), nodal involvement (P < 0.001), distant metastasis (P = 0.024) and TNM stage (P < 0.001). Higher TTK expression rates were observed in patients with normal CA 19-9 levels, moderately to well-differentiated tumors, T stages 1 + 2, negative nodal involvement, free distant metastasis and TNM stages Ⅰ + Ⅱ, in contrast to the ones with elevated CA 19-9 levels, lowly to undifferentiated tumors, T stage 3, positive nodal involvement, distant metastasis and TNM stages Ⅲ + Ⅳ, respectively.

Survival analysis

Clinical follow-up data were available among 65 of

Table 5 Univariate and multivariate analyses for gallbladder cancer

	χ^2	*P* value	OR (95%CI)
Univariate			
Age	2.221	0.136	
Gender	0.167	0.683	
Cholecystolithiasis	0.346	0.558	
Diabetes	0.165	0.685	
Fever	0.001	0.989	
Jaundice[1]	5.110	0.024[1]	
ALT[1]	7.781	0.005[1]	
AST[1]	5.708	0.017[1]	
TBil	0.241	0.516	
DBil[1]	6.645	0.010[1]	
GGT	0.899	0.343	
ALP[1]	4.099	0.043[1]	
CEA	3.137	0.077	
CA 19-9[1]	12.385	< 0.001[1]	
Surgical type[1]	20.715	< 0.001[1]	
Tumor size	0.099	0.754	
Differentiation[1]	12.385	< 0.001[1]	
T stage[1]	21.594	< 0.001[1]	
N stage[1]	19.887	< 0.001[1]	
M stage[1]	29.503	< 0.001[1]	
TNM stage[1]	33.062	< 0.001[1]	
TTK[1]	21.226	< 0.001[1]	
Multivariate			
Surgery type[1]		0.001[1]	4.250 (1.867-9.674)
T stage[1]		0.013[1]	2.927 (1.258-6.808)
TTK[1]		0.001[1]	0.076 (0.024-0.241)

[1]Statistically significant. ALT: Alanine aminotransferase; AST: Aspartate aminotransferase; GGT: Gamma-glutamyl transpeptidase; CEA: Carcinoembryonic antigen; TTK: Threonine and tyrosine kinase.

Table 6 Correlations between TTK expression and clinicopathological parameters

Parameter	TTK expression		χ^2	*P*-value
	Low expression	High expression		
Age (yr)				
≤ 65	16	17	0.059	0.808
> 65	18	17		
Gender				
Female	20	19	0.277	0.598
Male	13	16		
CEA				
Normal	20	22	3.512	0.061
Elevated	12	4		
CA 19-9[1]				
Normal	10	16	5.756	0.016[1]
Elevated	23	10		
Tumor size				
≤ 3	22	21	0.063	0.801
> 3	12	13		
Differentiation[1]				
Lowly-undifferentiated	11	4	4.191	0.041[1]
Moderately-well	23	30		
T stage[1]				
1 + 2	8	25	17.015	< 0.001[1]
3	26	9		
Nodal involvement[1]				
Negative	12	26	11.691	< 0.001[1]
Positive	22	8		
Metastasis[1]				
M0	27	33	5.100	0.024[1]
M1	7	1		
TNM stage[1]				
Ⅰ + Ⅱ	5	23	19.671	< 0.001[1]
Ⅲ + Ⅳ	29	11		

[1]Statistically significant. CEA: Carcinoembryonic antigen; TTK: Threonine and tyrosine kinase.

the 68 patients. Univariate survival analysis (Table 5) revealed that TTK expression ($P < 0.001$), jaundice ($P = 0.024$), concentrations of ALT ($P = 0.005$), AST ($P = 0.017$), ALP ($P = 0.043$), DBil ($P = 0.010$), CA 19-9 ($P < 0.001$), surgical type ($P < 0.001$), tumor differentiation ($P < 0.001$), T ($P < 0.001$), N ($P < 0.001$), M ($P < 0.001$) and TNM stages ($P < 0.001$) were associated with OS in patients with GBC, while age, gender, fever, cholecystolithiasis, diabetes, concentrations of TBil, GGT and CEA had no significant influence on the survival in our study.

Cox regression multivariate analysis revealed that surgical type, T stage and TTK expression were independent prognostic factors for OS (Table 5). Further, subgroup analysis by log-rank test indicated that patients with higher levels of TTK expression had longer OS and better prognosis, regardless of T, N, M, or TNM stage, in comparison with the ones with lower TTK expression (Figure 4 B-H).

DISCUSSION

On account of its critical role in maintaining chromosome stability, an increasing number of researchers have concentrated on the relationship between TTK and cancer. While TTK has been studied in many types of malignancies, no prior research has been found regarding its expression and clinical prognosis, in GBC.

In the present study, it was discovered that, the overall expression of TTK in tumor tissues was significantly lower than that in normal tissues, and GBC patients with higher TTK expression had a better prognosis. By contrast, TTK overexpression was found in numerous neoplasms, where they were concomitant with a worse prognosis. Consistent with our results, Xu *et al*[30] also found that increased TTK expression was related with prolonged disease free survival and OS in triple-negative breast cancer, but without comparisons between tumor and normal tissues. It may be suggested that TTK plays a certain role in the initiation of GBC. TTK is required for the execution of the SAC machinery during mitosis and conductive to the fidelity of chromosome segregations at the kinetochores. The inhibition of TTK activity could therefore compromise the function of the SAC and culminate in undesirable effects, including chromosomal instability (CIN), aneuploidy formation, cell death or carcinogenesis[31-35]. It is widely accepted that chromosomal instability is correlative with intratumor heterogeneity, chromosome aberrations and aneuploidy formations. In fact, aneuploidy has been found at the earliest stages of carcinogenesis and CIN is considered a fundamental process for cancer development[36]. So far, a premature

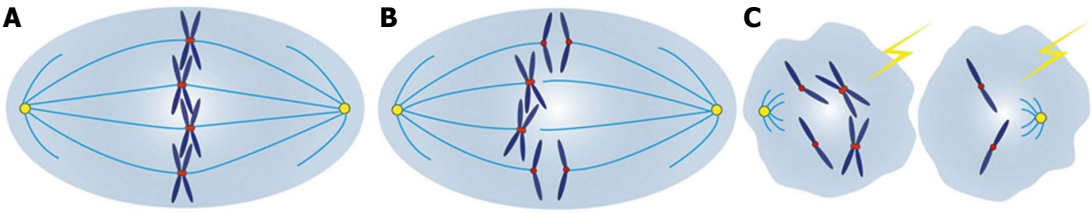

Figure 5 Diagram for possible mechanism concerning threonine and tyrosine kinase and carcinogenesis. A: Sister chromatids are properly arrayed in the equatorial plate at metaphase, with correct attachments to microtubules by kinetochores, attributed to the normal spindle assembly checkpoint (SAC) safeguard mechanism; B: Aberrant TTK expression, either increased or decreased expressions, could definitely compromise the functions of the SAC, with frequent chromosome missegregation errors; C: Severe chromosome missegregation errors, due to the override of SAC function, could result in chromosomal instabilities, aneuploidy formations, cell deaths and carcinogenesis; TTK: Threonine and tyrosine kinase.

termination of TTK synthesis, due to cancer-associated frameshift mutations, has been frequently found in gastric and colorectal cancers with microsatellite instability[37]. Whether the same process takes place in GBC remains to be explored afterwards.

Apart from the variances between tumor and normal tissues, it was revealed in our current study that there were significant negative correlations between TTK expression and tumor differentiation, T, N, M as well as TNM stages. Furthermore, it was discovered that lower levels of TTK expressions were more helpful for cancer infiltration, nodal involvement and distant metastasis. Patients with higher levels of TTK expression at the same stage had a longer OS than those with lower levels of TTK expression. Thus, TTK may serve as a positive biomarker indicative of prognosis and make a strategic choice for clinicians. For instance, patients with higher levels of TTK expression perhaps could benefit better from the adjuvant chemo- or radio-therapy, in contrast to the ones with lower expression. The use of TTK expression may be more important for patients with IGBC. Currently, the management of IGBC is primarily dictated by T stage alone, with a re-resection recommendation for T1b, T2, or T3 disease[38]. In terms of T1a patients, simple laparoscopic cholecystectomy is sufficient, with a 5-year survival rate of 95.5%[39]. If lower levels of TTK expression are detected in cancer specimens, more attention should be paid to these patients, due to a larger likelihood of nodal involvement and distant metastasis in the future. The survival of the remaining 4.5% of patients may be improved, with a combination of routine pathology and TTK expression.

Of note, our study may provide theoretical support for immunotherapy and targeted therapy in different tumors concerning TTK. TTK has been utilized as an immunogenic epitope to elicit potent and peptide-specific cytotoxic T lymphocyte activity against cancer cells. Its safety, immunogenicity and clinical response have been validated in some clinical trials, including lung cancer, esophageal cancer and biliary tract cancer[40-46]. Even, in a variety of human tumors, TTK has been used as a therapeutic target for innovative approaches in combating the malignancies, involving glioblastoma, breast cancer, hepatocellular carcinoma and pancreatic cancer[11,12,14-16,18-21]. TTK inhibitors could give rise to attenuated aggressiveness, reduced viability, augmented autophagy and increased apoptosis in these cancers. Further, phase I clinical trials of oral TTK inhibitors (BAY1161909, BAY1217389) have been performed in breast cancer (ClinicalTrials.gov ID: NCT02138812, NCT02366949). In terms of these tumors above, TTK overexpression is exploited and TTK-targeted therapies are available. Nevertheless, it should be cautious for these therapies applied in GBC, due to the low TTK expression.

To date, some mechanisms have been revealed in several tumors, concerning TTK and neoplasia. It was unveiled that, in hepatocellular carcinoma, demethylations of TTK promoters were conducive to its overexpression and highly expressed TTK could activate the Akt/mTOR pathway in a p53 dependent fashion[18]. Moreover, in melanoma, TTK/AKT and B-Raf^{WT}/ERK signaling constituted an auto-regulatory negative feedback loop together, and continuous phosphorylations of TTK through oncogenic B-Raf^{V600E} signaling were able to abrogate the negative feedback loop, leading to aberrant SAC function and tumorigenesis[47,48]. It was discovered that, in breast cancer, high levels of TTK expression were protective for aneuploidy and enabled these cells to tolerate aneuploidy[49]. While in colon cancer, overexpressed TTK could increase aneuploidy, owing to a weakened SAC function, and contribute to carcinogenesis[50]. Among studies available in the literature, it was demonstrated that overexpression of TTK correlated positively with tumor grades and poor survival. Conversely, it was indicated in our study that, lower expression of TTK correlated closely with tumor grade and dismal prognosis. Taken together, aberrant TTK expression, either increased or decreased expression, is clearly correlated with tumorigenesis, which may result from chromosomal instabilities and aneuploidy formations, as a result of compromised SAC functions (Figure 5). Therefore, TTK may play different roles in disparate malignancies, and more thorough research studies are still encouraged to verify the exact relationships between TTK and cancers, as well as the subtle mechanisms.

Recently, it has been found that TP53, KRAS and ERBB3 are the most frequent somatic mutations in the GBC spectrum[51]. Additionally, striking progress has

been made in the clarification of emergent intracellular signaling pathways, such as Hedgehog, PI3K/AKT/mTOR and Notch, which are activated in GBC[52]. These promising studies may provide valuable clues for the deep insight into the roles that TTK plays in GBC.

Our study has several limitations. Primarily, the study was retrospective, and all the information of each patient was collected from medical records, which may contribute to the selection bias. Next, it was a single-institutional investigation and the number of cases was relatively small, restricting the power of statistical analysis. Finally, some patients received postoperative chemotherapy or radiotherapy, and the effects of these adjuvant therapies on prognosis were not considered, in spite of limited survival benefits brought by them. For these reasons above, multi-institutional investigations and prospective studies are required to explore the expression of TTK in GBC, and further evaluate its clinical significance in a larger cohort of patients.

In conclusion, our data suggest that the expression of TTK in GBC is lower than that in normal tissues. Higher levels of TTK expression are concomitant with longer overall survival in GBC. TTK is a favorable prognostic biomarker for patients with GBC.

COMMENTS

Background

Threonine and tyrosine kinase (TTK) is a dual-specificity protein kinase capable of phosphorylating threonines/serines and tyrosines. It is the core component and major regulator of the spindle assembly checkpoint (SAC), which functions to ensure faithful chromosome segregation and maintain genome stability. Increased TTK levels could be readily discovered in many types of human tumors, including glioblastoma, thyroid carcinoma and breast cancer, and its overexpression closely correlates with early recurrence and poor survival. However, no prior studies were found regarding the expression of TTK in patients with gallbladder cancer (GBC). In this study, we detected the expression of TTK in GBC specimens and analyzed the associations between TTK expression and clinicopathological parameters and clinical prognosis.

Research frontiers

Numerous studies demonstrate that high levels of TTK are present in many types of human malignancies, and its overexpression closely correlates with early recurrence and poor survival. Several TTK inhibitors have been developed to combat the malignancies and they exhibit demonstrable survival benefits. Moreover, TTK has been used as an immunogenic epitope to elicit potent and peptide-specific cytotoxic T lymphocyte activity against cancer cells. Its safety, immunogenicity and clinical response have been validated in several clinical trials.

Innovations and breakthroughs

The results demonstrate that the expression of TTK in gallbladder cancer is lower than that in normal tissues. Higher levels of TTK expression are concomitant with longer overall survival in GBC. TTK is a favorable prognostic biomarker for patients with GBC.

Applications

This study suggests that TTK may serve as a positive biomarker indicative of prognosis, and it may also provide theoretical support for the immunotherapy and targeted therapy in different tumors concerning TTK.

Terminology

The SAC is a safeguard mechanism that functions to monitor improperly oriented chromosomes, generate correct bipolar attachments to the spindle and minimize chromosome missegregation errors prior to anaphase onset. TTK is a dual-specificity protein kinase that phosphorylates threonines/serines and tyrosines. TTK acts as the core component and major regulator of the SAC, which functions to recruit and orchestrate other SAC protein kinases to the kinetochore, thereby ensuring faithful chromosome segregation and maintaining genome stability.

Peer-review

This is an interesting study about the TTK in GBC. In this study, the authors investigated the expression of TTK in GBC specimens and the associations between TTK expression and clinicopathological parameters and clinical prognosis. The authors found that using the median H-score as the cutoff value, patients with higher levels of TTK expression in the nucleus had favorable overall survival. This study is overall well-designed and the manuscript is very well-written.

REFERENCES

1 **Cubertafond P**, Gainant A, Cucchiaro G. Surgical treatment of 724 carcinomas of the gallbladder. Results of the French Surgical Association Survey. *Ann Surg* 1994; **219**: 275-280 [PMID: 8147608 DOI: 10.1097/00000658-199403000-00007]

2 **Steinert R**, Nestler G, Sagynaliev E, Müller J, Lippert H, Reymond MA. Laparoscopic cholecystectomy and gallbladder cancer. *J Surg Oncol* 2006; **93**: 682-689 [PMID: 16724350 DOI: 10.1002/jso.20536]

3 **Kwon AH**, Imamura A, Kitade H, Kamiyama Y. Unsuspected gallbladder cancer diagnosed during or after laparoscopic cholecystectomy. *J Surg Oncol* 2008; **97**: 241-245 [PMID: 18095299 DOI: 10.1002/jso.20944]

4 **Hundal R**, Shaffer EA. Gallbladder cancer: epidemiology and outcome. *Clin Epidemiol* 2014; **6**: 99-109 [PMID: 24634588 DOI: 10.2147/CLEP.S37357]

5 **Levy AD**, Murakata LA, Rohrmann CA Jr. Gallbladder carcinoma: radiologic-pathologic correlation. *Radiographics* 2001; **21**: 295-314; questionnaire, 549-555 [PMID: 11259693 DOI: 10.1148/radiographics.21.2.g01mr16295]

6 **Lara-Gonzalez P**, Westhorpe FG, Taylor SS. The spindle assembly checkpoint. *Curr Biol* 2012; **22**: R966-R980 [PMID: 23174302 DOI: 10.1016/j.cub.2012.10.006]

7 **Vleugel M**, Hoogendoorn E, Snel B, Kops GJ. Evolution and function of the mitotic checkpoint. *Dev Cell* 2012; **23**: 239-250 [PMID: 22898774 DOI: 10.1016/j.devcel.2012.06.013]

8 **Fisk HA**, Mattison CP, Winey M. A field guide to the Mps1 family of protein kinases. *Cell Cycle* 2004; **3**: 439-442 [PMID: 14963409 DOI: 10.4161/cc.3.4.784]

9 **Sacristan C**, Kops GJ. Joined at the hip: kinetochores, microtubules, and spindle assembly checkpoint signaling. *Trends Cell Biol* 2015; **25**: 21-28 [PMID: 25220181 DOI: 10.1016/j.tcb.2014.08.006]

10 **Santaguida S**, Amon A. Short- and long-term effects of chromosome mis-segregation and aneuploidy. *Nat Rev Mol Cell Biol* 2015; **16**: 473-485 [PMID: 26204159 DOI: 10.1038/nrm4025]

11 **Tannous BA**, Kerami M, Van der Stoop PM, Kwiatkowski N, Wang J, Zhou W, Kessler AF, Lewandrowski G, Hiddingh L, Sol N, Lagerweij T, Wedekind L, Niers JM, Barazas M, Nilsson RJ, Geerts D, De Witt Hamer PC, Hagemann C, Vandertop WP, Van Tellingen O, Noske DP, Gray NS, Würdinger T. Effects of the selective MPS1 inhibitor MPS1-IN-3 on glioblastoma sensitivity to antimitotic drugs. *J Natl Cancer Inst* 2013; **105**: 1322-1331 [PMID: 23940287 DOI: 10.1093/jnci/djt168]

12 **Maachani UB**, Kramp T, Hanson R, Zhao S, Celiku O, Shankavaram U, Colombo R, Caplen NJ, Camphausen K, Tandle A. Targeting MPS1 Enhances Radiosensitization of Human Glioblastoma by Modulating DNA Repair Proteins. *Mol Cancer Res* 2015; **13**: 852-862 [PMID: 25722303 DOI: 10.1158/1541-7786.MCR-14-0462-T]

13 **Salvatore G**, Nappi TC, Salerno P, Jiang Y, Garbi C, Ugolini C, Miccoli P, Basolo F, Castellone MD, Cirafici AM, Melillo

RM, Fusco A, Bittner ML, Santoro M. A cell proliferation and chromosomal instability signature in anaplastic thyroid carcinoma. *Cancer Res* 2007; **67**: 10148-10158 [PMID: 17981789 DOI: 10.1158/0008-5472.can-07-1887]

14 **Maire V**, Baldeyron C, Richardson M, Tesson B, Vincent-Salomon A, Gravier E, Marty-Prouvost B, De Koning L, Rigaill G, Dumont A, Gentien D, Barillot E, Roman-Roman S, Depil S, Cruzalegui F, Pierré A, Tucker GC, Dubois T. TTK/hMPS1 is an attractive therapeutic target for triple-negative breast cancer. *PLoS One* 2013; **8**: e63712 [PMID: 23700430 DOI: 10.1371/journal.pone.0063712]

15 **Győrffy B**, Bottai G, Lehmann-Che J, Kéri G, Orfi L, Iwamoto T, Desmedt C, Bianchini G, Turner NC, de Thè H, André F, Sotiriou C, Hortobagyi GN, Di Leo A, Pusztai L, Santarpia L. TP53 mutation-correlated genes predict the risk of tumor relapse and identify MPS1 as a potential therapeutic kinase in TP53-mutated breast cancers. *Mol Oncol* 2014; **8**: 508-519 [PMID: 24462521 DOI: 10.1016/j.molonc.2013.12.018]

16 **Maia AR**, de Man J, Boon U, Janssen A, Song JY, Omerzu M, Sterrenburg JG, Prinsen MB, Willemsen-Seegers N, de Roos JA, van Doornmalen AM, Uitdehaag JC, Kops GJ, Jonkers J, Buijsman RC, Zaman GJ, Medema RH. Inhibition of the spindle assembly checkpoint kinase TTK enhances the efficacy of docetaxel in a triple-negative breast cancer model. *Ann Oncol* 2015; **26**: 2180-2192 [PMID: 26153498 DOI: 10.1093/annonc/mdv293]

17 **Miao R**, Luo H, Zhou H, Li G, Bu D, Yang X, Zhao X, Zhang H, Liu S, Zhong Y, Zou Z, Zhao Y, Yu K, He L, Sang X, Zhong S, Huang J, Wu Y, Miksad RA, Robson SC, Jiang C, Zhao Y, Zhao H. Identification of prognostic biomarkers in hepatitis B virus-related hepatocellular carcinoma and stratification by integrative multi-omics analysis. *J Hepatol* 2014; **61**: 840-849 [PMID: 24859455 DOI: 10.1016/j.jhep.2014.05.025]

18 **Liu X**, Liao W, Yuan Q, Ou Y, Huang J. TTK activates Akt and promotes proliferation and migration of hepatocellular carcinoma cells. *Oncotarget* 2015; **6**: 34309-34320 [PMID: 26418879 DOI: 10.18632/oncotarget.5295]

19 **Miao R**, Wu Y, Zhang H, Zhou H, Sun X, Csizmadia E, He L, Zhao Y, Jiang C, Miksad RA, Ghaziani T, Robson SC, Zhao H. Utility of the dual-specificity protein kinase TTK as a therapeutic target for intrahepatic spread of liver cancer. *Sci Rep* 2016; **6**: 33121 [PMID: 27618777 DOI: 10.1038/srep33121]

20 **Slee RB**, Grimes BR, Bansal R, Gore J, Blackburn C, Brown L, Gasaway R, Jeong J, Victorino J, March KL, Colombo R, Herbert BS, Korc M. Selective inhibition of pancreatic ductal adenocarcinoma cell growth by the mitotic MPS1 kinase inhibitor NMS-P715. *Mol Cancer Ther* 2014; **13**: 307-315 [PMID: 24282275 DOI: 10.1158/1535-7163.MCT-13-0324]

21 **Kaistha BP**, Honstein T, Müller V, Bielak S, Sauer M, Kreider R, Fassan M, Scarpa A, Schmees C, Volkmer H, Gress TM, Buchholz M. Key role of dual specificity kinase TTK in proliferation and survival of pancreatic cancer cells. *Br J Cancer* 2014; **111**: 1780-1787 [PMID: 25137017 DOI: 10.1038/bjc.2014.460]

22 **Shiraishi T**, Terada N, Zeng Y, Suyama T, Luo J, Trock B, Kulkarni P, Getzenberg RH. Cancer/Testis Antigens as potential predictors of biochemical recurrence of prostate cancer following radical prostatectomy. *J Transl Med* 2011; **9**: 153 [PMID: 21917134 DOI: 10.1186/1479-5876-9-153]

23 **Dahlman KB**, Parker JS, Shamu T, Hieronymus H, Chapinski C, Carver B, Chang K, Hannon GJ, Sawyers CL. Modulators of prostate cancer cell proliferation and viability identified by short-hairpin RNA library screening. *PLoS One* 2012; **7**: e34414 [PMID: 22509301 DOI: 10.1371/journal.pone.0034414]

24 **Xie Y**, Wang A, Lin J, Wu L, Zhang H, Yang X, Wan X, Miao R, Sang X, Zhao H. Mps1/TTK: a novel target and biomarker for cancer. *J Drug Target* 2017; **25**: 112-118 [PMID: 27819146 DOI: 10.1080/1061186X.2016.1258568]

25 **Yeo W**, Chan SL, Mo FK, Chu CM, Hui JW, Tong JH, Chan AW, Koh J, Hui EP, Loong H, Lee K, Li L, Ma B, To KF, Yu SC. Phase I/II study of temsirolimus for patients with unresectable Hepatocellular Carcinoma (HCC)- a correlative study to explore potential biomarkers for response. *BMC Cancer* 2015; **15**: 395 [PMID: 25962426 DOI: 10.1186/s12885-015-1334-6]

26 **Specht E**, Kaemmerer D, Sänger J, Wirtz RM, Schulz S, Lupp A. Comparison of immunoreactive score, HER2/neu score and H score for the immunohistochemical evaluation of somatostatin receptors in bronchopulmonary neuroendocrine neoplasms. *Histopathology* 2015; **67**: 368-377 [PMID: 25641082 DOI: 10.1111/his.12662]

27 **Liang PI**, Li CF, Chen LT, Sun DP, Chen TJ, Hsing CH, Hsu HP, Lin CY. BCL6 overexpression is associated with decreased p19 ARF expression and confers an independent prognosticator in gallbladder carcinoma. *Tumour Biol* 2014; **35**: 1417-1426 [PMID: 24114011 DOI: 10.1007/s13277-013-1195-z]

28 **Budwit-Novotny DA**, McCarty KS, Cox EB, Soper JT, Mutch DG, Creasman WT, Flowers JL, McCarty KS Jr. Immunohistochemical analyses of estrogen receptor in endometrial adenocarcinoma using a monoclonal antibody. *Cancer Res* 1986; **46**: 5419-5425 [PMID: 3756890]

29 **Christoph DC**, Kasper S, Gauler TC, Loesch C, Engelhard M, Theegarten D, Poettgen C, Hepp R, Peglow A, Loewendick H, Welter S, Stamatis G, Hirsch FR, Schuler M, Eberhardt WE, Wohlschlaeger J. βV-tubulin expression is associated with outcome following taxane-based chemotherapy in non-small cell lung cancer. *Br J Cancer* 2012; **107**: 823-830 [PMID: 22836512 DOI: 10.1038/bjc.2012.324]

30 **Xu Q**, Xu Y, Pan B, Wu L, Ren X, Zhou Y, Mao F, Lin Y, Guan J, Shen S, Zhang X, Wang C, Zhong Y, Zhou L, Liang Z, Zhao H, Sun Q. TTK is a favorable prognostic biomarker for triple-negative breast cancer survival. *Oncotarget* 2016; **7**: 81815-81829 [PMID: 27833085 DOI: 10.18632/oncotarget.13245]

31 **Colombo R**, Caldarelli M, Mennecozzi M, Giorgini ML, Sola F, Cappella P, Perrera C, Depaolini SR, Rusconi L, Cucchi U, Avanzi N, Bertrand JA, Bossi RT, Pesenti E, Galvani A, Isacchi A, Colotta F, Donati D, Moll J. Targeting the mitotic checkpoint for cancer therapy with NMS-P715, an inhibitor of MPS1 kinase. *Cancer Res* 2010; **70**: 10255-10264 [PMID: 21159646 DOI: 10.1158/0008-5472.CAN-10-2101]

32 **Hewitt L**, Tighe A, Santaguida S, White AM, Jones CD, Musacchio A, Green S, Taylor SS. Sustained Mps1 activity is required in mitosis to recruit O-Mad2 to the Mad1-C-Mad2 core complex. *J Cell Biol* 2010; **190**: 25-34 [PMID: 20624899 DOI: 10.1083/jcb.201002133]

33 **Jemaà M**, Galluzzi L, Kepp O, Senovilla L, Brands M, Boemer U, Koppitz M, Lienau P, Prechtl S, Schulze V, Siemeister G, Wengner AM, Mumberg D, Ziegelbauer K, Abrieu A, Castedo M, Vitale I, Kroemer G. Characterization of novel MPS1 inhibitors with preclinical anticancer activity. *Cell Death Differ* 2013; **20**: 1532-1545 [PMID: 23933817 DOI: 10.1038/cdd.2013.105]

34 **Kwiatkowski N**, Jelluma N, Filippakopoulos P, Soundararajan M, Manak MS, Kwon M, Choi HG, Sim T, Deveraux QL, Rottmann S, Pellman D, Shah JV, Kops GJ, Knapp S, Gray NS. Small-molecule kinase inhibitors provide insight into Mps1 cell cycle function. *Nat Chem Biol* 2010; **6**: 359-368 [PMID: 20383151 DOI: 10.1038/nchembio.345]

35 **Dodson CA**, Haq T, Yeoh S, Fry AM, Bayliss R. The structural mechanisms that underpin mitotic kinase activation. *Biochem Soc Trans* 2013; **41**: 1037-1041 [PMID: 23863175 DOI: 10.1042/BST20130066]

36 **Danielsen HE**, Pradhan M, Novelli M. Revisiting tumour aneuploidy - the place of ploidy assessment in the molecular era. *Nat Rev Clin Oncol* 2016; **13**: 291-304 [PMID: 26598944 DOI: 10.1038/nrclinonc.2015.208]

37 **Ahn CH**, Kim YR, Kim SS, Yoo NJ, Lee SH. Mutational analysis of TTK gene in gastric and colorectal cancers with microsatellite instability. *Cancer Res Treat* 2009; **41**: 224-228 [PMID: 20057968 DOI: 10.4143/crt.2009.41.4.224]

38 **Ethun CG**, Postlewait LM, Le N, Pawlik TM, Buettner S, Poultsides G, Tran T, Idrees K, Isom CA, Fields RC, Jin LX, Weber SM, Salem A, Martin RC, Scoggins C, Shen P, Mogal HD, Schmidt C, Beal E, Hatzaras I, Shenoy R, Merchant N, Cardona K, Maithel SK. A Novel Pathology-Based Preoperative Risk Score to

Predict Locoregional Residual and Distant Disease and Survival for Incidental Gallbladder Cancer: A 10-Institution Study from the U.S. Extrahepatic Biliary Malignancy Consortium. *Ann Surg Oncol* 2017; **24**: 1343-1350 [PMID: 27812827 DOI: 10.1245/s10434-016-5637-x]

39 **Tian YH**, Ji X, Liu B, Yang GY, Meng XF, Xia HT, Wang J, Huang ZQ, Dong JH. Surgical treatment of incidental gallbladder cancer discovered during or following laparoscopic cholecystectomy. *World J Surg* 2015; **39**: 746-752 [PMID: 25403888 DOI: 10.1007/s00268-014-2864-9]

40 **Suda T**, Tsunoda T, Daigo Y, Nakamura Y, Tahara H. Identification of human leukocyte antigen-A24-restricted epitope peptides derived from gene products upregulated in lung and esophageal cancers as novel targets for immunotherapy. *Cancer Sci* 2007; **98**: 1803-1808 [PMID: 17784873 DOI: 10.1111/j.1349-7006.2007.00603.x]

41 **Suzuki H**, Fukuhara M, Yamaura T, Mutoh S, Okabe N, Yaginuma H, Hasegawa T, Yonechi A, Osugi J, Hoshino M, Kimura T, Higuchi M, Shio Y, Ise K, Takeda K, Gotoh M. Multiple therapeutic peptide vaccines consisting of combined novel cancer testis antigens and anti-angiogenic peptides for patients with non-small cell lung cancer. *J Transl Med* 2013; **11**: 97 [PMID: 23578144 DOI: 10.1186/1479-5876-11-97]

42 **Mizukami Y**, Kono K, Daigo Y, Takano A, Tsunoda T, Kawaguchi Y, Nakamura Y, Fujii H. Detection of novel cancer-testis antigen-specific T-cell responses in TIL, regional lymph nodes, and PBL in patients with esophageal squamous cell carcinoma. *Cancer Sci* 2008; **99**: 1448-1454 [PMID: 18452554 DOI: 10.1111/j.1349-7006.2008.00844.x]

43 **Kono K**, Mizukami Y, Daigo Y, Takano A, Masuda K, Yoshida K, Tsunoda T, Kawaguchi Y, Nakamura Y, Fujii H. Vaccination with multiple peptides derived from novel cancer-testis antigens can induce specific T-cell responses and clinical responses in advanced esophageal cancer. *Cancer Sci* 2009; **100**: 1502-1509 [PMID: 19459850 DOI: 10.1111/j.1349-7006.2009.01200.x]

44 **Kono K**, Iinuma H, Akutsu Y, Tanaka H, Hayashi N, Uchikado Y, Noguchi T, Fujii H, Okinaka K, Fukushima R, Matsubara H, Ohira M, Baba H, Natsugoe S, Kitano S, Takeda K, Yoshida K, Tsunoda T, Nakamura Y. Multicenter, phase II clinical trial of cancer vaccination for advanced esophageal cancer with three peptides derived from novel cancer-testis antigens. *J Transl Med* 2012; **10**: 141 [PMID: 22776426 DOI: 10.1186/1479-5876-10-141]

45 **Iinuma H**, Fukushima R, Inaba T, Tamura J, Inoue T, Ogawa E, Horikawa M, Ikeda Y, Matsutani N, Takeda K, Yoshida K, Tsunoda T, Ikeda T, Nakamura Y, Okinaga K. Phase I clinical study of multiple epitope peptide vaccine combined with chemoradiation therapy in esophageal cancer patients. *J Transl Med* 2014; **12**: 84 [PMID: 24708624 DOI: 10.1186/1479-5876-12-84]

46 **Aruga A**, Takeshita N, Kotera Y, Okuyama R, Matsushita N, Ohta T, Takeda K, Yamamoto M. Long-term Vaccination with Multiple Peptides Derived from Cancer-Testis Antigens Can Maintain a Specific T-cell Response and Achieve Disease Stability in Advanced Biliary Tract Cancer. *Clin Cancer Res* 2013; **19**: 2224-2231 [PMID: 23479678 DOI: 10.1158/1078-0432.CCR-12-3592]

47 **Liu J**, Cheng X, Zhang Y, Li S, Cui H, Zhang L, Shi R, Zhao Z, He C, Wang C, Zhao H, Zhang C, Fisk HA, Guadagno TM, Cui Y. Phosphorylation of Mps1 by BRAFV600E prevents Mps1 degradation and contributes to chromosome instability in melanoma. *Oncogene* 2013; **32**: 713-723 [PMID: 22430208 DOI: 10.1038/onc.2012.94]

48 **Zhang L**, Shi R, He C, Cheng C, Song B, Cui H, Zhang Y, Zhao Z, Bi Y, Yang X, Miao X, Guo J, Chen X, Wang J, Li Y, Cheng X, Liu J, Cui Y. Oncogenic B-Raf(V600E) abrogates the AKT/B-Raf/Mps1 interaction in melanoma cells. *Cancer Lett* 2013; **337**: 125-132 [PMID: 23726842 DOI: 10.1016/j.canlet.2013.05.029]

49 **Daniel J**, Coulter J, Woo JH, Wilsbach K, Gabrielson E. High levels of the Mps1 checkpoint protein are protective of aneuploidy in breast cancer cells. *Proc Natl Acad Sci USA* 2011; **108**: 5384-5389 [PMID: 21402910 DOI: 10.1073/pnas.1007645108]

50 **Ling Y**, Zhang X, Bai Y, Li P, Wei C, Song T, Zheng Z, Guan K, Zhang Y, Zhang B, Liu X, Ma RZ, Cao C, Zhong H, Xu Q. Overexpression of Mps1 in colon cancer cells attenuates the spindle assembly checkpoint and increases aneuploidy. *Biochem Biophys Res Commun* 2014; **450**: 1690-1695 [PMID: 25063032 DOI: 10.1016/j.bbrc.2014.07.071]

51 **Li M**, Zhang Z, Li X, Ye J, Wu X, Tan Z, Liu C, Shen B, Wang XA, Wu W, Zhou D, Zhang D, Wang T, Liu B, Qu K, Ding Q, Weng H, Ding Q, Mu J, Shu Y, Bao R, Cao Y, Chen P, Liu T, Jiang L, Hu Y, Dong P, Gu J, Lu W, Shi W, Lu J, Gong W, Tang Z, Zhang Y, Wang X, Chin YE, Weng X, Zhang H, Tang W, Zheng Y, He L, Wang H, Liu Y, Liu Y. Whole-exome and targeted gene sequencing of gallbladder carcinoma identifies recurrent mutations in the ErbB pathway. *Nat Genet* 2014; **46**: 872-876 [PMID: 24997986 DOI: 10.1038/ng.3030]

52 **Bizama C**, García P, Espinoza JA, Weber H, Leal P, Nervi B, Roa JC. Targeting specific molecular pathways holds promise for advanced gallbladder cancer therapy. *Cancer Treat Rev* 2015; **41**: 222-234 [PMID: 25639632 DOI: 10.1016/j.ctrv.2015.01.003]

P- Reviewer: Deepak P, Zimmerman M **S- Editor**: Wang JL
L- Editor: Wang TQ **E- Editor**: Huang Y

World Journal of Gastroenterology

Submit a Manuscript: http://www.f6publishing.com

World J Gastroenterol 2017 August 21; 23(31): 5798-5808

DOI: 10.3748/wjg.v23.i31.5798

ISSN 1007-9327 (print) ISSN 2219-2840 (online)

ORIGINAL ARTICLE

Retrospective Study

Simple instruments facilitating achievement of transanal total mesorectal excision in male patients

Chang Xu, Hua-Yu Song, Shao-Liang Han, Shi-Chang Ni, Hu-Xiang Zhang, Chun-Gen Xing

Chang Xu, Chun-Gen Xing, Department of General Surgery, the Second Affiliated Hospital of Soochow University, Suzhou 215000, Jiangsu Province, China

Chang Xu, Hua-Yu Song, Shao-Liang Han, Shi-Chang Ni, Department of Colorectal Surgery, the First Affiliated Hospital of Wenzhou Medical University, Wenzhou 325000, Zhejiang Province, China

Hu-Xiang Zhang, Department of Pathology, the First Affiliated Hospital of Wenzhou Medical University, Wenzhou 325000, Zhejiang Province, China

Author contributions: Xu C, Song HY and Xing CG designed the research; Xu C, Song HY, Ni SC and Zhang HX performed the research; Xu C and Han SL analyzed the data; Xu C, Han SL and Xing CG wrote the paper.

Supported by (in part) Wenzhou Science and Technology Project, No. Y20160044; Suzhou Key Medical Center, No. LCZX201505; Soochow Development of Science and Technology Projects, No. SZS201618; Chinese Natural Science Foundation, No. 81672970; and Second Affiliated Hospital of Soochow University Preponderant Clinic Discipline Group Project, No. XKQ2015007.

Institutional review board statement: This study was approved by the Ethics Committee of the First Affiliated Hospital of Wenzhou Medical University. All procedures performed in studies involving human participants were in accordance with the ethical standards of the institutional and national research committee and with the 1964 Helsinki Declaration and its later amendments or comparable ethical standards.

Informed consent statement: Informed consent was obtained from all individual participants included in the study.

Conflict-of-interest statement: The authors declare that they have no conflict of interest.

Data sharing statement: No additional data are available.

Manuscript source: Unsolicited manuscript

Correspondence to: Chun-Gen Xing, MD, Professor, Department of General Surgery, the Second Affiliated Hospital of Soochow University, Suzhou 215000, Jiangsu Province, China. xingcg@suda.edu.cn
Telephone: +86-512-68284303
Fax: +86-512-68284303

Received: February 7, 2017
Peer-review started: February 9, 2017
First decision: May 12, 2017
Revised: June 18, 2017
Accepted: July 12, 2017
Article in press: July 12, 2017
Published online: August 21, 2017

Abstract

AIM

To assess the efficacy of a modified approach with transanal total mesorectal excision (taTME) using simple customized instruments in male patients with low rectal cancer.

METHODS

A total of 115 male patients with low rectal cancer from December 2006 to August 2015 were retrospectively studied. All patients had a bulky tumor (tumor diameter $\geqslant$ 40 mm). Forty-one patients (group A) underwent a classical approach of transabdominal total mesorectal excision (TME) and transanal intersphincteric resection (ISR), and the other 74 patients (group B) underwent a modified approach with transabdominal TME,

transanal ISR, and taTME. Some simple instruments including modified retractors and an anal dilator with a papilionaceous fixture were used to perform taTME. The operative time, quality of mesorectal excision, circumferential resection margin, local recurrence, and postoperative survival were evaluated.

RESULTS

All 115 patients had successful sphincter preservation. The operative time in group B (240 min, range: 160-330 min) was significantly shorter than that in group A (280 min, range: 200-360 min; P = 0.000). Compared with group A, more complete distal mesorectum and total mesorectum were achieved in group B (100% *vs* 75.6%, P = 0.000; 90.5% *vs* 70.7%, P = 0.008, respectively). After 46.1 ± 25.6 mo follow-up, group B had a lower local recurrence rate and higher disease-free survival rate compared with group A, but these differences were not statistically significant (5.4% *vs* 14.6%, P = 0.093; 79.5% *vs* 65.1%, P = 0.130).

CONCLUSION

Retrograde taTME with simple customized instruments can achieve high-quality TME, and it might be an effective and economical alternative for male patients with bulky tumors.

Key words: Rectal neoplasm; Total mesorectal excision; Transanal approach; Intersphincteric resection; Long-term outcome; Local recurrence

Core tip: Distal mesorectal excision is difficult in male patients with low rectal cancers, especially with a bulky tumor. We explored the application of simple instruments including modified retractors and an anal dilator with a papilionaceous fixture to perform transanal total mesorectal excision (taTME) in male patients with low rectal cancer. Our results showed that the modified approach with taTME achieved a shorter operative time and better quality of mesorectal excision as compared with the classical approach. This procedure may be an effective and economical alternative for taTME when a giant tumor is encountered in patients with low rectal cancer.

Xu C, Song HY, Han SL, Ni SC, Zhang HX, Xing CG. Simple instruments facilitating achievement of transanal total mesorectal excision in male patients. *World J Gastroenterol* 2017; 23(31): 5798-5808 Available from: URL: http://www.wjgnet.com/1007-9327/full/v23/i31/5798.htm DOI: http://dx.doi.org/10.3748/wjg.v23.i31.5798

INTRODUCTION

Rectal cancer is one of the most common malignant tumors that lead to high rates of morbidity and considerable mortality. High-quality surgery is of great importance in curing patients with rectal cancer. Total mesorectal excision (TME), which considers the rectum and mesorectum as one lymphovascular structure and requires its excision within an intact fascia propria[1], has been shown to significantly reduce the rate of local recurrence and increase the survival rate. Therefore, TME is generally accepted as the gold standard for surgical treatment of rectal cancer[2]. However, during the surgical procedure of TME, distal mesorectal excision becomes difficult when the tumor is low and near to the pelvic floor. Williams[3] described the area of the distal rectum that lies within the pelvic floor musculature as "no man's land" in rectal cancer surgery. The so-called "no man's land" cannot usually be reached from the abdomen and has been relatively inviolate as far as surgical exploration is concerned. It is particularly difficult to dissect the end of the rectum in some patients with low rectal cancers, such as those with a narrow pelvis and large tumor volume. These conditions may affect the surgical quality and lead to incomplete mesorectal excision and higher local recurrence rates, thus reducing the survival rate[4-6].

Recently, many studies have suggested that a transanal approach may resolve these issues[7,8] by greatly facilitating distal rectal dissection and providing high-quality TME specimens. Most of these studies used a specialized platform, such as a transanal endoscopic operation platform. However, few institutions around the world could perform this surgery. To date, most colorectal surgeons do not have access to the equipment needed for transanal endoscopic operation nor have they had formal training with this device. Moreover, application of transanal endoscopic operation has remained limited due to high costs and the complexity for surgeons.

During the past 10 years, we applied simple customized instruments to perform retrograde transanal TME for male patients with low rectal cancers. With the help of these simple instruments, we have been able to acquire clearer surgical exposure and easily cross the "no man's land" under direct observation. Here, we introduce this procedure employing simple instruments and present the operative results from our study.

MATERIALS AND METHODS

Patient selection

A total of 3497 consecutive patients underwent radical resection for rectal cancer (tumors located within 12 cm of the anal verge) at the First Affiliated Hospital of Wenzhou Medical University (China) between December 2006 and August 2015. Of these, 115 patients were enrolled in this study.

The inclusion criteria were as follows: (1) tumor margin located ⩽ 5 cm from the anal verge; (2) palpable resectable primary tumor detectable by

Figure 1 Preparation of special instruments. A: The retractors, which are modified from thyroid retractors, could be adapted to the curvature of the pelvis manually. Red dots show the turning point of the retractor during transanal operation; B: An anal dilator with a papilionaceous fixture from a stapler device for hemorrhoids, which was placed after completion of intersphincteric resection.

digital examination, and no tumor invasion in the external sphincter, levator ani, and puborectalis muscles by magnetic resonance imaging (MRI); (3) no distant metastasis found before operation; (4) refusal to undergo abdominoperineal resection of the rectal carcinoma and strong desire for sphincter preservation; and (5) huge tumor volume (tumor diameter $\geqslant$ 40 mm).

Since 2011, we have recommended temporal stoma to most patients to improve their quality of life in the early period after operation. All of the procedures were performed by three senior colorectal surgeons.

Preoperative adjuvant therapy

The preoperative clinical stage of rectal cancer was assessed by abdominal computed tomography (CT) and pelvic MRI with 3.0-T system. Patients with stage cTNM Ⅱ-Ⅲ were recommended to receive preoperative neoadjuvant chemoradiotherapy according to Clinical Guideline of Colorectal Cancer in China since 2010, but only 19 patients fulfilled the regimens, which was performed over a 5-wk period. A dose of 45-50 Gy in 25 fractions was administered along with capecitabine (825 mg/m^2 per day) to enhance the efficacy of radiotherapy. Surgery was performed in the 6th to 8th weeks after neoradiotherapy.

Surgical procedures

Step 1: Transabdominal TME. The dissection was started by high ligation of the inferior mesenteric vessels, followed by mobilization of the sigmoid colon, descending colon and splenic flexure of colon. The dissection was performed following the principles of TME working in "the holy plane", which ensured excision of the whole rectum and mesorectum as one distinct lymphovascular entity.

Step 2: Transanal ISR. The lower margin of the tumor was closed with submucosal purse-string sutures under direct observation, followed by retrograde irrigation of the anal canal with povidone-iodine solution. The rectum and anal canal were circumferentially dissected 2 cm below the tumor. The potential space between the internal and external sphincter was entered and dissected to the superior border of the anorectal ring.

Step 3: Retrograde transanal TME. For preparation of special instruments, two flexible retractors of 25 cm in length were modified from the thyroid retractor and could be adapted to the curvature of the pelvis manually. We also used an anal dilator with a papilionaceous fixture from a stapler device for hemorrhoids (Figure 1).

For retrograde dissection, a circular anal dilator with a diameter of 34 mm was introduced with an obturator device, which replaced the Lone Star Retractor for holding the anal canal open. The dilator was then sutured to the anal margin with four cardinal stitches. After removing the obturator, dissection of the distal mesorectum was pursued by alternating bilateral, posterior and anterior dissection (Figure 2). (1) Bilateral mobilization of the distal rectum (Figure 2A): Dissection was started along the natural boundary between the surface of the levator ani muscle and mesorectum toward the pelvic cavity assisted by two specially designed retractors. After the whole internal sphincter was dissected from the external sphincter, the space between the levator ani muscle and the mesorectum could be detected. The two retractors were inserted into this space and expanded it. The distance of bilateral mobilization toward the pelvic cavity could reach 10 cm according to the length of the retractors; (2) Posterior mobilization of the distal rectum (Figure 2B): The hiatal ligament was cut off after sharp dissection along the natural boundary between the surface of the levator ani muscle and mesorectum with an electrocautery or ultracision harmonic scalpel; and (3) Anterior mobilization of the distal rectum (Figure 2C): The rectourethral muscle was cut off, and the Denonvilliers fascia was sharply

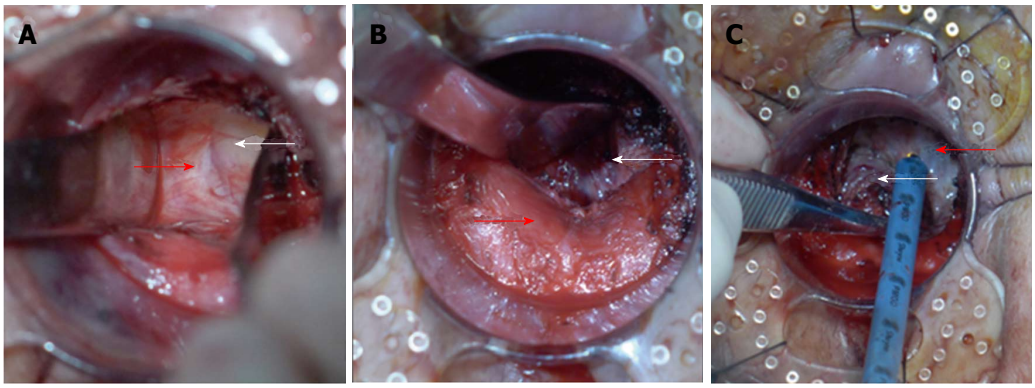

Figure 2 Dissection of the distal mesorectum in retrograde transanal total mesorectal excision. A: Bilateral mobilization of the distal rectum. Dissection is started along the natural boundary between the surface of the levator ani muscle and mesorectum toward the pelvic cavity assisted. The two retractors are inserted into this space and used to expand it. The distance of bilateral mobilization toward the pelvic cavity could reach 10 cm according to the length of the retractors; B: Posterior mobilization of the distal rectum. The hiatal ligament is cut off after sharp dissection along the natural boundary between the surface of the levator ani muscle and mesorectum with an electrocautery or ultracision harmonic scalpel; C: Anterior mobilization of the distal rectum. The rectourethral muscle is cut off, and the Denonvilliers fascia is sharply dissected between the anterior and posterior lobes. White arrows indicate the rectum and its mesorectum, and red arrow indicates the levator ani muscle or Denonvilliers fascia.

dissected between the anterior and posterior lobes. On both sides of the rear of the prostate, the components of the pelvic autonomic nervous plexus (Walsh bundle) were identified and protected. The dissection approached the superior border of the prostate anteriorly and coccygeal posteriorly. Histological evaluation of the invasion of tumor cells was performed on the dissected plane (the external sphincter and/or the levator ani) by microscopic examination of a frozen-section specimen. If any tumor cells were found, the procedure was suspended immediately and converted to abdominoperineal resection.

The tumor specimen was removed when the transanal operation met the gauzes previously placed at the pelvis transabdominally.

Step 4: Abdominal closure. The surgical field was rinsed, and the sigmoid stump was pulled down without tension to the anus. The colon and anal canal were interruptedly sutured using the absorbable 3-0 thread under assistance of an anal ligation device. The drainage tubes of the anal canal were placed across the coloanal anastomotic stoma.

The abdomen was closed, and an ileostomy was performed prophylactically. The classical approach was performed with Step 1 (transabdominal TME), Step 2 (transanal ISR) and Step 4 (abdominal closure), whereas the modified approach included Step 1 but only extending to the superior border of the anterior prostate and posterior coccygeal and then the perineal procedure was performed including Step 2, Step 3 (retrograde transanal TME) and Step 4.

Pathologic assessment of the resected specimen

Histopathological reports included TNM staging systems and other tumor prognostic factors, such as the status of circumferential resection margin (CRM) and distal margin. The CRM was considered to be involved when the tumor was within 1 mm of the resected CRM.

Each freshly excised specimen was evaluated by an experienced pathologist before formalin fixation. Macroscopic assessments of the resected specimen were made as follows:

Complete: intact mesorectum with only minor irregularities of a smooth mesorectal surface is observed macroscopically. No defect is deeper than 5 mm, and there is no coning toward the distal margin of the specimen. There is a smooth circumferential resection margin on slicing.

Nearly complete: moderate bulk to the mesorectum, but with irregularity of the mesorectum surface is observed macroscopically. Moderate coning of the specimen is allowed. At no site is the muscularis propria visible, with the exception of the insertion of the levator muscles.

Incomplete: little bulk to the mesorectum, with defects down onto the muscularis propria and/or very irregular circumferential resection margin is observed macroscopically.

Assessment of postoperative complications

Postoperative complications represent all complications that were recorded, and the Clavien-Dindo grade (grades Ⅰ-Ⅴ) was used to classify the complications within 30 d postoperatively[9].

Postoperative therapy

The patients were recommended to receive postoperative adjuvant radiotherapy and/or chemotherapy based on pTNM staging 3 wk after surgery. Radiation therapy fields should include the tumor bed, which should be defined by preoperative radiologic imaging and/or surgical clips. Radiation doses should be: 45-50 Gy in 25-28 fractions. 5-FU-based chemotherapy should be delivered concurrently with radiation. The

Table 1 Clinical characteristics of male patients with low rectal cancer *n* (%)

Variable	Group A, *n* = 41	Group B, *n* = 74	*P* value
Age in yr[1]	62.4 ± 11.2	59.0 ± 12.6	0.630
ASA score			0.787
1	6 (14.6)	8 (10.8)	
2	24 (58.5)	43 (58.1)	
3	11 (26.8)	23 (31.1)	
BMI[1]	24.8 ± 2.3	25.0 ± 2.8	0.193
Intertuberous diameter in mm[2]	98 (83-110)	99 (86-111)	0.426
Distance of tumors from the anal verge in mm[2]	4 (0.5-5)	4 (1-5)	0.160
Tumor diameter in mm[2]	50 (40-70)	50 (40-70)	0.679
Laparoscopy for abdominal operation	17 (41.5)	43 (58.1)	0.087
Ostomy	18 (43.9)	72 (97.3)	0.000
Operators			0.815
A	26 (63.4)	51 (68.9)	
B	9 (22.0)	13 (17.6)	
C	6 (14.6)	10 (13.5)	
Neoadjuvant radiotherapy	3 (12.5)	16 (35.6)	0.041
Adjuvant radiotherapy	2 (7.7)	4 (11.8)	0.602
Adjuvant chemotherapy	16 (55.2)	32 (64.0)	0.439
pT			0.458
pT1	2 (4.9)	4 (5.4)	
pT2	12 (29.3)	30 (40.5)	
pT3	27 (65.9)	40 (54.1)	
TNM stage			0.189
Stage Ⅰ	12 (29.3)	28 (37.8)	
Stage Ⅱ	13 (31.7)	29 (39.2)	
Stage Ⅲ	16 (39.0)	17 (23.0)	

[1]Values are mean ± SD; [2]Values are median (range). Group A: A classical approach; Group B: A modified approach with retrograde transanal total mesorectal excision. BMI: Body mass index; TNM: Tumor node metastasis.

chemotherapy regimen of FOLFOX6, m FOLFOX6 or XELOX was recommended to patients with TNM stage Ⅱ or Ⅲ. Six patients received postoperative adjuvant chemoradiotherapy, and 48 patients received postoperative adjuvant chemotherapy.

Follow-up protocol

Seven of the 115 patients were lost to follow-up. Patients were followed by serial clinical examination and carcinoembryonic antigen assessment every 3-6 mo for 2 year and then every 6 mo for a total of 5 year. Chest/abdominal/pelvic CT scanning was performed every 6-12 mo for up to 5 year. Colonoscopy was performed every 1 year. Local recurrence was defined as the first clinical, radiologic and/or pathologic evidence of a tumor of the same histological type within the pelvis. Distant recurrence was defined as clinical, radiologic and/or pathologic evidence of systemic disease outside the pelvis, at sites including but not limited to the liver, lungs, and para-aortic region.

Anal sphincter function assessment

Anal sphincter function was evaluated at 1 year after operation. Anorectal manometry was used to estimate anal function, and incontinence status was assessed by Wexner's score[10] and Kirwan's classification[11].

Statistical analysis

All data were analyzed using SPSS statistics software (version 21.0; Chicago, IL, United States). Quantitative data that followed a normal distribution are presented as mean ± SD and were compared by the *t*-test. Quantitative data that followed a non-normal distribution are presented as median (range) and were compared by Mann-Whitney *U* test. Comparisons were performed using the Pearson χ^2 test or Fisher exact test for categorical variables. In addition, the Wilcoxon Mann-Whitney test was applied to compare the Clavien-Dindo classifications of the two groups. Survival was estimated using the Kaplan-Meier method, and the log-rank test was used to compare survival curves. Overall survival was defined as the time from the date of surgery to the date of death or date of last follow-up for living patients. All of the tests were two-sided with a level of significance set at $P < 0.05$.

RESULTS

Clinical characteristics of patients with low rectal cancer

Successful sphincter preservation was achieved for all of the 115 male patients with lower rectal cancer. Among these patients, 41 patients underwent a classical approach (group A) and 74 patients underwent a modified approach with retrograde transanal TME (group B). There were no differences in age, ASA score, BMI, intertuberous diameter, distance of tumors from the anal verge, tumor diameter, rate of laparoscopy for abdominal operation, operators, pT stage or TNM stage between groups A and B (Table 1). We performed more "ostomy" procedures in group B (97.3%, 72/74)

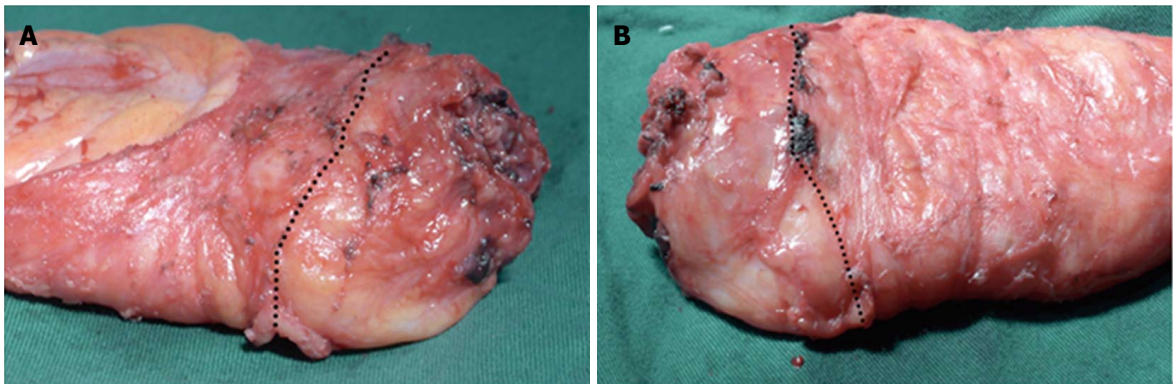

Figure 3 Specimen was examined by a pathologist. A: The anterior side of specimen; B: The posterior side of specimen. The black dotted line shows the boundary of transabdominal total mesorectal excision (TME) and retrograde transanal TME. The lower rectum had a smoother mesorectum surface compared with the upper rectum. TME: Total mesorectal excision.

Table 2 Clinicopathological outcomes *n* (%)

Variable	Group A, *n* = 41	Group B, *n* = 74	*P* value
Total operating time in min[2]	280 (200-360)	240 (160-330)	0.000
Blood loss in mL[2]	80 (20-500)	60 (20-300)	0.184
Hospital stays after operation[2]	8 (7-23)	8 (6-19)	0.341
Distance of tumors from distal margin in mm[1]	16.9 ± 5.3	17.9 ± 4.9	0.466
Distal mesorectum			0.000
Complete	31 (75.6)	74 (100)	
Nearly complete	7 (17.1)	0 (0)	
Incomplete	3 (7.3)	0 (0)	
Total mesorectum			0.008
Complete	29 (70.7)	67 (90.5)	
Nearly complete	9 (22.0)	7 (9.5)	
Incomplete	3 (7.3)	0	
Distal involvement			1.000
Positive	0 (0)	0 (0)	
Negative	41 (100)	74 (100)	
Circumferential resection margin			0.543
Positive	2 (4.9)	2 (2.7)	
Negative	39 (95.1)	72 (97.3)	

[1]Values are mean ± SD; [2]Values are median (range). Group A: A classical approach; Group B: A modified approach with transanal total mesorectal excision.

compared with group A (43.9%, 18/41; *P* = 0.000) to reduce the rate of anastomostic leakage. Twenty-four and forty-five patients had stage cTNM Ⅱ-Ⅲ cancer in groups A and B, respectively. Clinically, neoadjuvant radiotherapy was applied more frequently in group B (35.6%, 16/45) than in group A (12.5%, 3/24; *P* = 0.041). Four patients had down-staging. In group A, 26 and 29 patients were suggested to receive adjuvant radiotherapy and adjuvant chemotherapy, respectively. These numbers were 34 and 50 in group B, respectively. However, only some of them actually accepted adjuvant radiotherapy and chemotherapy (Table 1).

Surgical results

In this study, we assessed the surgery quality in the two groups by evaluating the operative time, the completeness of distal mesorectum and total mesorectum, circumferential resection margin, and distal margin. The operative time in group B (240 min, range: 160-330 min) was significantly shorter than that in group A (280 min, range: 200-360 min; *P* = 0.000). Moreover, compared with group A, the resected specimen in group B had a superior TME quality (Figure 3). The rates of complete distal mesorectum and complete total mesorectum were 100.0% and 90.5% in group B, and these were significantly higher than those in group A (75.6%, *P* = 0.000 and 70.7%, *P* = 0.008, respectively). There were no differences in the involvement of the circumferential resection margin and distal margin between the two groups (Table 2). The completion status of the surgery on the pelvic floor (the location of the distal rectum) could be clearly observed *via* the anus after removal of the specimen (Figure 4).

Postoperative complications of surgery

There were no perioperative deaths in this study, but 41 cases experienced postoperative complications, including anastomotic leakage in 4 cases, anastomotic

Table 3 Postoperative complications in male patients with low rectal cancer *n* (%)

Variable	Group A, *n* = 41	Group B, *n* = 74	*P* value
Anastomotic leakage	2 (4.9)	2 (2.7)	0.542
Anastomotic stricture	6 (14.6)	12 (16.2)	0.823
Postoperative inflammatory intestinal obstruction	2 (4.9)	4 (5.4)	0.903
Urinary tract infection	1 (2.4)	4 (5.4)	0.455
Wound infection	3 (7.3)	4 (5.4)	0.681
Urinary retention	3 (7.3)	5 (6.8)	0.91
Clavien-Dindo classification			0.85
Ⅰ	5 (12.2)	7 (9.5)	
Ⅱ	3 (7.3)	10 (13.5)	
Ⅲ	2 (4.9)	0	

Data are presented as *n* (%). Group A: A classic approach; Group B: A modified approach with retrograde transanal total mesorectal excision.

Table 4 Postoperative anal functional results of male patients with low rectal cancer *n* (%)

Items	Pre-operation			1 yr after operation		
	Group A	Group B	*P* value	Group A	Group B	*P* value
MRP in kPa	12.2 ± 2.2	13.1 ± 3.5	0.126	8.8 ± 2.3	9.0 ± 2.8	0.087
MSP in kPa	18.0 ± 3.6	17.3 ± 3.0	0.054	16.3 ± 3.3	17.6 ± 2.8	0.201
HZL in mm	32.2 ± 5.1	34.7 ± 5.5	0.7	24.9 ± 4.5	24.2 ± 5.9	0.080
Wexner score	0.4 ± 1.2	0.2 ± 0.8	0.112	2.7 ± 2.7	3.6 ± 3.8	0.099
Kirwan classification			0.591			0.617
Ⅰ	34 (82.9)	64 (86.5)		15 (36.6)	22 (29.7)	
Ⅱ	7 (17.1)	9 (12.2)		16 (39.0)	25 (33.8)	
Ⅲ	0	1 (1.4)		7 (17.1)	19 (25.7)	
Ⅳ	0	0		3 (7.3)	8 (10.8)	
Ⅴ	0	0		0	0	

Wexner scores are presented as number (SD): 0 = perfect continence; 20 = major incontinence. Kirwan classifications are presented as number: Grade Ⅰ = perfect; Grade Ⅱ = incontinence of flatus; Grade Ⅲ = occasional minor soiling; Grade Ⅳ = frequent major soiling; Grade Ⅴ = incontinence. HZL: High-pressure zone length; MRP: Maximum resting pressure; MSP: Maximum squeeze pressure.

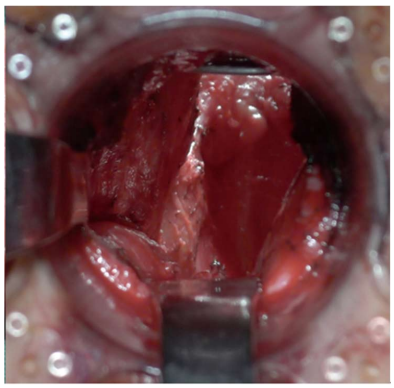

Figure 4 Completion status of the surgery on the pelvic floor (the location of the distal rectum) can be clearly observed transanally after removing the specimen.

stricture in 18 cases, early postoperative inflammatory intestinal obstruction in 6 cases, urinary tract infection in 5 cases, wound infection in 7 cases, and urinary retention in 8 cases. There were no differences in the incidence of postoperative complications between group A and group B ($P > 0.05$; Table 3).

Functional results

Functional results were recorded for 115 patients during follow-up (Table 4), and no differences were found in the values of the maximum resting pressure, maximum squeeze pressure and high-pressure zone length between the two groups preoperatively or at 1 year after operation. Similar results were observed for the Wexner continence score and Kirwan classification.

Survival and local recurrence

The mean duration of follow-up was 46.1 ± 25.6 mo (range: 12-122 mo), and 7 cases were lost to follow-up. Overall, 94 patients (91.3%) were followed up for more than 24 mo. No anastomotic recurrence was found in this study.

Twenty-one cases (18.3%, 21/115) experienced recurrence and metastasis. Among them, local recurrence was found in 10 cases (8.7%, 6 in group A and 4 in group B), which included pelvic lateral lymph node recurrence in 3 cases (1 underwent lateral lymph node dissection), sacrum recurrence in 4 cases, and pelvic muscles recurrence in 3 cases. Of the 115 patients, 14 patients (10.7%) experienced distant metastasis. Of these, 2 patients presented with liver metastases, 5 with lung metastases, and 7 with metastases to lymph nodes at the para-aortic region.

The 5-year survival rate for the study population was 78.9%, with rates of 75.5% in group A and 81.0% in group B, with no difference between the groups ($P = 0.228$). Group B had a lower local

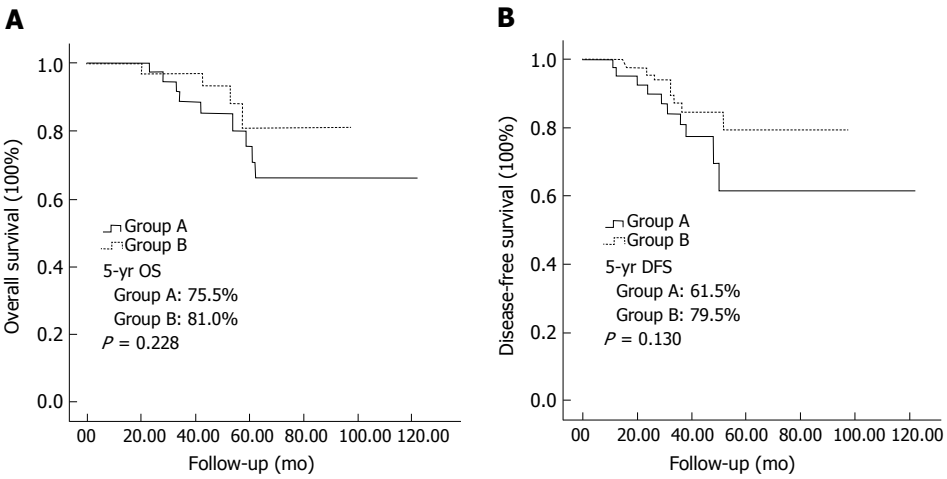

Figure 5 Survival curve for 115 male patients with low rectal cancer. A: Overall survival of the two groups; B: Disease-free survival of the two groups.

recurrence rate (5.4%) and higher disease-free survival rate (79.5%) comparing with group A (14.6% and 61.5%, respectively), but these differences were not statistically significant (P = 0.093 and P = 0.130, respectively; Figure 5).

DISCUSSION

Numerous studies have revealed a strong relationship between a low tumor level and poor TME quality, higher positive circumferential resection margin and recurrence[4,6,12]. Leonard *et al*[4] reported that the incomplete TME rate was only 15.4% (2/15) when the inferior margin of the tumor above the anal verge was > 10 cm, and the rate was 28.2% (35/124) for tumors between 5 to 10 cm from the anal verge. If it was < 5 cm, the incomplete TME rate increased to 39.3% (42/107). The positive rate at the circumferential resection margin of incomplete TME was twice that of complete TME[4]. Therefore, as the low rectal cancer is closer to the anus, TME is more difficult to perform. Narrow pelvises and giant tumors have been proven to lead to surgical difficulties and increase the risk of non-curative resection[13-15]. Approaching the pelvic floor, the failure of surgical exposure may be the cause of misunderstanding the anatomic plane and inaccurate surgical dissection.

Based on these considerations, the concept of the "down-to-up" procedure has been proposed in cases where transabdominal TME is difficult[16]. This procedure reduces the effects of pelvis factors on pelvic surgery, and the operating space is expanded from the anus towards the pelvic cavity. The end of the rectum and its mesentery could be excised precisely under direct observation by retrograde transanal TME. In the 1980s, Gerald Marks developed transabdominal transanal resection (TATA) to perform TME from below to upward, but this technique required specialized instruments with limited exposure, and thus, few were able to replicate this approach[17,18]. Recently, some researchers have tried to perform TME using a transanal endoscopic operation device[19-24]. This approach has great potential value for further applications. However, it still has the disadvantages of technical difficulties associated with limited maneuverability, which means an increased learning curve for surgeons. Because of the smaller operating space under an endoscopic device, this type of surgical procedure is not suitable if the tumor is relatively large and the mesorectum is relatively thick[19]. In addition, the device is still expensive.

For better exposure of the pelvic floor from down to up and to obtain a larger operating space, we inserted a circular anal dilator into the anal canal instead of the Lone Star Retractor or transanal endoscopic operation device. We have used an anal dilator with a round-shape fixture from a classical stapler device for hemorrhoids and found that it was blocked by ischial tuberosities when the patient had a short intertuberous diameter. Now we apply an anal dilator with a papilionaceous fixture for deeper insertion into the anal canal to keep the external sphincter of the upper anal canal out of the anal dilator. This step prevents the contracting muscle from the anorectal ring from blocking the view, which facilitates observation of the pelvic floor and the accurate surgical dissection of the distal mesorectum transanally. Meanwhile, we use specially designed retractors to further extend the exposure of the operative field. This ensures the dissection is performed along the accurate anatomic plane under direct observation.

In this study, 74 patients underwent a modified approach with retrograde transanal TME (group B), and the results revealed that the operative time with the modified approach (240 min, range: 160-330 min) was significantly shorter than that with the classical approach (280 min, range: 200-360 min; P = 0.000). Moreover, the resected specimens in group B showed optimal TME quality. Compared with group A, a complete distal mesorectum and complete

total mesorectum were achieved in group B (100% *vs* 75.6%, *P* = 0.000; 90.5% *vs* 70.7%, *P* = 0.008, respectively). The shorter procedure and better quality specimens observed in group B indicate that retrograde transanal TME with simple instruments facilitated the mobilization of the low rectum for male patients. Actually, several transanal surgery studies have already demonstrated that transanal TME can be performed safely with a promising amount of intact specimens and low rates of involved CRM[16,25-28]. Perdawood *et al*[29] reported a prospective study including 50 patients on the surgical results of transanal TME compared with laparoscopic TME (laTME) for rectal cancer. The circumferential resection margin was positive in 1 patient in their transanal TME group and 4 patients in their laTME group (*P* = 0.349). All patients in their transanal TME group had either complete or nearly complete specimen quality, while 4 patients in their laTME group had incomplete specimen quality (*P* = 0.113). Less blood loss, shorter operating time, and shorter hospital stay were observed in their transanal TME group. A meta-analysis including seven studies (transanal TME group, *n* = 270; laTME group, *n* = 303) indicated that the complete grade for the quality of the mesorectum was significantly higher for transanal TME than for laTME (OR = 1.75, 95%CI: 1.02-3.01, *P* = 0.04) and significantly fewer patients in the transanal TME group had a positive CRM (OR = 0.39, 95%CI: 0.17-0.86, *P* = 0.02)[30].

However, research studies on oncologic outcomes of transanal TME are still few. Rouanet *et al*[23] reported oncologic outcomes for a series of 30 transanal TME operations with locally advanced tumors. Overall survival rates after 12 and 24 mo were 96.6% and 80.5%, respectively. In the present study, our results revealed that group B had a lower local recurrence rate and higher 5-yr disease-free survival rate compared with group A (5.4% *vs* 14.6% and 79.5% *vs* 61.5%, respectively). However, these differences were not statistically significant, possibly due to the small number of patients in this study.

Furthermore, we also observed the anal sphincter function and incontinence status 1 year after operation. No differences were found between the two groups, and the mean Wexner score in group B (retrograde transanal TME) was 3.6, which was also close to that in other transanal TME studies[31,32]. This modified approach with retrograde transanal TME does not compromise anal function compared with the conventional approach for patients with low rectal cancer.

Taken together, the results of this study indicated that the modified approach is better than the classical approach for sphincter-preserving surgery in male patients with low rectal cancers, especially in those with bulky tumors. However, this study is limited mainly in its retrospective design, and a larger number of patients would be ideal. Additionally, only a few of the patients received neoadjuvant chemoradiation in this study because of rejections. In conclusion, our results indicate that the procedure of retrograde transanal TME with simple instruments can overcome the so-called the "no man's area" in rectal surgery to ensure TME completion at the distal rectum and can achieve a better quality specimen without lowering anorectal function.

ACKNOWLEDGMENTS

We would like to thank Xiu-Ling Wu and Zhong-Min Lin, Department of Pathology, the First Affiliated Hospital of Wenzhou Medical University for their assistance in pathologic assessment, and Xin-Jun Yang, Department of Preventive Medicine, the School of Public Health and Management, Wenzhou Medical University, for her assistance in statistical analysis.

COMMENTS

Background

High-quality total mesorectal excision (TME) is of great importance in curing patients with rectal cancer. However, distal mesorectal excision is difficult when the tumor is low, especially with a narrow pelvis and large tumor volume.

Research frontiers

Many studies have suggested that a transanal approach may resolve the issues derived from a narrow pelvis and large tumor volume. This procedure provides several advantages over conventional excision by offering much improved visualization and exposure. It greatly facilitates distal rectal dissection and provides high-quality TME specimens.

Innovations and breakthroughs

Most studies about the transanal approach used a specialized platform, such as a transanal endoscopic operation platform. However, the application of transanal endoscopic operation has remained limited due to the high costs of such platforms and the complexity for surgeons. The authors explored the application of simple instruments including modified retractors and an anal dilator with a papilionaceous fixture to perform transanal total mesorectal excision (taTME). These simple instruments facilitate observation of the pelvic floor and accurate surgical dissection of the distal mesorectum transanally.

Applications

The study results suggest that the modified approach with simple instruments achieved a shorter operative time and better quality of mesorectal excision, as compared with the classical approach. It is a better approach for sphincter-preserving surgery in male patients with low rectal cancers, especially in those with bulky tumors. This procedure may be a safe, effective and economical alternative for taTME.

Terminology

The intersphincteric resection technique allows a sphincter-saving resection for ultralow rectal cancer, mainly excluding cases with infiltration of the external sphincter. This technique consists of removing part of or the whole internal anal sphincter to obtain free distal margin. TME, which considers the rectum and mesorectum as one lymphovascular structure, requires its excision within an intact fascia propria. TaTME is a procedure in which the rectum is mobilized transanally in a retrograde fashion. It reduces the effects of pelvis factors on pelvic surgery, and the end of the rectum and its mesentery could be excised precisely under direct observation.

Peer-review

The authors have developed a unique surgical method for transanal TME using

simple instruments. The reviewer considers that their procedure is potentially good and the manuscript is well written. This is a very interesting study about a surgical technique that although described several decades ago, is only now being widely adopted by colorectal surgeons around the world.

REFERENCES

1 **Heald RJ**. The 'Holy Plane' of rectal surgery. *J R Soc Med* 1988; **81**: 503-508 [PMID: 3184105]
2 **Yang Q**, Xiu P, Qi X, Yi G, Xu L. Surgical margins and short-term results of laparoscopic total mesorectal excision for low rectal cancer. *JSLS* 2013; **17**: 212-218 [PMID: 23925014 DOI: 10.4293/108680813X13654754534675]
3 **Williams NS**. The rectal 'no man's land' and sphincter preservation during rectal excision. *Br J Surg* 2010; **97**: 1749-1751 [PMID: 20949555 DOI: 10.1002/bjs.7283]
4 **Leonard D**, Penninckx F, Fieuws S, Jouret-Mourin A, Sempoux C, Jehaes C, Van Eycken E; PROCARE, a multidisciplinary Belgian Project on Cancer of the Rectum. Factors predicting the quality of total mesorectal excision for rectal cancer. *Ann Surg* 2010; **252**: 982-988 [PMID: 21107108 DOI: 10.1097/SLA.0b013e3181efc142]
5 **Hiranyakas A**, da Silva G, Wexner SD, Ho YH, Allende D, Berho M. Factors influencing circumferential resection margin in rectal cancer. *Colorectal Dis* 2013; **15**: 298-303 [PMID: 22776435 DOI: 10.1111/j.1463-1318.2012.03179.x]
6 **Garlipp B**, Ptok H, Schmidt U, Stübs P, Scheidbach H, Meyer F, Gastinger I, Lippert H. Factors influencing the quality of total mesorectal excision. *Br J Surg* 2012; **99**: 714-720 [PMID: 22311576 DOI: 10.1002/bjs.8692]
7 **Nicholson G**, Knol J, Houben B, Cunningham C, Ashraf S, Hompes R. Optimal dissection for transanal total mesorectal excision using modified CO2 insufflation and smoke extraction. *Colorectal Dis* 2015; **17**: O265-O267 [PMID: 26218459 DOI: 10.1111/codi.13074]
8 **Araujo SE**, Crawshaw B, Mendes CR, Delaney CP. Transanal total mesorectal excision: a systematic review of the experimental and clinical evidence. *Tech Coloproctol* 2015; **19**: 69-82 [PMID: 25380741 DOI: 10.1007/s10151-014-1233-x]
9 **Dindo D**, Demartines N, Clavien PA. Classification of surgical complications: a new proposal with evaluation in a cohort of 6336 patients and results of a survey. *Ann Surg* 2004; **240**: 205-213 [PMID: 15273542 DOI: 10.1097/01.sla.0000133083.54934.ae]
10 **Jorge JM**, Wexner SD. Etiology and management of fecal incontinence. *Dis Colon Rectum* 1993; **36**: 77-97 [PMID: 8416784]
11 **Kirwan WO**, Turnbull RB Jr, Fazio VW, Weakley FL. Pullthrough operation with delayed anastomosis for rectal cancer. *Br J Surg* 1978; **65**: 695-698 [PMID: 709078]
12 **Oh SY**, Kim YB, Paek OJ, Suh KW. Does total mesorectal excision require a learning curve? Analysis from the database of a single surgeon's experience. *World J Surg* 2011; **35**: 1130-1136 [PMID: 21416172 DOI: 10.1007/s00268-011-1014-x]
13 **García-Granero E**, Faiz O, Flor-Lorente B, García-Botello S, Esclápez P, Cervantes A. Prognostic implications of circumferential location of distal rectal cancer. *Colorectal Dis* 2011; **13**: 650-657 [PMID: 20236143 DOI: 10.1111/j.1463-1318.2010.02249.x]
14 **Targarona EM**, Balague C, Pernas JC, Martinez C, Berindoague R, Gich I, Trias M. Can we predict immediate outcome after laparoscopic rectal surgery? Multivariate analysis of clinical, anatomic, and pathologic features after 3-dimensional reconstruction of the pelvic anatomy. *Ann Surg* 2008; **247**: 642-649 [PMID: 18362627 DOI: 10.1097/SLA.0b013e3181612c6a]
15 **You JF**, Tang R, Changchien CR, Chen JS, You YT, Chiang JM, Yeh CY, Hsieh PS, Tsai WS, Fan CW, Hung HY. Effect of body mass index on the outcome of patients with rectal cancer receiving curative anterior resection: disparity between the upper and lower rectum. *Ann Surg* 2009; **249**: 783-787 [PMID: 19387325 DOI: 10.1097/SLA.0b013e3181a3e52b]
16 **de Lacy AM**, Rattner DW, Adelsdorfer C, Tasende MM, Fernández M, Delgado S, Sylla P, Martínez-Palli G. Transanal natural orifice transluminal endoscopic surgery (NOTES) rectal resection: "down-to-up" total mesorectal excision (TME)--short-term outcomes in the first 20 cases. *Surg Endosc* 2013; **27**: 3165-3172 [PMID: 23519489 DOI: 10.1007/s00464-013-2872-0]
17 **Marks G**, Mohiuddin M, Rakinic J. New hope and promise for sphincter preservation in the management of cancer of the rectum. *Semin Oncol* 1991; **18**: 388-398 [PMID: 1862356]
18 **Atallah S**. Transanal total mesorectal excision: full steam ahead. *Tech Coloproctol* 2015; **19**: 57-61 [PMID: 25560966 DOI: 10.1007/s10151-014-1254-5]
19 **Zhang H**, Zhang YS, Jin XW, Li MZ, Fan JS, Yang ZH. Transanal single-port laparoscopic total mesorectal excision in the treatment of rectal cancer. *Tech Coloproctol* 2013; **17**: 117-123 [PMID: 22936590 DOI: 10.1007/s10151-012-0882-x]
20 **Atallah S**, Albert M, DeBeche-Adams T, Nassif G, Polavarapu H, Larach S. Transanal minimally invasive surgery for total mesorectal excision (TAMIS-TME): a stepwise description of the surgical technique with video demonstration. *Tech Coloproctol* 2013; **17**: 321-325 [PMID: 23377536 DOI: 10.1007/s10151-012-0971-x]
21 **Lacy AM**, Adelsdorfer C. Totally transrectal endoscopic total mesorectal excision (TME). *Colorectal Dis* 2011; **13** Suppl 7: 43-46 [PMID: 22098517 DOI: 10.1111/j.1463-1318.2011.02781.x]
22 **Velthuis S**, van den Boezem PB, van der Peet DL, Cuesta MA, Sietses C. Feasibility study of transanal total mesorectal excision. *Br J Surg* 2013; **100**: 828-831; discussion 831 [PMID: 23440708 DOI: 10.1002/bjs.9069]
23 **Rouanet P**, Mourregot A, Azar CC, Carrere S, Gutowski M, Quenet F, Saint-Aubert B, Colombo PE. Transanal endoscopic proctectomy: an innovative procedure for difficult resection of rectal tumors in men with narrow pelvis. *Dis Colon Rectum* 2013; **56**: 408-415 [PMID: 23478607 DOI: 10.1097/DCR.0b013e3182756fa0]
24 **Meng W**, Lau K. Synchronous laparoscopic low anterior and transanal endoscopic microsurgery total mesorectal resection. *Minim Invasive Ther Allied Technol* 2014; **23**: 70-73 [PMID: 24483132 DOI: 10.3109/13645706.2014.887022]
25 **Marks JH**, Montenegro GA, Salem JF, Shields MV, Marks GJ. Transanal TATA/TME: a case-matched study of taTME versus laparoscopic TME surgery for rectal cancer. *Tech Coloproctol* 2016; **20**: 467-473 [PMID: 27178183 DOI: 10.1007/s10151-016-1482-y]
26 **Veltcamp Helbach M**, Deijen CL, Velthuis S, Bonjer HJ, Tuynman JB, Sietses C. Transanal total mesorectal excision for rectal carcinoma: short-term outcomes and experience after 80 cases. *Surg Endosc* 2016; **30**: 464-470 [PMID: 25921202 DOI: 10.1007/s00464-015-4221-y]
27 **Tuech JJ**, Karoui M, Lelong B, De Chaisemartin C, Bridoux V, Manceau G, Delpero JR, Hanoun L, Michot F. A step toward NOTES total mesorectal excision for rectal cancer: endoscopic transanal proctectomy. *Ann Surg* 2015; **261**: 228-233 [PMID: 25361216 DOI: 10.1097/SLA.0000000000000994]
28 **Lacy AM**, Tasende MM, Delgado S, Fernandez-Hevia M, Jimenez M, De Lacy B, Castells A, Bravo R, Wexner SD, Heald RJ. Transanal Total Mesorectal Excision for Rectal Cancer: Outcomes after 140 Patients. *J Am Coll Surg* 2015; **221**: 415-423 [PMID: 26206640 DOI: 10.1016/j.jamcollsurg.2015.03.046]
29 **Perdawood SK**, Al Khefagie GA. Transanal vs laparoscopic total mesorectal excision for rectal cancer: initial experience from Denmark. *Colorectal Dis* 2016; **18**: 51-58 [PMID: 26603786 DOI: 10.1111/codi.13225]
30 **Ma B**, Gao P, Song Y, Zhang C, Zhang C, Wang L, Liu H, Wang Z. Transanal total mesorectal excision (taTME) for rectal cancer: a systematic review and meta-analysis of oncological and perioperative outcomes compared with laparoscopic total mesorectal excision. *BMC Cancer* 2016; **16**: 380 [PMID: 27377924 DOI: 10.1186/s12885-016-2428-5]
31 **Elmore U**, Fumagalli Romario U, Vignali A, Sosa MF, Angiolini MR, Rosati R. Laparoscopic anterior resection with transanal total

mesorectal excision for rectal cancer: preliminary experience and impact on postoperative bowel function. *J Laparoendosc Adv Surg Tech A* 2015; **25**: 364-369 [PMID: 25918836 DOI: 10.1089/lap.2014.0435]

32 **Dumont F**, Goéré D, Honoré C, Elias D. Transanal endoscopic total mesorectal excision combined with single-port laparoscopy. *Dis Colon Rectum* 2012; **55**: 996-1001 [PMID: 22874608 DOI: 10.1097/DCR.0b013e318260d3a0]

P- Reviewer: Allaix ME, Elpek GO, Horesh N, Kai K, Wani IA
S- Editor: Ma YJ **L- Editor**: Filipodia **E- Editor**: Huang Y

World Journal of Gastroenterology

Submit a Manuscript: http://www.f6publishing.com

World J Gastroenterol 2017 August 21; 23(31): 5809-5816

DOI: 10.3748/wjg.v23.i31.5809

ISSN 1007-9327 (print) ISSN 2219-2840 (online)

ORIGINAL ARTICLE

Retrospective Study

Donor-derived infections among Chinese donation after cardiac death liver recipients

Qi-Fa Ye, Wei Zhou, Qi-Quan Wan

Qi-Fa Ye, Wei Zhou, Qi-Quan Wan, Department of Transplant Surgery, the Third Xiangya Hospital of Central South University, Changsha 410013, Hunan Province, China

Qi-Fa Ye, Department of Transplant Surgery, Zhongnan Hospital of Wuhan University, Wuhan 430071, Hubei Province, China

Author contributions: Ye QF contributed to the study design and data analysis; Zhou W enrolled the study patients, performed the data collection, and contributed to the data analysis; Wan QQ drafted the manuscript and contributed to the study design and data analysis; all authors read and approved the final manuscript.

Supported by the New Xiangya Talent Project of The Third Xiangya Hospital of Central South University, No. 20170311.

Institutional review board statement: The study was reviewed and approved by the Institutional Review Board of The Third Xiangya Hospital of Central South University, Changsha, China (IRB No. 2017-S003).

Conflict-of-interest statement: All the authors declare they have no conflict of interest related to the manuscript.

Data sharing statement: There are no additional data available.

Manuscript source: Unsolicited manuscript

Correspondence to: Qi-Quan Wan, MD, Associate Professor, Department of Transplant Surgery, the Third Xiangya Hospital of Central South University, No. 138, Tongzipo Road, Changsha 410013, Hunan Province, China. 13548685542@163.com
Telephone: +86-731-88618312
Fax: +86-731-88618312

Received: March 20, 2017
Peer-review started: March 23, 2017
First decision: June 5, 2017
Revised: June 27, 2017
Accepted: July 22, 2017
Article in press: July 24, 2017
Published online: August 21, 2017

Abstract

AIM

To investigate blood cultures of deceased donors and report the confirmed transmission of bacterial infection from donors to liver recipients.

METHODS

We retrospectively studied the results of blood cultures among our donation after cardiac death (DCD) donors and calculated the donor-derived bacterial infection rates among liver recipients. Study participants underwent liver transplantation between January 1, 2010 and February 1, 2017. The study involved a total of 67 recipients of liver grafts from 67 DCD donors. We extracted the data of donors' and patients' characteristics, culture results and clinical outcomes, especially the post-transplant complications in liver recipients, from electronic medical records. We analyzed the characteristics of the donors and the corresponding liver recipients with emphasis put on donor-derived infections.

RESULTS

Head trauma was the most common origin of death among our 67 DCD donors (46.3%). Blood taken prior to the procurement operation was cultured for 53 of the donors, with 17 episodes of bloodstream infections developing from 13 donors. The predominant organism isolated from the blood of donors was Gram-positive bacteria (70.6%). Only three (4.5%) of 67 liver recipients developed confirmed donor-derived bacterial infections,

with two isolates of multidrug-resistant *Klebsiella pneumoniae* and one isolate of multidrug-resistant *Enterobacter aerogenes*. The liver recipients with donor-derived infections showed relation to higher crude mortality and graft loss rates (33.3% each) within 3 mo post transplantation, as compared to those without donor-derived infections (9.4% and 4.7%, respectively). All three liver recipients received appropriate antimicrobial therapy.

CONCLUSION

Liver recipients have high occurrence of donor-derived infections. The liver recipients with donor-derived multidrug-resistant *Enterobacteriaceae* infections can have good outcome if appropriate antimicrobial therapy is given.

Key words: Liver transplant; Donation after cardiac death donor; Infection; Multidrug resistant; Bacteria; Transmission

Core tip: This study aimed to investigate blood cultures of donation after cardiac death (DCD) liver donors and report the confirmed transmission of bacterial infection from donors to liver recipients. The predominant organism isolated from the blood of donors was Gram-positive bacteria (70.6%). Only three (4.5%) of 67 liver recipients developed confirmed donor-derived bacterial infections, with two isolates of multidrug-resistant *Klebsiella pneumoniae* and one isolate of multidrug-resistant *Enterobacter aerogenes*. Our findings support that liver grafts from DCD donors with bloodstream infections owing to multidrug-resistant *Enterobacteriaceae* can be used if the donors and recipients receive appropriate antimicrobial therapy.

Ye QF, Zhou W, Wan QQ. Donor-derived infections among Chinese donation after cardiac death liver recipients. *World J Gastroenterol* 2017; 23(31): 5809-5816 Available from: URL: http://www.wjgnet.com/1007-9327/full/v23/i31/5809.htm DOI: http://dx.doi.org/10.3748/wjg.v23.i31.5809

INTRODUCTION

Liver transplantation is currently considered the therapy of choice for patients with end-stage liver disease. Organs from infected donors after cardiac death (DCD), such as those with bacteremia, are now utilized in response to the disparity between the available graft pool and the organ need for liver transplantation, which carries risk of transmission of infectious diseases and death[1-5]. The risk of unanticipated disease transmission to liver recipients *via* donor grafts has been gaining research attention. Donor-derived transmission of infections remains a rare complication of liver transplantation and the studies have supported its overall safety and favorable outcomes[6-13]; however, the outcome of this type of infection itself among liver recipients is controversial and some authors suggest that it is associated with significant mortality[14,15].

As the volume of liver recipients increases, the number of infections transmitted through DCD donors can also be expected to rise. Unfortunately, the data of DCD donor-derived infections following liver transplantation are currently lacking in China. We, therefore, aimed to investigate the blood cultures of DCD donors and report the cases of confirmed (proven/probable) transmission of bacterial and fungal infections from donors to liver recipients. The current study provided, to our best knowledge, the first finding of liver recipients experiencing confirmed donor-derived bacterial infections in China and this report represents the largest series of liver recipients with donor-derived infections due to multidrug-resistant (MDR) *Enterobacteriaceae* in the world thus far.

MATERIALS AND METHODS

Study population

This retrospective analysis of a single-center population was conducted with the purpose of recording all liver recipients with donor-derived bacterial infections. All involved human participants had been initially recruited to the study between January 1, 2010 and February 1, 2017. We then searched the medical record systems of the Third Xiangya Hospital (Changsha, China) to identify all DCD donors and liver recipients who received grafts from DCD donors. The recorded information allowed for identification of individual participants during or after data collection.

The final study population consisted of 67 liver recipients of grafts from 67 DCD donors who had been admitted to the intensive care unit (ICU) of the Department of Transplant Surgery, the Third Xiangya Hospital of Central South University before organ procurement and transplantation. Multi-organ transplant recipients were excluded from the study. Data recorded included donor age, sex, category, length of ICU stay, number of donors with/without available results of blood cultures, bacteria and fungi isolated from donors, antibiotic administration, and cause of death. The procedures used for donor screening, donor treatment for bacterial and fungal infections, and obtainment of the liver graft were also recorded. Liver graft recipient data representing variables associated with donor-derived infections were collected from the medical records as well, and included age, sex, underlying liver diseases, site of infection, time of infection onset, organisms, antimicrobial use, immunosuppressive therapy, and crude mortality/graft loss. The data of post-liver transplant complications were collected for all liver recipients. For all liver graft recipients, the maintenance immunosuppression was tacrolimus/cyclosporin complemented with prednisone tapered to 5-10 mg/d. All liver graft recipients were followed for at least 3 mo post transplantation or until death.

Donor screening and treatment for bacterial and fungal infections

In our hospital, any DCD donor with a history or suspicion of prior bloodstream infection from whom a liver graft will be harvested is subject to a detailed and appropriate investigation to ensure that infection is not present in the liver. To rule out the presence of active infection, our hospital also takes a complete history from the donor's family and performs a thorough review of the medical records, including vital signs and findings of physical, radiographic and any available microbiologic tests. Most of the donors in this study also underwent routine culturing of blood, urine and sputum. Blood cultures were obtained to rule out occult donor infection, especially among donors at "increased" risk for bacteremia or fungemia[16]. Targeted antibiotics were administered to the infected donor for at least 24 h, with some degree of clinical response (improved white blood cell count and hemodynamics, and defervescence) and, if possible, the infected donor's treatment included documentation of the infection resolution prior to donation.

Obtaining liver grafts

All cases of organ donation were performed according to the protocols for China categories Ⅰ, Ⅱ and Ⅲ donors[17]. After informed consent was obtained from the donor's family, life supports were removed. After the legal 5-min standoff time, the donor immediately underwent a "super-rapid" procurement technique in the operating room. In brief, a rapid abdominal incision was made, followed by rapid cannulation of the abdominal aorta and superior mesenteric or portal vein. The liver was then perfused with University of Wisconsin solution and prompt hepatectomy was performed. The intra-abdominal organs were removed *en bloc*, submerged in University of Wisconsin solution at 4 ℃, and placed in cold storage. The bile duct was flushed with physiological saline solution *in situ* and preserved *ex situ* with University of Wisconsin solution.

Recipient prophylactic strategies and treatments for bacterial and fungal infections

Second- or third-generation cephalosporins, semisynthetic penicillins/beta-lactamase inhibitors, or carbapenems, were prescribed according to the pre-transplant results of cultures and administered 1 h before the liver transplantation, with an additional dose given at 72 h post transplantation to the liver recipients without donor-derived infections. Recipients of liver graft from a bacteremic donor were treated with a 7-d to 14-d course of targeted antibiotics. Antifungal therapy was administered within 2 wk to a recipient of liver graft from a donor with fungemia if the liver recipient had no evidence of infection. Cases of established fungal infection were administered a 4-wk to 6-wk course, with at least 6 wk of treatment, when vascular involvement was present.

Definitions

The deceased-organ donations were classified as follows: China category Ⅰ (C-Ⅰ), organ donation after brain death; China category Ⅱ (C-Ⅱ), organ donation after circulatory death; and China category Ⅲ (C-Ⅲ), organ donation after brain death followed by circulatory death[17].

Transmission of organisms was considered proven by clear evidence of the same infection in the donor and at least one of the recipients. Transmission of the organisms was considered probable by strong evidence suggesting but not proving infectious transmission, such as the infection being documented in more than one recipient but not diagnosed in the donor[18]. Both proven and probable transmissions were considered as confirmed transmission of infections[18]. Appropriate antimicrobial use in donors was considered when the infected donor had received targeted antimicrobial treatment for at least 24-48 h, optimally with some degree of clinical response[19]. Appropriate antimicrobial use in recipients was considered if the isolated organisms showed *in vitro* susceptibility to empirical antibiotics, which were administered within 48 h of sampling for culture[20].

We utilized the standardized definition of MDR *Enterobacteriaceae*, as previously defined by international consensus in 2012; specifically, MDR was considered with evidence of non-susceptibility to at least one agent in three or more appointed antimicrobial categories[21].

RESULTS

DCD donor characteristics

There were 67 liver recipients of grafts from 67 DCD donors during the study period. The characteristics of the donors are shown in Table 1. The DCD donors showed a male-dominated sex ratio (nearly 1:4) and were largely represented by young adults. The pre-retrieval ICU length of stay ranged from 1 d up to 41 d. Head trauma was the most common cause of death, followed by benign central nervous system tumor. The majority of donors were classified as China category Ⅲ, followed by China category Ⅱ.

Cases of infectious transmission from DCD donors to liver graft recipients

For 53 of the donors (79.1%), the blood samples taken prior to the procurement operation were cultured and produced evidence of 17 bloodstream infections from 13 of the donors. Appropriate antimicrobial use, according to the positive blood culture results, was administered in 10 of those 13 donors. The results of blood cultures from the donors are shown in Table 2. The majority of pathogens isolated from the donor's blood were coagulase-negative *Staphylococci*. Among the three donors who elicited infectious transmission to three liver recipients, one donor did not have an available result of blood culture and the other two donors had negative

Table 1 Characteristics of the 67 donation after cardiac death donors *n* (%)

Characteristic	Value
Age in years, median (IQR)	29.0 (19.0-44.0)
Sex	
Male	55 (82.1)
Female	12 (17.9)
Origin of death	
HT	31 (46.3)
Benign CNS tumor	18 (26.9)
CVA	15 (22.4)
Anoxia	2 (3.0)
Meningitis	1 (1.5)
China classification of donation	
I	5 (7.5)
II	8 (11.9)
III	54 (80.6)
ICU stay in days, median (IQR)	5 (3.0-10.0)
Donors with positive culture	13
Blood culture, *n*/*n*	
Donors with/without available results	53/14
Donors with appropriate antimicrobial use/all donors with positive blood culture results	10/13

CNS: Central nervous system; CVA: Cerebrovascular accident; DCD: Donation after cardiac death; HT: Head trauma; ICU: Intensive care unit; IQR, Interquartile range.

Table 2 Classification and percentage of organisms isolated from donors' bloodstream, *n* = 17

Organism	*n* (%)
Gram-positive bacteria	12 (70.6)
Staphylococcus aureus	3 (17.6)
Coagulase-negative *staphylococci*	9 (52.9)
S. epidermidis	4 (23.5)
S. hemolyticus	1 (5.9)
S. capitis	1 (5.9)
S. hominis	2 (11.8)
S. simulans	1 (5.9)
Gram-negative bacteria	3 (17.6)
Klebsiella pneumoniae	2 (11.8)
Acinetobacter baumannii	1 (5.9)
Fungi	2 (11.8)
Candida albicans	1 (5.9)
Candida parapsilosis	1 (5.9)

results of blood culture after being admitted to the ICU; none of these three donors underwent blood culture within 10 d prior to organ procurement.

Infectious agents transmitted from DCD donors to liver graft recipients

Table 3 shows the characteristics of these three donors (D1-D3) and their corresponding liver recipients (R1-R3, representing 4.5% of the total recipient population), highlighting the relationship between donors and recipients with infection transmission. Several cultures (blood, urine, and abdominal drainage fluid) were routinely taken from the recipients following the liver transplantation. The confirmed donor-derived MDR bacterial infections included two isolates of *Klebsiella pneumoniae* and one isolate of *Enterobacter aerogenes*. Both of the *Klebsiella pneumoniae* isolates were extended-spectrum beta lactamase-producing rods. All three of the isolates (all being *Enterobacteriaceae* family members) were carbapene-susceptible.

Recipient characteristics and outcomes of infectious transmissions from DCD donors to liver graft recipients

Additional isolates from four recipients of kidney grafts from these three donors (D1-D3) provided strong evidence of transmission of infectious bacteria through their similar resistance profiles. Thus, no recipient case of infection transmission could be classified as a proven donor-derived infection, and all three cases (R1-R3) were classified as probable donor-derived infections. No liver recipients developed donor-derived fungal infections. No recipients had a presumed or confirmed invasive bacterial or fungal infection before transplantation. The underlying liver diseases of these three recipients were polycystic liver disease, hepatocellular carcinoma and cirrhosis due to hepatitis B virus infection, and heredofamilial amyloidosis. All three donor-derived infections occurred within 3 d post transplantation, and were administered appropriate anti-microbial therapy prior to or immediately following diagnosis of the infection. All three recipients recovered from the donor-derived bacterial infections, but one died of septic shock with graft loss owing to other organisms. Liver recipients without donor-derived infections had lower rates of crude mortality and graft loss [6/64 (9.4%) and 3/64 (4.7%), respectively] within 3 mo post transplantation, as compared with those with donor-derived infections (33.3% each).

Post-liver transplant complications in liver graft recipients with and without DCD-derived infections

All complications experienced by the full liver recipient population (n = 67) are presented in Table 4. The most common complication was post-transplant infection; the 20 total infections occurred in the three liver recipients with donor-derived infections (4 infection episodes) and the 64 liver recipients without donor-derived infections (16 infection episodes). The next most common complication was vascular (9 vascular episodes), all cases of which occurred in the liver recipients without donor-derived infections. Tumor recurrence developed in six of the liver recipients without donor-derived infections and none of the recipients with donor-derived infections.

Survival of liver graft recipients with and without DCD-derived infections

Figure 1 shows the Kaplan-Meier curves for 3-mo survival after liver transplantation. There was no difference in survival between the liver recipients with and without donor-derived infection (log-rank test, P = 0.165).

DISCUSSION

Although there are numerous reports of fatal donor-

Table 3 Characteristics of donors and their corresponding liver recipients with donor-derived infections

Donor	Diagnosis	Blood culture result	Recipient (sex/age)	Underlying liver disease(s)	Culture result (specimen)/time to infection onset	Inappropriate antimicrobial/ immunosuppressive therapy	Outcome
D1	Head trauma	Negative[1]	R1[2] (Female/48 yr)	Polycystic liver disease	*K. pneumoniae* (Blood and abdominal drainage fluid)/1 d	No/Pred	Patient death and graft loss
D2	Head trauma	Negative[1]	R2[3] (Male/38 yr)	Hepatocellular carcinoma and cirrhosis due to hepatitis B virus infection	*K. pneumoniae* (Blood and abdominal drainage fluid)/1 d	No/FK506 + Pred	Patient and graft survival
D3	Head trauma	Not available	R3[3] (Male/69 yr)	Heredofamilial amyloidosis	*E. aerogenes* (Blood)/3 d	No/FK506 + Pred	Patient and graft survival

[1]Donors had a negative result of blood culture after being admitted to the intensive care unit, whereas they did not undergo blood culture within 10 d prior to organ procurement; [2]Two kidney recipients of graft from the common donor, with this liver recipient having developed organ-space surgical site infection owing to *Klebsiella pneumoniae* within 20 d following the transplantation; [3]One kidney recipient of graft from the common donor, with this liver recipient having also developed bloodstream infection owing to the same bacterium immediately after the transplantation.

Table 4 Comparison of post-liver-transplant complications in liver recipients with and without donor-derived infections

Complication	Episodes of complications in three liver recipients with donor-derived infections	Episodes of complications in 64 liver recipients without donor-derived infections
Infection	4	16
Pneumonia	1	7
Peritonitis	0	3
Bloodstream infection	3	5
Surgical site infection	0	1
Vascular complications	0	9
Portal vein thrombosis	0	1
Cerebral embolism	0	1
Hepatic artery thrombosis	0	1
Abdominal bleeding	0	5
Gastrointestinal bleeding	0	1
Biliary complications	3	2
Bile leakage	0	0
Biliary strictures	1	2
Stone formation	1	0
Bilomas	1	0
Recurrent tumor	0	6
Acute rejection	0	4
Graft-versus-host disease	0	2
Graft dysfunction	0	3
Adhesive ileus	0	1

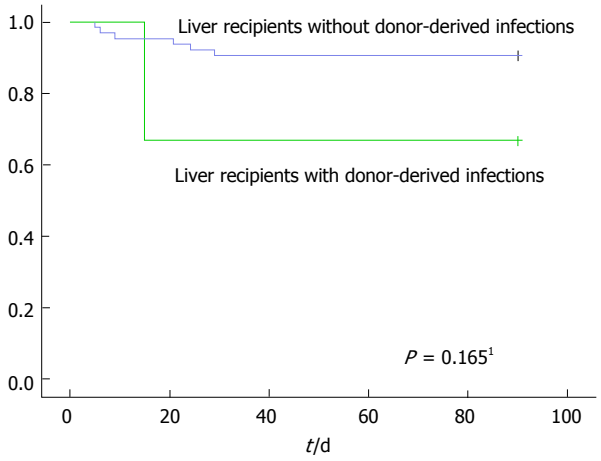

Figure 1 Kaplan-Meier curves for 3-mo survival after liver transplantation. [1]Log-rank test indicated no significant difference in survival between the two groups.

derived infections affecting around 3% of solid organ transplants, in the current era of organ shortage marginal organ donors are increasingly utilized[22,23]. More recent data demonstrate that most bacterial isolates appear to be irrelevant to subsequent recipient outcome and that the grafts from bacteremic donors may be safely used if bacteremia in the donor has been ideally treated and antibiotic therapy is continued in the organ recipient[2,6,7,24,25].

Our present study found 19.4% (13/67) of donors having available results of blood cultures developed bloodstream infections, which is in line with literature reports suggesting that about 5%-11.3% of all deceased donors have unrecognized bacteremia at the time of donation[2,6,8,25]. We also found that three (4.5%) of 67 donors transmitted bacterial infections to three liver recipients, which agrees with the 2013 report[26] from the Organ Procurement and Transplantation Network Ad Hoc Disease Transmission Advisory Committee that reported 15 (12.8%) out of 117 donors with infections developed proven/probable transmission of bacterial (except for tuberculosis) and fungal infections.

Doucette *et al*[3] proposed that the observed higher risk of transmission in liver recipients, as compared to other solid organ recipients, may be mainly attributed to bacterial retention in and poor antibiotic penetration of the liver graft. Some recipient-related factors were also proposed, such as a high Model for End-Stage Liver Disease (commonly known as MELD) score, leukopenia, and immunosuppression.

Coagulase-negative *Staphylococci* (such as *Staphylococcus epidermidis*) and *Staphylococcus aureus* represent the more commonly isolated microorganisms from donor blood cultures[7,8,25]. In our donor blood cultures, the majority of isolates were coagulase-negative *Staphylococci* and *S. aureus* (together 70.6%; 12 of 17 pathogens). Coagulase-negative *Staphylococci* also represent the most common microorganisms isolated from preservation fluid[2,15,27]. None of the cases

of donor-derived infections in liver recipients of our study were due to Gram-positive bacteria, agreeing with previous studies that have suggested lower risk of transmission of Gram-positive bacteria (*vs* Gram-negative bacteria) from a donor to a recipient[6,28-30]. This could be due to several reasons, such as low pathogenicity of coagulase-negative *Staphylococci*, potential contamination in donor culture (*i.e.*, not a true pathogen), or catheter line-associated infection in donor (*i.e.*, non-systemic infections).

All three donor-derived infections in our current study were caused by MDR Gram-negative bacteria, agreeing with a previous report suggesting that Gram-negative bacteria account for about 80% of transmissions to recipients[9]. Although rare, donor-derived infections caused by bacteria, in particular MDR bacteria, can have devastating consequences for organ transplant recipients[9-11,29,31]. The data reported to the United States' Organ Procurement and Transplantation Network from 2005 to 2011 showed the donor-derived infection-attributable recipient mortality rate to be 29.2% (19/65)[6]. These previous studies are consistent with our present study, wherein one (33.3%) of three liver recipients with MDR *Klebsiella pneumoniae* infection died from subsequent septic shock due to other organisms and the rate of graft loss was 33.3%. In contrast with our finding, however, others have reported a favorable outcome among liver recipients with donor-derived infections due to MDR Gram-negative bacteria or methicillin-resistant *S. aureus* (commonly known as MR SA)[3,5,9-11,23,32-34]. Further data are needed to assess the effects of donor-derived bacterial or fungal infections and appropriate antimicrobial use on allograft function and recipient survival over a long-term follow-up period.

The current study has provided, to the best of our knowledge, the first data of liver recipients with confirmed donor-derived bacterial infections treated in a single transplant center in China; in addition, the report represents the largest of liver recipients with donor-derived infections due to MDR *Enterobacteriaceae* in the world thus far. Since both the morbidity and mortality rates of donor-derived infections are high in China, the findings from the current study support future efforts towards a better understanding of potential risks for disease transmission and highlight the necessity for a standardized critical incident reporting system in the Chinese transplant system to improve short- and long-term allograft and recipient survival.

The principal limitation of our study was the single-center, retrospective study design, which did not allow for the investigation of donor-derived MDR bacterial infections by genetic or molecular analysis. Improvements in new screening technologies, such as the use of whole genome sequencing, have recently proven a powerful advance in the investigation of donor-derived MDR bacterial infections[35]. Since we used drug-sensitive test screening for donor-derived infections rather than a gene-level technique, it is possible that our testing algorithm over-estimated the transmission events.

Nonetheless, our findings underscore the importance of blood culture being performed as close to the donation time as possible and the importance of testing preservation fluid culture; since the reported contamination rates of the latter range widely (from 9.5% to 98.4%)[2,15,27], this sample was not routinely obtained at our institution. Our findings also indicate that donors with infections should receive antibiotics directed at the identified bacteria or fungi 24-48 h prior to procurement, optimally yielding evidence of clinical improvement.

In conclusion, DCD donors in our institute had a high rate of bacterial infection, with Gram-positive bacteria being the predominant isolate, whereas the donor-derived infections developed by liver recipients were Gram-negative predominant. Our findings strongly support organ donation as the common source of bacterial infection in the liver recipients. Although the number of these cases in our study was too small to draw conclusions, we support the use of liver grafts from the DCD donor pool, including those with infections owing to MDR *Enterobacteriaceae* if the donors and recipients receive appropriate antimicrobial therapy.

COMMENTS

Background

Nowadays, the use of bacteremic donors to fulfill the disparity between the limited donor pool and the increasing need for organs is an expanding practice, which may result in an increased risk of transmission of infectious diseases and death. However, the data of donation after cardiac death (DCD) donor-derived infections following liver transplantation are currently lacking in China. As limited data are available in Chinese liver recipients of grafts from DCD donors, this study aimed to investigate the blood cultures of DCD donors and report the cases of confirmed (proven/probable) transmission of bacterial and fungal infections from donors to liver recipients.

Research frontiers

The use of infectious donors to fulfill the disparity between the limited donor pool and the increasing need for organs has become an important issue in the field of transplantation. Furthermore, the use of donors with infections caused by multidrug-resistant (MDR) bacteria is controversial and the recipients with MDR infections have a high mortality. This study shows excellent outcome for liver recipients with donor-derived MDR infections.

Innovations and breakthroughs

This is the first study to analyze liver recipients experiencing confirmed donor-derived bacterial infections in China and the largest report of liver recipients with donor-derived infections due to MDR *Enterobacteriaceae* in the world thus far.

Applications

Liver grafts from the pool of DCD donors with bloodstream infections owing to MDR *Enterobacteriaceae* can be used if the donors have been treated and have documentation of resolution of infection prior to donation, and if the corresponding liver recipients are treated with a 7- to 14-d course of antibiotics targeted to the organism isolated from a bacteremic donor.

Terminology

Confirmed transmission includes a proven or probable transmission. A proven transmission was indicated by clear evidence of the same infectious disease in the donor and at least one of the recipients. A probable transmission was indicated by strong evidence suggesting, but not proving, a disease transmission, such as the disease being documented in more than one recipient but not being diagnosed in the donor. MDR bacteria were defined as those non-susceptible to at least one agent in three or more appointed antimicrobial categories.

Peer-review

Although sample size was small, this paper provides important information. This report shows excellent outcomes for recipients with donor-derived infections.

REFERENCES

1 **Wolfe RA**, Roys EC, Merion RM. Trends in organ donation and transplantation in the United States, 1999-2008. *Am J Transplant* 2010; **10**: 961-972 [PMID: 20420646 DOI: 10.1111/j.1600-6143.2010.03021.x]

2 **Cerutti E**, Stratta C, Romagnoli R, Serra R, Lepore M, Fop F, Mascia L, Lupo F, Franchello A, Panio A, Salizzoni M. Bacterial- and fungal-positive cultures in organ donors: clinical impact in liver transplantation. *Liver Transpl* 2006; **12**: 1253-1259 [PMID: 16724336 DOI: 10.1002/lt.20811]

3 **Doucette KE**, Al-Saif M, Kneteman N, Chui L, Tyrrell GJ, Kumar D, Humar A. Donor-derived bacteremia in liver transplant recipients despite antibiotic prophylaxis. *Am J Transplant* 2013; **13**: 1080-1083 [PMID: 23398841 DOI: 10.1111/ajt.12133]

4 **Camargo JF**. Donor-derived infections in solid organ transplant recipients: Challenging the 30-day paradigm. *Transpl Infect Dis* 2017; **19** [PMID: 28100037 DOI: 10.1111/tid.12665]

5 **Miceli MH**, Gonulalan M, Perri MB, Samuel L, Al Fares MA, Brown K, Bruno DA, Zervos M, Ramesh M, Alangaden G. Transmission of infection to liver transplant recipients from donors with infective endocarditis: lessons learned. *Transpl Infect Dis* 2015; **17**: 140-146 [PMID: 25586791 DOI: 10.1111/tid.12330]

6 **Ison MG**, Grossi P; AST Infectious Diseases Community of Practice. Donor-derived infections in solid organ transplantation. *Am J Transplant* 2013; **13** Suppl 4: 22-30 [PMID: 23464995 DOI: 10.1111/ajt.12095]

7 **Freeman RB**, Giatras I, Falagas ME, Supran S, O'Connor K, Bradley J, Snydman DR, Delmonico FL. Outcome of transplantation of organs procured from bacteremic donors. *Transplantation* 1999; **68**: 1107-1111 [PMID: 10551637]

8 **Lumbreras C**, Sanz F, González A, Pérez G, Ramos MJ, Aguado JM, Lizasoain M, Andrés A, Moreno E, Gómez MA, Noriega AR. Clinical significance of donor-unrecognized bacteremia in the outcome of solid-organ transplant recipients. *Clin Infect Dis* 2001; **33**: 722-726 [PMID: 11477528 DOI: 10.1086/322599]

9 **Mularoni A**, Bertani A, Vizzini G, Gona F, Campanella M, Spada M, Gruttadauria S, Vitulo P, Conaldi P, Luca A, Gridelli B, Grossi P. Outcome of Transplantation Using Organs From Donors Infected or Colonized With Carbapenem-Resistant Gram-Negative Bacteria. *Am J Transplant* 2015; **15**: 2674-2682 [PMID: 25981339 DOI: 10.1111/ajt.13317]

10 **Mills JP**, Wilck MB, Weikert BC, Porrett PM, Timko D, Alby K, Bonomo RA, Blumberg EA. Successful treatment of a disseminated infection with extensively drug-resistant Klebsiella pneumoniae in a liver transplant recipient with a fosfomycin-based multidrug regimen. *Transpl Infect Dis* 2016; **18**: 777-781 [PMID: 27458980 DOI: 10.1111/tid.12578]

11 **Ariza-Heredia EJ**, Patel R, Blumberg EA, Walker RC, Lewis R, Evans J, Sankar A, Willliams MD, Rogers J, Milano C, Razonable RR. Outcomes of transplantation using organs from a donor infected with Klebsiella pneumoniae carbapenemase (KPC)-producing K. pneumoniae. *Transpl Infect Dis* 2012; **14**: 229-236 [PMID: 22624726 DOI: 10.1111/j.1399-3062.2012.00742.x]

12 **Zibari GB**, Lipka J, Zizzi H, Abreo KD, Jacobbi L, McDonald JC. The use of contaminated donor organs in transplantation. *Clin Transplant* 2000; **14**: 397-400 [PMID: 10946778]

13 **Cohen J**, Michowiz R, Ashkenazi T, Pitlik S, Singer P. Successful organ transplantation from donors with Acinetobacter baumannii septic shock. *Transplantation* 2006; **81**: 853-855 [PMID: 16570007 DOI: 10.1097/01.tp.0000203804.95180.6e]

14 **van der Vliet JA**, Tidow G, Kootstra G, van Saene HF, Krom RA, Sloof MJ, Weening JJ, Tegzess AM, Meijer S, van Boven WP. Transplantation of contaminated organs. *Br J Surg* 1980; **67**: 596-598 [PMID: 7000231]

15 **Janny S**, Bert F, Dondero F, Durand F, Guerrini P, Merckx P, Nicolas-Chanoine MH, Belghiti J, Mantz J, Paugam-Burtz C. Microbiological findings of culture-positive preservation fluid in liver transplantation. *Transpl Infect Dis* 2011; **13**: 9-14 [PMID: 20738832 DOI: 10.1111/j.1399-3062.2010.00558.x]

16 **Fischer SA**, Lu K; AST Infectious Diseases Community of Practice. Screening of donor and recipient in solid organ transplantation. *Am J Transplant* 2013; **13** Suppl 4: 9-21 [PMID: 23464994 DOI: 10.1111/ajt.12094]

17 **Huang J**, Wang H, Fan ST, Zhao B, Zhang Z, Hao L, Huo F, Liu Y. The national program for deceased organ donation in China. *Transplantation* 2013; **96**: 5-9 [PMID: 23743728 DOI: 10.1097/TP.0b013e3182985491]

18 **Garzoni C**, Ison MG. Uniform definitions for donor-derived infectious disease transmissions in solid organ transplantation. *Transplantation* 2011; **92**: 1297-1300 [PMID: 21996654 DOI: 10.1097/TP.0b013e318236cd02]

19 **Fishman JA**, Greenwald MA, Grossi PA. Transmission of infection with human allografts: essential considerations in donor screening. *Clin Infect Dis* 2012; **55**: 720-727 [PMID: 22670038 DOI: 10.1093/cid/cis519]

20 **Gao F**, Ye Q, Wan Q, Liu S, Zhou J. Distribution and resistance of pathogens in liver transplant recipients with Acinetobacter baumannii infection. *Ther Clin Risk Manag* 2015; **11**: 501-505 [PMID: 25848296 DOI: 10.2147/TCRM.]

21 **Magiorakos AP**, Srinivasan A, Carey RB, Carmeli Y, Falagas ME, Giske CG, Harbarth S, Hindler JF, Kahlmeter G, Olsson-Liljequist B, Paterson DL, Rice LB, Stelling J, Struelens MJ, Vatopoulos A, Weber JT, Monnet DL. Multidrug-resistant, extensively drug-resistant and pandrug-resistant bacteria: an international expert proposal for interim standard definitions for acquired resistance. *Clin Microbiol Infect* 2012; **18**: 268-281 [PMID: 21793988 DOI: 10.1111/j.1469-0691.2011.03570.x]

22 **Kirchner VA**, Pruett TL. Receiving the Unwanted Gift: Infection Transmission through Organ Transplantation. *Surg Infect* (Larchmt) 2016; **17**: 318-322 [PMID: 27096745 DOI: 10.1089/sur.2016.009]

23 **Altman DR**, Sebra R, Hand J, Attie O, Deikus G, Carpini KW, Patel G, Rana M, Arvelakis A, Grewal P, Dutta J, Rose H, Shopsin B, Daefler S, Schadt E, Kasarskis A, van Bakel H, Bashir A, Huprikar S. Transmission of methicillin-resistant Staphylococcus aureus via deceased donor liver transplantation confirmed by whole genome sequencing. *Am J Transplant* 2014; **14**: 2640-2644 [PMID: 25250641 DOI: 10.1111/ajt.12897]

24 **Goldberg E**, Bishara J, Lev S, Singer P, Cohen J. Organ transplantation from a donor colonized with a multidrug-resistant organism: a case report. *Transpl Infect Dis* 2012; **14**: 296-299 [PMID: 22176504 DOI: 10.1111/j.1399-3062.2011.00697.x]

25 **González-Segura C**, Pascual M, García Huete L, Cañizares R, Torras J, Corral L, Santos P, Ramos R, Pujol M. Donors with positive blood culture: could they transmit infections to the recipients? *Transplant Proc* 2005; **37**: 3664-3666 [PMID: 16386498 DOI: 10.1016/j.transproceed.2005.08.053]

26 **Green M**, Covington S, Taranto S, Wolfe C, Bell W, Biggins SW, Conti D, DeStefano GD, Dominguez E, Ennis D, Gross T, Klassen-Fischer M, Kotton C, LaPointe-Rudow D, Law Y, Ludrosky K, Menegus M, Morris MI, Nalesnik MA, Pavlakis M, Pruett T, Sifri C, Kaul D. Donor-derived transmission events in 2013: a report of the Organ Procurement Transplant Network Ad Hoc Disease Transmission Advisory Committee. *Transplantation* 2015; **99**: 282-287 [PMID: 25594557 DOI: 10.1097/TP.0000000000000584]

27 **Ruiz P**, Gastaca M, Gonzalez J, Hernandez MJ, Ventoso A, Valdivieso A, Montejo M, Ortiz de Urbina J. Incidence and clinical relevance of bacterial contamination in preservation solution for liver transplantation. *Transplant Proc* 2009; **41**: 2169-2171 [PMID: 19715863 DOI: 10.1016/j.transproceed.2009.06.036]

28 **Sifri CD**, Ison MG. Highly resistant bacteria and donor-derived infections: treading in uncharted territory. *Transpl Infect Dis* 2012; **14**: 223-228 [PMID: 22676635 DOI: 10.1111/j.1399-3062.2012.00752.x]

29 **Watkins AC**, Vedula GV, Horan J, Dellicarpini K, Pak SW, Daly T, Samstein B, Kato T, Emond JC, Guarrera JV. The deceased organ

donor with an "open abdomen": proceed with caution. *Transpl Infect Dis* 2012; **14**: 311-315 [PMID: 22283979 DOI: 10.1111/j.1399-3062.2011.00712.x]

30 **Bull DA**, Stahl RD, McMahan DL, Jones KW, Hawkins JA, Renlund DG, Taylor DO, Karwande SV. The high risk heart donor: potential pitfalls. *J Heart Lung Transplant* 1995; **14**: 424-428 [PMID: 7654726]

31 **Martins N**, Martins IS, de Freitas WV, de Matos JA, Magalhães AC, Girão VB, Dias RC, de Souza TC, Pellegrino FL, Costa LD, Boasquevisque CH, Nouér SA, Riley LW, Santoro-Lopes G, Moreira BM. Severe infection in a lung transplant recipient caused by donor-transmitted carbapenem-resistant Acinetobacter baumannii. *Transpl Infect Dis* 2012; **14**: 316-320 [PMID: 22168176 DOI: 10.1111/j.1399-3062.2011.00701.x]

32 **Wendt JM**, Kaul D, Limbago BM, Ramesh M, Cohle S, Denison AM, Driebe EM, Rasheed JK, Zaki SR, Blau DM, Paddock CD, McDougal LK, Engelthaler DM, Keim PS, Roe CC, Akselrod H, Kuehnert MJ, Basavaraju SV. Transmission of methicillin-resistant Staphylococcus aureus infection through solid organ transplantation: confirmation via whole genome sequencing. *Am J Transplant* 2014; **14**: 2633-2639 [PMID: 25250717 DOI: 10.1111/ajt.12898]

33 **Johnston L**, Chui L, Chang N, Macdonald S, McKenzie M, Kennedy W, Haldane D, Bethune R, Taylor G, Hanakowski M, Tyrrell G. Cross-Canada spread of methicillin-resistant Staphylococcus aureus via transplant organs. *Clin Infect Dis* 1999; **29**: 819-823 [PMID: 10589896 DOI: 10.1086/520442]

34 **Giani T**, Conte V, Mandalà S, D'Andrea MM, Luzzaro F, Conaldi PG, Grossi P, Rossolini GM. Cross-infection of solid organ transplant recipients by a multidrug-resistant Klebsiella pneumoniae isolate producing the OXA-48 carbapenemase, likely derived from a multiorgan donor. *J Clin Microbiol* 2014; **52**: 2702-2705 [PMID: 24759725 DOI: 10.1128/JCM.00511-14]

35 **Fishman JA**, Grossi PA. Donor-derived infection--the challenge for transplant safety. *Nat Rev Nephrol* 2014; **10**: 663-672 [PMID: 25178971 DOI: 10.1038/nrneph.2014.159]

P- Reviewer: Boin IFSF, Hori T, Inoue K **S- Editor**: Gong ZM
L- Editor: Wang TQ **E- Editor**: Xu XR

World Journal of Gastroenterology

Submit a Manuscript: http://www.f6publishing.com

World J Gastroenterol 2017 August 21; 23(31): 5817-5822

DOI: 10.3748/wjg.v23.i31.5817

ISSN 1007-9327 (print) ISSN 2219-2840 (online)

CASE REPORT

Rarity among benign gastric tumors: Plexiform fibromyxoma - Report of two cases

Kinga Szurian, Holger Till, Eva Amerstorfer, Nicole Hinteregger, Hans-Jörg Mischinger, Bernadette Liegl-Atzwanger, Iva Brcic

Kinga Szurian, Bernadette Liegl-Atzwanger, Iva Brcic, Institute of Pathology, Medical University of Graz, 8036 Graz, Austria

Holger Till, Eva Amerstorfer, Department of Paediatric and Adolescent Surgery, Medical University of Graz, 8036 Graz, Austria

Nicole Hinteregger, Department of Radiology, Division of Neuroradiology, Vascular and Interventional Radiology, Medical University of Graz, 8036 Graz, Austria

Hans-Jörg Mischinger, Department of Surgery, Medical University of Graz, 8036 Graz, Austria

Author contributions: Szurian K and Brcic I designed the report; Till H, Amerstorfer E, Hinteregger N and Mischinger HJ collected the patients' clinical data; Szurian K, Till H, Amerstorfer E, Liegl-Atzwanger B and Brcic I analyzed the data and wrote the paper; Hinteregger N and Mischinger HJ revised the paper; All authors approved the final manuscript.

Institutional review board statement: Since medical treatment was conducted according to highest clinical standards, the present report of two cases is not of experimental character and does not require an ethical committee statement.

Informed consent statement: Informed consent was obtained from both patients.

Conflict-of-interest statement: The authors declare that they have no conflicts of interest.

Manuscript source: Unsolicited manuscript

Correspondence to: Iva Brcic, MD, Institute of Pathology, Medical University of Graz, Auenbruggerplatz 25, 8036 Graz, Austria. iva.brcic@medunigraz.at
Telephone: +43-316-38578031
Fax: +43-316-384329

Received: February 10, 2017
Peer-review started: February 12, 2017
First decision: March 16, 2017
Revised: April 3, 2017
Accepted: May 4, 2017
Article in press: May 4, 2017
Published online: August 21, 2017

Abstract

Plexiform fibromyxoma is a very rare mesenchymal tumor of the stomach, found almost exclusively in the antrum/pylorus region. The most common presenting symptoms are anemia, hematemesis, nausea and unintentional weight loss, without sex or age predilection. We describe here two cases of plexiform fibromyxoma, involving a 16-year-old female and a 34-year-old male. Both patients underwent complete resection (R0) by distal gastrectomy and retrocolic gastrojejunostomy (according to Billroth 2); for both, the postoperative course was uneventful. Histology showed multiple intramural and subserosal nodules with characteristic plexiform growth, featuring bland spindle cells situated in an abundant myxoid stroma with low mitotic activity. Immunohistochemistry showed α-smooth muscle actin-positive spindle cells, focal positivity for CD10, and negative staining for KIT, DOG1, CD34, S100, β-catenin, STAT-6 and anaplastic lymphoma kinase. One of the cases showed focal positivity for h-caldesmon and desmin. Upon follow-up, no sign of disease was found. In the differential diagnosis of plexiform fibromyxoma, it is important to exclude the more common gastrointestinal stromal tumors as they have greater potential for aggressive

behavior. Other lesions, like neuronal and vascular tumors, inflammatory fibroid polyps, abdominal desmoid-type fibromatosis, solitary fibrous tumors and smooth muscle tumors, must also be excluded.

Key words: Plexiform fibromyxoma; Plexiform angiomyxoid myofibroblastic tumor; Gastrointestinal stromal tumor; Stomach; Benign gastric tumor

Core tip: Plexiform fibromyxoma is a very rare benign mesenchymal tumor of the stomach. Here, we describe two cases of plexiform fibromyxoma, resolved with complete resection. The macroscopic, microscopic, immunohistochemical and molecular findings are reviewed. In the differential diagnosis of plexiform fibromyxoma, it is important to exclude the more common gastrointestinal stromal tumors as they have potentially more aggressive behavior.

Szurian K, Till H, Amerstorfer E, Hinteregger N, Mischinger HJ, Liegl-Atzwanger B, Brcic I. Rarity among benign gastric tumors: Plexiform fibromyxoma - Report of two cases. *World J Gastroenterol* 2017; 23(31): 5817-5822 Available from: URL: http://www.wjgnet.com/1007-9327/full/v23/i31/5817.htm DOI: http://dx.doi.org/10.3748/wjg.v23.i31.5817

INTRODUCTION

Gastrointestinal stromal tumors (GISTs) are the most common gastric mesenchymal tumors[1]. Immunohistologically, they show positive staining for *KIT* proto-oncogene receptor tyrosine kinase [KIT, cluster of differentiation (CD)117] and DOG1 (discovered on GIST-1), and the vast majority of cases harbor mutations in the *KIT* or *PDGFRα* (platelet-derived growth factor receptor alpha) genes. Plexiform fibromyxoma (PFM), also known as the plexiform angiomyxoid myofibroblastic tumor (PAMT), is a very rare benign mesenchymal gastric tumor, arising almost exclusively in the antrum/pylorus region. It was first described by Takahashi *et al*[2] in 2007. The cases reported to date have indicated no sex predilection and with a wide age range[3-5]. Clinical symptoms include anemia and hematemesis, which are consequent to tumor ulceration, nausea and weight loss.

Herein, we describe the specific histopathological features of two cases of PFM in regard to the current literature and discuss misleading differential diagnoses.

CASE REPORT

Case 1 presentation

A 16-year-old Caucasian female patient presented with refractory anemia, first detected following a skiing accident. She was treated in an outpatient setting, with iron, vitamin B12 and folic acid supplementation. In history taking, the patient reported recurrent nausea; otherwise, the medical history and physical examination were unremarkable. Laboratory findings showed no significantly altered values, except for a moderate, normochromic, normocytic anemia (hemoglobin 9.5 g/dL; normal range: 12.1-15.1 g/dL). During work-up, ultrasound examination detected a hypoechoic lesion in the gastric wall. Magnetic resonance imaging revealed a heterogeneously enhancing, lobulated, exophytic mass, situated intramural within the submucosa of the anterior wall of the gastric antrum (Figure 1). Positron emission tomography-computed tomography further revealed a hypermetabolic lesion in the dorsal part of the mass. Endoscopy confirmed a subepithelial lesion with partially ulcerated mucosa in the gastric antrum, necessitating a distal gastrectomy for complete resection.

Case 2 presentation

A 34-year-old obese male patient with unremarkable medical history presented with complaint of discomfort in the epigastric region accompanied by flatulence. Laboratory findings were within normal limits, except for slightly higher creatine kinase (227 U/L; normal range: 52-336 U/L) and elevated lactate dehydrogenase (377 U/L; normal range: 105-333 U/L). Gastroscopy revealed a pyloric submucosal lesion, suspicious of GIST. Biopsy showed foveolar hyperplasia of antral mucosa, with no submucosa.

Tumor characteristics for both cases

Both patients underwent distal gastrectomy for complete resection (R0) and retrocolic gastrojejunostomy (according to Billroth 2) (Figure 2). Gross examination of the specimens from both cases showed well-circumscribed lobulated tumors, with the largest diameter measuring 6.5 cm in case 1 and 1.6 cm in case 2. Examination of the cut surface showed both tumors to be well demarcated and solid, with mucoid consistency. A multinodular growth pattern was apparent, mostly involving the submucosa, muscularis propria and subserosal adipose tissue (Figure 3A). Overlying mucosa was focally ulcerated.

For both cases, histological analysis showed multiple intramural and subserosal nodules of characteristic plexiform growth, with cytological bland spindle cells situated in an abundant myxoid stroma having prominent capillary network and scattered inflammatory and mast cells (Figure 3B). Mitotic activity was low (up to 3/50 high power fields, HPF). Mucosal involvement with ulceration was observed; however, there was no necrosis and all resection margins were free of tumor.

Immunohistochemically, both cases showed positive reaction for alpha-smooth muscle actin (α-SMA) (Figure 3C) and focal positivity for CD10. Furthermore,

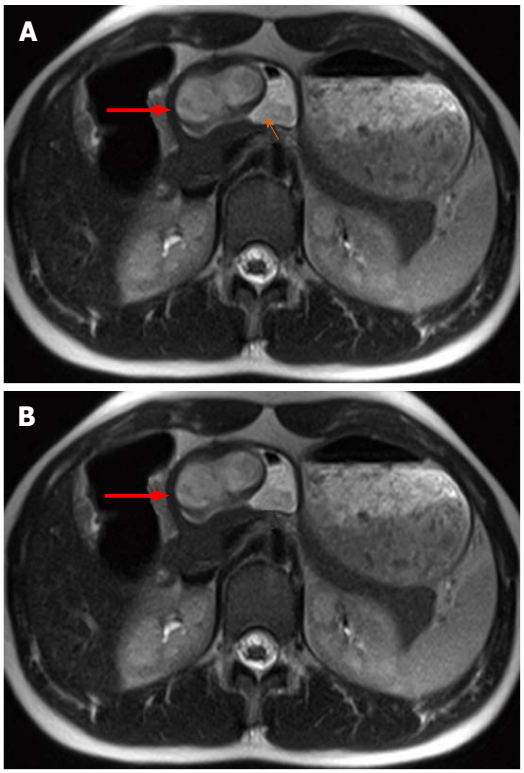

Figure 1 Magnetic resonance imaging findings for case 1, using transverse T2-and T1-weighted magnetic resonance imaging. A: Transverse T2-weighted magnetic resonance imaging (MRI) showing well circumscribed, endophytic mass (thick red arrow) of the gastric antrum which is partially filled with fluid (thin orange arrow); B: T1-weighted MRI after contrast media application showing homogeneous wall enhancement of the well circumscribed mass (thick red arrow).

the case 1 tumor cells showed focal positivity for h-caldesmon (Figure 3D) and desmin, while case 2 tumor cells showed negativity for h-caldesmon and desmin. In both cases, the tumor cells were negative for KIT (Figure 3E), DOG1 (Figure 3F), hematopoietic progenitor cell antigen CD34 (CD34), S100, β-catenin, signal transducer and activator of transcription 6, interleukin-4 induced (STAT-6) and anaplastic lymphoma kinase. Neither tumor was succinate dehydrogenase complex iron sulfur subunit B (SDHB)-deficient. Mutational status analysis was performed for case 1, and no mutations were found in *KIT* (exons 9, 11, 13, 17, 18 or 20) or *PDGFRA* (exons 12, 14 or 18) by direct sequencing using paraffin-embedded tissue samples (Custom Ion Torrent AmpliSeq Panel; Thermo Fisher Scientific, Waltham, MA, United States).

In both cases, these findings led to the final diagnosis of PFM. Postoperatively, case 1 developed pulmonary embolism, which was treated by administration of anticoagulants. The patient was discharged on postoperative day 9. The postoperative course of case 2 was uneventful and the patient was discharged on postoperative day 11. At the last follow-up (6 and 16 mo postoperative respectively), neither patient showed evidence of residual or recurrent disease, nor complained of symptoms of dumping syndrome, afferent loop syndrome or gastroesophageal reflux.

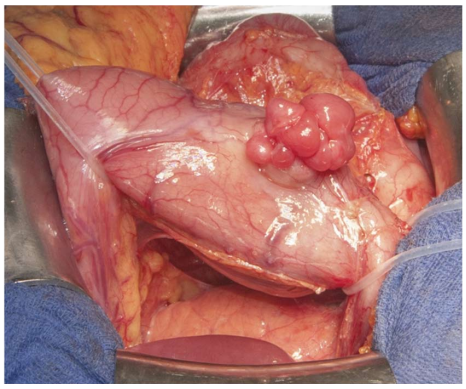

Figure 2 Gross appearance of the plexiform fibromyxoma during surgery (case 2). The tumor is lobulated, protrudes from the gastric serosa and is located in the lower part (antrum) of the stomach near the pylorus. Underneath the stomach, normal appearing pancreas can be appreciated.

DISCUSSION

PFMs are very rare gastric mesenchymal tumors. To date, various names have been proposed to describe this benign spindle cell tumor, including fibromyxoma, plexiform angiomyxoid tumor, and PAMT[2,6]. In 2009, Miettinen *et al*[4] described 12 cases of benign gastric antral fibromyxoid tumors, designating them as PFM. In 2010, this term was accepted and these tumors became recognized as a distinct entity, according to World Health Organization's classification of tumors of the digestive system[7].

Cases of PMFs reported show no trend in age (range: 7-75 years) but indicate an almost exclusive location in the gastric antrum and pyloric region, with up to 20% of cases spreading to the duodenal bulb[4]. Like in our patients, extension to the exterior surface of the stomach and proximal duodenum has been described. The size can range from 1.5 to 15 cm[5]. Two-thirds of the tumors are ulcerated, putting these patients at risk of gastrointestinal bleeding and secondary anemia. Other clinical features include abdominal pain, nausea, vomiting and unintentional weight loss. These symptoms can also be found in patients with GIST, a mesenchymal tumor that is common in the stomach and more aggressive, and which must always be considered as a differential diagnosis for PMF. PMFs are asymptomatic, and thus primarily discovered incidentally. Our first patient presented with refractory anemia, and the tumor was detected by ultrasound examination. The second patient complained of discomfort in the epigastric region.

On gross examination, these tumors are not encapsulated and present as (multi)nodular lesions, variably involving the intramucosal to subserosal and serosal parts of the stomach. In fact, tumor projection toward the serosal surface is commonly encountered in this entity. Histological features are quite typical

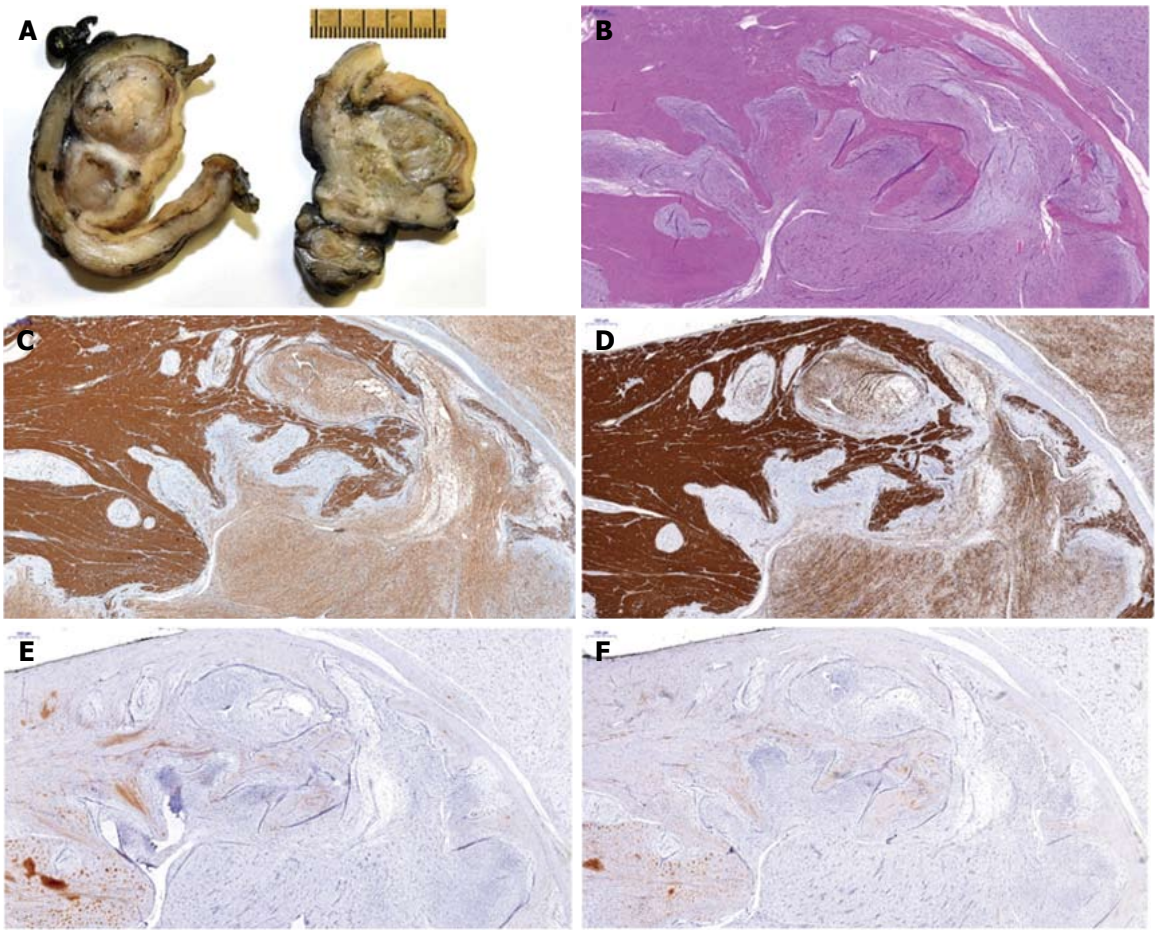

Figure 3 Macroscopic, microscopic and immunohistochemical features of plexiform fibromyxoma. A: Cut section showing multinodular, solid glistening translucid tumor within the gastric wall and subserosa; B: Histological analysis of the tumor showing composition of ovoid to spindled-shaped cells in a myxoid or fibromyxoid stroma with a plexiform intramural growth pattern; C-F: Immunohistochemical analysis showing positivity for alpha-smooth muscle actin (C) and h-caldesmon (D), but negativity for KIT (E) and DOG1 (F).

and show a plexiform growth pattern with multiple nodules composed of abundant paucicellular to moderately cellular myxoid or fibromyxoid stroma, and having prominent small vessels and bland-looking monomorphic tumor cells within the gastric wall and subserosa. In some cases, more collagenous stroma is observed-feature most commonly seen in the extramural extension. The tumor cells range from oval to spindle in shape, and show no atypia. Mitoses are rare (up to 7/50 HPF)[4,5,8]. Ulceration and invasion of the mucosa can be found. Miettinen *et al*[4] reported vascular invasion in 4 patients, suggesting possible intravascular tumor spread within the gastric wall and subserosa. In our cases, multiple tumor nodules were displayed in all gastric layers. Serosa was intact and no intravascular component was noted. Tumor cells were bland-looking, embedded in mildly cellular stroma that was more collagenous in the extramural parts of the tumors. Up to 3 mitotic figures were found on 50 HPF. In addition, an extensive capillary network and scattered inflammatory and mast cells were found within the stroma.

Immunohistochemically, tumor cells usually show focal to diffuse positive reaction with vimentin, α-SMA and CD10, and sometimes with desmin and/or h-caldesmon or calponin[2,4-6,9,10]. This immunoprofile indicates that these tumors contain cells with myofibroblastic and fibroblastic and/or smooth muscle cell characteristics, all of which were observed as present in one of our cases. However, the predominant cell type is myofibroblastic in the majority of the reported cases. Quero *et al*[6] compiled the clinicopathologic characteristics of all cases published up to March 2016. We present in Table 1 the collective immunohistochemical findings for desmin and h-caldesmon/calponin, as well as the findings for the two newest cases presented herein. The expression of myogenic markers in some of the tumors suggests that a subset of these tumors contain not only tumor cells with myofibroblastic-fibroblastic phenotype but also tumor cells with true smooth muscle differentiation[9]. For those tumors, some authors prefer to use the term "PAMT"; this would suggest that PMFs, plexiform myofibroblastic tumors and PAMTs are slightly different entities in the spectrum of benign plexiform myxoid (myo)fibroblastic lesions of the stomach.

In all of these tumor types, negativity for immunohistochemical staining with KIT, DOG1, CD34,

Table 1 Myogenic markers in 61 published cases of plexiform fibromyxoma *n* (%)

	Desmin	h-Caldesmon/Calponin
(-)	23 (37.7)	15 (24.6)
f (+)	14 (22.9)	10 (16.4)
(+)	4 (6.4)	4 (6.6)
NA	20 (33.0)	32 (52.4)
Total	61 (100.0)	61 (100.0)

NA: Not available; f: Focal; (+): Positive; (-): Negative.

epithelial membrane antigen, beta-catenin and S100 has been reported[2,4-6,9,10]. A negative finding for KIT and DOG1 excludes GIST, especially for the plexiform myxoid type, while a negative finding for S100 excludes neuronal tumors (*i.e.,* schwannoma and neurofibroma). Vascular lesions should show positivity for CD34, CD31 and ETS-related gene, which is a distinguishing feature from PMF. Other differential diagnoses include fibroblastic tumors [*i.e.,* inflammatory fibroid polyp, abdominal desmoid-type fibromatosis (nuclear β-catenin staining) and solitary fibrous tumor (CD34 and nuclear STAT6 expression)] and smooth muscle tumors (*i.e.,* leiomyoma and leiomyosarcoma). Quero *et al*[6] reported that only four of the published cases showed positive expression for h-caldesmon or calponin, albeit diffuse.

The tumor from one of our patients showed focal positivity for h-caldesmon. These cases can be diagnostically challenging and difficult to differentiate from myxoid leiomyomas. They more commonly arise in the gastric cardia or fundus, have plexiform architecture and contain, at least, focal fascicles of tumor cells with typical eosinophil cytoplasm (*i.e.,* morphological features compatible with smooth muscle differentiation)[1,11]. The discontinuous plexiform multinodular pattern is more of a characteristic of PFM. In female patients, metastatic low-grade endometrial stromal sarcoma (ESS) should be ruled out by testing for status of estrogen receptor (ER) and progesterone receptor (PR) expression, positivity for both of which is characteristic of low-grade ESS. Furthermore, in low-grade ESS, the following translocations have been described: JAZF1-SUZ12 and MEAF6-PHF1. On the other hand, high-grade ESSs are ER- and PR-negative, and can have YWHAE-FAM22 translocation.

Mutational analysis has been performed in some of the cases published, but none reported detection of *KIT* or *PDGFRα* mutations[4-6]. The same results were found in one of our cases (the other was not tested). In contrast, GIST typically bear *KIT* or *PDGFRα* activating mutations; however, approximately 10% of GISTs in adults and more than 90% in children lack these mutations, and are then classified as wild-type GISTs[12], being either succinate dehydrogenase (SDH)-deficient or non-SDH-deficient[13,14]. The SDH-deficient type encompasses cases of Carney triad and Carney Stratakis syndrome, as well as some sporadic cases. These tumors are usually found in young women, typically occur in the antrum and show a characteristic multifocal/multinodular and plexiform growth pattern. However, the tumors are more cellular, composed of epithelioid cells that are immunohistochemically positive for KIT and DOG1. Further, *PDGFRα* mutations have also been described in inflammatory fibroid polyps. Recently, Spans *et al*[15] described a recurrent translocation-t(11;12)(q11;q13), involving the long non-coding gene metastases-associated lung adenocarcinoma transcript 1 and the gene glioma-associated oncogene homologue 1 (*GLI1*)-in a subgroup of PMTs.

Surgery with negative resection margins is the treatment of choice. This tumor is considered to be a benign lesion, and to date no cases of recurrence or distant metastases after complete surgical resection have been reported[4]. Upon follow-up of our 2 patients, no sign of disease was found.

In summary, different terms have been used to describe the benign gastric tumor with prominent plexiform and myxoid pattern. Current histomorphological and immunohistochemical findings suggest that PMFs, plexiform myofibroblastic tumors and PAMTs are slightly different entities in the spectrum of benign plexiform myxoid (myo)fibroblastic (spindle cell) lesions of the stomach. Most importantly, it is crucial to differentiate these tumors from the more common GISTs, as the latter have greater potential for aggressive behavior. GISTs and other gastric myxoid tumors are distinguishable upon investigation of a wide panel of immunohistochemical markers and mutational status analysis of both the *KIT* and *PDGFRα* genes.

COMMENTS

Case characteristics

Two cases of plexiform fibromyxoma presented with discrete symptoms. The first was a 16-year-old female, with incidentally found refractory anemia, and the second was a 34-year-old male, who presented with discomfort in the epigastric region accompanied by flatulence.

Clinical diagnosis

Physical examination of both patients was unremarkable. On gastroscopy, however, submucosal tumor was observed, situated in the antral region.

Differential diagnosis

Gastrointestinal stromal tumor (GIST), inflammatory fibroid polyp, abdominal desmoid-type fibromatosis, solitary fibrous tumor, leiomyoma and leiomyosarcoma.

Laboratory diagnosis

In the first case, laboratory findings showed moderate, normochromic, normocytic anemia (hemoglobin of 9.5 g/L). The second case showed a slight increase in creatine kinase (227 U/L) and elevated lactate dehydrogenase (377 U/L).

Imaging diagnosis

In the first case, ultrasound examination of the abdomen displayed a hypoechoic lesion in the gastric wall, magnetic resonance imaging revealed a heterogeneously enhancing, lobulated, exophytic mass, situated intramural

within the submucosa of the anterior wall of the gastric antrum, and positron emission tomography-computed tomography showed a hypermetabolic lesion. In the second case, only gastroscopy was performed, and it revealed a 3-cm large submucosal lesion.

Pathological diagnosis

For both cases, histology showed multiple intramural and subserosal nodules with characteristic plexiform growth featuring bland spindle cells situated in an abundant myxoid stroma with a prominent capillary network.

Treatment

Both patients underwent distal gastrectomy and retrocolic gastrojejunostomy (according to Billroth 2).

Related reports

Reports of cases of plexiform fibromyxoma in the literature are rare. Macroscopic, microscopic, immunohistochemical and molecular findings are crucial for exclusion of the more common gastrointestinal stromal tumors, which have potentially more aggressive behavior.

Term explanation

Plexiform fibromyxoma, also known as a plexiform angiomyxoid myofibroblastic tumor, is a very rare mesenchymal tumor of the stomach, found almost exclusively in the antrum/pylorus region.

Experiences and lessons

This report presents the characteristic findings of plexiform fibromyxoma. Gastric GIST should be excluded in the differential diagnosis.

Peer-review

The authors have described two cases of very rare gastric plexiform fibromyxoma that were successfully resected. The article highlights the macroscopic, histologic, immunohistochemical and molecular findings typical of theses tumors and provides insights into the correct diagnosis.

REFERENCES

1 **Lee HH**, Hur H, Jung H, Jeon HM, Park CH, Song KY. Analysis of 151 consecutive gastric submucosal tumors according to tumor location. *J Surg Oncol* 2011; **104**: 72-75 [PMID: 21031420 DOI: 10.1002/jso.21771]

2 **Takahashi Y**, Shimizu S, Ishida T, Aita K, Toida S, Fukusato T, Mori S. Plexiform angiomyxoid myofibroblastic tumor of the stomach. *Am J Surg Pathol* 2007; **31**: 724-728 [PMID: 17460456 DOI: 10.1097/01.pas.0000213448.54643.2f]

3 **Wang LM**, Chetty R. Selected unusual tumors of the stomach: a review. *Int J Surg Pathol* 2012; **20**: 5-14 [PMID: 22134628 DOI: 10.1177/1066896911429300]

4 **Miettinen M**, Makhlouf HR, Sobin LH, Lasota J. Plexiform fibromyxoma: a distinctive benign gastric antral neoplasm not to be confused with a myxoid GIST. *Am J Surg Pathol* 2009; **33**: 1624-1632 [PMID: 19675452 DOI: 10.1097/PAS.0b013e3181ae666a]

5 **Takahashi Y**, Suzuki M, Fukusato T. Plexiform angiomyxoid myofibroblastic tumor of the stomach. *World J Gastroenterol* 2010; **16**: 2835-2840 [PMID: 20556828 DOI: 10.3748/wjg.v16.i23.2835]

6 **Quero G**, Musarra T, Carrato A, Fici M, Martini M, Dei Tos AP, Alfieri S, Ricci R. Unusual focal keratin expression in plexiform angiomyxoid myofibroblastic tumor: A case report and review of the literature. *Medicine* (Baltimore) 2016; **95**: e4207 [PMID: 27428222 DOI: 10.1097/MD.0000000000004207]

7 **Miettinen M,** Fletcher CD, Kindblom LG, Tsui WM. Mesenchymal tumors of the stomach. In: Bosman FT, Carneiro F, Hruban R, Teise ND. WHO classification of tumors of the digestive system 4th ed. Lyon: IARC; 2010: 74-79

8 **Kane JR**, Lewis N, Lin R, Villa C, Larson A, Wayne JD, Yeldandi AV, Laskin WB. Plexiform fibromyxoma with cotyledon-like serosal growth: A case report of a rare gastric tumor and review of the literature. *Oncol Lett* 2016; **11**: 2189-2194 [PMID: 26998147 DOI: 10.3892/ol.2016.4185]

9 **Li P**, Yang S, Wang C, Li Y, Geng M. Presence of smooth muscle cell differentiation in plexiform angiomyxoid myofibroblastic tumor of the stomach: a case report. *Int J Clin Exp Pathol* 2014; **7**: 823-827 [PMID: 24551311]

10 **Duckworth LV**, Gonzalez RS, Martelli M, Liu C, Coffin CM, Reith JD. Plexiform fibromyxoma: report of two pediatric cases and review of the literature. *Pediatr Dev Pathol* 2014; **17**: 21-27 [PMID: 24160555 DOI: 10.2350/13-09-1373-OA.1]

11 **Miettinen MM,** Quade B. Leiomyoma of deep soft tissue. In: Fletcher CDM, Bridge JA, Hogendoorn PCW, Mertens F. WHO classification of tumors of soft tissue and bone 4th ed. Lyon: IARC; 2013: 110-111

12 **Joensuu H**, Hohenberger P, Corless CL. Gastrointestinal stromal tumour. *Lancet* 2013; **382**: 973-983 [PMID: 23623056 DOI: 10.1016/S0140-6736(13)60106-3]

13 **Wada R**, Arai H, Kure S, Peng WX, Naito Z. "Wild type" GIST: Clinicopathological features and clinical practice. *Pathol Int* 2016; **66**: 431-437 [PMID: 27427238 DOI: 10.1111/pin.12431]

14 **Janeway KA**, Kim SY, Lodish M, Nosé V, Rustin P, Gaal J, Dahia PL, Liegl B, Ball ER, Raygada M, Lai AH, Kelly L, Hornick JL; NIH Pediatric and Wild-Type GIST Clinic, O'Sullivan M, de Krijger RR, Dinjens WN, Demetri GD, Antonescu CR, Fletcher JA, Helman L, Stratakis CA. Defects in succinate dehydrogenase in gastrointestinal stromal tumors lacking KIT and PDGFRA mutations. *Proc Natl Acad Sci USA* 2011; **108**: 314-318 [PMID: 21173220 DOI: 10.1073/pnas.1009199108]

15 **Spans L**, Fletcher CD, Antonescu CR, Rouquette A, Coindre JM, Sciot R, Debiec-Rychter M. Recurrent MALAT1-GLI1 oncogenic fusion and GLI1 up-regulation define a subset of plexiform fibromyxoma. *J Pathol* 2016; **239**: 335-343 [PMID: 27101025 DOI: 10.1002/path.4730]

P- Reviewer: Lee JI, Park WS, Tovey FI **S- Editor**: Ma YJ
L- Editor: A **E- Editor**: Huang Y

World Journal of Gastroenterology

Submit a Manuscript: http://www.f6publishing.com

World J Gastroenterol 2017 August 21; 23(31): 5823-5828

DOI: 10.3748/wjg.v23.i31.5823

ISSN 1007-9327 (print) ISSN 2219-2840 (online)

CASE REPORT

Tegafur-uracil-induced rapid development of advanced hepatic fibrosis

Shuya Honda, Koji Sawada, Takumu Hasebe, Shunsuke Nakajima, Mikihiro Fujiya, Toshikatsu Okumura

Shuya Honda, Koji Sawada, Takumu Hasebe, Shunsuke Nakajima, Mikihiro Fujiya, Toshikatsu Okumura, Division of Gastroenterology and Hematology/Oncology, Department of Medicine, Asahikawa Medical University, Asahikawa, Hokkaido 078-8510, Japan

Author contributions: Honda S, Sawada K, Hasebe T and Nakajima S treated this patient; Sawada K, Fujiya M and Okumura T wrote the paper.

Institutional review board statement: This study was approved by the Institutional Review Board of Asahikawa Medical University.

Informed consent statement: Written informed consent was obtained prior to this manuscript preparation.

Conflict-of-interest statement: All the authors have no conflicts of interests to declare.

Manuscript source: Unsolicited manuscript

Correspondence to: Koji Sawada, MD, PhD, Division of Gastroenterology and Hematology/Oncology, Department of Medicine, Asahikawa Medical University, 2-1 Midorigaoka-higashi, Asahikawa, Hokkaido 078-8510, Japan. k-sawada@asahikawa-med.ac.jp
Telephone: +81-166-682462
Fax: +81-166-682469

Received: February 21, 2017
Peer-review started: February 22, 2017
First decision: June 5, 2017
Revised: June 22, 2017
Accepted: July 22, 2017

Article in press: July 24, 2017
Published online: August 21, 2017

Abstract

Tegafur-uracil has been reported to have only minor adverse effects and is associated with liver injury in 1.79% of Japanese patients. The development of tegafur-uracil-induced hepatic fibrosis with portal hypertension is rare. Here, we report a case of a 74-year-old woman with rapidly developing tegafur-uracil-induced hepatic fibrosis. The patient had no history of liver disease and had been treated with tegafur-uracil for 8 mo after breast cancer surgery. The patient was admitted to our hospital for abdominal distension and leg edema associated with liver dysfunction. Computed tomography imaging revealed massive ascites and splenomegaly, and a non-invasive assessment of liver fibrosis indicated advanced fibrosis. The histopathological findings revealed periportal fibrosis and bridging fibrosis with septation. The massive ascites resolved after discontinuing tegafur-uracil. These findings suggest that advanced hepatic fibrosis can develop from a relatively short-term administration of tegafur-uracil and that non-invasive assessment is useful for predicting hepatic fibrosis.

Key words: Tegafur-uracil; Drug-induced liver injury; Hepatic fibrosis; Portal hypertension; Non-invasive assessment

Core tip: This case report presents a rapid development of hepatic fibrosis induced by tegafur-uracil and the usefulness of a non-invasive assessment of hepatic fibrosis. Tegafur-uracil is often administered in patients with various cancers; therefore, when liver dysfunction progresses in patients treated with tegafur-uracil, the

development of hepatic fibrosis should be considered, even for short-term administration.

Honda S, Sawada K, Hasebe T, Nakajima S, Fujiya M, Okumura T. Tegafur-uracil-induced rapid development of advanced hepatic fibrosis. *World J Gastroenterol* 2017; 23(31): 5823-5828 Available from: URL: http://www.wjgnet.com/1007-9327/full/v23/i31/5823.htm DOI: http://dx.doi.org/10.3748/wjg.v23.i31.5823

INTRODUCTION

Tegafur-uracil is used worldwide as a treatment for various cancers, such as those of the lung, colon, liver, and breast. The oral administration of tegafur-uracil has been reported to have only minor adverse effects and, as such, is considered suitable for long-term administration[1,2]. Studies with a special focus on drug-induced liver injury (DILI) and drug safety have reported that tegafur-uracil is associated with liver injury in 1.79% of Japanese patients. The development of associated advanced hepatic fibrosis is unusual. In fact, studies have shown that advanced hepatic fibrosis develops only after the long-term administration of tegafur-uracil[1,3]. Here, we report a case that rapidly progressed to advanced hepatic fibrosis with portal hypertension. The patient had been treated with short-term tegafur-uracil chemotherapy, and a non-invasive assessment was useful for the diagnosis and prediction of hepatic fibrosis.

CASE REPORT

A 74-year-old woman who was treated with amlodipine for hypertension for more than 10 years was admitted to our hospital for abdominal distension and leg edema. The patient had undergone a muscle-sparing mastectomy for breast cancer in the left breast 9 mo prior. The histopathological examination showed stage Ⅰ estrogen receptor- and progesterone receptor-negative apocrine carcinoma. The patient was therefore put on a regimen of tegafur-uracil (400 mg daily) for 8 mo. There was no history of liver disease or alcohol abuse, and there was no family history of liver disease. Before breast cancer surgery, computed tomography (CT) imaging demonstrated neither chronic liver disease nor splenomegaly (Figure 1A), and a blood examination showed normal platelet counts (19.2 × $10^4/\mu L$), no coagulopathy (prothrombin time activity 104%), and no liver dysfunction (total bilirubin 0.5 mg/dL, aspartate aminotransferase 22 U/L, alanine aminotransferase 14 U/L, alkaline phosphatase 320 mg/dL, gamma-glutamyl transferase 24 U/L). Two months after the administration of tegafur-uracil, her blood examination revealed increased serum transaminase levels. She was therefore prescribed ursodeoxycholic acid as a supportive liver therapy because of a suspicion of DILI. However, upon admission, her blood examination showed low platelet counts, persistent liver dysfunction, and increased levels of fibrosis markers such as type 4 collagen 7S and hyaluronic acid. The anti-hepatitis-B core (HBc) test was weakly positive; however, the HBV-DNA test was negative, suggesting a past infection (Table 1). CT imaging revealed the presence of massive ascites and splenomegaly (Figure 1B), and upper gastrointestinal endoscopy showed grade 1 esophageal varices without red spots (Figure 1C). The magnetic resonance (MR) elastography and Virtual Touch Quantification (VTQ) values were 7.0 kPa and 2.54 m/s, respectively (Figure 2A and B). These findings suggested that the patient had hepatic failure accompanied by portal hypertension and advanced hepatic fibrosis. Although her serum immunoglobulin levels were normal, she was positive for anti-nuclear antibody (ANA) (anti-centromere type) (Table 1). A liver biopsy was performed because primary biliary cholangitis (PBC) was suspected. Histopathological examination revealed spotty necrosis in zone 3 and interface hepatitis, including lymphocytes, neutrophils, and eosinophils, all in zone 1 (Figure 3A and B). A Marked ballooning of hepatocytes with Mallory bodies was noted (Figure 3C). Periportal fibrosis and bridging fibrosis with partial septation were observed (Figure 3D). The intralobular bile ducts had partially degenerated, but neither chronic non-suppurative destructive cholangitis nor cholestasis were detected. There was no pathological copper or iron accumulation. Therefore, the patient was diagnosed with tegafur-uracil-induced liver injury with a rapid development of advanced hepatic fibrosis. Discontinuation of tegafur-uracil combined with conservative treatment, including a diuretic, immediately improved the patient's serum transaminase levels and prothrombin activity. The massive ascites was improved after 1 mo (Figure 4). Thirteen months after drug discontinuation, the patient's type Ⅳ collagen 7S and hyaluronic acid levels were improved from 16 ng/mL to 6.5 ng/mL and from 653.4 ng/mL to 112.2 ng/mL, respectively, suggesting an alleviation of hepatic fibrosis.

DISCUSSION

Only five cases of tegafur-uracil-induced hepatic fibrosis with portal hypertension have been described in the literature[1,3,4] (Table 2). These patients were treated with tegafur-uracil over a long period (23-54 mo; mean 39.6 mo), and their pathological findings showed periportal fibrosis and bridging fibrosis following liver biopsy. In our case, massive ascites, esophageal varices, and splenomegaly appeared 8 mo after drug administration. Hepatic fibrosis has been previously described in patients treated with tegafur-uracil over 23-54 mo, but the present case developed liver fibrosis only 8 mo after the administration of this medication, which suggested that a relatively short-term treatment

Table 1 Laboratory data on admission

WBC	5750/μL	ALP	670 mg/dL	Type 4 collagen 7S	16 ng/mL
RBC	2.99×10^6/μL	LDH	386 mg/dL	Hyaluronic acid	653.4 ng/mL
Hb	11.7 g/dL	γGTP	97 U/L		
PLT	5.3×10^6/μL	ChE	68 U/L	ANA	× 1280
		T. Cho	120 g/dL	(anti-centromere type)	
PT%	40%	BUN	18.6 mg/dL	AMA	(-)
PT-INR	1.63	Cre	0.65 mg/dL	ASMA	(-)
		Na	140 mEq/L		
T.P.	6.1 g/dL	K	3.9 mEq/L	HBs Ag	(-)
Alb	2.9 g/dL	Cl	105 mEq/L	HBc Ab	9.36 S/CO
T. Bil	1.7 mg/dL	NH3	44 μg/dL	HBV DNA	(-)
D. Bil	0.8 mg/dL	IgG	1591.2 mg/dL	HCV Ab	(-)
AST	130 U/L	IgA	636.4 mg/dL		
ALT	80 U/L	IgM	107.4 mg/dL		

WBC: White blood cell count; RBC: Red blood cell count; Hb: Hemoglobin; PLT: Platelet count; PT%: Prothrombin time; PT-INR: Prothrombin time-international normalized ratio; T.P.: Total protein; Alb: Albumin; T.Bil: Total bilirubin; D.Bil: Direct bilirubin; AST: Aspartate aminotransferase; ALT: Alanine aminotransferase; ALP: Alkaline phosphatase; LDH: Lactate dehydrogenase; γGTP: Gamma-glutamyl transferase; ChE: Cholinesterase; T.Cho: Total cholesterol; BUN: Blood urea nitrogen; Cre: Creatinine; NH3: Ammonia; IgG: Immunoglobulin G; IgA: Immunoglobulin A; IgM: Immunoglobulin M; ANA: Anti-nuclear antibody; AMA: Anti-mitochondrial antibody; ASMA: Anti-smooth muscle antibody; HBsAg; Hepatitis B surface antigen; HBcAb: Hepatitis B core antibody; HBV: Hepatitis B virus; HCV Ab: Hepatitis C virus antibody.

Table 2 Tegafur-uracil-induced hepatic fibrosis

Cases	Age (yr)	Sex	Daily dose (mg)	Duration (mo)	Type 4 collagen 7S (ng/mL)	Hepatic fibrosis	Portal hypertension
1[1]	81	M	400	48	12	Bridging fibrosis	Esophageal varices Ascites
2[3]	76	F	NA	24	NA	Bridging fibrosis	Ascites
3[4]	82	M	300	48	12	Bridging fibrosis	NA
4[4]	73	M	300	23	11	Bridging fibrosis	NA
5[4]	68	F	400	55	12	Bridging fibrosis	NA
Our case	74	F	400	8	16	Bridging fibrosis With septation	Esophageal varices Ascites Splenomegaly

M: Male; F: Female; NA: Not available.

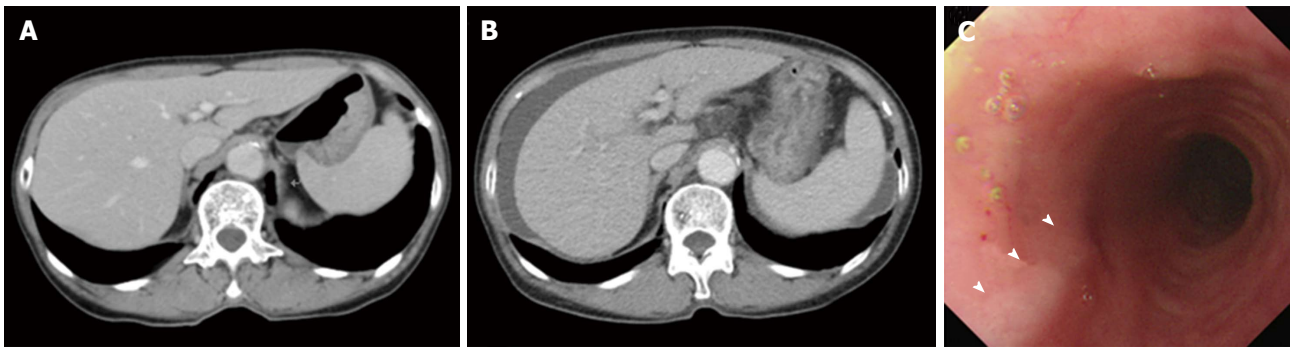

Figure 1 Computed tomography and upper gastrointestinal endoscopy images. A: CT imaging showed neither chronic liver disease nor splenomegaly before breast cancer surgery; B: Eight months after treatment with tegafur-uracil, CT imaging revealed the presence of massive ascites and splenomegaly; C: Upper gastrointestinal endoscopy showed grade 1 esophageal varices (arrowheads).

with tegafur-uracil induced advanced hepatic fibrosis with portal hypertension. We initially suspected tegafur-uracil-induced liver dysfunction on the basis of previous chronic liver disease. In particular, because anti-centromere type ANA is a significant risk factor for the development of portal hypertension in patients with PBC[5,6], we suspected PBC in this patient, and a liver biopsy was performed. Histopathological examination revealed the marked ballooning of hepatocytes and infiltration of neutrophils and eosinophils. However, contrary to our expectations, features consistent with PBC were not observed. In addition, the patient did not have a history of chronic liver disease or alcohol abuse, and a previous CT imaging did not show chronic liver

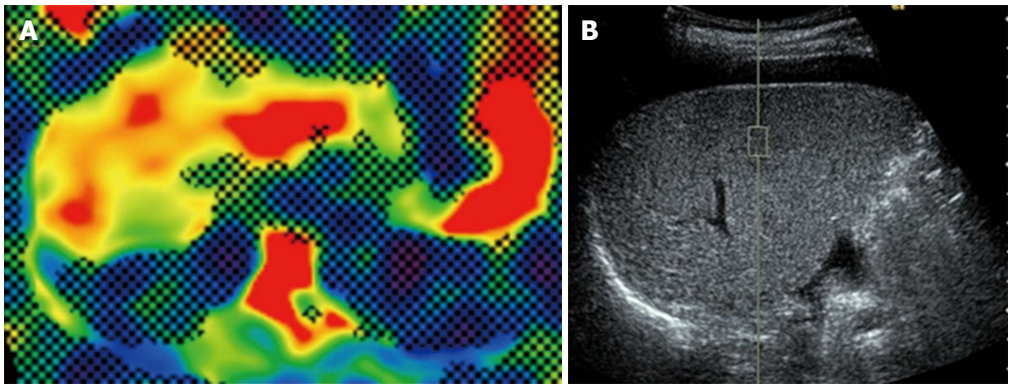

Figure 2 Magnetic resonance elastography and virtual touch quantification in the liver. A: Elastography showed that the shear stiffness of the liver was 7.0 kPa; B: A region of interest was placed the right lobe and the median value of the measured shear wave velocity was 2.54 m/s.

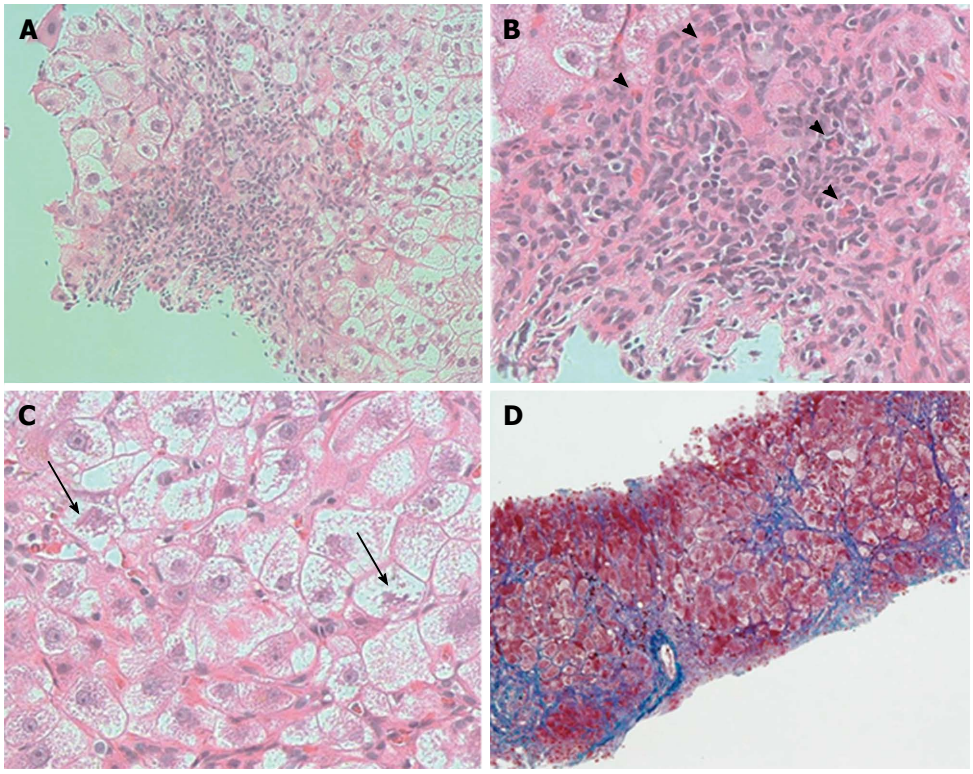

Figure 3 Histopathological analysis of the liver. A: Histopathological examination showed interface hepatitis; B: Infiltration of lymphocytes, neutrophils, and eosinophils (arrowheads); C: Markedly ballooning of hepatocytes with Mallory bodies was observed (arrows) (hematoxylin-eosin staining, magnification A: × 200, B: × 400, C: × 400); D: Azan staining showed periportal fibrosis and bridging fibrosis with partial septation (Azan staining, magnification: × 100).

disease or splenomegaly. It is difficult to diagnose atypical PBC, even if historical analysis is performed; however, PBC usually develops slowly without an acute onset or acute exacerbation[7,8]. The clinical course necessitated the discontinuation of tegafur-uracil therapy. This treatment plan improved the patient's liver dysfunction. Therefore, it appeared that advanced hepatic fibrosis was induced by the short-term administration of tegafur-uracil.

Autoimmunity is related to liver injury induced by some drugs, such as herbal products, minocycline, diclofenac, statins, and other biological agents[9,10]. In our case, the mechanism underlying the rapid development of hepatic fibrosis was unclear. However, certain mechanisms that underlie autoimmune reactions may have been associated with the rapid progression of fibrosis.

Recent studies have suggested that non-invasive assessments of liver fibrosis, including approaches that use MR elastography[11,12] and VTQ[13-15], are useful for predicting hepatic fibrosis in patients with liver disease, particularly in those with chronic hepatitis C. Suou *et al*[1,4] reported that hepatic fibrosis without elevated transaminase levels could be induced by the long-term oral administration of tegafur-uracil and that certain serum fibrosis markers, such as type Ⅳ collagen 7S,

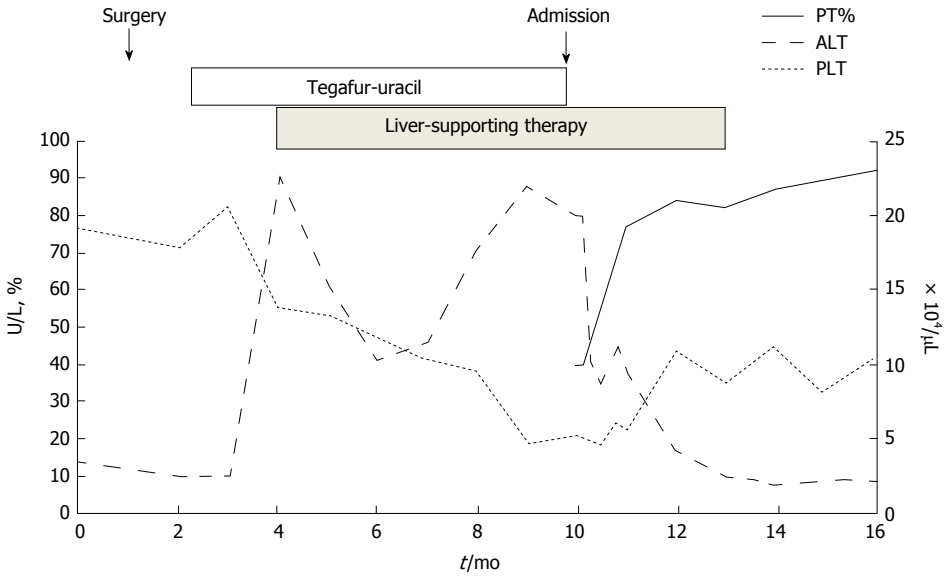

Figure 4 Clinical course. Serum ALT levels increased after the administration of tegafur-uracil. With liver-supporting treatment, the serum ALT levels temporarily improved. However, serum ALT levels increased again, and the patient was referred to our hospital after 8 mo. Discontinuation of tegafur-uracil combined with conservative treatment improved serum ALT levels, platelet counts, and prothrombin activity. PT%: Prothrombin time; ALT: Alanine aminotransferase.

were useful for the diagnosis of tegafur-uracil-induced hepatic fibrosis[1,4]. In our case, serum fibrosis markers, MR elastography, and VTQ indicated the presence of advanced hepatic fibrosis. Histopathological findings from liver biopsy specimens supported the findings obtained using the abovementioned techniques. These data suggest that non-invasive approaches may be useful in diagnosing hepatic fibrosis in patients with DILI.

In conclusion, our case suggests that short-term treatment with tegafur-uracil may lead to the rapid development of hepatic fibrosis with portal hypertension. Tegafur-uracil can occasionally induce liver injury, which may develop into advanced hepatic fibrosis with portal hypertension. However, hepatic fibrosis is not evaluated in many cases. Thus, when liver dysfunction progresses in patients who are treated with tegafur-uracil even for short periods, oncologists should consider hepatic fibrosis and perform a non-invasive assessment to rule out this possibility.

COMMENTS

Case characteristics

A 74-year-old Japanese woman who was treated with tegafur-uracil for 8 mo after breast cancer surgery presented with abdominal distension and leg edema.

Clinical diagnosis

Massive ascites and leg edema.

Differential diagnosis

Primary biliary cholangitis.

Laboratory diagnosis

Laboratory examination revealed low platelet counts, liver dysfunction, and high hepatic fibrosis markers such as type 4 collagen 7S and hyaluronic acid.

Imaging diagnosis

CT imaging revealed massive ascites and splenomegaly, and both of MR elastography and VTQ indicated advanced hepatic fibrosis.

Pathological diagnosis

Pathological examination revealed bridging fibrosis with septation, suggesting advanced hepatic fibrosis.

Treatment

Discontinuation of tegafur-uracil combined with conservative treatment.

Related reports

Some studies have shown the development of hepatic fibrosis induced by tegafur-uracil. However, all of the previously described patients had been treated with tegafur-uracil for a long period of time.

Term explanation

Tegafur-uracil has minor adverse effects and is associated with liver injury in only 1.79% of Japanese patients. Tegafur-uracil-induced hepatic fibrosis is rare.

Experiences and lesson

The present case suggests that tegafur-uracil may lead to the rapid development of hepatic fibrosis with portal hypertension, even when administered for a short period of time.

Peer-review

This is a well written case report. The case is rare and unusual in view of the rapid progression of the fibrosis.

REFERENCES

1 **Suou T**, Tanaka K, Okano J, Shiota G, Horie Y, Horie Y, Kawasaki H. A case with hepatic fibrosis showing ascites and esophageal varices induced by oral UFT(R) administration. *Hepatol Res* 2002; **22**: 161-165 [PMID: 11818256]
2 **Palmeri S**, Gebbia V, Russo A, Armata MG, Gebbia N, Rausa L. Oral tegafur in the treatment of gastrointestinal tract cancers: a phase II study. *Br J Cancer* 1990; **61**: 475-478 [PMID: 2109630]
3 **Kobayashi F**, Ikeda T, Sakamoto N, Kurosaki M, Tozuka S,

Sakamoto S, Fukuma T, Marumo F, Sato C. Severe chronic active hepatitis induced by UFTR containing tegafur and uracil. *Dig Dis Sci* 1995; **40**: 2434-2437 [PMID: 7587827]

4 **Suou T**, Maruyama S, Nakamura H, Kishimoto Y, Abe J, Tanida O, Yamada S, Kawasaki H. Increase in serum 7S domain of type IV collagen and N-terminal propeptide of type III procollagen levels with normal serum transaminase levels after long-term oral administration of Tegaful-Uracil. *Hepatol Res* 2002; **24**: 184 [PMID: 12270748]

5 **Nakamura M**, Kondo H, Mori T, Komori A, Matsuyama M, Ito M, Takii Y, Koyabu M, Yokoyama T, Migita K, Daikoku M, Abiru S, Yatsuhashi H, Takezaki E, Masaki N, Sugi K, Honda K, Adachi H, Nishi H, Watanabe Y, Nakamura Y, Shimada M, Komatsu T, Saito A, Saoshiro T, Harada H, Sodeyama T, Hayashi S, Masumoto A, Sando T, Yamamoto T, Sakai H, Kobayashi M, Muro T, Koga M, Shums Z, Norman GL, Ishibashi H. Anti-gp210 and anti-centromere antibodies are different risk factors for the progression of primary biliary cirrhosis. *Hepatology* 2007; **45**: 118-127 [PMID: 17187436 DOI: 10.1002/hep.21472]

6 **Ishibashi H**, Komori A, Shimoda S, Ambrosini YM, Gershwin ME, Nakamura M. Risk factors and prediction of long-term outcome in primary biliary cirrhosis. *Intern Med* 2011; **50**: 1-10 [PMID: 21212566]

7 **Kaplan MM**. Primary biliary cirrhosis. *N Engl J Med* 1996; **335**: 1570-1580 [PMID: 8900092 DOI: 10.1056/NEJM199611213352107]

8 **Neuberger J**. Primary biliary cirrhosis. *Lancet* 1997; **350**: 875-879 [PMID: 9310614 DOI: 10.1016/S0140-6736(97)05419-6]

9 **Ortega-Alonso A**, Stephens C, Lucena MI, Andrade RJ. Case Characterization, Clinical Features and Risk Factors in Drug-Induced Liver Injury. *Int J Mol Sci* 2016; **17**: pii: E714 [PMID: 27187363 DOI: 10.3390/ijms17050714]

10 **deLemos AS**, Foureau DM, Jacobs C, Ahrens W, Russo MW, Bonkovsky HL. Drug-induced liver injury with autoimmune features. *Semin Liver Dis* 2014; **34**: 194-204 [PMID: 24879983 DOI: 10.1055/s-0034-1375959]

11 **Shire NJ**, Yin M, Chen J, Railkar RA, Fox-Bosetti S, Johnson SM, Beals CR, Dardzinski BJ, Sanderson SO, Talwalkar JA, Ehman RL. Test-retest repeatability of MR elastography for noninvasive liver fibrosis assessment in hepatitis C. *J Magn Reson Imaging* 2011; **34**: 947-955 [PMID: 21751289 DOI: 10.1002/jmri.22716]

12 **Motosugi U**, Ichikawa T, Sano K, Sou H, Muhi A, Koshiishi T, Ehman RL, Araki T. Magnetic resonance elastography of the liver: preliminary results and estimation of inter-rater reliability. *Jpn J Radiol* 2010; **28**: 623-627 [PMID: 20972864 DOI: 10.1007/s11604-010-0478-1]

13 **Friedrich-Rust M**, Nierhoff J, Lupsor M, Sporea I, Fierbinteanu-Braticevici C, Strobel D, Takahashi H, Yoneda M, Suda T, Zeuzem S, Herrmann E. Performance of Acoustic Radiation Force Impulse imaging for the staging of liver fibrosis: a pooled meta-analysis. *J Viral Hepat* 2012; **19**: e212-e219 [PMID: 22239521 DOI: 10.1111/j.1365-2893.2011.01537.x]

14 **Kircheis G**, Sagir A, Vogt C, Vom Dahl S, Kubitz R, Häussinger D. Evaluation of acoustic radiation force impulse imaging for determination of liver stiffness using transient elastography as a reference. *World J Gastroenterol* 2012; **18**: 1077-1084 [PMID: 22416182 DOI: 10.3748/wjg.v18.i10.1077]

15 **Nightingale K**. Acoustic Radiation Force Impulse (ARFI) Imaging: a Review. *Curr Med Imaging Rev* 2011; **7**: 328-339 [PMID: 22545033 DOI: 10.2174/157340511798038657]

P- Reviewer: Buechler C, Snyder N **S- Editor**: Gong ZM
L- Editor: A **E- Editor**: Li D

Published by **Baishideng Publishing Group Inc**
7901 Stoneridge Drive, Suite 501, Pleasanton, CA 94588, USA
Telephone: +1-925-223-8242
Fax: +1-925-223-8243
E-mail: bpgoffice@wjgnet.com
Help Desk: http://www.f6publishing.com/helpdesk
http://www.wjgnet.com

ISSN 1007-9327